Untersuchungen zur Molekulargewichtsverteilung von Polyäthylenterephthalat*

KLAUS GEHRKE† und GERHARD REINISCH, *Deutsche Akademie der Wissenschaften zu Berlin, Institut für Faserstoff-Forschung, Teltow-Seehof, Deutsche Demokratische Republik*

Synopsis

The molecular weight distribution of carefully prepared thermostabilized poly(ethylene terephthalate) was determined immediately after polycondensation *in vacuo* ($\bar{P}_n = 121$) and after the melt was stirred at 280°C for 5.5 hr under nitrogen ($\bar{P}_n = 123$). The fractionation was carried out by successive precipitation in liquid phases. The samples were separated into 25 fractions including refractionation. The Flory distribution was observed in all samples.

Einleitung

Zur genaueren Charakterisierung von Polymeren dient neben der Bestimmung des mittleren Polymerisationsgrades die Festlegung der Molekulargewichtsverteilungskurve. Bisher bekannte Untersuchungen zur Molekulargewichtsverteilung von Polyäthylenterephthalat behandeln Veränderungen in unstabilisierten Proben verschieden langer Schmelzeverweilzeiten bzw. während des Abbaus. So fand Ciampa,[3] dass bei verhältnismässig gleicher Viskosität im Laufe eines Spinnvorganges eine Verbreiterung der Molekulargewichtsverteilung eintritt, während Turska und Skwarski[4] mitteilten, dass mit fortlaufendem Abbau eine Verschmälerung gegenüber der von Flory[5] und Schulz[6] für Polykondensate berechneten Molekulargewichtsverteilung eintritt. Als Ursache für diese gegensätzlichen Effekte wurden in beiden Arbeiten Reaktionen zwischen Endgruppen und binnenständigen Estergruppen der Polymerketten angenommen. Solche Kettenaustauschreaktionen sind aber nach Flory bereits bei der Aufstellung der theoretischen Molekulargewichtsverteilung berücksichtigt worden.

In unstabilisierten Polyäthylenterephthalatschmelzen verlaufen Zwischenkettenaustausch- und Abbaureaktionen nebeneinander, so dass sich beide Einflüsse auf die Molekulargewichtsverteilung überlagern. Sta-

bilisierte Polyäthylenterephthalatschmelzen, in denen nach Zimmermann[7] erst nach 8–10 Stdn ein Viskositätsabfall eintritt, gestatten es nun, die Zusammenhänge zwischen den rasch und reversibel verlaufenden Zwischenkettenaustauschreaktionen und der Molekulargewichtsverteilung getrennt vom Einfluss des irreversiblen Kettenabbaus festzustellen. Auch in diesen Schmelzen werden zwar Polymerketten in gewissem Umfang statistisch gespalten. Das Polymere enthält aber infolge schonender Herstellung noch genügend Hydroxylgruppen, die mit den Vinylesterendgruppen des einen Spaltstückes sogleich wieder unter Kettenverlängerung reagieren können.[8] Die Reaktion ähnelt also insgesamt einem Zwischenkettenaustausch. Nach Kenntnis des Zusammenhanges von Zwischenkettenaustausch und Molekulargewichtsverteilung gestatten dann abgebaute Proben, in denen beide Reaktionen parallel laufen, eine Aussage über den Einfluss des irreversiblen Kettenabbaus.

Die Ergebnisse unserer Untersuchungen über die Polymerisationsgradverteilung während des Auf- und Abbaustadiums der Schmelzepolykondensation von Polyäthylenterephthalat haben wir bereits veröffentlicht.[9] Die Publikation der vorangegangenen Versuche an thermostabilisierten Schmelzen[1] hat sich leider wegen technischer Schwierigkeiten stark verzögert. Wir meinen aber, dass diese Ergebnisse für das Gesamtbild und für die Praxis der Polyäthylenterephthalatherstellung auch jetzt noch von Interesse sind und haben das Angebot des Herausgebers der Symposiumsbände gern angenommen, die Arbeit doch noch zu publizieren. Zur Unterschung der Molekulargewichtsverteilung von schmelzestabilisiertem Polyäthylenterephthalat benutzten wir zwei Proben aus einem 22 Mol-Ansatz (V4A-Rührautoklav), wobei die erste Probe nach Beendigung der Polykondensation entnommen worden war und den Polymerisationsgrad 121 besass. Für die zweite Probe nach einer Schmelzeverweilzeit von $5^1/_2$ Stdn wurde der Polymerisationsgrad 123 gemessen.

Fraktioniermethode

Erfolgreich sind bis jetzt zur Ermittlung der Molekulargewichtsverteilung von Polyäthylenterephthalat die Methode der Lösefraktionierung[10] und die fraktionierte Fällung angewandt worden. Die fraktionierte Fällung kann entweder in Form von Niederschlägen oder als Verteilung zwischen zwei flüssigen Phasen ausgeführt werden. Von G. V. Schulz[11] wurde gezeigt, dass letztere Variante für kristallisierende Polymere eine bessere Selektivität zeigt. Wir benutzten deshalb das Sukzessivverfahren.[12,13] Als Lösungsmittel diente Phenol/Tetrachloräthan (1:1, m:m) und als Fällmittel n-Heptan.

Zu einer 1% Lösung des Polymeren wurde n-Heptan bis zur Trübung zugegeben und anschliessend durch 7 Stdn. Rühren garantiert, dass das Gleichgewicht der Verteilung des Polymeren zwischen beiden flüssigen Phasen erreicht wird. Dann wurde 10 Stdn absitzen lassen und die untere flüssige Schicht, die die höhermolekularen Anteile enthält, abgetrennt. Entsprechend wurden so sieben bis acht Originalfraktionen erhalten.

Diese Originalfraktionen wurden auf dieselbe Weise in drei bis vier Unter-
fraktionen aufgeteilt. Die Bestimmung der Polymerenmenge in den
Fraktionen erfolgte gravimetrisch, die rel. Lösungsviskosität wurde in
Phenol/Tetrachloräthan (1:1) bei 20°C vermessen. Für die Umrechnung
zum Polymerisationsgrad wurden die Gleichungen von Frind[14] und Koepp
und Werner[15] benutzt. Aus den so erhaltenen Werten und dem Mengen-
prozentanteil der einzelnen Fraktionen wurde nach G. V. Schulz[16] die
Integralkurve konstruiert, die durch graphische Differentiation in die
Differentialkurve überführt wurde.

Ergebnisse und Diskussion

Die integrale Molekulargewichtsverteilung des stabilisierten Poly-
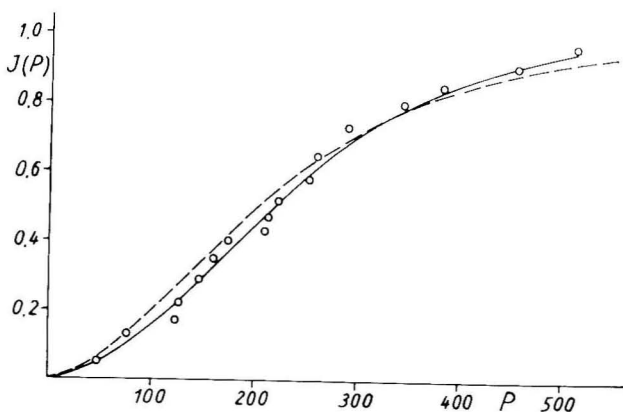äthylenterephthalats ist in Bild 1 und 2 dargestellt. Die Kurve in Bild 1

Abb. 1. Integralverteilungskurve von stabilisiertem Polyäthylenterephthalat, $\bar{P}_n = 121$,
im Vergleich zur theoretischen Kurve nach Flory (gestrichelte Kurve).

charakterisiert stabilisiertes Polyäthylenterephthalat nach der Beendigung
der Polykondensation (Probe K 1), die Kurve in Bild 2 das gleiche Polymere
nach 5½ Stdn. Schmelzeverweilzeit bei 280°C (Probe K 2). Die gestri-
chelten Kurven wurden aus dem mittleren Polymerisationsgrad der Aus-
gangsprobe nach Flory[5] berechnet. Die Fraktionierungen wurden je
einmal wiederholt. Dabei wurde festgestellt, dass die Verteilungskurven
reproduzierbar waren. Es ist von Grichl[17] bewiesen worden, dass mit
weiterer Aufteilung der Fraktionen eine Annäherung an die theoretische
Kurve möglich ist. Ca. 15 Fraktionen stellen nach unserer Meinung für
unser Problem einen Kompromiss zwischen Genauigkeit und Arbeits- und
Zeitaufwand dar.

Unter Berücksichtigung dieser Gesichtspunkte kann man aus unseren
Kurven den Schluss ziehen, dass thermostabilisiertes Polyäthylentere-
phthalat nach Beendigung der Kondensation sowie auch in der Schmelze bei
280°C über die Zeit, in der Viskositätskonstanz vorliegt, eine Flory-Vertei-
lung aufweist.

TABELLE I
Fraktionierung von stabilisiertem Polyäthylenterephthalat

$I(P)$, % Probe K 1	P	$I(P)$ % Probe K 2	P
4,57	48,2	1,58	29,2
12,79	77,5	4,70	54,3
17,43	123,7	8,82	92,7
22,42	127,5	14,01	94,1
28,98	145,0	18,33	103,0
35,46	161,4	22,53	113,8
40,74	172,8	25,74	140,1
43,46	210,2	29,43	141,8
47,28	212,0	35,30	179,5
52,10	224,1	39,54	184,6
57,85	252,3	43,02	188,0
64,61	258,5	47,58	210,2
73,56	290,0	52,54	215,4
80,19	345,8	57,14	252,4
85,09	381,4	61,36	275,7
91,43	457,1	65,63	277,4
97,09	513,8	70,50	321,4
		75,81	323,1
		79,26	332,8
		81,54	350,0
		83,70	355,0
		85,68	366,2
		88,29	448,4
		91,32	473,5
		95,50	496,8

Im Bild 3 sind die Differentialkurven für die beiden stabilisierten Polyäthylenterephthalatproben angeführt. Zusätzlich zu dem aus den Integralverteilungskurven gezogenen Schluss, dass hier eine Flory-Verteilung vorliegt, ist noch zu erkennen, dass sich die Molekulargewichtsverteilung während der Schmelzeverweilzeit nicht wesentlich verändert hat. Dies ist
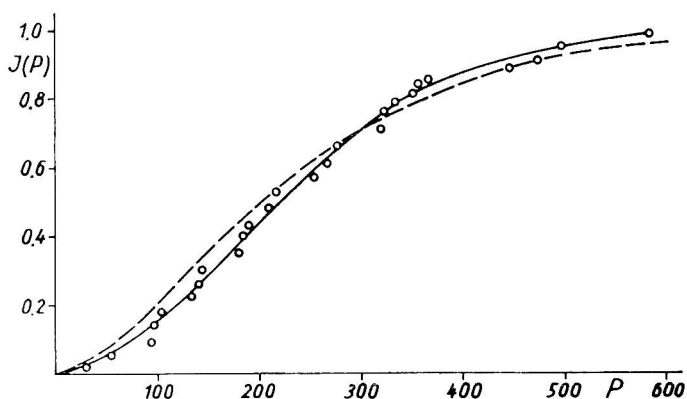

Abb. 2. Integralverteilungskurve von stabilisiertem Polyäthylenterephthalat nach einer Schmelzeverweilzeit von 5,5 Stdn bei 280°, $\bar{P}_n = 123$, (gestrichelte Kurve nach Flory).
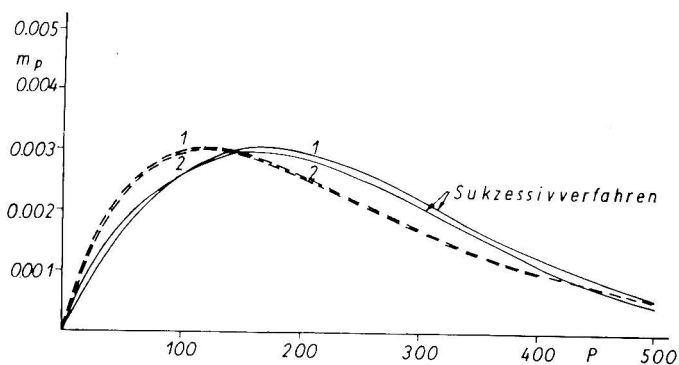
Abb. 3. Molekulargewichtsvereilungskurven von stabilisiertem Polyäthylenterephthalat vor (Kurve *1*) und nach (Kurve *2*) einer Schmelzeverweilzeit von 5,5 Stdn (gestrichelte Kurve nach Flory).

auch zu erwarten, da der mittlere Polymerisationsgrad beider Ausgangsproben fast identisch ist und für beide Proben eine Flory-Verteilung gefunden wurde.

Auf Grund der Übereinstimmung unserer Ergebnisse mit der theoretischen Verteilung nach Flory muss man annehmen, dass der Zwischenkettenaustausch in schonend hergestellten Polyäthylenterephthalatschmelzen, die unter guter Durchmischung im offenen System gehalten werden, nach statistischen Gesetzen erfolgt.

Experimenteller Teil

Das stabilisierte Polyäthylenterephthalat wurde aus 22 Mol Dimethylterephthalat und 66 Mol Glykol unter Verwendung von 0,03 Mol/Mol Mangan (II)-acetat, 0,03 Mol/Mol Antimon (III)-acetat und 0,06 Mol/ Mol Triphenylphosphat bei $277 \pm 1°C$ und 0,6 Torr unter Reinststickstoff hergestellt. Nach Beendigung der Polykondensation wurde das Vakuum mit Stickstoff aufgehoben. Während der $5^{1}/_{2}$ Std. Schmelzeverweilzeit bei 280°C wurde mit 60 U/min gerührt und ein Stickstoffstrom von 4 1/Std. übergeleitet.

Die Einsatzmengen für die Sukzessivfraktionierungen betrugen 13 g. Die wiedergewonnene Menge Polymeres nach der Fraktionierung betrug 96,2% (K 1) und 94,86% (K 2). Die Fraktionierung einer jeden Probe wurde wiederholt. Die Verteilungskurven waren reproduzierbar. Umkehrungen bei der Gewinnung der Originalfraktionen traten nicht auf.

Literatur

1. K. Gehrke und Reinisch, G., Vortrag Internat. Symposium über Makromolekulare Chemie, Prag 1965, Preprint 444.

2. H. Zimmermann, G. Reinisch, K. Gehrke, E Leibnitz, und P. Lohmann, *Abh. deut. Akad. Wiss. Berlin, Kl. Chem., Geol., Biol.*, **1965,** No. 3, 19.

3. G. Ciampa und R. Paolillo, *Atti Acad. Naz. Lincei, Rend. Cl. Sci. Fis. Mat. Nat.* **26**, 459 (1959).

4. E. Turska und T. Skwarski, Makromolekulares Symposium Wiesbaden 1959, III B 13.

5. P. J. Flory, *J. Amer. Chem. Soc.*, **58**, 1877 (1936).

6. G. V. Schulz, *Z. Physik. Chem.*, **A182**, 127 (1938).

7. H. Zimmermann, *Faserforsch. Textiltech.*, **13**, 481 (1962).

8. H. Zimmermann und E. Leibnitz, *Faserforsch. Textiltech.*, **16**, 282 (1965).

9. K. Gehrke und G. Reinisch, *Faserforsch. Textiltech.*, **17**, 201 (1966).

10. O. Fuchs, *Z. Elektrochem.*, **60**, 229 (1956).

11. G. V. Schulz und E. Nordt, *J. Prakt. Chem.*, **155**, 115 (1940).

12. A. Gordijenko, *Faserforsch. Textiltech.*, **4**, 499 (1953).

13. E. Turska und T. Skwarski, *Zeszyty Nauk Politechn. Lodz, Chem.*, **5**, 21 (1957).

14. H. Frind, *Faserforsch. Textiltech.*, **5**, 290 (1954).

15. H. Koepp und H. Werner, *Makromol. Chem.*, **32**, 79 (1959).

16. G. V. Schulz und A. Dinglinger, *Z. Physik. Chem.*, **43B**, 47 (1939).

17. W. Griehl und H. Lückert, *J. Polym. Sci.*, **30**, 399 (1958).

Alternating Copolymerization of Polar Vinyl Monomers in the Presence of Zinc Chloride. I. Propagation and Initiation of the Copolymerization of Acrylonitrile with Styrene

SHIGERU YABUMOTO, KIYOSHI ISHII, and KOICHIRO ARITA,
Central Research Laboratory, Daicel Limited, Irumagun, Saitama, Japan

Synopsis

Copolymerization of acrylonitrile with styrene spontaneously occurred on addition of zinc chloride without addition of any other radical initiator. The composition of the copolymer approached that of strictly alternating copolymer as zinc chloride added to the copolymerization system increased. The significance of the apparent monomer reactivity ratios of this copolymerization system was studied from a kinetic point of view, and it was shown that the monomer sequence distribution is indicated by the apparent monomer reactivity ratios. Further, equations which represent the relation between the apparent monomer reactivity ratios and Q,e values at a given salt concentration were derived. These equations reasonably accounted for the decrease of the apparent monomer reactivity ratios of the copolymerization of acrylonitrile with styrene in the presence of zinc chloride and the behavior of the other acrylonitrile copolymerization systems in the presence of zinc chloride. The initiation step of the spontaneous radical copolymerization of acrylonitrile with styrene in the presence of zinc chloride was explained by a cross-initiation mechanism.

INTRODUCTION

In recent years, it has been found by several groups of workers,[1-8] that the copolymerization reactivity of polar vinyl monomers having nitrogen or oxygen atoms in their side chains is altered by complexing with Lewis acids. In view of the results of the spectroscopic study[9] and the LCAO calculation[10] of complexed monomers, it seems to be reasonable to explain the change of the copolymerization reactivity in terms of Q,e values of the complexed monomers.

The change of monomer reactivity ratios for acrylonitrile (AN) has been reported by Imoto et al.[1] for the case of copolymerization with vinylidene chloride in the presence of $ZnCl_2$. The $AN \cdot ZnCl_2$ complex is so poorly soluble in vinylidene chloride that the copolymerization can not be carried if all of AN in the copolymerization system forms complex with $ZnCl_2$. There are thus three kinds of monomers in the copolymerization system: $AN \cdot ZnCl_2$ complex, free AN, and vinylidene chloride, and there are corresponding three kinds of polymer radicals. Therefore this copoly-

merization system can not be dealt with as an ordinary two-component copolymerization system, and it is not quite obvious that the Lewis-Mayo equation can be applied to such a copolymerization system.

AN–styrene(St) copolymer (AS copolymer) is an industrially produced plastic which has however the shortcoming of thermal coloration. Several reactions may be involved in the coloration, but, as is the case with the thermal coloration of AN homopolymer,[11–16] the contribution of the cyclization reaction of cyano groups in a long AN sequence in the copolymer may be predominant.

From the results of the AN–vinylidene chloride copolymerization in the presence of $ZnCl_2$,[1] it was expected that alternating AN–St copolymer of high thermostability might be obtained by copolymerization in the presence of $ZnCl_2$. In the course of the experiments following facts were found: (1) the apparent monomer reactivity ratios of the AN–St copolymerization in the presence of $ZnCl_2$ decrease as $ZnCl_2$ added to the copolymerization system increases; (2) the radical copolymerization occurs spontaneously with addition of $ZnCl_2$ without addition of any other radical initiator.

In the present report, it is discussed from the kinetic point of view whether the Lewis-Mayo equation can be applied to this copolymerization system. The relation of the apparent monomer reactivity ratios to the monomer sequence distribution in the copolymer and to the Q,e scheme is elucidated. The spontaneous initiation of the copolymerization of AN with St in the presence of $ZnCl_2$ is explained by a cross-initiation mechanism.

Subsequent reports in this series will discuss some properties of the AS copolymer obtained by copolymerization in the presence of $ZnCl_2$ and will deal with the copolymerization of methyl methacrylate with St in the presence of $ZnCl_2$.

EXPERIMENTAL

Materials

Monomers as commercially obtained were dried over anhydrous sodium sulfate and distilled in a stream of dry nitrogen.

$ZnCl_2$ was the Guaranteed Reagent grade and was used without further purification.

Copolymerization Procedure

$ZnCl_2$ was dissolved in AN at a given concentration, and this solution and St were introduced into a glass tube in a dry nitrogen stream. The glass tube was sealed off and kept in a thermostat maintained at a constant temperature to allow polymerization to take place. The resulting copolymer was purified repeatedly by dissolution in acetone and precipitation into methanol, and the elimination of $ZnCl_2$ from the copolymer was confirmed by an acetone solution of dithizone.

Analysis of Copolymer Composition and Reactivity Ratios

Copolymer composition was determined at less than 5% conversion by nitrogen analysis by the micro-Dumas method (Coleman nitrogen analyzer). Monomer reactivity ratios were determined by the line intersection method. The copolymer contained no cyclohexane-soluble material, indicating that cationic polymerization of St did not take place.

RESULTS AND DISCUSSION

Copolymerization of AN with St in the Presence of $ZnCl_2$

The composition of the AN copolymer obtained by the copolymerization in the presence of $ZnCl_2$ approaches equimolar composition, as the quantity
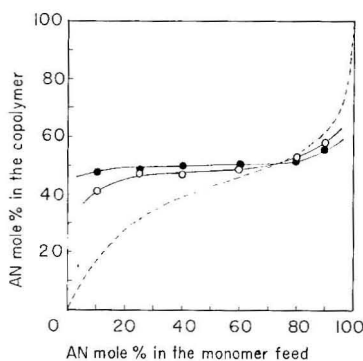

Fig. 1. Composition of the AN–St copolymer obtained in the presence of $ZnCl_2$ at 60°C: ($\bullet$) $ZnCl_2/AN = 0.10$ (mole ratio), ($\circ$) $ZnCl_2/AN = 0.03$; (--) copolymer composition of ordinary radical copolymerization; $r_1 = 0.04$, $r_2 = 0.4$.
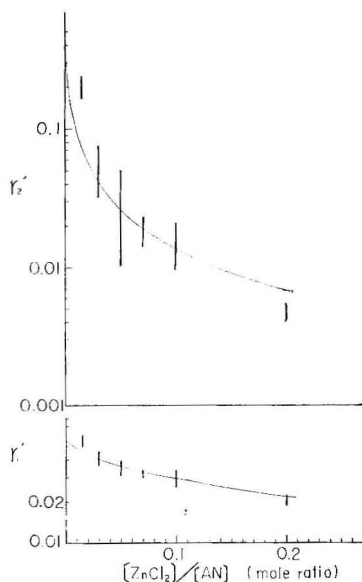

Fig. 2. Apparent monomer reactivity ratios vs. $ZnCl_2$ concentration.

of ZnCl$_2$ added to the copolymerization system increases.   Some examples are shown in Figure 1.

The change of the apparent monomer reactivity ratios with increasing concentration of ZnCl$_2$ is shown in Figure 2.   In the case of ordinary copolymerization, such a copolymer composition curve indicates strongly an alternating copolymerization, but, as mentioned above, this copolymerization is substantially a three-component copolymerization system, and therefore the meaning of the apparent monomer reactivity ratios should be elucidated from a kinetic point of view, before the monomer sequence distribution in the copolymer is discussed.

Copolymer Equation in the Presence of a Salt

In the case of that monomer A is capable of forming complex with a salt and monomer B is not capable of forming complex, the copolymer equation for the copolymerization of these monomers at a given salt concentration is derived as follows.

We let M$_1$, M$_2$, and M$_3$ represent free monomer A, monomer A complexed with a salt, and monomer B, respectively, and M$_1\cdot$, M$_2\cdot$, and M$_3\cdot$ represent the growing polymer radicals having monomers M$_1$, M$_2$ and M$_3$ as their terminal, free-radical-bearing units, respectively.   There are nine possible chain-propagating reactions, i.e.

the reaction is:

$$M_i\cdot + M_j \rightarrow M_j\cdot \quad i = 1,2,3 \quad\quad j = 1,2,3$$
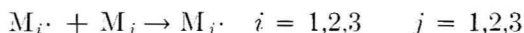
the rate being $k_{ij}[M_i\cdot][M_j]$.

The probability of the addition of monomer B to the polymer radical, the terminal group of which is free or complexed monomer A, is given by

$$P_{ab} = \frac{k_{13}[M_1\cdot][M_3] + k_{23}[M_2\cdot][M_3]}{k_{11}[M_1\cdot][M_1] + k_{12}[M_1\cdot][M_2] + k_{22}[M_2\cdot][M_2] + k_{21}[M_2\cdot][M_1] + k_{13}[M_1\cdot][M_3] + k_{23}[M_2\cdot][M_3]} \quad (1)$$

If the ratio of the concentrations of M$_1$ and M$_2$ and the ratio of the concentrations of M$_1\cdot$ and M$_2\cdot$ are represented as shown in eqs. (2) and (3), the probability of P_{ab} is as given in eq. (1)

$$[M_2]/[M_1] = t/(1 - t) \quad (2)$$

$$[M_2\cdot]/[M_1\cdot] = s/(1 - s) \quad (3)$$

$$P_{ab} = \frac{[M_3]\{(1-s)k_{13} + sk_{23}\}}{\{[M_1] + [M_2]\}\{(1-t)k_{11} + (1-t)sk_{21} + t(1-s)k_{12} + tsk_{22}\} + [M_3]\{(1-s)k_{13} + sk_{23}\}}$$

$$= \frac{[M_3]}{[M_3] + r_1'([M_1] + [M_2])} \quad (4)$$

where

$$r_1' = \frac{(1 - t)(1 - s)k_{11} + (1 - t)sk_{21} + t(1 - s)k_{12} + tsk_{22}}{(1 - s)k_{13} + sk_{23}} \quad (5)$$

The other probabilities of the propagating reactions are given in the same way.

$$P_{ba} = \frac{[M_1] + [M_2]}{r_2'[M_3] + [M_1] + [M_2]} \tag{6}$$

where

$$r_2' = \frac{k_{33}}{(1 - t)k_{31} + tk_{32}} \tag{7}$$

and

$$P_{aa} = 1 - P_{ab} = \frac{r_1'([M_1] + [M_2])}{[M_3] + r_1'([M_1] + [M_2])} \tag{8}$$

$$P_{bb} = 1 - P_{ba} = \frac{r_2'[M_3]}{r_2'[M_3] + [M_1] + [M_2]} \tag{9}$$

Goldfinger[17] derived the next equation for copolymer composition,

$$P_{ba}/P_{ab} = a/b \tag{10}$$

where a and b are the mole fractions of monomer A and B, respectively, in the copolymer.

Substituting eqs. (4) and (6) in eq. (10) yields

$$a/b = d([M_1] + [M_2])/d[M_3]$$

$$= \frac{[M_1] + [M_2]}{[M_3]} \frac{r_1'([M_1] + [M_2]) + [M_3]}{r_2'[M_3] + ([M_1] + [M_2])} \tag{11}$$

This equation has an identical form with the Mayo-Lewis copolymer equation. It is quite obvious that r'_1 and r'_2 are the apparent monomer reactivity ratios which are obtained by dealing with the copolymerization in the presence of a salt as an ordinary copolymerization. In the case that s defined by eq. (3) is constant all over the range of monomer composition in the feed, r'_1 can be obtained as a constant, and the monomer sequence distribution in the copolymer can be calculated by eqs. (4), (6), (8), and (9) in the same way as the calculation of the monomer sequence distribution for an ordinary copolymer.

If the transfer of ligands between salts in the copolymerization system easily takes place, the possibility of the following equilibrium will be assumed:

$$[M_1\cdot] + [M_2] \overset{K}{\rightleftharpoons} [M_2\cdot] + [M_1]$$

$$[M_1\cdot][M_2] = K[M_2\cdot][M_1] \tag{12}$$
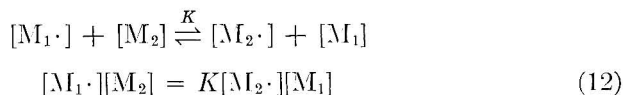
where K is an equilibrium constant.

Substituting eqs. (2) and (3) in eq. (12) yields

$$s/(1 - s) = Kt/(1 - t) \tag{13}$$

Apparently, in this case s is constant at a given t which is determined by the ratio of the concentration of complexed A monomer to the concentration of free A monomer.

In the case of the copolymerization of AN with St in the presence of $ZnCl_2$, considering the rather poor stability[18] of the $AN \cdot ZnCl_2$ complex in polar solvents, the equilibrium described above can be reasonably assumed. Thus the monomer sequence distribution of the AS copolymer obtained by the copolymerization in the presence of $ZnCl_2$ can be described by apparent reactivity ratios, and small values of those indicate the alternating tendency of the copolymer.

Relation between the Apparent Monomer Reactivity Ratios and Q,e Values

Following the Alfrey-Price treatment, the nine rate constants of the copolymerization in the presence of a salt are written as follows:

$$k_{ij} = P_i Q_j e^{-e_{ij}} \qquad i = 1,2,3 \qquad j = 1,2,3 \qquad (14)$$

Substituting eqs. (13) and (14) in eqs. (5) and (7) yields

$$r_1' = \frac{(1-t)^2 Q_1 \exp\{-e_1^2\} + t(1-t)(Q_2 + PQ_1)\exp\{-e_1 e_2\} + t^2 PQ_2 \exp\{-e_2^2\}}{(1-t)Q_3 \exp\{-e_1 e_3\} + tPQ_3 \exp\{-e_2 e_3\}} \qquad (15)$$

$$r_2' = \frac{Q_3 \exp\{-e_3^2\}}{(1-t)Q_1 \exp\{-e_1 e_3\} + tQ_2 \exp\{-e_2 e_3\}} \qquad (16)$$

where

$$P = KP_2/P_1 \qquad (17)$$

P is an inherent constant in the combination of monomer A and the salt.

In the case of the copolymerization of AN with St in the presence of $ZnCl_2$, M_1 is AN, M_2 is $AN \cdot ZnCl_2$ complex, and M_3 is St. Q,e values of AN and St are known from the literature,[19] but P, Q_2, and e_2 are unknown. These values were estimated by a curve fitting method in the experimental results of Figure 2. Thus $P = 5.39$, $Q_2 = 24$, $e_2 = 2.53$ are obtained.

The curve resulting from this calculation is shown in Figure 2. The decrease of the apparent reactivity ratios of the copolymerization of AN with St with increase of the quantity of $ZnCl_2$ added was successfully explained. To calculate t in eqs. (15) and (16), the composition of the $AN \cdot ZnCl_2$ complex was assumed to be in a molar ratio of 2:1, on the basis of the results reported by Sumitomo et al.[20]

To ascertain the validity of eqs. (15) and (16) other copolymerization systems of AN in the presence of $ZnCl_2$ were investigated. The results of the copolymerization of AN with α-methylstyrene in the presence of $ZnCl_2$ are shown by the points in Figure 3. The copolymerization curve, plotted in Figure 3 was calculated from the apparent reactivity ratios, which were predicted by means of eqs. (15) and (16), Q,e values of
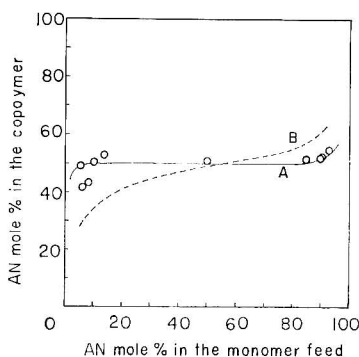
Fig. 3. AN–α-methylstyrene copolymerization in the presence of ZnCl$_2$, ZnCl$_2$/AN = 0.10 (mole ratio): (A) the curve predicted by eqs. (15) and (16), (B) ordinary radical copolymerization curve from literature.[21]
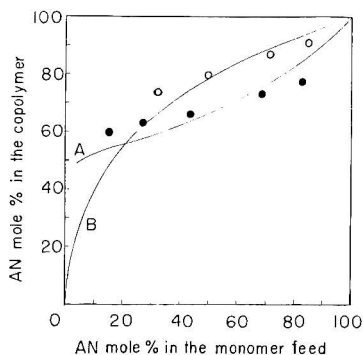

Fig. 4. Copolymerization of AN–ZnCl$_2$ complex with allyl chloride, (A and B) the copolymer composition curve predicted by Q,e: (●) in the presence of ZnCl$_2$, (○) in the absence of ZnCl$_2$; Experimental results are from Imoto et al.[3]

α-methylstyrene[19] ($Q_3 = 0.98$, $e_3 = -1.27$), and P, Q, e values of AN·ZnCl$_2$ complex (described above). The experimental results fit the curve well.

In Table I the apparent monomer reactivity ratios obtained by Imoto et al.[1] for the copolymerization of AN with vinylidene chloride in the presence of ZnCl$_2$ are compared with those calculated by eqs. (15) and

TABLE I

Apparent Monomer Reactivity Ratios of the AN–Vinylidene Chloride Copolymerization

ZnCl$_2$/AN (mole ratio)	Calculated by eqs. (15) and (16)		Observed by Imoto et al.[1]	
	r_1'	r_2'	r_1'	r_2'
0	0.91	0.37	0.91	0.22
0.023	1.18	0.24	1.10	0.12
0.071	1.40	0.11	1.16	0.05
0.122	1.48	0.07	1.20	0.01

(16) and Q,e values (Q,e values of vinylidene chloride;[19] $Q_3 = 0.22$, $e_3 = 0.36$).

The calculated r_1' values are in better agreement with the observed values than the r_2' values are. Since the observed values of r_2' were estimated from copolymerization experiments at rather low vinylidene chloride contents in the feed monomer, and the absolute values of r_2' were very small, the agreement between the observed and calculated r_2''s seems to be satisfactory.

In Figure 4 the results of the copolymerization of $AN \cdot ZnCl_2$ complex with allyl chloride by Imoto et al.[3] are compared with the copolymerization curve calculated from monomer reactivity ratios which are estimated from Q,e values (Q,e values of allyl chloride,[19] $Q = 0.056$, $e = 0.11$). Considering the latitude of the uncertainty of Q,e values, the agreement between observation and calculation shown in Figure 4 seems to be satisfactory.

Thus it has been shown that P,Q,e values of $AN \cdot ZnCl_2$ complex obtained from the copolymerization of AN with St in the presence of $ZnCl_2$ and eqs. (15) and (16) can be applied to other copolymerization systems of AN in the presence of $ZnCl_2$.

In view of these facts it seems to be reasonable to assume that the concept described above about the propagation step of the copolymerization in the presence of a salt is valid, at least in the case of the copolymerization of AN in the presence of $ZnCl_2$.

Initiation of Copolymerization of AN with St in the Presence of $ZnCl_2$

The copolymerization of AN with St occurred spontaneously on addition of $ZnCl_2$ alone, without addition of any other radical initiator. Similar phenomena were observed also in the copolymerization of AN with styrene derivatives and that of methacrylonitrile with styrene derivatives. These acceleration effects of $ZnCl_2$ for the copolymerizations are shown in Table

TABLE II
Acceleration Effect of $ZnCl_2$ on the Copolymerizations

| Copolymerization system (M_1–M_2)[a] | Overall rate of copolymerization, wt-%/hr | | R_p/R_{p0} | $ZnCl_2/M_1$ (mole ratio) |
	In the absence of $ZnCl_2$ (R_{p0})	In the presence of $ZnCl_2$ (R_p)		
AN–St	0.29	3.28	11.6	0.10
AN–α-methylstyrene	0.12	1.87	15.5	0.10
Methacrylonitrile–α-methylstyrene	~0	2.59		0.10
AN–vinyltoluene	0.28	6.30	22.5	0.10
Methacrylonitrile–St	~0	2.38		0.21

[a] All the copolymerizations were carried out at 60°C, and the monomer composition in the feed was 1:1 mole ratio.

TABLE III
Effect of Hydroquinone on the AN·ZnCl$_2$–St Copolymerization

Hydroquinone/AN (mole ratio)	Polymerization conditions		Monomer composition in the feed, AN mole-%	ZnCl$_2$/AN (mole ratio)	Yield, %
	Temp, °C	Time, hr			
2.3 × 10^{-2}	20–25	48	60	0.10	0
0	20–25	48	60	0.10	≧98

II. The copolymerizations were inhibited by addition of hydroquinone, as shown in Table III. The 520 mμ absorption band of diphenyl picryl hydrazyl (DPPH) in the AN–ZnCl$_2$–DPPH solution (1:0.13:1.5 × 10^{-5} mole ratio) disappeared on addition of an equivalent volume of St, and a similar phenomenon was observed with iodine. The rates of the copolymerizations were accelerated by addition of lauroyl peroxide or 2,2′-azobis-isobutyronitrile, but the copolymer composition was identical with that of the copolymerization on addition of ZnCl$_2$ only, as shown in Table IV.

Recently it was reported that the formation of a charge-transfer complex of monomers was involved in the propagation and initiation steps of alternating copolymerizations.[22-29] In these copolymerization systems generally the absorption band of the charge-transfer complex was observed, but in the present copolymerization systems neither coloration (which indicated the formation of charge-transfer complex) nor a particular absorption band in the ultraviolet spectra of the copolymerization systems was observed.

In view of the above facts, the initiation step of the copolymerizations might be thermal initiation.

Walling[30] observed a large rate of thermal initiation for the copolymerizations of alternating pairs of monomers, and he named this phenomenon

TABLE IV
Effect of Lauroyl Peroxide (LPO) on the AN–St Copolymerization in the Presence of ZnCl$_2$[a]

Monomer composition in the feed, AN mole-%	LPO, wt-%	ZnCl$_2$/AN (mole ratio)	R_p, wt-%/hr	Copolymer composition, AN mole-%
10.0	0.20	0.10		47.1
25.0	0.20	0.10	20.4	49.1
40.2	0.22	0.10	27.8	49.8
80.0	0.20	0.10	19.8	52.3
10.2	0	0.10	0.3	47.3
25.2	0	0.10	2.7	48.6
40.0	0	0.10	4.0	50.4
79.5	0	0.10	2.3	52.2

[a] All the copolymerizations were carried out at 60°C.

cross initiation. The initiation step of the copolymerizations described here seems to belong to this category.

The formation of radicals by thermal initiation is assumed to be caused by hydrogen transfer between monomers.[31] In the reaction (18),
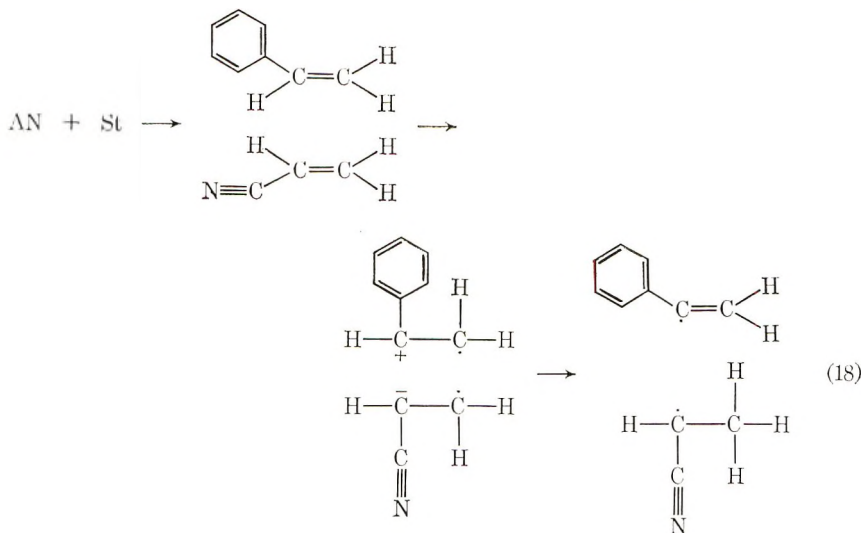
if AN is complexed with $ZnCl_2$, the polarity of AN may increase, the transition state of the reaction may be stabilized, and the reaction may take place more easily.

The alternating copolymerization of vinylidene cyanide with styrene occurs spontaneously without addition of radical initiator, and the initiation step of this copolymerization is a typical cross-initiation.[32] The Q,e values of vinylidene cyanide are $Q = 20.13$ and $e = 2.58$.[19] These values are close to the Q,e values of $AN \cdot ZnCl_2$ complex as estimated in this report, and this fact, too, seems to suggest the cross-initiation mechanism of the copolymerization of AN with St in the presence of $ZnCl_2$.
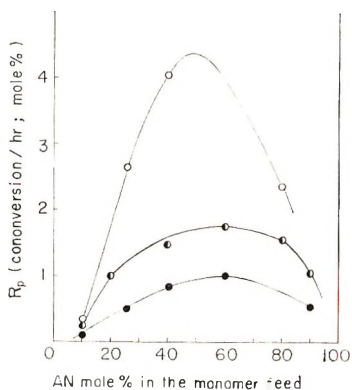

Fig. 5. Rp vs. monomer composition in the feed: (○) $ZnCl_2/AN = 0.10$ (mole ratio) at 60°C., (◑) $ZnCl_2/AN = 0.07$ at 60°C, (●) $RnCl_2/AN = 0.07$ at 40°C.

The overall rate of the copolymerization of AN with St in the presence of $ZnCl_2$ is shown in Figure 5 as a function of the composition of monomers in the feed.

The overall rate of the copolymerizations in the presence of a salt can be written as in eq. (19) in an identical form with the overall rate equation for an ordinary copolymerization, which was derived by Melville et al.,[33]

$$\frac{d\{[M_1] + [M_2] + [M_3]\}}{dt} =$$

$$\frac{I^{1/2}\{r_1'([M_1]+[M_2])^2+2([M_1]+[M_2])[M_3]+r_2[M_3]^2\}}{\{r_1'^2\delta_1'^2([M_1]+[M_2])^2+2\varphi r'_1 r'_2 \delta_1' \delta_2([M_1]+[M_2])[M_3]+r_2'^2\delta_2^2[M_3]^2\}^{1/2}} \quad (19)$$

where notations are the same as in the copolymer equation in the presence of a salt; I is the rate of the initiation, r_1' and r_2' are defined by eqs. (5) and (7). If k_{tij} is defined as a rate constant of the termination reaction,

$$\text{Mi·} + \text{Mj·} \rightarrow \text{inactive polymer}$$
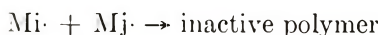
then

$$\delta_1' = \frac{\{k_{t11}(1-s)^2 + 2s(1-s)k_{t12} + s^2 k_{t22}\}^{1/2}}{(1-t)(1-s)k_{11} + t(1-s)k_{12} + s(1-t)k_{21} + tsk_{22}} \quad (20)$$

$$\delta_2 = k_{t33}^{1/2}/k_{33} \quad (21)$$

$$\varphi = \frac{sk_{t23} + (1-s)k_{t13}}{\{k_{t11}(1-s)^2 + 2s(1-s)k_{t12} + s^2 k_{t22}\}^{1/2}k_{t33}^{1/2}} \quad (22)$$

where k_{ij} is a propagation rate constant and t and s are defined by eqs. (2) and (3).

It is shown in Figure 5 that the overall rate of the copolymerization of AN with St in the presence of $ZnCl_2$ has a maximum. In the case of the copolymerization of two monomers which possess substituents inducing dissimilar polarity, the overall rate of copolymerization frequently has a minimum at a constant initiation rate,[34] since φ is generally greater than unity. Therefore the fact that the overall rate of the copolymerization in Figure 5 has a maximum suggests that the initiation rate has a maximum with the change of monomer composition; this is consistent with the assumption of the cross-initiation mechanism.

To discuss this problem more quantitatively, kinetic investigations to calculate δ_1' and φ values will be needed.

References

1. M. Imoto, T. Otsu, and K. Murata, *Kogyo Kagaku Zasshi*, **66**, 1900 (1963).
2. M. Imoto, T. Otsu, and Y. Harada, *Makromol. Chem.*, **65**, 180 (1963).
3. M. Imoto, T. Otsu, B. Yamada, and A. Shimizu, *Makromol. Chem.*, **82**, 277 (1965).
4. M. Imoto, T. Otsu, and B. Yamada, *Kogyo Kagaku Zasshi*, **68**, 1132 (1965).
5. Esso Research and Engineering Co., Brit. Pat. 946,052 (January 26, 1962).
6. M. Ibonai and T. Kato, *Kogyo Kagaku Zasshi*, **70**, 2078 (1967).

7. S. Tazuke, N. Sato, and S. Okamura, *J. Polym. Sci. A-1*, **4**, 2461 (1966).

8. S. Tazuke and S. Okamura, *J. Polym. Sci. A-1*, **5**, 1083 (1967).

9. S. Tazuke and S. Okamura, *J. Polym. Sci. B*, **5**, 95 (1967).

10. S. Tazuke, K. Tsuji, T. Yonezawa, and S. Okamura, *J. Phys. Chem.*, **71**, 2957 (1967).

11. N. Grassie and I. C. McNeill, *J. Polym. Sci.*, **27**, 207 (1958); *ibid.*, **31**, 205 (1958); *ibid.*, **39**, 211 (1959).

12. N. Grassie and I. N. Hay, *J. Polym. Sci.*, **56**, 189 (1962).

13. E. M. LaCombe, *J. Polym. Sci.*, **24**, 152 (1957).

14. H. Kobayashi, *Kobunshi Kagaku*, **10**, 496 (1953); *ibid.*, **11**, 84 (1954).

15. T. Takata, I. Hiroi, and M. Taniyama, *J. Polym. Sci. A*, **2**, 1567 (1964).

16. T. Takata, *Kobunshi Kagaku*, **19**, 641, 653, 682, 690 (1962).

17. G. Goldfinger, *J. Polym. Sci.*, **3**, 462 (1948).

18. M. Imoto, T. Otsu, and M. Nakabayashi, *Makromol. Chem.*, **65**, 194 (1963).

19. G. E. Ham, *Copolymerization*, Interscience, New York, 1964, pp. 845–863.

20. H. Sumitomo, K. Kobayashi, and Y. Yahama, *Kogyo Kagaku Zasshi*, **67**, 1658 (1964).

21. R. G. Fordyce, E. C. Chapin, and G. E. Ham, *J. Amer. Chem. Soc.*, **70**, 2489 (1948).

22. P. D. Bartlett and K. Nozaki, *J. Amer. Chem. Soc.*, **68**, 1495 (1946).

23. S. Iwatsuki and Y. Yamashita, *Kogyo Kagaku Zasshi*, **67**, 1470 (1964).

24. S. Iwatsuki, Y. Tanaka, and Y. Yamashita, *Kogyo Kagaku Zasshi*, **67**, 1467 (1964).

25. S. Iwatsuki and Y. Yamashita, *Kogyo Kagaku Zasshi*, **68**, 1138, 1963 (1965).

26. S. Iwatsuki, M. Murakami, and Y. Yamashita, *Kogyo Kagaku Zasshi*, **68**, 1967 (1965).

27. S. Iwatsuki and Y. Yamashita, *Makromol. Chem.*, **89**, 205 (1965).

28. S. Iwatsuki, M. Shin, and Y. Yamashita, *Makromol. Chem.*, **102**, 232 (1967).

29. S. Iwatsuki and Y. Yamashita, *J. Polym. Sci. A-1*, **5**, 1753 (1967).

30. C. Walling, *J. Amer. Chem. Soc.*, **71**, 1930 (1949).

31. M. Imoto and K. Fujishiro, *Kobunshi Kagaku Kyotei*, Asakura, Tokyo, 1965, pp. 43–45.

32. H. Gilbert, F. F. Miller, S. J. Averill, E. J. Carlson, V. L. Folt, H. J. Heller, F. D. Stewart, R. F. Schmidt, and H. L. Trumbull, *J. Amer. Chem. Soc.*, **78**, 1669 (1956).

33. H. W. Melville, B. Noble, and W. F. Watson, *J. Polym. Sci.*, **2**, 229 (1947).

34. C. H. Bamford, W. G. Barb, A. D. Jenkins, and P. F. Onyon, *The Kinetics of Vinyl Polymerization by Radical Mechanisms*, Butterworths, London, 1958, p. 176.

Aromatic Copolyimide–Amides II

W. WRASIDLO and J. M. AUGL, *U. S. Naval Ordnance Laboratory, White Oak, Silver Spring, Maryland 20910*

Synopsis

Six thermally stable polyimide-*co*-amides have been synthesized from sulfuryl-bis[*N*-(4′-phenylene)-4-(chloroformyl)-phthalimide] and various aromatic diamines. Linear, high molecular weight final polymers were obtained by one step low-temperature solution condensations in dimethylacetamide. Thermal properties such as glass transition and polymer decomposition temperatures and solution properties such as viscosities and solubilities varied significantly with polymer structure. Tough, flexible films of these polymers were cast from solution. The thermal-oxidative stabilities of films were strongly dependent on structure, solvents used, and impurities present.

INTRODUCTION

In a previous publication[1] it was shown that polyimide-*co*-amides made from monomers containing preformed imide rings have several advantages over those prepared by the polyamic acid route. On comparing polymers of varying structures, it was also demonstrated[1] that the introduction of diphenylsulfone linkages into the chain significantly improved solubility and isothermal oxidative stability. To further investigate these observations, a new series of polyimide-*co*-amides was prepared from a monomer containing the diphenylsulfone moiety between the preformed imide rings. It was anticipated that this group would favorably affect solubility and thermal properties with these polymers.
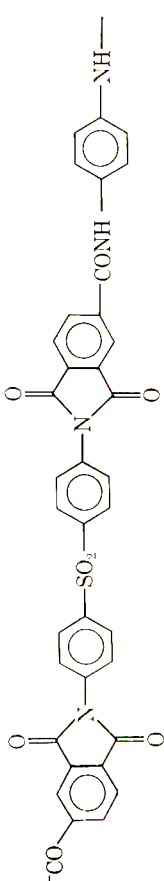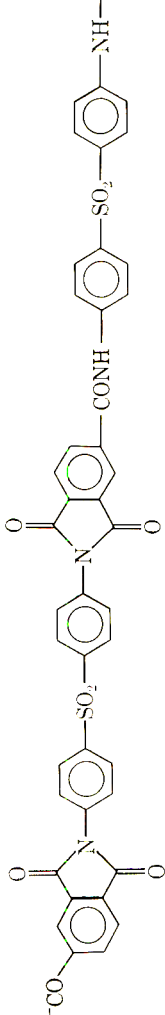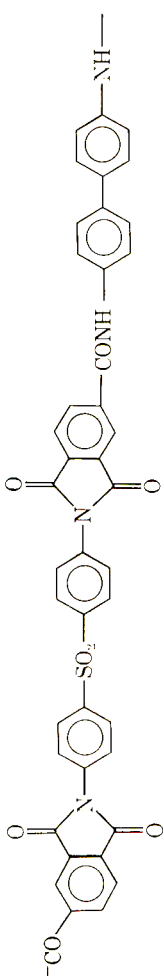
EXPERIMENTAL

Monomer Synthesis

Sulfuryl - bis[*N* - (4′ - phenylene) - 4 - (chloroformyl) - phthalimide]. This monomer was prepared as previously described.[1] Condensation of trimellitic acid anhydride with 4,4′-diaminodiphenylsulfone, followed by imidization using acetic anhydride and pyridine and treatment of the acid with thionyl chloride led to a 71% overall yield of the diacid chloride, mp 301–302°C.

Aromatic Diamines. The diamines used in this study are commercially available and were purified to obtain polymer grade materials.

TABLE I
Elemental Analysis of Imide–Amide Copolymers

No.	Polymer structure		C, %	H, %	N, %	S, %
I		Calcd	69.53	3.52	7.54	
		Found	66.32	3.56	7.38	
II		Calcd	64.57	3.15	8.36	
		Found	63.04	3.25	8.25	
III		Calcd	66.31	3.18	7.36	4.21
		Found	64.55	3.22	6.98	4.44

IV   —CO ... SO_2 ... —CONH ... —NH—

| | Calcd | 64.57 | 3.15 | 8.36 | |
| | Found | 61.93 | 3.16 | 8.25 | |

V   —CO ... SO_2 ... —CONH ... SO_2 ... —NH—

| | Calcd | 62.37 | 2.99 | 6.93 | 7.93 |
| | Found | 60.20 | 2.97 | 6.82 | 8.07 |

VI   —CO ... SO_2 ... —CONH ... —NH—

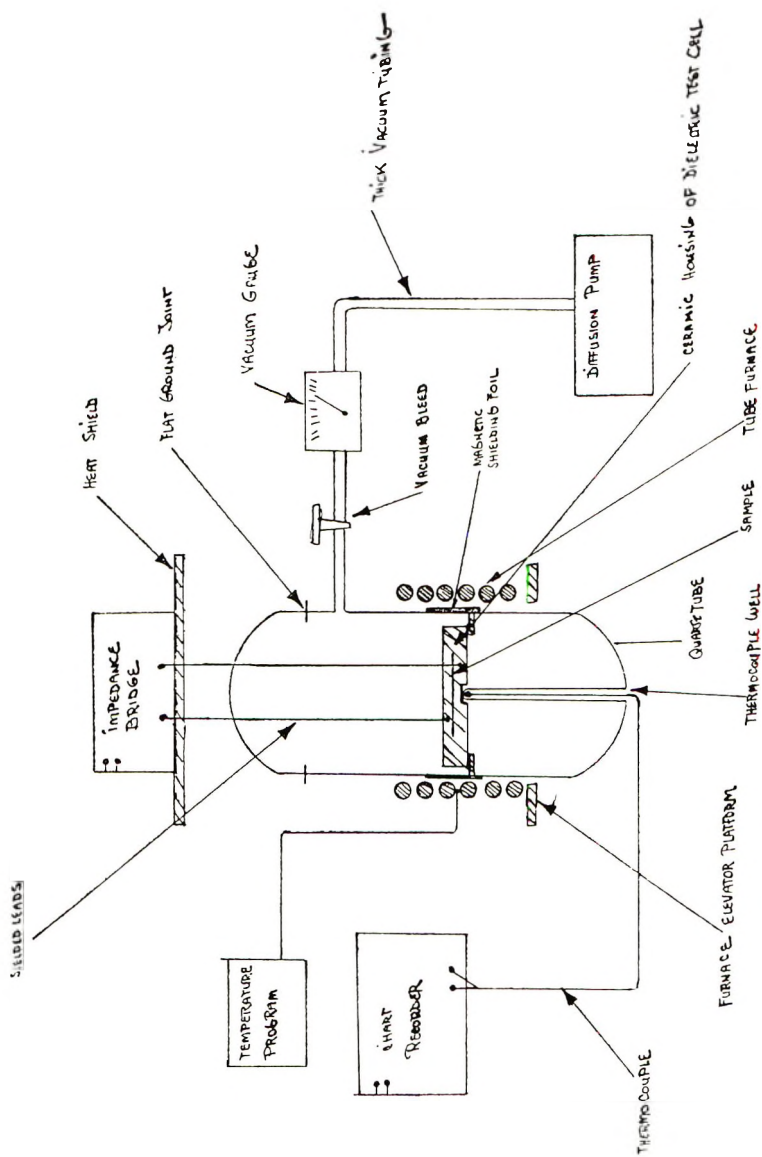| | Calcd | 67.74 | 3.25 | 7.52 | |
| | Found | 66.40 | 3.51 | 7.16 | |

Fig. 1. Schematic drawing of apparatus for measurement of glass transition temperatures: Furnace, Marshall (2000°F); recorder, Bristol, 11 in. chart; bridge, General Radio, type 1650A; temperature programer, West Instrument, Model JS6R 2; vacuum gauge, A. F. Smith, Pompano Beach, Florida; shielding foil, Perfection Mica Company, Chicago, Ill.

Polymer Synthesis

All six polymers were synthesized under essentially identical reaction conditions. Sulfuryl-bis[N-(4-phenylene)-4'-(chloroformyl)-phthalimide] (0.010 mole) was added to a solution of 0.010 mole of aromatic diamine in dimethylacetamide (DMAc) at −15°C. Then, the solution temperature was allowed to rise to 25°C within a period of 1 hr. The resulting viscous clear polymer solution (∼10% solids) was neutralized with pyridine and the polymer precipitated from water. Purification was accomplished by washing the precipitate three times with water and twice with acetone in a Waring Blendor. The resulting finely divided powder was then dried at 140°C under reduced pressure, and could readily be redissolved in dimethylacetamide to obtain 10% solutions from which films were cast.

Polymer Characterization

The polymers were characterized by infrared spectra and elemental analysis. The infrared spectra showed imide bands at $1\,785$ cm^{-1} due to symmetrical carbonyl stretching vibrations, at $1\,730$ cm^{-1} due to asymmetrical carbonyl stretching vibrations, at 725 cm^{-1} possibly due to ring carbonyl deformations, and at $1\,158$ cm^{-1}, assigned to S=O stretching modes. Repeat unit structures and elemental analyses are shown in Table I.

Measurements

Polymer decomposition temperatures were determined by dynamic thermogravimetric analysis in vacuum at a heating rate of 5°C/min with the use of an Ainsworth electronic vacuum balance. Measurements were made on powdered samples of purified polymers. The decomposition temperature (PDT) was defined as the temperature of onset of weight loss.

The thermal stability of polymers was measured under isothermal conditions in air at 300 and 400°C in a preheated furnace. The interior of the furnace was lined with aluminum foil to obtain uniform heat distribution. Polymer solutions were cast in aluminum cups and the solvent removed at 140°C under oil pump pressure. Coated specimens were then heated and periodically checked for retention of film creasability. A second set of samples was simultaneously heated in Coor's crucibles and weight losses periodically recorded.

Glass transition temperatures were determined of polymer coatings on chromium plated steel electrodes by means of dielectric loss measurements at a programed heating rate of 5°C/min. The apparatus designed for this purpose is shown in Figure 1.

Intrinsic viscosities [η] of polymers were determined in DMAc at 30 ± 0.05°C in an Ubbelohde viscometer.

RESULTS AND DISCUSSION

The six new polyimide-*co*-amides synthesized in this study had the general structure:
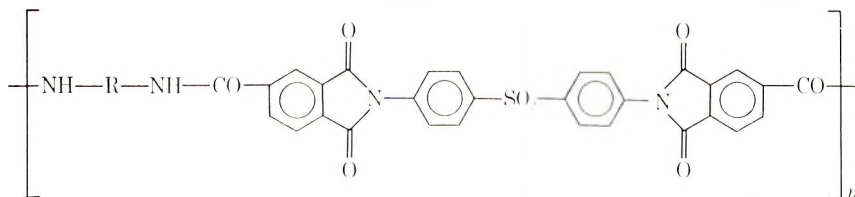
where R = 4,4'-diphenylmethane (I), *m*-phenylene (II), 4,4'-diphenyl ether (III), *p*-phenylene (IV), 4,4'-diphenylsulfone (V), or 4,4'-biphenylene (VI).   Some thermal and solution properties of these polymers are given in Table II.   From TGA data obtained in vacuum the relative order of thermal stability is I < II < III < IV < V < VI.

Polymer I containing the diphenylmethane linkage was the least stable, and VI containing the biphenylene linkage was the most stable, the difference being 80°C.

The glass transition temperatures of all six polymers were high.   Polymers I, II, and V, containing flexibilizing groups such as the methylene, ether, or sulfone linkage, or polymer II containing the *m*-phenylene moiety
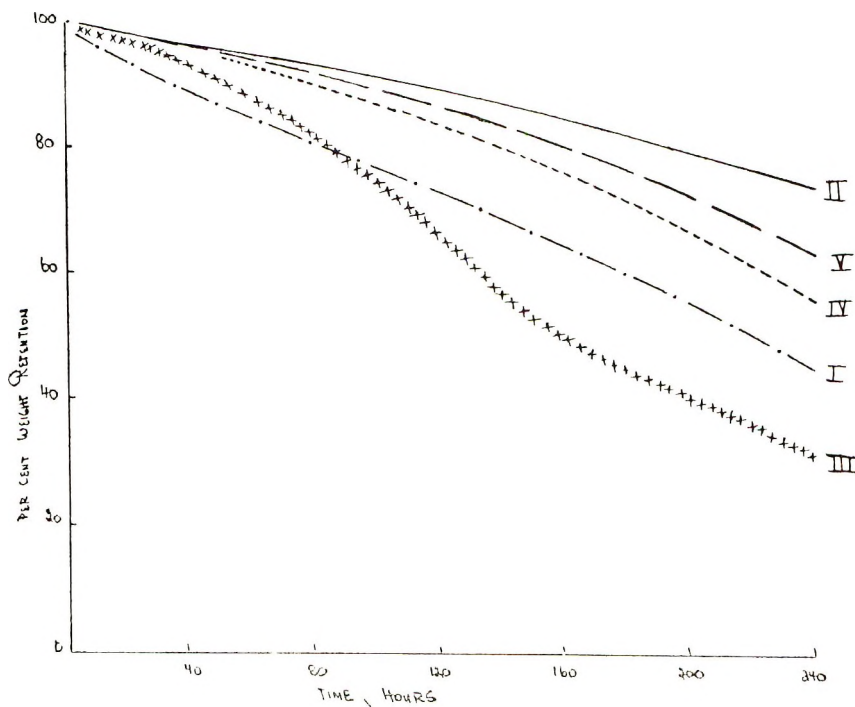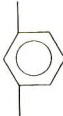

Fig. 2. Isothermal weight loss of films at 400°C in static air.

TABLE II
Polymer Properties

No.	R group	PDT, °C[a]	T_g, °C[b]	$[\eta]$, dl/g[c]	Solubility in DMAc	Thermal stability in air[d]	
						at 300°C	at 400°C
I	(–CH₂– bridged bis-phenyl structure)	400	324	1.2	+	3 days	16 hr
II	(meta-linked bis-phenyl structure)	425	311	1.6	+	>1 month	~40 hr
III	(–O– bridged bis-phenyl structure)	440	310	0.8	+	>3 weeks	3 days
IV	(para-linked bis-phenyl structure)	450	368	1.8	+	>1 month	1 week
V	(–SO₂– bridged bis-phenyl structure)	470	307	0.7	+	>1 month	3 days
VI	(biphenyl structure)	480	370	0.7	–[e]	24 hr	16 hr

[a] Determined by TGA in vacuum ($\Delta T/\Delta t = 5°C/min$).
[b] From dielectric loss measurements.
[c] In DMAc at 30°C.
[d] As measured by retention of film creasability.
[e] Film made from 5% LiCl–DMAc solution.

Fig. 3. Effect of impurities on isothermal weight loss of ASO_2i-$PhSO_2Ph$ film at $400°C$ in static air: (——) purified; (- -) unpurified.

which introduces chain irregularity showed glass transition temperatures between 307 and 324°C. This is 50–60°C lower than for polymers IV and VI containing the chain-stiffening p-phenylene and biphenylene linkages. The latter two polymers had T_g's of 368°C and 370°C, respectively.

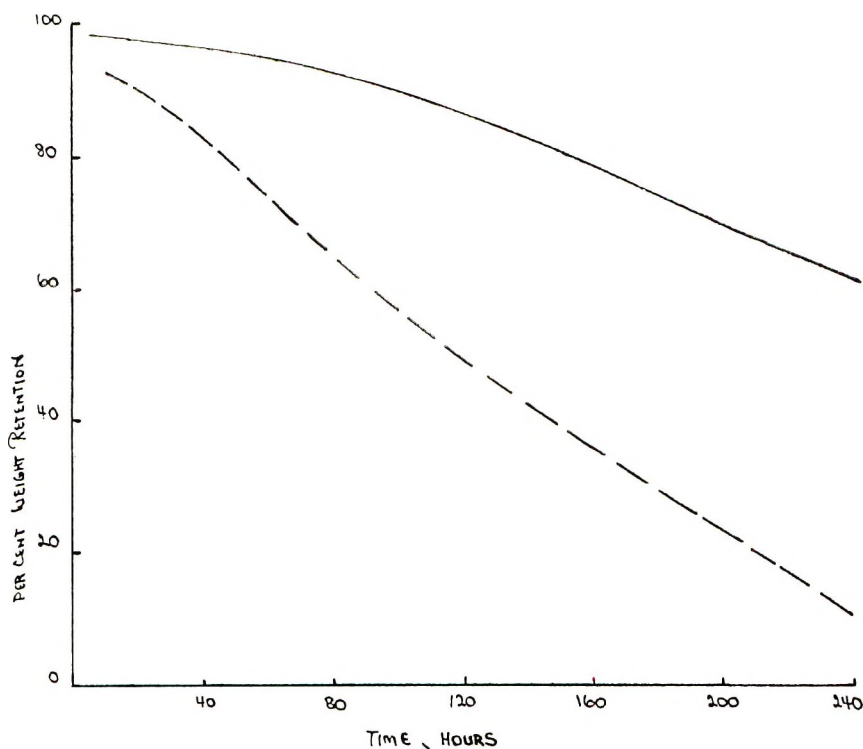All polymers synthesized in this study were of high molecular weight, as indicated by intrinsic viscosities ranging from 0.7 to 1.8 dl/g. With the exception of VI all polymers could readily be dissolved in concentrations up to about 20 wt-% in solvents such as DMAc, m-cresol, N-methylpyrrolidone or hexamethyl phosphoramide (HMPA). Polymer VI was however soluble in DMAc containing 5% lithium chloride.

The thermal stability in air of polymers shown in Table II as measured by retention of film creasability varied considerably depending upon polymer structure. At 300°C, I retained its flexibility for about three days, III for about three weeks, and II, IV and V were still creasable after one month, at the end of the test period. A film of Polymer VI embrittled after 24 hr. However, this result cannot be compared with those of the other polymers since it was made from a solution containing lithium chloride. Lithium chloride strongly accelerates the decomposition of these polymers in air, as was shown in several cases. Isothermal aging at
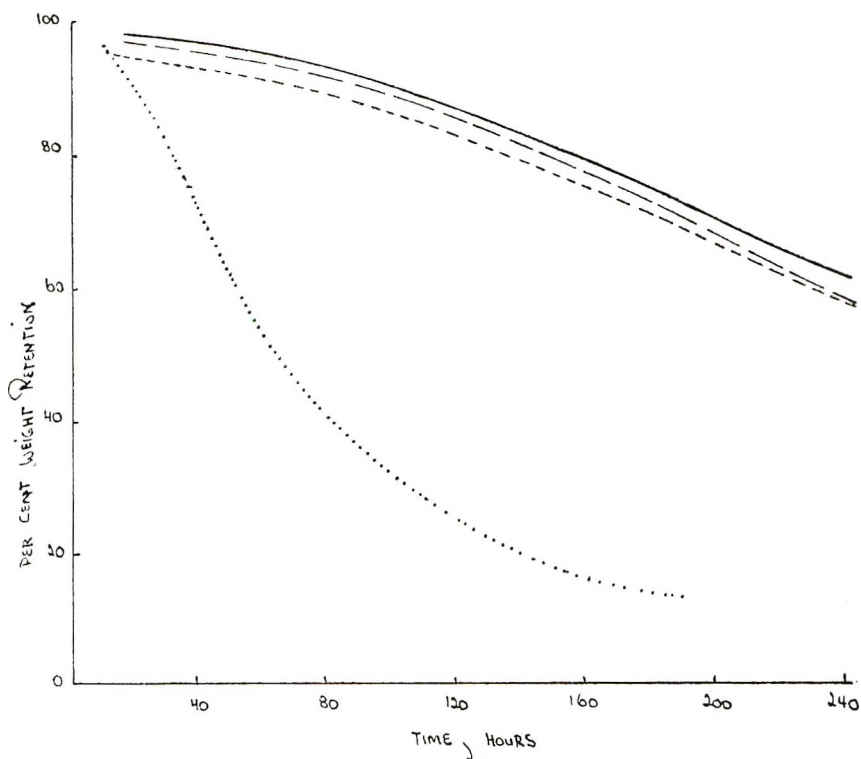
Fig. 4. Effect of solvents on isothermal weight loss of ASO₂i-Ph-SO₂Ph films at 400°C in static air: (———) DMAc; (– –) m-cresol; (- -) N-methylpyrrolidone; (. . .) HMPA.

400°C in air decreased the flex life of films considerably, varying from a few hours to a few days (Table II, column 7). Simultaneously measured were the weight losses of separate films at this temperature (Fig. 2). As expected, no correlation between retention of creasability and retention of sample weight could be drawn. This became especially apparent by comparing polymer III with I. After exposure to air at 400°C for 3 days both polymer films retained about 85% of their original weight but polymer III was still creasable, while Polymer I became extremely brittle after 16 hr of exposure.

The effect of impurities on the thermal stability of polymer films was demonstrated by isothermal weight loss measurements of polymer V in air at 400°C (Fig. 3). After 10 days a film made from the original neutralized polymer solution retained 10% of its weight, while a film made from a solution of isolated and purified polymer retained 70% of its original weight.

Films of polymer V made from solutions of different solvents were heated at 400°C in air (Fig. 4). Of the four solvents chosen, DMAc, m-cresol and N-methylpyrrolidone had only minor effects on the isothermal weight loss of films, while the use of hexamethyl phosphoramide degraded the polymer much more rapidly.

Of the six polymers studied, II and V had the best balance of thermal and solution properties.

Reference

1. W. Wrasidlo and J. M. Augl, *J. Polym. Sci.*, in press.

Thermal Decomposition Products of Polypropylene

YOSHIO TSUCHIYA and KIKUO SUMI, *National Research Council of Canada, Division of Building Research, Ottawa, Canada*

Synopsis

Isotactic polypropylene was decomposed under vacuum at 360, 380, and 400°C, and the volatile products from C_1 to C_{12} hydrocarbons were analyzed by gas chromatography. The formation of the main products is discussed on the basis of a free-radical mechanism in which intramolecular radical transfer is assumed to play an important role. The mechanism of the formation of a number of products suggested by previous workers is criticized on the basis of the results of a more comprehensive analysis of this investigation.

Decomposition products of polypropylene have been determined by several investigators in order to explain the mechanism of decomposition of this polymer. Madorsky and Straus[1] used mass spectrometry and analyzed products having one to six carbon atoms, but did not separate any isomers. Moiseev, Khloplyankina et al., Bailey et al., and van Schooten and Evenhuis[2-6] used gas chromatography. Moiseev and his co-workers[2,3] presented a good picture of the mechanism of decomposition by assuming intramolecular radical transfer. The chromatograms presented suggest, however, that more precise experimental data could be obtained by using some newer techniques of gas chromatography. Bailey[4,5] determined the products from C_1 to C_5 hydrocarbons and explained the formation of the major fragments. van Schooten and Evenhuis[6] simplified the analysis by converting all the olefins to the paraffins and presented data in which the products having the same carbon skeleton were combined. They extended the analysis to C_{12} hydrocarbons and presented a mechanism of decomposition that was more comprehensive than those presented by others. The limitation imposed by combining the olefins and the paraffins precluded, however, a more complete explanation of the mechanism.

The authors of the present paper believe that more comprehensive data in which the paraffins and the individual olefins are separated should be useful in discussing the mechanism of decomposition of polypropylene. Products from C_1 to C_{12} hydrocarbons were analyzed by gas chromatography.

EXPERIMENTAL

Material

A commercial grade of isotactic polypropylene having a specific gravity of 0.905 and a crystal melting point of 166°C was used. The sample was first treated with methyl ethyl ketone in a Soxhlet extraction apparatus for 50 hr and dried under vacuum, to remove the amorphous portion.

Thermal Decomposition

The apparatus and procedure were similar to those used in the previous studies on polyisobutylene.[7] A horizontal quartz tube containing 1 g of sample was evacuated to 1×10^{-4} mm Hg. The vacuum line to the pump was then closed, and an electric furnace provided with wheels was moved quickly along steel tracks to position the sample in the hot zone. The sample was pyrolyzed at 360, 380, and 400°C.

Analysis

The gas chromatographic conditions that were used for the analysis were the same as in the previous studies.[7] A silica gel-packed column and a support-coated open tubular column with squalane as the liquid phase were used with a flame ionization detector.

RESULTS AND DISCUSSION

Analysis of the Products

The decomposition products of polypropylene pyrolyzed at 400°C are presented in Figure 1. The relative areas of the peaks of the chromatograms are represented by line charts against the retention indices both for the pyrolysis products and the hydrogenated pyrolysis products.

The decomposition products were composed of five different homologous series as shown in Figure 2. The products that did not belong to these series amounted to only 0.3% by weight of the products analyzed. The five homologous series each produced a straight line parallel to one another.

A doublet corresponding to product a-3 (which is three monomer units greater than the smallest fragment of series "a") was found in the chromatograms. A doublet corresponding to product b-3 was also found. van Schooten and Evenhuis[6] identified a-3 as 4,6-dimethylnonane and the hydrogenated product of b-3 as 2,4,6-trimethylnonane by infrared and mass spectrometric analysis. They assumed that the two doublets are stereoisomers. The present experimental results support the suggestion that the doublets are due to stereoisomers. As indicated earlier, the retention indices of the two doublets fit the positions of series a and b, but did not fit any other series and these products are expected from a knowledge of the mechanism of decomposition of polymers. The boiling point of a-3, estimated from retention index–boiling point data, was 179°C,
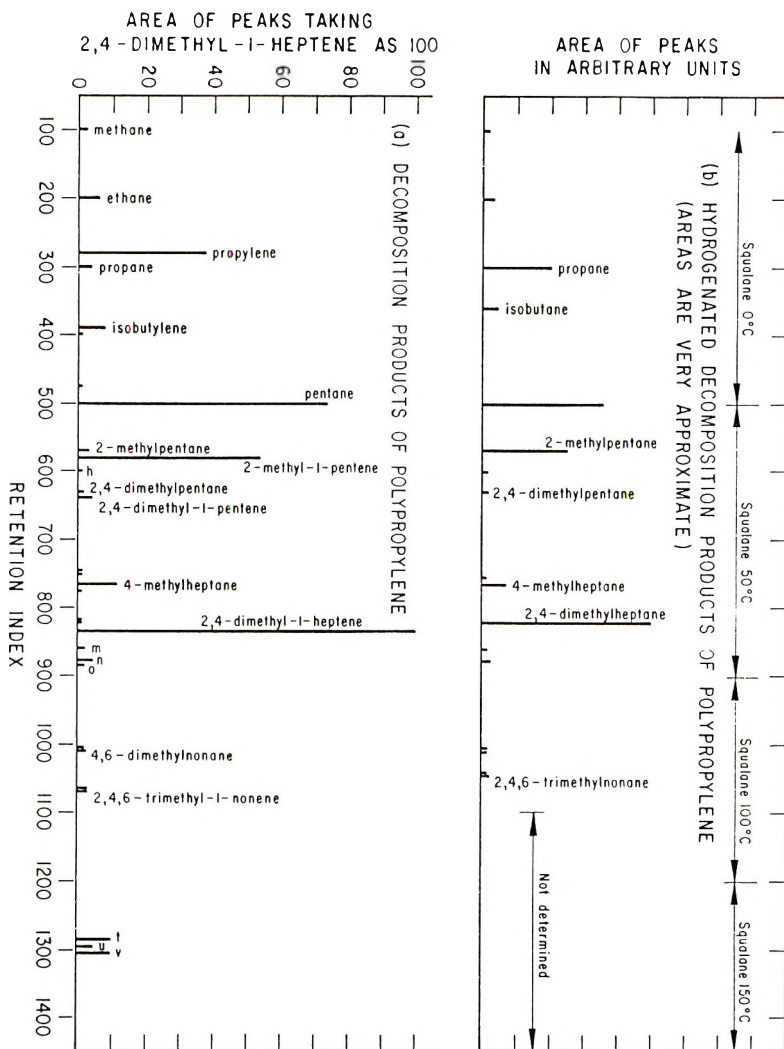
Fig. 1. Area of peaks vs. retention index.

whereas that of 4,6-dimethylnonane found in the literature[8] was 179.8°C. None of the other saturated hydrocarbons having boiling points of 179.8 ± 2.0°C had the carbon skeleton corresponding to fragments from polypropylene.[8] A similar method to support the identification b-3 was not conducted because of lack of sufficient data on compounds having boiling points in the range of that of b-3.

The results of the quantitative analysis are presented in Table I.

Mechanism of Decomposition

The mechanism of decomposition of polypropylene is given in Scheme 1; the decomposition of secondary radical II only is shown. The initiation re-

TABLE I
Thermal Decomposition Products of Polypropylene

	360°C		380°C		400°C	
	Wt-% of polymer	Mole-% of volatiles	Wt-% of polymer	Mole-% of volatiles[a]	Wt-% of polymer	Mole-% of volatiles[a]
Methane	0.0055	7.7	0.021	7.0	0.057	3.9
Ethane	0.0057	4.2	0.030	5.4	0.13	4.8
Propane	0.0021	1.1			0.078	1.9
Propylene	0.0296	15.7	0.131	13.2	0.83	21.4
Isobutylene	0.0083	3.3	0.069	6.6	0.16	3.0
Butane			0.001	0.09	0.004	0.07
2-Methyl-1-butene			0.002	0.14	0.010	0.15
1-Pentene					0.008	0.12
Pentane	0.102	31.6	0.421	31.5	1.62	24.3
2-Pentene, cis and trans			0.002	0.12	0.015	0.23
2-Methylpentane	0.0066	1.7	0.017	1.1	0.074	0.93
2-Methyl-1-pentene	0.079	20.9	0.249	16.0	1.19	15.4
Peak h			0.003	0.2	0.029	0.4
2,4-Dimethylpentane			0.004	0.22	0.032	0.34
2,4-Dimethyl-1-pentene	0.0019	0.43	0.013	0.72	0.089	0.98
4-Methylheptane	0.013	2.6	0.052	2.5	0.24	2.3
2,4-Dimethyl-1-heptene	0.040	7.1	0.26	11.2	2.20	18.9
Peak m			0.005	0.20	0.059	0.5
Peak n			0.007	0.25	0.098	0.75
Peak o			0.006	0.23	0.044	0.35
4,6-Dimethylnonane, threo form	0.0039	0.55	0.011	0.38	0.042	0.29
4,6-Dimethylnonane, erythro form	0.0046	0.66	0.014	0.49	0.052	0.36
2,4,6-Trimethyl-1-nonene, threo form	0.0130	1.73	0.040	1.3	0.055	0.36
2,4,6-Trimethyl-1-nonene, erythro form	0.0134	1.78	0.045	1.4	0.066	0.44
Total volatiles analyzed	0.326	100	1.41	100	7.05	100
100-residue wt-%	2.7		4.4		19.8	

[a] Molecular weights of unidentified compounds were estimated from their retention indices.
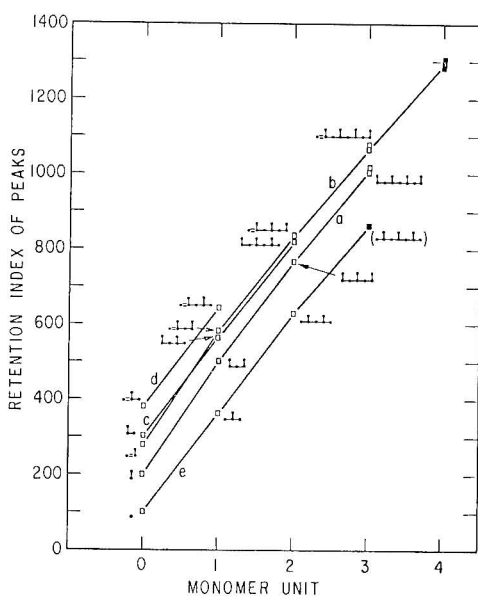
Fig. 2. Retention index of products: (□) identified peak; (■) unidentified peak.

TABLE II
Decomposition Products Resulting from Intramolecular
Radical Transfer at 400°C

From		Transfer to nth carbon		
	n	Decomposition product	Amount of product, mole-% of volatiles	
Secondary radical	3	Ethane	4.8	
	3	2-Methyl-1-pentene	15.4	
CH—CH₂—ĊH				
| |	5	Pentane	24.3	
CH₃ CH₃				
	5	2,4-Dimethyl-1-heptene	18.9	
	7	4-Methylheptane	2.3	
	7	2,4,6-Trimethyl-1-nonene	0.80	
	9	4,6-Dimethylnonane	0.65	
Primary radical	4	Propane	1.9	
⁓CH—CH₂—CH—ĊH₂	4	2,4-Dimethyl-1-pentene	0.98	
| |				
CH₃ CH₃	6	2-Methylpentane	0.93	
	6	2,4,6-Trimethyl-1-heptene	a	
	8	2,4-Dimethylheptane	<0.1	

ª Not determined.
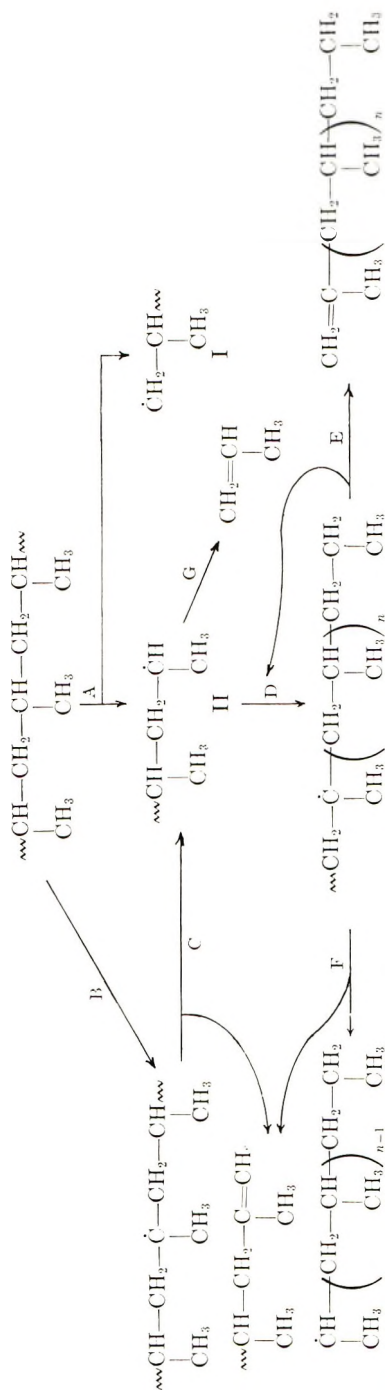
Scheme 1. The thermal decomposition of polypropylene.

action (A) occurs by random scission of the main chain, yielding two types of radicals: primary (I) and secondary (II). The production of radical II is more favorable than the production of radical I during the decomposition because the former is also produced by intermolecular and intramolecular radical transfer to tertiary carbon followed by β-scission (B, C, D, and E).
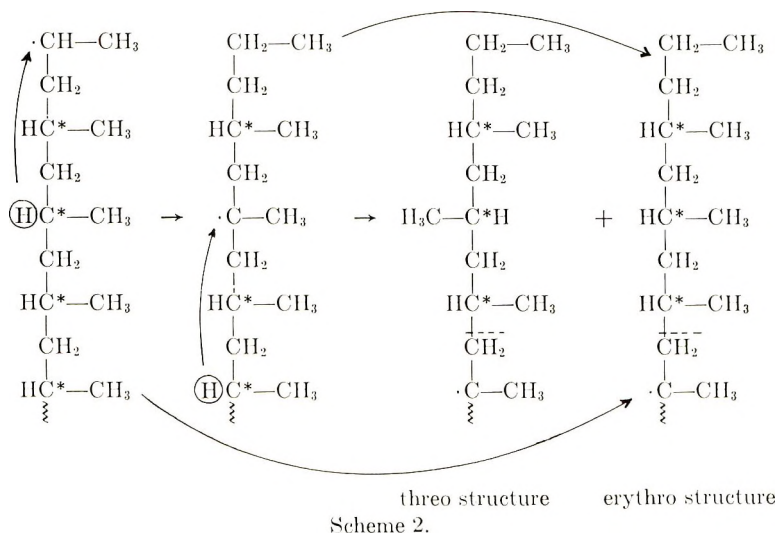
Intramolecular radical transfer and propagation (G) reactions can account for the production of most volatiles. The quantitative results of the products formed at 400°C are presented in Table II by assuming the occurrence of intramolecular radical transfer. The experimental results indicate that the radical transfer was mainly to the tertiary carbons. The amounts of the products formed following radical transfer to the primary and secondary carbons were small; these reactions were therefore neglected in preparing Table II. The ease of radical transfer to the tertiary carbons increases the amount of radical II as compared with radical I. Thus, the amounts of products formed from radical II were much greater than those from radical I.

Stereoisomers were found in the decomposition products of isotactic polypropylene. The presence of some stereoisomers in the products can be explained by stepwise radical transfer, as shown in Scheme 2, for the

$$
\begin{array}{ccccc}
\cdot CH-CH_3 & CH_2-CH_3 & & CH_2-CH_3 & CH_2-CH_3 \\
| & | & & | & | \\
CH_2 & CH_2 & & CH_2 & CH_2 \\
| & | & & | & | \\
HC^*-CH_3 & HC^*-CH_3 & & HC^*-CH_3 & HC^*-CH_3 \\
| & | & & | & | \\
\textcircled{H}C^*-CH_3 \rightarrow & \cdot C-CH_3 \rightarrow & H_3C-C^*H & + & HC^*-CH_3 \\
| & | & | & & | \\
CH_2 & CH_2 & CH_2 & & CH_2 \\
| & | & | & & | \\
HC^*-CH_3 & HC^*-CH_3 & HC^*-CH_3 & & HC^*-CH_3 \\
| & | & | & & | \\
CH_2 & CH_2 & CH_2 & & CH_2 \\
| & | & | & & | \\
HC^*-CH_3 & \textcircled{H}C^*-CH_3 & \cdot C-CH_3 & & \cdot C-CH_3 \\
\end{array}
$$

threo structure   erythro structure

Scheme 2.

formation of 4,6-dimethylnonane, where the asterisks denote asymmetric carbons. The occurrence of stepwise radical transfer during the thermal decomposition of polymethylene has been reported earlier.[9]

Equal amounts of the threo and erythro structures should be expected from stepwise radical transfer. The experimental results showed that the latter peak of this doublet was always greater than the former. This suggests that direct radical transfer to the ninth carbon of the chain has also

taken place, and that the former peak is due to the threo and the latter to the erythro structure.

The analytical data of the hydrogenated decomposition products obtained by van Schooten and Evenhuis[6] agreed well with the experimental results of the present investigation. By separating the individual olefins from the paraffins, the present authors were able to obtain a better understanding of the mechanism of decomposition of polypropylene.

van Schooten and Evenhuis suggested three different routes for the formation of 2-methylpentane in the hydrogenated products: two for 2-methylpentane prior to hydrogenation and one for 4-methyl-1-pentene. In the present experiments both of these products were found to be minor ones. The main product with the carbon skeleton of 2-methylpentane was 2-methyl-1-pentene, which could be formed by intramolecular radical transfer from a secondary macroradical (II) to the third carbon (which is tertiary) followed by β scission.

van Schooten and Evenhuis believed that 2,4-dimethylpentane is an important product formed by a radical transfer from a primary macroradical (I) to a secondary carbon, followed by β scission. In the present experiments the amount of 2,4-dimethyl-1-pentene was found to be much greater than the paraffin having the same carbon skeleton. This olefin could be produced by a radical transfer from a primary macroradical (I) to the fourth carbon of the chain (which is tertiary), followed by β scission.

van Schooten and Evenhuis suggested five different routes for the formation of 2,4-dimethylheptane. They believed that two of these routes leading to the formation of 2,4-dimethyl-1-heptene and 4,6-dimethyl-2-heptene were the important ones. The present experiments showed that only the former olefin is a major product; the latter was less than 1 per cent of the former.

The above examples illustrate the advantage of separating individual products in order to explain the mechanism of thermal decomposition of polymers. van Schooten and Evenhuis neglected radical transfer to the third and fourth carbons of the polypropylene chain, which is important, as shown in Table II. Also, they were not aware of the greater yield of products from the secondary macroradical (II), as compared with that from the primary (I), as this was not apparent from their experimental data.

Khloplyankina et al.[3] found large amounts of 1-pentene and 2-pentene in the decomposition products of polypropylene. They attributed the formation of these two products to intramolecular radical transfer from secondary macroradical (II) to primary carbon and to secondary carbon, respectively, followed by β scission. In the present experiments, only small amounts of pentenes were found. This result is consistent with overall data obtained in that the products that were formed after radical transfer to the primary and secondary carbons were found in small amounts.

Bailey et al.[4,5] found large amounts of propane, especially at low pyrolysis temperatures. They explained this result by suggesting the presence of

head-to-head structures in their polymer sample. According to the present knowledge of the mechanism of decomposition of polymers, approximately equal amounts of 2-methyl-1-hexene and propane should be produced by the mechanism:
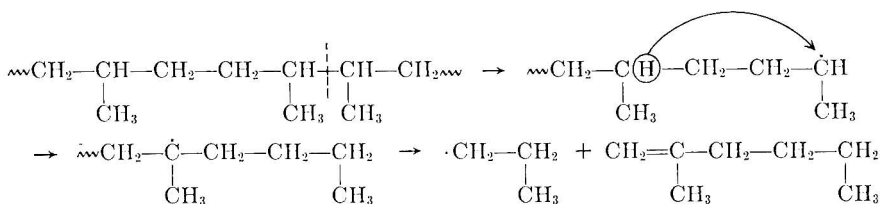
The present authors believe that it is necessary to determine the amount of 2-methyl-1-hexene produced to confirm that the irregularity in the polymer suggested by Bailey was the main reason for the large yield of propane. In the present experiments, a smaller amount of propane was found and the amount of 2-methyl-1-hexene at a retention index of 678 was less than one-tenth of the amount of propane.

Madorsky presented a mechanism of decomposition whereby scission of a C—C bond in the chain is accompanied by a transfer of hydrogen at the site.[10] According to this mechanism, a saturated end and an unsaturated end are produced in equal amounts. If volatiles were produced by this mechanism, alkanes, alkenes with a terminal double bond, and alkadienes with two terminal double bonds should be produced in the ratio of $1:2:1$. The present results do not agree with this mechanism because only small amounts of alkadienes were found.

References

1. S. Madorsky and S. Straus, *J. Res. Nat. Bur. Stand.*, **53**, 361 (1954).

2. V. D. Moiseev, *Plasticheskie Massy*, 1963, No. 12, 3; English transl., *Soviet Plastics*, 1964, No. 12, 6.

3. M. S. Khloplyankina, M. B. Nieman, and V. D. Moiseev, *Plasticheskie Massy*, 1961, No. 2, 9; English transl., *Soviet Plastics*, 1962, No. 2, 11.

4. W. J. Bailey and C. N. Lieske, paper presented to Division of Polymer Chemistry, American Chemical Society Meeting, (New York) 1963; *Preprints*, **4**, No. 2, 589 (1963).

5. W. J. Bailey and C. L. Liotta, paper presented to Division of Polymer Chemistry, American Chemical Society Meeting (Chicago), 1964; *Preprints*, **5**, No. 2, 333 (1964).

6. J. van Schooten and J. K. Evenhuis, *Polymer*, **6**, 343 (1965).

7. Y. Tsuchiya and K. Sumi, *J. Polym. Sci. A-1*, in press.

8. S. W. Ferris, *Handbook of Hydrocarbons*, Academic Press, New York, 1959, pp. 53–55.

9. Y. Tsuchiya and K. Sumi, *J. Polym. Sci. B*, **6**, 357 (1968).

10. S. L. Madorsky, *Thermal Degradation of Organic Polymers*, Interscience, New York, 1964; p. 117.

Mechanism of Decoloration by Solvent of Thermally Degraded Poly(vinyl Chloride)*

TSUNETAKA MATSUMOTO, ISAO MUNE, and SEIJI WATATANI,
Department of Industrial Chemistry, Kobe University, Kobe, Japan

Synopsis

The mechanism of decoloration of thermally degraded poly(vinyl chloride) (PVC) by solvents has been investigated systematically. The main results obtained are as follows. Good solvents for PVC, especially tetrahydrofuran, methyl ethyl ketone, and dioxane are effective for decoloration. The solvent peroxide which is formed by autoxidation of solvent contributes to decoloration. The number of double bonds in degraded PVC decreases as the decoloration proceeds and at the same time the solvent peroxide existing in solvent is consumed. Moreover, the existence of solvent fragments in decolored PVC is recognized. From these results, it is most reasonable to conclude that the decoloration mechanism is as follows: the solvent partially is changed to a solvent peroxide by autoxidation, and the solvent peroxide reacts with polyene double bonds of degraded PVC and breaks down conjugated double bonds, and consequently degraded PVC is decolored.

INTRODUCTION

The thermal degradation of poly(vinyl chloride) (PVC) has been studied by a number of workers.[1–3] It is known that the decomposition reaction involves mainly loss of hydrogen chloride, and the degraded PVC has a reddish-brown color. This discoloration seems to be caused by the formation of long sequences of conjugated double bonds. Meanwhile, a few investigators[4–7] have found that the degraded PVC is decolored easily by several organic solvents at room temperature.

Imoto and co-workers[4] pointed out that the color of degraded PVC became faint during repeated precipitation from tetrahydrofuran (THF) solution with methyl alcohol. They attributed this phenomenon to oxidation of the double bonds oxidized by oxygen and formation of comparatively short-chain polyenes. Konishi[5] found that degraded PVC was decolored by dissolving in solvents such as methyl ethyl ketone (MEK) and THF. From this fact, he suggested that this phenomenon occurred as result of reaction between solvents and the polymer radicals which are considered to be the colored materials in degraded PVC. As Atchison[6] indicated, in case of dissolution of irradiated PVC in THF, the THF

* Presented in part at the 15th annual meeting of the Society of Polymer Science, Japan, May 1966.

solution became deep reddish brown and then gradually changed to light yellow and finally to colorless.   At the same time, he recognized that the air and light exposure was effective for the color fading.   Similar fading of a degraded PVC in THF solution had been observed by Wippler.[7]   Furthermore, we recognized[8] that the color of THF solution changed from reddish brown to light yellow during solution polymerization of methyl methacrylate in THF in the presence of degraded PVC.

From these facts, it is logical to consider that decoloration of degraded PVC by organic solvents involves radicals, but evidence for the mechanism has not yet been presented.   Therefore, our purpose in this paper is to investigate the mechanism of decoloration of degraded PVC and 1,8-diphenyloctatetraene(DPOT) in solvents by means of measuring the absorption spectra at the ultraviolet and visible regions.   Here, we considered DPOT as a model compound for the polyene structure of degraded PVC.

EXPERIMENTAL

The material used was a commercial PVC powder obtained by suspension polymerization having granule size of 150–200 μ (Sumilit Sx-8, Sumitomo Chemical Industry Ltd.) and a degree of polymerization of 800.   This material was immersed in methyl alcohol and refluxed at 70°C for 4 hr, then washed with methyl alcohol and dried under reduced pressure.   The PVC was degraded thermally at 170°C for 2 hr under a nitrogen atmosphere.

The degraded PVC (0.1 g) was dissolved or dispersed with 10 ml. solvent. The decoloration reaction by solvent was carried out qualitatively in a 50-ml Erlenmeyer flask at a concentration of 0.5 g PVC/20 ml solvent at a room temperature.   On the other hand, the reaction was carried out quantitatively in a 25-ml flame-sealed test tube at a concentration of 0.5 g PVC/20 ml solvent at 70°C.   In the case of adding radical sources or radical scavengers in acetone or THF, benzoyl peroxide (BPO), 2,2-azobisisobutyronitrile (AIBN), 1,1-diphenyl-2-picrylhydrazyl (DPPH) and hydroquinone were added in amounts of 1 wt-% to degraded PVC.

The degree of decoloration was obtained by comparison of transmittance or optical density with that of a 1 wt-% THF solution of PVC purified by precipitation from THF solution with methyl alcohol.   The optical density was measured mainly at 500 mμ by using Shimazu MPS-50 type spectrophotometer.

Special grade chemicals were used as solvents for decoloration without further purification, and first grade THF was used after purification by the method of Morikawa et al.[9]   Purified THF was stored at a room temperature for a fixed time in order to obtain the desired quantity of peroxide. The amounts of peroxide in solvents were measured by iodometric titration.[10]

On the other hand, quantitative analysis of double bonds in degraded or decolored PVC was carried out by the pyridine sulfuric acid bromine method,[11] by which Mizutani[12] and Takemoto[13] had obtained good results.

The number of carbonyl groups in PVC was determined by the method of Morikawa.[14] The method is as follows. Carbonyl groups in PVC were converted to Schiff's bases by condensation with p-nitrophenylhydrazine; the content of Schiff bases was calculated by an experimental expression from the ultraviolet maximum absorbance of the reaction products. The existence of carbonyl groups was observed by infrared absorption spectra. Nitrogen contents in the PVC decolored by dimethylformamide (DMF) were determined by the Kjeldahl method. Furthermore, the intrinsic viscosity was measured at 30°C in THF.

The model compound, DPOT, was synthesized[15] from cinnamic aldehyde and succinic acid. DPOT was decolored by solvents in a 25-ml flame-sealed test tube in a nitrogen atmosphere. In this case, dioxane, THF, and carbon tetrachloride were mainly used as solvents. Chlorine contents of the model compound decolored by carbon tetrachloride were determined by the flask combustion method.[16]

RESULTS AND DISCUSSION

Decoloration of Degraded PVC by Solvents

In the previous section, it was pointed out that a few organic solvents were capable of decoloring degraded colored PVC. Therefore, we first examined the decoloring ability of several solvents and other reagents.

Figure 1 shows the ultraviolet and visible spectra of PVC decolored under different conditions. The degraded PVC has many fine absorption spectral bands in the range from ultraviolet to the visible region. This fine structure is the characteristic of the absorption spectra of long-chain polyenes.[17-19] The fine structure peaks show maxima at 475, 450, 432, 410, 387, 365, 339, 332, 309, 288, 275, and 240 mμ. Especially, strong
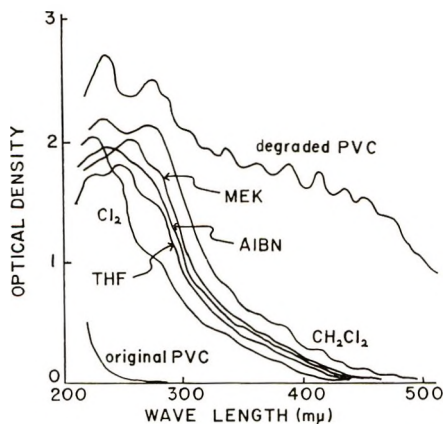

Fig. 1. Visible and ultraviolet spectra of degraded PVC and PVC decolored under different conditions: Decoloration conditions: THF, MEK, 70°C, 5 hr in acetone; methylene chloride at room temperature in diffused daylight for 72 hr; chlorine, bubble in dichloroethane solution of PVC for 30 min.

peaks appear at 432, 410, 387, 275, and 240 mμ.   While work by Bohlmann and Mannhardt[17] on compounds of the type CH_3—(—CH=CH—)$_n$—CH_3 shows that these compounds obey the Lewis-Calvin relationship[18] ($\lambda_{max} = Kn$) fairly well.

From this relationship, in our case an n value of approximately 9 is calculated.   However, we have considered that degraded PVC contains from long ($n = 9$) to short polyene chains ($n = 2$).

These fine structure absorptions diminished and disappeared under different decoloration conditions.   The decoloration was most effective with chlorine, and then THF, MEK, and methylene chloride.   Furthermore, degraded PVC was decolored by AIBN in acetone.
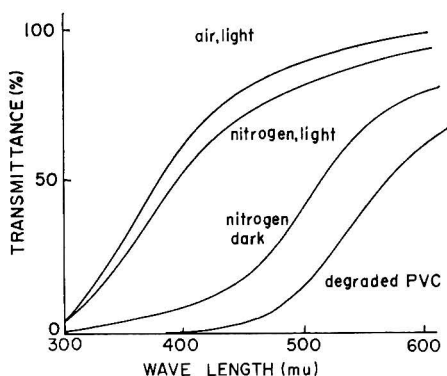

Fig. 2. Effect of light and air on the decoloration of degraded PVC by methyl ethyl ketone for 72 hr at room temperature.   PVC concentration, 0.5 g/20 ml MEK.

However, the absorption at 275 mμ did not diminish appreciably, even after degraded PVC was decolored.   This absorption may be due to short-chain polyene ($n = 3$) or carbonyl groups.   Here, carbonyl groups are probably formed by the thermal oxidation of PVC and absorb near 275 mμ.

The effects of light and air on decoloration are shown in Figure 2.   The experiments were made in MEK at room temperature.   Degraded PVC was most highly decolored in diffused daylight in an air atmosphere. On being kept in a dark room in a nitrogen atmosphere, slight decoloration occurred.   These results indicate that decoloration seems to be accelerated by exposure to air and light.   This fact agrees with the results obtained by Atchison on the decoloration of irradiated PVC in THF.[6]

Table I shows the degree of decoloration by many kinds of solvents. The most effective solvents on decoloration are methylene chloride as halide; MEK, methyl isobutyl ketone (MIBK) and cyclohexanone as ketones; THF and dioxane as cyclic ether; and methyl methacrylate and methyl acrylate as vinyl compounds.   Benzene, chloroform, and methyl acetate show some effectiveness for decoloration, but methyl alcohol and n-hexane have no effect.   Although good solvents for PVC are generally

TABLE I

Decoloration of Degraded PVC by Various Solvents in Diffused Daylight for 14 Days

Degree of decoloration, $\%^a$	Alcohols and hydrocarbons	Halides	Ketones and aldehydes	Esters and acids	Ethers	Nitrogen compounds	Monomers
100–80 (white)		Methylene chloride	MEK, MIBK, cyclohexanone, acetoaldehyde		THF, dioxane	DMF	MMA, MA, EA, vinyl acetate
80–60 (light yellow)	Benzene, xylene	Dichloroethane, chloroform	DIBK, aceto-phenone	Methyl acetate, ethyl acetate		Methylaniline, pyridine	Styrene, acrylonitrile
60–40 (yellow)	Toluene	Chlorobenzene, trichloroethane	Acetone, butyl-aldehyde	Butyl acetate, maleic anhydride	Dimethyl-ether	Nitrobenzene	
40–20 (brown)		Carbon tetra-chloride, tetra-chloroethane	Diacetone alcohol	Formic acid (80%)		Aniline, morpholine, ethanolamine	
20–0 (reddish brown)	Glycerine, n-hexane, isooctane			Acetic acid		Acetonitrile	Acrylic acid, methacrylic acid

ª Expressed as value of transmittance at a concentration of 0.1 g/10 ml. THF at 500 mμ.
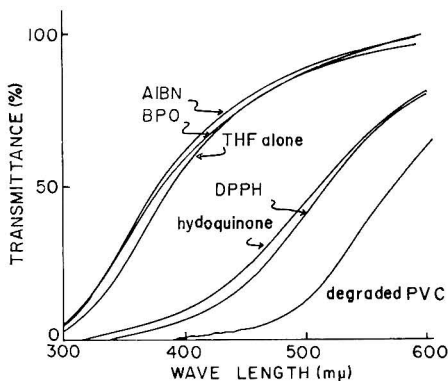
Fig. 3. Decoloration by THF in the presence of various radical sources at 70°C for 4 hr. PVC concentration, 0.5 g/20 ml THF.
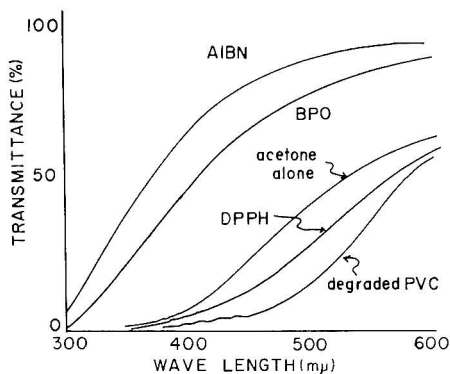

Fig. 4. Decoloration by acetone in the presence of various radical sources at 70°C for 4 hr. PVC concentration, 0.5 g/20 ml acetone.
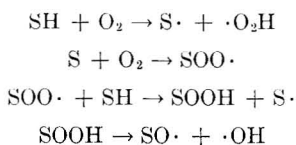
effective for decoloring, morpholine, pyridine, and nitrobenzene are not effective.

Considering the above results, it may safely be said that the decoloring reaction seems to proceed radically. From this point of view, the decoloring reaction was studied in the presence of several radical sources in various solvents. Figure 3 shows the results of decoloration in case of the addition of BPO, AIBN, hydroquinone and DPPH in THF. Degraded PVC was decolored greatly by THF alone. Even in case of addition of BPO or AIBN to THF, the degree of decoloration was almost the same with THF alone. On the contrary, it was very small when hydroquinone or DPPH which acts as a radical scavenger, was added to THF. Furthermore, Figure 4 shows the results of decoloration in acetone. The degraded PVC was decolored slightly by acetone alone. However, the degree of decoloration was considerable when BPO or AIBN were added to acetone. Hydroquinone or DPPH retarded the decoloration.

It is most suitable to suppose the existence of solvent radicals in order to explain the phenomenon of decoloration in the presence of radical sources; that is, the promoting effect of added AIBN or BPO on decoloration is considered to be caused by the reaction of the decomposed radicals and solvent radicals with degraded PVC. On the other hand, the retarding effect of decoloration with hydroquinone or DPPH is considered due to the fact that solvent radicals cannot react with degraded PVC because of capture by stable radicals such as DPPH before solvent radicals react with degraded PVC.

Autoxidation of Solvent and Decoloration by Solvent

The solvent radicals are probably peroxy radicals of solvent or decomposed radicals of solvent peroxide. Ketone, THF, and dioxane are easily autoxidized by oxygen in the air, because of the active hydrogen atoms in their molecules. In general, the autoxidation of a solvent may proceed as shown in eqs. (1)–(4):

$$SH + O_2 \rightarrow S\cdot + \cdot O_2H$$
$$S + O_2 \rightarrow SOO\cdot$$
$$SOO\cdot + SH \rightarrow SOOH + S\cdot$$
$$SOOH \rightarrow SO\cdot + \cdot OH$$

where SH is a solvent molecule. On the basis of this scheme, it may be considered that some kinds of radicals exist in a solvent.

THF, dioxane, and MEK (these three were kept beside window for 3 days) show absorption bands at $3\,400$ cm^{-1} (ν_{O-H}), $1\,115$ cm^{-1}, and 850 cm^{-1} (ν_{C-O}),[20] which seem to be due to the peroxide or hydroperoxide. Furthermore, according to the quantitative analyses of peroxide by
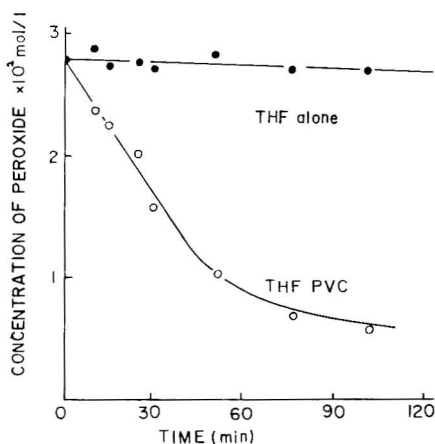

Fig. 5. Variation of the amount of peroxide in THF with decoloration in air at 70°C at a concentration of 0.1 g/10 ml THF. Initial concentration of peroxide in THF, 2.8×10^{-2} mole/l.
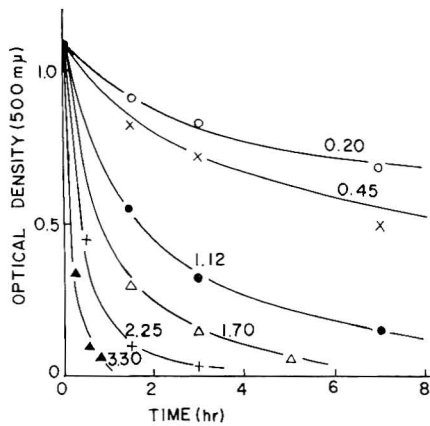
Fig. 6. Relationships between the amount of peroxide in THF and the rate of decoloration of degraded PVC at a concentration of 0.5 g/20 ml THF at 70°C. Figures on curves show initial concentration of peroxide in THF in units of moles/l. $\times$ 10^2.
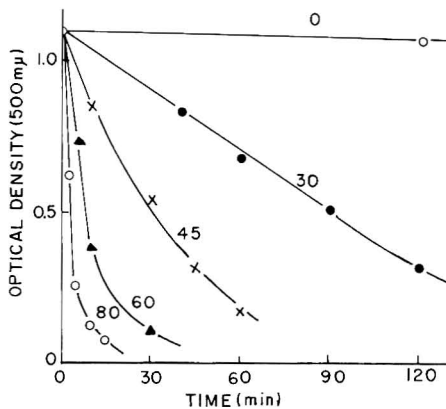
Fig. 7. Effect of temperature on decoloration of degraded PVC at a concentration of 0.1 g PVC/10 ml THF. Initial concentration of peroxide in THF, 7×10^{-2} mole/l. Figures on curves denote the decolorization temperature, in °C.

iodometric titration, the amounts of peroxide in these solvents were about 10^{-2} mole-eq/l.

From these results, it is suggested that the peroxy radicals formed in process of autoxidation or the decomposed radicals or peroxide play an important role in the decoloration by ketone or THF. We therefore studied the relationships between the amounts of peroxide in the solvent and the degree of decoloration of degraded PVC. These results are shown in Figure 5.

The amounts of peroxide in THF alone remain unchanged in the range we studied. However, in case of dissolution of degraded PVC with THF, the amounts of peroxide in THF solution decreases as the decoloration proceeds. From these results it is most reasonable to conclude that the

degraded PVC consumes the THF peroxide and is decolored. Moreover, the relationships between the degree of decoloration and the amounts of peroxide in THF are shown in Figure 6. The rate of decoloration became greater as the amounts of peroxide in THF increased. Here, although it has not been shown in detail, the rate of decoloration is in proportion to the amounts of peroxide in the range of limited amounts.

Figure 7 shows the effects of temperature on the rate of decoloration. The rate of decoloration became faster with increasing temperature. Here, the remarkable point is that the rate of decoloration was quite great even at room temperature. From the relationships between the rate of decoloration and the reciprocal of the absolute temperature, the value of the apparent energy of activation was about 15 kcal/mole, while the activation energy with AIBN in acetone was 30 kcal/mole. These values will be discussed later.

Decolored PVC

As the fine structure absorption due to the polyene structure disappears on decoloration, it is expected that the number of double bonds in decolored PVC decreases. Figure 8 shows the decrease of the number of double bonds as the decoloration by THF and methylene chloride proceeds. In case of THF, the rate of decoloration is fast, but the number of double bonds decreases little. On the other hand, the rate of decoloration by methylene chloride is slow and the number of double bonds decreases gradually. It is very hard to interpret the slowness of decrease in the number of double bonds of the PVC decolored by THF.

Therefore, we tried to determine the trend in the number of double bonds of PVC decolored by other organic solvents or decoloring reagents. At the same time, some characteristics of decolored PVC were examined.
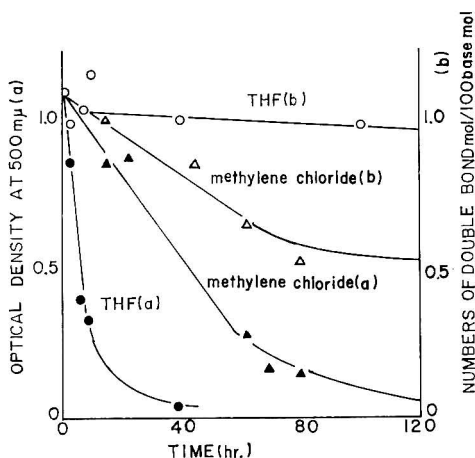

Fig. 8. Variation of double bonds in degraded PVC with the time of decoloration by THF and methylene chloride under diffused daylight at 30°C.

TABLE II
Characteristics of Decolored PVC

PVC	Transmittance, %	$[\eta]$, dl/g	Number of carbonyl groups, mole/100 base mole	Number of double bonds, mole/100 base mole
Original	98.0	0.620	0.003	0.16
Degraded	10.2	0.675	0.020	1.09
Decolored				
Cl_2	97.6	0.655	0.019	0.00
AIBN	95.3	0.640		0.59
THF	98.2	0.605	0.044	0.98
MEK	95.9	0.620	0.047	0.73
CH_2Cl_2	73.8	0.650	0.023	0.58

These results are summarized in Table II. From the value of transmittance of decolored PVC, it is apparent that degraded PVC is decolored well by any reagents. The intrinsic viscosity increases a little on thermal degradation. This may be the result of a crosslinking reaction. On the other hand, the viscosity of decolored PVC is slightly smaller than the value for degraded PVC. Notably, the viscosity of the PVC decolored by THF or MEK is smaller than that of other decolored PVC.

Meanwhile, the spectra of infrared absorption of degraded PVC were measured. The spectra of degraded PVC are almost the same as those of the original PVC. For the PVC decolored by THF or MEK, a new absorption was observed at 1730 cm^{-1} which is due to carbonyl groups. These results are shown in Figure 9. It is apparent from the spectra that PVC decolored by solvents such as THF, MEK, and dioxane contains carbonyl groups.

Table II shows the amounts of carbonyl groups analyzed by the method of Morikawa.[14] The PVC decolored by THF or MEK contains more carbonyl groups than the others. However, this value is only 0.045
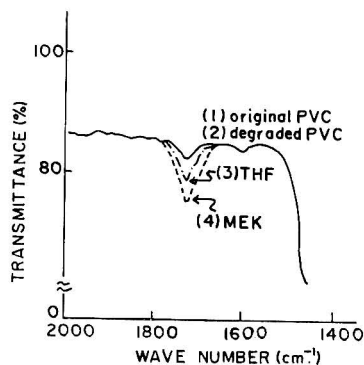

Fig. 9. Infrared spectra of decolored PVC: (1) original PVC; (2) degraded PVC; (3) PVC decolored by THF; (4) PVC decolored by MEK.

mole-eq/100 base mole of PVC. Degraded PVC has also carbonyl groups (0.020 mole-eq/100 base mole). In case of the decoloration by chlorine or methylene chloride, there is no change in the amount of carbonyl groups. In case of THF or MEK, the number of carbonyl groups in decolored PVC increases as the decoloration proceeds. This phenomenon seems to be due to partial oxidation of polyene or the addition of solvents to polyene. As the autoxidized THF and MEK have carbonyl groups in themselves, it may be reasonable to consider that these solvents (an intermediate in process of autoxidation) add to polyene and then the number of carbonyl groups in decolored PVC increases.

As shown in Table II, a remarkably large number of double bonds seem to remain, except for the PVC decolored by chlorine. Especially, the PVC decolored by THF has as many double bonds as degraded PVC has, in spite of the decoloration caused by breaking of conjugated polyene structure, there are still many double bonds remaining. It is hard to understand why PVC decolored by THF has many double bonds. Therefore, it is most reasonable to consider that it simply appears as if many double bonds were remaining in the PVC decolored by THF while actually bromine is consumed by another active species in the determination of the number of double bonds by the pyridine–sulfuric acid–bromine method.

TABLE III
Bromine Consumption by THF[a]

No.	Peroxide in THF, mole/l. $\times 10^4$	Consumed Br_2, mole $\times 10^4$
1	0.0	0.945
2	0.83	1.245
3	3.40	1.040
4	4.92	1.335

[a] THF, 1.23×10^{-4} mole; 15°C; 20 hr.

The fact that the number of double bonds remained unchanged with decoloration is a characteristic of the PVC decolored by THF; this characteristic may be related to the reactivity of THF or THF fragments. It may be due to the addition or substitution reaction of bromine to THF or its intermediates in process of the autoxidation. The reaction between THF and bromine is not yet known. So, the amount of bromine consumed with THF was measured in the same way as in the analysis for double bonds. In this experiment, we used amounts of THF equivalent to the amounts which were supposed to be consumed by double bonds. The results are shown in Table III.

As seen from Table III, THF consumes about the same amount of bromine, and this value is independent of the amount of peroxide in THF. This result is explained as follows. In analysis for the number of double bonds in the PVC decolored by THF, bromine is consumed by both the residual double bonds and the added THF in the decolored PVC. Accord-

ingly, many double bonds seem to remain in decolored PVC. Thus, it may be considered that solvent fragments exist in decolored PVC.

Table IV shows the results of the decoloration by DMF. As nitrogen atoms are observed in decolored PVC, it is evident that DMF fragments exist in decolored PVC. At the same time, the number of double bonds in decolored PVC decreases. From these results, the mechanism of decoloration by solvent seems to be the addition of solvent or solvent fragments to polyene double bonds in degraded PVC. However, it is very difficult to discuss the decoloration mechanism, since the number of double bonds of degraded PVC is very small (about 8 per molecule on the average).

TABLE IV

Analyses of Nitrogen and Double Bond in PVC Decolored by DMF[a]

	Nitrogen, mole/100 base mole PVC	Double bond, mole/100 base mole PVC
Original	0.00	0.16
Degraded	0.01	1.09
Decolored	0.45	0.35

[a] Decoloration conditions; PVC concentration 1 g/40 ml DMF; 20 days, 30°C.

Decoloration of Model Compound by Solvent

Figure 10 shows the changes of ultraviolet and visible absorption spectra of DPOT, the model compound, decolored by dioxane. The peak of the maximum absorption wavelength (379 mμ) of DPOT decreases with the
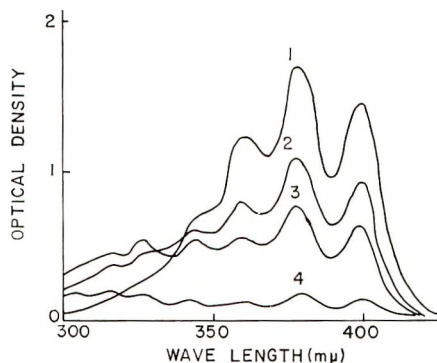
Fig. 10. Change in ultraviolet and visible spectra of DPOT decolored by dioxane at a concentration of 1.7×10^{-5} mole/l. at 70°C; (1) original; (2) after 1 hr; (3) after 2 hr; (4) after 5 hr.

decoloring time; at the same time, the yellow color of the solution changes to colorless. In this case, a new absorption peak that appears near 327 mμ increases at first and later decreases gradually as the decoloration pro-

ceeds. The number of conjugated double bonds in DPOT is 4, but there exist benzene rings at each end related to these conjugated double bonds. Accordingly, the polyene chain length of DPOT is assumed to be 7. At the early stage of decoloration by dioxane, a new absorption appears near 327 mμ, and the absorption of 379 mμ disappears. From the Lewis-Calvin relationship, the absorption at 327 mμ corresponds to a polyene chain length of 4–5. From this result, it may be considered that the double bond next to the benzene ring is broken by dioxane at first.

According to more detailed results, the rate of decoloration of DPOT by solvents is fast on exposure to air and light but very slow under a nitrogen atmosphere in a dark room. Even in the dark some solvents, such as dioxane, cyclohexanone, THF, and MEK, have the ability to produce decoloration under the air atmosphere. Thus, the decoloration of DPOT seems to be caused by the peroxide in solvents. On calculating the apparent energy of activation for decoloration of DPOT by solvents, the values of 14 kcal/mole for THF, 27 kcal/mole for MEK, and 28 kcal/mole for AIBN in benzene were obtained. These values of activation energy agreed well with those for decoloration of degraded PVC by THF or AIBN.

TABLE V
Decoloration of DPOT by CCl₄ at 20°C in
Diffused Daylight for 120 hr

Compound	Weight, mg	Cl content, wt %	Number of double bonds, mole/mole
DPOT	100	—	3.95
Decolored DPOT	171	39	1.53

In order to study the structure of decolored DPOT, carbon tetrachloride was used instead of THF, because the separation of the decolored product of DPOT by THF from the autoxidized products of THF was difficult. Table V shows the changes in the number of double bonds, chlorine contents, and weight of the DPOT decolored by carbon tetrachloride. The double bonds decrease as the decoloration proceeds, but some still remain in the decolored DPOT. Meanwhile, the analysis shows that chlorine content of decolored DPOT is 39 wt-%. The weight increased by decoloration of DPOT agrees with the weight of chlorine added to DPOT. Carbon tetrachloride does not produce peroxy radical with oxygen, but easily produces the radical by the reaction (5) on exposure to daylight.

$$CCl_4 \xrightarrow{h\nu} Cl\cdot + CCl_3\cdot \tag{5}$$
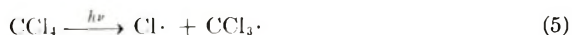
Accordingly, it is assumed that decoloration by carbon tetrachloride is caused by addition of Cl· or CCl₃· radicals in the solvent to conjugated double bonds in DPOT.

Mechanism of Decoloration

If it is considered that the decoloration of degraded PVC is due to the addition reaction of solvent radical to a polyene structure, the decoloration phenomena can be well explained. From the above results, it is possible to propose the following condition and mechanisms for decoloration.

A necessary condition for the decoloration is that the solvents must be good solvents for PVC. The decoloration may proceed with two types of solvents.

(1) Decoloration by solvents which are easily autoxidized proceeds by autoxidation of solvents (where SH denotes a solvent molecule):

$$SH \xrightarrow{-H} S\cdot \xrightarrow{O_2} SOO\cdot \xrightarrow{+H} SOOH \longrightarrow SO\cdot + \cdot OH$$
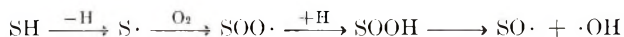
and subsequent addition of solvent radicals to polyene double bonds:
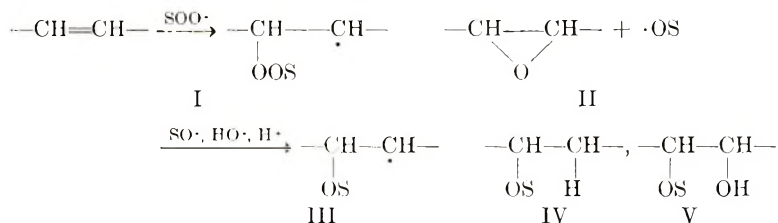
(2) Decoloration by solvents which are easily excited by exposure to light (e.g., CCl_4) proceeds by a different set of reactions, yielding VI and VII.
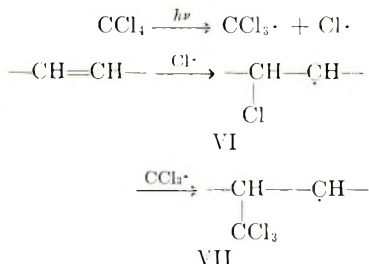
It is a necessary condition that solvent must be a good one for dissolving PVC. For example, the model compound was decolored by carbon tetrachloride, but degraded PVC was not decolored by it as CCl_4 is a poor solvent for degraded PVC.

In case of decoloration by autoxidized solvents for the structure of decolored PVC, none of the postulate types (products I–V) could be observed by the analyses of infrared spectra. However, the existence of peroxide groups in decolored PVC is indicated by iodometric titration, so the existence of structure I is possible. Since structure I can easily change into the structure II, the latter structure may exist. Nitrogen atoms are observed in PVC decolored by DMF, which indicates the existence of solvent fragments in decolored PVC. Therefore, the decoloration reaction may proceed by the addition of peroxy radicals of solvents to polyene double bonds. In this case, the hydroperoxide is considered to be solvent

peroxide, but other types of peroxides also may have to be considered. Moreover, although we have neglected it in this paper, it may have to be considered that the decoloration occurs partially by scission of the main chain in degraded PVC by solvent peroxide. We are currently studying these points.

On the other hand, in case of decoloration by solvents excited by light, as chlorine atoms were found in the model compound decolored by carbon tetrachloride, decoloration must be caused by the addition of Cl· or CCl₃· radicals to polyene double bonds. Therefore, in this case, the structure VI or VII is possible.

Thus, it is concluded from the results of this investigation that the decoloration of degraded PVC by solvents such as THF is due to peroxides of solvents, and the mechanism is considered to be the addition of peroxy radicals of solvents to conjugated double bonds in degraded PVC.

References

1. E. J. Arlman, *J. Polymer Sci.*, **12**, 543 (1954).
2. B. Baum and L. H. Wartman, *J. Polym. Sci.*, **28**, 537 (1958).
3. D. E. Winkler, *J. Polym. Sci.*, **35**, 3 (1959).
4. M. Yamaguchi, T. Otsu, and M. Imoto, *Kogyo Kagaku Zasshi*, **58**, 472 (1955).
5. A. Konishi, *Nippon Kagaku Zasshi*, **78**, 1517 (1957).
6. G. J. Atchison, *J. Polym. Sci.*, **49**, 385 (1961).
7. C. Wippler, *Nucleonics*, **18**, 68 (1960).
8. T. Matsumoto, unpublished results.
9. T. Morikawa and K. Yoshida, *Kagaku to Kogyo*, **37**, 107 (1963).
10. C. D. Wagner, R. H. Smith, and E. D. Peters, *Ind. Eng. Chem. Anal. Ed.*, **19**, 976 (1947).
11. K. W. Rosenmund and B. Laukivitz, *Angew. Chem.*, **37**, 58 (1924).
12. H. Mizutani, *Kobunshi Kagaku*, **8**, 181 (1951).
13. K. Takemoto, *Kogyo Kagaku Zasshi*, **63**, 183 (1960).
14. T. Morikawa, *Kobunshi Kagaku*, **24**, 592 (1967).
15. R. Kuhn, *Ber.*, **69**, 98 (1936).
16. A. Steyermark, *Quantitative Organic Microanalysis*, 2nd Ed., Academic Press, New York, 1961.
17. F. Bohlmann and H. Mannhardt, *Ber.*, **89**, 1307 (1956).
18. G. N. Lewis and M. Calvin, *Chem. Revs.*, **25**, 273 (1939).
19. K. Hirayama, *J. Amer. Chem. Soc.*, **77**, 373 (1955).
20. H. R. Williams and H. S. Mosher, *Anal. Chem.*, **27**, 517 (1955).

Oxidative Polymerization of Diethynyl Compounds

ALLAN S. HAY, *General Electric Research and Development Center Schenectady, New York 12301*

Synopsis

Diethynyl compounds are readily polymerized to high molecular weight linear polymers by oxidative coupling with oxygen in the presence of an amine complex of a copper salt as catalyst. Organometallic moieties can also be introduced into these polymers. Thus polymers in which silicon, arsenic, and mercury are part of the polymer backbone have been synthesized.

INTRODUCTION

It was shown previously[1] that the oxidative coupling reaction

$$\tfrac{1}{2}O_2 + 2RC \equiv CH \rightarrow RC \equiv C - C \equiv CR + H_2O \tag{1}$$

could be performed in a variety of solvents at room temperature in the presence of a small amount of an amine complex of a copper (I) salt as catalyst. Since in most cases the yields obtained were practically quantitative, the oxidation of diethynyl compounds would then be expected to yield high molecular weight linear polymers, i.e.,

$$n/_2O_2 + n\ HC \equiv C - R - C \equiv CH \rightarrow \leftarrow C \equiv C - R - C \equiv C \rightarrow_n + nH_2O \tag{2}$$
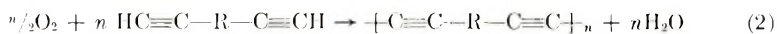
The preparation and properties of some polymers of this type is the subject of the present paper. Polymers of this class have also been synthesized recently by Kotlyarevskii and co-workers.[2] Almost any diethynyl compound can be polymerized by this method; hence the scope of the reaction is very large, and even organometallic moieties can readily be incorporated into this class of polymers.

EXPERIMENTAL

Polymerization of Acetylene

To a 250-ml Erlenmeyer flask was added 1 g CuCl, 2.4 g of N,N,N',N'-tetramethylethylenediamine, and 135 ml of pyridine. The reaction was vigorously stirred and oxygen was passed into the reaction. Acetylene was then bubbled into the reaction mixture slowly for 3 min. The temperature rose from 30 to 38°C during this time. After the acetylene was stopped, the reaction continued. In 7 min the temperature rose to 55°C, then began to subside. After 3 min the reaction mixture was filtered and washed

with methanol containing some HCl. The solid on the filter which looked like carbon black was dried for 4 hr at 100°C under high vacuum to give 2 g of a finely divided solid which has no melting point. The material is insoluble in all solvents and is very finely divided; analysis showed C, 62.3%; H, 4.0%. Some of the material was heated to about 600°C in a test tube; the analysis was then C, 82.8%; H, 2.2%.

In the oxidation, if a diamine is not used, only a very slow reaction occurs. The reaction can be run in many solvents other than pyridine.

Polymerization of *m*-Diethynylbenzene

To a 250-ml Erlenmeyer flask, was added 0.59 g CuCl and 125 ml of pyridine. Oxygen was passed through the vigorously stirred solution; then there was added 2.37 g of *m*-diethynylbenzene. A vigorous reaction ensued. In 14 min the temperature rose to 40°C and a precipitate began to settle from solution. The reaction was continued for 2 min longer, then precipitated in methanol and filtered, then washed with methanol containing a little HCl, and dried *in vacuo*. There was obtained 2.25 g of an almost colorless powder that begins to decompose at about 180°C and gradually darkens as the temperature is raised.

ANAL. Calcd for $(C_{10}H_4)_n$: C, 96.75%; H, 3.25%. Found: C, 96.4%; H, 3.5%.

The material is soluble in most organic aromatic solvents, such as chlorobenzene and nitrobenzene, and in chlorinated hydrocarbons, such as *s*-tetrachloroethane, above 100°C. If a nitrobenzene solution is evaporated at 170°C, a tough, transparent film remains that has a tensile strength of 5000–8000 psi. When ignited in air a vigorous reaction ensues, the net result of which is removal of most of the hydrogen. Thus a piece of film weighing 0.068 g was ignited, and the residue after ignition weighed 0.0648 g, i.e., the loss was 0.0032 g or 4.7%. This material now contained 96.2% carbon and 0.8% hydrogen. When heated *in vacuo* rapidly to ca. 200°C a violent reaction occurred, and gases were evolved that analyzed for approximately 90% hydrogen and 10% methane. During the decomposition the residue became red hot.

If the oxidation is run with the use of N,N,N',N'-tetramethylethylenediamine as ligand the reaction is much faster, e.g., the maximum temperature is reached in 2–3 min; however, the product is the same but is of higher molecular weight.

Reaction of Mercury (II) Chloride and 1,4-Phenylenediethynylenedilithium

To a solution of 16 g (0.10 mole) of bromobenzene in 150 ml of anhydrous ether was added 1.4 g (0.20 g atoms) of lithium wire. After 2.5 hr at reflux the lithium had reacted and there was added 12.7 g (0.10 mole) of *p*-diethynylbenzene. An immediate reaction occurred, and there was deposited a colorless solid. After 1 hr at reflux there was added 13.7 g (0.05 mole) of mercury (II) chloride and the reaction mixture refluxed for 1 hr further.

The reaction mixture was filtered and the precipitate boiled in ethanol to remove lithium chloride and filtered hot. There was obtained 15.2 g of a colorless solid (VI) that is insoluble in hot pyridine, o-dichlorobenzene, nitrobenzene, N,N-dimethylformamide, tetrahydrofuran, N,N-dimethylacetamide, and dioxane. The solid begins to decompose at about 200°C.

ANAL. Calcd for $C_{20}H_{10}Hg$: C, 52.7%; H, 2.2%. Calcd for $C_{10}H_4Hg$: C, 36.9%; H, 1.24%. Found: C, 40.3%; H, 1.9%.

When the material is ignited the residue is a highly expanded (ca. 20 times) carbonaceous material that conducts electricity.

Reaction of Mercury (II) Chloride and 1,6-Heptadiynylenedilithium

The reaction was run as the preceding one with the use of 1.5 g (0.22 g-atom) of lithium wire, 17 g (0.11 mole) of bromobenzene, 9.9 g (0.11 mole) of 1.6-heptadiyne, and 14.5 g (0.053 mole) of mercury (II) chloride. There was obtained 19.1 g of an insoluble, colorless solid (VII) that softens at about 190°C, then resolidifies above 200°C, and gradually darkens up to 300°C.

ANAL. Calcd for $C_{14}H_{12}Hg$: C, 44.0%; H, 3.7%. Calcd for C_7H_6Hg: C, 28.9%; H, 2.1%. Found: C, 31.2%; H, 2.6%.

1,7,13,19-Eicosatetrayne and Mercury (II) Chloride

To a solution containing 11 g of mercury (II) chloride, 27 g of potassium iodide, 27 ml of water, and 21 ml of 10% sodium hydroxide solution in an ice bath was added a solution of 10.7 g of 1,7,13,19-eicosatetrayne in 100 ml of ethanol. After stirring for 10 min, the colorless solid was removed by filtration and washed with cold ethanol. There was obtained 18.5 g of a colorless powder (VIII) that begins to soften at 65°C and is all melted at 100°C.

ANAL. Found: C, 52.9%; H, 5.7%; Hg, 18.1%.

Oxidative Coupling of (VIII)

To a solution of 1 g of copper (I) chloride in 135 ml of pyridine was added 5 g of VIII. Oxygen was passed through the vigorously stirred solution for 70 min, and then the reaction mixture was precipitated in methanol and filtered. There was obtained 3 g of a colorless solid, IX, softening at 105–115°C.

ANAL. Found: C, 59.5%; H, 6.6%; Hg, 33.3%. This corresponds to the empirical formula $C_{29.8}H_{39.8}Hg$ or approximately 1.5 eicosatetraynes per mercury.

A solution of this polymer is s-tetrachloroethane was evaporated at 140°C. On cooling there remained a tough, flexible film.

Reaction of Diphenyldichlorosilane and Phenylethynyllithium

To a solution of phenyllithium from 7.7 g (1.1 g-atom) of lithium and 87.5 g (0.56 mole) of bromobenzene prepared in 500 ml ether was added 56.5 g

(0.55 mole) of phenylacetylene. To this solution, at reflux, there was added, dropwise, 70.5 g (0.29 mole) of diphenyldichlorosilane. After 1 hr, the ether layer was washed with water, dried, and evaporated on the steam bath. To the residue was added a small amount of ethanol and a solid separated out, 82 g (0.214 mole; 74%); mp 79–80°C. Recrystallization from ethanol raised the melting point to 82°C.

ANAL. Calcd for $C_{26}H_{20}Si$: C, 86.7%; H, 5.6%; Si, 7.3%. Found: C, 87.3%; H, 5.5%; Si, 7.5%.

Methylphenylbis(phenylethynyl)silane

Dichloromethylphenylsilane (42 g; 0.22 mole) was added dropwise to an ethereal solution of phenylethynyllithium prepared in the usual manner from 6.9 g (1 g-atom) of lithium wire and 78 g (0.5 mole) of phenylacetylene. There was obtained 41 g (0.126 mole, 57%) of methylphenylbis(phenylethynyl)silane, mp 69–71°C.

ANAL. Calcd for $C_{23}H_{18}Si$: C, 85.5%; H, 5.6%. Found: C, 85.2%; H, 5.4%.

Diethyldichlorosilane and 1,4-Phenylenediethynylenedilithium

The reaction was run in the usual fashion with 1.0 g (0.144 g-atom) of lithium, 11.3 g (0.072 mole) of bromobenzene, 4.55 g (0.036 mole) of p-diethynylbenzene, and 4.5 g (0.028 mole) of dichlorodiethylsilane in 250 ml of ether. There was isolated a semisolid which was added to 135 ml of pyridine containing 1.0 g of copper (I) chloride. Oxygen was bubbled through the vigorously stirred solution, and in 5 min the temperature rose to 46°C and the reaction mixture became viscous. After precipitation in methanol there was isolated 3.3 g of a bright yellow solid (XII) that was soluble in hot s-tetrachloroethane and could be cast into a transparent, flexible film.

ANAL. Found: C, 82.5%; H, 6.1%; Si, 9.4%. This corresponds to the approximate formula:
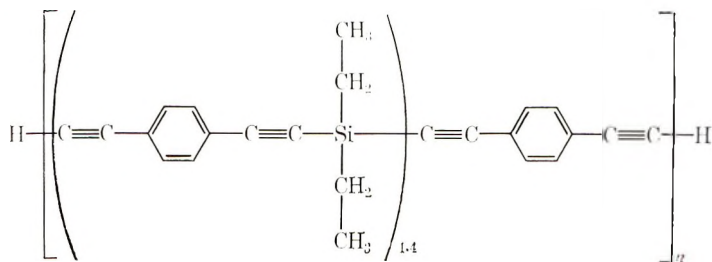
Diiodophenylarsine and 1,4-Phenylenediethynylenedilithium

To a suspension of 1,4-phenylenediethynylenedilithium in 500 ml of anhydrous ether prepared from 23.4 g (0.15 mole) of bromobenzene, 2.05 g (0.3 mole) of lithium wire, and 9.3 g (0.074 mole) of p-diethynylbenzene was added 25 g (0.062 mole) of diiodophenylarsine. The mixture was refluxed

for 2 hr; then water was cautiously added. The ether layer was evaporated and the residue triturated with alcohol. After drying there was obtained 10.2 g of an almost colorless solid (X) that could be cast into a very brittle film.

ANAL. Calcd for $(C_{16}H_9As)_n$: C, 69.6%; H, 3.28%; As, 27.1%. Found: C, 68.8%; H, 3.0%; As, 26.9%.

This low molecular weight polymer (9 g) was added to a solution of 2 g of copper (I) chloride in 150 ml of pyridine, and oxygen was passed through the vigorously stirred solution for 1 hr. The product was isolated by precipitation into methanol and filtration. After redissolving in chloroform, filtering, reprecipitating into methanol and drying, there was obtained a polymer (XI) of intrinsic viscosity 0.175 dl/g (in $CHCl_3$ at 25°C) which gave a flexible film when cast from s-tetrachloroethane at 110°C.

ANAL. Found: C, 69.3%; H, 3.1%; As, 25.2%.

DISCUSSION

The polymer (I) obtained by oxidative coupling of m-diethynylbenzene[3]

I
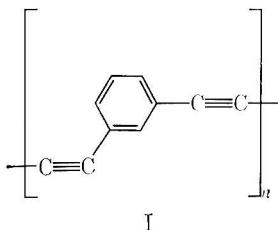
is a pale yellow solid that is practically insoluble in all solvents at room temperature. It is practically amorphous as obtained from the reaction mixture. Nitrobenzene is one of the best solvents for the polymer, and light yellow films of the polymer which are tough and flexible can be cast from this solvent at 160°C; thus, it is completely miscible at this temperature. When cast at lower temperatures from nitrobenzene and other solvents (e.g., at 130°C from s-tetrachloroethane), translucent to opaque films which are brittle are obtained due to a high degree of crystallinity. The amorphous polymer is readily crystallized by tetrahydrofuran.[4] A 1% suspension of the polymer in nitrobenzene on slow heating only becomes completely soluble at about 110°C. Yet because the polymerization reaction is extremely fast, high molecular weight polymers are readily obtained when the polymerization proceeds at room temperature even though the polymer precipitates from the reaction mixture at the end of the polymerization.

The molecular weight of these polymers can be roughly estimated from the intense ethynyl carbon–hydrogen stretching band in the infrared at 3310 cm^{-1}. Intrinsic viscosities of the polymers have also been determined in nitrobenzene at 140°C. Since the polymer is insoluble in the reaction mix-

ture, the polymerization must be performed rapidly.   This restriction does not, of course, apply to reactions with yield soluble polymers.   The highest molecular weights are obtained by using the most effective catalysts and increasing the temperature as would be expected.   When the polymerization was performed at 30°C in pyridine solvent, a polymer with intrinsic viscosity 0.19 dl/g (nitrobenzene at 140°C) was obtained.   This polymer had a molecular weight (infrared determination of endgroups) of 8700. Increasing the reaction temperature to 40°C gave a polymer with an intrinsic viscosity of 0.35 dl/g and molecular weight of 12400.   When the polymerization was performed at 40°C in a mixed nitrobenzene–pyridine (80/20) solvent with the use of a N,N,N',N'-tetramethylethylenediamine–CuCl catalyst which is exceptionally effective for the oxidative coupling of acetylenes,[1] a polymer with an intrinsic viscosity of 0.41 dl/g and molecular

TABLE I

$C_6H_5C{\equiv}CH$, mole-%	$[\eta]$, dl/g	Molecular weight (calcd)
25	0.12	1200
11	0.16	2480
5	0.22	5080
2.5	0.27	10200
1.25	0.29	20000

TABLE II

Compound	Increase in weight, %
Diphenyl ether	5.2
n-Decane	6.6, 7.8
Cumene	13.5
Aniline	12.8, 15.0
Phenol	16.5
o-Cresol	18.2, 20.0

weight of 30000 was obtained.   The first polymer, when cast into a film from nitrobenzene at 160°C, was brittle.   The last polymer gave a very tough and flexible film.   The properties of the polymer have been described elsewhere.[4]

The polymerization can also be chain-stopped by the addition of a monoethynyl compound.   A solution of m-diethynylbenzene and phenylacetylene was added to the reaction mixture dropwise over a 4–5 min period.   Intrinsic viscosities of the resulting polymers were determined in nitrobenzene at 140°C.   Results are given in Table I.

The calculated molecular weights are only very roughly in agreement with molecular weights determined on non-chain-stopped polymers of the same intrinsic viscosity by end group analysis (infrared).

The polymer when heated above 180°C rapidly becomes insoluble.[4] It was of interest to determine how the polymer would behave when heated

in the presence of organic compounds. The procedure was as follows. A 0.2000-g portion of polymer (molecular weight 20000) was heated in a sealed tube at 200°C with 5 ml of the organic compound for 15 min. After cooling the solid was removed by filtration and dried for 0.5 hr at 210°C *in vacuo* (0.5 mm). The residue was then weighed, the increase in weight indicating the amount of the organic carbon incorporated in the residual carbonaceous polymer (Table II).

It is apparent that there is considerable reaction with organic compounds containing active hydrogens and much less with compounds containing no functional groups.

The polymer obtained by oxidative coupling of *p*-diethynylbenzene is bright yellow and highly crystalline.[3] It begins rapidly to decompose about 100°C, and since it is completely insoluble no further work was done on it. The oxidative coupling of *p*-diethynylbenzene has also been described elsewhere.[5,6] However, unsubstituted polyynes are highly unstable.[7] Oxidative coupling of acetylene yielded an insoluble material that looked like finely divided carbon; however, it contained only about 60% carbon, the remainder being hydrogen and oxygen. The infrared spectrum of the material indicated the presence of triple bonds as well as quite intense but diffuse absorption in the carbonyl region. Apparently, coupling occurs, but the conjugated triple bond system then rearranges and picks up oxygen giving a complex material.

In recent years, one of the areas of acetylene chemistry that has been looked at intensively in a number of laboratories is the preparation and chemistry of metallo-organic acetylenes.

Bis(phenylethynyl)mercury has been known for a number of years and is comparable in stability to diphenylmercury.[8]

Hartmann[9] has prepared phenylethynyl compounds of tin, phosphorus, arsenic, and antimony, i.e., $Sn(C\equiv CC_6H_5)_4$, $P(C\equiv CC_6H_5)_3$, $As(C\equiv CC_6H_5)_3$, and $Sb(C\equiv CC_6H_5)_3$. He has also prepared various other alkynyl and ethynylene derivatives of arsenic, antimony, tin, lead, zinc, boron, germanium, and silicon.[2] All of these compounds are prepared by conventional methods involving generally the reaction of the acetylenic Grignard reagent or lithium derivative with the organometallic halide. The phenylethynyl derivatives are particularly noteworthy because of their stability, tetrakis(phenylethynyl)tin has a melting point without decomposition of 174°C, and they are all easily purified and prepared in high yield.

Nast[10] has prepared phenylethynyl derivatives of transition metals in which the phenylethynyl anion acts in the same way as cyanide as a ligand (II):

$$K_4[Fe(C\equiv C_6H_5)_6]$$
$$II$$
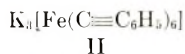
Chatt[11] has prepared relatively stable covalent acetylenic derivatives of platinum and palladium and nickel. The complexes (III) are stabilized by coordination with trialkyl phosphines.

$$C_6H_5C{\equiv}C-P\left(\begin{array}{c}(Et)_3 \\ | \\ P \\ | \\ \\ | \\ P \\ | \\ (Et)_3\end{array}\right)-C{\equiv}CC_6H_5$$

III
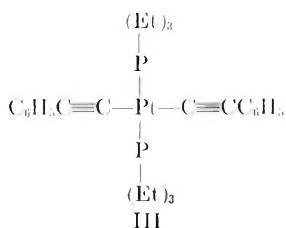
In a series of papers Arens[12] has explored extensively the chemistry of acetylenic ethers and thioethers, and Montanori[13] has also recently studied acetylenic thioethers.

The preceding work indicated that phenylethynyl derivatives of varying stability could be readily prepared from derivatives of most elements of the periodic table. We proposed to incorporate structures of this type in high molecular weight polymers by preparing similar derivatives of diethynyl compounds and then converting them to high molecular weight polymers by oxidative coupling:

$$HC{\equiv}CRC{\equiv}C-M-C{\equiv}CRC{\equiv}CH \rightarrow$$

$$+C{\equiv}C-R-C{\equiv}C-M-C{\equiv}C-R-C{\equiv}C+_n \quad (3)$$
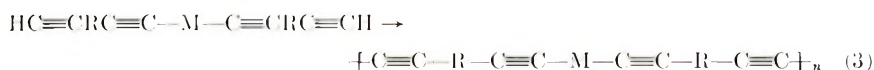
where R denotes a hydrocarbon and M a metal or organometallic residue. Polymers of this type should be unique, in that many of the heteroatoms we propose to incorporate in the polymers have never before been introduced into the backbone of a polymer chain.

To evaluate the feasibility of preparing polymers of the type described containing various heteroatoms in the backbone we attempted the synthesis of three types: (1) polymers containing a divalent atom, i.e., mercury (II); (2) polymers containing a trivalent atom, i.e., arsenic (III); and (3) polymers containing a tetravalent atom, silicon. These three types will be considered in the order given and were chosen because of the availability of the starting materials.

Polymers Containing Mercury

Ideally, we would like to react a diethynyl compound such as m- or p-diethynylbenzene or an alkadiyne with a Grignard reagent or an alkyl or aryl lithium compound to produce the corresponding acetylene organometallic (IV).

$$HC{\equiv}C-R-C{\equiv}CH \xrightarrow{RLi} HC{\equiv}C-R-C{\equiv}CLi \xrightarrow{HgX_2} (HC{\equiv}CR-C{\equiv}C)_2Hg \quad (4)$$

IV   V
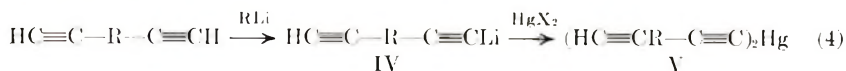
This could then be reacted with a mercury (II) halide, for example, to give the monomer (V) required for oxidative coupling to a high polymer. By using m- or p-diethynylbenzene it was found that the dilithium derivatives, which are insoluble in ether, were formed preferentially. Reaction with mercury (II) chloride gave insoluble, infusible solids. The analysis would indicate that a low polymer (VI) was formed.

$$\left[C\equiv C-\text{<benzene ring>}-C\equiv C-Hg \right]_n$$

VI
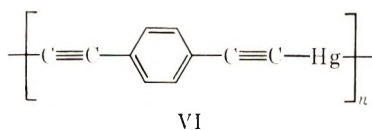
Similar results were obtained with aliphatic diynes. From 1,6-heptadiyne an insoluble polymer was obtained which softened at 190°C. The analysis indicates that the product has approximately the structure VII.

$$+ C\equiv C-(CH_2)_3-C\equiv C-Hg +_n$$

VII
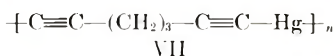
Since the former polymers were insoluble, we attempted a synthesis using a long-chain diyne, 1,7,13,19-eicosatetrayne. The low polymer VIII obtained, which was soluble in organic solvents, was oxidatively coupled to give a high polymer (IX) that could be cast into a tough, flexible film. The analysis corresponded approximately to 1.5 eicosatetraynes per mercury. This is the first example of a high polymer containing mercury as part of the polymer backbone.

Polymers Containing Arsenic

Diiodophenylarsene was used to prepare polymers containing arsenic. Since the monolithium compound (II) from *m*- or *p*-diethynylbenzene could not be prepared because of the insolubility of the dilithium compound, an excess of the latter was reacted with diiodophenylarsene to give a low polymer (X), which was then
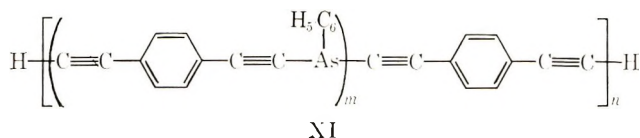
$$H-\left[\left(C\equiv C-\text{<benzene ring>}-C\equiv C-\underset{\underset{m}{|}}{As}\right)-C\equiv C-\text{<benzene ring>}-C\equiv C\right]_n-H$$

XI

oxidatively coupled to a high polymer (XI). Polymers containing up to 25% As by weight were readily obtained in this manner. The low polymer, X, could also be copolymerized with *m*-diethynylbenzene to give polymers containing lesser amounts of arsenic.

Polymers Containing Silicon

Initially some simple tetrasubstituted silanes were prepared. Tetrakis-(phenylethynyl)silane was found to melt at 193°C, diphenylbis(phenylethynyl)silane at 79°C, and methylphenylbis(phenylethynyl)-silane at 69°C.

As in the previous cases with mercury and arsenic, the simple monomers, such as XII

$$(HC\equiv C-\text{<benzene ring>}-C\equiv C)-SiR_2$$

XII
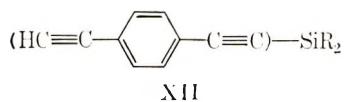
could not be prepared by using p-diethynylbenzene.   Low polymers (XIII) were then prepared by reacting the dilithium derivative of the diacetylene in excess with the dichlorosilane.

$$\text{H}(\text{C}\equiv\text{C}-\text{R}-\text{C}\equiv\text{C}-\underset{\underset{\text{R}_2}{|}}{\overset{\overset{\text{R}_1}{|}}{\text{Si}}})_n\text{C}\equiv\text{C}-\text{R}-\text{C}\equiv\text{CH}$$

XIII

This low polymer was then oxidatively coupled to a high polymer.

By using p-diethynylbenzene or m-diethynylbenzene with dichloro-diphenylsilane or dichlorodimethylsilane, insoluble and infusible polymers were obtained.   However, with dichlorodiethylsilane, p-diethynylbenzene gave a soluble polymer.   Presumably, m-diethynylbenzene would also give a soluble polymer.

References

1. A. S. Hay, *J. Org. Chem.*, **27**, 3320 (1961).

2. I. L. Kotlyarevskii, A. S. Zanina, and N. M. Gusenkova, *Izv. Akad. Nauk, SSSR Ser. Khim.*, **1967**, 900; see also previous papers in this series.

3. A. S. Hay, *J. Org. Chem.*, **25**, 637 (1960).

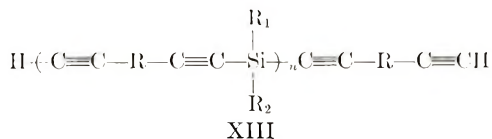4. A. E. Newkirk, A. S. Hay, and R. S. McDonald, *J. Polym. Sci. A*, **2**, 2217 (1964).

5. I. L. Kotlyarevskii, L. B. Fisher, A. A. Dulov, and A. A. Slinkin, *Izv. Akad. Nauk, SSSR Otdel. Khim. Nauk*, **1960**, 950.

6. V. V. Korshak, A. M. Sladkov, and Yu. P. Kudryavtsev, *Vysokomol. Soedin.*, **2**, 1824 (1960).

7. R. A. Raphael, *Acetylenic Compounds in Organic Synthesis*, Academic Press, New York, 1955, p. 131.

8. J. R. Johnson and W. L. McEwen, *J. Amer. Chem. Soc.*, **48**, 469 (1926).

9. H. Hartmann, H. Niemüller, W. Reiss, and B. Karbstein, *Naturwiss.* **46**, 321 (1959) and previous papers.

10. R. Nast and H. Griesshammer, *Chem. Ber.*, **90**, 1315 (1957) and previous papers.

11. J. Chatt and B. L. Shaw, *J. Chem. Soc.*, **1959**, 4020.

12. J. F. Arens, *Advan. Org. Chem.*, **2**, 177 (1960).

13. F. Montanori and A. Negrini, *Ricerca Sci.*, **27**, 467 (1957); CA **52**, 9985(1958).

Received July 25, 1968

Gel-Permeation Chromatography of Cellulose Esters. Effect of Average DP, DS, Substituent Size, and Primary Hydroxyl Content

R. J. BREWER* and L. J. TANGHE, *Polymer Technology Division,* and S. BAILEY, *Industrial Laboratory, Eastman Kodak Company, Rochester, New York 14650*

Synopsis

Hydrolyzed cellulose acetates and cellulose tripropionates prepared over wide ranges of intrinsic viscosity (DP) were fractionated by gel-permeation chromatography (GPC). An increase was observed in the polystyrene equivalent length (PSEL) at 50% cumulative height with increasing DP of the ester. Cellulose acetates and propionates over wide range of acyl content (DS), and a homologous series of triesters (propionate through heptanoate) of the same DP were fractionated by GPC. Increased amount and size of acyl gave relatively small increases in PSEL. The molecular size of cellulose acetates was not affected by the amount of primary hydroxyl present in the esters. The breadth of molecular weight distribution of the cellulose esters, as measured by the weight-average to number-average molecular size ratio, $\overline{M}_w/\overline{M}_n$, was not affected by any variation in the composition of the esters. A blend of cellulose tripropionates of widely differing DP gave a broadened GPC curve in agreement with that calculated from the components of the blend.

INTRODUCTION

Gel-permeation chromatography (GPC) has recently become a widely used, effective analytical tool for the characterization of molecular weight distributions. Although most of the literature concerns synthetic polymers, some work has been reported on cellulose esters. Segal[1-3] and Meyerhoff[4] fractionated cellulose nitrates by GPC and found this ester suitable for determining molecular weight distribution. Maley[5] and Cazes[6,7] reported some work on GPC fractionation of cellulose esters, but gave no data. We recently employed[8] the tricarbanilate derivative, obtained by way of regenerated cellulose, to fractionate two cellulose acetates prepared by different methods of acetylation.

Although GPC has proved useful for fractionating cellulose esters, little is known about the effects of variation in degree of polymerization (DP), size and amount (DS) of acyl substituent, and primary hydroxyl on apparent molecular size. All of these are common variables associated

* Presents Address: Research Laboratories, Tennessee Eastman Company, Division of Eastman Kodak, Kingsport, Tennessee 37662.

with the preparation of cellulose esters and they can greatly influence the physical properties of the ester.

This paper, therefore, summarizes some of our work on the effects of these variables on the behavior of cellulose esters during GPC fractionation.

EXPERIMENTAL

Preparation of Hydrolyzed Cellulose Acetate Viscosity Series

Cotton linters were acetylated at a 9:1 (liquid:cellulose) ratio with acetic acid, acetic anhydride, and sulfuric acid catalyst according to general procedures previously described.[9] The reaction solution was free from fiber and grain after an esterification time of 30 min, and samples were removed at intervals during the following $1^1/_2$ hr as the temperature was raised from 100 to 140°F. The samples were diluted with aqueous acetic acid containing enough $MgCO_3$ to neutralize half of the sulfuric acid catalyst. The ester in solution was hydrolyzed at 110°F to approximately 39.5% acetyl, and the solution was poured into distilled water to precipitate the ester.

Preparation of Cellulose Tripropionate Viscosity Series

Dewatered cotton linters were esterified in a stainless steel mixer using 0.7 part of propionic acid, 4.2 parts of propionic anhydride, and sulfuric acid catalyst. The esterification solution was free from fiber and grain after 6 hr, and samples were removed at intervals during the following 3 hr as the temperature was raised from 100 to 140°F. The samples were diluted with aqueous propionic acid, held at room temperature for 2 hr, and poured into distilled water to recover the esters.

Preparation of Cellulose Acetate Hydrolysis Series

Cotton linters were acetylated with acetic anhydride and sulfuric acid as previously described[9] and after 65 min total reaction time the esterification solution was diluted with aqueous acetic acid containing enough $MgCO_3$ to neutralize half of the sulfuric acid catalyst. Samples of the solution were removed and held at 110°F to hydrolyze the ester for specified times. After the desired hydrolysis time, the solution was poured into distilled water to precipitate the ester.

Preparation of Cellulose Propionate Hydrolysis Series

A cellulose tripropionate prepared from cotton linters was hydrolyzed according to procedures previously described[10] with the use of 0.05M sulfuric acid in aqueous propionic acid. The hydrolysis was started in 90% aqueous propionic acid at 15:1 solvent:ester ratio. After a hydrolysis time of 96 hr, the water content was increased to 15% at 20:1 solvent:ester ratio to minimize the viscosity reduction.[10] Samples of the hydrolysis

solution were removed at intervals and poured into distilled water to precipitate the ester.

Preparation of Homologous Cellulose Triesters

The propionate, butyrate, and propionate–pentanoate triesters were prepared by esterifying cotton linters with the appropriate anhydride using sulfuric acid catalyst according to procedures previously described.[9,11] The pentanoate, hexanoate, and heptanoate triesters were prepared from regenerated cellulose using the appropriate acid chloride in pyridine solvent according to Malm et al.[12]

Preparation of Cellulose Acetates With Progressively Lower Amounts of Primary Hydroxyl

Starting with a sample of cellulose acetate whose hydroxyl was 46% primary, samples of lower primary hydroxyl content were prepared by equilibration[13] and by preferential reesterification.[14]

Fractionation of Cellulose Esters by Gel-Permeation Chromatography

The molecular size distribution of the cellulose esters was obtained on a Model 100 Waters gel-permeation chromatograph. The basic characteristics and operation of the instrument have been described by Maley[5] and Cazes.[6,7] The chromatograph was operated at ambient temperatures by using 1 ml of 0.5% solution of the ester in Eastman White Label tetrahydrofuran injected into columns with upper permeability ranges of 100 000, 8 000, and 3 000 Å.

Molecular size values for the esters were obtained from the GPC fractionation data according to the method described by Cazes.[7] The method was translated into Fortran language for computer calculations. The calculated molecular size values are equivalent to those of the polystyrene standards used to calibrate the instrument.

RESULTS AND DISCUSSION

Table I gives the results of GPC fractionation of the hydrolyzed cellulose acetate viscosity series. All the samples contained approximately 39.5% acetyl (60.5% cellulose). The intrinsic viscosities were corrected by a factor of 50.4/60.5,[15] so that the equation of Tamblyn et al.,[16] DP $= 140[\eta]^{1.20}$, which is based on samples containing 50.4% cellulose, could be used to calculate molecular weight.

For instrument calibration, narrow DP fractions of cellulose esters would be desirable. However, the preparation and characterization of such fractions were beyond the scope of this work. Our instrument was calibrated using polystyrene standards and the results herein are reported as polystyrene equivalent lengths (PSEL).

There is a very good correlation between the polystyrene equivalent lengths (PSEL) at 50% cumulative height of the esters and their intrinsic

TABLE I
Hydrolyzed Cellulose Acetate Viscosity Series[a]

Sample	Intrinsic viscosity			GPC analysis[e]	
	Ester[b]	Regenerated cellulose[c]	Molecular weight[d]	PSEL[f]	$\overline{M}_w/\overline{M}_n$[g]
1	2.19	2.60	75400	4700	2.4
2	2.01	2.38	67600	4000	3.1
3	1.87	2.22	61100	3900, 3500	2.3, 2.8
4	1.79	2.13	58500	3500	2.5
5	1.54	1.70	48900	3000, 2900	2.8, 2.6
6	1.36	1.63	42100	2600	2.8
7	1.05	1.30	30700	1900	2.5
8	0.72	0.89	19800	1200	2.4
9	0.56	0.64	14800	660	2.3

[a] Prepared from cotton linters.

[b] In acetone.

[c] In iron–sodium tartrate (FeTNa); cellulose regenerated from esters with $0.5M$ $NaOCH_3$ in CH_3OH.

[d] Calculated from ester intrinsic viscosity according to the method of Tamblyn et al.[16] with modifications by Genung.[15]

[e] In tetrahydrofuran, 0.5% solution (w/w).

[f] Polystyrene equivalent length (Å) at 50% cumulative height from GPC chromatograms.

[g] Weight-average to number-average molecular size (Å) ratio calculated by computer from GPC fractionation data.

viscosities. This relationship is shown graphically in Figure 1, where a straight line is observed over the intrinsic viscosity range studied.

The weight-average to number-average molecular size ratios ($\overline{M}_w/\overline{M}_n$), a measure of molecular heterogeneity, for the hydrolyzed cellulose acetates
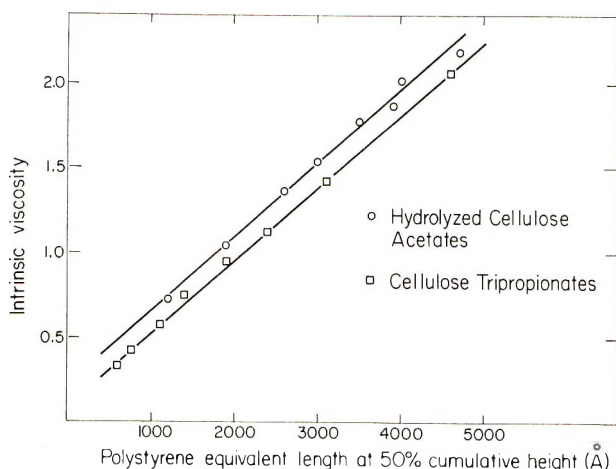
Fig. 1. Relation of average intrinsic viscosity of cellulose esters to their molecular size as determined by GPC.
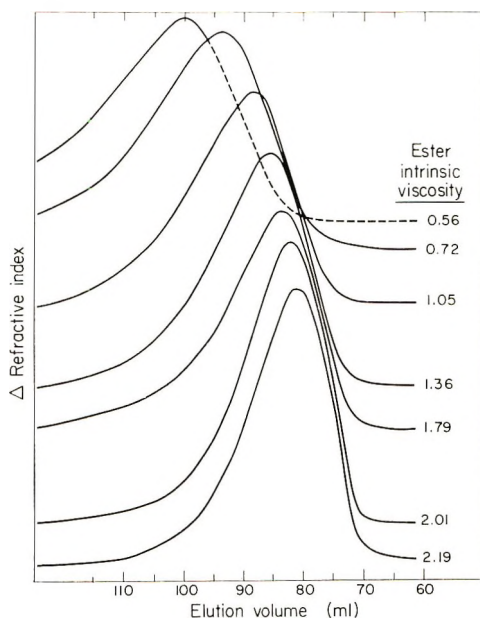
Fig. 2. GPC chromatograms of hydrolyzed lint cellulose acetate viscosity series.
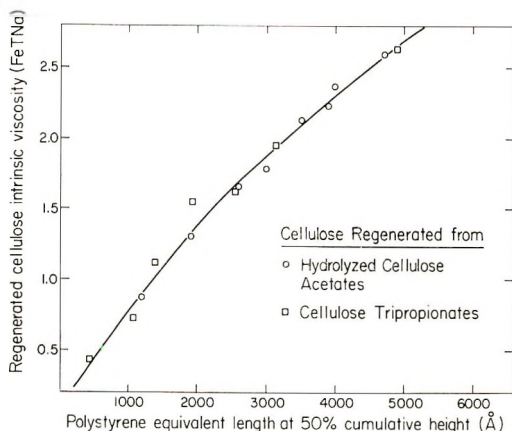
Fig. 3. Relation of cellulose ester molecular size as determined by GPC to regenerated cellulose intrinsic viscosity.

do not vary to any extent with intrinsic viscosity but the elution curves become broader as the ester intrinsic viscosity is reduced (Fig. 2). However, this is not reflected by an increase in the $\overline{M}_w/\overline{M}_n$ ratio. Similar variations in the shape of the distribution curves were observed in the tripropionate viscosity series.

The results for the GPC fractionation of the cellulose tripropionate viscosity series are presented in Table II. Again the ester intrinsic viscosities correlate quite well with the PSEL values. Figure 1 shows the

data as a straight line parallel to the hydrolyzed cellulose acetate data line
but located at slightly higher molecular size values.   This is because the
intrinsic viscosity is based on the weight of cellulose ester and a given
weight of cellulose tripropionate contains less cellulose than the same
weight of hydrolyzed cellulose acetate.   When the PSEL value is plotted
against the regenerated cellulose intrinsic viscosity in iron–sodium tartrate
(FeTNa), both series lie on the same line (Fig. 3).

TABLE II
Tripropionate Viscosity Series[a]

| | Intrinsic viscosity | | | GPC analysis[e] | |
Sample	Ester[b]	Regenerated cellulose[c]	Molecular weight[d]	PSEL[f]	$\bar{M}_w/\bar{M}_n$[g]
1	2.05	2.64	102000	4800, 4900	2.9, 2.2
2	1.41	1.95	69000	3100, 3200	2.7, 2.4
3	1.11	1.62	52800	2400, 2700	2.9, 2.5
4	0.95	1.56	42900	1900	3.0
5	0.75	1.11	29400	1400	2.9
6	0.58	0.73	24100	1100	2.8
7	0.42	0.54	16300	790	2.4
8	0.34	0.44	14500	500	2.4

  [a] Prepared from cotton linters.

  [b] In acetone.

  [c] In iron–sodium tartrate.

  [d] Calculated from ester intrinsic viscosity according to method of Tamblyn, et al.[16]
and Genung.[15]

  [e] In tetrahydrofuran, 0.5% solution (w/w).

  [f] Polystyrene Equivalent Length (Å) at 50% cumulative height from GPC chromato-
grams.

  [g] Weight-average to number-average molecular size (Å) ratio calculated by computer
from GPC fractionation data.

The $\bar{M}_w/\bar{M}_n$ ratios for the tripropionates (Table II) show no variation
over the intrinsic viscosity range studied, again showing that the nature of
the molecular weight distribution remains unchanged when the average
intrinsic viscosity (DP) is altered.

Effect of Average DS on GPC Molecular Size of Cellulose Esters

The effect of variations in the degree of substitution (DS) on the GPC
molecular size of cellulose esters is shown in Tables III and IV for the
cellulose acetates and propionates, respectively.   The PSEL value of the
cellulose acetates remained essentially unchanged as the acetyl content
increased from 38.0 to 42.1% (Table III).   The PSEL of the propionates
increased slightly (2700 to 3000 Å) as the propionyl content increased from
38.7 to 51.5% (Table IV).   The calculated unit molecular weights for
these degrees of substitution are 260 and 328, respectively.   At an intrinsic

viscosity of 1.32, the DP is 196 corresponding to molecular weights of 51 000 and 64 300.

The $\bar{M}_w/\bar{M}_n$ ratios of the esters in both cases were not affected by variation in the degree of substitution.

TABLE III
Cellulose Acetate Hydrolysis Series[a]

Sample	Acetyl, %[b]	Intrinsic viscosity[c]	GPC analysis[d]	
			PSEL[e]	$\bar{M}_w/\bar{M}_n$[f]
1	42.7	1.24	Insoluble in THF	
2	42.1	1.22	2900	2.7
3	41.6	1.26	2500	3.2
4	40.9	1.24	2700	2.6
5	40.5	1.24	2400	2.3
6	40.1	1.23	2700	2.4
7	39.6	1.20	2600	2.4
8	39.3	1.22	2500	3.0
9	38.7	1.22	2300	2.5
10	38.0	1.26	2600	2.3
11	36.1	1.27	Insoluble in THF	

[a] Prepared from cotton linters.

[b] Calculated from per cent hydroxyl as determined by the carbanilation method (17).

[c] In $CH_2Cl_2 : CH_3OH$ (9:1 by weight).

[d] In tetrahydrofuran, 0.5% solution (w/w).

[e] Polystyrene equivalent length (Å) at 50% cumulative height from GPC chromatograms.

[f] Weight-average to number-average molecular size (Å) ratio calculated by computer from GPC fractionation data.

TABLE IV
Cellulose Propionate Hydrolysis Series[a]

Sample	Propionyl, %[b]	Intrinsic viscosity[c]	GPC analysis[d]	
			PSEL[e]	$\bar{M}_w/\bar{M}_n$[f]
1	51.5	1.28	2900	3.1
2	51.1	1.32	2900	2.8
3	49.5	1.30	3100	2.3
4	44.8	1.38	2900	2.3
5	43.7	1.38	2800	2.7
6	42.3	1.39	2800	2.3
7	40.9	1.43	2700	2.7
8	40.3	1.37	2700	2.6
9	38.7	1.40	2700	2.7

[a] Prepared from cotton linters.

[b] Calculated from per cent hydroxyl as determined by the carbanilation method.[17]

[c] In acetone.

[d] In tetrahydrofuran, 0.5% solution (w/w).

[e] Polystyrene equivalent length (Å) at 50% cumulative height from GPC chromatograms.

[f] Weight-average to number-average molecular size (Å) ratio calculated by computer from GPC fractionation data.

Effect of Substituent Size on GPC Molecular Size of Cellulose Esters

Table V shows the effect of varying the size of acyl substituents in cellulose esters on their apparent molecular size. These esters were prepared at the same DP level as evidenced by their regenerated cellulose intrinsic viscosities. The ester intrinsic viscosity decreased with increasing acyl size except for the tripropionate. This tripropionate behavior has been observed previously[12] and probably is due to its solubility characteristics in acetone.

TABLE V
Homologous Cellulose Triester Series

Cellulose triester	Unit molecular weight	Intrinsic viscosity		GPC analysis[c]	
		Ester[a]	Regenerated cellulose[b]	PSEL[d]	$\bar{M}_w/\bar{M}_n$[e]
Propionate	330	1.11	1.62	2400	2.8
Butyrate	372	1.30	1.65	2600	2.8
Isobutyrate	372	1.25	1.67	2700	2.6
Propionate–pentanoate	400	1.20	1.62	2600	2.7
Pentanoate	414	1.14	1.65	3100	2.9
Hexanoate	456	0.96	1.64	3300	2.8
Heptanoate	498	0.81	1.57	3200	2.9

[a] In acetone.

[b] In iron–sodium tartrate.

[c] In tetrahydrofuran, 0.5% solution (w/w).

[d] Polystyrene equivalent length (Å) at 50% cumulative height from GPC chromatograms.

[e] Weight-average to number-average molecular size (Å) ratio calculated by computer from GPC fractionation data.

The PSEL values for the homologous triesters (Table V) increased from 2400 to 3200 Å in going from the tripropionate (unit molecular weight 330) to the triheptanoate (unit molecular weight 498). Based on these unit molecular weights and a constant DP of 158, this represents an increase in molecular weight from 52200 to 79000.

The $\bar{M}_w/\bar{M}_n$ ratio was not affected by variations in the acyl size (Table V).

Effect of Primary Hydroxyl Content on GPC Molecular Size of Cellulose Acetates

Variations in the primary hydroxyl content of cellulose acetates of the same DP level had no effect on their apparent molecular size or molecular size distribution ($\bar{M}_w/\bar{M}_n$) as is shown in Table VI. The samples, whose primary hydroxyl content decreased from 46 to 19%, gave the same PSEL value (3000 Å). Sample 5 (23% primary hydroxyl) gave a lower PSEL value (2200 Å), but this sample had a lower intrinsic viscosity.

TABLE VI
Primary Hydroxyl Series[a]

Sample	Primary hydroxyl, %[b]	Intrinsic viscosity		GPC analysis[e]	
		Ester[c]	Regenerated cellulose[d]	PSEL[f]	$\overline{M}_w/\overline{M}_n$[g]
1	46	1.46	1.68	3100	2.8
2	38	—	—	3000	2.5
3	31	1.44	1.64	3000	2.7
4	30	1.40	1.62	2900	2.4
5	23	1.14	1.34	2200	2.3
6	19	1.55	1.65	3100	2.4

[a] Cellulose acetates prepared from linters.

[b] By the tritylation method;[17] all samples contained $3.90 \pm 0.15\%$ total hydroxyl as determined by the carbanilation method.[17]

[c] In $CH_2Cl_2 : CH_3OH$ (9:1).

[d] In iron–sodium tartrate.

[e] In tetrahydrofuran, 0.5% solution (w/w).

[f] Polystyrene equivalent length (Å) at 50% cumulative height from GPC chromatograms.

[g] Weight-average to number-average molecular size (Å) ratio calculated by computer from GPC fractionation data.

Comparison of Changes in the GPC Molecular Size of Cellulose Esters Caused by Changes in Average DP, DS, and Size of Acyl

Table VII summarizes and compares the effects of varying the composition of cellulose esters on their GPC molecular size.

The solubility of cellulose acetates in tetrahydrofuran limited the range of acetyl which could be investigated by GPC (42.1–38.0% acetyl). Thus the change in molecular weight of the acetates was too small to be detected by a change in PSEL. There is good agreement in the change of PSEL per thousand increase in molecular weight between the propionate hydrolysis series (Table VII, 24 Å increase) and the homologous triesters (Table VII, 30 Å increase). This change in PSEL represents an increase in the *diameter* of the cellulose ester molecules.

For the hydrolyzed cellulose acetate viscosity series and the tripropionate viscosity series, the increases in PSEL per thousand increase in molecular weight (Table VII, 52 and 50 Å, respectively) are in good agreement and represent an increase in the *length* of the cellulose ester molecules.

It is evident from these results that the PSEL of cellulose esters is affected to a much greater degree by changes in average intrinsic viscosity (DP) than by changes in the size and/or amount (DS) of acyl substituent.

GPC Fractionation of a Blend of High and Low Intrinsic Viscosity Cellulose Tripropionates

Figure 4 shows GPC chromatograms of high and low intrinsic viscosity cellulose tripropionates (Table II; samples 1 and 7, 2.05 and 0.42 intrinsic

TABLE VII

Change in GPC Molecular Size of Cellulose Esters Due to Changes in DP and in Size and Amount of Acyl Substituent

| Series | Change in | | | Increase in PSEL, Å, per thousand increase in molecular weight |
	Composition	Molecular weight	PSEL[a]	
Acetate hydrolysis	42.1 to 38.0% acetyl	38,500 to 36,200[b]	Nil[c]	Nil
Propionate hydrolysis	51.5 to 38.7% propionyl	64,300 to 51,000[d]	3000 to 2700	24
Homologous triester	Heptanoate to propionate	79,000 to 52,200[e]	3200 to 2400	30
Acetate viscosity	2.19 to 0.56 intrinsic viscosity	94,500 to 18,500	4700 to 660	52
Propionate viscosity	2.05 to 0.34 intrinsic viscosity	102,000 to 14,500	4850 to 500	50

[a] Polystyrene equivalent length (Å) at 50% cumulative height from GPC chromatograms.

[b] Based on intrinsic viscosity 1.20 of acetate at 39.6% acetyl; calculated by method of Tamblyn et al.[16] and Genung.[15]

[c] Change too small for accurate measurement.

[d] Based on intrinsic viscosity 1.32 of tripropionate; calculated by method of Tamblyn et al.[16] and Genung.[15]

[e] Based on the same intrinsic viscosity of regenerated cellulose throughout the series and on an intrinsic viscosity of 1.11 for cellulose tripropionate, corresponding to a DP of 158.

viscosity, respectively) along with a 50:50 blend of these esters. The curve for the blend is much broader than for either of the components and shows bimodal characteristics. This is reflected in the high $\bar{M}_w/\bar{M}_n$ ratio (4.3) for the blend as compared to the component esters (Table II; $\bar{M}_w/\bar{M}_n$ 2.9 and 2.4 for samples 1 and 7, respectively).
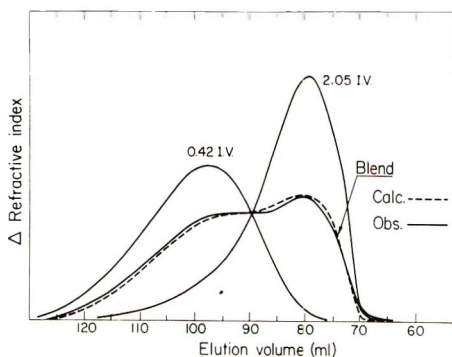

Fig. 4. GPC fractionation of a blend of cellulose tripropionates of high and low intrinsic viscosity.

There is excellent agreement between the observed and calculated GPC chromatograms (Fig. 4) for the blend of cellulose tripropionates. Similar results were obtained on a blend of hydrolyzed cellulose acetates having comparable intrinsic viscosities of 2.19 and 0.56.

References

1. L. Segal, *J. Polym. Sci. B*, **4**, 1011 (1966).

2. L. Segal, paper presented to Division of Carbohydrate Chemistry, 153rd Meeting, American Chemical Society, Miami Beach, Fla., April 1967; *Abstract of Papers*, Paper No. 34.

3. L. Segal, paper presented at Symposium on Analytical Gel-Permeation Chromatography, 154th Meeting, American Chemical Society, Chicago, September 1967; *Abstracts of Papers*, Paper No. 96.

4. G. Meyerhoff and S. Jovanovic, *J. Polym. Sci. B*, **5**, 495 (1967).

5. L. E. Maley, *Analysis and Fractionation of Polymers*, *J. Polym. Sci. C*, **8**, F. W. Billmeyer, Jr., Ed., Interscience, New York, 1965, pp. 253–268.

6. J. Cazes, *J. Chem. Educ.*, **43**, A567 (1966).

7. J. Cazes, *J. Chem. Educ.*, **43**, A625 (1966).

8. R. J. Brewer, L. J. Tanghe, S. Bailey, and J. T. Burr, *J. Polym. Sci. A-1*, **6**, 1697 (1968).

9. C. J. Malm, L. J. Tanghe, and B. C. Laird, *Ind. Eng. Chem.*, **38**, 77 (1946).

10. C. J. Malm, R. E. Glegg, J. T. Salzer, D. F. Ingerick, and L. J. Tanghe, *Ind. Eng. Chem. Process Design Devel.*, **5**, 81 (1966).

11. J. W. Mench, B. Fulkerson, and G. D. Hiatt, *Ind. Eng. Chem. Process Design Devel.*, **5**, 110 (1966).

12. C. J. Malm, J. W. Mench, D. L. Kendall, and G. D. Hiatt, *Ind. Eng. Chem.*, **43**, 684 (1951).

13. C. J. Malm, L. J. Tanghe, B. C. Laird, and G. D. Smith, *J. Amer. Chem. Soc.*, **74**, 4105 (1952).

14. C. J. Malm, L. J. Tanghe, B. C. Laird, and G. D. Smith, *J. Amer. Chem. Soc.*, **75**, 80 (1953).

15. L. B. Genung, *Anal. Chem.*, **36**, 1817 (1964).

16. J. W. Tamblyn, D. R. Morey, and R. H. Wagner, *Ind. Eng. Chem.*, **37**, 573 (1945).

17. C. J. Malm, L. J. Tanghe, B. C. Laird, and G. D. Smith, *Anal. Chem.*, **26**, 188 (1954).

Grafting of Maleic Anhydride on Polyethylene. III. Influence of Polyethylene Concentration on the Course of the Reaction in a Homogeneous Medium

STANISŁAW POREJKO, WŁODZIMIERZ GABARA,
TERESA BŁAŻEJEWICZ, and MARIA ŁECKA, *Department of
the Technology of Polymers, Polytechnic Institute of Warsaw, Warsaw, Poland*

Synopsis

The effect of the polymer concentration on the grafting of maleic anhydride on polyethylene was studied at different temperatures and at different monomer and initiator concentrations. The character of the curves obtained suggests the importance of the termination reactions and the appearance of the gel effect at higher polymer concentrations.

INTRODUCTION

Our previous papers[1-4] dealt with different methods of grafting maleic anhydride on polyethylene. It was found that during grafting, reactions between macroradicals play an important role. Investigations of grafting in a solution[2] showed that polyethylene and maleic anhydride constitute an interesting model system for further study of the phenomena which occur during grafting. If the reaction is carried out in aromatic hydrocarbons, poly(maleic anhydride) precipitates from the solution during the grafting. Under such conditions it would seem that the effect of poly(maleic anhydride) should be negligible. This also suggested that detailed studies of the influence of polyethylene concentration on the course of grafting may give interesting information on the reactions of macroradicals in the solution, especially since some of the results of previous investigations[2] suggested that the gel effect may occur.

Moreover, these problems have, so far, not been extensively investigated and the published results are often contradictory.[5-7]

EXPERIMENTAL

The method of grafting was similar to that already described.[2] Polyethylene and xylene were placed in a three-necked flask equipped with a stirrer, condenser, and thermometer. The temperature in the flask, which was heated in an oil bath, was maintained with an accuracy of ±0.5°C. When the polymer was dissolved and the determined reaction temperature

reached, maleic anhydride and benzoyl peroxide were added. Oxygen was removed from the reaction medium by passing oxygen-free, dry nitrogen through the reaction mixture during the whole time of reaction. After a determined time, the solution was poured into acetone; the precipitated product was centrifuged and washed in acetone until the solution over the precipitate was colorless. [Poly(maleic anhydride) is easily soluble in acetone and gives red solutions.] The product was subsequently dried at 50°C *in vacuo* to constant weight.

The degree of grafting was determined on the basis of change in the polymer weight during reaction. The accuracy of this method for the determination of the percentage of grafting was checked in our previous work.[2]
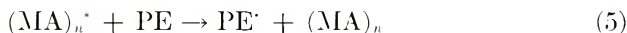
Grafting was carried out on low-density polyethylene (molecular weight 15,600) and on linear polyethylenes of the Rigidex type (British Hydrocarbon Chemicals Ltd.): Rigidex 50, Rigidex 25, and Rigidex X4RR, having intrinsic viscosities in xylene at 105°C of 0.875, 1.107, and 1.195, respectively. Before reaction all polymers were purified by dissolving in xylene and precipitation in acetone.

Maleic anhydride, benzoyl peroxide, xylene, and acetone were chemically pure and were not additionally purified.
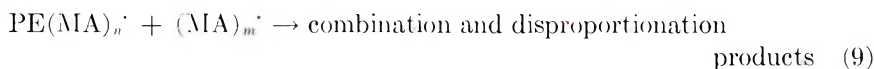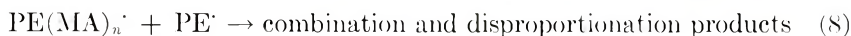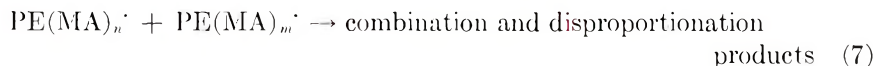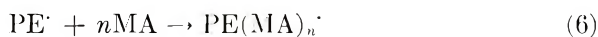
The polyethylene and benzoyl peroxide concentrations are, throughout the article, given in grams per 100 g of the mixture of xylene and maleic anhydride.

RESULTS AND DISCUSSION

Out of the very complex system, the scheme shown in eqs. (1)–(9) presents only some of the reactions taking place. In these equations PE denotes polyethylene; MA, maleic anhydride; BP, benzoyl peroxide. Only those reactions which may bear upon the discussed problems were chosen.

$$BP \rightarrow 2R^{\cdot} \tag{1}$$

$$R^{\cdot} + MA \rightarrow R(MA)^{\cdot} \tag{2}$$

$$R(MA)^{\cdot} + MA \rightarrow R(MA)_2^{\cdot} \tag{3}$$

$$R^{\cdot} + PE \rightarrow PE^{\cdot} + RH \tag{4}$$

$$(MA)_n^{\cdot} + PE \rightarrow PE^{\cdot} + (MA)_n \tag{5}$$

The formation of polyethylene macroradicals might also be due (especially in the case of high-density polyethylene) to the addition of radicals to double bonds.

$$PE^{\cdot} + nMA \rightarrow PE(MA)_n^{\cdot} \tag{6}$$

$$PE(MA)_n^{\cdot} + PE(MA)_m^{\cdot} \rightarrow \text{combination and disproportionation products} \tag{7}$$

$$PE(MA)_n^{\cdot} + PE^{\cdot} \rightarrow \text{combination and disproportionation products} \tag{8}$$

$$PE(MA)_n^{\cdot} + (MA)_m^{\cdot} \rightarrow \text{combination and disproportionation products} \tag{9}$$

Grafting on Low-Density Polyethylene

Influence of Temperature

Figure 1 shows the interdependence of the percentage of grafting and polyethylene concentration at different temperatures.

Unlike the dependencies described in literature, the curves have two maxima. In the following discussion the maximum which appears at a low polyethylene concentration will be termed maximum I, and that at high polyethylene concentration, maximum II.
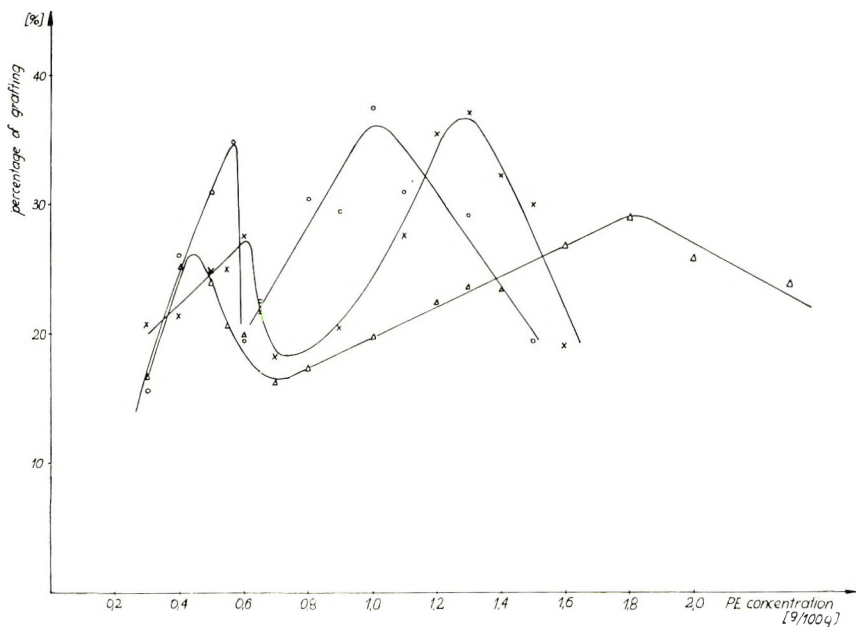

Fig. 1. Percentage of grafting vs. concentration of low-density polyethylene at various temperatures: (×) 90°C, (○) 110°C, (△) 130°C. Benzoyl peroxide concentration, 1.5 g/100 g; maleic anhydride concentration, 10 wt-%; time of reaction, 5 hr.

Maximum I. It seems that maximum I is the result of two opposing tendencies. The generally accepted view that an increase in the polymer concentration increases the probability of reaction between radicals and the polymer [reaction (4)], explains the initial increase of the percentage of grafting. However, the increase in the concentration of macroradicals also increases the rate of termination reactions [reactions (7) and (8)], which is proportional to it in the second power. The end result is a decrease in the percentage of grafting. This important influence of polyethylene concentration is most probably due to the negligible direct role which poly(maleic anhydride) macroradicals play in grafting [reactions (5) and (9)], which in turn may be caused by the insolubility of poly(maleic anhydride) in the reaction mixture. In such a situation mainly poly-

ethylene macroradicals and those of the graft copolymer would take part in the termination reactions.

This hypothesis is confirmed by the direction in which maximum I shifts with changing temperature: at 90°C it appears at polyethylene concentration 0.6 g/100 g; at 110°C, 0.55 g/100 g; and at 130°C, 0.4 g/100 g. The higher the temperature, the higher the rate of transfer reaction, and the higher the concentration of polyethylene macroradicals. If in the investigated system the increase in the viscosity had played a decisive role, as described in the paper cited above, maximum I would have shifted in the opposite direction, since viscosity decreases with the increase of temperature.

The above discussed hypothesis is to a large extent based on the assumption of the negligible role of poly(maleic anhydride) macroradicals. This fact was confirmed by a clear difference between the percentage of grafting in the presence of benzoyl peroxide and azobisisobutyronitrile described in our previous article.[2] Looking for further confirmation of this hypothesis, we compared the results of reactions when the order of adding the reactants was different. For example: when the whole reaction mixture is heated

TABLE I
Influence of the Order of Addition of Reactants[a]

No.	Added at reaction temp	Poly-ethylene, g	Benzoyl peroxide, g	Maleic anhydride, g	Xylene, g	Temp, °C	Graft-ing, %
1	Benzoyl per-oxide and maleic an-hydride	0.0514	1.4984	10.0027	90.1750	110	73.0
2	Benzoyl per-oxide	0.0504	1.4984	10.0001	90.0207	110	64.6
3	—	0.0505	1.5007	9.9985	89.9465	110	24.6
4	—	0.0507	1.4993	10.0027	90.0706	110	18.8

[a] Time of reaction, 5 hr.

from room temperature to reaction temperature (110°C), the part of benzoyl peroxide used up in the homopolymerization [reaction (2)] should be larger. The difference in the activation energy of the transfer and addition reactions is the reason why at lower temperatures poly(maleic anhydride) macroradicals constitute the major part of all macroradicals present in the system. This, in turn, should result in a lower percentage of grafting in comparison to the situation when benzoyl peroxide is added at reaction temperature, as proved by the results in Table I.

The second assumption on which we based our explanation of the appearance of maximum I is the fact that the increase in polyethylene concentration causes an increase in the concentration of polyethylene macroradicals, which in turn is the result of an increase in the rate of the transfer reaction to the polymer [reaction (4)]. Previous studies[3,4] of the

grafting of maleic anhydride on polyethylene in a heterogeneous medium showed an important influence of polyethylene oxidation on the course of grafting. Moreover, when the quantity of oxygen in the reaction medium is small and limited, the percentage of grafting decreases with an increase in the quantity of polyethylene.
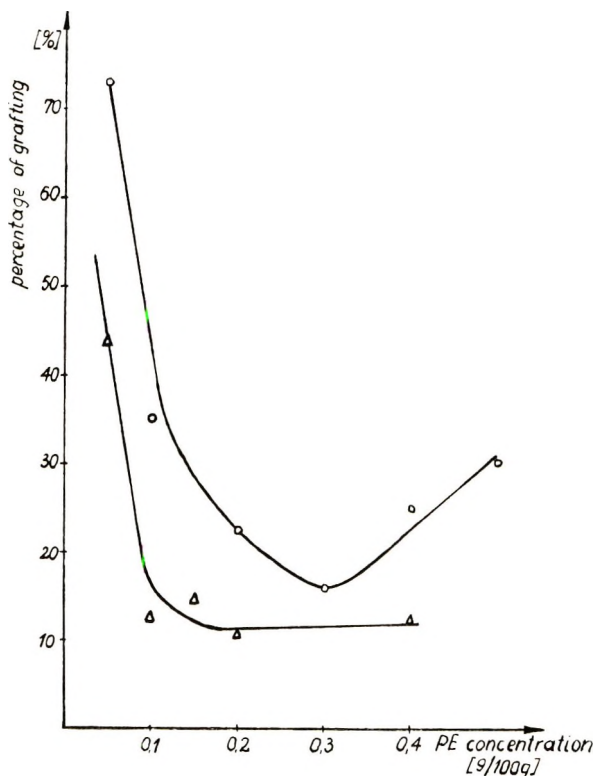

Fig. 2. Percentage of grafting vs. concentration of low-density polyethylene at various maleic anhydride concentrations: (O) 10 wt-%; (△) 5 wt-%. Benzoyl peroxide concentration, 1.5 g/100 g; temperature, 110°C; time of reaction, 5 hr.

Figure 2 shows the effect of polyethylene concentration on the percentage of grafting in the range of very low polymer concentrations. The character of the curves is similar to that for heterogeneous grafting.[3,4] Since oxygen was removed from the reaction medium only by passing oxygen-free nitrogen through it, part of the dissolved oxygen may still be present, and the situation is similar to that described for heterogeneous grafting. To establish the influence of oxygen, the solution was degassed under vacuum before the reaction. All reactants were divided into two parts, and each of them was degassed in room temperature. The first one consisted of xylene and polyethylene, and the second one of xylene, benzoyl peroxide, and maleic anhydride. The first part was heated to 130°C, then the second part was quickly added. The temperature went down to 110°C and was

TABLE II
Influence of Oxygen on the Percentage of Grafting[a]

No.	Reaction mixture	Poly-ethylene, g	Benzoyl peroxide, g	Maleic anhydride, g	Xylene, g	Temp, °C	Graft-ing, %
1	Degassed	0.0500	1.5007	10.0010	90.0010	110	15.4
2	Not degassed	0.0514	1.4984	10.0027	90.1750	110	73.0
3	Degassed	0.4005	1.4995	10.0010	90.1050	110	27.0
4	Not degassed	0.4001	1.5000	10.0002	90.1192	110	25.6

[a] Time of reaction, 5 hr.

subsequently stabilized at this level. During the whole time of reaction, oxygen-free nitrogen was passed through the solution.

The results in Table II show that the role of oxygen at very low polyethylene concentrations is important. At higher polymer concentrations no such influence was observed. Since oxygen takes part in the reaction in both cases, these results indicate that, at a higher polymer concentration, the quantity of polyethylene macroradicals formed in effect of oxidation is negligible in comparison to that of the macroradicals formed as the result of the transfer reaction. This proves that the higher the polyethylene concentration, the greater the probability of a transfer reaction to the polymer.

Maximum II. The above discussion showed that the decrease of the percentage of grafting beyond maximum I is due to the important role of termination reactions. Figure 1 shows that further increase in polyethylene concentration causes an increase in the percentage of grafting. This is most probably related to the appearance of the gel effect. The increase in the viscosity of the reaction mixture results in a decrease of the termination reaction constant and, in effect, in the increase of the rate of grafting. A complete and definitive explanation of the decrease of the percentage of grafting beyond maximum II is made very difficult by the complexity of the system. Most probably this too is related to increasing viscosity. The increase in viscosity may, for example, result in: (1) a decrease of the constant of propagation reaction [reaction (6)], (2) a decrease of the initiation effectiveness,[8] (3) a decrease of the constant of the transfer reaction to the polymer [reaction (4)].

This raises a new problem—the nature of chief element determining the position of maximum II. Is it the primary viscosity (related to the polymer concentration) or the changes in viscosity during grafting? If primary viscosity plays a decisive role, then, with the increase of temperature maximum II should shift in the direction of higher polymer concentrations. This hypothesis would not justify the position of maximum II for 110°C (maximum II appears at polyethylene concentration of 1.30 g/100 g at 90°C, 1.05 g/100 g at 110°C, and 1.80 g/100 g at 130°C). These results suggest that the occurrence of the gel effect is connected also with viscosity changes during reaction.

Influence of Monomer Concentration

Results presented in Figure 3 show that the occurrence of two maxima is the effect of special reaction conditions. For maleic anhydride concentration of 20 wt-%, the curve has only one maximum, while for a concentration of 5 wt-%, the percentage of grafting practically does not change with the increase in polyethylene concentration. The maximum for the monomer concentration of 20 wt-% is high and broad (when compared with the curve for 10 wt-%) which suggests that it is maximum II rather than maximum I. The increase in maleic anhydride concentration creates more favorable conditions for homopolymerization (at the same polymer concentration, the ratio monomer/polymer increases) and the concentration of polyethylene macroradicals should decrease. Thus, maximum I shifts in the direction of higher polymer concentrations. At the same time, a higher percentage of grafting increases the viscosity of the solution and maximum II shifts in the direction of lower polymer concentrations. As a result, both maxima coincide.
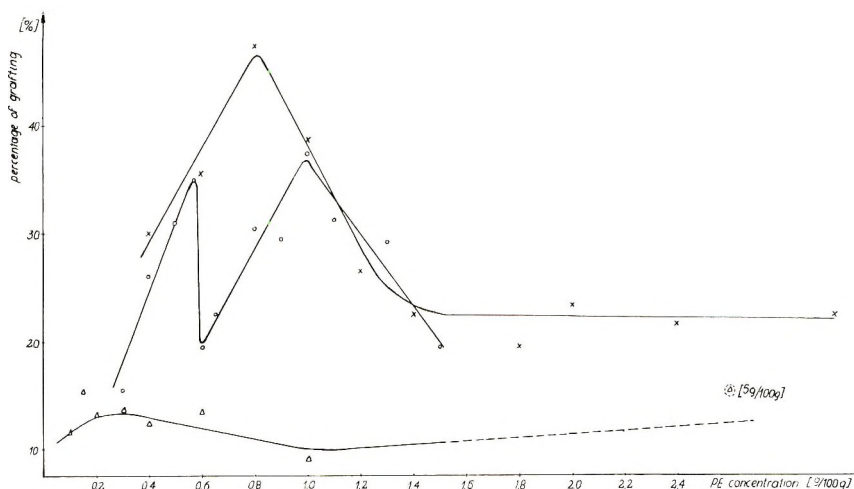

Fig. 3. Percentage of grafting vs. concentration of low-density polyethylene at various maleic anhydride concentrations: ($\triangle$) 5 wt-%; ($\bigcirc$) 10 wt-%; ($\times$) 20 wt-%. Benzoyl peroxide concentration, 1.5 g/100 g; temperature, 110°C; time of reaction, 5 hr.

At the monomer concentration of 5 wt-%, the percentage of grafting is relatively low, and the observed changes are of the same magnitude as the accuracy of the method of percentage of grafting determination. Maximum I is very small, but its position in comparison with that for 10 wt-% further supports the proposed hypothesis. The almost straight line beyond maximum I suggests that the main role in the appearance of maximum II should be attributed to viscosity changes during the reaction. But the fact that the percentage of grafting does not diminish suggests that the gel effect occurs in this case also.

Grafting on Linear Polyethylene

To find whether analogous effects occur in the case of linear polyethylene, the influence of polymer concentration on the percentage of grafting was studied on three types of polyethylene: Rigidex 50, Rigidex 25 and Rigidex X4RR. The results are presented in Figure 4. The curves, similar to those for low-density polyethylene, have two maxima.

For all types of polyethylene maximum I appears at practically the same polymer concentration (0.50–0.55 g/100 g). The only difference is in the percentage of grafting. For the polymer with the lowest molecular weight (Rigidex 50), the percentage of grafting at maximum I is about 60%, for
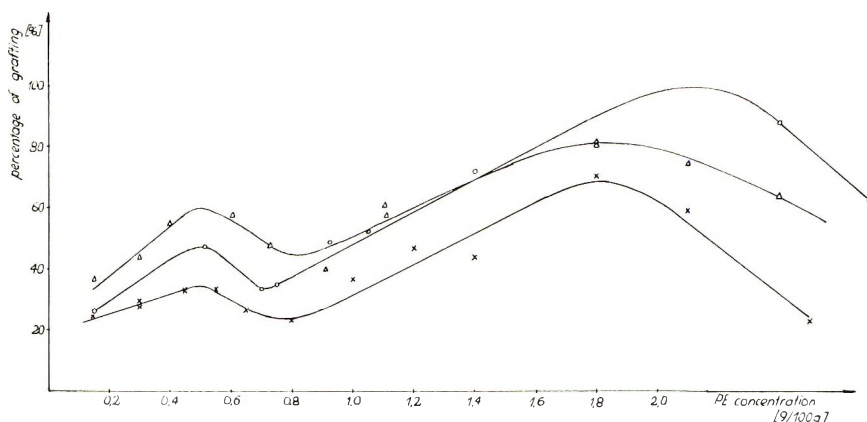

Fig. 4. Percentage of grafting vs. concentration of linear polyethylene at various molecular weights: (×) Rigidex X4RR (intrinsic viscosity, 1.195); (○) Rigidex 25 (intrinsic viscosity, 1.107); (△) Rigidex 50 (intrinsic viscosity, 0.875). Benzoyl peroxide concentration, 1.5 g/100 g; temperature, 110°C; maleic anhydride concentration, 10 wt-%; time of reaction, 5 hr.

Rigidex 25 (medium molecular weight) it is about 47%, and for that with the highest molecular weight (Rigidex X4RR), about 33%. This is, most probably, the result of the important role played by the unsaturated bonds, already observed during grafting on poly(methyl methacrylate).[10,11] The infrared spectra of those three polyethylenes showed that intensities of bands of unsaturated bonds at 912 cm^{-1} (—CH=CH$_2$), 992 cm^{-1} (—CH=CH$_2$), and 1642 cm^{-1} (C=C) are highest for Rigidex 50 and lowest for Rigidex X4RR.

If primary viscosity were the decisive factor in the occurrence of the gel effect, then, with the increase of molecular weight, maximum II would shift in the direction of lower polyethylene concentrations. The positions of maximum II for Rigidex X4RR (1.8 g/100 g) and Rigidex 25 (2.1 g/100 g) fit this hypothesis. The appearance of maximum II for Rigidex 50 at a relatively low polymer concentration (1.8 g/100 g) indicates that the decrease of the percentage of grafting beyond maximum II is caused not

only by primary viscosity. Moreover, the fact that the percentages of grafting for Rigidex 25 and Rigidex 50 in the rising part of the curve are close suggests that the changes of viscosity during the reaction are influenced not only by the percentage of grafting but also by the structure of the copolymer. The same percentage of grafting can be reached when a small number of long side chains, or a greater number of shorter ones, is grafted onto the polymer.

The regulation of the reaction rate is achieved most readily by controlling initiator concentration. The curves for different initiator concentrations are presented in Figure 5. The higher the initiator concentration, the higher the concentration of polyethylene macroradicals. Thus, with the
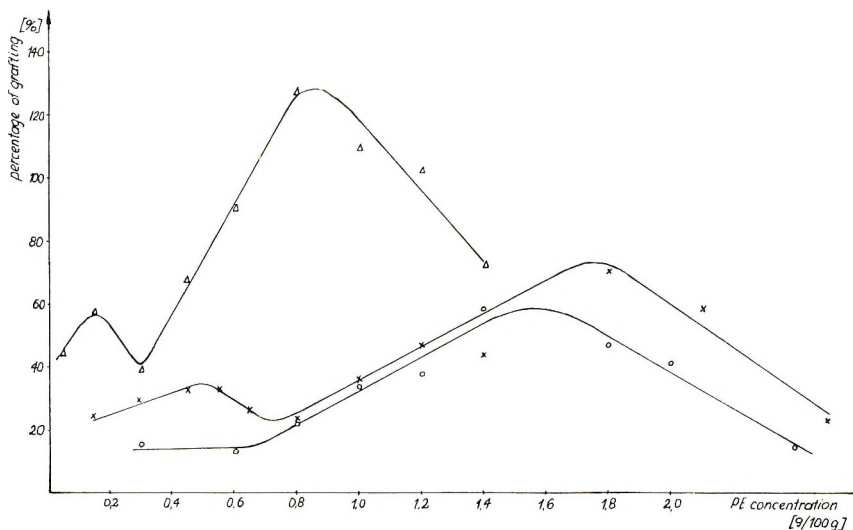
Fig. 5. Percentage of grafting vs. concentration of linear polyethylene (Rigidex X4RR) at various benzoyl peroxide concentrations: (○) 0.5 g/100 g; (×) 1.5 g/100 g; (△) 3.0 g/100 g. Temperature, 110°C; maleic anhydride concentration, 10 wt-%; time of reaction, 5 hr.

increase of benzoyl peroxide concentration, maximum I shifts in the direction of lower polymer concentrations. For a benzoyl peroxide concentration of 3.0 g/100 g, maximum I appears at polymer concentration of about 0.2 g/100 g, and for 1.5 g/100 g at 0.55 g/100 g. For the initiator concentration of 0.5 g/100 g maximum I does not appear at all. This is most probably related to the fact that the concentration of polyethylene macroradicals reaches the appropriate level (at which, as a result of termination reactions, the percentage of grafting diminishes) at higher polymer concentrations at which the gel effect plays already an important role.

The shifting of maximum II in the direction of lower polyethylene concentrations with the increase of initiator concentration supports the hypothesis that not only primary viscosity but also the viscosity changes during reaction influence the gel effect.

CONCLUSIONS

The curves of dependence between the percentage of grafting and polymer concentration, both in the case of low-density and high-density polyethylene, have two maxima.

Maximum I is the result of the important role of termination reactions between the macroradicals of polyethylene and those of the graft copolymer. Maximum II is, most probably, connected with the occurrence of the gel effect.

The course of the interdependence of the percentage of grafting and polyethylene concentration for different temperatures, molecular weights, and initiator concentrations shows that the occurrence of the gel effect (maximum II and its shiftings) is influenced not only by primary viscosity but also by viscosity changes during reaction.

References

1. W. Gabara and S. Porejko, *J. Polym. Sci. A-1*, **5**, 1547 (1967).

2. S. Porejko, W. Gabara, and J. Kulesza, *J. Polym. Sci. A-1*, **5**, 1563 (1967).

3. W. Gabara and S. Porejko, *J. Polym. Sci. A-1*, **5**, 1539 (1967).

4. W. Gabara and S. Porejko, *Polimery*, **12**, 151, 196 (1967).

5. V. A. Kuznetsova, U. G. Krazev, Z. A. Rogovin, and T. N. Troptseva, *Zh. Prikl. Khim.*, **37**, 1334 (1964).

6. J. Potts, E. Bonner, R. Turbett, and F. Rugg, paper presented at American Chemical Society Meeting-in-Miniature, January (1957).

7. V. Lazar and J. Pavlinec, *J. Polym. Sci. A*, **2**, 3197 (1964).

8. G. V. Schulz and G. Harborth, *Makromol. Chem.*, **1**, 106 (1947).

9. S. S. Ivantchev, L. V. Skubilina, and J. T. Denisov, *Vysokomol. Soedin.*, **B9**, 706 (1967).

10. G. V. Schulz, G. Henrici-Olivé, and S. Olivé, *J. Polym. Sci.*, **17**, 45 (1955).

11. G. Henrici-Olivé, S. Olivé, and G. V. Schulz, *Makromol. Chem.*, **23**, 207 (1957).

Radiation-Induced Solid-State Polymerization of Derivatives of Methacrylic Acid. II. Postirradiation Polymerization of Octadecyl Methacrylate

M. J. BOWDEN and J. H. O'DONNELL, *Chemistry Department, University of Queensland, Brisbane, Australia*

Synopsis

Octadecyl methacrylate (mpc $\approx 12°C.$) polymerized readily in the solid state in the temperature range -30 to $+12°C.$ after gamma irradiation at $-196°C$. The initial rate of polymerization and the "limiting" conversion increased with radiation dose and temperature. The temperature dependence of the rate corresponded to an "apparent" activation energy of 20 kcal./mole. Difficulties were experienced with polymerization during separation of the polymer from residual monomer, but these were minimized by using low radiation doses and a hot, selective solvent. The maximum conversion achieved was 70%. The polymer was crosslinked, even at low conversions.

INTRODUCTION

This work is part of an investigation of the effect of the size and shape of the ester group on the polymerizability of acrylate and methacrylate esters in the solid state. Apparently the hydrocarbon chains decrease the rigidity of the lattice and increase the polymerizability. Hydrocarbon chains would be expected also to crystallize in a parallel arrangement, which would align the double bonds in layers, and this should favor polymerization. The radiation-induced polymerization of vinyl stearate in the orthorhombic form apparently is due to this effect, and the retention of paraffin crystallinity is strong evidence of topochemical influence.[1] It has been demonstrated that although methyl methacrylate does not polymerize[2] in the crystalline solid, or does so only with difficulty,[3,4] it polymerizes in a mixture with paraffin oil, but not pure octadecane.[2]

The polymerization of octadecyl methacrylate (ODMA) in the solid state has been reported by Fee and his co-workers.[5] They achieved 79% yield of polymer after 1 Mrad of gamma irradiation at $-10°C$. and measured K and a values for the Mark-Houwink relationship between viscosity and molecular weight. They did not investigate the solid-state polymerization in detail, and their separation procedure, which was to melt the irradiated sample, is unsatisfactory. Hardy and his co-workers[6,7] have investigated the radiation-induced solid-state polymerization of cetyl methacrylate and reported that the polymerization rate in the solid

increased as the temperature decreased down to $-196°C$. but did not give any kinetic curves. Our electron spin resonance studies of methacrylate systems have shown that relatively small quantities of the methacrylate propagating radical are present at $-196°C$. and that the reaction of the initial radical species occurs in the region of $-100°C$. Therefore a careful investigation of the solid-state polymerization of octadecyl methacrylate was undertaken.

EXPERIMENTAL

Octadecyl methacrylate (Borden Chemical Co., pure grade) was purified from inhibitor by shaking three times with an equal volume of 10% w/v aqueous NaOH, followed by three washes with distilled water. It was then dried over anhydrous magnesium sulfate and calcium hydride, filtered,

TABLE I
Postirradiation Polymerization of Octadecyl Methacrylate

Dose, Mrad	Time, hr.	Temp., °C.	Polymer yield, %
0.1	168	-80	0.0
0.1	168	-37	2.5
0.1	168	-28	9.3
0.1	4	-20	8.5
0.1	2	-10	18.5
0.1	1	0	30.7
0.2	1	0	45.3
1.0	1	0	56.3
0.1	1	10	56.9

and stored at $0°C$. The monomer had a refractive index of 1.4406 at $50°C$. and melting point of approximately $12°C$. The melting point is rather indefinite, apparently due to the existence of at least one, and probably two, liquid crystal phases. The absolute purity of the octadecyl methacrylate (ODMA) is difficult to assess. The melting point suggests that there are some impurities, but differential thermal analysis did not show any large abnormalities. Further purification was not undertaken, because of the difficulties involved and the quantities required. Similar problems have been experienced in purification of octadecanol for synthesis.

Samples of monomer (4 g.) were degassed in glass tubes by alternate freezing at $-78°C$. and melting and then were sealed under vacuum (10^{-5} mm. Hg). They were shock-frozen from the melt by immersion in liquid nitrogen and stored at this temperature.

Irradiations were carried out at $-196°C$. with ^{60}Co gamma-rays, and the irradiated samples were stored at $-196°C$. Kinetic runs were carried out by placing the samples in a thermostatted bath (-20 to $10°C$.), removing them after successive time intervals, and freezing immediately in liquid nitrogen, to prevent further polymerization. Slush baths of

diethyl sulfate and anisole were used for obtaining temperatures of -28 and $-37°C$., respectively.

Determinations of the yield of polymer were made by selectively dissolving the residual monomer. This was done by transferring the sample to a large volume of hot solvent containing a small quantity of hydroquinone, to inhibit polymerization in solution. The procedure for separating polymer from monomer was investigated thoroughly, because difficulty was experienced with polymerization during the solution or melting stage, and the best results were obtained by crushing the sample and stirring it vigorously into isopropanol at 75°C.

RESULTS AND DISCUSSION

Polymerization during Separation

Serious difficulties were experienced with polymerization during separation of the polymer from residual monomer. Any solution process involves a phase change similar to melting, and there is ample evidence that high polymerization rates and even explosive polymerization can occur during melting,[8-10] sometimes even without previous irradiation.[11-13] Therefore the possibility of polymerization during dissolution is to be generally expected, although it is normally neglected.

At first high yields (up to 75%) were obtained from irradiated ODMA on separating immediately after warming from $-196°C$. Therefore, polymerization was actually occurring during irradiation at $-196°C$., or during warming at a solid-solid phase change, or during warming because of the time taken in warming, or during the solution process.

A number of techniques were used for investigating this problem.

First, the temperature of the solvent was increased, so as to increase the solution rate. This caused a marked decrease in polymer yield: from 75 to 10%, as the solvent temperature was raised from 20 to 120°C.

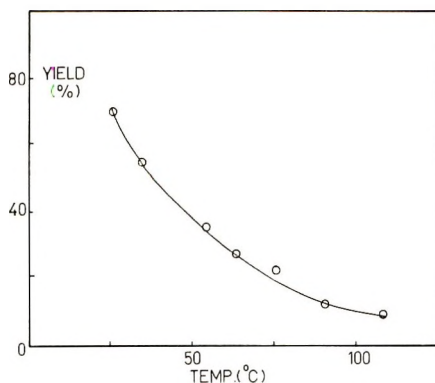Fig. 1. Effect of temperature of solvent used for separating polymer and monomer on the zero-time polymer yield after 1 Mrad of gamma irradiation at $-196°C$.

(Fig. 1). Difficulties arise in that (1) the solvent boiling point may be exceeded (therefore methanol, isopropanol, and n-butanol were used progressively), (2) the solubility of the polymer, particularly one of low molecular weight, may increase, and (3) high temperatures may increase the rate of polymerization at the interface between the solid and the solvent. Second, the particle size of the sample was reduced so as to increase the rate of solution and to decrease the time at which the solid monomer was near the melting point. The samples of monomer were originally solidified by shock-freezing in liquid nitrogen and, consequently, were in one piece. Fragmentation was achieved best by breaking open the glass tubes, transferring the cylindrical plug of sample to a stainless-steel cup containing liquid nitrogen, and then using a stainless-steel hammer, which fitted closely into the cup. Initiation of polymerization in irradiated formaldehyde at −196°C. by mechanical shock has been reported[14] but did not occur in ODMA. Third, the total radiation dose was reduced. This decreased the polymer yield under all separation conditions.

Careful attention to these three factors resulted in zero yields of polymer at zero time, i.e., from samples dissolved immediately on removal from storage at −196°C.

Therefore we consider that no polymerization occurs at −196°C. during or after irradiation. Furthermore, we suggest that polymerization apparently occurring at such low temperatures, and which is determined by solution separation, should be viewed with caution. Measurements that are made by melting the irradiated monomer are especially prone to error. For instance, we have found that methyl methacrylate irradiated to 1 Mrad with gamma-rays, will partly polymerize on melting, the polymer yield depending on the rapidity of melting. Although we have shown that polymerization does not occur at −196°C. in ODMA, there are reports of polymerization in other monomers at this temperature, e.g., acrylonitrile,[15,16] and even at 4.2°K.[17]

Elimination of the zero-time polymer yield does not ensure that the measured polymer yields after various polymerization times are correct. The rate of solution of residual monomer definitely depends on the proportion of insoluble polymer in the sample; consequently, the yields may be progressively inflated at higher conversions. This problem is minimized by rapid solution but cannot be checked.

Effect of Dose

The yields of polymer after various intervals at 0°C. after radiation doses of 0.05 to 1.0 Mrad are shown in Figure 2. The general shape of the conversion curves are typical of postirradiation polymerization, i.e., a rapid initial rate which decreases to very low rate, approximating to a "limiting" conversion. There is no induction period, and the initial rates are very high. Both the initial rates and the "limiting" conversions increase with dose.
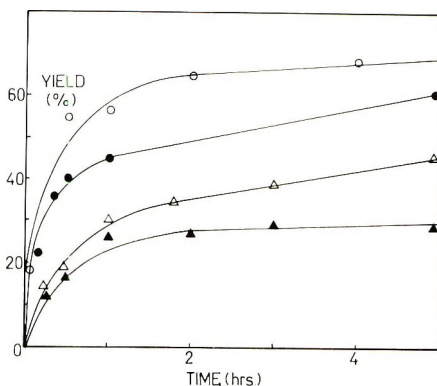
Fig. 2. Effect of radiation dose on polymerization of ODMA at 0°C. Dose (Mrad): (○) 1; (●) 0.2; (△) 0.1; (▲) 0.05.

Effect of Temperature

Conversion curves for polymerization at different temperatures after 0.1 Mrad of gamma irradiation are shown in Figure 3. There is a marked increase in both initial rate and "limiting" conversion with increase in temperature in the range −20 to 10°C. The initial rates give a linear Arrhenius plot (Fig. 4), from which an apparent activation energy of 20 kcal./mole may be derived. This differs markedly from the value of −0.7 kcal./mole reported for cetyl methacrylate,[6] although one would expect these monomers to show similar polymerizability.

The Arrhenius plot suggests that the rate of polymerization should be negligible below about −35°C., and it was found that a sample kept at −37°C. for 7 days yielded only 2% polymer.

The reason for the existence of a "limiting" conversion is unknown. It is a function of both radiation dose and temperature and is well below complete conversion. Most probably it is associated with a process of
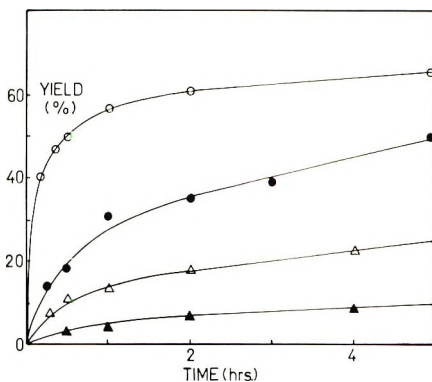

Fig. 3. Effect of temperature on polymerization of ODMA after 0.1 Mrad of gamma irradiation at −196°C. Temperature (°C.): (○) 10; (●) 0; (△) −10; (▲) −20.
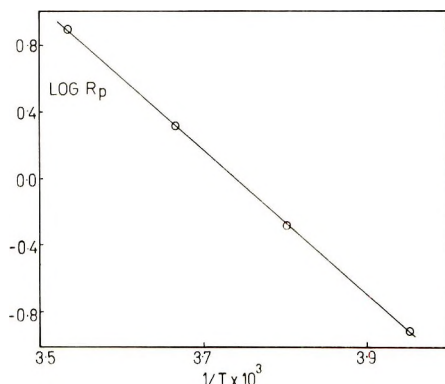
Fig. 4. Arrhenius plot of initial polymerization rates (R_p) for ODMA after 0.1 Mrad of gamma irradiation at $-196°C$.

physical trapping of the growing chains, which is supported by observations that the total concentration of free radicals is constant in some monomers during postirradiation polymerization.[11]   The way in which the radicals are trapped is still open to speculation.   It is possible that propagation occurs within the crystallites and stops at intercrystalline boundaries, requiring an activation energy to cross them.   Adler has obtained micrographs of polymer chains bridging intercrystalline boundaries in trioxane.[18] There is also evidence that polymerization proceeds at the boundary between an amorphous polymer phase and a crystalline monomer phase.[19]

Effect of Oxygen

When the samples were sealed under air instead of in vacuum, the polymerization rate was decreased, as shown in Figure 5.   This suggests that the polymerization occurs by a free-radical mechanism, of which oxygen is a well-known inhibitor in the liquid phase.   The wax-like structure of
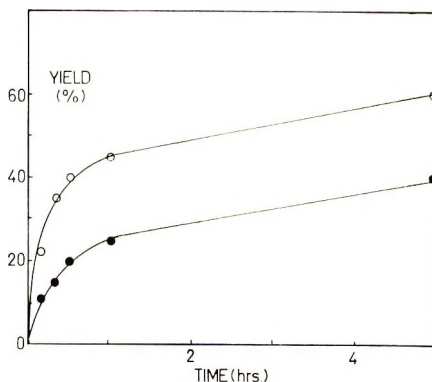

Fig. 5. Effect of oxygen on polymerization of ODMA at 0°C. after 0.2 Mrad of gamma irradiation at $-196°C$.: (O) sample in vacuum; (●) sample in atmosphere of air.

ODMA would be expected to retain oxygen during solidification and to be reasonably permeable to gaseous diffusion.

CONCLUSIONS

The rapid polymerization of ODMA in the solid state from about $-30°C$. to the melting point indicates that the monomer molecules or the growing chains have considerable mobility in the solid in this temperature range or that local melting of monomer occurs around the growing ends of the chains, resulting in pseudoliquid polymerization, or that the spatial arrangement of the double bonds in the lattice is favorable for polymerization.

Diffusion of ODMA molecules in the solid would not be expected to be significant. Meakins[20] suggests that only rotation about the long axis of the hydrocarbon chain occurs below the melting point in similar compounds, such as alcohols and acids, according to dielectric-loss measurements. Although the role of defects is unknown, they must increase molecular motion. It is difficult to exclude the second possibility cited above, but if this is the mechanism, then the rate of polymerization would be expected to fall off more rapidly at lower dose rates and to proceed during irradiation at low temperatures. Solid–solid phase transitions in paraffin-type solids are well known, and the existence of a transition in ODMA at $-30°C$. has been shown. Similarly, a phase change in cetyl methacrylate has been observed at $-16°C$.[6] Therefore it seems likely that above $-30°C$. the spatial arrangement of the monomer molecules places the double bonds in a suitable relationship for polymerization. Further, the mobility now available, even if it is restricted to segmental rotation, enables the reaction to proceed.

The separated polymer was insoluble, apparently because of crosslinking and suggesting either that some of the initiating radicals were produced on the hydrocarbon chain or that chain transfer to monomer occurred readily.

References

1. N. Morosoff, H. Morawetz, and B. Post, *J. Am. Chem. Soc.*, **87**, 3035 (1965).

2. R. Bensasson, M. Durup, A. Dworkin, M. Magat, R. Marx, and H. Szwarc, *Discussions Faraday Soc.*, **36**, 177 (1963).

3. I. M. Barkalov, V. I. Goldanskii, N. S. Enikolopyan, S. F. Terekhova, and G. M. Trofimova, in *Macromolecular Chemistry, Paris* **1963** (*J. Polym. Sci. C*, **4**), M. Magat, Ed., Interscience, New York, 1964, p. 909.

4. N. T. Lipscomb and E. C. Weber, *J. Polym. Sci. A-1*, **5**, 779 (1967).

5. J. G. Fee, W. S. Port, and L. P. Witnauer, *J. Polym. Sci.*, **33**, 95 (1958).

6. G. Y. Hardy, K. Nyitrai, J. Varga, G. Kovacs, and N. Fedorova, in *Macromolecular Chemistry, Paris*, **1963** (*J. Polym. Sci. C*, **4**), M. Magat, Ed., Interscience, New York, 1964, p. 923.

7. G. Hardy, K. Nyitrai, G. Kovacs, N. Fedorova, and J. Varga, Radiation Chemistry Symposium, Tihany, 1962, J. Dabo, Ed., Hungarian Acad. Sci., Budapest, 1964.

8. M. Letort and A. J. Richard, *J. Chim. Phys.*, **57**, 752 (1960).

9. C. Chachaty, M. Magat, and L. Ter Minassian, *J. Polym. Sci.*, **48**, 139 (1960).

10. R. B. Mesrobian, P. Ander, D. S. Ballantine, and C. J. Dienes, *J. Chem. Phys.*, **22**, 565 (1954).

11. T. A. Fadner and H. Morawetz, *J. Polym. Sci.*, **45**, 475 (1960).

12. Rohm and Haas Bulletin, *Glacial Methacrylic Acid-Glacial Acrylic Acid* (1960).

13. A. V. Samarina, V. I. Arulik, and L. I. Efimov, *Vysokomolekul. Soedin*, **8**, 1660 (1966).

14. Y. Tsuda, *J. Polymer Sci.*, **49**, 369 (1961).

15. I. M. Barkalov, V. I. Goldanskii, N. J. Enikolopyan, S. F. Terekhova, and G. M. Trofimova, in *Macromolecular Chemistry, Paris*, **1963** (*J. Polym. Sci. C*, **4**), M. Magat, Ed., Interscience, 1964, p. 897.

16. H. Sobue and Y. Tabata, *J. Polym. Sci.*, **43**, 459 (1960).

17. I. M. Barkalov, D. A. Gareeva, V. I. Goldanskii, N. S. Enikolopyan, and A. A. Berlin, *Vysokomolekul. Soedin*, **8**, 1140 (1966).

18. G. Adler, *J. Polym. Sci. A-1*, **4**, 2883 (1966).

19. G. Adler and W. Reams, *J. Chem. Phys.*, **32**, 1698 (1960).

20. R. J. Meakins, in *Progress in Dielectrics*, Vol. 3, J. B. Birks and J. Hart, Eds., Wiley, New York, 1961, p. 151.

Radiation-Induced Solid-State Polymerization of Derivatives of Methacrylic Acid. III. An Electron Spin Resonance Study of Radical Reactions in Irradiated Octadecyl Methacrylate

M. J. BOWDEN and J. H. O'DONNELL, *Chemistry Department, University of Queensland, Brisbane, Australia*

Synopsis

The electron spin resonance spectrum of gamma-irradiated octadecyl methacrylate (m.p. ≈ 12°C.) was due to a mixture of three radicals formed by (*1*) loss of a hydrogen atom from the paraffin chain, (*2*) addition of a hydrogen atom to the double bond, and (*3*) addition of a monomer molecule to radicals formed by (*1*) or (*2*). On warming monomer added to radicals (*1*) and (*2*) between −170 and −50°C., and above −50°C. the spectrum was solely due to propagating methacrylate radicals. The total radical concentration decreased slightly at −150°C. and was then constant up to −30°C. A marked decrease in radical concentration occurred from −30 to +12°C., it took place rapidly and reached an equilibrium value after each successive increase in temperature. Differential thermal analysis indicated a solid–solid phase change at −30°C. When the sample was kept at 0°C. there was no further decrease in radical concentration even with 50% conversion to polymer. With 2% added chloranil the (chloranil)⁻ was observed to be of about the same concentration as methacrylate radicals. The initial total radical concentration was lower and decreased to zero by 0°C. on warming. No polymer was obtained.

INTRODUCTION

A major difficulty in studying chemical reactions in the solid state is the lack of nondestructive methods of observing the reactions in situ. Further, the techniques used for the liquid phase are usually unsatisfactory. Additives either are expelled into isolated pockets during solidification or disrupt the crystalline lattice, altering the physical properties of the system. Consequently, ideas about the mechanism of a reaction are usually derived by analogy with the liquid phase. Electron spin resonance (ESR) should be a powerful tool for observing reactions of radicals with molecules in the solid state, but so far most studies have been confined to observing stationary concentrations of radicals or the disappearance of radicals.[1–3]

The polymerization of methacrylate esters in the liquid phase, which can be initiated by free-radical[4] or anionic species,[5] has been extensively studied. High-energy irradiation can produce cationic, free-radical and

anionic centers in organic solids,[6] and all three of these species are believed
to initiate polymerization in suitable monomers. However, it seems most
probable that irradiated methacrylates polymerize by a free-radical
mechanism in the solid state. Bamford et al.[7] have observed that crystals
of methacrylic acid polymerize inward from the surface during and after
illumination with ultraviolet light, which must almost certainly produce a
free-radical reaction. O'Donnell et al.[8] found the ESR spectrum of the
propagating methacrylate radical in partly polymerized barium methacry-
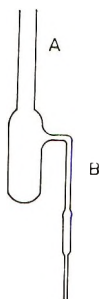late dihydrate.

Fig. 1. Arrangement for obtaining sample of degassed ODMA in ESR tube.

The present investigation was undertaken to show that the propagating
methacrylate radical was present in octadecyl methacrylate (ODMA)
during solid-state postirradiation polymerization; such would support the
postulate of a free-radical mechanism. It was also hoped that a trans-
formation from initial radicals to propagating radicals at about $-30°C.$,
where polymerization commences on warming, would be observed. Fur-
ther, it was planned that the relative radical concentrations at different
stages in warm-up and polymerization be measured.

EXPERIMENTAL

Samples of ODMA (Borden Chemical Co. pure grade), purified free of
inhibitor and water, were degassed by freeze-thaw cycles in a Pyrex glass
tube connected to the ESR sample tube and a vacuum line at 10^{-5} mm. Hg
(Fig. 1). After thorough degassing, which required about six cycles with
such a viscous monomer, the two-tube system was sealed at A in Fig. 1.
The ODMA was melted and a suitable amount (0.2 ml.) transferred to
the ESR tube by tilting the combination. The ESR tube was then
sealed at B. This tube was made from 3 cm. of Spectrosil ultrahigh-purity
silica tubing (Thermal Syndicate Ltd.) of 4 mm. o.d. and 0.5 mm. wall
thickness, joined to 3 cm. of 4 mm. o.d. quartz tubing and then through
a graded seal to Pyrex glass tubing. The Spectrosil tubing did not show
any measurable radical concentration after gamma irradiation at the doses
used for the monomer. The prepared samples were frozen, irradiated
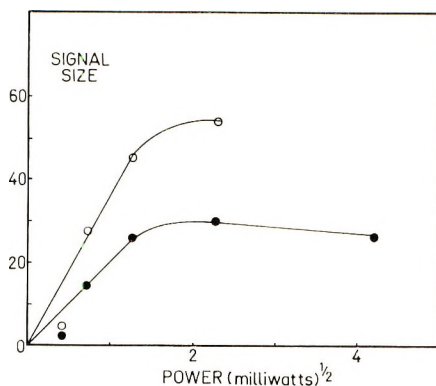with ^{60}Co gamma-rays, and stored in liquid nitrogen.

Fig. 2. Effect of microwave power on intensity of ESR spectrum of gamma-irradiated ODMA: (○) −170°C.; (●) −120°C.

The ESR spectra were obtained with a Varian V-4502 instrument, with a 9 in. magnet. A liquid-nitrogen Dewar was inserted in the cavity for measurements at −196°C., and a Varian variable-temperature cavity utilizing a flow of nitrogen gas was used for measurements between −180 and +12°C. The spectra saturated very easily; therefore, the effect of microwave power was examined (Fig. 2) and a value of 0.52 mwatt (25 db.) chosen for all quantitative work.

A Perkin-Elmer differential scanning calorimeter, model 1B, was used for investigating phase changes in the solid monomer. This instrument measures the heat input required to maintain the sample and a standard at the same temperature during warming, and small samples (10 mg.) ensure that thermal conductivity differences do not give misleading results. Unfortunately, measurements could not be carried out at very low temperatures or with irradiated samples.

RESULTS AND DISCUSSION

ESR Spectrum at −196°C.

The ESR spectrum of gamma-irradiated ODMA at −196°C. is shown in Fig. 3A. It consists of five broad lines (peak width between positions of maximum slope in absorption curve, 7 gauss) with a hyperfine splitting of 23 gauss. On closer examination (Fig. 3B) two further lines are seen with the same splitting, indicating that at least part of the five-line spectrum is due to a seven-line spectrum arising from radical (II), formed by addition of a hydrogen atom to the double bond. The predominant trapped radical in gamma-irradiated vinyl monomers at low temperatures is usually formed in this way.[9] In gamma-irradiated barium methacrylate dihydrate at −196°C. the spectrum is mainly a seven-line one, owing to this species.[8] A comparison of the spectrum of ODMA with gamma-irradiated docosane and octadecane (Fig. 3C) suggests that the spectrum is also due partly to
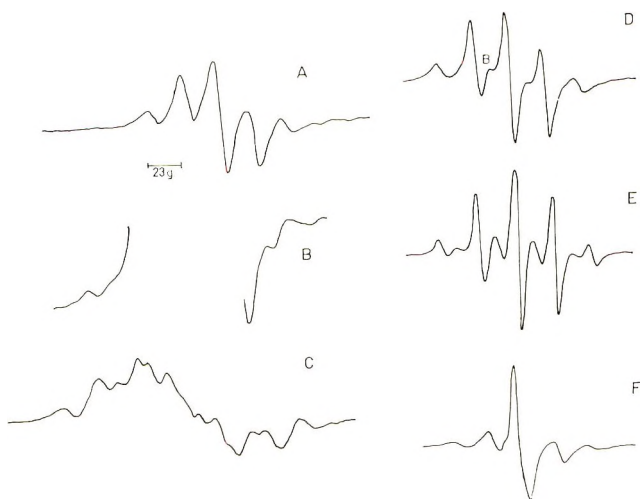
Fig. 3. Electron spin resonance spectra: (A) gamma-irradiated ODMA at $-196°C.$; (B) magnification of outer peaks of A; (C) gamma-irradiated octadecane at $-196°C.$; (D) gamma-irradiated ODMA warmed to $-80°C.$, ESR spectrum at $-170°C.$; (E) gamma-irradiated ODMA warmed to $-20°C.$, ESR spectrum at $-170°C.$; (F) gamma-irradiated ODMA containing 2% w/v chloranil at $-196°C.$ Dose, 0.2 Mrad in all cases.

$$
\begin{array}{ccc}
& CH_3 & CH_3 \\
& | & | \\
CH_2{=}C & \rightsquigarrow CH_2{=}C & + \; H\cdot \\
& | & | \\
& CO_2R & CO_2R'\cdot \\
& & (I)
\end{array} \tag{1}
$$

$$
\begin{array}{cc}
& CH_3 & CH_3 \\
& | & | \\
H\cdot + CH_2{=}C & \rightarrow CH_3{-}C\cdot \\
& | & | \\
& CO_2R & CO_2R \\
& & (II)
\end{array} \tag{2}
$$

$$
\begin{array}{cc}
& CH_3 & H \quad CH_3 \\
& | & | \quad | \\
R\cdot + CH_2{=}C & \rightarrow R{-}C{-}C\cdot \\
& | & | \quad | \\
& CO_2R & H \quad CO_2R \\
& & (III)
\end{array} \tag{3}
$$
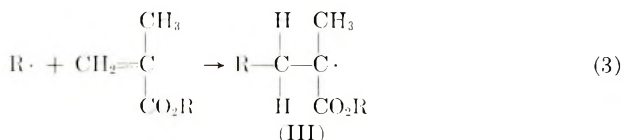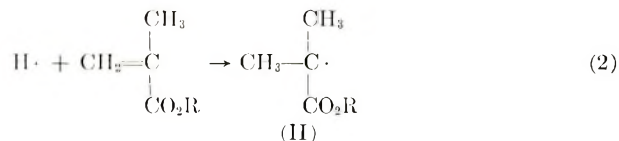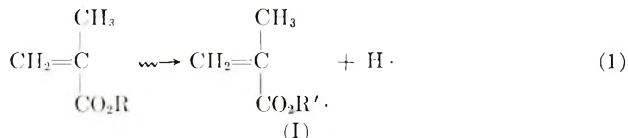
the alkyl radical (I), formed by loss of a hydrogen atom from the hydrocarbon chain.   The very broad lines of the spectrum are normal for solid paraffin hydrocarbons[10] and prevent satisfactory analysis giving the proportions of the three types of radical present in ODMA.   A small proportion of the spectrum also is due to the propagating radical (III), as in barium methacrylate.

Warming

The ODMA was warmed by progressive stages to the melting point (12°C.) and the spectrum measured at the temperature of each stage and

on cooling back to −170°C. on each occasion. The spectrum underwent a transition between −120 and −50°C., with the loss of the outer two lines and the appearance of intermediate peaks (Fig. 3D). Above −50°C. the spectrum (Fig. 3E) showed no further change in shape (Fig. 3F is discussed in another section). This nine-line spectrum of alternating intensity, with splittings of 11.5 gauss, is attributed to the methacrylate propagating radical (III). This is the spectrum observed in barium methacrylate dihydrate[8] and methacrylic acid[11] polymerizing in the solid state. There has been a long controversy over whether this spectrum results from one radical or two, but it is now clear that it results from one radical.[8,11−13]

Therefore reaction (3), in which R· refers to both (I) and (II), must have gone to completion at below −50°C., although no polymer can be separated. Of course, the ESR spectrum gives no indication of the number of monomer units which have added.

Radical Concentration

The effect of warming on the total radical concentration was determined by integrating the first-derivative spectrum obtained at −170°C. after each progressive stage of warming up and then measuring the area of this absorption spectrum. This double integration was performed on a computer by feeding in values of the first-derivative spectrum for incremental increases in magnetic field and integrating by Simpson's rule. A problem with any integration of a differential spectrum is drift in the baseline of the integrated spectrum or drift in the baseline of the first-derivative spectrum. This can be overcome by measuring the area of the integrated spectrum above the sloping baseline or, when an electronic integrator is being used, by reversing the leads to the integrator and taking half of the total area obtained.[14] However, the problem was found to be, not the integration or the original baseline, but asymmetry in the first-derivative spectrum produced by the ESR spectrometer. The center peak showed the main asymmetry and, being the largest peak, it had a significant effect. The asymmetry was not inherent in the spectra but was an instrumental effect due to the automatic frequency control. This is a key feature of the spectrometer, since it locks the magnetic field and
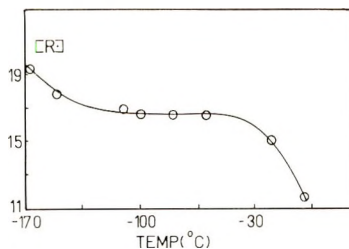

Fig. 4. Variation in total radical concentration [R·] in gamma-irradiated ODMA during warming from −170°C. to the melting point. Dose, 0.2 Mrad.

the microwave frequency, but unless the automatic frequency-control current was zero (i.e., there was perfect natural balance of the instrument, a very difficult condition to maintain for any period), asymmetry developed in the central peak. With careful operation symmetrical spectra were obtained, and the deviation of the baseline in the integrated absorption spectrum was negligible; hence, errors in the area were insignificant.

The resultant total radical concentration is shown as a function of temperature in Fig. 4. There is a slight decrease in radical concentration between -170 and $-150°C$. but then there is little change up to $-30°C$., above which it drops rapidly. The area of the differential spectrum (measured at $-170°C$.) increased twofold between -170 and $-30°C$., suggesting that there was an increase in the total radical concentration on warming. This is quite misleading and illustrates that first-derivative spectra should not be used for measuring relative radical concentrations when temperature changes have occurred.

There was no change in the shape of the spectrum on cooling back from $+10$ to $-170°C$.; the intermediate peaks of the alternating spectrum did not alter relative to the major peaks.

When the sample that had been warmed progressively to $10°C$. and cooled back to $-170°C$. was warmed up again, no further changes in the shape of the spectrum were observed. Therefore the changes observed during the first warm-up can be attributed to chemical reaction.

Time Dependence

The transformation in the spectrum between -150 and $-50°C$. was examined in detail. The reaction at $-120°C$. was followed as a function of time, with the height of the first intermediate peak (B in Fig. 3D) as a measure of the extent of the reaction. A first-order dependence on the concentration of initial radicals was observed, as shown in Fig. 5. The interpretation of kinetic curves for solid-state reactions is difficult, but these results indicate that the reaction is controlled by the physical or chemical properties of the initial radicals.

When the irradiated monomer was warmed to above $-30°C$., the radical concentration was strongly temperature-dependent but did not change with time; that is, the reaction causing loss of radicals occurred in the interval during which the instrument was reaching temperature equilibrium, less than 5 min. The disappearance of radicals in ODMA by mutual reaction would necessitate a diffusion of propagating radicals, which must be at least dimers, requiring considerable molecular mobility. The disappearance of radicals could result from a hydrogen-transfer reaction occurring over long distances. This would eliminate the requirement for diffusion of the dimeric or larger propagating radicals, but then all the radicals should disappear.

The rapid decrease in radical concentration with each rise in temperature shows that there must be either an equilibrium or a temperature-controlled limitation on the reaction. It seems likely that the distribution

of radicals through the medium is not uniform and that those which are closest together combine first. There must be increasing disorder and molecular mobility in ODMA from -30 to $+12°C.$, and the disappearance of radicals progressively on warming may reflect the distribution of distances separating them. It is well known that molecules can show unusually high mobilities in some organic solids.

A detailed crystallographic study of ODMA over a range of temperature is required, as is the case for all monomers that polymerize in the solid state. This is particularly difficult for ODMA, since it must be done from -100 to $+12°C.$

ODMA polymerizes rapidly at $0°C.$, reaching a "limiting" conversion to polymer of 50% after 3 hr. The ESR spectrum of a sample kept at $0°C.$ for 3 hr. in the spectrometer cavity and examined periodically showed no change in shape or intensity, indicating that no termination took place during polymerization. Hence, the marked decrease in the rate of polymerization must result from trapping of the propagating radicals. When
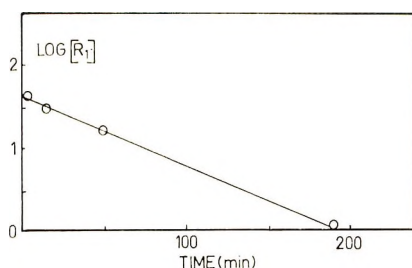
Fig. 5. First-order kinetic plot for conversion of initial radicals to propagating radicals at $-120°C.$ in gamma-irradiated ODMA.

the sample, partly polymerized at $0°C.$, was warmed to $+10°C.$, there was no decrease in radical concentration. Therefore the radicals which disappear during the initial warming up must be relatively small and mobile, i.e. dimers. This indicates that the disappearance of radicals on warming is not due to proton-transfer between immobile radicals, since this mechanism should be equally effective for small and large radicals. In fact, the polymer radicals are so immobile that no decrease in their concentration is observed, even when the melting point of the monomer is exceeded. This also provides evidence that all of the radicals are polymeric, that is, all of the radicals are involved in long-chain polymerization. It is interesting to note that the trapped radicals disappeared rapidly when the sample was warmed to above $20°C.$, which was the glass-transition temperature of the polymer, as indicated by visual observation of a change from a waxy to a tacky form and a peak in the differential thermal analysis curve. This observation confirms that the propagating radicals are terminated by mutual reaction, which can take place only between trapped long-chain radicals when movement is possible.

Effect of Chloranil

The spectrum at $-196°C$. obtained from gamma-irradiated ODMA containing 2% w/v chloranil (Fig. 3F) shows a reduction in the total radical concentration and the presence of the radical formed by addition of an electron to the chloranil,[15] in approximately the same concentrations as the ODMA radicals. This suggests that the electron is a precursor of some of the ODMA radicals, probably as a precursor of H atoms, as observed in other systems.[16] The importance of electrons in the radiolysis of organic solids has only recently been recognized[17] and the decrease in H_2 yield by addition of electron scavengers demonstrated.[18]

When the sample was warmed, the transformation to the propagating radical occurred at $-120°C$. There was a marked decrease in the radical concentration at $-40°C$., and by $0°C$. it was reduced to zero. Furthermore, when the sample was melted, no polymer was obtained. This is more evidence that transformation to the propagating radical in methacrylates, observed by ESR, corresponds to the formation, not of long chains but, probably, only of dimer. It is also evidence that a small concentration of an impurity may completely change the characteristics of a solid-state reaction. In this case it is probably radical-scavenging by the chloranil which prevents polymerization. Although additives are frequently ineffectual in solid monomers, the fairly flexible structure of ODMA probably accommodates the chloranil with a reasonably uniform distribution. Moreover, the greatly increased number of defects in the structure should increase the mobility of the radicals and hence increase the rate of their combination.

Differential Thermal Analysis

A typical differential thermal analysis curve obtained for ODMA with the Perkin-Elmer differential scanning calorimeter is shown in Fig. 6. The strongly endothermic peak A corresponds to the melting point. There is a definite endothermic peak commencing at $-30°C$. (peak B), which
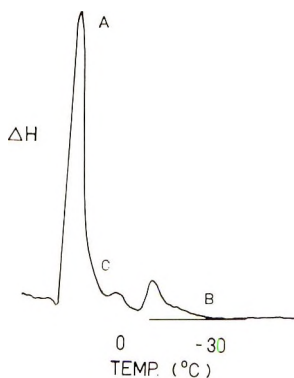

Fig. 6. Differential thermal analysis of ODMA.

apparently results from a solid–solid phase change. The small peak at 0°C. (peak C) may be due to a futher phase change, but no correlation with changes in the ESR spectra or polymerization rates has been observed.

CONCLUSIONS

The polymerization of ODMA in the solid state between −30 and +12°C. has been shown to proceed by a free-radical mechanism.

It is most important to distinguish between addition of the first monomer to the initial radical and long-chain polymerization. The first-monomer addition occurred at as much as 100°C. below the onset of long-chain polymerization. When chloranil was present, the addition of one monomer molecule occurred, although there was no long-chain polymerization on further warming.

There must be considerable molecular mobility in ODMA at temperatures above −30°C. for radicals to disappear, and this apparently results from a phase transition at −30°C. to a relatively "loose" structure. Polymerization proceeded in the "high-temperature" phase, but there was no rapid polymerization at the phase-transition temperature, as has been observed in other monomers.[19]

The total radical concentration varied with temperature. Consequently, the apparent activation energy for postirradiation polymerization includes a contribution from an "initiation" step.

References

1. S. E. Bresler and E. N. Kazbekov, *Fortschr. Hochpolymer Forsch.*, **3**, 688 (1964).

2. H. Szwarc, *J. Chim. Phys.*, **63**, 137 (1966).

3. H. Ueda and Z. Kuri, *J. Polym. Sci.*, **61**, 333 (1962).

4. T. Otsu, T. Ito, and M. Imoto, *J. Polym. Sci. A*, **2**, 2901 (1964).

5. F. A. Bovey and G. V. D. Tiers, *J. Polym. Sci.*, **44**, 173 (1960).

6. A. J. Swallow, *Radiation Chemistry of Organic Compounds*, Pergamon, London, 1960.

7. C. H. Bamford, G. C. Eastmond, and J. C. Ward, *Proc. Roy. Soc. (London)*, **A271**, 357 (1963).

8. J. H. O'Donnell, B. McGarvey, and H. Morawetz, *J. Am. Chem. Soc.*, **86**, 2322 (1964).

9. C. Chachaty and M. C. Schmidt, *J. Chim. Phys.*, **62**, 527 (1965).

10. D. Libby, M. G. Ormerod, and A. Charlesby, *Polymer*, **1**, 212 (1960).

11. H. Fischer, *J. Polym. Sci. B*, **2**, 529 (1964).

12. M. C. R. Symons, *J. Chem. Soc.*, **1963**, 1186.

13. D. Kourim and K. Vacek, *Trans. Faraday Soc.*, **61**, 415 (1965).

14. J. G. Kenworthy, G. F. Longster, and R. E. Richards, *Trans. Faraday Soc.*, **62**, 534 (1966).

15. J. E. Wertz and J. L. Vivo, *J. Chem. Phys.*, **23**, 2441 (1955).

16. L. Kevan and C. Fine, *J. Am. Chem. Soc.*, **88**, 869 (1966).

17. W. V. Skerman, *J. Chem. Soc. A*, 599 (1966).

18. D. W. Skelly and W. H. Hamill, *J. Chem. Phys.*, **44**, 2891 (1966).

19. V. A. Kargin, V. A. Kabanov, and I. M. Papissov, in *Macromolecular Chemistry, Paris,* **1963** (*J. Polym. Sci. C*, **4**), M. Magat, Ed., Interscience, New York, 1964, p. 767.

Copolymers of Modified Starches with Polyacrylonitrile

GEORGE F. FANTA, ROBERT C. BURR,
C. R. RUSSELL, and C. E. RIST,
*Northern Regional Research Laboratory, Northern Utilization
Research and Development Division, Agricultural Research
Service, U.S. Department of Agriculture, Peoria, Illinois 61604*

Synopsis

A study was made of the ceric ammonium nitrate-initiated graft polymerization of acrylonitrile (AN) onto a number of modified starches that had been reduced in molecular weight by either acid, hypochlorite, or enzyme treatment. With highly soluble starches, much of the starting material was recovered as ungrafted carbohydrate, and the reaction product was largely dimethylformamide-soluble polymer with a high polyacrylonitrile (PAN) content. The molecular weight of grafted PAN was lower when the modified starches existed as granules in water dispersion; however, heating (60°C) an aqueous slurry of an acid-modified corn starch (with intact granules) before the reaction had relatively little effect on the composition of the copolymer. Decreasing the concentrations in water of modified starch and AN resulted in more frequent and lower molecular weight grafts of PAN. Aqueous methanol as a reaction medium for an acid-modified starch with intact granules led to more frequent grafting of lower molecular weight PAN than when water alone was used. The number of grafted chains, however, was fewer than found with unmodified wheat starch under comparable conditions. A modified starch with the granule structure completely broken down gave no detectable reaction in aqueous methanol.

INTRODUCTION

Graft copolymers of unmodified starch and polyacrylonitrile (PAN), formed through ceric ammonium nitrate initiation, have been studied in this laboratory to determine what factors govern the frequency of grafting and the molecular weight of grafted PAN. We found three reaction variables that influence these two properties: the extent of swelling and disruption of the starch granule,[1] the medium in which the reaction is run,[2] and the reactant concentration.[3] To extend our study, we examined the grafting of PAN onto a series of modified starches, which are produced commercially by reacting starch with acid, enzyme, or hypochlorite. In a program aimed at starch utilization, it is important to know how such starches behave under the conditions of the grafting reaction. Our latest work shows that modified starches give results significantly different from any of our previously reported work.[1–3]

EXPERIMENTAL

Materials

Acrylonitrile (Eastman Kodak, practical grade) was fractionated at atmospheric pressure through a 15-in. Vigreux column. A center cut was collected and stored in amber glass at 5°C.

The initiator solution was prepared by dissolving 13.9 g of ceric ammonium nitrate in 250 ml of $1N$ nitric acid.

The modified starches are listed in Table I along with their intrinsic

TABLE I
Modified Starches

Starch[a]	Type	$[\eta]$[b]	Solubility, %[c]
Flojel 75	Acid modified	0.52	3
Claro 5591	Hypochlorite-oxidized	0.50	6
Flojel 90	Acid-modified	0.22	23
Stadex 60	Dextrin	0.094	62
Modified wheat starch	Enzyme-modified	0.18	76
Amidex B518	Thin boiling pregelatinized	0.12	86
Stadex 120	Dextrin	0.090	97

[a] Except for enzyme-modified wheat starch, all commercial starches were derived from corn starch. List of manufacturers: Stadex 60 and Stadex 120, A. E. Staley Manufacturing Co.; Flojel 90 and Flojel 75, National Starch and Chemical Corp.; Amidex B518 and Claro 5591, Corn Products Co.

[b] Intrinsic viscosity in 90:10 (by volume) dimethyl sulfoxide–water dl/g.

[c] A mixture of 21.9 g (dry basis) starch and 500 ml water was stirred for 2 hr at 25°C and centrifuged at 1600 g for 35 min. From the weight of solid found in an aliquot of the supernatant, the weight percentage dissolved was calculated.

viscosities in 90:10 (by volume) dimethyl sulfoxide–water and also their per cent solubilities in water at the concentrations most often used for graft polymerization (4.4% slurry). All but the enzyme-modified starch were commercial products. The enzyme-modified starch was prepared by slurrying 89.6 g (dry basis) of wheat starch in 300 ml of water. A 0.3-g portion of calcium chloride was added, the pH adjusted to 6.8, and 0.016 g of α-amylase dissolved in the slurry. The stirred mixture was heated to 89°C for 1 hr and held at this temperature for 20 min. The mixture was cooled and the starch precipitated by addition to 1 l. of 95% ethanol. The solid was washed with ethanol, vacuum-dried at 60°C, and ground to pass a 120-mesh sieve. Final traces of ethanol were removed by air-equilibrating, drying again under vacuum, and air-equilibrating a second time. Final moisture content was 10.1%.

Aqueous slurries of Flojel 75, Claro 5591, Flojel 90, and Stadex 60 at room temperature were similar in appearance when viewed by light microscopy, and each sample showed intact starch granules. The slurry of enzyme-modified starch contained some highly swollen, irregularly shaped

particles but no intact granules.   No discrete particles could be seen on microscopic examination of slurries of Amidex B518 and Stadex 120.

Graft Polymerization

For reactions at normal dilution, modified starch (21.9 g, dry basis) was slurried in 500 ml of water and the stirred mixture purged with a slow stream of nitrogen for 1 hr.   Acrylonitrile (AN) (31.8 g) was added and after 5 min, 7.5 ml of initiator solution was added.   The mixture was stirred for 3 hr at 25°C (temperature controlled with an ice bath), hydroquinone added, and the mixture filtered.   The solid was washed first with water and then with ethanol and finally vacuum-dried.   In some preparations, an appreciable amount of carbohydrate was recovered from the aqueous filtrate; however, this material contained little or no PAN (by infrared).

In the reactions run at high dilution, 3.0 g of modified starch (dry basis), 800 ml of water, 10.0 g of AN, and 12.0 ml of initiator solution were used.

For the reaction of Flojel 75 in aqueous methanol, a stream of nitrogen was bubbled for 1 hr through a thick slurry of 21.9 g (dry basis) of starch in 25 ml of water.   Initiator solution (7.5 ml) was added to the stirred starch slurry followed after 5 min by a solution of 31.8 g of AN in 115 ml of nitrogen-purged methanol.   In the reaction with Amidex B518, 30 ml of water was used because of increased swelling of the starch.

The crude product from each reaction was extracted with dimethylformamide (DMF) to remove ungrafted PAN;[4,5] however, some carbohydrate-containing polymer also was extracted.   The copolymer insoluble in DMF was then analyzed for nitrogen.   To determine the molecular weight of grafted PAN chains, the starch moiety was removed by refluxing in dilute hydrochloric acid followed by treatment with periodate and base.[6]   The molecular weight of grafted PAN was determined by intrinsic viscosity measurements,[4] and the grafting frequency was then calculated.

RESULTS AND DISCUSSION

Six commercial modified starches and one enzyme-modified starch prepared in this laboratory were grafted with AN (ceric ammonium nitrate initiator).   The type of modification, the intrinsic viscosity, and the per cent solubility in water at the concentration most often used for grafting are given in Table I for each starch.   These starches were chosen because they represent ones most commonly used industrially and encompass a broad range of water solubilities and degree of granule disruption.

The first series of reactions (Table II) was conducted at concentrations used in our earlier work[1] (21.9 g of starch, dry basis, 500 ml of water, 31.8 g of AN, 7.5 ml of initiator solution).   These concentrations will be subsequently referred to as normal dilution as opposed to the more dilute reactions to be described later.   The DMF solubles, except for the fraction from Flojel 75, contained more than trace amounts of carbohydrate, as

evidenced by both infrared and nitrogen analyses; and the carbohydrate content tended to increase with increased solubility in water of the modified starch.

Since the amount of DMF solubles was larger than observed in previous work with unmodified wheat starch,[1] we suspected grafting to small carbohydrate fragments in the modified starches. If such grafting occurred, the resulting polymer would contain mainly PAN and would, therefore, be readily dissolved by DMF. To test this hypothesis, Claro 5591 was extracted with water at room temperature to remove soluble, low molecular weight material. The extracted and air-dried product was grafted with AN and then separated into fractions in the usual manner to give 6.8 g of DMF-soluble polymer containing 88.2% PAN. The DMF-insoluble fraction (41.9 g) contained 48.0% PAN of molecular weight 171,000 and had a calculated grafting frequency of 1110 anhydroglucose units (AGU)/graft.

TABLE II
Products of Reaction of Acrylonitrile with Modified Starches[a]

		DMF-soluble		DMF-insoluble			
Starch[b]	Water-soluble, g	Weight, g	PAN content, %	Weight, g	PAN content, %	Molecular weight of grafted PAN	Grafting frequency, AGU/graft
Flojel 75	0.5	10.5	99.8	30.8	31.6	214000	2850
Claro 5591	0.8	15.1	96.0	31.6	36.4	185000	1990
Flojel 90	3.9	11.8	93.3	32.4	51.1	183000	1080
Stadex 60	14.4	21.4	90.3	11.8	61.3	319000	1240
Enzyme-modified	17.0	25.7	87.7	8.0	69.8	716000	1910
Amidex B518	15.2	24.8	93.9	2.5	55.1	522000	2620
Stadex 120	23.5	Weight of water-insolubles: 0.1 g (not further examined)					

[a] Polymerization recipe: 21.9 g (dry basis) starch, 31.8 g AN, 500 ml water, 7.5 ml initiator solution. Reaction time: 3 hr.
[b] See Table I.

When these results are compared with those in Table II for Claro 5591, it is apparent that water extraction before graft polymerization reduced both the weight of DMF solubles and the amount of PAN in this fraction. These two results lend support to the proposed hypothesis. Although the molecular weights for grafted PAN did not greatly differ between the two DMF-insoluble fractions, the fraction from water-extracted Claro 5591 had a larger number of grafted chains.

Other than the run with Stadex 120, in which little or no reaction occurred, the tendency was an increase in both the amount of DMF and water solubles, a reduction in the amount of DMF insolubles, and an increase in the PAN content of the DMF-insoluble fraction with increasing water solubility of the modified starch used. With highly soluble starches, therefore, much of the starting material was recovered as ungrafted carbo-

hydrate (water-soluble fraction) and the reaction product was largely DMF-soluble polymer with a high PAN content.

Since Flojel 75 (acid-modified) and Claro 5591 (hypochlorite-oxidized) in water were similar in microscopic appearance, solubility, and intrinsic viscosity, the effect of modification method on copolymer composition was estimated by comparing the amounts and composition of the two sets of fractions. The DMF-insoluble starch-PAN copolymer from hypochlorite-oxidized starch had slightly shorter PAN chains and was more frequently grafted than the product derived from acid-modified starch.

In Flojel 75, Claro 5591, and Flojel 90, where the granules of starch are largely intact, molecular weights for grafted PAN were lower than for enzyme-modified starch and Amidex B518, where the structure of the granule is completely disrupted. Stadex 60 was 62% soluble at the concentration used for grafting but still contained some intact starch granules. In this case, the molecular weight of grafted PAN was intermediate between the granular and the disrupted starches. The dependence of molecular weight on the physical state of the starch was not surprising in view of results we reported earlier for unmodified wheat starch.[1] Table II, however, shows no correlation between granule disruption and grafting frequency.

Although the molecular weight of grafted PAN seemed to depend on whether the modified starches existed as granules in water dispersion, Flojel 75, a modified starch in which the granules were intact, was relatively insensitive to the changes in pretreatment conditions that caused large variations in copolymer structure with unmodified wheat starch. The polymer produced when Flojel 75 was slurried in water at 60°C before grafting was similar to that formed after room temperature pretreatment (Table III). This result is in sharp contrast to unmodified wheat starch, where a pretreatment temperature of 60°C caused about a fivefold increase

TABLE III
Effect of Pretreatment on Composition of Flojel 75–Polyacrylonitrile Copolymers[a]

		DMF-soluble		DMF-insoluble			
Starch pretreatment[b]	Water-soluble, g	Weight, g	PAN content, %	Weight, g	PAN content, %	Molecular weight of grafted PAN	Grafting frequency, AGU/graft
Added dry	1.6	6.6	—	27.2	22.1	235000	5110
1 hr, 25°C	0.5	10.5	99.8	30.8	31.6	214000	2850
1 hr, 60°C	2.5	10.6	96.7	31.2	35.8	236000	2610

[a] Polymerization recipe: 21.9 g (dry basis) Flojel 75, 31.8 g AN, 500 ml water, 7.5 ml initiator solution. Reaction time: 3 hr.

[b] In the first reaction, water and initiator were sparged with nitrogen for 1 hr. Monomer was then added followed immediately by Flojel 75 (powder). In the other reactions, starch–water slurries were sparged with nitrogen at 25 or 60°C. Monomer was then added to the starch slurries at 25°C, followed after 5 min by the initiator solution.

in the molecular weight of grafted PAN and about a fourfold decrease in the number of grafted chains as compared with 25°C.[1]   When Flojel 75 was added as a dry powder to an aqueous solution of monomer and initiator (Table III), the molecular weight of grafted PAN was not appreciably different from that resulting when Flojel 75 was slurried in water before the reaction, although the number of chains grafted was significantly lower.

We had previously found for unmodified wheat starch that a reduction in the molecular weight of grafted PAN and an increase in the number of grafted chains could be achieved by decreasing the concentrations of reactants[3] (3.0 g starch, dry basis, 800 ml water, 10.0 g AN, and 12 ml initiator solution).   When the modified starches were grafted under these conditions, which will subsequently be referred to as high dilution, the DMF-insoluble fractions (Table IV) also had shorter and more frequent

TABLE IV
Products of Reaction of Acrylonitrile with Modified Starches (High Dilution)[a]

	DMF-soluble		DMF-insoluble			
Starch[b]	Weight, g	PAN content, %	Weight, g	PAN content, %	Molecular weight of grafted PAN	Grafting frequency, AGU/graft
Flojel 75	0.4	94.4	4.6	38.3	41400	411
Claro 5591	1.6	93.5	4.4	38.6	77300	757
Flojel 90	4.9	90.2	3.8	44.5	69700	536
Stadex 60	4.1	77.3	1.6	59.2	150000	637
Enzyme-modified	4.0	72.7	0.8	33.4	92000	1130
Amidex B518	8.0	81.5	0.2	—	—	—

[a] Polymerization recipe: 3.0 g (dry basis) starch, 10.0 g AN, 800 ml water, 12.0 ml initiator solution.   Reaction time: 3 hr.
[b] See Table I.

branches than their counterparts in Table II.   The weight of water solubles was not determined, but increased water solubility of the modified starch tended to increase the amount of DMF-soluble polymer and to lower the conversion to DMF-insoluble graft copolymer, similar to the series of reactions made at normal dilution.   Also, the PAN content of the DMF-soluble fraction followed the same general trend observed in Table II.   The molecular weights of grafted PAN, however, did not show the dependence on granule disruption seen in Table II.   Claro 5591 (hypochlorite-oxidized) again gave more DMF-soluble polymer than Flojel 75 (acid-modified); however, contrary to Table II, the DMF-insoluble product from Claro 5591 was less frequently grafted with PAN of higher molecular weight than the product from Flojel 75.

With unmodified wheat starch, the use of aqueous methanol as a reaction medium also gave a more frequently grafted product with lower molecular weight PAN.[2]   In this procedure, starch was slurried in a minimum amount of water, ceric ammonium nitrate solution added, and a solution

of AN in methanol added to the starch–ceric complex. When this method was used with Flojel 75, the product, after DMF extraction, contained 8.5% PAN of molecular weight 21300; and a grafting frequency of 1420 AGU/graft was calculated. Although a greater number of chains was grafted to Flojel 75 in the presence of methanol than in its absence (Table II), the number of grafted chains was not so large as expected. For unmodified wheat starch, either aqueous methanol or high dilution conditions in water gave a copolymer with about the same grafting frequency. With Flojel 75, however, fewer chains were grafted in aqueous methanol than under high dilution (1420 compared to 411 AGU/graft). This difference might result from a more facile migration of methanol to the free-radical sites within the Flojel 75 granule (as opposed to an unmodified wheat starch granule). Free radicals might then be destroyed by chain transfer before they can react with AN to form grafted PAN. If this explanation is correct, even fewer chains should be grafted to a modified starch where the granule structure has been completely disrupted. When Amidex B518 was grafted with AN in aqueous methanol under conditions comparable to those used for Flojel 75, no graft polymerization occurred, as evidenced by the lack of nitrile absorption in the infrared spectrum of the isolated product.

References

1. R. C. Burr, G. F. Fanta, C. R. Russell, and C. E. Rist, *J. Macromol. Sci.*, **A1**, 1381 (1967).

2. R. C. Burr, G. F. Fanta, C. R. Russell, and C. E. Rist, *J. Macromol. Sci.*, **A2**, 93 (1968).

3. G. F. Fanta, R. C. Burr, C. R. Russell, and C. E. Rist, *J. Appl. Polym. Sci.*, in press.

4. G. F. Fanta, R. C. Burr, C. R. Russell, and C. E. Rist, *J. Appl. Polym. Sci.*, **10**, 929 (1966).

5. C. E. Brockway and P. A. Seaberg, *J. Polym. Sci. A-1*, **5**, 1313 (1967).

6. L. A. Gugliemelli, M. O. Weaver, and C. R. Russell, *J. Polym. Sci. B*, **6**, 599 (1968).

Alternating Copolymerization of Polar Vinyl Monomers in the Presence of Zinc Chloride.   II. Properties of Acrylonitrile–Styrene Copolymer*

SHIGERU YABUMOTO, KIYOSHI ISHII, MASAKIYO
KAWAMORI, KOICHIRO ARITA, and HIROSHI YANO,
Central Research Laboratory, Daicel Ltd., Iruma-gun, Saitama, Japan

Synopsis

The properties of the acrylonitrile–styrene copolymer prepared in the presence of zinc chloride were investigated in comparison with those of a copolymer having the same overall composition and prepared by the ordinary radical procedure.   The characteristics of the polymer prepared with $ZnCl_2$ were as follows: (1) less coloration by alkali treatment, (2) less coloration by thermal treatment and (3) higher glass transition temperature.   These features may be attributed principally to the structure of the copolymer, which has more unlike bonds and less long sequences as described in the first article of this series.   The effects of residual salt in the copolymer on the properties were also investigated.

INTRODUCTION

In recent years, the properties of copolymers have been studied in relation not only to their overall composition but also to the fine structure such as sequence length distribution or the distribution of the like and the unlike bonds.

Several papers have reported on the sequence length or bond distributions of acrylonitrile–styrene copolymers (AS copolymers), the properties of which are the object of this article.   Shibasaki[1] studied the mechanism of instantaneous thermal decomposition of AS copolymers at temperatures higher than 400°C by pyrolysis gas chromatography and interpreted the distribution of the decomposition products by introducing the penultimate effect on the monomer releasing rate at the radical end of the decomposing polymer chain.   Igarashi and Kambe[2] reported that the decomposition residue increases more than proportional to the acrylonitrile component over the temperature range from 250 to 450°C, and proposed that the sequence length distribution be considered to explain the phenomenon.   Uematsu,[3] assuming the stiffness energies of the like and the unlike bonds in the copolymer, tried to explain the shift of the glass transition temperature on the basis of variation in the copolymer composition.

---

* This work was reported on the 16th Annual Congress of the Kobunshi-Gakkai, Tokyo University, May 26–28, 1967.

In the preceding article of this series,[1] it was shown that the apparent reactivity ratios in the copolymerization in the presence of zinc chloride (ZAS copolymer) were smaller than those of ordinary radical copolymerization (AS copolymer), and this fact led us to expect that ZAS copolymer may have some special properties due to its highly alternative character. In this article, an attempt to elucidate the features of ZAS copolymer in relation to the sequence length distribution was carried out.

EXPERIMENTAL

Preparation of Copolymers

The monomers purified as described in the preceding report were polymerized in nitrogen atmosphere at 50–70°C. The polymer yield was in the range 5–15 wt-% except for copolymer ZAS 2223, the conversion of which was ca. 40 wt-%. The polymers purified by repeated precipitations into methanol from acetone solution contained the less than 0.01 wt-% residual zinc chloride.

Copolymer ZAS 2223 alone contained ca. 0.3 wt-% residual salt because it was precipitated only once to obtain a large amount of the sample to permit various examinations. The content of residual salt was measured quantitatively by spectrophotometry as described in the preceding article. The polymer samples are listed in Table I.

Reagents

Commercial guaranteed grade reagents were used except for the monomers.

Coloration by Alkali Treatment

A 100-mg portion of well dried sample was dissolved in 100 ml of dimethylformamide (DMF) in an Erlenmeyer flask. After 24 hr, 2 ml of aqueous 1N sodium hydroxide was added to the solution with stirring at 30°C. After 10 min, the absorption spectrum in the visible region was measured by using a Beckman DK 2 spectrophotometer. The sampling and the measurement were repeated at 20-min intervals.

Coloration by Thermal Treatment

A 100-mg portion of well dried sample weighed in an aluminum foil vessel was placed in a pretreating chamber of the furnace, then the chamber was repeatedly evacuated and charged with nitrogen gas. After the treatment, the vessel was moved into the heating chamber maintained at 240 or 280°C. After 1 hr, the vessel was cooled and the sample was dissolved in 10 ml of DMF. The coloration was measured by using Beckman DK2 spectrophotometer.

TABLE I
Properties of the Samples

Copolymer sample	ZnCl₂, parts	Phase of polymerization	$[\eta]$, dl/g	AN component, mole-%[a]	Unlike bonds, mole-%[b]	Isotactic AN sequences longer than 4 monomer units, mole-%[b]	Properties examined
ZAS 26	3	Bulk	—	50	96	2.1×10^{-5}	Alkali and thermal coloration
ZAS 39	3	MIBK	1.80	50	96	2.1×10^{-5}	
ZAS 2223	3	solution	1.29	49	96	4.5×10^{-6}	η_{melt}, $T(E'')$, T_f, tensile and impact strength
AS 0			0.41	0	0	0	
AS 25			0.90	27	52	4.9×10^{-7}	
AS 38			1.15	36	68	3.1×10^{-5}	Alkali coloration, thermal coloration, $T(E'')$
AS 46		Bulk	1.18	46	85	7.0×10^{-4}	
AS 55	0		1.58	53	85	1.8×10^{-2}	
AS 67			1.69	64	68	0.24	
AS 73			1.82	73	52	0.55	
AS 85			3.05	85	29	1.45	
AS 100		MeOH solution	1.50	100	0	$6.25\ (= 2^{-4} \times 100)$	
AS 49		MIBK	—	49	86	2.1×10^{-3}	$T(E'')$, T_f, tensile and impact strength
AS 50		solution	1.22	50	86	3.1×10^{-3}	
AS 52			1.95	52	85	7.0×10^{-3}	Alkali and thermal coloration η_{melt}

[a] Observed by micro-Dumas method (Coleman analyzer).
[b] Calculated by using reactivity ratios.

Glass Transition Temperature

Dynamic mechanical moduli were observed at 110 Hz with a Vibron DDV-II, a nonresonance forced-vibration type viscoelastometer, over the temperature range 20–140°C. The specimens (0.3 × 3.0 × 50 mm) were cut out of the sheets made by hot pressing at 180°C for 10 min at 130 kg/cm² pressure. To confirm the results obtained, the softening temperature by the Clash-Berg method (ASTM D1043-61T) was determined on specimens (1.0 × 6.3 × 60 mm) cut out of the sheets made by the same procedure. Little residual monomer was detected in the specimens.

Tensile Strength

Specimens were cut out of the sheets (1 mm thick) by stamping according to ASTM D638-61T. The specimens were examined by using a Tensilon, an Instron-type testing machine, with a grip span of 60 mm and a drawing speed of 5 mm/min at 20°C.

Impact Strength

Specimens (1.0 × 10 × 50 mm) cut out of the sheets were examined by using a modified Izod-type testing machine with the impact-support span of 2.5 mm.

Melt Viscosity

A $1^1/_2$ g portion of well dried sample was pressed into a vertical cylinder of 1 cm² cross section equipped with a nozzle (1 mm diameter, 10 mm length) at the bottom and a plunger at the top; all were maintained at 230°C. The degassed sample was held in the cylinder for 5 or 65 min. Then a pressure of 40 or 100 kg/cm² was applied through the plunger to force the sample out through the nozzle.

Effects of Residual Zinc Chloride

To elucidate the effects of residual salt on the properties of the copolymers, AS copolymer with zinc chloride added was examined in comparison with pure AS copolymer. The salt was added to an acetone solution of the copolymer and the polymer was precipitated into methanol. The content of the salt was determined by the method presented above.

RESULTS AND DISCUSSION

Coloration by Alkali Treatment

Typical spectra are shown in Figure 1. The AS copolymers treated with alkali under the conditions described above develop yellow to brown color with absorption peaks at 290, 362, and 400 (shoulder) mμ. The color developed by ZAS copolymer was about one fourth as intense as that developed by the AS copolymer of the same composition.
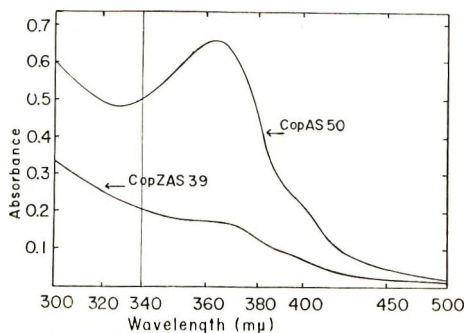
Fig. 1. Absorption spectra of alkali-treated AS copolymers: (ZAS 39) polymerized in the presence of zinc chloride, (AS 50) polymerized by ordinary methods. Both containing 50 mole-% AN component.

It is well known that alkali coloration of polyacrylonitrile (PAN) in dilute solution is due to the formation of conjugated polyimines, $(-C=N-)_n$, along the polymer chain.[5-7] Polystyrene (PSt), on the other hand, develops no color at all under the same conditions. It is supposed, therefore, that the coloration of AS copolymer is due to the formation of conjugated polyimines in the acrylonitrile (AN) sequences long enough to yield the structure. In addition to the length, the tacticity of the sequence must restrict the formation of the structure between the pendant cyano groups within an AN sequence. In the case of isotactic sequences, the increase in the number of conjugated imines brings about little or no distortion of the skeleton. In the case of syndiotactic sequences, on the contrary, the third imine structure adding to the diimine formed already cannot be formed without a great deal of distortion, which might destroy the ring structure. Recently the effect of tacticity on the alkali coloration of PAN was reported.[3] The PAN obtained in urea adducts by x-ray irradiation (the meso-racemic ratio was 6:1) developed four to five times the color developed by the radically polymerized PAN (meso–racemic ratio, 1:1). So, it may be assumed that in the alkali coloration of AS copolymers, isotactic AN sequences longer than n monomer units alone can yield the $(-C=N-)_n$ structure.

To examine this assumption, a series of AS copolymers of various compositions and hence various sequence length distributions which could be calculated from the reactivity ratios and the compositions of the copolymers were treated with alkali. Instead of $1N$ sodium hydroxide aqueous solution, $0.02N$ ethanol solution was used with this series to avoid too deep coloration of the samples rich in AN component. As shown in Figure 2, the absorption at 362 mμ of the polymer treated with alkali increases more than proportional to the AN component. This absorption, presumably due to the tetraimines, was plotted in Figure 3 against the amount of isotactic AN sequences longer than four monomer units. The linear correlation obtained may be considered to support the assumption. To
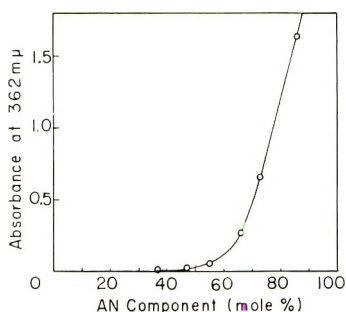
Fig. 2. Absorption at 362mμ of alkali-treated AS copolymers polymerized by ordinary methods, as a function of the composition.
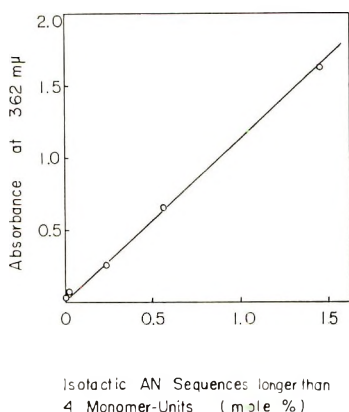

Fig. 3. Absorbance at 362mμ of alkali-treated AS copolymers polymerized by ordinary methods, as a function of the amount of the isotactic AN sequences longer than 4 monomer units.

confirm this correlation for the samples treated with $1N$ sodium hydroxide aqueous solution, a pair of samples, copolymer AS 50 and a blend of copolymers AS 46 and AS 55 prepared by coprecipitation, was examined. A linear correlation was obtained between the coloration and the amount of the isotactic AN sequences longer than four monomer units as shown in Table II.

The results shown in Figure 1 may be interpreted as indicating that the amount of isotactic AN sequences longer than four monomer units in ZAS 39 copolymer is one fourth that of AS 50 copolymer having the same overall composition. However, the ratio calculated from the reactivity ratios is 1/150 instead of 1/4 as shown in Table I.

There is some question whether the presence of zinc chloride at the copolymerization stage does affect the tacticity of AN sequences in ZAS copolymer. For poly(methyl methacrylate) (PMMA), Otsu et al.[9] reported that the presence of the salt did not affect the tacticity of PMMA. On the contrary, Makishima et al.[10] reported that an influence was ob-

served, since the tacticity of the polymer was insensitive to the polymerization temperature in the presence of the salt.   The difference in the tacticity, however, was not marked.   It would thus seem rather unlikely that variation in the tacticity is the cause of the discrepancy.   For more elaborate

TABLE II
Alkali Coloration of Homogeneous and Blended AS Copolymers

Copolymer sample	AN component, mole-%	Isotactic AN sequence, mole-%	Absorbance at 362 mμ	Absorption per isotactic sequence longer than 4 monomer units
AS 50	50	3.1×10^{-3}	0.48	1.6×10^2
Blend of AS 46 and AS 55	50	10.4×10^{-3}	1.55	1.6×10^2

discussions, it would be necessary for the tacticity of PAN obtained in the presence of $ZnCl_2$ to differ from that of ordinary PAN, since the determination of the tacticity of PAN by means of NMR spectroscopy seems to be established.[11]

As another factor which may affect the alkali coloration, the effect of the residual zinc chloride was examined, though less than 0.01 wt-% of
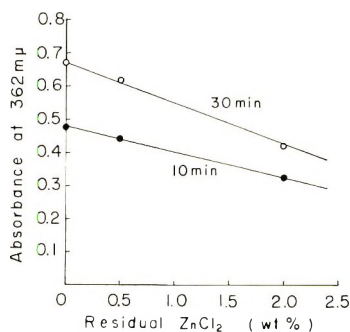
Fig. 4. Absorption at 362 mμ of alkali-treated AS copolymers as a function of residual zinc chloride.

salt remains in ZAS copolymer, because the salt may activate the cyano groups by coordination and act as a catalyst for coloration.   The residual salt, however, reduced the alkali coloration, as shown in Figure 4.   It is also shown in Figure 4 that a sample containing less than 0.1 wt-% salt is hardly influenced by the salt in the alkali coloration.

The cause of the discrepancy is still unknown.

Thermal Coloration

Typical absorption spectra of the thermally colored AS copolymers in the visible region are shown in Figure 5.   Unlike the case of alkali coloration, ZAS copolymers differ only a little from AS copolymers in the thermal coloration.

In thermally treated PAN, the conjugated polyimine structure was also assumed as one of the principal sources of the color which readily develops even below 200°C.[12]   As shown in Figure 6, the coloration takes place principally in the long AN sequences.   In thermal treatment at above 200°C, however, double bonds formed in the polymer main chain may release the steric distortion of racemic links to form the conjugated polyimine ring structure.   In addition, the thermal treatment in bulk, in contrast with the alkali treatment in dilute solutions, may cause formation of a conjugate polyimine structure between the cyano groups belonging to different AN sequences.   PAN, when heated in bulk, yields not only polyimines, but also hydrogen cyanide, ammonia, hydrogen, monomer, and low molecular weight cyano compounds, of which the latter two are

Fig. 5. Absorption spectra of thermally treated AS copolymers: (ZAS 39) polymerized in the presence of zinc chloride; (AS 50) polymerized by ordinary methods. Both contain 50/mole-% AN component.

Fig. 6. Absorption at 400 mμ of thermally treated AS copolymers prepared by ordinary methods, as a function of the isotactic AN sequences longer than 4 monomer units.   Heating temperature was 240°C.
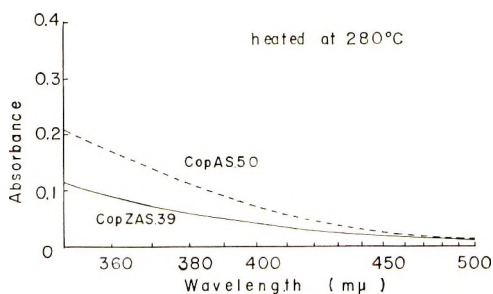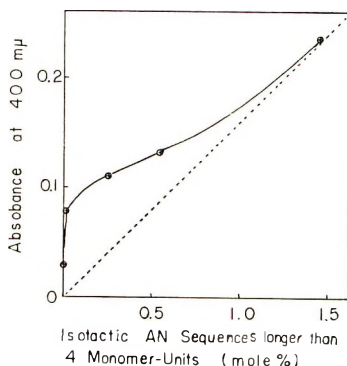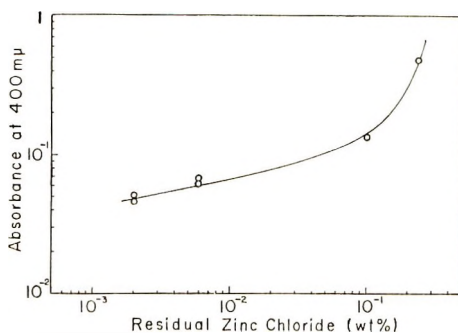
Fig. 7. Absorbance at 400 mμ of thermally treated AS copolymers as a function of residual zinc chloride. Heating temperature was 240°C.

evidently the products of main chain scission.[13–17]   Moreover, PSt develops color, though pale, on the thermal treatment.   These factors may yield strong color sources (other than polyimines formed from the isotactic AN sequences longer than four monomer units) and hence weaken the dependence of the thermal coloration on the sequences, as shown in Figure 6.

It may be also supposed that some weak links such as carbon–carbon double bonds, styryl or keteneimine structures, were produced in the main chain of ZAS copolymer, and that the result was acceleration of coloration so much as to mask the effect of fewer long AN sequences.

As shown in Figure 7, the residual zinc chloride promotes thermal coloration of AS copolymer.   Residual salt in amounts more than 0.1 wt-%, accelerates the coloration markedly, and this is accompanied with some gelation.   The effect decreases rapidly, however, with decreasing the salt content, becoming so small for concentrations less than 0.01 wt-%, that it is not necessary to take the effect into consideration on the results shown in Figure 5.

Glass Transition Temperature

The temperature of the maximum loss modulus, $T(E'')$ is plotted in Figure 8 against composition.   The $T(E'')$ of copolymer ZAS 2223 is above the curve, being higher by ca. 7°C than that of copolymer AS of the same composition.   The glass transition temperatures T_g observed by Beevers et al.[18] are also shown in Figure 8.   Although the absolute values are different, Beevers' values obtained by the measurement of refractive indices also form another curve similar to ours.   The difference between the $T(E'')$ of AS copolymer and the composition-weighted mean calculated from the $T(E'')$ of PSt and PAN, which is equal to the vertical distance between the curve and the dotted line, is plotted in Figure 9 against the amount of the unlike bonds (AN–St links) in the copolymer.   The $T(E'')$ of PAN assumed to be 100°C by the extrapolation of the curve is in good accordance with values of 105°C at 5 Hz observed by Schmieder and Wolf[19] and 99°C
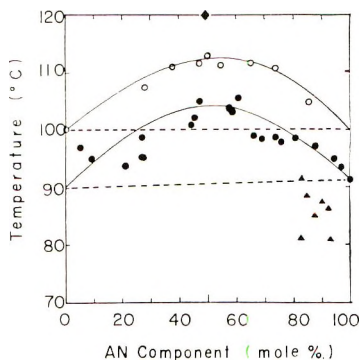
Fig. 8. Loss peak temperature $T(E'')$, and the glass transition temperature T_g observed by Beevers et al. of AS copolymers prepared by ordinary methods, as a function of the composition. $T(E'')$ of AS copolymers are represented by (O), $T(E'')$ of ZAS 2223, by (◆) and Tg observed by Beevers et al. by (●) and (▲).
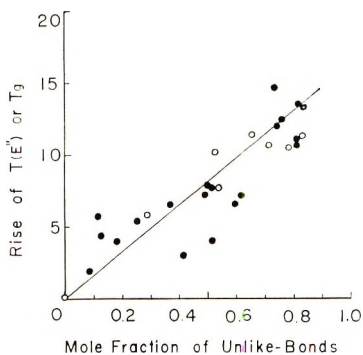
Fig. 9. The increase of $T(E'')$ or T_g of AS copolymer from the composition-weighted mean of those of the homopolymers, as a function of mole fraction of unlike bonds.

at 200–300 Hz reported by Cotten and Schneider.[20]   In Figure 9, the T_g observed by Beevers et al. are also shown in the same way.   As shown in Figure 9, a linear correlation was obtained, although some data are scattered.   The correlation may be interpreted as indicating that the increase in the $T(E'')$ or T_g of AS copolymer from the composition weighted mean of those of homopolymers is due to and proportional to the amount of the unlike bonds in the copolymer.

TABLE III
Transition Temperatures

Copolymer sample	AN component, mole-%	$[\eta]$, dl/g	$T(E'')$, °C	T_f, °C
ZAS 2223	49	1.29	120	110
AS 50	50	1.22	113	105

The observed increase in the $T(E'')$ of copolymer ZAS 2223 compared to that of copolymer AS 50 is ca. 7°C, and the increase in the softening temperatures T_f observed by the Clash-Berg method is ca. 5°C, as shown in Table III, while the temperature increase due to the increase in the unlike bonds is calculated to be ca. 2°C.

The effect of the residual salt on the T_f is shown in Figure 10, where the addition of 0.24 wt-% salt raises the T_f of copolymer AS by ca. 2°C. Therefore, the discrepancy of ca. 3°C must be due to the 0.3 wt-% residual salt contained in the sample used (copolymer ZAS 2223).
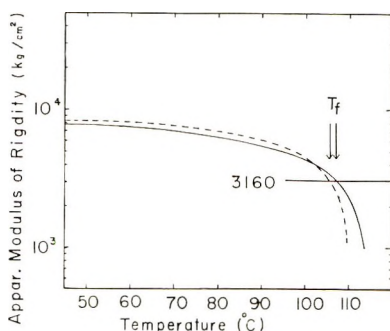
Fig. 10. Apparent moduli of rigidity of copolymer AS 50 with 0.24 wt-% zinc chloride added and pure copolymer AS 50; observed as a function of temperature by Clash-Berg method.

Other Properties

No significant difference in tensile and impact strengths of ZAS and AS copolymers was observed, as shown in Table IV.

The melt viscosity depression which took place during storage of the samples for 65 min in a cylinder kept at 230 or 280°C was less for ZAS copolymer than for AS copolymer. However, the addition of zinc chloride to AS copolymer decreased the depression of the melt viscosity, as shown in Table IV, presumably by promoting the intermolecular reactions. So, this phenomenon cannot be regarded as one of the essential characteristics of ZAS copolymer.

APPENDIX

The amount of the isotactic AN sequences longer than four monomer units was calculated as follows.

The number of AN sequences as long as n monomer units may be expressed as;

$$S_A(n) = m_A \, q_A^2 \, p_A^{n-1}$$

where m_A is the mole fraction of the AN component, $q_A = S/(r_A A + S)$, $p_A = 1 - q_A$, r_A and r_S are reactivity ratios defined by $r_A = k_{AA}/k_{AS}$ and

TABLE IV
Mechanical and Flow Properties

Copolymer sample	AN component, mole-%	$[\eta]$, dl/g	Tensile strength, kg/cm^2	Impact strength, kg/cm	Melt viscosity $\times$ 10^3, poise	Depression of melt viscosity after 1 hr, %
ZAS 2223	49	1.29	860	0.8	52	3
AS 52 with added ZnCl$_2$ (0.3%)	52	1.95	—	—	550	5
AS 52 (pure)	52	1.95	990	0.9	560	22

$r_S = k_{SS}/k_{SA}$, respectively, A is the mole fraction of AN in the monomer feed in the copolymerization, and $S = (1-A)$ is mole fraction of St in the monomer feed in the copolymerization.

The number of isotactic sequences in the AN sequences as long as n monomer units, $\mu(n|r)$, may be described as;

$$\mu(n|r) = \mu^{n-1} + \sum_{t=r+1}^{n-1} \{2\rho + (n - 1 - t)\rho^2\}\mu^{t-1}$$

$$= \mu^r\{1 + \rho(n - 1 - r)\}$$

where μ is the probability of meso linkage, (no penultimate effect was assumed); $\rho = (1-\mu)$ is the probability of racemic linkage, n ($>r$); r, and t are integers.

The meso–racemic ratio of AS copolymers being nearly unity, the probability may be described as:

$$\mu(n|r) = (n + 1 - r)/2^{r+1}$$

Then, the amount of the sequences, $S(r = 4)$ which is able to yield the conjugated tetraimines may be presented as;

$$S(4) = \sum_{n=5}^{\infty} \mu(n|r = 4)S_A(n)$$

$$= m_A(1 - q_A{}^2)p_A{}^3/2^5.$$

Strictly, the contributions of the isotactic sequences in the calculation of $\mu(n|r)$ should have been weighted by factors of 2 for the sequences longer than $2r$, 3 for those longer than $3r$, and so on. This correction, however, is trivial for the sequences not longer than $2r$ or $3r$. In addition, the abundance of AN sequences longer than 10 monomer units is very small for the copolymers dealt with in this article, and hence the actual correction in $S(4)$ is not necessary.

References

1. Y. Shibasaki, *J. Polym. Sci. A-1*, **5**, 21 (1967).
2. S. Igarashi and H. Kambe, *Makromol. Chem.*, **79**, 180 (1964).
3. I. Uematsu, *Kobunshi*, **15**, 324 (1966).
4. S. Yabumoto, K. Ishii, and K. Arita, *J. Polym. Sci. A-1*, in press.
5. T. Takata, *Kobunshi Kagaku*, **19**, 641 (1962).
6. T. Takata, *Kobunshi Kagaku*, **19**, 653 (1962).
7. T. Takata and I. Hiroi, *J. Polym. Sci. A*, **2**, 1567 (1964).
8. T. Yoshino and H. Kenjo, paper presented at the 16th Kobunshi-Toronkai, Kyushu University, Japan, Oct. 19–21, 1967; *Preprints*, **2**, 116 (1967).
9. T. Otsu, B. Yamada, and M. Imoto, *J. Macromol. Sci.*, **A1**, 61 (1967).

10. S. Makishima, H. Hiarai, and S. Okusawa, paper presented at 18th Annual Congress of the Chemical Society of Japan, Kwansai University, Apr. 2–5, 1965; *Preprints*, p. 54.

11. K. Matsuzaki, T. Uryu, M. Okada, and H. Shiraki, *J. Polym. Sci. A-1*, **6**, 1475 (1968).

12. L. H. Peebles, Jr. and J. Brandrup, *Makromol. Chem.*, **98**, 189 (1966).

13. S. L. Madorsky, *Thermal Degradation of Organic Polymers*, Interscience, New York, 1964, pp. 194–202.

14. H. Nagao, M. Uchida and A. Yamaguchi, *Kogyo Kagaku Zasshi*, **59**, 698 (1956).

15. H. Nagao, M. Uchida and A. Yamaguchi, *Kogyo Kagaku Zasshi*, **59**, 940 (1956).

16. Y. Takayama, *Kogyo Kagaku Zasshi*, **61**, 1021 (1958).

17. H. Zahn and P. Shafer, *Makromol. Chem.*, **30**, 225 (1959).

18. R. B. Beevers and E. F. T. White, *J. Polym. Sci. B*, **1**, 171 (1963).

19. K. Schmieder and K. Wolf, *Kolloid-Z.*, **134**, 149 (1953).

20. G. R. Cotten and W. C. Schneider, *Kolloid-Z.*, **192**, 16 (1963).

Thermogravitational Effect in Macromolecular Solutions

F. S. GAETA and N. M. CURSIO, *International Laboratory of Genetics and Biophysics (C.N.R.), Napoli, Italy*

Synopsis

We have investigated in a thermogravitational apparatus the behavior of solutions containing macromolecular solutes and of suspensions of ultramicroscopic particles such as viruses and ribosomes. We have obtained very high separation ratios with all the solutes studied, the value of the separation being characteristic of each solution. The reproducibility of the results is good, and the dependence on the geometrical and physical parameters involved fits the predictions of the phenomenological theory. Our results prove that fractionation of very high molecular weight particles is feasible by this method, and also that the characterization of the macromolecular species and the determination of the mass and shape of the particles of the solute seem to be within the possibilities of the thermogravitational method when this is applied to very high molecular weight materials.

INTRODUCTION

Since the pioneer works of Ludwig[1] and Soret[2–5] in the last century, the diffusion of solutes in a liquid medium in presence of a thermal gradient has been extensively studied.

If one has two horizontal plane and parallel surfaces, constituting, respectively, the bottom and top of a container filled with a liquid solution, and the upper surface is maintained at a higher temperature than the lower one, heat flows in the interposed liquid in conditions of gravitational equilibrium—that is, in absence of convective motions. (A few exceptions to the latter behavior do exist, water between 0 and 4°C being an important one.) The flow of heat is combined with a flow of matter, the solute migrating towards the cold wall, except in a few cases, so that after a while the solution becomes concentrated near the cold wall and diluted near the hot wall.

Over the past 80 years, continuous attention has been paid by many workers to both the experimental and theoretical aspects of thermal diffusion. There has lately been a revival of interest in the problem since it has started to be treated with the methods of the recently developed nonequilibrium thermodynamics,[6] in which thermal diffusion has become one of the favorite topics.[7–12] Much attention has also been paid to a derived[13] effect—the thermogravitational effect—brilliantly exploited by

Clusius and Dickel[14-16] in gases, and applied to the liquid state first by Korshing and Wirtz[17-21] and immediately afterwards by Clusius and Dickel themselves.[22]

In an apparatus of the thermogravitational kind, the hot and cold walls are so inclined that a convection current develops which constantly brings fresh solution between the plates. These can be placed very close to each other so that strong temperature gradients are produced in the gap and the separation process is therefore much quicker and the unmixing more pronounced.

During the last thirty years more than a hundred papers have been published on this last line of research alone, but no practical application of the effect to systems in the liquid state has yet been found, and the only available theories are empirical, inasmuch as they describe the time dependence of the flow of matter, as well as its dependence from the geometry of the apparatus and from some physical parameters of the solution in terms of a parameter D' (called the coefficient of thermal diffusion) that can be obtained only experimentally. No indication on the way in which D' should be expected to vary, for instance, with the molecular mass of the particles of the solute is given by such theories.

Of the many workers who have studied thermodiffusion in liquid solutions, Debye and Bueche,[23] Emery and Drickamer,[24] Ham,[25] and Whitmore,[26] and later Langhammer[27-30] are among the very few who have worked with relatively high molecular weight materials, indicating the possibility of obtaining fractionation of components having different molecular mass by means of the thermogravitational process.

It would be interesting if the results could be extended to materials of much higher molecular weight, especially those of biological importance like proteins and nucleic acids as well as to ultramicroscopic structures like viruses and ribosomes. Moreover, it would be useful to exploit the observed behavior of the macromolecules themselves in a thermogravitational experiment, to derive from it information on inherently important molecular parameters as the mass and shape of the dissolved particles. This would give us another analytical tool in the field of biochemistry and of the physical chemistry of high polymers. With these aims we undertook the experiments described in the present paper.

THERMAL DIFFUSION METHODS AND PHENOMENOLOGICAL THEORY

Choice of Method

As mentioned above, there are basically two types of apparatus with which one can study diffusion of solutes in the presence of a thermal gradient. One of these consists essentially of two horizontal plates at different temperatures, and in this device every convective motion of the interposed liquid is accurately avoided. The other, instead, uses tilted (or vertical) hot and cold surfaces and the convective motions which arise

arc exploited to bring continuously fresh solution to the region of the thermal gradient.

The few references that we could find in the literature to other workers who have investigated the behavior of rather big molecules in thermal diffusion experiments practically all referred to experiments performed with apparatus of the thermogravitational kind,[23,27-30] the only exceptions to this being the studies by Emery and Drickamer,[24] and Whitmore,[26] who employed an apparatus of the Soret type in a study on solutions of polystyrene in toluene and in other nonaqueous solvents. Furthermore, the thermogravitational kind of apparatus gives comparatively greater separations in a shorter time. In view of these considerations we decided to construct an apparatus of the thermogravitational type for our first investigation, notwithstanding the relatively low degree of precision obtainable with such an apparatus.

Phenomenological Theory of the Thermogravitational Method

A satisfactory phenomenological theory of the thermogravitational apparatus was established by de Groot[31,32] following the line of thought already developed by Hiby and Wirtz[33] and extending to the liquids the ideas of W. H. Furry et al.[34] Here we can only briefly state the basic assumptions of de Groot's theory and the conclusions arrived at, in the form of working equations.

The result of a thermogravitational run is basically the production of a certain degree of unmixing between solute and solvent, in general the solute being pushed towards the cold plate and brought into the lower reservoir, while the solvent, remaining near the hot wall, is conveyed to the upper reservoir. The fresh solution arriving between the plates from the reservoirs undergoes the same process and the concentration of the solute is therefore gradually increased in the lower reservoir and decreased in the upper one.

This process goes on until the concentration difference in the reservoirs becomes equal to the maximum separation that can be produced by thermal diffusion in the solution during the time of flow between the plates. The degree of unmixing of solute and solvent can be conveniently expressed in terms of the ratios C_i/C_0 and C_s/C_0, where C_0 is the initial concentration (in grams per cubic centimeter) and C_i and C_s are the concentrations in the upper and lower reservoirs, respectively. Other convenient expressions are the "separation ratio" C_i/C_s and the "reduced separation ratio" $[(C_i/C_s) - 1]$.

Two groups of parameters influence the separations obtained, and one, which we could call of the group of "external" parameters, is constituted by the dimensions of the apparatus, the angle of inclination given to the plates, the average temperature, and the temperature difference applied, while the other comprises such intrinsic properties of the system under study as the viscosity and thermal expansion coefficient of the solution and the concentration of solute, as well as the molecular characteristics of

solvent and solute. The effects of the interaction of the thermal gradient with the dissolved particles are then described in terms of a coefficient D' (in square centimeters per second per degree) which is called the coefficient of thermal diffusion, alternatively described in terms of the Soret coefficient s, which is defined as the ratio of the coefficient of thermal diffusion D' to the coefficient of isothermal diffusion D (in square centimeters per second). The dimensions of s are therefore equal to the inverse of a temperature.

If one supposes that D and D' (and hence s) are independent of the concentration (which, particularly in the case of macromolecular solutes, will be true only in the range of very small concentrations), if the temperature gradient is assumed to be uniform between the plates and the hydrodynamic flow of the liquid is laminar, and if the whole process is approximately stationary, then the ratios C_i/C_s and C_s/C_0 vary in the course of time as:[32a]

$$C_i/C_0 = 1 + \tanh\alpha(1 - e^{-\gamma \cot h\alpha})$$
$$C_s/C_0 = 1 - \tanh\alpha(1 - e^{-\gamma \cot h\alpha}) \tag{1}$$

with

$$\alpha = 252\eta D'h/\beta\rho g a^4 \tag{2}$$

and

$$\gamma = (\beta\rho g b a^3 D't/720VD)(\Delta T)^2 \tag{3}$$

where h is the height of the plates; b is the width of the plates; a is the distance between the hot and cold plate; V is the volume of the reservoirs; ΔT is the temperature difference; ρ, β, and η are, respectively, the density, the coefficient of thermal expansion, and the viscosity of the solution; t is the time of duration of the run (expressed in seconds) and g is the gravitational constant. The calculations quoted above, leading to the expressions (1), (2), and (3) as well as to the expressions (4)–(8), are simplified not taking into account the temperature dependence of the density ρ, of the thermal expansion coefficient β and of the coefficient of diffusion D, so that the values of these parameters which are to be introduced into the expressions are the respective values at a temperature equal to the average of the temperatures of the two plates. The same applies in practice also to the coefficient of viscosity η since the effect of the temperature variation of η involves only small variations of α and γ.[32b] Therefore also the value of η to be used is the one at the average temperature

$$T_{av} = (T_1 + T_2)/2$$

T_1 and T_2 being the temperatures of the hot and cold plate, respectively.

For runs long enough to attain the steady state, one gets[32c]

$$C_i/C_s = e^{2\alpha} = \exp\{504\eta D'h/\beta\rho g a^4\} \tag{4}$$

while for short runs the "reduced separation ratio" is given by[32d] $C_i = 1 + \gamma$; $C_s = 1 - \gamma$; consequently:

$$(C_i/C_s) - 1 \simeq 2\gamma = (\beta\rho g b a^3 D't/360\eta VD)(\Delta T)^2 \tag{5}$$

and hence

$$s = (D'/D) = (360\eta V/\beta\rho g b a^3 \Delta T^2)[(C_i/C_s) - 1](1/t) \qquad (6)$$

in such a way that the Soret coefficients can be calculated, in the course of short runs, by measuring reduced separation ratios in function of time and temperature difference between the plates. The thermal diffusion coefficient D' can be obtained from runs of long duration and then, through the value of the ordinary diffusion coefficient D, the Soret coefficients can be independently calculated again.

EXPERIMENTAL

Design of Apparatus

We used two apparatuses, henceforth referred to as numbers 1 and 2, both following substantially the design of the separation column described by de Groot in his thesis.[32] The theory outlined above is therefore directly applicable to our results.

Apparatus 1 (Figs. 1 and 2) was made of two thick brass plates, each one having a plane surface coated with a thick silver layer and then highly polished to 1 μ or more. The two polished surfaces were placed one in
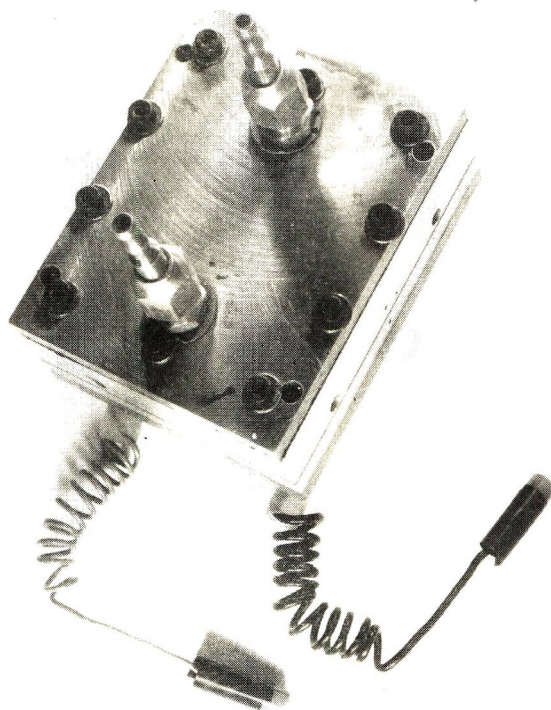

Fig. 1. Thermogravitational apparatus 1, assembled.
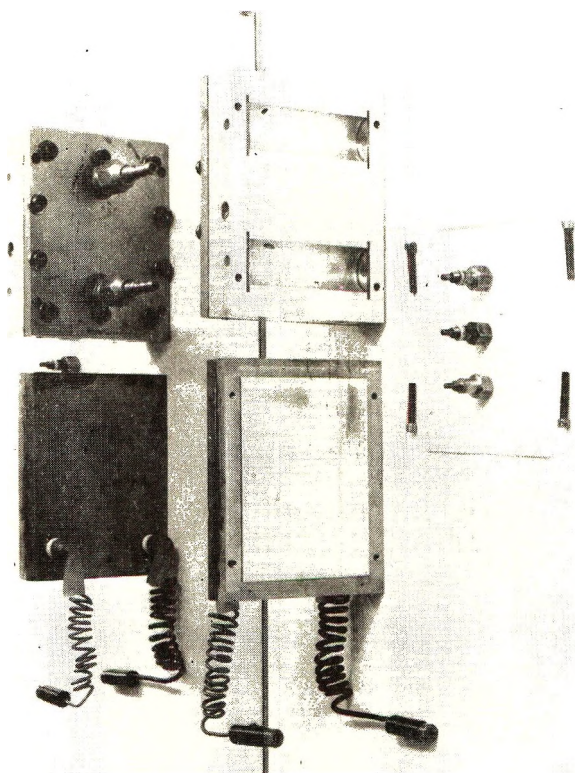
Fig. 2. Thermogravitational apparatus 1, disassembled.

front of the other and held parallel at a small distance adjustable by means
of a gasket (hard rubber, Teflon, or polyethylene) and positioning screws;
by varying the thickness of the gasket the distance between the surfaces
could be adjusted to different values. Before each run the distance a
between the two surfaces facing each other was measured by means of a
micrometer with a precision of ±0.002 cm. One plate was heated by an
electric 1-kw resistance and, since the power in it could be regulated, the
temperature of the hot surface could be fixed at any desired value within a
wide range.

At the back of the cold plate 45 channels were machined, through which
cold water is circulated. (The cooling water was circulated in a closed
circuit comprising a cooling unit so that the temperature of the cold wall
could also be varied within a certain range, if required.) Into this same
plate, which is 2.4 cm thick, two semicylindrical reservoirs were machined;
the volume of each was $(15.2 + 2.2 \, a.b)$ cm^3.

Three holes fitted with sealing nuts were also provided, one leading into
the upper reservoir and two into the lower, for filling and sampling of the
solutions.

The whole apparatus was mounted on a tilt-plane resting on micrometric screws, with which a small inclination can be given to the whole apparatus (4° in most runs) so that the hot surface is higher than the cold one. A series of automatic control and measuring devices was also built, to check the temperatures and the flow of the cooling fluid and to allow the necessary securities during the overnight runs. At the end of each run, specially built syringes could be fitted to each of the three holes so that samples of the liquid could be drawn for analysis; the tip of each needle was able to reach fixed positions within the reservoirs..

Apparatus 2 was essentially identical to apparatus 1, apart from some modifications to be discussed later.

Making a Run

Each part of the apparatus was well washed in a mildly alkaline bath, followed by rinsing with water, then alcohol, and finally distilled, deionized water. The apparatus was then assembled and filled with the solution under study. Whenever possible the solvent was boiled just before preparing the solution and the run be started immediately after, because in
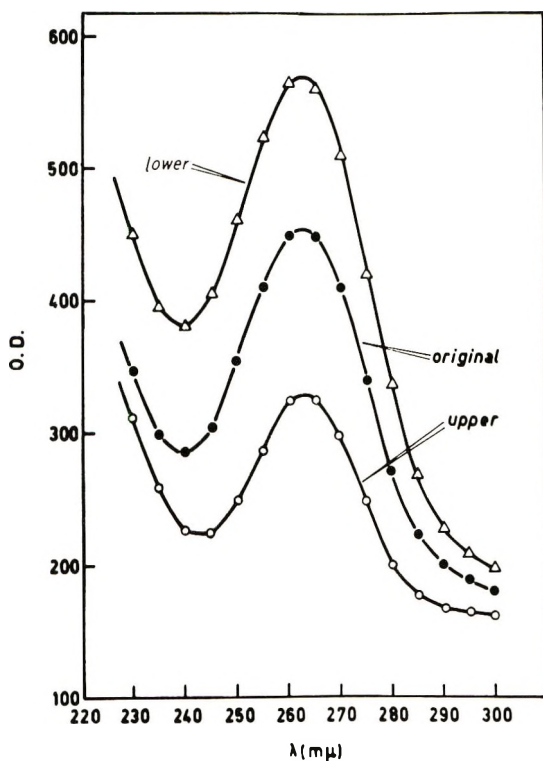

Fig. 3. Absorption spectra: (●) original DNA solution, before being run; (△) enriched DNA solution, derived at the end of the run from the lower reservoir; (○) impoverished DNA solution, derived at the end of the run from the upper reservoir.

this way the formation of bubbles on the working surfaces was avoided or strongly reduced and one of the major sources of error in this way eliminated.

After filling of the apparatus, the cooling and heating systems were connected, the apparatus was tilted the desired amount, the thermocouples and the resistance thermometer inserted, and after 4–5 min a stationary state in the flow of heat was reached, as evidenced by the constancy of the temperatures attained at all points of the apparatus. The automatic control devices were switched on at this point to control the temperature for the rest of the run.   This combined control of heating and cooling allowed us to achieve a stability of 0.5°C over periods of time exceeding 48 hr in some cases.   At the end of the run a sample of approximately 1 ml was withdrawn from the apparatus by means of a syringe inserted in the upper filling hole, and an equal amount of liquid was then withdrawn from the lower reservoir through the middle filling hole.

The adsorption spectrum of each of the two samples was then determined by means of a spectrophotometer and compared with the spectrum of the original untreated solution.   In this way not only was the separation of the solvent from the solution measured, but also contamination or alteration of the materials produced during the run was detected.   Figure 3 shows a typical absorption spectrum of each of the three samples analyzed in a run with DNA.   When necessary, other kinds of measurement were also carried out, as reported later.

Materials and Methods

The deoxyribonucleic acid (DNA) used in our experiments was derived from two sources: the sperm of the sea urchin *Arbacia lixula* and coliphage T4.   The extraction of DNA from these was carried out with a method employing SDS and cold phenol[35] and yielded high molecular weight DNA. For each of our preparations, the determination of the molecular weight was made by determining the coefficient of sedimentation in a Spinco Model E analytical ultracentrifuge and by successive applications of the equation of Mendelkern and Flory[36,37] in the simplified form elaborated for DNA by Rice and Doty.[38]   The T4 coliphages were produced in a single preparation at a final titer of 5×10^{12} phage particles/ml, by the standard procedure, and then stored in the cold.   All experiments with phage were made with particles derived from this original preparation.

Ribosomes were derived from *E. coli*, Cambridge strain MRE600, which are RNAase−. The *E. coli* were grown in Medium L during the logarithmic phase.   The bacteria were mechanically disrupted by grinding with alumina (Alcoa) in 10^{-2} N Tris buffer of pH 7.4 plus $MgCl_2$, $2.5 \times 10^{-4}N$. After repeated centrifugation, treatment with DNAase, resuspension and recentrifugation, a pellet of separated 30 S and 50 S ribosomes was obtained. The runs in our thermogravitational apparatus were made by resuspending the ribosomes in the Tris buffer used for the preparation.

To understand better the results to be presented here, one should re-

member that, according to current views, the two ribosomal subunits (the 30 S and 50 S) are extremely similar in composition (both being super-molecular aggregates of protein and RNA, of not too different a shape, and both being assimilable to a prolate ellipsoid) and that the 50 S material has about twice the molecular mass of the 30 S particles. In our case the weights proved to be ~1.8 × 10^6 and ~0.9 × 10^6, respectively. Other materials, such as hemoglobin and high molecular weight dextrans, were obtained from current commercial sources.

RESULTS

Solutes of Small Molecular Weight

A thermogravitational device of the kind built by us contains many adjustable parameters, the optimal value of which must be found empirically. Most important among these are the distance a between the plates and the inclination θ given to the apparatus. Both these affect strongly the flow of the solution in the gap between the plates; we therefore investigated these points carefully.

We used a CuSO$_4$ solution and made a series of runs of fixed duration at a fixed value of θ, varying the parameter a by using gaskets of different thickness, and measuring a in the way described above in the section dealing with design of the apparatus. We found that maximal separations of the solute from the solution were obtained by using a value of $a = 0.045$ cm. Above or below this value the separation was found to decrease very quickly.

As for the influence of the angle of inclination θ, we found that a 4° inclination gave satisfactory results and varying θ between 3° and 5° left the results practically unchanged. Angles smaller than 2° often (but not always) upset the hydrodynamic flow of the solution in the gap, resulting in the mixing of the ascending and descending currents, with consequent failure of the run, while at inclinations greater than 5° the time taken to achieve equilibrium increased. We therefore decided, in the following experiments, to adopt a fixed inclination of 4° in all our runs with only very few exceptions. We also checked that the optimal values of a and θ remained the same for all durations of the runs.

Two other geometrical parameters which influence[31,32] the results are the length h of the gap between the two flat plates and the volume V of the reservoirs [see eqs. (2)–(6)]. In our apparatus 2 both these parameters were varied with respect to those in apparatus 1 and, in addition, we investigated separately the effect of altering the volume V alone, in each of our two models, by adding material on the walls of the existing reservoirs. This decrease of V has the effect mainly of decreasing the time needed to reach the stationary state, although too much reduction of the volume of the reservoirs or altering their shape occasionally leads to irregularities of function appearing in the form of reduced separations and inequality of percentage decrease of concentration in the upper reservoir with respect to

increase of concentration in the lower one The reason for this must be the formation of zones of incomplete mixing of the solution flowing from the gap into the reservoirs with the material already contained in them.

The decrease of h from 9 to 5.5 cm in model 2 with respect to model 1 had the effect of slightly decreasing the time needed to achieve the equilibrium separation, without noticeably altering the value of the final separation itself.

Quantitatively, all the separations obtained in the runs with $CuSO_4$ compared well with the results found, for instance, by de Groot[32] with the same substance.

Macromolecular Solutes

Having obtained results similar to the ones found in the literature for solutes of small molecular weight, we proceeded to experiment with macromolecular substances.
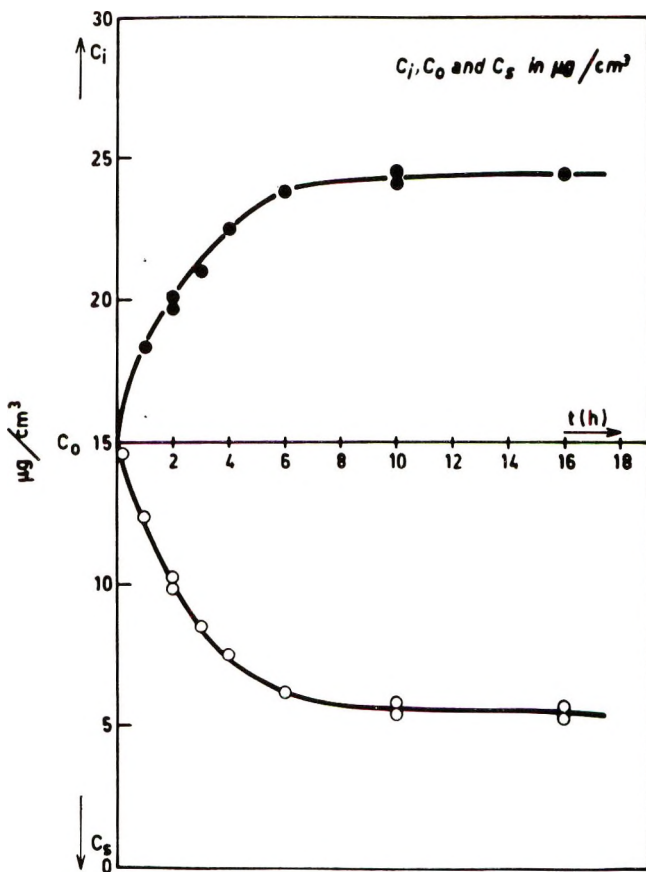

Fig. 4. Concentrations of DNA solutions contained in the upper and lower reservoirs, after runs of various duration: (●) solutions from the lower reservoir; (○) solutions from the upper reservoir. The concentrations were obtained through spectrophotometric analysis of the kind described in Fig. 3.
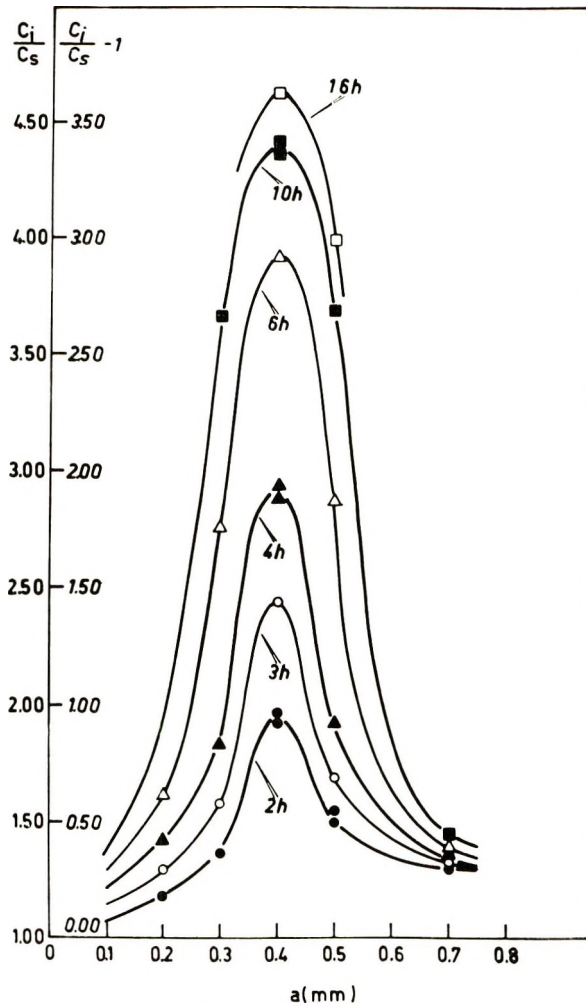
Fig. 5. Separation ratios C_i/C_s and reduced separation ratios $(C_i/C_s) - 1$ as a function of the distance a between hot and cold plate, for various durations of the runs: (●) 2 hr; (○) 3 hr; (▲) 4 hr; (△) 6 hr; (■) 10 hr; (□) 16 hr.

We used DNA having a molecular weight of 10^7 and extracted from sea urchin sperm as described in the materials and methods section, which was then denatured by heating for 15 min at 90°C before being introduced into our thermogravitational apparatus for a run. The denatured material is a skein of a single-strand DNA tightly wound on itself in a nearly spherical coil of molecular weight $\sim 5 \times 10^6$; when run in our apparatus it gave the results summarized in Figures 5–9. Subsequently, DNA extracted from coliphage T4 treated in a similar way gave analogous results, not included among these data. In each case the denatured DNA was suspended in a $0.15N$ sodium chloride–$0.015N$ sodium citrate (SSC) buffer solution.
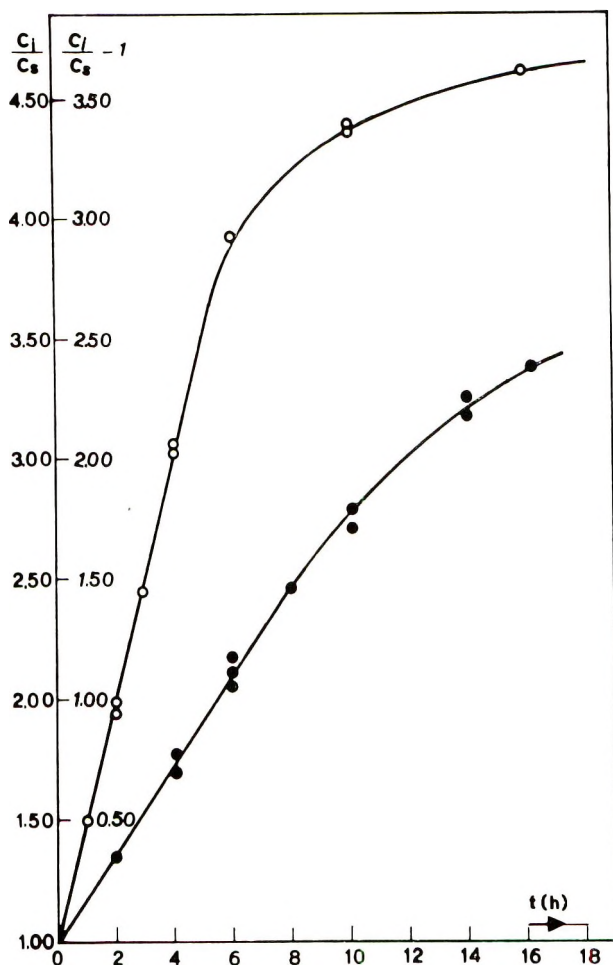
Fig. 6. Separation ratios C_i/C_s and reduced separation ratios $(C_i/C_s) - 1$, in function of the duration of the runs: ($\circ$) $\Delta T = 30°C$; ($\bullet$) $\Delta T = 20°C$. The values at $\Delta T = 30°C$ are the ones of Figure 5 corresponding to the value of $a = 0.04$ cm.

From an examination of these results and by comparison with the data found in the literature, one notices at once that our separation ratios C_i/C_s are bigger than any found with materials of smaller molecular weight.

In Figure 4 are plotted the concentrations of DNA reached in the upper and lower reservoirs after runs of increasing duration. In each of these runs the initial concentration of DNA in the solution was 15 $\mu g/cm^3$, and all runs were made under the same experimental conditions.

In Figure 5 the ratios C_i/C_s and $(C_i/C_s) - 1$ [see eq. (5)] are plotted against the values of a for different durations of the runs. While the values of the separation ratios are higher than those obtained with materials of smaller size, the dependence on a is qualitatively the same as for the latter. In particular, the highest separations are found at a value of
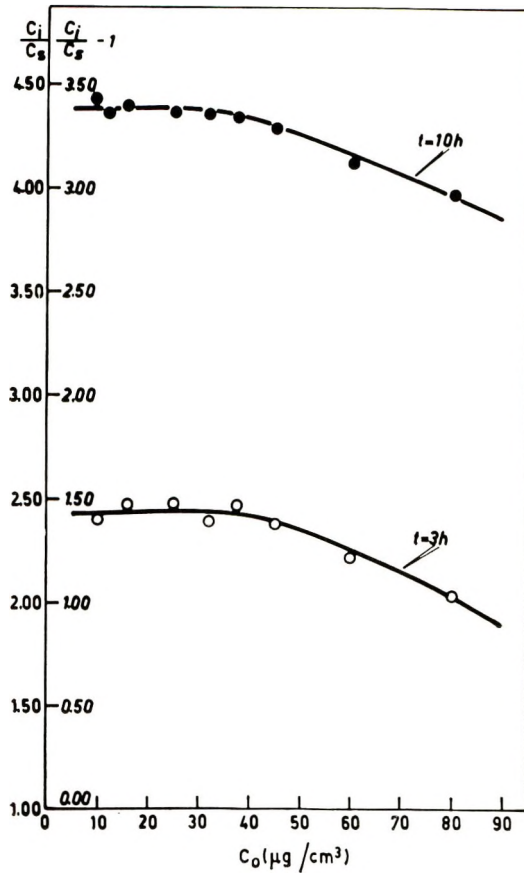
Fig. 7. Concentration dependence of the separation ratios for DNA solutions: (○) at $t = 3$ hr; (●) at $t = 10$ hr.

$a = 0.04$ cm, and above or below this value the separation ratios decrease as predicted by the phenomenological theory. Indeed this theory[32] predicts an increase of the separation ratio with a^3 for small a, and a decrease with a higher power of a for values of this parameter greater than optimal.

Now, a characteristic time θ can be defined for each given set of values of the "external" and "intrinsic" parameters. The theory gives the following expression for θ:

$$\theta = (V/H) \tanh \alpha \tag{7}$$

where V is the volume of the reservoirs, α is given by eq. (2) and H is given by:

$$H = (1/362880)(\beta \rho g/\eta)^2 (1/D) b a^7 (\Delta T)^2 \tag{8}$$

A run can be considered short if its duration is $t \ll \theta$ and long when $t \gg \theta$.

In Figure 6 the separation ratios and reduced separation ratios obtained with denatured DNA and corresponding to $a = 0.04$ cm are plotted against the duration of the run for the temperature differences $\Delta T' = 30°C$ and $\Delta T = 20°C$. Equation (5), which is valid for runs of short duration, predicts a linear dependence on time, and one can see that the curve corresponding to $\Delta T' = 30°C$ is indeed linear up to 5–6 hr of run, while the one corresponding to $\Delta T = 20°C$ is linear up to 11 hr, in very good accord with eqs. (7) and (8); this fact incidentally provides us with an operative definition of the term short referred to the duration of a particular run.

This means that the approximations introduced by de Groot into phenomenological theory to solve the empirical equations can be still considered legitimate in the case of our macromolecular suspensions, since our results check quite well the dependence of the separation ratios on the parameters a, $(\Delta T)^2$, and t, to which they are most sensitive.

A more subtle point arises now: namely, up to which point can we consider our molecular suspensions to be infinitely diluted? Since in our case there is a strong dependence of such important parameters as η on the concentration of the macromolecular component, one has to find an answer to this question by experiment. We therefore conducted a series of runs with varying concentrations of denatured DNA, from 9 $\mu g/cm^3$ up to 80 $\mu g/cm^3$; the results are represented in graphical form in Figure 7. One can see that already at relatively small concentrations (about 40 $\mu g/cm^3$) the solutions show a concentration dependence on the separation ratios, probably entirely due to the increase of η [see eq. (5)] and to its influence on the hydrodynamical flow of the liquid between the plates.

Effect of Difference of Temperature of the Plates

Another point that had to be checked with great care was the dependence of the separation ratios C_i/C_s on the difference of temperature T between the plates. The phenomenological theory [eq. (5)] predicts an increase of the separation ratios proportional to $(\Delta T)^2$. On the other hand, the variation of temperature also affect, various parameters included in the expression given above, especially the viscosity η of the fluid and the diffusion coefficient D. One is therefore compelled to consider whether the proportionality of the separation ratios to $(\Delta T)^2$ predicted by phenomenological theory continues to hold for the case of macromolecular solutions notwithstanding the great influence of the temperature on both viscosity η and diffusion constant D of these solutions.

An analysis of the phenomenological theory as developed by de Groot shows that, in the case of solutions of denatured DNA, and within the limits of the temperature differences used by us, the assumptions underlying the phenomenological theory are still valid and one can use for η and D the values corresponding to the average temperature $(T_1 + T_2)/2$. To check this point we made a series of runs with denatured DNA of molecular weight 5×10^6 at temperature differences of 8, 14, 18, 20, 22, 28, and 30°C, having taken care to assign the temperatures of the hot and cold
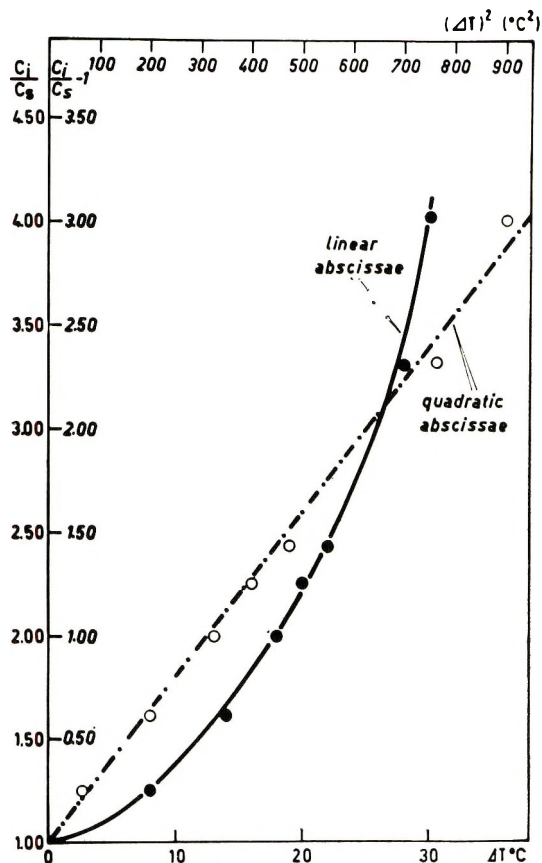
Fig. 8. Separation ratios as a function of the temperature difference ΔT, between hot and cold plate, at constant average temperature: (–·–) linear dependence in $(\Delta T)^2$ (upper scale abscissae); (——) refers to lower scale abscissae, linear in ΔT.

plates in such a way that the average temperature would always be 21°C. In this way the separation ratios of Figure 8 have been obtained, and one can see that the law of proportionality to $(\Delta T)^2$ is rather well satisfied. On the contrary, when the temperature difference is increased while the temperature of the cold plate is kept constant, the separation ratios follow less well the proportionality to $(\Delta T)^2$, as we shall see in the next section.

Dependence of Separation Ratios on the Nature of the Solutes

To investigate the dependence of the separation ratios on the nature of the suspended particles, we made many runs with proteins, polymeric dextrans of high molecular weight, and some supermolecular particles, namely ribosomes and viruses. These experiments were all made with our apparatus 2. It must be remembered, in comparing them with the preceding ones, that at all the different values of T employed, the temperature of the cold plate was always kept constant (at $+8$°C), while the tempera-
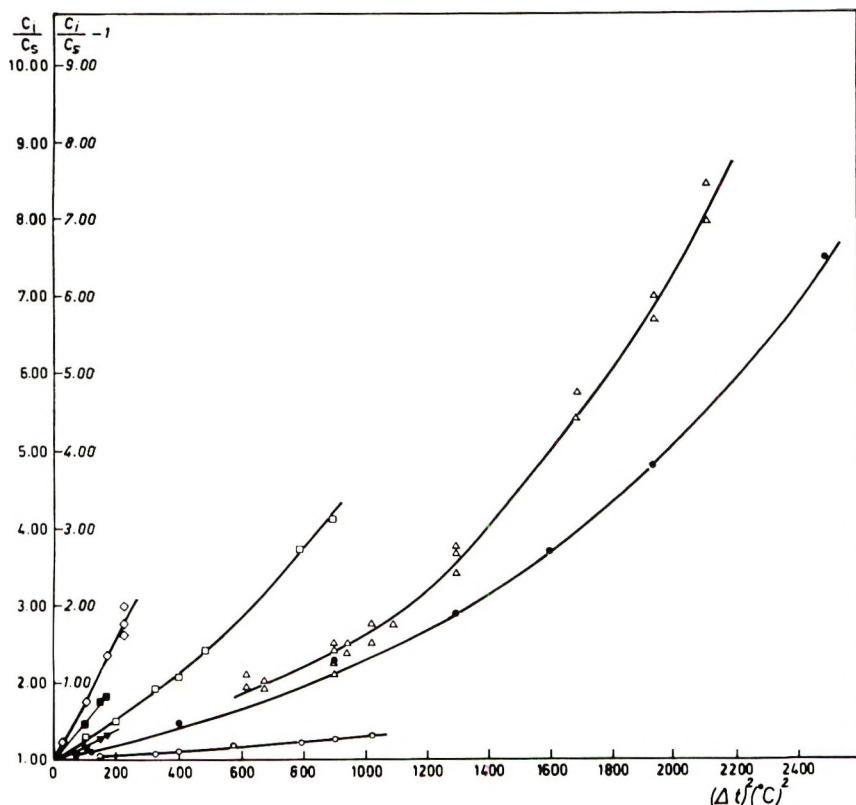
Fig. 9. Separation ratios as a function of the temperature difference ΔT between hot and cold plate. The temperature of the cold plate is held constant. For description of the characteristics of the various materials see text ($\Diamond$: ϕT_4; $\square$: denatured DNA; $\triangle$: ϕT_4 debris; $\bullet$: dextran 2000; $\bigcirc$: hemoglobin; $\blacksquare$: 50_s ribosomes; $\blacktriangledown$: 30_s ribosomes).

ture of the hot plate was varied, so that the average temperature also varied from one run to another. The results are summarized in graphical form in Figure 9.

One observes the following facts from these results: in the first place, the dependence on the temperature difference no longer follows closely the law of proportionality to $(\Delta T)^2$. This is readily explainable in terms of the variation of the physical properties of the liquid between the plates with increasing temperature and the consequent variation of both the thermal sedimentation of the particles and the hydrodynamical regime of flow of the liquid as a whole.

Much more interesting is the fact that different materials give different separations at all ΔT's employed. As one can see the general tendency is for an increase of the separation ratios with increasing dimensions and increasing density of the suspended particles. Compare, for instance, the results obtained with dextran 2000 and denatured DNA, both having been

run in the same solvent, the DNA being denser than dextran and having a molecular weight about 2.5 times higher.

Particles of T4 virus, which are assemblies of a structurally complex protein coat and a nucleus of high molecular weight, double-stranded DNA, having a total molecular weight of 2.4×10^8, gave by far the highest separation ratios observed. Even if for such massive particles some separation due to their redistribution in the gravitational field is to be expected, this separation would be much smaller than the ones observed in our thermogravitational experiments, furthermore would require much longer time to establish itself, and finally would require a completely
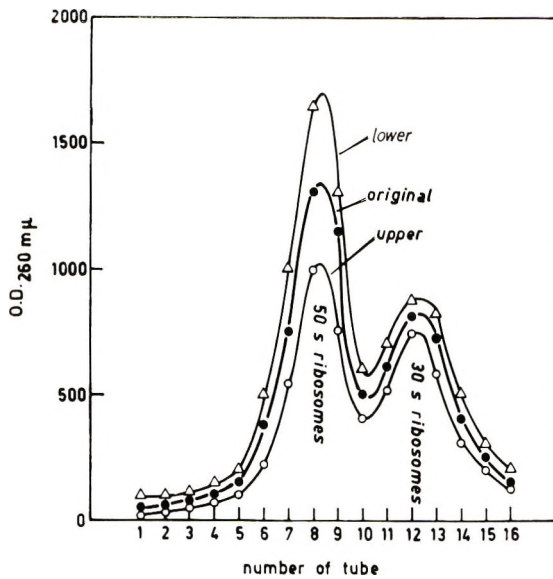
Fig. 10. Ribosomes derived from ($\triangle$) the enriched solution of the lower reservoir and from ($\circ$) the impoverished solution of the upper reservoir are fractionated in a preformed sucrose gradient in a centrifuge tube, and then the fractions are collected in various tubes in order of decreasing sedimentation coefficient.

immobile liquid to form, while the convective movement existing in our apparatus would be sufficient to destroy completely the gravitational separation if one would start the circulation of the liquid by itself after the particles have sedimented. This proves that the separation ratios observed in the case of the T4 viruses must be ascribed to the effect of thermogravitation. Unfortunately we could not employ temperature differences higher than 15°C because the phage particles became disrupted. On the other hand, by predisrupting the phages by osmotic shock prior to introduction into our apparatus, we could study the behavior of these debris to much higher temperatures. This material consists of loose complexes of relatively low-density proteins and DNA having various shapes and masses, these being of the order of 10^6.

The case of *E. coli* ribosomes is also very interesting, even if no direct quantitative comparison with the other materials can be made because, owing to their nature, we had to run the ribosomes in a solvent different from the usual saline solution normally employed. The nature and the mass of these particles, as well as the kind of solvent in which they were run, were described in the section on materials and methods. The results of the thermogravitational runs are represented by the six points in Figure 9, and the detailed analysis of the materials derived from the upper and lower reservoirs of our apparatus after the run is given in Figure 10.

A few drops of the solutions derived from each reservoir were layered on sucrose solution in a centrifuge tube and then spun down for about 2 hr. The tube was then extracted from the centrifuge, punctured on the bottom, and the contents, flowing down drop by drop, collected in successive tubes. The contents of these tubes were then analyzed spectrophotometrically. Hence the optical densities on the ordinates of Figure 10 are proportional to the number of ribosomes of the corresponding layer in the ultracentrifuge tube. As will be seen, heavier particles come down first (tubes 7, 8, and 9) and lighter particles follow later (tubes 11, 12, and 13).

It is important to observe that the separation ratios obtained for the two types of particles, namely the 50 S and the 30 S (run simultaneously in each case), have different values, the value of the separation being 1.7 for the 50 S and 1.18 for the 30 S material. These two values are almost precisely in the same ratio as the sedimentation coefficients of the two types of particles in a centrifugal field: 50 and 30. Now the 50 S and 30 S ribosomes are approximately round particles, both being aggregates of proteins and ribonucleic acid in the same ratio; furthermore, in our runs both kinds of particles were contained in the same solution. The fact that one gets different separation ratios for the two shows that C_i/C_s is dependent on the mass of the suspended particles.

Since the molecular mass does not figure in the phenomenological equations, it must be contained in the coefficient D'. The fact that the ratio of the thermogravitational separations in this case—in which all other factors are the same—turns out to be equal to the ratio of the respective centrifugal coefficients, is obviously an important point that sheds some light on the nature of D'.

DISCUSSION

First we would stress that all the above results agree well with the phenomenological equations worked out for this type of apparatus by de Groot.[31,32] Indeed the dependence of the separation ratios C_i/C_s on a, $(\Delta T)^2$ and t, which are considered crucial tests for the applicability of the phenomenological theory,[30,33] all conform well to the equations worked out.

We can therefore say that the thermogravitational method can be employed to study solutions (or suspensions) of materials having very high molecular weight and a high degree of structural complexity. The

fact that our separation ratios turn out to be higher than any obtained with materials of small molecular weight makes the method particularly appropriate for the study of macromolecules or submicroscopic particles.

Especially interesting is the finding that the separation ratios obtained are dependent on such parameters as the molecular mass and the nature of the suspended particles. Even if these parameters do not figure as such in the phenomenological theory, this finding does not contradict our previous statement that the phenomenological theory applies to our case, since molecular mass and shape are indeed included in the coefficient of thermal diffusion D'. The fact that molecular parameters are determinant of the value of D'—or of the separation ratios, which is the same—not only confirms that fractionation of different molecular species is feasible by the thermogravitational method also in the field of high polymers, as already proposed by some other workers,[24,27] but also that this method can be applied to another, completely new, and subtle purpose, namely the characterization of macromolecular species in terms of the observed C_i/C_s and also perhaps the determination of specific molecular parameters and their dependence on the nature of the solvent.

The development of such a new tool in high polymer science and in biological and biochemical research seems to be very attractive, and we intend to devote more effort in this field. The different materials must be studied systematically with respect to each of the structural parameters playing a role in the phenomenon of thermal diffusion.

More advanced apparatus must be developed, from which more accurate and complete data can be obtained. Furthermore, for the fulfilment of our program a good phenomenological theory is not sufficient—what one needs is an understanding of the nature of the physical forces responsible for the sedimentation of particles in a thermal gradient. In other words one must be able to explain in physical terms the dependence of D' on molecular properties. The preliminary results presented in this paper have already given us useful indications of the physical nature of the forces responsible for thermodiffusion. These indications will doubtlessly contribute to the development of a more satisfactory theoretical approach.

References

1. C. Ludwig, S-B *Akad. Wiss.*, Wien, **20**, 539 (1856).
2. Ch. Soret, *Arch. Sci. Phys. Nat.*, Genève (*3*), **2**, 48 (1879).
3. Ch. Soret, *C. R. Acad. Sci.* (Paris), **91**, 289 (1880).

4. Ch. Soret, *Arch. Sci. Phys. Nat., Genève* (3), **4**, 209 (1880).

5. Ch. Soret, *Ann. Chim. Phys.* (5), **22**, 293 (1888).

6. D. D. Fitts, Nonequilibrium Thermodynamic, McGraw-Hill, New York, 1962, p. 101ff.

7. R. L. Saxton, E. L. Dougherty, and H. G. Drickamer, *J. Chem. Phys.*, **22**, 1166 (1945).

8. R. L. Saxton and H. G. Drickamer, *J. Chem. Phys.*, **22**, 1287 (1954).

9. W. M. Rutherford and H. G. Drickamer, *J. Chem. Phys.*, **22**, 1284 (1954).

10. W. M. Rutherford, E. L. Dougherty, Jr., and H. G. Drickamer, *J. Chem. Phys.*, **22**, 1289 (1954).

11. E. L. Dougherty, Jr. and H. G. Drickamer, *J. Chem. Phys.*, **23**, 295 (1955).

12. I. Prigogine, *Introduction to Thermodynamics of Irreversible Processes*, Thomas, Springfield, Ill., 1955.

13. S. R. de Groot, *Thermodynamics of Irreversible Processes*, Interscience, New York, 1951.

14. K. Clusius and G. Dickel, *Naturwiss.*, **26**, 546 (1938).

15. K. Clusius and G. Dickel, *Z. Phys. Chem.* (Leipzig) **B44**, 397 (1939).

16. K. Clusius and G. Dickel, *Naturwiss.*, **27**, 487 (1939).

17. H. Korsching and K. Wirtz, *Naturwiss.*, **27**, 110 (1939).

18. H. Korsching and K. Wirtz, *Naturwiss.*, **27**, 267 (1939).

19. H. Korsching and K. Wirtz, *Angew. Chem.*, **52**, 499 (1939).

20. H. Korsching and K. Wirtz, *Abh. Preuss. Akad. Wiss.*, No. 3 (1939).

21. H. Korsching and K. Wirtz, *Ber. Dtsch. Chem. Ges.*, **73**, 249 (1940).

22. K. Clusius and G. Dickel, *Naturwiss.*, **27**, 148 (1939).

23. P. Debye and A. M. Bueche, *High Polymer Physics*, H. A. Robinson, Ed., Chemical Publishing Co., Brooklyn, 1948, pp. 497–527.

24. A. H. Emery and H. C. Drickamer, *J. Chem. Phys.*, **23**, 2252 (1955).

25. J. B. Ham, *J. Appl. Phys.*, **31**, 1853 (1960).

26. F. C. Whitmore, *J. Appl. Phys.*, **31**, 1858 (1960).

27. G. Langhammer, *Naturwiss.*, **41**, 525 (1954).

28. G. Langhammer and K. Quitzsch, *Makromol. Chem.*, **17**, 74 (1955).

29. G. Langhammer, *Kolloid-Z.*, **44**, 146 (1956).

30. G. Langhammer, *J. Chim. Phys.*, **54**, 885 (1957).

31. S. R. de Groot, *Physica*, **9**, 801 (1942).

32. S. R. de Groot, *L'Effet Soret. Diffusion Thermique dans les Phases Condensées*, Academisch Proefschcift, North Holland, Amsterdam, 1945, (a) p. 94, eqs. (216) and (217); (b) pp. 95–97; (c) p. 98, eq. (238); (d) p. 98, eqs. (234) and (235); (e) p. 112.

33. J. W. Hiby and K. Wirtz, *Physik. Z.*, **41**, 77 (1940).

34. H. W. Furry, R. C. Jones, and L. Onsanger, *Phys. Rev.*, **55**, 1083 (1939).

35. S. Aurisicchio and G. Quagliarotti, in press.

36. L. Mandelkern and P. J. Flory, *J. Chem. Phys.*, **20**, 212 (1952).

37. L. Mandelkern, W. R. Krigbaum, H. A. Sheraga, and P. J. Flory, *J. Chem. Phys.*, **20**, 1392 (1952).

38. P. Doty, B. B. McGill, and S. A. Rice, *Proc. Nat. Acad. Sci.*, U. S., **44**, 432 (1958).

Dehydration Kinetics and Glass Transition of Poly(acrylic Acid)

A. EISENBERG and T. YOKOYAMA,* *Department of Chemistry, McGill University, Montreal, Canada* and EMMA SAMBALIDO, *Department of Chemistry, University of California, Los Angeles, California*

Synopsis

The kinetics of dehydration and decarboxylation as well as the glass transition temperature as a function of anhydride content were measured for poly(acrylic acid). It was found that the glass transition of PAA is of the order of 103°C and increases with increasing anhydride content, reaching an extrapolated value of 140°C for the pure linear anhydride. Anhydride formation is a first-order reaction, as is also decarboxylation, the latter being much slower than the former. The rate constants are for dehydration, $k_a = 2.5 \times 10^9 \exp\{-26000/RT\}$; for decarboxylation, $k_d = 2.9 \times 10^8 \exp\{-27000/RT\}$. Anhydride formation occurs primarily by an intramolecular process.

INTRODUCTION

Acrylic and methacrylic acid are two of the most important constituents of ionic polymers. In recent years, interest in the bulk properties of these polymers has increased sharply, as evidenced in several publications[1–5] and a symposium.[6] Since the authors hope, as part of systematic study of ionic forces in polymers,[5,7] to investigate some viscoelastic and thermal properties of ionized acrylic acid and some of its copolymers, it was thought advisable first to study the un-ionized homopolymer itself.

This article will report our work on the glass transition of the polymer and partial anhydride as well as on the rate of anhydride formation in the material, and also give some speculations on the mechanism of anhydride formation. The problem of the glass transition interested us because literature values as divergent as 88 and 166°C have been reported.[8,9] The study of the kinetics of anhydride formation was important because ionization of the material increases the glass transition temperature drastically, and, for partially ionized polymers, drying of the resultant material leads to some dehydration. It is therefore important to know the kinetic factors of the anhydride formation to insure a minimum of structural change consistent with maximum of dryness.

The results of the work indicate that (1) the glass transition of PAA is of the order of 103°C and increases with increasing anhydride concentration; (2) that the anhydride formation occurs by a first-order process and thus

* Present address: Kyushu University, Fukuoka, Japan.

seems to be quite different from the process in poly(methacrylic acid);[10] (3) that it occurs primarily by intramolecular reactions; and finally (4) that decarboxylation also occurs simultaneously with water elimination, but at a very much slower rate. While many of these facts may have been known qualitatively,[11] we could find no description of quantitative work on the kinetics of anhydride formation or the glass transition as a function of anhydride content.

EXPERIMENTAL PROCEDURES

Polymerization

The acrylic acid (Matheson, Coleman and Bell) was distilled, and the fraction boiling at 54°C under pressure of 22 mm Hg was collected and stored in the dark, at low temperature, until used.

The polymerization was carried out by dropwise addition of a solution of benzoyl peroxide to an agitated refluxing solution of acrylic acid in benzene. The polymer precipitated during polymerization; it was collected, washed three times with benzene, dried in vacuum at 97°C for two days, and stored over P_2O_5. The polymer as well as the filtrate proved to be free from unsaturation by use of bromine as well as by infrared spectroscopy. The molecular weight, as determined by intrinsic viscosity from the equation,[12] $[\eta] = 8.5 \times 10^{-4} M^{1/2}$, ranged from 1.80×10^4 to 3.13×10^5, depending on the concentration of initiator.

Dehydrations

The dehydrations were carried out by passing nitrogen through a sample of powdery polymer until the desired weight loss was achieved. The dehydration temperatures depended on the experiment. For glass transition samples they were 170°C, for stress relaxation 125°C, and for the kinetic runs 140, 155, and 170°C.

Glass Transition Measurements

The partially dehydrated powders obtained by the above procedure were molded in a cylindrical sample mold at 132°C under a calculated pressure of ca. 10000 kg/cm² (the actual pressure on the sample was undoubtedly lower). The resultant cylinders were brownish and translucent. The glass transitions were determined on an instrument and by a technique described before,[13] which is based on the determination of the linear expansion coefficient of the material.

Stress Relaxation

The samples for stress relaxation were prepared by molding of undehydrated PAA (at 153–171°C and ca. 700 kg/cm²) and subsequent dehydration. The runs themselves were performed in a vacuum instrument which was described briefly before.[14]

Spectroscopic Studies

Infrared spectra of PAA and dehydrated PAA were measured by using a KBr pellet technique and the Perkin-Elmer Model 21 spectrophotometer. In the preparation of the specimens care was taken to prevent absorbtion of water from the atmosphere.

Kinetic Studies

The precise kinetic runs were performed on a sample of PAA in powder form.   The polymer was embedded in glass wool, maintained at a constant temperature, and preheated N_2 was passed slowly through the material.   The N_2 flowing out of the polymer tube was passed through Anhydrone (anhydrous magnesium perchlorate) and through Ascarite (NaOH-coated asbestos) to determine the amount of H_2O and CO_2 evolved. The Anhydrone and the Ascarite were weighed periodically, as was also the tube containing the polymer, so that plots of total weight loss, loss of H_2O, and loss of CO_2 could be obtained separately.   Runs were performed at three temperatures, 140, 155, and 170°C.

RESULTS

Glass Transition Temperature

Figure 1 reproduces the results of the glass transition temperature as a function of percentage weight loss.   The value of 103°C obtained for the zero weight loss sample agrees well with that of 106°C obtained by Hughes
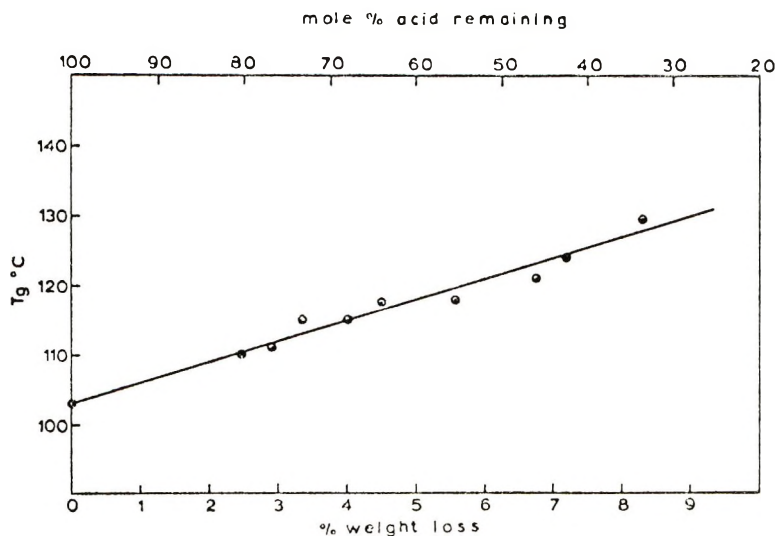
Fig. 1. T_g vs. per cent weight loss or mole-% acid remaining in partially dehydrated poly(acrylic acid).

and Fordyce.[15] The relation between anhydride concentration and T_g seems to be linear, extrapolating to a value of 140°C for the pure anhydride.

One drying run for a prolonged period under less well controlled conditions yielded values of the order of 180°C for the glass transition. This will be discussed once our view of the dehydration mechanism has been presented.

Stress Relaxation

The results of the stress relaxation runs at 125°C for a sample stored for successively longer periods are shown in Figure 2. Curves 1–9 were
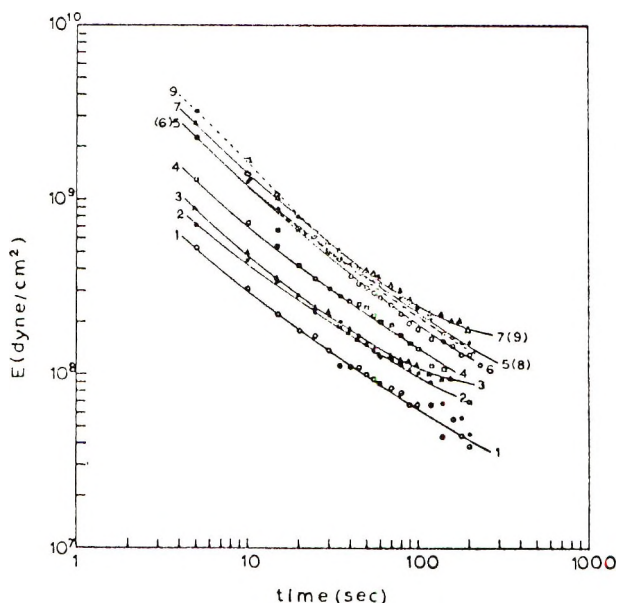
Fig. 2. Stress relaxation curves as a function of storage time at 125°C for PAA, log $E_r(t)$ vs. log t: (1) 1.5 hr; (2) 4.0 hr; (3) 6.5 hr; (4) 14.0 hr; (5) 24.0 hr; (6) 35.0 hr; (7) 46.0 hr; (8) 55.0 hr; (9) 720 hr.

obtained for storage times after insertion into the oven ranging from 1.5 to 720 hr. It is perhaps useful to present the change in the isochronal (here 10-sec) modulus with storage time, and this is done in Figure 3. Because of the relatively rapid change of the modulus with storage time even at 125°C, a temperature relatively close to T_g, it seems useless to attempt the construction of a master curve for the material.

Spectroscopy and Elemental Analysis

The weight loss of the samples upon heating, the change in T_g, and the change in the relaxation modulus suggest that we are most probably observing the formation of the anhydride. This is confirmed by elemental
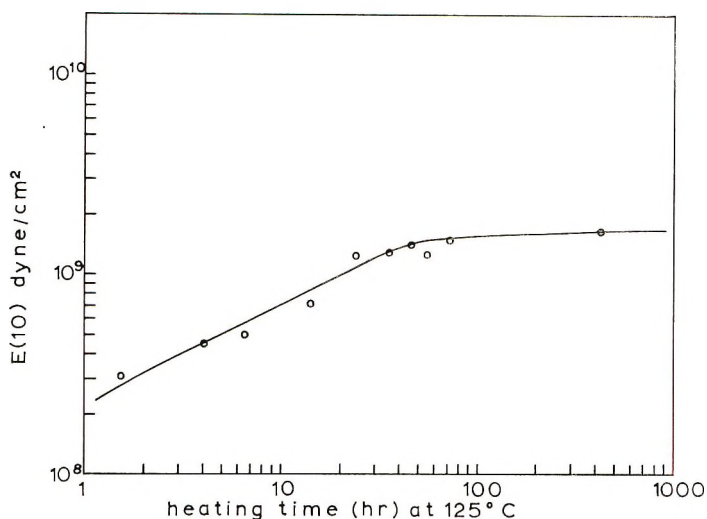
Fig. 3. Isochroual (10-sec) modulus vs. storage time for PAA log E_r (10) vs. log t.

analysis and spectroscopic studies. The results of the elemental analysis for a dry PAA sample and for one heated at 155°C for 43 hr are shown in Table I and compared with those calculated for the complete anhydride. It is clear that the heated sample corresponds much more to the anhydride than to the pure PAA. The discrepancy, particularly in the C content, will be discussed later in terms of partial anhydride formation.

The change in the infrared spectra upon heating is shown in Figure 4a and 4b. Figure 4a shows the results for dry PAA, while spectrum 4b has been obtained from a material heated at 155°C for 43 hr. It is seen that the relatively sharp carbonyl band of the original PAA (at 1700 cm^{-1})[16] becomes weak, and new bands appear at 1750 and 1800 cm^{-1}. These bands can safely be assigned to the carboxylic anhydride group.[16] The new band at 1020 cm^{-1} is also assigned to C—O—C bending vibration of the acid anhydride.[16] Finally, in the 3μ region, the —COOH band of PAA has nearly completely disappeared in the heated material.

TABLE I

	C, %			H, %		
	Found	Calcd		Found	Calcd	
PAA	49.71, 49.73	50.00		6.06, 6.01	5.60	
PAA heated at 155°C for 43 hr	56.02	57.14[a]	56.06[b]	5.18	4.80[a]	4.92[b]

[a] Assuming complete dehydration.

[b] Assuming 86.5% dehydration.
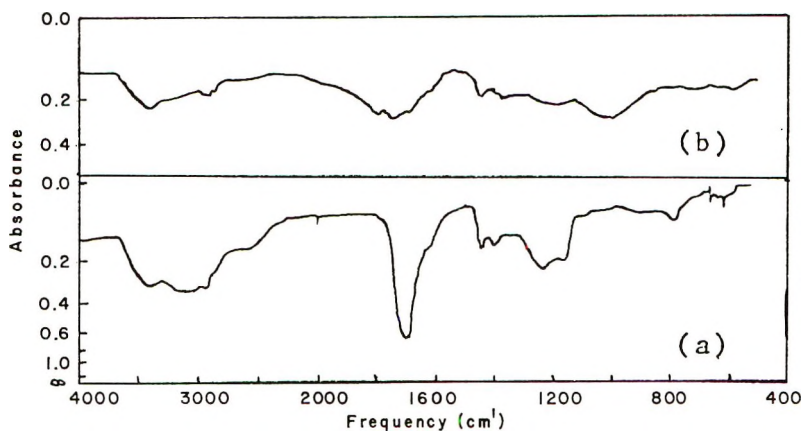
Fig. 4. Infrared spectra of (a) poly(acrylic acid) and (b) the product obtained by dehydration after 43 hr at 155°C.

Kinetic Studies

A plot of total weight loss, loss of H_2O, and loss of CO_2 versus time at 170°C is shown in Figure 5.   It is evident that the sum of the loss of H_2O and CO_2 is smaller than the total weight loss.   However, a plot (not shown) of the difference between total weight loss and the sum of H_2O and CO_2
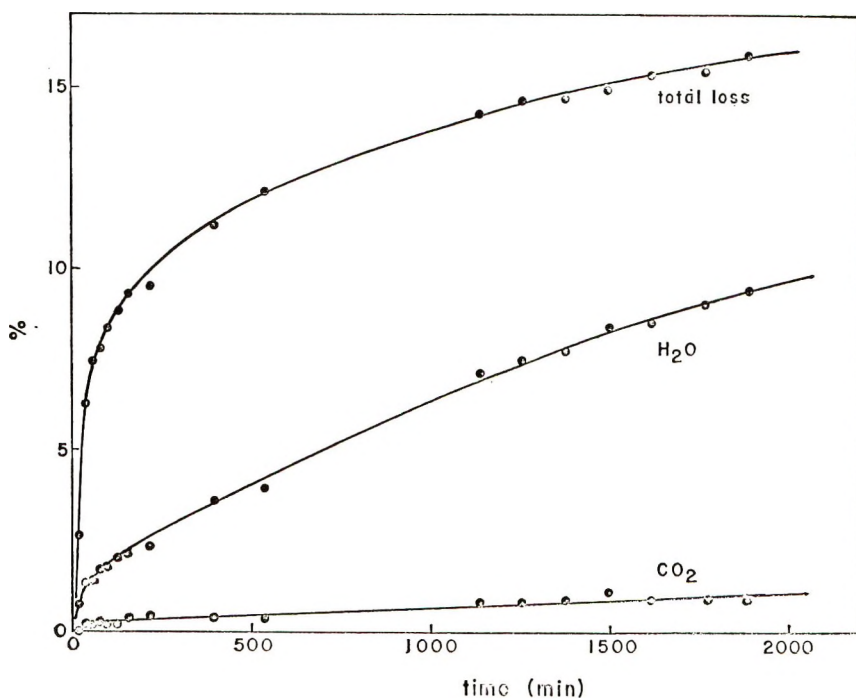
Fig. 5. Weight loss as a function of time at 170°C: (top) total weight loss, %; (middle) percent loss of H_2O: (bottom) per cent loss of CO_2.

lost indicates that most of the difference results from a rapid evaporation, mostly of benzene. After the initial evaporation the difference between H_2O and CO_2 and total weight loss remains practically constant, showing a very slight decline after 900 min. The benzene which is responsible for the initial weight loss was identified by mass spectrometry, which, incidentally, also revealed small traces of propionic acid, which is probably an impurity of the acrylic acid. In samples heated for long periods of time, benzoic acid was also detected. It is due most probably to the use of benzyol peroxide as initiator and some resulting decomposition. The benzene itself, it should be recalled, was used as a solvent in the polymerization. No monomeric acrylic acid was found, in contrast to the situation with poly (methacrylic acid).
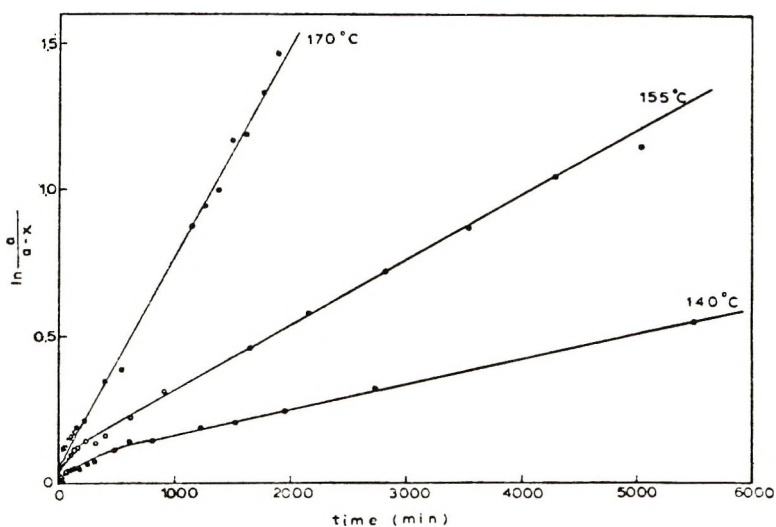
Fig. 6. First-order rate plots for weight loss vs. time plotted as $\ln [a/(a - x)]$ vs. t, where a is initial concentration of carboxyl groups and $a - x$ is the residual concentration at time t.

It was shown before that poly(methacrylic acid) forms the anhydride by a second-order process.[10] A plot of our data for the reciprocal of residual COOH(moles) versus time did not yield a straight line, indicating that second-order kinetics are not obeyed. However, a plot (reproduced in Fig. 6) of $\ln [a/(a-x)]$ versus time, where a is moles of initial COOH and x is moles of reacted COOH (a and x were obtained from the weight of PAA, H_2O, and CO_2) yielded a set of straight lines indicating first-order kinetics for the decrease in concentration of COOH groups due to both anhydride formation and decarboxylation. The initial nonlinearity is most probably due to incomplete drying of the PAA used; the absorbed water would presumably evaporate first, yielding an apparently rapid initial reaction. The value of the rate constant will be given below. To ensure that the first order kinetics were not an experimental artifact, due
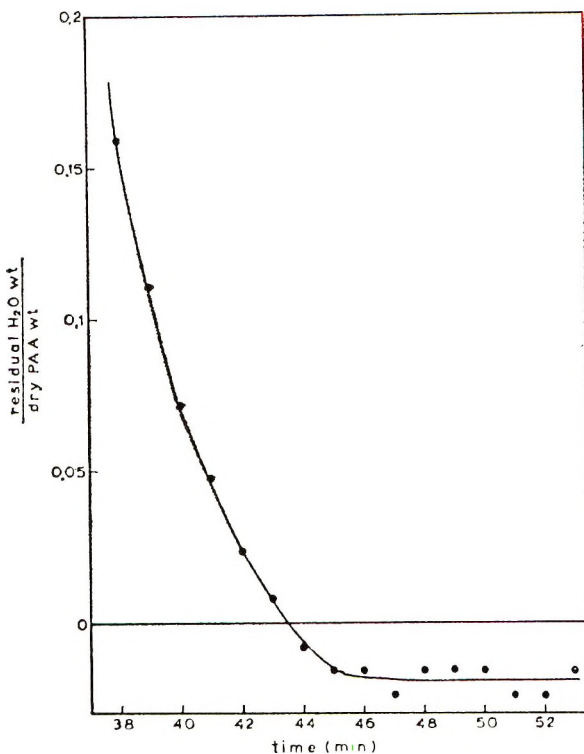
Fig. 7. Evaporation of water from concentrated solution of PAA. Plotted as residual H$_2$O weight/dry PAA weight vs. time; 0.01 on ordinate corresponds to 1.0 mg. The terminal portion of the curve lies below zero since the material taken as "dry" PAA actually contained a small amount of adsorbed water.

perhaps to the slow rate of diffusion of water through the acid, a 19.5% solution of PAA was heated at 110°C (considerably below the temperatures of the kinetic runs) and its weight monitored as a function of time. The terminal portion of that curve is shown in Figure 7 indicating that the drying process is over after approximately 45 min, and that its kinetics thus do not interfere with the dehydration kinetics. The fact that methacrylic acid forms the anhydride by a second-order reaction could conceivably be explained by the increased chain stiffness of the methacrylic acid relative to acrylic acid. The increase in chain stiffness might make intermolecular anhydride formation kinetically more favorable than intramolecular anhydride formation.

Solubility Studies

In order to determine whether the anhydride was formed inter- or intramolecularly, the solubility of the anhydride (prepared by heating at 155°C for 43 hr) was determined. Since the anhydride dissolves almost completely in dimethylformamide and in dimethyl sulfoxide, intramolecular anhydride formation seems to occur almost exclusively.

DISCUSSION

Mechanism of Anhydride Formation

It might seem strange that anhydride formation, which involves the elimination of water from two COOH residues, should proceed by a mechanism which yields first-order kinetics. There may be two possible reasons for this phenomenon.

(1) Spectroscopic evidence, i.e., the width of the carboxyl band at ca. 3000 cm^{-1} and the position of the carbonyl band at 1700 cm^{-1}, indicates that most of the COOH residues are hydrogen-bonded in the form of dimers.[16] Water elimination might thus proceed from the dimer, leading to an intermolecular anhydride. This would be consistent with first-order kinetics, but would yield a crosslinked insoluble material. However, the solubility studies discussed above indicate that practically no inter-molecular anhydride formation occurs This possibility must therefore be ruled out.

(2) Since the anhydride formation is intramolecular and the reaction is first-order, it seems reasonable to assume that the mechanisms would be predominantly water elimination from neighboring carboxyl groups along the chain. This process might require that at least one of the two carboxyl residues not be hydrogen-bonded, but this is quite feasible: the equilibrium constant for dimerization in liquid propionic acid is known,[17] and an extrapolation to 155°C gives the value of 8.7 (in reciprocal mole fraction), indicating that approximately 20% of the acid residues are present as the monomer. Even if this value is one or two orders of magnitude too high, the presumably short lifetime of a hydrogen bonded pair above glass transition would ensure that a steady supply of unbonded residues is available. Additional supporting evidence comes from the high entropy of activation for the anhydride formation process, which will be discussed in the next section.

Kinetic Parameters for Anhydride Formation and Decarboxylation

Now that we have a reasonable mechanism to work with, an attempt can be made to determine the individual rate constants. The assumption is made that anhydride formation occurs by water elimination from neigh-boring COOH groups along the same chain, while decarboxylation can occur both from paired groups or from single COOH groups. The con-centration of pairs along the same chain will be called [A$_2$], while that of isolated —COOH groups [A$_1$]; the total concentration of carboxyl groups, [A], is equal to 2[A$_2$] + [A$_1$]; the rate constant for anhydride formation will be called k_a, while that for decarboxylation will be called k_d. The total rate of disappearance of COOH groups, due to both anhydride for-mation and decarboxylation, can now be given as

$$-d[-\text{COOH}]/dt = -d[\text{A}]/dt = k_d[\text{A}] + 2k_a[\text{A}_2] = k_d([\text{A}_1] + 2[\text{A}_2])$$
$$+ 2k_a[\text{A}_2]$$

Experimentally, it is known (Fig. 5) that decarboxylation occurs very much more slowly than anhydride formation. Furthermore, if we confine our attention to the initial stages of the reaction, were $[A_1] \ll 2[A_2]$, then the above equation can be written in a somewhat simplified form, i.e.,

$$- d[A]/dt \simeq 2k_d[A_2] + 2k_a[A_2]$$

$$\simeq (2k_d + 2k_a)\,[A_2]$$

$$\simeq k'[A_2] \simeq k[A]$$

or first-order overall, as was observed experimentally. [A] and $[A_2]$ are related by the dimerization equilibrium constant.

Both k_d and k_a can now be calculated. By taking the total number of —COOH groups from the weight of material present (simple stoichiometry) and setting the loss of one water molecule equivalent to two COOH groups and one CO_2 molecule to one COOH group, we obtain:

$$k_a = 2.5 \times 10^9 \exp\{-26000/RT\}$$

$$\Delta H°\dagger = 25 \text{ kcal}$$

and

$$\Delta S°\dagger = -18 \text{ cal/deg-mole}$$

$$k_d = 2.9 \times 10^8 \exp\{-27000/RT\}$$

$$\Delta H°\dagger = 26 \text{ kcal}$$

$$\Delta S°\dagger = -23 \text{ cal/deg mole}$$

Due to the very small amount of CO_2 given off at the temperatures of the experiment, the accuracy of k_d is much smaller than that of k_a. It should also be pointed out that the high entropy of activation for the process of anhydride formation suggests a very high degree of ordering for the transition state, which might very well be due to the partial immobilization of neighboring COOH groups. At this time, we can offer no explanation for the identity of the enthalpies of activation for the anhydride formation and decarboxylation reactions, but these values are very normal for reactions of this type.

Additional Comments

Two additional factors should be brought out; one of these deals with glass transition determinations while the other deals with the discrepancy between the calculated and experimental elemental composition for the most strongly dehydrated sample. Both of these are connected, so they will be discussed together.

By our usual dehydration procedure we were unable to obtain samples with a T_g higher than approximately 130°C. However, the value for T_g of the pure anhydride, obtained by extrapolation of the linear portion of the curve to 12.5% weight loss, yields a value of approximately 140°C. It is clear that if anhydride formation occurs by water elimination from

among neighboring pairs, occasionally isolated COOH groups will be left which cannot dehydrate by that mechanism, but must do so through intermolecular anhydride formation. Presumably temperatures in excess of 170°C would be required for that reaction to proceed at an appreciable rate; also, crosslinking would result from that reaction, which would possibly lead to drastic increases in T_g. As a matter of fact, one experiment involving a dehydration temperature of over 200°C yielded a value for T_g of about 180°C. This was presumably due to a very high crosslinking density, although no further experiments were performed due to the complete intractability of the sample.

The partial dehydration mentioned above is also confirmed by the discrepancy between the experimental C and H content of the sample and the value calculated for complete dehydration (see Table I). Flory[18] and Wall[19] calculated the percent dehydrohalogenation of PVC for reaction involving neighboring groups, and obtained a value of 86.5% for maximum extent of reaction. A recalculation of the expected C and H content for that degree of reaction is also shown in Table I, and a much better agreement is found.

References

1. W. E. Fitzgerald and L. E. Nielsen, *Proc. Roy. Soc.* (London), **A282**, 137 (1964).

2. R. W. Rees and D. J. Vaughn, paper presented to the Division of Polymer Chemistry, American Chemical Society, Detroit, Michigan, April 1965; *Polymer Preprints*, **6**, No. 1, 278, 296 (1965).

3. N. Z. Erdi and H. Morawetz, *J. Colloid Sci.*, **19**, 708 (1964).

4. J. Moacanin and E. F. Cuddihy, paper presented to the Division of Polymer Chemistry, American Chemical Society, Atlantic City N.J., September 1965; *Polymer Preprints*, **6**, No. 2, 799 (1965).

5. A. Eisenberg, *Adv. Polym. Sci.*, **5**, 59 (1967).

6. American Chemical Society, San Francisco Meeting, April 1968, Symposium on effect of ions on the bulk properties of polymers.

7. A. Eisenberg and T. Yokoyama, *Polymer Preprints*, **7**, 617 (1968).

8. E. Jenckel and E. Brauker, *Z. Physik. Chem.*, **A185**, 465 (1940).

9. K. H. Illers, *Z. Elektrochem.*, **70**, 353 (1966).

10. D. H. Grant and N. Grassie, *Polymer*, **1**, 125 (1960).

11. *Encyclopedia of Polymer Science and Technology*, Vol. 1, Kirk and Othmer, Eds. Interscience, New York, 1964, p. 197.

12. S. Newman, W. R. Krigbaum, C. Laugier, and P. J. Flory, *J. Polym. Sci.*, **14**, 451 (1954).

13. A. Eisenberg and T. T. Sasada, *Proceedings of the International Conference* "Physics of Non-Crystalline Solids" *Delft*, 1964. J. A. Prins, ed. No. Holland Publ. Co., 1965.

14. A. Eisenberg and T. Sasada, paper presented at IUPAC Macromolecular Symposium, Prague, 1965, *J. Poly. Sci. C*, **16**, 3473 (1968).

15. L. J. T. Hughes and D. B. Fordyce, *J. Polymer Sci.*, **22**, 509 (1956).

16. L. J. Bellamy, *The Infra-red Spectra of Complex Molecules*, Wiley, New York, 1954.

17. G. C. Pimentel and A. L. McClellan, *The Hydrogen Bond*, Freeman, San Francisco, 1960, p. 367.

18. P. J. Flory, *J. Amer. Chem. Soc.*, **61**, 1518 (1939).

19. F. T. Wall, *J. Amer. Chem. Soc.*, **62**, 803 (1940); *ibid*, **63**, 821 (1941).

Molecular Weight Distribution in Radiation-Induced Polymerization. I. γ-Radiation-Induced Free-Radical Polymerization of Liquid Styrene

R. Y. M. HUANG, J. F. WESTLAKE, and S. C. SHARMA,
*Department of Chemical Engineering, University of Waterloo,
Waterloo, Ontario, Canada*

Synopsis

The kinetics of γ-radiation-induced free-radical polymerization of styrene were studied over the temperature range 0–50°C at radiation intensities of 9.5×10^4, 3.1×10^5, 4.0×10^5, and 1.0×10^6 rad/hr. The overall rate of polymerization was found to be proportional to the 0.44–0.49 power of radiation intensity, and the overall activation energy for the radiation-induced free-radical polymerization of styrene was 6.0–6.3 kcal/mole. Values of the kinetic constants, $k_p{}^2/k_t$ and k_{trm}/k_p, were calculated from the overall polymerization rates and the number-average molecular weights. Gel-permeation chromatography was used to determine the number-average molecular weight $\bar{M}_n$, the weight-average molecular weight $\bar{M}_w$, and the polydispersity ratio $\bar{M}_w/\bar{M}_n$, of the product polystyrene. The polydispersity ratios of the radiation-polymerized polystyrene were found to lie between 1.80 and 2.00. Significant differences were observed in the polydispersity ratios of chemically initiated and radiation-induced polystyrenes. The radiation chemical yield, G(styrene), was calculated to be 0.5–0.8.

INTRODUCTION

Radiation-induced polymerization of vinyl monomers has been the subject of extensive studies during the past two decades. Starting with the work of Chapiro in 1950, early kinetic studies have shown that the polymerization proceeds via a free-radical mechanism. Kinetic data obtained in these studies could be well explained in terms of conventional free-radical polymerization mechanisms. An excellent review of radiation-induced polymerization covering the period up to 1962 is contained in the book by Chapiro.[1]

Recently, however, two new developments in radiation-induced polymerization have stimulated interest in this field. Chen and Stamm[2] reported evidence for the simultaneous existence of ionic and free-radical mechanisms in the radiation-induced polymerization of styrene at low temperatures. Okamura et al.[3] and Johnson et al.[4] independently reported that the radiation-induced polymerization of liquid styrene in extremely "dry" systems proceeds via an ionic mechanism. Okamura et al.[5] found that the

presence of water or ammonia in excess of 10^{-3} mole/l. completely suppresses the ionic mechanism, and thus only free-radical polymerization was observed in earlier studies where no special precautions had been taken to remove the last traces of water from the styrene monomer. Considerably faster polymerization rates and high G(styrene) values were obtained in the ionic polymerization when compared to the free radical polymerization.

In the field of polymer analytical techniques, gel-permeation chromatography has emerged in recent years as a major new tool for characterizing the molecular weight distribution of polymers. Gel-permeation chromatography represents an important experimental technique in studying polymerization kinetics, since the molecular weight disrtibution of a polymer is a function of its polymerization mechanism. The present investigations are concerned with experimental studies of the kinetics of selected vinyl monomers in both the "wet" and the "dry" systems over a wide temperature range and by using gel-permeation chromatography for characterization of molecular weight distribution. This paper deals with the γ-ray-induced free-radical ("wet" system) polymerization of liquid styrene over the temperature range 0–50°C.

EXPERIMENTAL

Materials

Monomer. Styrene (Eastman Organic Chemicals, highest purity) was washed with 10% sodium hydroxide and distilled water to remove the inhibitor. It was dried overnight over anhydrous calcium chloride. The styrene was then distilled at 40–45°C/16–20 mm Hg absolute pressure in a distillation flask fitted with an air-cooled reflux condenser, and stored in a refrigerator.

Methanol. Methanol (ACS Grade, Fisher Scientific Company) was used as obtained for the precipitation of polystyrene from the reaction mixture.

Tetrahydrofuran. THF (Fisher Certified ACS Grade) was used as obtained as the eluting solvent for the gel-permeation chromatograph and for the determination of molecular weight and molecular weight distribution of the product polystyrene.

Polystyrene Standards. Eleven standard monodisperse ($\bar{M}_w/\bar{M}_n$ = 1.06–1.20) polystyrene samples with molecular weights of 900, 2 100, 4 800, 10 300, 19 800, 51 000, 97 200, 160 000, 411 000, 860 000, and 1 800 000, respectively were obtained from the Pressure Chemical Company of Pittsburgh, Pennsylvania, and used for the calibration of the gel-permeation chromatograph.

Radiation Facility

The irradiations were carried out in a Gamma-Cell 220 ^{60}Co γ-ray irradiation facility, located in the Department of Chemical Engineering,

University of Waterloo. This unit contains 13 000 Ci of ^{60}Co and had a central field radiation intensity of 1×10^6 rad/hr in the sample chamber. It was designed and built by the Commercial Products Division, Atomic Energy of Canada Ltd., Ottawa, Ontario. A series of lead attenuators was used in the sample chamber in order to vary the radiation intensities. Three lead attenuators of different thickness were used to attenuate the radiation dose rate to 4×10^5, 3×10^5, and 9.5×10^4 rad/hr, respectively. Radiation intensities were measured by using ferrous–ferric (Fricke) dosimetry.

Polymerization Reaction Vessel

A line sketch of the polymerization reaction vessel is shown in Figure 1. It consists of a jacketed glass vessel 12 cm in height and about 3.0 cm in diameter (ID). The outside diameter of the jacket is 5.2 cm. The temperature of the reactants can be maintained at the desired level by circulating a heating/cooling fluid through the jacket. The capacity of the reaction vessel is about 80 ml. Size requirements were restricted by the maximum possible space available in the sample chamber when using the thickest lead attenuator (to obtain the lowest dose rate).

The gas dispersion tube extending down to about 1.0 cm from the bottom is used to maintain a nitrogen atmosphere inside the reaction vessel. It
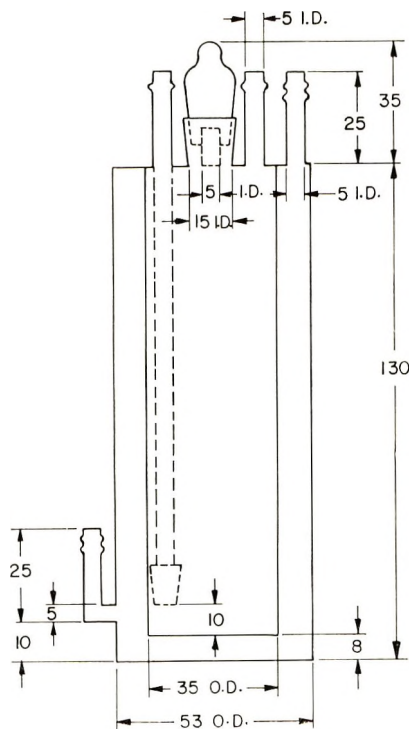

Fig. 1. Polymerization reaction vessel.

also provides the necessary stirring action needed to have uniform conditions inside the reaction vessel. A 1.5-cm ID neck fitted with a ground-glass stopper permits withdrawal of the desired amount of reaction sample at various time intervals.

Temperature Control

Haake Constant-Temperature Circulating Bath. Temperatures between 20 and 50°C were obtained and maintained in the polymerization reaction vessel by circulating water through the jacket. A constant-temperature Haake circulation bath was employed for this purpose. It controlled the reaction temperature to ±0.5°C.

Lauda Kryomat Constant Temperature Circulating Bath. Temperatures below 20°C were obtained by using a Lauda Table Model Kryomat, Model TK 30, supplied by Lauda Instruments Incorporated, Westbury, N. Y. Temperatures between −38°C and +38°C could be maintained by using this bath with circulating methanol.

The temperature of the circulating fluid at the outlet of the jacket was taken to be the reaction temperature. A check on the reaction temperature was made by measuring the temperature while withdrawing the sample.

Polymerization Rates

Approximately 80 ml of distilled styrene was poured into the reaction vessel, and nitrogen was bubbled continuously through the system. The desired reaction temperature was maintained by circulating water or methanol (depending upon the temperature desired) through the outer jacket of the polymerization vessel from a constant temperature circulation bath. It took about 5–6 min for the temperature of styrene to reach the desired level, and in the meantime a nitrogen atmosphere was established inside the vessel. The nitrogen used had a purity of 99.7%.

Irradiations were conducted for desired time intervals after the required temperature was reached inside the polymerization vessel. Following the irradiation, 20–40 ml of the sample was withdrawn, depending on the irradiation time or the conversion, and poured into a 10–20-fold excess of chilled methanol with continuous vigorous stirring. The precipitated polystyrene was filtered on sintered glass Gooch crucibles and then dried to constant weight at 55–65°C in a vacuum oven. The per cent conversion was determined gravimetrically.

Polymerization runs were carried out at six different temperatures of −0.3, 9.5, 19.3, 29.5, 40.0, and 49.5°C. Experiments at each temperature were performed at four average radiation dose rates of 1×10^6, 4×10^5, 3.1×10^5, and 9.5×10^4 rad/hr for a total of 24 runs. In most cases the maximum per cent conversion was kept below 8% in order to minimize the viscosity effects. The maximum reaction time for the polymerization runs varied from 6 to 40 hr, depending upon the dose rate and the temperature.

Gel-Permeation Chromatography

The molecular weight and the molecular weight distribution of the product polystyrene was determined by using gel-permeation chromatography.

A Waters GPC unit, Model 200, fitted with four columns of cross-linked polystyrene gel of pore sizes 10^6, 10^5, 10^4, and 10^3 Å, was used. Eleven standard monodisperse ($\bar{M}_w/\bar{M}_n = 1.06$–$1.20$) polystyrene samples, having average molecular weights of 900, 2100, 4800, 10300, 19800, 51000, 97000, 160000, 411000, 860000, and 1800000, were obtained from the Pressure Chemical Company, Pittsburgh, Pennsylvania, and used for the calibration of the gel-permeation chromatograph. Tetrahydrofuran (THF)
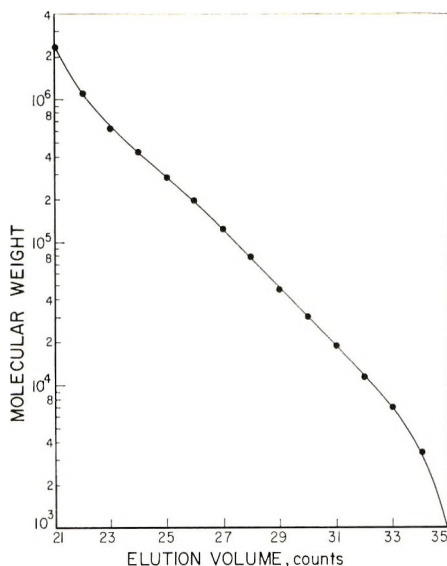
Fig. 2. Polystyrene calibration curve for gel-permeation chromatograph plot of log molecular weight vs. elution volume (counts). Eluting solvent, tetrahydrofuran; temperature, 25°C.

was used as the eluting solvent. Samples with concentrations of 0.5%, 0.25%, 0.125%, and 0.0625% by weight of these standards in tetrahydrofuran were prepared. A 2-ml portion of each of these samples was injected and a solvent flow rate of 1.0 ml/min was maintained. The oven temperature was kept at 25 ± 0.5°C. The elution volume or the count at the peak of each sample was determined. Extrapolation to zero concentration was made to correct for possible concentration effects. The extrapolated value of each count at the corresponding molecular weight was plotted against the log of molecular weight. Figure 2 shows the calibration plot for the gel-permeation chromatograph.

Molecular Weights and Molecular Weight Distributions

Two polystyrene samples were selected from each run. A 0.25% by weight solution of each was made in tetrahydrofuran (THF) in a 25-ml volumetric flask. These were allowed to stand overnight and then filtered under nitrogen pressure to remove any foreign materials which might clog the pores of the polystyrene gel in the gel permeation chromatograph.

The injection inlet of the gel-permeation chromatograph was washed twice with pure tetrahydrofuran and then rinsed with the filtered polymer solution. The polymer solution was then injected, an injection time of 60 sec. being used. A flow rate of 1 ml/min of the solvent was maintained, and the oven temperature was kept at 25 ± 0.5°C.

The number-average ($\bar{M}_n$) and the weight-average ($\bar{M}_w$) molecular weights were calculated from the gel permeation chromatograph elution curve and the calibration curve (Fig. 2) according to the standard method recommended by Waters Associates. Tung's method[16] was used to correct for imperfect resolution resulting from axial dispersion. A computer program was written in Fortran IV to facilitate calculations required for this correction. All computations were carried out on the University of Waterloo IBM 7040 and 360/75 digital computers.

RESULTS

Experimental data for the per cent polymerization versus reaction time for styrene polymerization at various dose rates and temperatures are plotted in Figures 3–8. In most cases the per cent conversion was kept
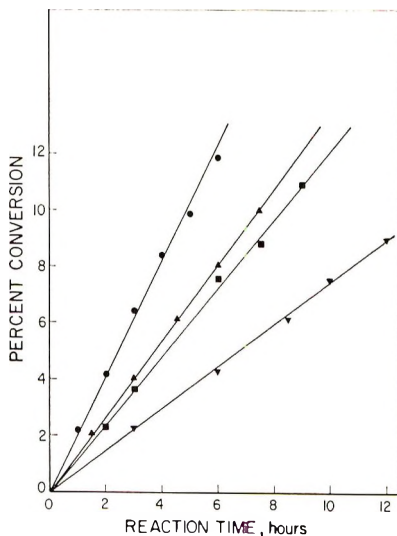
Fig. 3. γ-Ray-induced polymerization of bulk styrene. Plot of per cent conversion vs. reaction time at various dose rates. Temperature, 49.5°C; Dose Rate, M. Rads/ Hour; ●: 1.000; ▲: 0.400: ■: 0.310; ▼: 0.095.
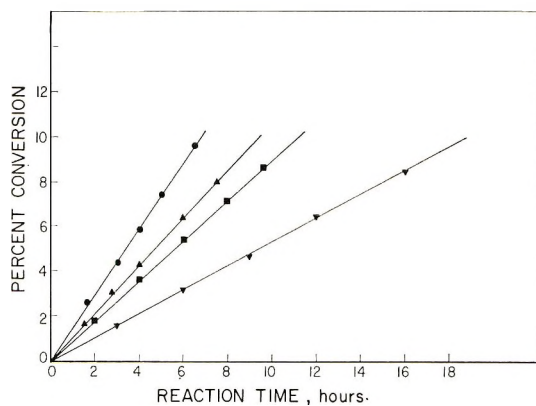
Fig. 4. γ-Ray-induced polymerization of bulk styrene. Plot of per cent conversion vs. reaction time at various dose rates. Temperature, 40°C; Dose Rate, M. Rads/ Hour; ●: 1.000; ▲: 0.400; ■: 0.310; ▼: 0.095.
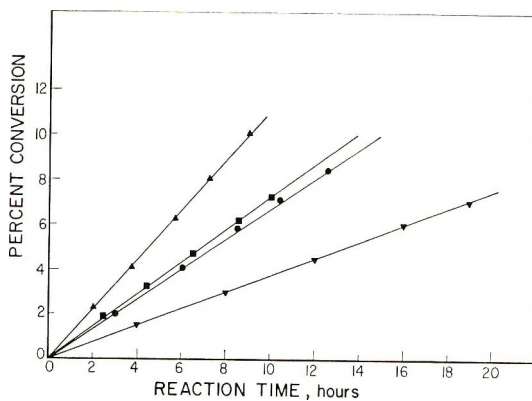
Fig. 5. γ-Ray-induced polymerization of bulk styrene. Plot of per cent conversion vs. reaction time at various dose rates. Temperature, 29.5°C; Dose Rate, M. Rads/ Hour; ▲: 1.000; ■: 0.400; ●: 0.310; ▼: 0.095.
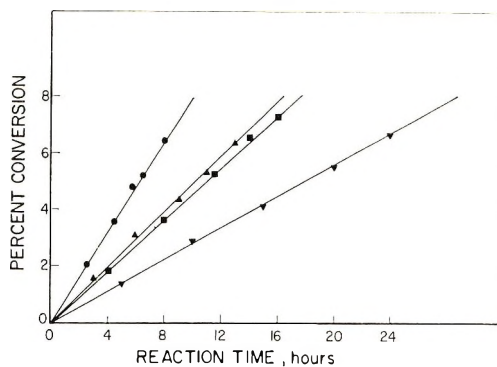
Fig. 6. γ-Ray-induced polymerization of bulk styrene. Plot of per cent conversion vs. reaction time at various dose rates. Temperature, 19.3°C; Dose Rate, M.Rads/ Hour; ●: 1.000; ▲: 0.400; ■: 0.310; ▼: 0.095.
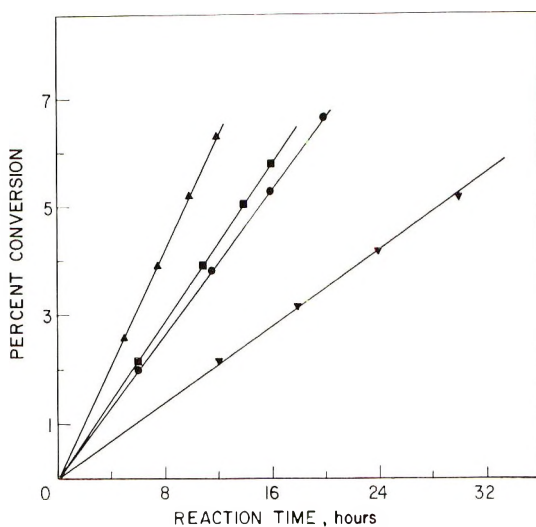
Fig. 7. γ-Ray-induced polymerization of bulk styrene. Plot of per cent conversion vs. reaction time at various dose rates. Temperature, 9.5°C; Dose Rate, M.Rads/Hour ●: 1.000; ▲: 0.400; ■: 0.310; ▼: 0.095.
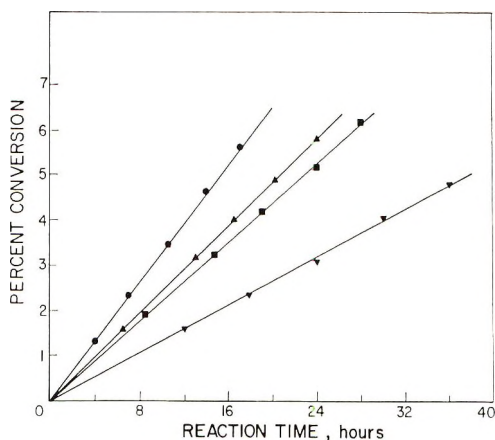
Fig. 8. γ-Ray-induced polymerization of bulk styrene. Plot of per cent conversion vs. reaction time at various dose rates. Temperature, −0.3°C; Dose Rate, M.Rads/Hour; ●: 1.000; ▲: 0.400; ■:0.310; ▼: 0.095.

below 8% to avoid the Trommsdorf effect. The slope of each line gives the polymerization rate (per cent conversion/hour) at the corresponding dose rate and temperature. Figure 9 shows the dependence of polymerization rate on dose rate at a given temperature. Each of the six lines refers to a particular temperature employed. The exponents of radiation intensity (dose-rate) calculated from Figure 9 are found to lie between 0.44 and 0.49 (Table I). The overall activation energy for the γ-ray-induced polymerization of styrene was determined from an Arrhenius plot of polymerization
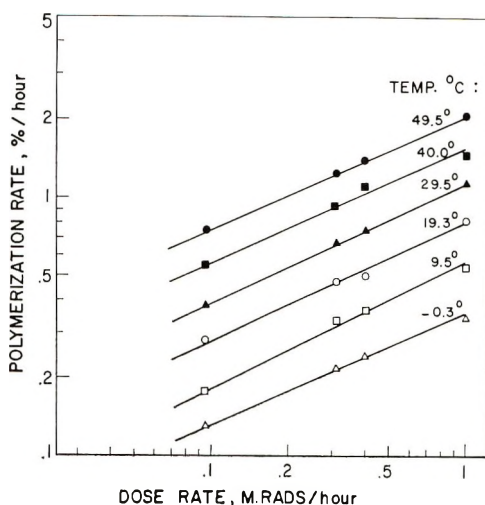
Fig. 9. Dose rate dependence of polymerization rate. Plot of polymerization rate vs. radiation intensity.

rate vs. $1/T$. Such a plot is shown in Figure 10 for each of the four dose-rates used. The overall activation energies calculated from the slope of each of these lines were found to be 6.3, 6.1, 6.0, and 6.1 kcal/mole, respectively (Table II).

TABLE I
Dose Rate Dependence of Polymerization Rate[a]

Temperature, °C	Slope
49.5	0.44
40.0	0.44
29.5	0.46
19.3	0.45
9.5	0.49
−0.3	0.44

[a] See Figure 9.

TABLE II
Overall Activation Energy for Radiation-Induced
Polymerization of Styrene[a]

Dose rate, Mrad/hr	Activation energy, kcal/mole
1.0	6.3
0.40	6.1
0.31	6.0
0.095	6.1

[a] See Figure 10.
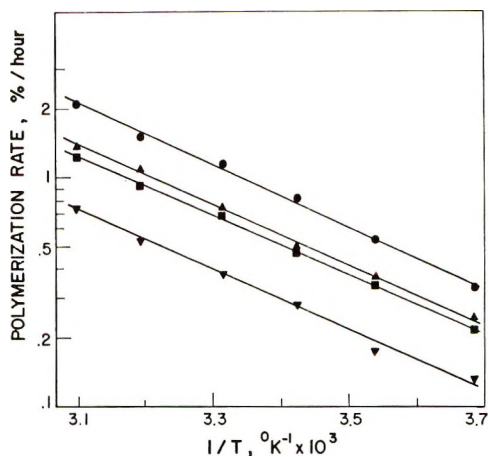
Fig. 10. Overall activation energy for radiation-induced polymerization vs. $1/T$. Dose Rate, M.Rads/Hour; ●: 1.000; ▲: 0.400; ■: 0.310; ▼: 0.095.
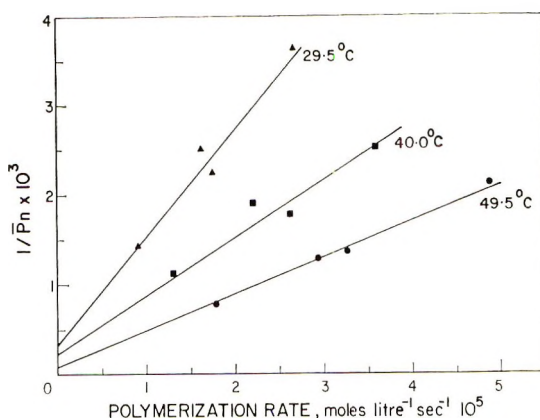
Fig. 11. Plot of $1/P_n$ vs. polymerization rate.

From steady-state free radical polymerization kinetics, the following relationship can be derived,[6] assuming chain transfer to monomer and termination by combination:

$$\frac{1}{\bar{P}_n} = \frac{k_t}{2k_p{}^2}\left(\frac{R_p}{[M]^2}\right) + \frac{k_{trm}}{k_p} \tag{1}$$

In Figures 11 and 12, the reciprocal of the number-average degree of polymerization, $\bar{P}_n$, is plotted against the overall rate of polymerization for each of the six temperatures. The number-average degree of polymerization was determined by using gel-permeation chromatography. As expected from eq. (1), straight line relationships were obtained for each temperature. Values of $k_p{}^2/k_t$ were calculated from the slopes of these lines while the intercept gave the values of k_{trm}/k_p at the corresponding
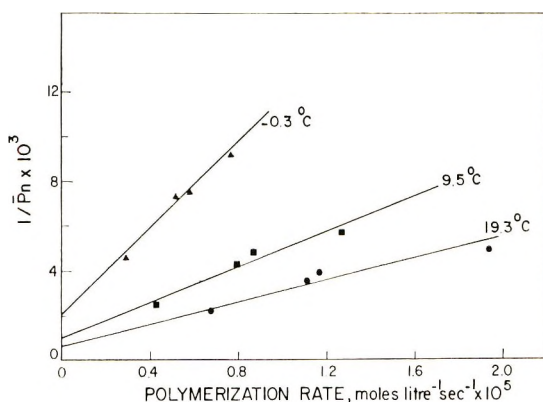
Fig. 12. Plot of $1/\bar{P}_n$ vs. polymerization rate.
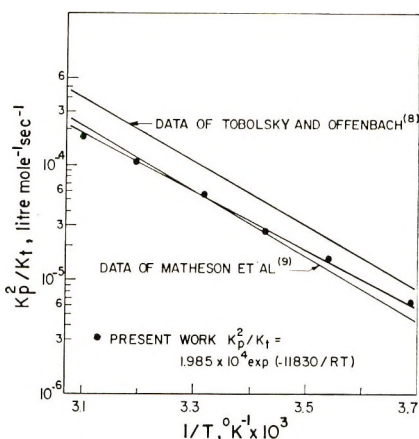
Fig. 13. Radiation-induced polymerization of styrene. Plot of $k_p{}^2/k_t$ vs. $1/T$.

temperature (Table III). The values of $k_p{}^2/k_t$ and k_{trm}/k_p (calculated from Figs. 11 and 12) are plotted against $1/T$ in Figures 13 and 14, respectively. The resulting Arrhenius type relationships for the temperature dependence of $k_p{}^2/k_t$ and k_{trm}/k_p were calculated and expressed as:

$$k_p{}^2/k_t = 1.985 \times 10^4 \exp\{-11830/RT\} \tag{2}$$

$$k_{trm}/k_p = 4.57 \times 10^{-11} \exp\{9490/RT\} \tag{3}$$

The G values for styrene polymerization were calculated from the $k_p{}^2/k_t$ values and the overall polymerization rates, by using eq. (4):[1]

$$G(\text{styrene}) = 6.02 \times 10^{22} \frac{k_t}{k_p{}^2}\left(\frac{R_p{}^2}{[M]^2}\right)\frac{1}{Ie_{(\text{styrene})}} \tag{4}$$

where $G(\text{styrene})$ is the G value for radical initiation of styrene polymerization, I is the radiation intensity (in rads/second), and $e_{(\text{styrene})}$ is the

TABLE III

Data from Plots of $1/\bar{P}_n$ vs. Polymerization Rate[a]

Temperature, °C	$k_t/2k_p{}^2$	$k_{trm}/k_p \times 10^5$
49.5	3 000	9.5
40.0	4 600	24.0
29.5	9 000	34.0
19.3	18 800	60
9.5	32 000	100
−0.3	74 600	200

[a] See Figures 11 and 12.

amount of energy absorbed per rad in styrene, expressed in electron-volts per gram.

Table IV shows the G(styrene) values calculated from the data obtained in this work. As can be seen, the G(styrene) values range from 0.50 to

TABLE IV

Polydispersity Ratios $\bar{M}_w/\bar{M}_n$ and G(styrene) Values in Radiation-Induced Styrene Polymerization

Temperature, °C	Dose rate I, rad/sec	$R_p \times 10^5$, mole/l.-sec	$\bar{M}_w \times 10^{-3}$	$\bar{M}_n \times 10^{-3}$	$\bar{M}_w/\bar{M}_n$	G(styrene)[a]
	278.0	4.880	94.0	46.5	1.81	0.50
	111.0	3.270	142.0	78.0	1.82	0.61
49.5	86.2	2.930	158.0	83.0	1.90	0.68
	26.4	1.785	288.0	145.0	1.99	0.78
	278.0	3.580	73.5	40.5	1.81	0.53
	111.0	2.612	112.0	59.0	1.90	0.70
40.0	86.2	2.195	111.0	55.5	2.00	0.64
	26.4	1.302	223.0	93.0	2.40	0.74
	278.0	2.682	54.0	28.5	1.90	0.60
	111.0	1.764	87.0	47.0	1.85	0.65
29.5	86.2	1.620	78.0	41.5	1.88	0.71
	26.4	0.914	155.0	73.5	2.11	0.73
	278.0	1.933	43.5	21.0	2.06	0.61
	111.0	1.170	49.0	26.5	1.84	0.56
19.3	86.2	1.116	56.0	29.5	1.90	0.66
	26.4	0.677	97.0	49.5	1.96	0.79
	278.0	1.268	36.0	19.0	1.88	0.51
	111.0	0.865	37.0	22.0	1.69	0.60
9.5	86.2	0.800	45.5	24.5	1.86	0.65
	26.4	0.425	77.5	43.0	1.81	0.60
	278.0	0.785	21.5	11.5	1.85	0.46
	111.0	0.582	27.0	14.0	1.92	0.64
−0.3	86.2	0.529	25.0	14.5	1.76	0.70
	26.4	0.318	49.5	24.5	2.03	0.80

[a] G(styrene) = G value for radical initiation of styrene polymerization.
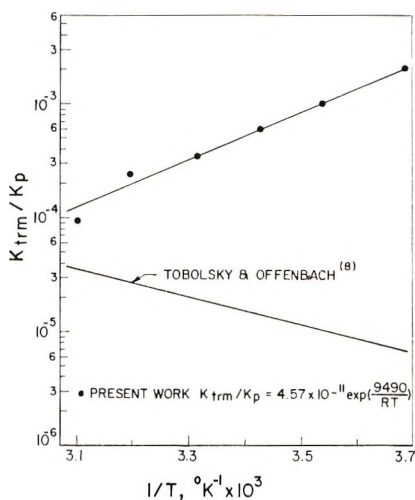
Fig. 14. Chain transfer to monomer in the radiation-induced polymerization of styrene. Plot of k_{trm}/k_p vs. $1/T$.
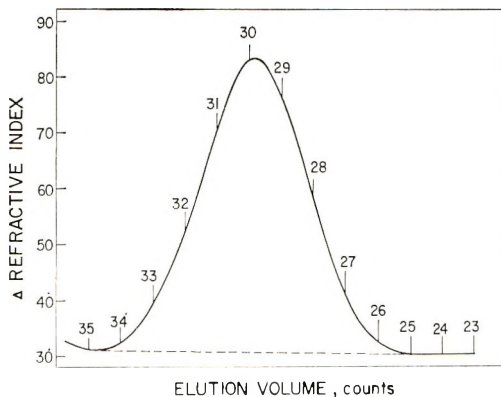
Fig. 15. Typical gel-permeation chromatogram of radiation-induced polystyrene.

0.80. Gel-permeation chromatography was used to determine the number-average molecular weight $\bar{M}_n$, the weight-average molecular weight $\bar{M}_w$, and the polydispersity ratios $\bar{M}_w/\bar{M}_n$. The results are listed in Table IV for all the 24 polymerization runs. It is seen that the experimental values of the polydispersity ratio lie, for the most part, between 1.80 and 2.00. A typical GPC chromatogram of radiation polymerized polystyrene is shown in Figure 15.

DISCUSSION

The dependence of the polymerization rate on radiation dose-rate at a given temperature is shown in Figure 9. The exponents of the radiation intensity are found to lie between 0.44 and 0.49. Based on steady-state

polymerization kinetics, the theoretical value for the exponents of the radiation intensity should be 0.50. Values reported in the literature for this quantity are close to 0.50 at low dose rates[1] but tend to decrease slightly below 0.50 at high dose rates. The values obtained in this work agree fairly well with those reported in the literature.

The overall activation energy for the γ-ray-induced polymerization of styrene as calculated from Figure 10, was found to lie between 6.0 and 6.3 kcal/mole. Table V compares values from the literature for the overall activation energy of styrene polymerization with those obtained in the present work. The present experimental values for the overall activation energy are in good agreement with previously reported values using photochemical methods of initiation. However, they are somewhat lower than the activation energy reported by Ballantine et al.[7] (recalculated by Chapiro[1]) for the γ-ray-induced polymerization of styrene. It should be noted that the original value of Ballantine et al. was derived from experimental data at three temperatures (72°C, 25°C, and −18°C) and a different dose rate was used at each temperature. The polymerization rate data from two of these dose rates were apparently normalized to the third dose rate, assuming a square-root intensity dependence for the polymerization rate.

In Figure 13 the values of k_p^2/k_t are plotted against $1/T$. The data of Tobolsky and Offenbach[8] and of Matheson et al.[9] are also included for comparison with the data obtained in this work. The present results show closer agreement with the data of Matheson et al. as compared with those of Tobolsky and Offenbach over the entire temperature range studied.

The k_{trm}/k_p values obtained in this work are compared with the corresponding data of Tobolsky and Offenbach[8] in Figure 14. The present values are not only considerably higher than the values of Tobolsky and Offenbach but also show an opposite trend with temperature. The reason for this discrepancy is not understood at present, and is under further investigation. As can be seen from Table IV, the G(styrene) values obtained in this work range from 0.50 to 0.80. Chapiro[1] has calculated G(styrene) values from various polymerization rate data in the literature. They range from 0.30 to 0.80 depending upon the dose rate. For the range of dose rates used in the present experiments, Chapiro's collected data indicate G(styrene) values between 0.30 and 0.50. However, it is important to note that in his calculations for the G(styrene) values, Chapiro has used the

TABLE V
Overall Activation Energy ($E_p - \frac{1}{2} E_t$) of Styrene Polymerization

Initiation	$E_p - \frac{1}{2}E_t$	Reference
UV light and thermal	6.3	Tobolsky and Offenbach[8]
UV light	6.6	Matheson et al.[9]
γ-rays	7.15	Ballantine et al.[7] (Corrected value by Chapiro[1])
γ-rays	6.0–6.3	Present work

$k_t/k_p{}^2$ values of Tobolsky and Offenbach,[3] which are only 60–70% of the values obtained in the present work. This results in the lower values obtained by Chapiro. If this difference is taken into account, the G(styrene) values obtained in this work are in reasonably good agreement with those of Chapiro.

The number-average molecular weights $\bar{M}_n$, the weight-average molecular weights $\bar{M}_w$, and the polydispersity ratios $\bar{M}_w/\bar{M}_n$ were determined by gel-permeation chromatography. The results are listed in Table IV for the polystyrene sample obtained in all the 24 polymerization runs. The polydispersity ratio is a measure of the molecular weight heterogeneity of the polymer and also provides valuable information concerning the polymerization kinetics, especially the termination step. It can be seen from Table IV that the experimental values for the polydispersity ratio lie, for the most part, between 1.80 and 2.00.

For styrene polymerization, it is generally accepted that the termination occurs predominantly by combination[10–12] and chain transfer to monomer is negligible. If this is the case, the polydispersity ratio should be 1.50.[6] Experimental results obtained in this work show, however, that the values of polydispersity ratio lie between 1.80 and 2.00. In this connection, it is important to note that only a few experimental studies have been reported on this important problem of characterizing the molecular weight distribution of polymers and to relate them to the polymerization kinetics. In the past, this has been mainly due to the lack of a convenient and reliable technique for the determination of molecular weight distributions of polymers. Prior to the advent of gel-permeation chromatography, Baker and Williams[13] used their chromatographic technique to study the molecular weight distribution of polystyrene prepared by chemical means of initiation. They reported that the experimental molecular weight distribution is in good agreement with polymerization theory, assuming termination by combination. Recently, Hamielec et al.[14,15] polymerized styrene in batch and continuous stirred tank reactors using benzoyl peroxide initiator and determined the molecular weight distribution using gel-permeation chromatography. Their results support the view that in styrene polymerization, the radical chains terminate predominantly by combination.

The results of the present work suggest, therefore, that there are certain differences in the polymerization mechanism when radiation and chemical means of initiation are used. To further test this view and also to check the present experimental procedure, a series of polystyrenes were prepared with the use of azobisisobutyronitrile as the initiator and then characterized by gel-permeation chromatography. The results obtained are shown in Table VI. It can be seen from Table VI that the polydispersity ratios for this series of polystyrenes are close to 1.50. This is in good agreement with polymerization kinetics involving termination by combination.

A satisfactory quantitative explanation for the high polydispersity ratio obtained for radiation-induced polymerization of styrene cannot be made at

TABLE VI
Polydispersity Ratios for Polystyrenes Prepared with
Azobisisobutyronitrile Initiator

Run no.	$\bar{M}_w \times 10^{-3}$	$\bar{M}_n \times 10^{-3}$	$\bar{M}_w/\bar{M}_n$*
31	34.0	22.0	1.54
32	79.0	50.0	1.58
33	52.5	34.0	1.54
34	60.5	39.0	1.55

present. However, it is possible that chain transfer to monomer and chain branching may cause the discrepancies observed in the molecular weight distributions. If the initiation is monoradical and the termination is exclusively by combination, the polydispersity ratio should be 1.50. For this case, any abnormal chain transfer to monomer will tend to pull the polydispersity ratio from 1.50 towards 2.00. The values of k_{trm}/k_p obtained in the present work are considerably higher than the corresponding values of Tobolsky and Offenbach.[8]

A theoretical kinetic analysis and computation of polydispersity ratios taking into account the chain transfer data obtained in the present work was carried out. Details of the kinetic equations and the computational procedures are described in the Appendix. The results of these computations are shown in Table VII. Predicted polydispersity ratios range from 1.55 at 49.5°C to a maximum of 1.67 at 9.5°C. These calculations show that chain transfer to monomer is one of the contributing factors which tends to push the polydispersity ratio from 1.50 towards 2.00. However, this factor alone cannot account for the high polydispersity ratios obtained in the present work.

Polystyrene is reported to be more sensitive towards radiolysis than styrene monomer.[1] Chapiro[1] has suggested a G(polystyrene) value of

TABLE VII
Comparison of Experimental and Theoretical Number-Average and Weight-Average
Molecular Weights Assuming Chain Transfer to Monomer and Termination
by Combination

Tempera-ture, °C	Dose rate, rads/sec	Experimental			Theoretical		
		$\bar{M}_w \times 10^{-3}$	$\bar{M}_n \times 10^{-3}$	$\bar{M}_w/\bar{M}_n$	$\bar{M}_w \times 10^{-3}$	$\bar{M}_n \times 10^{-3}$	$\bar{M}_w/\bar{M}_n$
49.5	278.0	84.0	46.5	1.81	88.0	57.0	1.53
	111.0	142.0	78.0	1.82	130.0	84.0	1.55
	86.2	158.0	83.0	1.90	133.0	86.0	1.55
	26.4	288.0	145.0	1.99	226.0	143.0	1.58
9.5	278.0	36.0	19.0	1.88	24.5	15.5	1.56
	111.0	37.0	22.0	1.69	34.0	21.5	1.59
	86.2	45.5	24.5	1.86	36.0	22.5	1.60
	26.4	77.5	43.0	1.81	59.5	35.5	1.67

about 1.5. Since polystyrene is produced in the reaction mixture, free-radical sites can be initiated on a polystyrene molecule as a result of irradiation. This could result in chain branching or graft copolymerization, resulting in higher apparent polydispersity ratios being monitored by gel-permeation chromatography. The high polydispersity ratios obtained in the present work could also result from contributing factors arising from the many assumptions made in the simplified free radical polymerization kinetic scheme. Possible side reactions, such as diradical initiation, termination by disproportionation, chain transfer to polymer, etc. have been neglected or assumed not to make any significant contribution to the overall kinetics. Further work on molecular weight distributions in radiation-induced polymerization is currently in progress at this laboratory, which may provide a better quantitative explanation for the observed discrepancy in polydispersity ratios.

APPENDIX

Method for Calculating the Theoretical Molecular Weight Distribution Assuming Chain Transfer to Monomer and Termination by Combination

Equation (5) has been derived by Bamford et al.[6] for molecular weight distribution in free-radical vinyl polymerization. It includes the effect of chain transfer to monomer and to solvent and termination both by combination and by disproportionation.

$$[W_n] = \frac{[\Delta M]}{k_p[M]} (1 - x)x^{n-1} \left(k_{trs}[S] + k_{trm}[M] + \left(\frac{R_i}{k_t + k_t'} \right)^{1/2} \right.$$

$$\left. \times \left\{ \frac{(x - 1)k_t(k_{trs}[S] + k_{trm}[M] + R_i(k_t + k_t')^{1/2})}{2k_p[M]} \right\} \right) \quad (5)$$

where

$$x = \frac{k_p[M]}{k_p[M] + k_{trs}[S] + k_{trm}[M] + R_i(k_t + k_t')^{1/2}}$$

and where k_p, k_t, k_t', k_{trm}, and k_{trs} are the reaction rate constants for propagation, termination by combination, termination by disproportionation, chain transfer to monomer, and chain transfer to solvent, respectively; $[M]$ is concentration of monomer; $[\Delta M]$ is the change in the concentration of monomer; n is the degree of polymerization; $[W_n]$ is the concentration of polymer with degree of polymerization n; R_i is the rate of initiation; and $[S]$ is the concentration of solvent.

For bulk polymerization, $[S] = 0$. If termination by combination alone is considered,

$$k_t' = 0$$

Therefore, eq. (5) reduces to

$$[W_n] = \frac{[\Delta M]}{k_p[M]} (1 - x)x^{n-1} \left(k_{trm}[M] \right.$$
$$\left. + \left(\frac{R_i}{k_t}\right)^{1/2} \left\{ \frac{(x - 1)k_t(k_{trm}[M] + (R_ik_t)^{1/2})}{2k_p[M]} \right\} \right) \quad (6)$$

and

$$x = \frac{k_p[M]}{k_p[M] + k_{trm}[M] + (R_ik_t)^{1/2}}$$

$$R_i^{1/2} = \frac{R_p}{[M]\left(\dfrac{k_p}{\sqrt{k_t}} + \dfrac{k_{trm}}{\sqrt{k_t}}\right)} \quad (7)$$

Therefore,

$$(R_ik_t)^{1/2} = \frac{R_p k_t}{[M](k_p + k_{trm})} \quad (8)$$

where R_p is the overall rate of polymerization.

From eqs. (6) and (8),

$$[W_n] = [\Delta M](1 - x)x^{n-1}\left[\frac{k_{trm}}{k_p} + \frac{x - 1}{2y}\left(\frac{R_p}{[M]^2}\frac{k_{trm}}{k_p}\right) + \frac{R_p}{y[M]^2}\right] \quad (9)$$

where,

$$y = \frac{k_p^2}{k_t} + \frac{k_{trm}k_p^2}{k_pk_t} \quad (10)$$

and

$$x = \frac{1}{1 + (k_{trm}/k_p) + (R_p/y[M]^2)} \quad (11)$$

The values of k_p^2/k_t and k_{trm}/k_p are known at each of the six temperatures (data from Figs. 13 and 14). R_p is known for each run and $[M]$ is also known.

$[\Delta M]$ which is the change in the concentration of monomer is equal to the per cent conversion $\times [M]/100$. Per cent conversion is known for every sample used for the experimental molecular weight distribution. Thus $[W_n]$ can be calculated for different values of n. This gives the theoretical molecular weight distribution. From the theoretical molecular weight distribution, the number-average molecular weight $\bar{M}_n$, the weight-average molecular weight $\bar{M}_w$, and the polydispersity ratio $\bar{M}_w/\bar{M}_n$ were calculated by using the relationships (12) and (13):

$$\bar{M}_n = \frac{\displaystyle\sum_n n[W_n]}{\displaystyle\sum [W_n]} \times \text{molecular weight of styrene monomer} \quad (12)$$

and

$$\bar{M}_w = \frac{\sum_n n^2[W_n]}{\sum_n n[W_n]} \times \text{molecular weight of styrene monomer} \qquad (13)$$

A computer program was written in Fortran IV to facilitate these calculations. All the computations were carried out on the University of Waterloo IBM 7040 and 360/75 computers.

References

1. A. Chapiro, *Radiation Chemistry of Polymeric Systems*, Wiley, New York, 1962.

2. C. S. H. Chen and R. F. Stamm, *J. Polym. Sci.*, **58**, 369 (1962).

3. S. Okamura, K. Ueno, and K. Hayashi, *J. Polym. Sci. B*, **3**, 363 (1965).

4. R. C. Potter, C. L. Johnson, D. J. Metz, and R. H. Bretton, *J. Polym. Sci. A-1*, **4**, 419 (1966).

5. K. Ueno, K. Hayashi, and S. Okamura, *Polymer*, **7**, 431 (1966).

6. C. H. Bamford, W. G. Barb, A. D. Jenkins, and P. F. Onyon, *The Kinetics of Vinyl Polymerization by Radical Mechanisms*, Butterworths, London, 1958.

7. D. S. Ballantine, P. Colombo, A. Glines, and B. Manowitz, *Chem. Eng. Prog. Symp. Ser. (Nuclear Eng.)*, **50**, No. 11, 267 (1954).

8. A. V. Tobolsky and J. Offenbach, *J. Polym. Sci.*, **16**, 311 (1955).

9. M. S. Matheson, E. E. Auer, E. B. Bevilacqua, and E. J. Hart, *J. Amer. Chem. Soc.*, **73**, 1700 (1951).

10. F. R. Mayo, R. A. Gregg, and M. S. Matheson, *J. Amer. Chem. Soc.*, **73**, 1691 (1951).

11. J. C. Beavington, H. W. Melville, and R. P. Taylor, *J. Polym. Sci.*, **12**, 449 (1954).

12. J. C. Beavington, H. W. Melville, and R. P. Taylor, *J. Polym. Sci.*, **14**, 463 (1954).

13. C. A. Baker and R. J. B. Williams, *J. Chem. Soc.*, **1956**, 2352.

14. J. H. Duerksen, A. E. Hamielec, and J. W. Hodgins, *A.I.Ch.E. J.*, **13**, 1081 (1967).

15. A. E. Hamielec, J. W. Hodgins, and K. Tebbens, *A.I.Ch.E. J.*, **13**, 1087 (1967).

16. L. H. Tung, *J. Appl. Polym. Sci.*, **10**, 375 (1966).

Change with Temperature of the ESR Spectra of Methacrylic Acid Radicals*

YOSHIRO SAKAI and MACHIO IWASAKI, *Government Industrial Research Institute, Hirate-machi, Kita-ku, Nagoya, Japan*

Synopsis

In order to elucidate the structure of methacrylic acid radicals, the change with observation temperature of the ESR spectrum of free radicals trapped in solid methacrylic acid γ-irradiated at −196°C was studied. Below −80°C, we found a 9-line spectrum, which is similar to the ordinary 9-line spectrum observed in irradiated poly(methacrylic acid) or poly(methyl methacrylate), but which differs in the stronger intensity of the so-called 4-line component. Our 9-line spectrum changes reversibly into a 13-line spectrum above −80°C. With broad-line NMR measurements of methacrylic acid, it was found that there is such an unusual crystalline transition around −30°C that the line width is narrower in the lower-temperature region (phase II) than that in the higher-temperature region (phase I). The change of the ESR spectrum can be interpreted in terms of the exchange of the two β-protons due to the hindered oscillation around the C_α—C_β bond of the single radical $\cdots C_\beta H_2 \dot{C}_\alpha (CH_3)COOH$ if one assumes the gradual change of the hindering potential barrier caused by the crystalline transition and the lower barrier in phase II. The modified Bloch treatment gave the hindering potential barrier to be 7.2 kcal/mole in phase I and 1.5 kcal/mole in phase II. The difference between our 9-line spectrum and the ordinary one with the very weak 4-line component comes from the difference of the surrounding matrix.

INTRODUCTION

Although it is well known that the methacrylic radical exhibits the so-called 9-line spectrum in the solid state, the origin of this spectrum is still open to question. There have been a tremendous number of papers concerning whether this spectrum is attributable to a single radical species or not, including discussions concerning the conformation of the radical.

The ESR spectra of the free radicals formed in methacrylic acid have been studied by several authors.[1–9] Most of them have reported on the ESR spectrum in the solid state. Recently Bamford and his co-workers[5,8] studied the ESR spectrum of methacrylic acid which was exposed to ultraviolet light in the solid state. They measured all the spectra at −196°C but did not study the change in spectra with temperature. In their case, an ordinary 9-line spectrum was observed when the monomer was exposed above −5°C, while in the temperature range from −5°C to −30°C each line of the so-called four-line component splitted into a doublet resulting

in a 13-line spectrum.   Furthermore, this 13-line spectrum changed to the ordinary 9-line spectrum when the sample was annealed at 0°C.   They suggested that by assuming the existence of the propagating radical I,

$$
\begin{array}{c}
CH_3 \\
| \\
-C_\beta H_2 - \underset{a}{\overset{\cdot}{C}} \\
| \\
COOH
\end{array}
$$

I
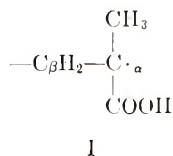
the ordinary 9-line spectrum is attributable to a symmetrical conformation of the half-filled p-orbital relative to the C_β—H bond, that is $\theta_1 = \theta_2 = 60°$ in Figure 1, while the 13-line spectrum is attributable to a radical species with slightly deformed conformations from the symmetrical position. They also suggested that the variation of the ESR spectrum due to the crystallization temperature is attributable to the change of the mixing ratio of the deformed and symmetrical conformations.   The change of the
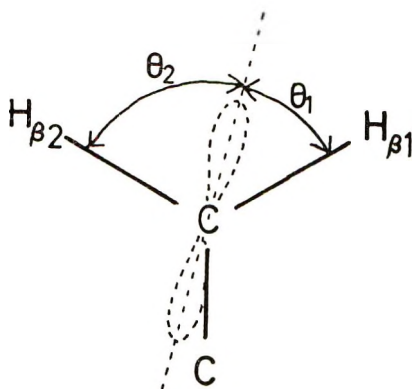
Fig. 1. Conformation of the half-filled p-orbital of methacrylic acid radicals, —$C_\beta H_2$—$C_a(CH_3)COOH$.

mixing ratio was attributed to the formation of crystal imperfections and the crystalline transitions at about $-12°$ and $+3°$, which were observed with broad-line NMR measurements.[8]

On the other hand, Fisher and Giacometti[6,7,9] observed the ESR spectra of the propagating radicals of methacrylic acid in an aqueous solution by using a flow system.   In the flow system the spectrum consists of 16 lines in place of the ordinary 9 lines.   This spectrum was assigned to a single conformation of the propagating radical whose two β protons have different coupling constants, corresponding to the deformed conformation. The alternation of the line width of the hyperfine components due to $\sum M_I = 0$ was well explained by assuming the hindered oscillation around the C_a—C_β bond.   According to Fisher, the ordinary 9-line spectrum for the solid polymers is thought to be an unresolved 16-line spectrum.

The 13-line spectrum found in solid methacrylic acid is essentially the same spectrum as the 16-line spectrum. The difference comes from the occasional overlapping of some lines. Consequently it would be expected that if the hindered oscillation around the C_α—C_β bond has some role in the solid state, then the spectral line shape should exhibit a temperature dependence. If the hyperfine components corresponding to $\sum M_I = 0$ coagulate due to the oscillational effect, the 9-line spectrum may be observed at higher temperature and the 13-line spectrum at lower temperature.

From this point of view, methacrylic acid radicals were produced by γ-irradiation of the solid monomer and the change of the ESR spectrum of the trapped radicals with observation temperature was studied. However, it was found unexpectedly that the propagating radical in methacrylic acid shows a 9-line spectrum at lower temperature, while with rising temperature the spectrum gradually changes into a 13-line structure, and this change with temperature takes place reversibly. In order to elucidate the cause of this temperature change of the spectrum which is contrary to expected behavior, the crystalline transition of the monomer was studied by broad-line NMR measurements, and an unusual transition was found at $-30°C$. The temperature change of the ESR spectrum found is seemingly explained with reference to this unusual crystalline transition.

EXPERIMENTAL

Methacrylic acid was purified as described previously by Bamford et al.,[10] and then the occluded air was degassed by repeated freezing and melting *in vacuo*. Methacrylic acid was then distilled into Spectrosil ESR sample tubes and was sealed off under a pressure of 10^{-5} mm Hg. The polycrystalline samples formed by freezing at $-196°C$ were irradiated with γ-rays from a ^{60}Co source at $-196°C$. The total dose was 2×10^5R at a dose rate of 3.1×10^4R/hr. A Japan Electron Optics Model 3BSX spectrometer was used for recording the ESR spectra in the range of $-196°C$ to $+10°C$ at 9.4 Gcps with 100 Kcps modulation. For the broad-line NMR measurements, purified methacrylic acid was sealed in a thin glass tube. Polycrystalline samples were prepared at two different temperatures: one was crystallized at $-196°C$ and the other at $+10°C$. Broad-line NMR spectra were recorded with Japan Electron Optics broad-line NMR spectrometer in the range of -150 to $+16°C$ at 30 Mcps.

RESULTS

Change with Temperature of ESR Spectrum

The change with observation temperature of the ESR spectrum of methacrylic acid irradiated at $-196°C$ is shown in Figure 2. The 7-line spectrum at $-196°C$ shown in Figure 2a corresponds to the monomer radical II which was formed by addition of a hydrogen atom to the double bond.[11]

$$CH_3-\underset{\underset{\displaystyle COOH}{|}}{\overset{\overset{\displaystyle CH_3}{|}}{C}}\cdot$$
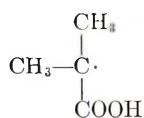
II

The spectrum is consistent with a coupling value of 21.4 G for the equivalent 6 protons involved in the two freely rotating methyl groups.
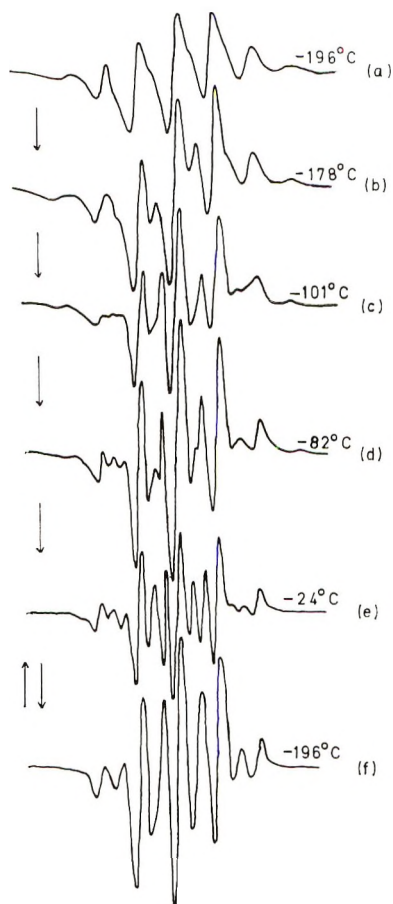
Fig. 2. Change with observation temperatures of the ESR spectra of methacrylic acid γ-irradiated at −196°C. Temperatures indicated in the figure are the observation temperatures of the spectra. The change between curves (e) and (f) is reversible.

With increasing temperature from −196 to −178°C, the spectrum changed gradually into a 9-line spectrum. This indicates that the monomer radical begins to react with neighboring monomers to form the propagating radical I

$$H \quad CH_3$$
$$-\overset{|}{\underset{|}{C}}_\beta - \overset{|}{\underset{|}{C}}_\alpha \cdot$$
$$H \quad COOH$$
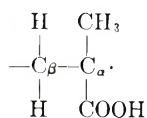
I

although it is the assignment of the 9-line spectrum to this radical which is presently under consideration. As the temperature increased further to $-101°C$, the monomer radicals almost disappeared, leaving the 9-line spectrum as shown in Figure 2c. When the temperature increased further to $-82°C$, each line of the 4-line component of the 9-line spectrum began to split into a doublet as shown in Figure 2d, and as a result the overall number of lines became 13 (5 + 8), as shown in Figure 2e. This 13-line spectrum at $-24°C$ is essentially the same as the one that was obtained with methacrylic acid irradiated with ultraviolet light below $-5°C$.[5,8]

On recooling the sample very slowly $(20–30°C/hr)$ from $-24°C$ to $-196°C$, a 9-line spectrum was again obtained, as is shown in Figure 2f. It should be noted here that although this 9-line spectrum is similar to that of methacrylic acid irradiated by ultraviolet light above $-5°C$ or that of irradiated poly(methacrylic acid), the intensity of the so-called
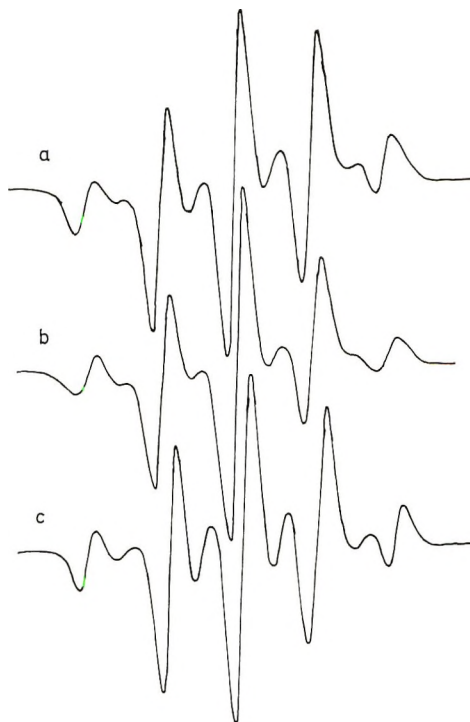
Fig. 3. ESR spectra of methacrylic acid radicals produced by γ-irradiation at 0°C: (a) methacrylic acid monomers; (b) poly(methacrylic acid); (c) simulated spectrum by the method described in the text.

four-line component is very much stronger when measured at $-196°C$. It is further to be noted that this change with temperature between 13-line and 9-line spectra took place reversibly many times. The intermediate spectra of this reversible change, for several temperatures, are given in Figure 7a (p. 1759). On the other hand, if the sample was cooled to $-196°C$ very rapidly, the 13-line spectrum did not change the 9-line spectrum.

If the sample was irradiated at 0°C, for a low dose, for which no appreciable polymerization was observed, then a 13-line spectrum which is essentially the same as that indicated in Figure 2e was obtained, but after prolonged irradiation with appreciable polymerization, the ordinary 9-line spectrum having a very weak 4-line component was obtained, as shown in Figure 3a. This spectrum is quite similar to the 9-line spectrum obtained by the irradiation of poly(methacrylic acid) shown in Figure 3b. In addition, the ordinary 9-line spectrum having a very weak 4-line component did not show the temperature dependence of the line shape of the 4-line component which is described above.

Unusual Transition of Methacrylic Acid Crystals

In connection with the temperature dependence of the ESR spectrum, the broad-line NMR spectra of the monomer were measured at various temperatures. Figure 4 shows the temperature change of the maximum
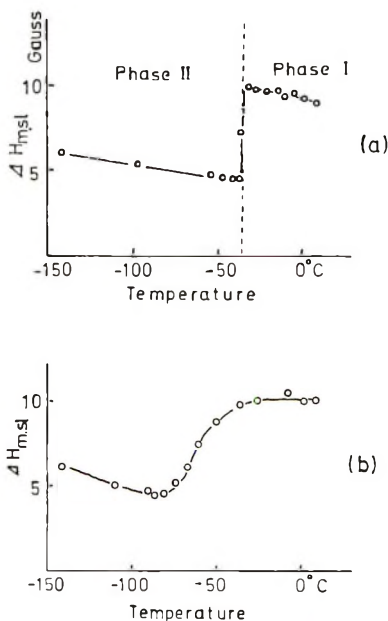
Fig. 4. Change of the maximum slope distance (ΔH_{msl}) with temperature of the broad-line NMR spectra of methacrylic acid: (a) sample rapidly cooled to $-196°C$ directly from the liquid phase; (b) sample crystallized by keeping 1.5 hr at $+10°C$ and then cooled to $-196°C$.

slope distance ΔH_{msl} of the NMR spectrum of methacrylic acid. When the monomer sample was rapidly cooled to $-196°C$ from $+20°C$, at which temperature the monomer is in a liquid phase, ΔH_{msl} gradually decreased with increasing temperature from $-196°C$, but when the temperature reached around $-30°C$, ΔH_{msl} suddenly increased by about 5 gauss as is indicated in Figure 4a. Moreover, this sudden change of ΔH_{msl} was found to occur reversibly. It should be noted that, in contrast to the ordinary case, in the lower-temperature phase (phase II) the ΔH_{msl} is narrower than that at higher temperature (phase I). If phase II is the supercooled liquid phase which is supposed to have a narrower ΔH_{msl} and the broadening at $-30°C$ corresponds to crystallization, one can not expect to find the sudden change at $-30°C$ when the temperature is lowered from phase I. Therefore, the fact that the change of ΔH_{msl} is reversible strongly suggests that phase II is not a supercooled liquid phase, but a different crystalline phase from phase I, stable at higher temperature.

On the other hand, another liquid monomer sample for the NMR measurement was crystallized rather slowly by keeping the sample at $+10°C$ (phase I) for $1\frac{1}{2}$ hr and then cooling the sample down to $-196°C$, rapidly passing through the transition point at $-30°C$. The results are shown in Figure 4b. In this case, the change of ΔH_{msl} due to the crystalline transition started at a lower temperature ($-80°C$) than in the case shown in Figure 4a, although both changes ended at the same temperature ($-30°C$). The reason for this is that in the latter case the crystal of phase I grown at $+10°C$ was rapidly cooled to the temperature of phase II, passing through the transition point at $-30°C$, so that a small amount of crystals of phase I may be mixed as an impurity in the crystalline lattice of phase II, resulting in the lowering of the starting temperature of the transition.

This crystalline transition was also confirmed by differential thermal calorimetry. Details of the crystalline transition and the behavior of the trapped radicals, such as the radical build-up and decay related to this transition, will be reported elsewhere in connection with the solid-state polymerization of this monomer. All these experiments were quite consistent with this unusual crystalline transition.

In our experiments we could not find the transitions at $-12°$ and $+3°C$ found by Bamford et al. These transitions are accompanied by an ordinary decrease of ΔH_{msl} due to the motional freedom of the molecules near the melting point.

ANALYSIS AND DISCUSSION

Qualitative Interpretation of the Spectral Change with Temperature

Fisher et al.[6,7] observed a 16-line spectrum of methacrylic acid radicals produced in redox system in an aqueous solution and showed that the two protons of the methylene group give different coupling constants, that is, $a_{\beta H_1}$ is 13.75 G and $a_{\beta H_2}$ is 11.04 G. In our case, the 13-line spectrum

observed at $-24°C$ is interpreted by assuming that a_{CH_3} for the freely ro-
tating CH_3 group is 22.2 G, $a_{\beta H_1}$ is 14.7 G, and $a_{\beta H_2}$ is 7.5 G.   Accidentally
a_{CH_3} is nearly equal to $a_{\beta H_1} + a_{\beta H_2}$, so that the 4th, 7th, and 10th line of
the 13 lines are actually composed of two lines, because of an occasional
overlapping in our case in comparison with the 16-line spectrum obtained
by Fisher et al.[6,7] (see Fig. 5).   The coupling value of 14.7 G for the $H_{\beta 1}$
gives the conformational angle of the half-filled p-orbital to the C_β—H
bond to be 55°, while the value of 7.5 G for the $H_{\beta 2}$ gives 65°, if we assume
$B = 46$ G in the so-called $B \cos^2\theta$ rule.   Therefore, the direction of the
p-orbital is slightly tilted from the symmetrical position, that is, from 60°.
If the system is rigid enough and no oscillation around the C_α—C_β bond
occurred, the intensity ratio of each line would be 1:1:1:4:3:3:6:3:3:4:
1:1:1 as is shown in Fig. 5.   The observed spectrum at $-24°C$ has an
intensity ratio fairly close to this predicted spectrum.
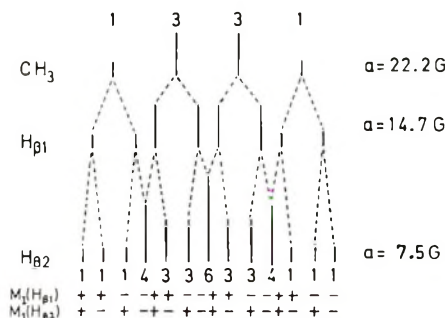
Fig. 5. Decomposition of the 13-line spectrum and the relative intensities of the lines.
Signs on the lowest line indicate those of nuclear spins of the two β-protons in the
methylene group of the radical.

In the 9-line spectrum, however, each of four groups of the two lines
corresponding to $\sum M_I = 0$, for the two β-protons in the 13-line spectrum,
i.e., the 2nd and 3rd, the 5th and 6th, the 8th and 9th, and the 11th and
12th lines in Figure 5, becomes a single line resulting in formation of the
so-called 4-line component and as a result the overall number of lines be-
comes 9.   In our experiments, while the 5-line component corresponding
to $\sum M_I = \pm 1$ did not change with temperature, the so-called 4-line com-
ponent corresponding to $\sum M_I = 0$ showed variation between 4 and 8 lines
with temperature as shown in Figure 7a.   Besides this, in referring to the
reversibility of the change of the lines corresponding to $\sum M_I = 0$, it seems
possible to interpret this change of the spectrum in terms of the exchange
of the two β-protons due to the hindered oscillation around the C_α—C_β
bond, because the $\sum M_I = 0$ lines are affected by the exchange of the two
β-protons, while the $\sum M_I = \pm 1$ lines are not.   In this proton-exchange
model, when the average lifetime of the proton exchange τ is long enough
compared with $^1/_{2\pi\Delta\nu_{spl}}$ ($\tau \gg {}^1/_{2\pi\Delta\nu_{spl}}$), where $\Delta\nu_{spl}$ is the difference of the

resonance frequencies for the two protons, each of the $\sum M_I = 0$ lines, that is, the so-called 4-line component, should clearly split to form a spectrum as illustrated in Figure 5. As τ becomes shorter $(\tau \approx 1/2\pi\Delta\nu_{spl})$, the $\sum M_I = 0$ lines become broader and weaker, and the separation of the two lines becomes smaller. Eventually the two lines appear as a single line at the averaged position of the two lines when τ becomes much smaller than $1/2\pi\Delta\nu_{spl}$ $(\tau \ll 1/2\pi\Delta\nu_{spl})$.

In ordinary cases, the mean lifetime of the proton exchange τ becomes longer as the temperature decreases. Therefore, in the case of the methacrylic acid radical the 9-line spectrum should appear in the higher-temperature region, while the 13-line spectrum should be observed in the lower-temperature region in which τ is longer. The results of the observation
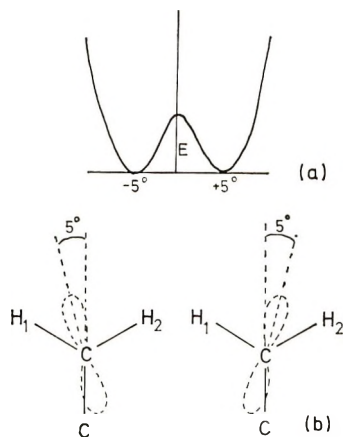
Fig. 6. (a) Schematic potential energy curve of the methacrylic acid radical for hindered oscillation around the C_α—C_β bond; (b) two stable conformations which are the mirror images of each other. Rapid exchange of the two sites takes place in phase II, and the potential barrier E varies during the crystalline transition.

are, however, completely opposed to this expectation. These unexpected experimental results, nevertheless, can be reasonably interpreted if the unusual crystalline transition observed in the broad-line NMR measurements is taken into consideration. According to our NMR measurements, ΔH_{msl} is unusually narrow in the lower temperature region (phase II). This may mean that the intermolecular interactions are weaker in phase II than those in phase I. In the crystalline solids, the potential barrier to internal rotation of the trapped radical may be much affected by the intermolecular interaction with surroundings, so that the potential barrier E between the two conformations corresponding to the mirror images as illustrated in Figure 6 may be higher in phase I than in phase II, that is, longer τ in phase I and shorter τ in phase II.

If this is the case, one can expect an opposite temperature change of the

4-line component due to the change of the potential barrier between the two different phases.*

Quantitative Analysis of the Spectral Change by Bloch Equations

On assuming the change of the hindering potential barrier caused by the crystalline transition and the lower barrier in phase II, the ESR simulation was carried out by solving the modified Bloch equations. The problem of the ESR spectrum of a system which presents variation in the β-proton hyperfine coupling values and the intensities with temperature have been treated by several authors[13-18] as a problem of hindered oscillation of a certain group of the radical. The same procedure can be applied to the present case.[13,14]

The modified Bloch equations for the oscillating methylene group are simply expressed by the treatment for the two-site exchange A and B.

$$dG_A/dt + [1/T_2 + 1/\tau - ig\beta(H_A - H)/\hbar] = ig\beta H_1 M_{Az}/\hbar + G_B/\tau \quad (1)$$

$$dG_B/dt + [1/T_2 + 1/\tau - ig\beta(H_B - H)/\hbar] = ig\beta H_1 M_{Bz}/\hbar + G_A/\tau \quad (2)$$

The solution of eqs. (1) and (2) is

$$G = G_A + G_B = i\tau(g\beta/\hbar)H_1 M_0(f_A + f_B)/2(1 - f_A - f_B) \quad (3)$$

$$dG/dH = \tau^2(g\beta/\hbar)^2 H_1 M_0(f_A^2 + f_B^2)/2(1 - f_A - f_B)^2 \quad (4)$$

where

$$M_0 = M_{Az} + M_{Bz} \quad (5)$$

$$f_A = [2 + \tau/T_2 - i\tau(g\beta/\hbar)(H_A - H)]^{-1} \quad (6)$$

$$f_B = [2 + \tau/T_2 - i\tau(g\beta/\hbar)(H_B - H)]^{-1} \quad (7)$$

Therefore the normalized derivative curve of the ESR absorption is

$$g(H) = \text{Imag.} (8/3\sqrt{3})(\tau/T_2)^2(f_A^2 + f_B^2)/(1 - f_A - f_B)^2 \quad (8)$$

For the very large τ, the line shape approaches the Lorentzian. Equation (8) is normalized so as $g(H) = 1$ at the maximum slope point $H = H_A \pm \hbar/\sqrt{3}g\beta T_2$ for $\tau = \infty$. T_2 was obtained from the ΔH_{msl} of the $\sum M_I = \pm 1$ line, the width of which is independent of temperature, by using the relation, $\Delta H_{msl} = 2\hbar/\sqrt{3}g\beta T_2$.

In the present case, the shapes of the $\sum M_I = 0$ lines must be expressed by eq. (8). The ESR spectra of our radical are simulated in the following way. As the 5-line component does not change with temperature, these lines are assumed to be independent of the τ value. As for the 4-line com-

* After finishing this work, we found Bowden and O'Donnell's paper[12] on ESR spectra of barium methacrylate dihydrate. They found just the expected normal temperature change of the spectrum. This is evidently due to the absence of an anomalous phase transition in barium methacrylate dihydrate. Our assumption is strongly confirmed by their results.
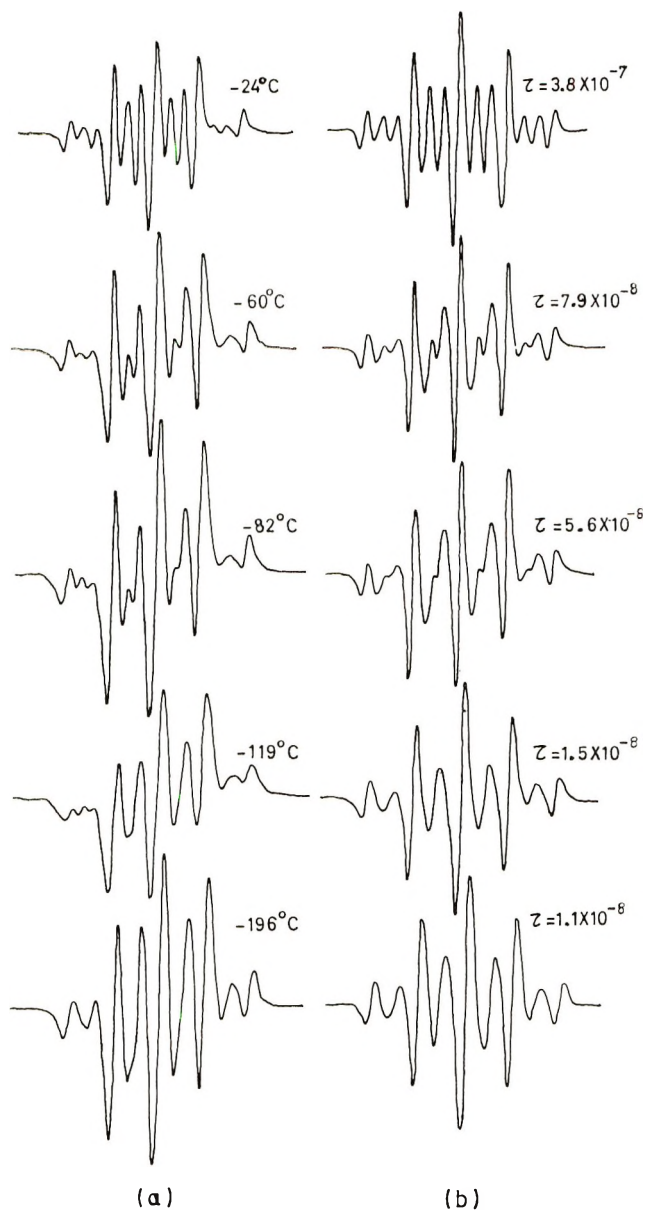
Fig. 7. Comparison of the observed ESR spectra of (a) methacrylic acid radicals at various temperatures with (b) simulated spectra for the various τ values.

ponent, the line shape of each line was calculated with eq. (8) for the several τ values by using a digital computer. The simulated spectra thus obtained are given in Figure 7b. It is clearly shown that the spectrum changes between the 13- and 9-line spectra according to the τ value. The simulated spectra are in good agreement with the observed ones shown in Figure 7a. From this beautiful agreement it seems that proton exchange

due to hindered oscillation may well be the cause of the temperature dependence of the spectrum. By comparing both spectra, the τ values at several temperatures were obtained.

Estimation of the Potential Barriers

In the usual case, a potential barrier is independent of temperature, and correlation time of the exchange τ is given as

$$\tau = \tau_0 \exp\{E/RT\} \tag{9}$$

or

$$E = RT \ln (\tau/\tau_0) \tag{10}$$

where τ_0 is the reciprocal of the frequency factor.

In the present case, however, the potential barrier of the proton exchange was assumed to change with temperature due to the rearrangement of the surrounding matrix of the trapped radical. Therefore, the potential barrier E should be considered as a function of temperature T. Therefore

$$E(T) = RT \ln (\tau/\tau_0) \tag{11}$$

If one assumes the value of τ_0, the potential barriers at various temperatures can be estimated from the τ values determined in the foregoing section. The frequency factor is given by the equation $f_0 = \tau_0^{-1} = kT/h$ from the absolute rate theory.[19] Therefore the τ_0 values are calculated for the various temperatures at which our observations were made. By using these values, the potential barriers at various temperature were obtained by eq. (11). The results are plotted in Figure 8. The fact that the potential barrier does not change suddenly at the crystalline transition point but increases gradually may be due to the impedance by the long propagating radical of the rapid rearrangement of the surrounding molecules and due to the impurity effect already mentioned in the section on NMR measurements. The fact that the rapid cooling did not produce a spectral change from a 13-line to a 9-line spectrum may be also due to the same cause.
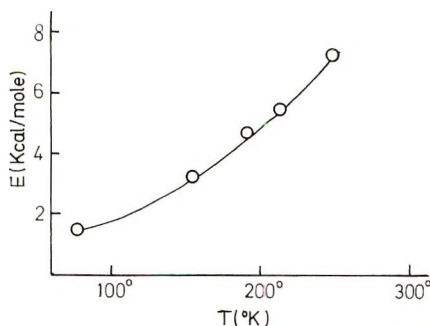
Fig. 8. Temperature change of the potential barrier for the hindered oscillation around the C_α—C_β bond of methacrylic acid radicals during the crystalline transition.

The values of E vary from 1.5 kcal/mole at $-196°C$ (phase II) to 7.2 kcal/mole at $-24°C$ (phase I). The value of E is not so sensitive to the assumed value of the frequency factor, that the order of magnitude obtained is considered to be fairly reliable. Moreover, the order of magnitude of the potential barrier thus obtained seems quite reasonable for the hindering potential of the internal rotation. These values may be compared with the value of 410 cal/mole in the case of allyl radical—CH_2—CH—$CH=CHCH_2$— in polyethylene[15] and the value of 2.4 kcal/mole in the case of the fumaric acid radical $HOOC$—CH_2—CH—$COOH$ formed in a single crystal of a urea–fumaric acid addition compound.[16] A recent observation by Ohigashi and Kurita for $\cdot CH_2COO^-$ in a single crystal of zinc acetate dihydrate gave a value of 5.8 kcal/mole.[18] The fact that the potential barriers in our case have reasonable values compared with other cases also tends to support our interpretation.

Another Possible Interpretation

There may be another possibility of the interpretation of the spectral change with temperature such as Bamford et al.[8] suggested. In their postulate, the two conformations with $\theta_1 = \theta_2 = 60°$ and $\theta_1 = 60° - \alpha$, $\theta_2 = 60_2 + \alpha$ are considered to make up the difference of the spectra by varying the mixing ratio of the two conformations. Therefore, another possibility is that phase II is favored for the former conformation and phase I for the latter conformation. Consequently during the crystalline transition the two conformations might be mixed.

We have carried out ESR simulations with several mixing ratios of the conformation of $\theta_1 = \theta_2 = 60°$ and that of $\alpha = 5°$. The results are shown in Figure 9. Some of them resemble the observed spectra while others do not. From these computations, the hindered-oscillation model seems more probable than the two-conformation postulate. However, if the tilt angle α from the symmetrical position varies gradually from $0°$ to $5°$ during the molecular rearrangement, we should take into consideration the various conformations between $0°$ and $5°$ for the intermediate range of the transition. Although it is not feasible to make such a computation, if this were the case, a closer resemblance of the simulated curves with the observed ones might be obtained. Therefore, this sort of explanation may not be definitely excluded at the present stage, although the hindered-oscillation model seems more reasonable.

Difference between the 9-Line Spectrum
and the Usual Spectrum

As already mentioned, the 9-line spectrum we obtained on the low-temperature irradiation has a much stronger intensity due to the 4-line component than that of the ordinary 9-line spectrum obtained by the irradiation at $0°C$ or by ultraviolet irradiation above $-5°C$.* It should be

---

* There is no indication of the 9-line spectrum in the paper of Bamford et al.[8] We tried the same experiment and got the ordinary 9-line spectrum.

noted that the latter spectrum is very similar to that obtained by the irradiation of poly(methacrylic acid) as shown in Figure 3b. It should be also mentioned that if we assume the symmetrical structure $\theta_1 = \theta_2 = 60°$ for the ordinary 9-line spectrum, we should expect much stronger intensity for the 4-line component. The intensity ratio of the 9 lines should be 1:2:4:6:6:6:4:2:1. However, the ordinary 9-line spectrum has a very
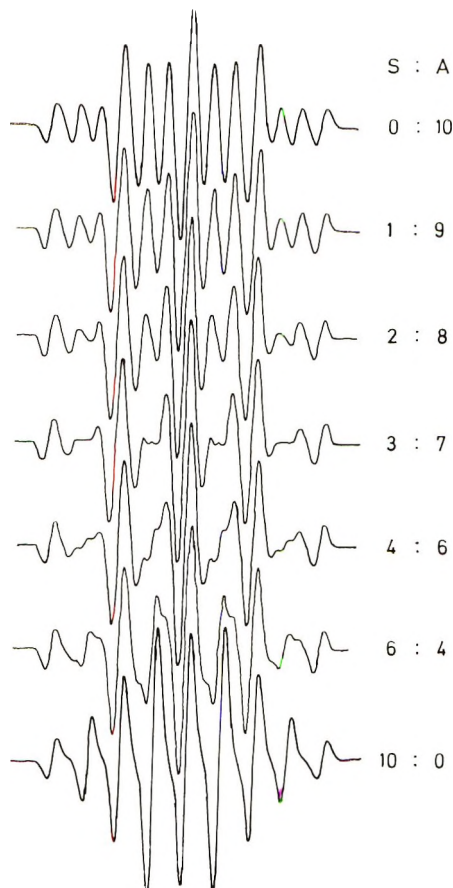
Fig. 9. Simulated spectra for the mixtures of the radicals having two conformations, S ($\theta_1 = \theta_2 = 60°$) and A ($\theta_1 = 55°$, $\theta_2 = 65°$). S:A denotes the mixing ratio of the two conformations.

much weaker intensity for the 4-line component. According to our computation, it is also impossible to reveal such a weak intensity even if we introduce the exchange of the two β-protons with $\tau \approx 1/2\pi\nu_{spl}$ for which we would have the weakest 4-line component.

There is another important experimental fact that should be emphasized. The ordinary 9-line spectrum does not give an appreciable change with temperature of the intensity of the 4-line component in the range from

−196°C to room temperature. In our opinion, therefore, we should distinguish the ordinary 9-line spectrum from ours having the fairly strong 4-line component which can be interpreted by proton exchange.

Now, if this is the case, one should consider why the 13-line spectrum was obtained by the irradiation at 0°C after low dose, while the ordinary 9-line spectrum was obtained by the prolonged irradiation at 0°C in our experiments. In the case of ultraviolet irradiation, Bamford et al.[5,8] also reported that the ordinary 9-line spectrum was obtained above −5°C and that annealing of the sample gave the 13-line spectrum.* As already mentioned, this 9-line spectrum is essentially the same as that obtained in the irradiated poly(methacrylic acid). Therefore, in the case of γ-irradiation at 0°C or ultraviolet irradiation above −5°C, it is considered that the polymerization of the monomers took place during the irradiation and the trapped radicals are surrounded by polymer molecules which are formed during irradiation.

If the tilt angle of the half-filled p-orbital is affected by the surrounding matrix, the conformational angle of the p-orbital may not have the fixed angle θ in the case of irregular surroundings of the noncrystalline poly(methacrylic acid). If this is the case, the width of the 4-line component is broadened and its intensity is lowered. We have tried ESR simulation for such a model. If we assume the most probable tilt angle of 5°, that is, $\theta_1 = 55°$ and $\theta_2 = 65°$, and the Gaussian distribution around this position with the half-height width of 5°, we could successfully simulate the ESR spectrum which quite resembles the observed ordinary 9-line spectrum as shown in Figure 3c. Therefore, it is probable that the propagating radical giving the ordinary 9-line spectrum is surrounded by irregular matrices of polymer molecules, resulting in the situation that the spectrum is not affected by the crystalline transition of the monomer molecules. If the potential barrier to hindered oscillation in a polymeric matrix is around 10 kcal/mole, one may not observe the temperature variation of the 4-line component between −196° and room temperature.[18] The details of the computations of the ESR simulation of the ordinary 9-line spectrum will be given in a subsequent paper.

CONCLUSIONS

Based on the considerations mentioned in the last section and the abnormally small ΔH_{msl} of the broad line NMR spectra in phase II, the temperature change of the ESR spectrum is well interpreted by proton exchange due to the oscillation around the C_α—C_β bond of the single radical species —$C_\beta H_2$—$\dot{C}_\alpha(CH_3)COOH$ trapped in the monomer lattice, if one assume that the potential barrier gradually changes due to the crystalline transition accompanied by the rearrangement of the surrounding molecules of the trapped radicals and that the potential barrier is lower in phase II

---

* The reason that the 13-line spectrum was observed at −196°C is simply that the samples were cooled rapidly down to −196°C.

than that in phase I. The conformational angles of the half-filled p-orbital to the two C_β—H bonds of this radical are $55°$ and $65°$, respectively.

References

1. S. E. Bresler, E. N. Kasbekov, and E. M. Saminskii, *Vvsokomol. Soedin.*, **1**, 1374 (1959).

2. C. H. Bamford and J. C. Ward, *Polymer*, **2**, 277 (1961).

3. C. H. Bamford and J. C. Ward, paper presented at Fifth International Symposium on Free Radicals, Uppsala, Sweden, 1961.

4. R. Bensasson, A. Bernas, M. Bodard, and R. Marx, *J. Chim. Phys.*, **60**, 950 (1963).

5. H. Bamford, G. C. Eastmond, and Y. Sakai, *Nature*, **200**, 1284 (1963).

6. H. Fischer, *J. Polym. Sci. B*, **2**, 529 (1964).

7. H. Fischer, *Z. Naturforsch.*, **19A**, 866 (1964).

8. C. H. Bamford, A. Bibby, and G. C. Eastmond, in *International Symposium on Macromolecular Chemistry, Prague 1965*, (*J. Polym. Sci. C*, **16**), O. Wichterle and B. Sedláček, Eds., Interscience, New York, 1967, p. 2417.

9. H. Fischer and G. Giacometti, in *International Symposium on Macromolecular Chemistry, Prague, 1965, J. Polym. Sci. C*, **16**, O. Wichterle and B. Sedláček, Eds., Interscience, New York, 1967, p. 2763.

10. C. H. Bamford, G. C. Eastmond, and J. C. Ward, *Proc. Roy. Soc. (London)*, **A271**, 357 (1963).

11. D. W. Ovenall, *J. Polym. Sci.*, **41**, 199 (1959).

12. M. J. Bowden and J. H. O'Donnell, *J. Phys. Chem.*, **72**, 1577 (1968).

13. I. Miyagawa and K. Itoh, *J. Chem. Phys.*, **36**, 2157 (1962).

14. M. Kashiwagi and Y. Kurita, *J. Chem. Phys.*, **39**, 3165 (1963).

15. S. Onishi, S. Sugimoto, and I. Nitta, *J. Chem. Phys.*, **37**, 1283 (1962).

16. C. Corvaja, *J. Chem. Phys.*, **44**, 1958 (1966).

17. C. Corvaja, *Trans Faraday Soc.*, **63**, 26 (1967).

18. H. Ohigashi and Y. Kurita, *Bull. Chem. Soc. Japan*, **41**, 275 (1968).

19. S. Glasstone, K. J. Leidler, and H. Eyring, *The Theory of Rate Processes*, McGraw-Hill, New York, 1941, Chap. 4.

Properties of Swollen Block Copolymer Elastomers

STUART L. COOPER, *Department of Chemical Engineering, University of Wisconsin, Madison, Wisconsin 53706*

Synopsis

The linear polyester–urethane block copolymer Estane is soluble in solutions having a solubility parameter of about 10.5. In benzene–methanol mixtures having solubility parameters sufficiently above and below 10.5, it is possible to swell this polymer to a quasi-equilibrium state. For samples swollen to the same swelling ratio, those in the more polar swelling medium display lower tensile properties. This indicates that, although swelling involves solvation of both the associated rubbery polyester and aromatic urethane segments, the aromatic segments function primarily as quasi-crosslinks which lead to enhanced physical properties. This is in agreement with previous observations on the mechanical properties of the unswollen elastomer.

INTRODUCTION

The polymeric solid state has been variously described as a supercooled glass, a bowl of tangled spaghetti, and a van der Waals bonded solid. Only recently have some new concepts been brought forward regarding glassy polymers as having reasonably heterogeneous bonding capabilities in the solid form.[1,2] As one example, Andrews[1] proposed that pure polyacrylonitrile contains both van der Waals bonding and dipole–dipole association. Another form of heterogeneous bonding is observed in block copolymer elastomers which may be found in a noncrosslinked, amorphous state. Examples of two commercially available systems are the styrene–butadiene–styrene block copolymers and certain polyether and polyester urethanes. It appears that interaction between the harder segments of the copolymer leads to a reinforcement of the system with aggregations of the hard segments acting as quasi-crosslinks.[3,4] The nature of the bonding within the reinforcing segments is not completely understood, and it appears that several possibilities may exist, depending on the system.[5,6] Two possibilities are that either the reinforcement is due to an aggregation of glassy amorphous segments or small semicrystalline regions.[6] Although it is unlikely that microcrystallites exist in the styrene–butadiene system, the rubbery state enhancement in the urethane systems may be more complicated with varying contributions arising both from crystallites and glassy segments.

In the particular case of the polyester–urethane[7] Estane (B. F. Goodrich), it is reasonably certain that primary covalent crosslinking is absent as was

demonstrated by Estane's solubility in nonreactive solvents such as tetrahydrofuran (THF) and dioxane, at room temperature. It appears that the solubility parameter δ, defined as the molar energy of vaporization per molar volume (a measure or solvent polarity), for this polymer lies near 10.5 in moderate hydrogen-bonding solvents.[8,9]

At values of solvent solubility parameter somewhat above and below 10.5, it was possible to swell Estane 5740–100 to a quasi-equilibrium condition. Some exploratory viscoelastic measurements were performed on the polymer in this swollen state.

EXPERIMENTAL

Swelling Measurements

In order to vary the solubility parameter of the swelling system easily and reproducibly, a mixture of polar and nonpolar solvents was chosen. The swelling measurements were made with mixtures of methanol ($\delta = 14.5$) and benzene ($\delta = 9.2$). The solubility parameter of the mixtures used was determined by using an equation proposed by Small,[10]

$$\delta_{\mathrm{mix}} = (x_1 v_1 \delta_1 + x_2 v_2 \delta_2)/(x_1 v_1 + x_2 v_2) \tag{1}$$

where x_1 is the mole fraction, v_1, the molar volume, and δ_1, the solubility parameter of species 1.

In the methanol–benzene system, calculation of δ_{mix} from eq. (1) reveals almost a linear relation between the solubility parameter of the mixture and the weight percent benzene in the mixture. Samples of compression-molded Estane 5740-100 were added to solutions of methanol and benzene (MeOH–$\mathrm{C_6H_6}$). It was found that at concentrations of 15–35% MeOH ($\delta = 10.1$–11.2) the polymer dissolved. On the other hand, when samples were immersed either in more or less polar solutions on either side of the solubility range, the samples did not dissolve.

Weighed samples were immersed in solvent mixtures with concentrations ranging from 0 to 5% MeOH and from 60 to 100% MeOH for periods from 30 to 60 hr. At 30-min intervals the samples were removed from the swelling medium, blotted quickly, and weighed. After 5 hr a quasi-equilibrium was reached, with very little change in weight with time. Subsequent weighings were made at longer intervals. The samples were finally dried and reweighed to determine the extent of solubility. These results are presented in Table I. In all of the samples used in stress-relaxation experiments, the extent of solubility was less than 5%.

The volume ratio of the swollen material q was computed from eq. (2),

$$q = V_f/V_0 = \frac{(W_{\mathrm{M}}/\rho_{\mathrm{M}}) + (W_{\mathrm{B}}/\rho_{\mathrm{B}}) + (1/\rho_{\mathrm{P}})}{(1/\rho_{\mathrm{P}})} \tag{2}$$

where ρ_{M} is the density of methanol, ρ_{B}, the density of benzene, W_i, the weight fractions of each component absorbed, and ρ_{P}, the density of the
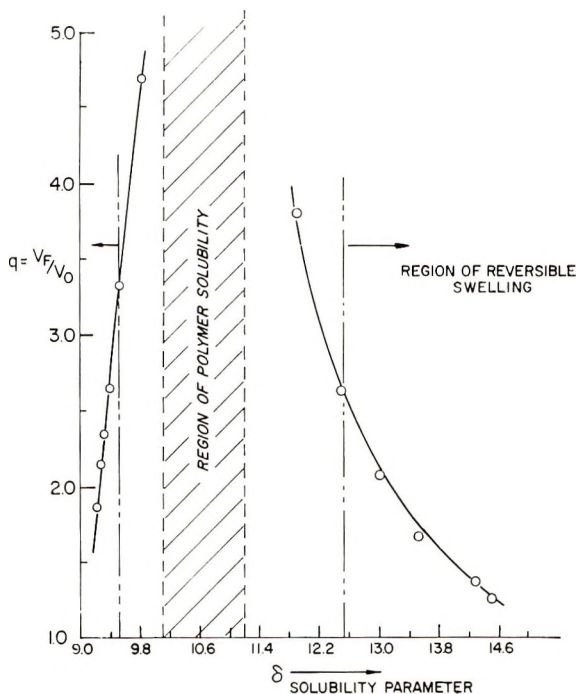
Fig. 1. Swelling ratio vs. solubility parameter for Estane 5740-100.

polymer. This calculation assumes that the concentration of the swelling species is the same as that of the swelling medium and that there is volume additivity. The results of the calculation of eq. (2) also appear in Table I and are displayed in Figure 1. Figure 1 illustrates the range of polymer solubility, and designates the regions in which the swelling was substantially

TABLE I

Swelling Ratios of Estane 5740-100 in Methanol–Benzene Solutions

Concentration, wt-%		Swelling,	Weight	
MeOH	Benzene	wt-%	loss, %	$q = V_f/V_0$
100		16	1.7	1.26
95	5	25	1.9	1.38
90	10	32	2.1	1.48
80	20	47	2.3	1.68
70	30	74	2.3	2.08
60	40	113	4.2	2.64
5	95	170	3.2	3.34
3	97	120	2.1	2.64
2	98	100	1.7	2.36
1	99	85	1.3	2.16
	100	64	1.0	1.87

reversible. In the latter regions stress relaxation experiments were carried out.

Measurements of Relaxation Modulus in Swollen Polymers

Modulus decay of swollen, strained samples was observed. For this purpose a suitably designed brass cell with a glass window was used in a standard stress relaxation experiment. The samples were swollen *in situ* for 5 hr, after which stress relaxation experiments were carried out in the solvent medium. The unstrained length of the sample was measured in the swollen state after which the sample was strained 8.5%. The decay of modulus as a function of time in different swelling solutions was followed. The modulus relaxation runs were made in duplicate which verified their reproducibility. Data were obtained in the range of 0–5% and 60–100% McOH solutions, and all runs were made at room temperature, 25°C. The equation appearing in Figure 4 was used for computing all relaxation moduli.[11]
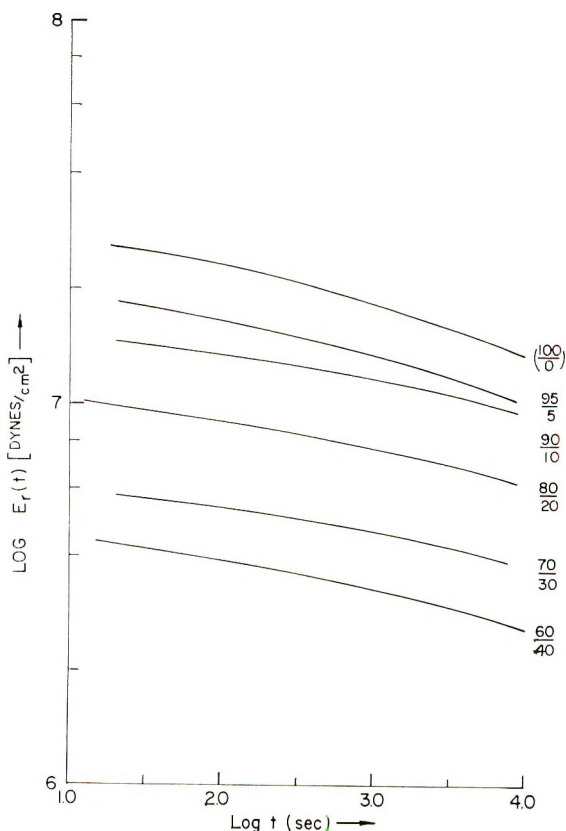
Fig. 2. Stress relaxation of swollen Estane 5740-100 (methanol-rich). Modulus vs. time.

RESULTS AND DISCUSSION

Figure 2 presents relaxation modulus data for 60–100% MeOH swelling solutions, and Figure 3 presents similar data in the concentration range 0–5% MeOH. In both cases as the solubility parameter approaches that of the polymer, the swelling ratio increases and the modulus decreases. It appears that the stress and modulus level are determined by the degree of solvation of the urethane reinforcing segments, while solvation of the associated rubbery segments also occurs and governs the overall degree of swelling.
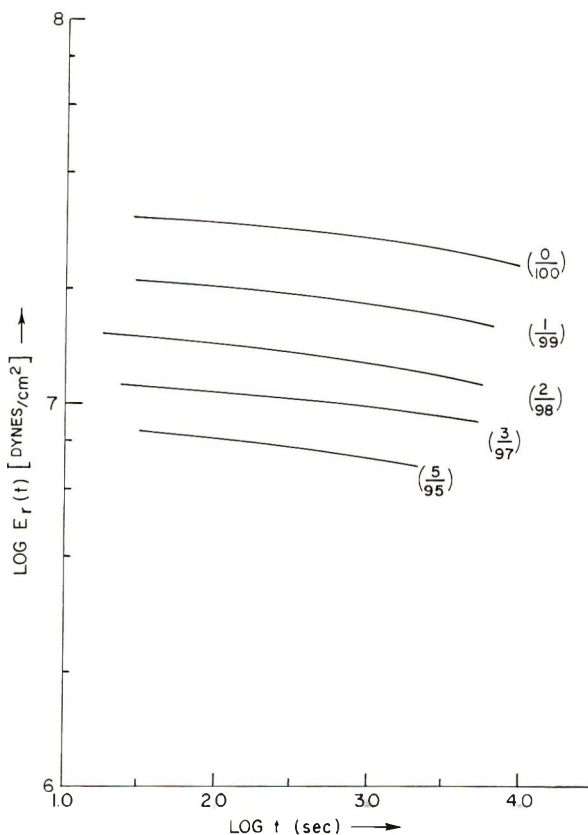
Fig. 3. Stress relaxation of swollen Estane 5740-100 (benzene-rich). Modulus vs. time.

It also appears that the aromatic urethane regions are held together by relatively strong forces. Stress relaxations were made at strain levels of from 8 to 85% in an 80% MeOH solution without affecting the modulus level. Also as a check, several runs were carried out for as long as 100 hr without a drastic reduction in the sample's retractive forces. The series of runs at different strains is presented in Figure 4.
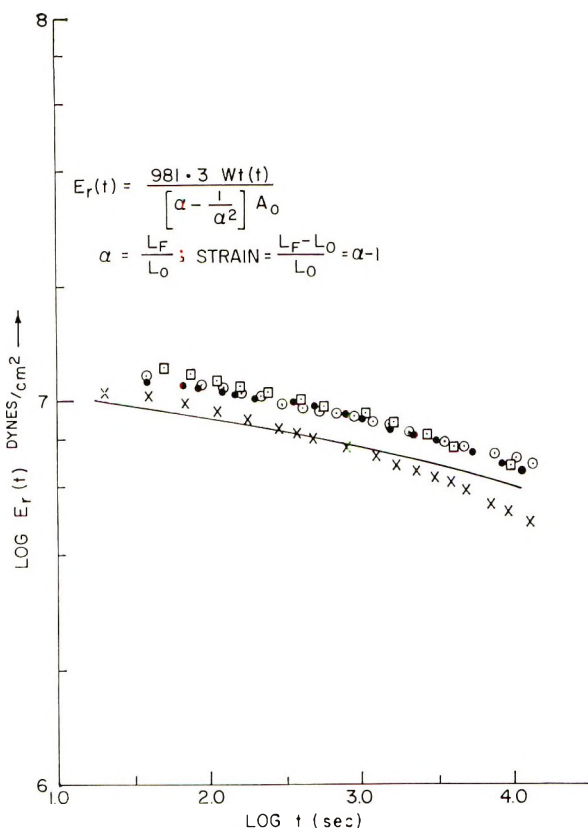
Fig. 4. Modulus vs. time for 80/20 methanol–benzene solutions at different strains: —, 8.5% strain; ⊙, 15.1% strain; ●, 26.6% strain; ⊡, 40.2% strain; X, 85.6% strain.

Some interesting features are revealed by a log–log plot of modulus versus swelling ratio for the swollen Estane system. This appears as Figure 5 where data are presented for both the McOH-rich and the benzene-rich swelling solutions. Since the modulus was time-dependent, as can be seen from the modulus decay experiments, it was arbitrarily decided to choose the modulus at 100 sec after deformation for presentation in Figure 5.

The data in Figure 5 follow a linear curve with a slope of approximately -3.1 for the benzene-rich system and a slope of -2.8 for the McOH-rich system.

It is noteworthy that at the same swelling ratio the modulus values in the benzene-rich samples were almost three times those of the methanol-rich samples. This supplies evidence that swelling in these systems involves not only solvation of the aromatic quasi-crosslinks but also a partial solvation of the intermolecular bonds between the associated rubbery segments. Thus, in the benzene-rich systems the nonpolar benzene easily swells the hydrocarbon backbone of the polyester segments
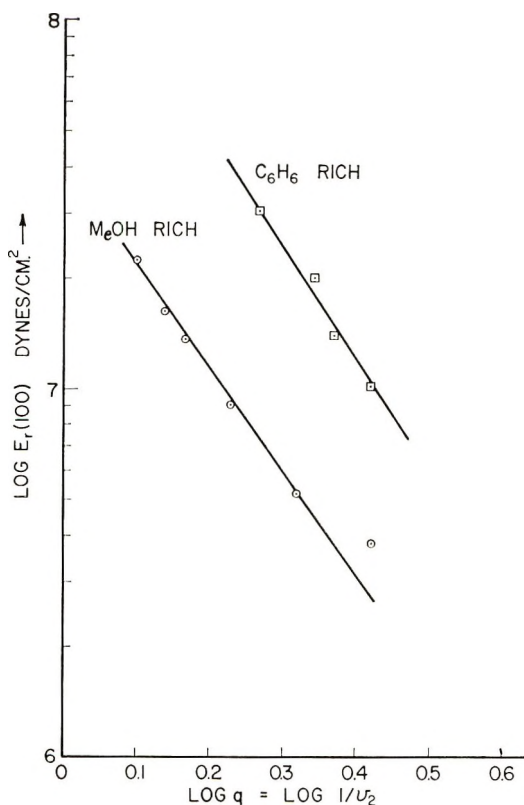
Fig. 5. Modulus vs. swelling ratio in swollen Estane 5740-100.

which are the rubbery segments at room temperature. In contrast to this, in the MeOH system, because of its greater polarity, more of the solvent can associate with the aromatic urethane linkages causing a greater solvation of the reinforcing tie points at the same swelling ratio.

CONCLUSIONS

The following conclusions may be drawn from these experiments: First, the aromatic urethane portions of polyester–urethanes are responsible for the enhanced modulus in these segmented elastomers and act as quasi-crosslinks. These juncture points appear to be intermolecularly associated and subject to solvation by appropriate solvents.

Secondly, in sufficiently poor solvents, these elastomers can be swollen and viscoelastic measurements made. Increased swelling produced by variation of the swelling medium solvates greater amounts of intermolecular tie points and results in lower tensile properties.

Finally, the chemical nature of the solvating agent markedly affects the level of modulus. Different modulus values at the same swelling ratio for

two swelling systems indicate that solvation of both the associated aromatic urethane and rubbery segments occurs.

Further research on the characterization of secondary bonding in block copolymer elastomers is underway in our laboratory.

References

1. R. D. Andrews and R. M. Kimmel, *J. Polym. Sci. B*, **3**, 167 (1965).

2. R. D. Andrews, *Transitions and Relaxations in Polymers*, (*J. Polym. Sci. C*, **14**), R. F. Boyer, Ed., Interscience, New York, 1966, p. 261.

3. S. L. Cooper and A. V. Tobolsky, *J. Appl. Polym. Sci.*, **10**, 1837 (1966).

4. S. L. Cooper and A. V. Tobolsky, *J. Appl. Polym. Sci.*, **11**, 1361 (1967).

5. D. Puett, *J. Polym. Sci. A-2*, **5**, 839 (1967).

6. R. Bonart, *J. Macromol. Sci. B*, **2**, 115 (1968).

7. C. S. Schollenberger (to B. F. Goodrich), U. S. Pat. No. 2,871,218 (January 27, 1959).

8. H. Burrell, *Off. Dig.*, **27**, 726 (1955).

9. *Polymer Handbook*, J. Brandrup and E. H. Immergut, Eds., Interscience, New York, 1965.

10. P. A. Small, *J. Appl. Chem.*, **3**, 71 (1953).

11. A. V. Tobolsky, *Properties and Structure of Polymers*, Wiley, New York, 1960, Chap. 4, 8A, pp. 88–97.

ESR Study of Radical Sites in Crystalline Texture of Irradiated Polypropylene by Means of Nitric Acid Etching

NAOSHI KUSUMOTO, KAZUKI MATSUMOTO, and MOTOWO TAKAYANAGI, *Department of Applied Chemistry, Faculty of Engineering, Kyushu University, Fukuoka, Japan*

Synopsis

Bulk-crystallized isotactic polypropylene samples with different crystalline textures were etched by fuming nitric acid to remove the disordered region. The radicals produced by irradiation of γ-rays or ultraviolet light on these etched samples in vacuum at liquid nitrogen temperature were investigated by the ESR method. A triplet spectrum in addition to the original spectrum of polypropylene radicals was separated for the etched samples. It was concluded that this triplet was caused by radical species associated with nitro groups introduced on the surface of the crystalline residues by etching. The difference in the intensity of this triplet among the samples was ascribed to differences in crystalline textures and interpreted in a quantitative way. The concentration of polypropylene radicals corrected for the triplet differed among the quenched, annealed, and cold-drawn samples and the sample annealed one after drawing. This fact was interpreted on the basis of the hypothesis that radical sites were almost concentrated in the defects of crystal domain. The well known nonet spectrum, which can be observed at liquid nitrogen temperature after annealing the irradiated samples at room temperature, was also confirmed to be attributable to the defects of crystals. The behavior of free methyl radicals induced by ultraviolet irradiation was also found to be strongly dependent on the state of aggregation of the polymer molecules.

INTRODUCTION

In recent years, ESR techniques have been used extensively as a method of studying the effect of ionizing radiation of crystalline polymers. Studies of radical species induced by high-energy radiation and of their behavior have been quite detailed.

A large number of reports, however, do not discuss in detail the influence of the higher-order structure of crystalline polymers on formation and behavior of radicals. The state of the amorphous phase, lamellar crystals, and defects in the crystal are important factors which determine the physical and chemical properties of crystalline polymers. They are also considered to affect the formation and the behavior of radicals.

One of the difficulties involved in the investigation of this problem was the fact that we could hardly distinguish the spectral components of the radicals trapped in different regions of the crystalline texture of the original

sample. Therefore, in the current study, attempts were made to obtain information about the sites of trapped radicals in the individual phase of the isotactic polypropylene samples by treating them with nitric acid and removing the disordered regions in stepwise.

The purpose of this paper is to confirm which phase within the sample is responsible for the nonet[1,2] spectrum of polypropylene, which was observed at −196°C for a sample irradiated at room temperature. Kusumoto[3] previously suggested the possibility that the radical responsible for the nonet exists preferentially in some loosened structure, such as chain-folded lamellar surface and/or defects in the crystalline phase. In this paper we intended to confirm this prediction.

EXPERIMENTAL

Pellets of isotactic polypropylene (Avisun 1021) were extracted with n-heptane for 48 hr and with n-hexane and benzene for 24 hr and were compressively into 1 mm × 20 mm × 80 mm sheets. These sheets were heat-treated or drawn to give different crystalline textures as listed in Table

TABLE I
Polypropylene Samples

Sample	Preparation	X_c, %
A	Annealed at 130°C for 24 hr	69
Q	Quenched into ice water from melted state	51
D	Drawn 8× at 72°C	70
D_A	Drawn 8× at 72°C and annealed at 130°C for 24 hr	76

I. The degree of crystallinity X_c, as determined by the x-ray method, is also listed in Table I.

Next, the sheets were treated with fuming nitric acid at 75°C for 0.5–12 hr. This oxidation method was used by a number of investigators to study the crystalline texture of polyethylene[4-10] and polypropylene.[11] The oxidized samples were taken out of the reaction vessel at various times during the progress of etching, extracted with acetone for 24 hr to remove the low molecular weight materials produced by etching, and dried under reduced pressure.

The weight of the etched samples was measured to assess the process of etching. The density of the samples was also measured by the flotation method to elucidate the removal of the disordered region by etching. Elemental analysis was also carried out to detect nitrogen atoms introduced as nitro groups by oxidation.

The etched samples were sealed in glass tubes evacuated to less than 10^{-4} mm Hg, and irradiated by γ-rays from a ^{60}Co source at a dose rate of 1.4×10^5 rad/hr to a total dose of 10^7 rad at −196°C. The bundle of sample tubes was rotated around its axis to allow uniform irradiation. Within a few hours after finishing the irradiation, the electron spin reso-

nance (ESR) spectra were measured. In the ultraviolet irradiation, the samples were sealed in evacuated quartz tubes and irradiated at −196°C in a rotating quartz Dewar vessel with light from a low-pressure mercury lamp.

A Hitachi MPU magnetic resonance spectrometer (X-band, 100 Kcps modulation) was employed for measurement of ESR spectra. Absolute values of the spin concentration of the irradiated samples were evaluated by comparing the integrated intensity of the resultant spectrum with that of an irradiated Teflon sample whose spin concentration was previously calibrated by a solution of DPPH in benzene. Viscoelastic measurements of the etched samples were conducted at 110 cps by use of direct-reading dynamic viscoelastometers to study the movable chains which compose the amorphous region. The instrument used was a Vibron model DDV-II (Toyo Measuring Instruments Co., Ltd.).

RESULTS AND DISCUSSION

Crystalline Texture of the Etched Samples

The weight of the sheets increased slightly in the early stage of oxidation and decreased after 5 hr. The density of the sheets increased linearly with the elapse of the oxidation time up to 6 hr. Hock[11] has reported on the oxidation of bulk-crystallized isotactic polypropylene by 70% nitric acid at 120°C. The tendency of the densities and the weight of the sheets to increase in our case was similar to those reported by Hock.[11] In our case, however, the oxidation progressed more slowly due to the lower oxidation temperature, although we used a higher concentration of the acid than that employed by Hock.[11]

Viscoelastic measurement of sample A oxidized with nitric acid for 6 hr revealed that the α_a dispersion due to the initiation of the micro-Brownian motion of molecular chains in the amorphous region vanished, while the original sample showed marked α_a dispersion. On the other hand, the crystalline dispersion α_c associated with the crystalline region increased with the progress of etching in the same way as shown by Minami et al.[12] These results means that the etching has selectively removed the movable chains capable of micro-Brownian motion above the glass transition temperature, which compose the amorphous region.

The x-ray crystallinity of sample A reached its maximum value of 87% after etching for 6 hr. Elemental analysis showed that the relative number of carbon atoms per nitrogen atom is 706 at 3 hr oxidation, 116 at 6 hr, and 97 at 9 hr. Since nitrogen is present in nitro groups[4,9] introduced by oxidation, the lamellar thickness can be estimated as 72 Å from the number of carbon atoms at 6 hr by assuming that nitro groups are combined with both cut ends of the polymer chain at both surfaces of the lamellar crystal. If one nitro group is combined at the lamellar surface to one cut end of a polymer chain and one carboxyl group is combined at the other cut end,

a value of 144 Å is obtained. This value coincides with the lamellar thickness estimated by Hock.[11]

Thus, it can be concluded that the amorphous region of the samples was removed selectively by acid treatment for more than 6 hr. We use hereafter the term "etching" to denote this oxidation process because the oxidation selectively etches the disordered region in the crystalline texture.

ESR Spectrum Peculiar to the Etched Samples

Figure 1 shows the ESR spectra of the γ-irradiated samples A, Q, D, and D_A (Table I) at different etching times. The original, unetched samples showed the well known octet spectra. It can be seen that the spectra of the etched samples resemble those of the original samples but become asymmetric with respect to the resonant center of the static magnetic field with increasing etching time. The asymmetry of the spectra of etched samples decreases markedly on heat treatment of the samples at −150 to −120°C. Figure 2a shows the spectrum of sample A at −196°C. This irradiated sample was heated to −130°C for 3 min and recooled to −196°C. It is noteworthy that the characteristic peak of the asymmetrical spectrum, (indicated by an arrow in Fig. 2a), disappeared on heating to −130°C as shown in Figure 2b. The residual spectrum obtained by subtracting the spectrum b from a in Figure 2 is an asymmetrical triplet as shown in Figure 2c, which further shows some fine structure. Since this triplet can not be found in the untreated samples and increases its intensity with increasing etching time, this triplet must be associated with chemical groups such as nitro and/or carboxyl groups introduced by oxidation with nitric acid.
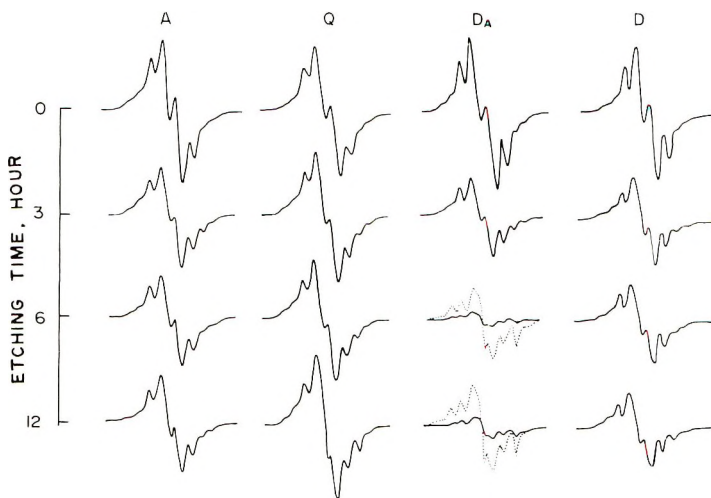
Fig. 1. ESR spectra of the samples at different etching times at −196°C. The preparation of samples A, Q, D and D_A is given in Table I.

On the other hand, the spectrum of sample A, which had been etched for 6 hr and irradiated by ultraviolet light at −196°C (Fig. 3b), showed a spectral pattern quite different from that of the etched sample A receiving γ-irradiation (Fig. 2a). The triplet spectrum of the etched sample irradiated by ultraviolet light as shown in Figure 3b almost matches that of
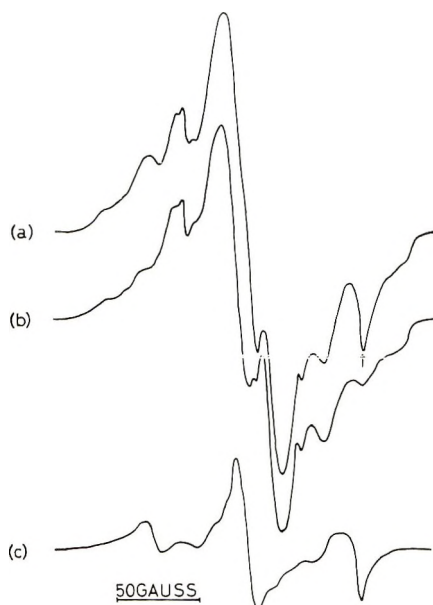
Fig. 2. ESR spectra of etched sample A (6 hr): (a) spectrum at −196°C before annealing; (b) spectrum at −196°C after heating the sample at −138°C for 3 min; (c) residual spectrum obtained by subtracting spectrum (b) from (a).
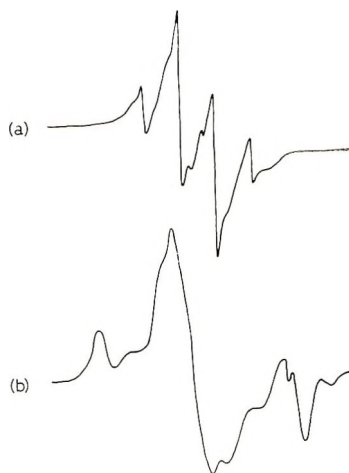
Fig. 3. ESR spectra of sample A irradiated by ultraviolet light at −196°C: (a) spectrum of unetched sample, (b) spectrum of sample etched 6 hr.

Figure 2c. This is attributed to the introduction of chemical groups such as nitro and carboxyl groups by etching which densely cover the surface of the lamellar crystals and absorb the ultraviolet light. The fact that the triplet radical is very unstable compared with the other radicals is due to the circumstance that the triplet radicals are located at very movable points of the molecular chains such as the ends cut by etching.

The outermost peaks of the triplet can be considered to be due to either (1) anisotropy of the g value or (2) hyperfine structure. The principal values of the g tensor are evaluated as $g_1 = 1.9641$, $g_2 = 2.0071$, and $g_3 = 2.0463$ from the line shape of the triplet. However, the range of these values is too wide compared with the case[13] of NO_2 and CO_2^- radicals. Thus, the cause of the peaks might be ascribed to the hyperfine structure of nitrogen or hydrogen atoms. The hyperfine separation (60 gauss) is too large to ascribe to hydrogen atom, but almost coincides with that of nitrogen atom in NO_2.[13] The intensity of the triplet spectrum during the etching time was estimated by subtracting the triplet shown in Figure 2c from the original spectrum, the intensity of the triplet being adjusted to leave the symmetrical spectrum. Thus, it can be concluded that this triplet spectrum is associated with the nitrogen atom in the nitro groups introduced by etching. The center peak in the triplet is considered to be intensified by superposition of the other spectra to the spectrum of nitro group radicals, since the nitrogen atom has a spin number $I = 1$ and, thus, hyperfine separation by a nitrogen atom must be a triplet with hyperfine components of equal intensity.

Interpretation of the Behavior of the Triplet Based on Change of the Crystalline Texture by Annealing

Figure 1 shows that the line shape, especially the symmetry, of the spectrum differs markedly with different samples which are etched for 6 hr. One of the reasons for this is that the intensity of the triplet spectrum from nitro groups relative to that of the spectrum of radicals in polypropylene itself differs with different samples. Table II lists the concentration of these radicals for different types of the samples.

Since the radicals of the triplet spectrum are present on the surface of the crystalline residues after etching, the radical concentration of samples

TABLE II
Concentration of Triplet Radicals and
Polypropylene Radicals for the Crystal Domain of the Samples

| Sample | Radical concentration, spins/g | |
	Triplet radical	Polypropylene radical
A	5.1×10^{18}	6.3×10^{19}
Q	1.0×10^{19}	1.17×10^{20}
D	5.3×10^{18}	7.2×10^{19}
D_A	2.1×10^{18}	1.3×10^{19}
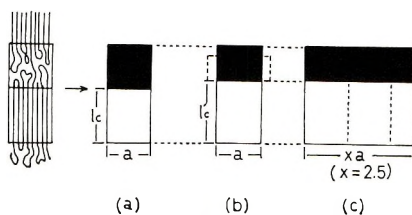
Fig. 4. Schematic representation of elements of crystalline texture (side view of the square blocks): (a) the element of cold-drawn film (sample D, $X_c = 70\%$), (b) the element of cold-drawn film after annealing (sample D_A, $X_c = 76\%$) in which the crystalline phase grew along the draw direction on annealing; (c) the element of cold-drawn film after annealing (sample D_A) which grew along the side. l_c and l_c' represent the lamellar thickness. The area surrounded by the broken line in (b) shows the amorphous region in the case where the sample shrinks on annealing due to the relaxation of the amorphous region. The filled area represents material removed by etching.

in which the disordered region has been removed by etching for 6 hr will be proportional to the surface area per unit weight of the lamellar crystals. The results in Table II show that the radical concentration of the triplet of the annealed samples is smaller than that of the samples before annealing. This is interpreted on the assumption that the crystal domain was developed to form larger crystals, and, thus, the ratio of the surface area to weight was largely decreased by annealing.

Next, we will inspect this assumption in more detail. Figure 4a shows a square block model which represents an element of the crystalline texture as shown at the left of the figure. The open squares represent the crystalline region and the filled squares represent the interlamellar disordered region. A detailed discussion of the latter region, such as the possibility of folding, is not important for our discussion. The degree of crystallinity of the cold drawn sample was increased from 70% to 76% by annealing. The question is whether we can interpret the decrease in the surface area per unit weight of the sample D by annealing in the way shown in Figure 4b, i.e., growth of the crystalline region accompanied by no change of the width of the element. If we adopt the structural change shown in Figure 4, where a is the width of the element and l_c is the thickness of the crystal phase of lamella, the etched surface area S_a of the crystal per unit volume for the model of Figure 4a can be calculated as shown in eq. (1) by taking into account the fact that the amorphous region is removed by etching:

$$S_a = (2a^2 + 4al_c)/a^2l_c \qquad (1).$$

In the case shown in Figure 4b, the corresponding surface area S_b, is

$$S_b = (2a^2 + 4al_c')/a^2l_c' \qquad (2),$$

where l_c' is the thickened length of the crystal phase after annealing. Dividing eq. (1) by eq. (2), we obtain the ratio R of S_a to S_b as follows:

$$R = S_a/S_b = (a^2 + 2al_c)l_c'/(a^2 + 2al_c')l_c \qquad (3)$$

Substituting $l_c = (70/76)l_c'$ and $R = (5.3 \times 10^{18})/(2.1 \times 10^{18}) = 2.5$ for samples D and D_A into eq. (3), we obtain

$$l_c'/a = (152/70 - 5)/6 < 0$$

This negative value of l_c'/a has no physical meaning and the annealing process from the model of Figure 4a to that of Figure 4b should be discarded from the viewpoint of radical behavior. Another possibility of interpreting the value of $R = 2.5$ is to make the value of a increase by annealing by a factor of x.

We assume here x^2 pieces of the crystal elements are united into one block side by side by annealing as shown in Figure 4c. For the process from the model of Figure 4a to that of 4c, the area ratio becomes

$$R = S_a/S_c = x^2 l_c'(a^2 + 2al_c)/[(ax)^2 + 2axl_c]l_c \tag{4},$$

substituting $l_c = (70/76)l_c'$ and $R = 2.5$ into eq. (4), we obtain

$$2.5 = (76/70 + 2l_c'/a)/(1 + 2l_c'/ax) \tag{5}.$$

The model in Figure 4c is acceptable when l_c'/a takes a positive value, that is,

$$l_c'/a = (152/70 - 5)/(10/x - 4) > 0 \tag{6}$$
$$x > 2.5$$

This means that, on annealing, about six or more ($>2.5^2$) blocks of the original crystal elements unite to form a more developed crystal plate, which is extended perpendicularly to the draw axis.

The polycrystalline texture of a well annealed oriented polymer is actually considered on the basis of various experimental facts (two meridional diffraction spots in the x-ray small-angle scattering, as seen in isotactic polypropylene annealed at 155°C or polyethylene drawn at high temperature) to have such a superstructure. On the other hand, polypropylene cold-drawn at 60°C does not show any such a diffraction pattern except for the diffused diffraction around the primary beam. Hosemann[14] has proposed a model from the analysis of the cold- and hot-drawn films of polyethylene. Figures 5a and 5b show a checkered pattern and a striped pattern for the cold-drawn and hot-drawn samples, respectively. The sides of crystal block are closely bound by the shift of ultrafibrils along the draw axis by annealing to show two meridional diffraction spots in the x-ray small-angle scattering. These models are quite suitable for the purpose of interpreting the ESR data in this study. Takayanagi et al.[15] have found support for these models from the anisotropy of the tensile storage modulus of oriented polyethylene, isotactic polypropylene, and several kinds of polyethers as a function of temperature. At the temperature of the primary absorption (around T_g'), the 0° modulus along the draw direction crosses the 90° modulus; above T_g the 90° modulus has a higher value than 0° modulus. This fact can be interpreted only by the model cited above.
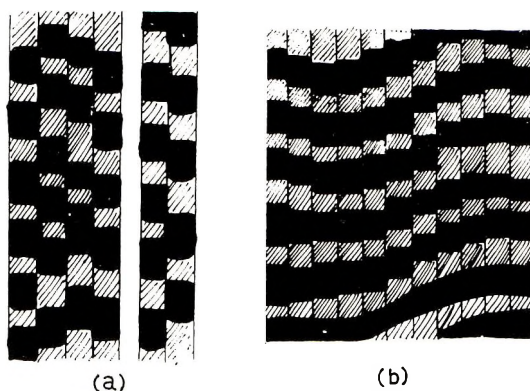
Fig. 5. Schematic representation of microfibrils:[14] (a) cold-drawn polyethylene film; (b) hot-drawn polyethylene film. The filled area shows the amorphous region.

In our experiment l_c' was estimated as 175 Å from the long period and the degree of crystallinity. By substituting this value into eq. (6) it can be deduced that 6 to 8 elements are to be united when the side length of the elemental crystal a is more than 100 Å, and 13 to 9 blocks when a is 50–100 Å. As for the structural change from quenched sample Q to annealed sample A, the same estimation mentioned above is also possible, and $x > 2.0$ is obtained, when the change of the degree of crystallinity from 56% to 73% by annealing is taken into account. Thus, it will be understood that the original crystal blocks must be united when the quenched sample is annealed.

Change of Radical Concentration Corrected for the Triplet with Etching Time

Figure 6 shows plots of radical concentrations at −196°C against etching time. The concentrations markedly vary with etching time. In this figure the intensity of the triplet spectrum was eliminated as far as possible by the method described above. The radical concentration of the quenched sample Q increases in the early stage of etching, reaches a maximum at 3 hr and decreases thereafter. In the other samples, the radical concentration decreases with increasing etching time. For all samples, however, the concentration becomes constant after 6 hr. The period of 6 hr agrees with the time required for the complete removal of the amorphous region of the samples as mentioned above. Thus, the radical concentrations at this time are considered to correspond to the radical concentration in the lamellae after removal of the disordered region.

The relation between the radical concentrations and etching time can be interpreted by the following considerations. The radical concentration in the amorphous region is larger than that in the crystalline region. The radical concentration in the sample decreases with as the degree of crystallinity increases by etching. When the amorphous region is wholly removed
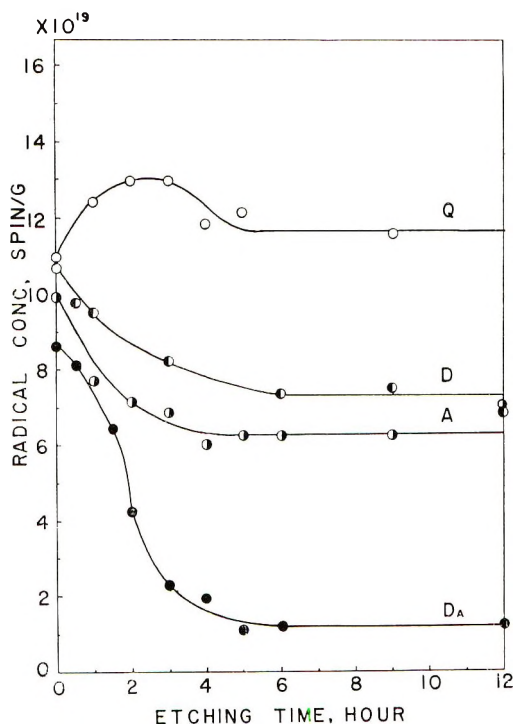
Fig. 6. Plots of radical concentrations corrected for the triplet at $-196°C$ against etching time.

at 6 hr, the leveling-off radical concentration corrected for the triplet coincides with that in the lamellar crystals. There do exist contradictory facts, namely, that a maximum is seen for the curve of sample Q in Figure 6 and that the radical concentrations of all the unetched samples (zero time values of the curves in Fig. 6) exceed the radical concentration of completely amorphous, atactic sample (7.2×10^{19} spins/g). These facts suggest that a certain phase, intermediate between the amorphous and the crystalline phase is present which can trap radicals with higher concentration than the completely amorphous or the crystalline region.

So far, we have seen that the state of aggregation of polymer molecules strongly affects the trapping ability of radicals of the polymer matrix. The results obtained above indicate the trapping ability in the crystalline texture decreases in the order: the phase with intermediate regularity between those of the crystalline and the amorphous state > the amorphous phase > the crystalline phase including defects or defect regions. This order will be considered reasonable after the following discussion.

To trap radicals stably it may be necessary that (1) the conformation of molecular chain is changed at the radical site, (2) the paired radicals produced by scission of a chemical bond are separated enough to prevent their recombination, and (3) the radicals do not migrate so far to react

with other radicals. Probability of being hit by quanta of radiation may be almost the same for molecules in any phase of the polymer matrix. However, the conditions (1) and (2) are difficult to satisfy in the completely crystalline phase because the mobility of molecules are largely inhibited and consequently the radicals recombine immediately after scission of a chemical bond by hitting. In the amorphous region, condition (3) will not be satisfied because of the larger mobility of molecular chains. Thus, the optimum condition for trapping the radicals will be found in the region of intermediate regularity in the polymer matrix. The mobility of polymer chains in this region will be intermediate between those in the typically crystalline and the amorphous phases.

Radical Sites Associated with Lamellar Crystals

According to the structural concept introduced above, the leveling-off values of the curve in Figure 6 correspond to the radical concentrations existing within the lamellar crystal themselves. They are considerably different among the samples Q, A, D, and D_A. The magnitudes of these values are in the order of Q, D, A, and D_A. This experimental fact can not be interpreted by formation of equal density of the radical sites over a whole domain of crystalline region, as it is independent of its crystalline texture. This must be interpreted by a mechanism in which the radicals are formed mainly in the defects of lamellar crystals and the amounts of defects are different among the samples; thus, the radical concentrations at the final stage of etching are different for each sample. In the case of single crystals of inorganic materials, irregular yields of radicals were often experienced, depending upon the conditions of preparation of the crystal.[17] Miura et al.[17] reported that they could not observe an ESR spectrum for a single crystal of pure sodium polyphosphate irradiated by γ-rays, but succeeded in observation of radicals for the crystal doped by a small amount of sodium sulfate to introduce defects into the crystal. These facts seem to support the mechanism presented here. Therefore, the final radical concentration of the lamellar crystal will give a measure of the number of defects existing within the lamellar crystals themselves. The fact that quenched sample Q has much higher radical concentration than annealed sample A is explained by the circumstance that sample Q has more defects than sample A.

It is most interesting that the difference between the radical concentration of the cold-drawn film D and that of the drawn and annealed sample D_A is extremely large. Annealing of the cold-drawn film depresses the trapping ability of radicals existing within the lamellar crystals to one fifth of the original sample. This fact indicates that the annealing of the cold-drawn film makes the crystalline region more highly developed and decreases the disordered region including defects. The secondary crystallization induced by annealing for cold-drawn sample D is considered to develop crystals more completely compared with that of the bulk samples, since the orientation of molecular chains is previously arranged in the draw

direction and is preferable to development of an extended crystalline lamella.

Radical Sites of the Nonet Spectrum

It has been recognized that the nonet ESR spectrum is always observed at liquid nitrogen temperature for isotactic polypropylene irradiated by γ-rays at room temperature in vacuum, while the octet is found for samples irradiated at liquid nitrogen temperature. Since this nonet could not be found for an atactic polypropylene sample,[1,3] the radical species is expected to be closely related to the crystalline regions. The interpretation for the cause of this spectrum has been made by two conflicting interpretations, which involve alkyl radicals[1,18,19] in one hand and allylic radicals[2,20,21] on the other hand. In either case, however, the molecular chains would need distortion of their backbone to form the radicals if they are in the crystalline lattice. For this difficulty it was suggested that the radicals are trapped preferentially in the lamellar surface composed of folded chains and/or some defects in the crystal.[3]

After the unetched bulk-crystallized samples were heated to room temperature and recooled to liquid nitrogen temperature the ESR spectrum showed a nonet structure very similar to those cited in the literature.[1,2] The same nonet spectrum was also obtained for sample A which had been etched for 6 hr. Figure 7 shows the ESR spectra before and after etching in our case. They agree very well with each other. Thus, it can be concluded that the nonet radicals are trapped in the lamellar crystals, presumably in the defects of crystals.

Figure 8 shows the spectra of samples Q and Da etched for 6 hr obtained by subtraction of the triplet spectrum from the original one. The figure shows that the spectrum of sample Q is close to the octet of the unetched
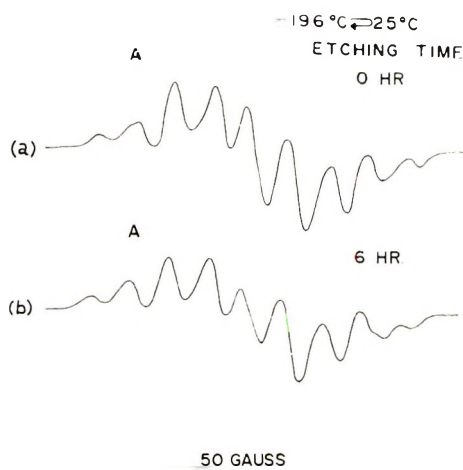
Fig. 7. Nonet spectra obtained from the samples before and after etching (a) spectrum of unetched sample A, (b) spectrum of etched sample A (6 hr).

sample, while the spectrum of sample D_A is close to the nonet. As for the radicals of polypropylene induced by γ-ray irradiation, many investigators have made identification of radicals on different bases. By utilizing the facts that the spectrum disappearing on annealing was the octet and that
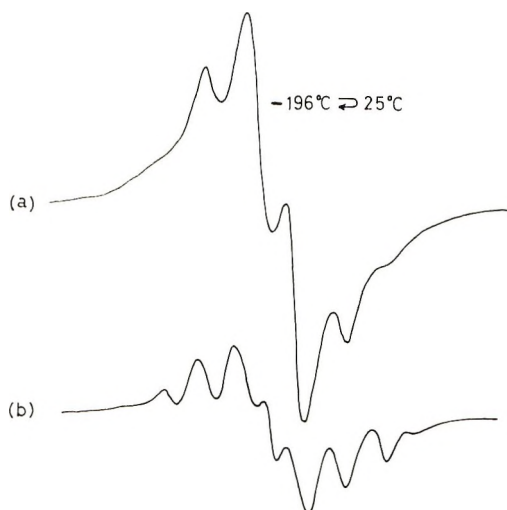
Fig. 8. Residual ESR spectra of samples etched 6 hr obtained by subtracting of the triplet spectrum from the original spectra: (a) sample Q; (b) sample D_A.

the nonet is relatively stable at room temperature, we can evaluate the intensity of both spectra for the samples Q, A, and D_A etched for 6 hr. Table III, which lists the results obtained by this method, shows that the concentration of the nonet radicals increases as the total radical concentration is increased, while the concentration ratio of the nonet radical to that

TABLE III
Concentration of Polypropylene Radicals in the Crystal Domain of the Samples

| Sample | Radical concentration, spins/g | | | |
	Octet	Nonet	Nonet/octet	Total
Q	9.2×10^{19}	2.5×10^{19}	0.27	1.17×10^{20}
A	3.9×10^{19}	2.4×10^{19}	0.62	6.3×10^{19}
D_A	3.4×10^{18}	9.6×10^{18}	2.8	1.3×10^{19}

of the octet radical is decreased. The ratio of thermally stable radicals (nonet) relative to unstable radicals (octet) increases as the crystal domain becomes perfect. This ratio is considered as a measure for expressing the perfection of the crystalline region. Thus, we can conclude that the radical species induced is sensitively dependent upon the crystal defects.

Free Methyl Radicals Produced by Irradiation
with Ultraviolet Light

Yoshida and Rånby[22] have reported that a very narrow quartet spectrum, which they assigned to the free methyl radical, was found for the bulk-crystallized polypropylene sample irradiated by ultraviolet light in vacuum at liquid nitrogen temperature, but could not be found in the case of γ-irradiation. They explained these facts by the much smaller kinetic energy for reaction with other radicals of the radicals produced by ultra-violet light irradiation compared to those produced by γ-ray irradiation.

In our experiment, this quartet spectrum was also observed for the bulk-crystallized sample A, as shown in Figure 9a; this spectrum is almost the same as cited in the literature.[22] However, we could not find the quartet spectrum for a completely atactic polypropylene sample which was irra-diated under the same conditions as mentioned above. The spectrum obtained for atactic polypropylene is shown in Figure 9b. This experi-mental result may be explained on the basis of the effect of the crystalline texture on formation and trapping of radicals. The radicals formed in the amorphous region react more rapidly than in the crystalline region, so that we could not detect the methyl radicals in the atactic sample.

Kusumoto et al.[23] found that free methyl radicals produced by ultraviolet light irradiation in the single crystal sample of poly-4-methyl-1-pentene react more rapidly than those in the bulk-crystallized sample. This is considered to be due to the fact that methyl radicals diffuse more easily to react with other radicals because the packing of molecular chains in the crystalline phase (density at room temperature is 0.823 g/ml) is looser than that in the amorphous phase (0.839 g/ml) below 50°C.[24] In the case of polypropylene, the density of the amorphous phase (0.85 g/ml) is smaller
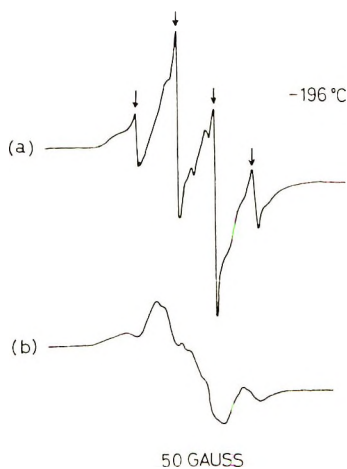
Fig. 9. ESR spectra obtained after ultraviolet irradiation: (a) bulk-crystallized sample A (the peaks characteristic of methyl radicals i.e., quartet spectrum, are indicated by arrows); (b) completely atactic (amorphous) sample.

than that of the crystalline phase (0.92 g/ml), so that methyl radicals in the amorphous phase diffuse and react more rapidly than those in the crystalline phase. Therefore, it can be said that not only the chemical structure of polymer molecules but also the state of aggregation of molecules plays a very important role in trapping of the free methyl radicals generated.

References

1. B. R. Loy, *J. Polym. Sci. A*, **1**, 2251 (1963).
2. H. Fisher and K. H. Hellwege, *J. Polym. Sci.*, **56**, 33 (1962).
3. N. Kusumoto, *J. Polym. Sci. C, Symposium on Macromolecular Chemistry, Tokyo-Kyoto*, 1966, in press.
4. R. P. Palmer and A. J. Cobbold, *Makromol. Chem.*, **74**, 174 (1964).
5. A. Keller and S. Sawada, *Makromol. Chem.*, **74**, 190 (1964).
6. I. L. Hay and A. Keller, *Nature*, **204**, 862 (1964).
7. A. Peterlin and G. Meinel, *J. Polym. Sci. B*, **3**, 1059 (1965).
8. A. Peterlin, G. Meinel, and H. G. Olf, *J. Polym. Sci. B*, **4**, 399 (1966).
9. G. Meinel and A. Peterlin, *J. Polym. Sci. B*, **5**, 197 (1967).
10. F. H. Winslow, M. Y. Hellman, W. Matreyek, and R. Salovey, *J. Polym. Sci. B*, **5**, 90 (1967).
11. C. W. Hock, *J. Polym. Sci. A-2*, **4**, 227 (1966).
12. S. Minami, H. Sato, and N. Yamada, *Rept. Progr. Polymer Phys. Japan*, **10**, 325 (1967).
13. Cited in *Kagaku* (17th Suppl.), p. 81 (1965).
14. R. Hosemann, *J. Appl. Phys.* **34**, 25 (1963).
15. M. Takayanagi, K. Imada, and T. Kajiyama, in *U. S.–Japan Seminar on Polymer Physics, J. Polym. Sci. C*, **15**, R. S. Stein and S. Onogi, Eds., Interscience, New York, 1966, p. 263.
16. K. Aiki, Dept. of Physics, Faculty of Sci., Kyushu Univ., private communication.
17. M. Miura, A. Hasegawa, and T. Fukui, *Bull. Chem. Soc. Japan*, **39**, 1432 (1966).
18. P. B. Ayscough and S. Munari, *J. Polym. Sci. B*, **4**, 503 (1966).
19. M. Iwasaki, T. Ichikawa, and K. Toriyama, *J. Polym. Sci. B*, **5**, 423 (1967).
20. V. K. Milinchuk and S. Ya. Pshezhetskii, *Dokl. Akad. Nauk SSSR*, **152**, 665 (1963).
21. H. Yoshida and B. Rånby, *Acta Chem. Scand.*, **19**, 72 (1965).
22. B. Ranby and H. Yoshida, in *Perspectives in Polymer Science (J. Polym. Sci. C*, 12), E. S. Proskauer, E. H. Imnergut, and C. G. Overberger, Eds., Interscience, New York, 1966, p. 263.
23. N. Kusumoto, K. Shirano, and M. Takayanagi, *Rept. Progr. Polym. Phys. Japan*, **10**, 519 (1967).
24. B. Rånby, *J. Polym. Sci.*, **44**, 369 (1960).

Salt Effect on Polymer Solutions

SHUJI SAITO,

Momotani Juntenkan, Ltd., Minatoku, Osaka, Japan

Synopsis

The salt effect was investigated by measurements of viscosity, cloud point, and solubility of aqueous solutions of poly(vinyl alcohol–acetate) copolymers, as these copolymers in water are sensitive in various ways to addition of various electrolytes. The major role in the salt effect is played by the anions, and water-structure breaking anions produce salting-in of the copolymers. Tetraalkylammonium halides (bromides and iodides) cause salting-in of the copolymers more effectively with increase of size of the hydrophobic cations. The Setschenow equation does not hold for the polymers except for very dilute polymer concentration. In salts of monoalkyl-substituted anions (R—COONa and R—SO₄Na) and cations (R—NH₃Cl and Br), so long as the alkyl chain is short, the salt effect is also dominated by the anions. With increase of the alkyl chain length, sodium salts of the monoalkyl-substituted anions exert a stronger salting-in effect upon the polymers than chlorides of similar long-chain cations. The significance of the counteranions is suggested for the interaction of nonionic polymers and the long-chain cations. The action of the salts on the copolymers is discussed in terms of medium effects (change of the water structure) and of the binding effect of the single ions to the polymers.

INTRODUCTION

The nature of aqueous solutions of a substance reflects mainly the interaction of the solute with the hydrogen-bonded structure of water.[1,2] This is also true for aqueous solutions of macromolecules. Since water is essential for the functions of proteins, their relations to water have been intensively studied through influences induced by various additives.[3] For example, urea,[4] ethanol,[5] and inorganic salts[6] are agents which perturb the water structure, and their addition to an aqueous solution of a protein causes significant configurational and functional changes referred to as denaturation.[7]

As for synthetic macromolecules, configurations of hydrophilic polymers such as poly(vinyl alcohol), polyvinylpyrrolidone, and poly(ethylene oxide) in water are rather insensitive to addition of urea, but those of water-insoluble or difficultly soluble copolymers such as poly(vinyl alcohol-acetate) and poly(vinylpyrrolidone-acetate) are markedly affected by urea, and in fact some of these copolymers are dissolved in aqueous urea media.[8] With these copolymers some changes of their state in solution are expected on addition of salts.

Compared with the accumulation of data of salt effect on small nonionic substances,[9-12] studies on nonionic macromolecules are rather rare.[13-16] The purpose of this report is to investigate effects of inorganic and organic salts, including surface-active long-chain salts, on solutions of these copolymers in relation to specific properties of the individual ions in water. The interactions of polymers and ionic surfactants have been discussed in detail elsewhere.[17]

EXPERIMENTAL

Materials

Polymers. Poly(vinyl alcohol) (PVA) was the same as used previously[8] and has an average degree of polymerization of 2000 with 0.6% acetate. Its electrolytic impurities were removed by passage through ion-exchange resins. Three kinds of poly(vinyl alcohol-acetate) copolymers (PVA-Ac) were the same as used before.[8,17,18] The acetate content and degree of polymerization of PVA-Ac(A) are 19.7% and 2300 respectively, those of PVA-Ac(B) are 30.0% and 2000, respectively and those of PVA-Ac(C) are 54% and 1400, respectively.

Inorganic Salts. All the inorganic salts were the special reagent-grade products of Wako Pure Chemicals Co., Japan.

Organic Salts. Tetramethylammonium bromide (abbreviated Me₄NBr, and so on), Et₄NCl, Et₄NBr, Et₄NI, n-Pr₄NI, monomethylammonium chloride (abbr. MeNH₃Cl, and so on), EtNH₃Cl, EtNH₃Br, and n-BuNH₃Cl were guaranteed reagent grade products of Tokyo Kasei Kogyo Co., Japan. n-Pr₄NBr and n-Bu₄NBr were the products of Eastman Organic Chemicals Co., U.S.A. The octyl and dodecyl derivatives, n-C$_8$H$_{17}$NH$_3$Cl and n-C$_{12}$H$_{25}$NH$_3$Cl, were made from the respective amines by neutralization with anhydrous HCl in acetone, and were recrystallized several times from ethanol. The pure n-octylamine was supplied from the Research Laboratory of Japan Oils & Fats Co., Japan, and the n-dodecylamine was an extra pure grade product of Tokyo Kasei Kogyo Co.

Sodium methylsulfate monohydrate was the guaranteed reagent grade reagent of Tokyo Kasei Kogyo Co. Sodium ethylsulfate monohydrate was a product of Hayashi Pure Chemicals Co., Japan, and was recrystallized several times from water and dried over silica gel. In order to determine its purity, the salt was first decomposed with strong HCl, and the free sulfate ion thus produced was determined gravimetrically as $BaSO_4$. The purity was at least 99.9% as monohydrate. Sodium butyl sulfate was synthesized in this laboratory from n-butanol and chlorosulfonic acid. The flat crystals were repeatedly recrystallized from water. The salt was dried over silica gel. The melting point was 190–193°C. Its purity was at least 99.9% as anhydride. Pure sodium n-hexyl sulfate and sodium n-octyl sulfate were supplied from the Research Laboratory of Kao Soap Co., Wakayama, Japan. Sodium n-dodecyl sulfate was the pure product (Texapon L 100) of Henkel GmbH., Düsseldorf, and recrystallized from ethanol.

Sodium formate, acetate, n-propionate, and n-butyrate were the reagent-grade products of Wako Pure Chemicals Co., Japan.

Distilled water was boiled before use.

Experimental Methods

Viscosity and cloud point measurements were carried out as reported previously.[8,18] The cloud point was determined as the temperature ($\pm 0.25°C$) at which the transparent copolymer solution became cloudy on slow warning. From a cloud point-salt concentration relationship at a definite polymer concentration like one shown in Figure 4, the solubility of the polymer at 25°C was determined. Similar curves were made at different polymer concentrations around 25°C. In this way solubilities of the polymer at various salt concentrations at 25°C were obtained.

RESULTS

PVA and PVA-Ac(A) solutions are transparent at room temperature, but PVA-Ac(B) is soluble in water only at low temperature. Cloud points of PVA-Ac(B) solutions of various concentrations are 24.0°C at 0.05%; 21.0°C at 0.1%; 18.5°C at 0.2%; 17.5°C at 0.3%; and 17.5°C at 0.6%.

Changes of intrinsic viscosity $[\eta]$ of aqueous solutions of PVA and the copolymers, PVA-Ac(A) and PVA-Ac(B) by addition of inorganic salts at 25°C are shown in Figures 1 and 2, respectively. Whereas KSCN increases the intrinsic viscosity of the PVA solution, KI produces almost no change, and KF and KCl decrease it; these tendencies appear more markedly in the copolymers. Evidently the hydrophilic parts (—OH) of the copolymers are less susceptible to addition of the salts than the hydrophobic parts (acetate) are. PVA-Ac(B) is soluble in KSCN and KI solutions at
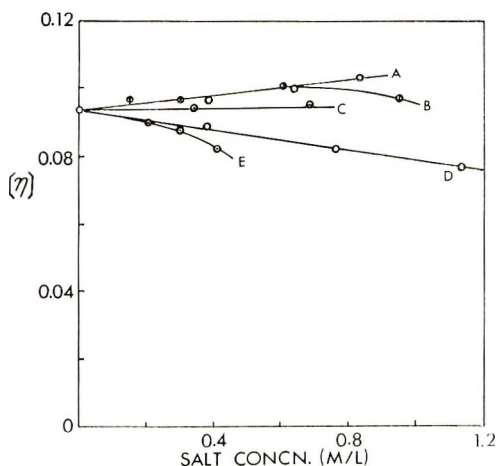
Fig. 1. Change of intrinsic viscosity $[\eta]$ of PVA solution by addition of inorganic salts at 25°C: (A) KSCN; (B) NaSCN; (C) KI; (D) KCl; (E) KF.
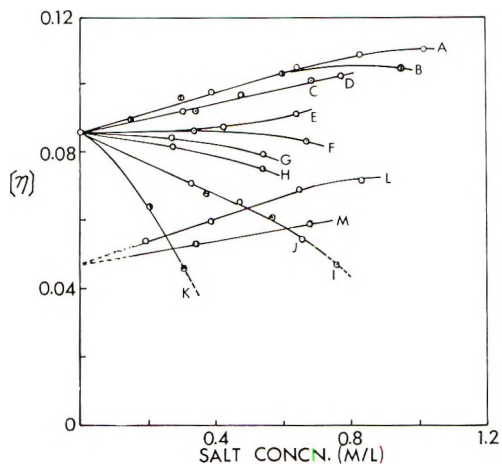
Fig. 2. Change of intrinsic viscosity (η) of PVA-Ac(A) and PVA-Ac(B) solutions by addition of inorganic salts at 25°C: (*A*) KSCN, PVA-Ac(A); (*B*) NaSCN, PVA-Ac(A); (*C*) KI, PVA-Ac(A); (*D*) NaI, PVA-Ac(A); (*E*) NaClO$_4$, PVA-Ac(A); (*F*) KBr, PVA-Ac(A); (*G*) LiCl, PVA-Ac(A); (*H*) NH$_4$Cl, PVA-Ac(A); (*I*) KCl, PVA-Ac(A); (*J*) NaI, PVA-Ac(A); (*K*) KF, PVA-Ac(A); (*L*) KSCN, PVA-Ac(B); (*M*) KI, PVA-Ac(B). The dotted portions were cloudy.
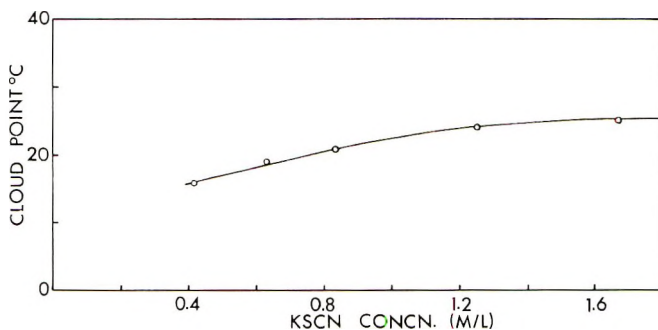
Fig. 3. Change of cloud point of 0.28% PVA-Ac(C) solution by addition of KSCN.

25°C above a critical salt concentration (Figs. 2 and 4). In order to dissolve PVA-Ac(C) in KSCN solution at 25°C, a higher salt concentration is required than for other copolymers with lower acetate contents (Fig. 3). There seems to exist an optimal acetate content of the copolymers for studying the salt effect conveniently, and thereafter the effect of salts was examined extensively on PVA-Ac(B) solutions.

Figure 4 demonstrates changes of the cloud point of a 0.21% PVA-Ac(B) solution on addition of various salts. In Figure 5, log S/S_0 was plotted against salt concentration (C_s) for some salts. Here S_0 (0.042%) and S are solubilities of PVA-Ac(B) in water and in the salt solution at a concentration C_s at 25°C. From the data plotted in Figures 4 and 5, salts at low salt concentrations at 25°C follow the following sequence from

strongest salting-in to strongest salting-out effects: $NH_4SCN = KSCN = NaSCN > NH_4I > KI = NaI > NaClO_4 > KNO_3 > LiBr > NH_4Br > NaBr > LiCl > NH_4Cl > CsCl = KCl = NaCl > KF = NaF = KIO_3.$
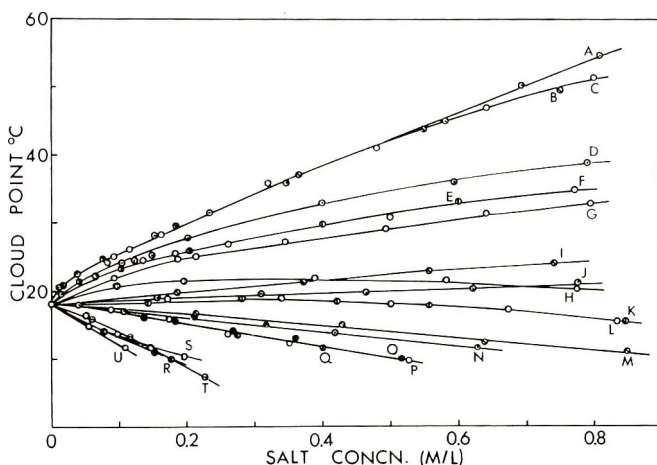
Fig. 4. Change of cloud point of 0.21% PVA-Ac(B) solution by addition of inorganic salts: (A) NH_4SCN; (B) $NaSCN$; (C) $KSCN$; (D) NH_4I; (E) NaI; (F) KI; (G) $NaClO_4$; (H) KNO_3; (I) $LiBr$; (J) NH_4Br; (K) $NaBr$; (L) KBr; (M) $LiCl$; (N) NH_4Cl; (O) $CsCl$; (P) KCl; (Q) $NaCl$; (R) NaF; (S) KF; (T) KIO_3; (U) $^1/_2$ Na_2SO_4.
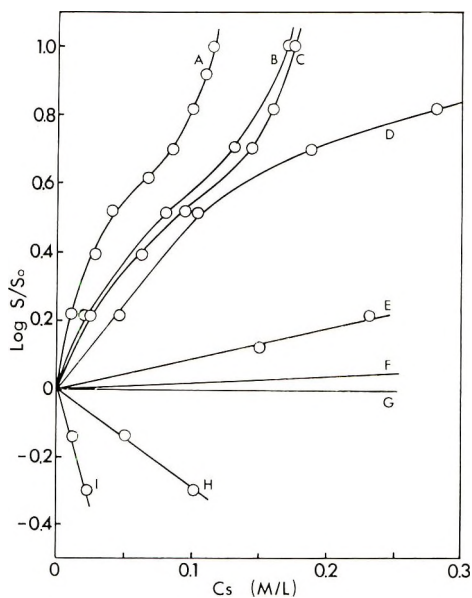
Fig. 5. Plots of log S/S_0 against salt concentration C_s: (A) $KSCN$; (B) NH_4I; (C) KI; (D) $NaClO_4$; (E) KNO_3; (F) $LiBr$; (G) KBr; (H) KCl; (I) KF. S_0 (0.042%) and S are solubilities of PVA-Ac(B) in water and in salt solution at concentration C_s, respectively, at 25°C.

In dilute salt solutions, the relative effect of single ions may be estimated from that of various salts with common counterions. The anionic order for the salt effect at around 25°C becomes then: $SCN^- > I^- > ClO_4^- > NO_3^- > Br^- > Cl^- > F^- = IO_3^- > \frac{1}{2} SO_4^=$.

This anionic order seems to be independent of the type of counter cations and is in line with Hofmeister's lyotropic series for anions. The differences
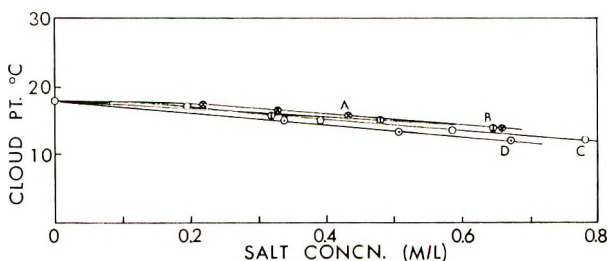
Fig. 6. Change of cloud point of 0.21% PVA-Ac(B) solution by addition of chlorides of polyvalent cations: (A) $\frac{1}{3}$ AlCl$_3$; (B) $\frac{1}{2}$ MgCl$_2$; (C) $\frac{1}{2}$ CaCl$_2$; (D) $\frac{1}{2}$ BaCl$_2$.
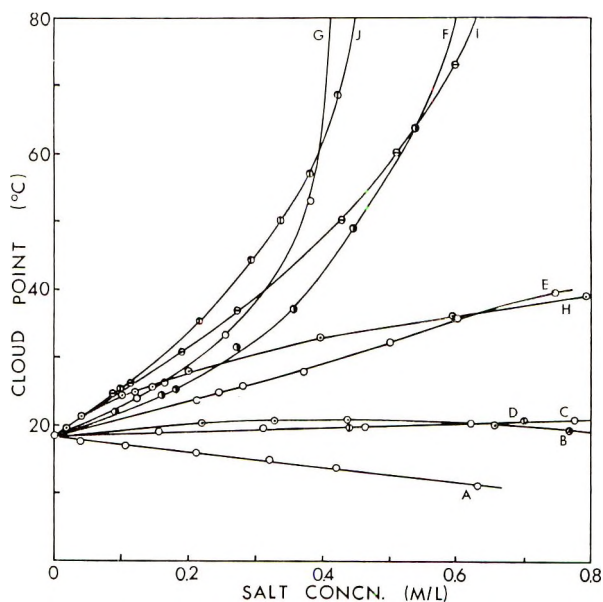
Fig. 7. Change of cloud point of 0.21% PVA-Ac(B) solution by addition of ammonium and tetraalkylammonium halides: (A) NH$_4$Cl; (B) Et$_4$NCl; (C) NH$_4$Br; (D) Me$_4$NBr; (E) Et$_4$NBr; (F) Pr$_4$NBr; (G) Bu$_4$NBr; (H) NH$_4$I; (I) Et$_4$NI; (J) Pr$_4$NI.

among the cations are rather small compared with those among the anions. This is the general tendency encountered in lyotropic phenomena.[19]

Figure 6 shows the effects of chlorides of di- and trivalent monatomic cations, and Figure 7 illustrates those of quaternary ammonium halides; the results for Bu$_4$NBr and Me$_4$NBr were already reported.[8] For com-
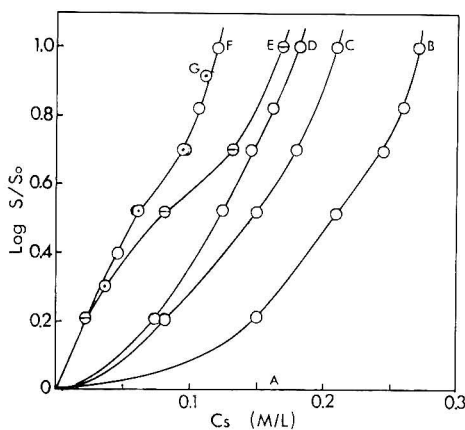
Fig. 8. Plots of log S/S_0 against salt concentration C_s: (A) NH$_4$Br = Me$_4$NBr (and Et$_4$NCl); (B) Et$_4$NBr; (C) Pr$_4$NBr; (D) Bu$_4$NBr; (E) NH$_4$I; (F) Et$_4$NI; (G) Pr$_4$NI. S_0 (0.042%) and S are solubilities of PVA-Ac B) in water and in salt solution at concentration C_s, respectively, at 25°C.
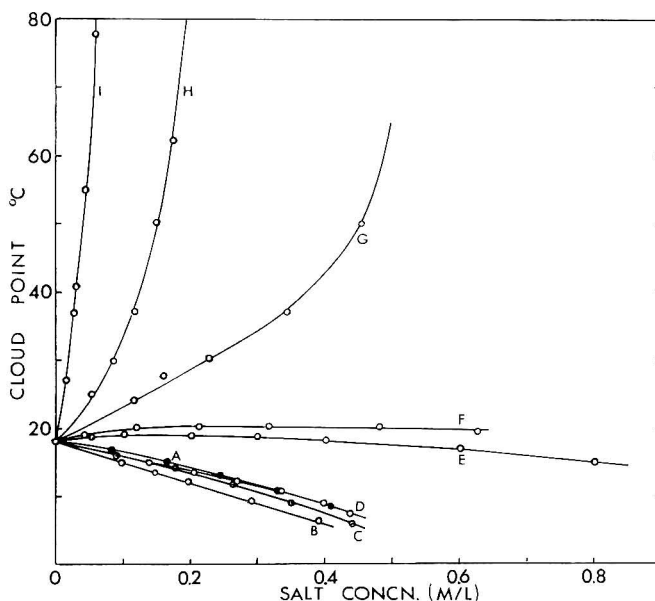
Fig. 9. Change of cloud point of 0.21% PVA-Ac(B) solution by addition of sodium alkylcarboxylates and sodium alkylsulfates: (A) Na formate; (B) Na acetate; (C) Na propionate; (D) Na butyrate; (E) MeSO$_4$Na; (F) EtSO$_4$Na; (G) BuSO$_4$Na; (H) C$_6$H$_{13}$SO$_4$Na; (I) C$_3$H$_{17}$SO$_4$Na.

parison with the effect of inorganic salts, the curves for three ammonium halides are also shown in Figure 7.

In view of the different nature of the effect of inorganic and organic cations on water,[1] their salt effects should be considered separately. The orders for mono- and polyvalent cations are as follows: Li$^+$ > Cs$^+$ =

$K^+ = Na^+$; $\frac{1}{3} Al^{+++} > \frac{1}{2} Mg^{++} > \frac{1}{2} Ca^{++} > \frac{1}{2} Ba^{++}$; and $Bu_4N^+ > Pr_4N^+ > Et_4N^+ > Me_4N^+ = NH_4^+$.

The dependence of the effect on the water structure on the ionic size of the mono- and polyvalent inorganic and organic cations is opposite to that of halide ions, and this is consistent with the results of the salt effect on the solubility of small nonelectrolytes.[9,10,20]

Figure 8 shows logs S/S_0 plots for PVA-Ac(B) solubility in some R_4NX solutions at 25°C as a function of the salt concentration C_s. The large tetraalkylammonium salts produce salting-in of the copolymer.

Figures 9 and 10 show changes of the cloud point of PVA-Ac(B) solution on addition of various salts of monoalkyl-substituted anions ($RCOONa$
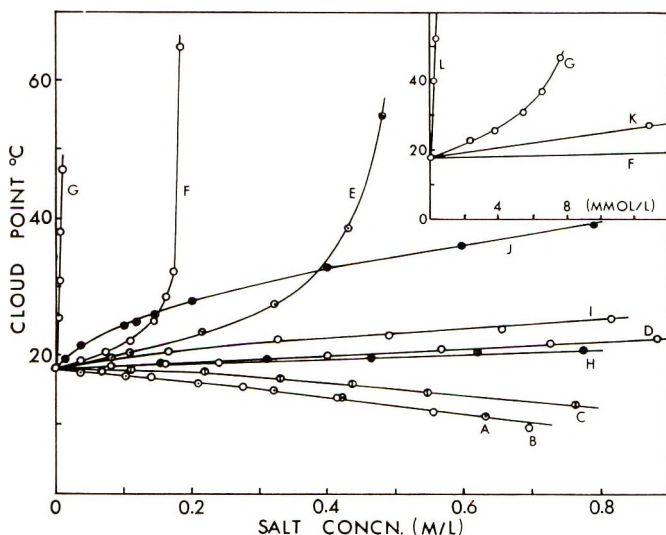
Fig. 10. Change of cloud point of 0.21% PVA-Ac(B) solution by addition of ammonium and monoalkylammonium halides. Insert: Comparison of sodium alkylsulfates and alkylammonium chlorides with the same alkyl chain lengths: (*A*) NH_4Cl; (*B*) Methyl-NH_3Cl, (*C*) Ethyl-NH_3Cl, (*D*) Butyl-NH_3Cl, (*E*) Hexyl-NH_3Cl, (*F*) Octyl-NH_3Cl, (*G*) Dodecyl-NH_3Cl, (*H*) NH_4Br, (*I*) Ethyl-NH_3Br, (*J*) NH_4I, (*K*) Octyl-SO_4Na, (*L*) Dodecyl-SO_4Na.

and RSO_4Na) and cations (RNH_3Cl and Br), respectively. In CO_2-free distilled water, these sodium carboxylates produce only a trace of the free acids.[21] As the cloud points immediately after addition of sodium butyrate and those after several hours were the same, the possibility of hydrolysis of the acetate groups of the copolymer by these sodium carboxylates is considered to be negligible. In the cases of cationic surfactants, in order to avoid errors due to their adsorption on the glass wall, the test tubes for measurements of the cloud point were rinsed with the same solution as that for the measurements. The salting-in order for these alkyl ions is: formate$^-$ > butyrate$^-$ > propionate$^-$ > acetate$^-$; dodecyl-SO_4^- > octyl-SO_4^- > hexyl-SO_4^- > butyl-SO_4^- > ethyl-SO_4^- > methyl-SO_4^-; and

dodecyl-NH_3^+ > octyl-NH_3^+ > hexyl-NH_3^+ > butyl-NH_3^+ > ethyl-NH_3^+ > methyl-NH_3^+ = NH_4^+.

In the alkyl-substituted organic ions, as long as the alkyl chains are short, a change of a few methylene units produces relatively small differences in the cloud point. Even surface-active $C_8H_{17}NH_3Cl$ gives rise to quite small an effect below its critical micelle concentration (CMC) (0.25 mole/l., determined by the dye solubilization method). However, with sodium alkylsulfates with chains longer than butyl, particularly with hexyl-SO_4Na and the higher homologs, a striking interaction is observed far below the CMC.

DISCUSSION

Inorganic Salts

The overall shape of a PVA-Ac chain in water depends on the balance between the hydrophobic attraction between acetate groups and the expansive hydrophilic interaction between the hydroxyl groups and the solvent water. The hydrophobic attraction in water is a consequence of the ordered water structure (the icebergs) in the hydrophobic regions.[2] When a water-structure-breaking, nonelectrolytic substance like urea or formamide is added to a PVA-Ac system,[8] it weakens the hydrophobic interaction and restores expansion of the whole polymer coil. On the other hand, addition of sucrose, which lowers water activity,[22] reinforces the attraction in the polymer chain.[23]

It is generally accepted that, when a salt is added to water, it modifies the water structure, and at low concentrations each ion brings about specific changes in the water surrounding the ion resulting from the balance of the water structure and the disturbing electrostatic effect in the vicinity of the ion.[1,6] Large ions such as SCN^-, ClO_4^-, I^-, Br^-, Cs^+, and Rb^+ are classified as water-structure breakers, while small and/or highly charged, strongly electrostrictive ions such as F^-, OH^-, H^+, Li^+, Na^+, Ca^{++}, Mg^{++}, and Al^{+++}, are assigned as water-structure makers.[1,6] Although the size of IO_3^- is big, this anion is considered a structure maker, because its negative charge is localized at the periphery and therefore it has a high charge density.[24] Among the intermediate ions in the lyotropic series, NH_4^+, K^+, and Cl^- have little effect on water structure.[25]

Modern theories of the salt effect on solubility of nonelectrolytes in water take the specificity of this solvent into consideration.[9-12] The forces underlying the general salt effect are primarily of electrostatic nature,[9-12] so the effects of the electrolytic and nonelectrolytic modifiers of water structure are basically different. Generally speaking, the strongly electrostrictive, positively hydrating ions cause salting-out, and the weakly electrostrictive ions which break the water structure, reduce this tendency or reverse it to salting-in, depending on the polarity of the nonelectrolytic solutes.[9-12,19] As is evident from Figures 1 and 2, the salts affect the hydrophobic acetate groups rather than the hydrophilic groups in the

copolymers; particularly KSCN, KI, and NaClO$_4$ help stabilize the acetate groups in water, while KF, KIO$_3$, and KCl tend to reject them, and KI is almost without effect on PVA. On the other hand, ethyl acetate is salted out by most salts, including even KI.[20]

In the copolymers, the hydrophobic interaction is weakened by insertion of hydroxyl groups between acetate groups. KSCN, KI, and NaClO$_4$ attack the weakened hydrophobic bonds in the copolymers, unlock the inner expansive forces, and thus cause salting-in. As seen in Figures 4 and 5, the anions essentially determine the properties of hydrophobic regions of the copolymer in water and lead to a wide spectrum of the salt effect. The predominance of anions over cations is related to the fact that with inorganic salts, the anions determine most of the effect on water in bulk[26,27] as well as its properties at the air and hydrophobic interfaces.[28-30]

Studies on the surface potential and surface tension of aqueous solutions of inorganic salts[28-30] concluded that a deficiency of the ions exists close to the interface, and that this effect follows the lyotropic series; SCN$^-$ is closest to and F$^-$ farthest from the interface, while the strongly hydrated cations have little effect.

Thus, inorganic ions modify the configuration of the polymers in water by the effect on solvent water (medium effect) at the polymer interface and in bulk. In this respect, their effect is entirely different from some characteristic reactions between functional groups of specific polymers and salts,[31-33] and also from the effect of some organic salts, as will be mentioned subsequently.

This interpretation applies to salt effects on cloud point and on CMC of nonionic surfactant solutions,[34-37] and to the viscosity of some polymer solutions.[14-16] In the former cases the salt effect arises from dehydration of the hydrophilic groups, i.e., ether oxygens of poly oxyethylene. In analogy with the general salt effect on nonpolar substances,[9,10,38,39] it seems more appropriate to consider the salt effect also on the hydrophobic parts.[37]

Figure 5 shows that the Setschenow equation for the salt effect on small nonelectrolytes:[9,10,18]

$$\log S/S_0 = KC_s$$

where S_0 is the solubility in water and S the solubility at a salt concentration C_s with K being a constant does not hold for the polymer except for very dilute polymer solutions. Each curve for KSCN, KI, and NH$_4$I seems to be divided into two portions; a portion with a decreasing slope at lower salt concentration and one with a steeper slope at higher salt concentration. It is considered that the curve for NaClO$_4$ and those for KSCN, KI, and NH$_4$I in their lower salt concentration regions may arise from the polymer–polymer interaction in the salt solutions, since for small nonelectrolytes the Setschenow equation applies up to several molar salt solutions. The steeper portions of the curves for KSCN, KI, and NH$_4$I at higher salt concentration, as seen also in the next section (Fig. 8), may

be caused by increasing direct contact of the anions with the polymers, which overwhelms the effect of the polymer–polymer interaction.

Organic Salts

Tetraalkylammonium Salts. Me_4N^+ is still slightly water-structure-breaking, but other larger tetraalkylammonium ions (R_4N^+), especially Bu_4N^+, are distinctly water-structure-making[40,41] in a fundamentally different way from that of small inorganic ions such as F^-, OH^-, H^+, and Li^+. Whereas these strongly electrostrictive ions cause orientation of water dipoles around them by concentric electrostatic forces, large R_4N^+, trialkylsulfonium cations,[42] or in general, nonpolar substances enhance the hydrogen-bonded structure of water because of their very hydrophobic nature,[1,2] The large R_4N^+ produce salting-in not only of small nonelectrolytes[43,44] but also of some polymers following the order $Bu_4N^+ >$ $Pr_4N^+ > Et_4N^+ > Me_4N^+$ (Figs. 7 and 8). The binding of these cations supposedly gives the hydrophobic polymers a hydrophilic polyelectrolytic character.[8] However, at low salt concentrations, I^-, a strong breaker, still is the dominant factor (Fig. 8). It is noted that NH_4Br and Me_4NBr exert the same effect on the copolymer (Fig. 7).

Since the water structure[1,56,45] and therefore the binding equilibria are dependent on temperature, the behavior of individual ions suggested from the cloud point data over a wide temperature range is rather complicated. However, a comparison of the rates of cloud point change by addition of $Et_4N^+X^-$ (where X^- is Cl^- and Br^-) relative to those of the corresponding ammonium halides around 18°C (Fig. 7) may indicate that the actions of halide ions and the organic cations seem to be additive, as are inorganic anions and cations in the salt effect on small nonelectrolytes[9,10,19] and on PVA-Ac(B) (Fig. 4). Hence, in very dilute salt solutions, these hydrophobic cations may not interfere much with halide ions in their salt effect. In these cases two effects may be at work independently to change the solution state of the polymer: the binding of the hydrophobic cations, and the medium effect of the inorganic counter anion.

A comparison of the effect of the R_4NBr and R_4NI in Figure 8 shows, however, that the interaction of the polymer and R_4N^+ is under the influence of the anion. Here the additivity of both effects clearly does not hold and the more strongly structure-breaking counteranion ($I^- > Br^-$) seems to interfere appreciably with the cation on the polymer. From the activity measurements of R_4NX salts in water it was concluded that the R_4N^+ and halide ion interact with each other in specific ways with respect to their structural influences upon water: a more strongly structure-breaking anion ($I^- > Br^- > Cl^-$) lets the more structure-making cation ($Bu_4N^+ > Pr_4N^+ > Et_4N^+$) more compatible with each other because the breaker anion makes free water molecules available for the self-salting in, or association, of the hydrophobic cations.[46] Therefore, both I^- and R_4N^+ may approach the polymer more closely and interfere with each other on it more strongly than do bromide and chloride ions.

The Setschenow plots for the polymer in R_4NX solutions also deviate from linearity (Fig. 8). The slopes of the curves increase with the salt concentration, since it is assumed that the distribution of the organic cations and inorganic anions in the neighborhood of the polymer is not uniform and it is found that the binding of the cation to the polymer increases with increasing salt concentration. In these cases it is considered that the polymer–polymer interaction may be covered by the binding effect. In the cases of R_4NI salts where the curves for Et_4NI and Pr_4NI at 25°C overlap, the mechanism seems to be more complex, as mentioned above. As shown in Figure 7, with a rise of temperature the difference between Et_4NI and Pr_4NI widens, because the water structure around the cations is decreased.

Monoalkyl-Substituted Ions. The marked depression of the cloud point by four sodium alkylcarboxylates (formate, acetate, propionate, and butyrate) shown in Figure 9 is due to the $—COO^-$ group which provides an intense electrical field in water.[25] Therefore, like F^- and OH^-, formate ion immobilizes water around it, but acetate ion may, because of its hydrophobic methyl group, approach more closely to the hydrophobic region of the polymer, and carry out a more efficient salting-out effect. In propionate and butyrate ions, this tendency may persist, but these alkyl ions may be not only attracted to the polymer but also weakly bound, and may thus raise the solubility of the polymer as the balance of the two effects. The binding is favored by an increasing length of the alkyl chains of these ions. For example, addition of sodium acetate reduces the viscosity of a PVA solution (by the medium effect), but that of sodium laurate enhances it significantly (by the binding effect).[47]

As understood from the cloud point data of $MeSO_4Na$ (Fig. 9) $MeNH_3Cl$ (Fig. 10), the $—SO_4^-$ and $—NH_3^+$ groups do not probably alter the water structure much, so the cloud point always rises on addition of the sodium alkylsulfates and of alkylammonium chlorides and bromides. The rate of the increase per ethylene unit of sodium alkylsulfates is bigger than that of alkylammonium chlorides in dilute solutions around room temperatures. The moderately surface-active $C_8H_{17}NH_3Cl$ does not show any special thermal effect upon PVA-Ac(B) up to its CMC (0.25 mole/l.): its effect below 0.1 mole/l. seems to be normal as extrapolated from the effects of the series of the lower homologs (Fig. 10). However, an abrupt rise of the cloud point near the CMC is clearly attributable to the binding of the surface-active cation in quantity, presumably to micelle-like binding. On the other hand, the polymer interacts considerably with $BuSO_4Na$ despite its inability to form micelles,[48] and with $C_6H_{13}SO_4Na$ (CMC: 1.2 mole/l.) and $C_8H_{17}SO_4Na$ (CMC: 0.13 mole/l.) even far below their CMC's (Fig. 9). The action of $BuSO_4Na$ suggests that even this anion brings about some binding effect, in contrast with $BuNH_3Cl$. The difference in the cloud point phenomena between the typical ionic surfactants, $C_{12}H_{25}SO_4Na$ (CMC: 8 mmole/l.) and $C_{12}H_{25}NH_3Cl$ (CMC: 14 mmole/l.), is striking (Fig. 10, insert). In view of the strong salting-in effect of NH_4I compared

with the effect of Bu_4NBr or $C_8H_{17}NH_3Cl$ at low concentrations, as illustrated in Figures 8 and 10, the medium effect by inorganic counteranions still prevails over the binding effect of the organic cations to the polymer.

When a polymer is hydrophilic like polyvinylpyrrolidone (PVP), sodium alkylsulfates with alkyl chains shorter than octyl,[49] and $C_{12}H_{25}NH_3Cl$ even above the CMC, are scarcely bound to it.[47] A special binding ability of other organic anions to nonionic polymers has been generally recognized.[14,17,50] Thus, the extent of the interaction depends not only upon mutual hydrophobic and steric relations of the partners but also upon the ionic nature.[17] Recently it was found that in the presence of SCN^-, $C_{12}H_{25}NH_3^+$ shows a strong interaction with PVP.[51] This fact may suggest that counteranions play an important part in the interaction of polymers and long-chain cations.

References

1. J. L. Kavanau, *Water and Solute-Water Interactions*, Holden-Day, San Francisco, 1964.

2. G. Némethy, *Angew. Chem. Intern. Ed.*, **6**, 195 (1967).

3. J. F. Brandt, and L. Hunt, *J. Amer. Chem. Soc.*, **89**, 4826 (1967).

4. D. B. Wetlaufer, S. K. Malik, L. Stoller, and R. L. Coffin, *J. Amer. Chem. Soc.*, **86**, 508 (1964).

5. F. Franks and D. J. G. Ives, *Quart. Rev.*, **20**, 1 (1966).

6. H. S. Frank and W. Y. Wen, *Discussions Faraday Soc.*, **24**, 133 (1957).

7. J. A. Gordon and W. P. Jencks, *Biochemistry*, **2**, 47 (1963).

8. S. Saito and T. Otsuka, *J. Colloid Interface Sci.*, **25**, 531 (1967).

9. F. A. Long and W. F. McDevit, *Chem. Rev.*, **51**, 119 (1952).

10. N. C. Deno and C. H. Spink, *J. Phys. Chem.*, **67**, 1347 (1963).

11. B. E. Conway, J. E. Desnoyers, and A. C. Smith, *Phil. Trans. Roy. Soc. (London)*, **A256**, 389 (1964).

12. P. Ruetschi and R. F. Amlie, *J. Phys. Chem.*, **70**, 718 (1966).

13. H. Morawetz, *Macromolecules in Solution*, Interscience, New York, 1965, p. 81.

14. J. Eliassaf, F. Eriksson, and F. R. Eirich, *J. Polym. Sci.*, **47**, 193 (1960).

15. J. Eliassaf, *J. Appl. Polym. Sci.*, **3**, 372 (1960).

16. F. E. Bailey and J. V. Koleske, in *Non-ionic Surfactants*, M. J. Schick, Ed., Dekker, New York, 1967, p. 794.

17. S. Saito, *J. Colloid Interface Sci.*, **24**, 227 (1967).

18. S. Saito, *Kolloid Z. Z. Polym.*, **226**, 10 (1968).

19. J. T. Edsall and J. Wyman, *Biophysical Chemistry*, Vol. 1, Academic Press, New York, 1958, p. 263.

20. H. S. Harned and B. B. Owen, *The Physical Chemistry of Electrolytic Solutions*, 3rd ed., Reinhold, New York, 1958, p. 531.

21. L. Pauling, *General Chemistry*, Freeman, San Francisco, 1947, Chap. 21.

22. R. A. Robinson and R. H. Stokes, *J. Phys. Chem.*, **65**, 1954 (1961).

23. S. Saito, unpublished data.

24. E. R. Nightingale, *J. Phys. Chem.*, **64**, 162 (1960).

25. R. W. Gurney, *Ionic Processes in Solutions*, McGraw-Hill, New York, 1953, p. 159.

26. J. Greyson, *J. Phys. Chem.*, **71**, 2210 (1967).

27. B. E. Conway, R. E. Verrall, and J. E. Desnoyers, *Z. Physik. Chem.*, **230,** 157 (1965).

28. J. E. B. Randles, *Discussions Faraday Soc.*, **24,** 194 (1957).

29. N. L. Jarvis and M. A. Scheiman, *J. Phys. Chem.*, **72,** 74 (1968).

30. N. K. Adam, *The Physics and Chemistry of Surfaces*, 2nd ed., Oxford Univ. Press, London, 1938, p. 360.

31. S. Saito, H. Okuyama, H. Kishimoto, and Y. Fujiyama, *Kolloid-Z.*, **144,** 41 (1955).

32. S. Saito and H. Okuyama, *Kolloid-Z.*, **139,** 150 (1954).

33. H. G. Nadeau and S. Siggia, in *Non-ionic Surfantants*, M. J. Schick, Ed., Dekker, New York, 1967, p. 838.

34. P. Becher, in *Non-ionic Surfactants*, M. J. Schick, Ed., Dekker, New York, 1967, p. 500.

35. P. Becher, *J. Phys. Chem.*, **68,** 3585 (1964).

36. W. Luck, *Ber. Bunsenges. Phys. Chem.*, **69,** 69 (1965).

37. P. Mukerjee, *J. Phys. Chem.*, **69,** 4038 (1965).

38. T. J. Morrison and N. B. B. Johnstone, *J. Chem. Soc.*, **1955,** 3655.

39. A. Ben-Naim and M. Egel-Thal, *J. Phys. Chem.*, **69,** 3250 (1965).

40. W. Y. Wen and S. Saito, *J. Phys. Chem.*, **68,** 2639 (1964).

41. F. Franks and H. T. Smith, *Trans. Faraday Soc.*, **63,** 2586 (1967).

42. S. Lindenbaum, *J. Phys. Chem.*, **72,** 212 (1968).

43. J. E. Desnoyers, G. E. Pelletier, and C. Jolicoeur, *Can. J. Chem.*, **43,** 3232 (1965).

44. H. E. Wirth and A. LoSurdo, *J. Phys. Chem.*, **72,** 751 (1968).

45. O. D. Bonner and G. B. Woolsey, *J. Phys. Chem.*, **72,** 899 (1968).

46. W. Y. Wen, S. Saito, and C. M. Lee, *J. Phys. Chem.*, **70,** 1244 (1966).

47. S. Saito, *Kolloid-Z.*, **137,** 98 (1954).

48. J. Clifford and B. A. Pethica, *Trans. Faraday Soc.*, **60,** 1483 (1964).

49. S. Barkin, Ph.D. Thesis, Polytechnic Institute of Brooklyn, 1957.

50. P. Molyneux and H. P. Frank, *J. Amer. Chem. Soc.*, **83,** 3169 (1961).

51. S. Saito and M. Yukawa, *J. Colloid Interface Sci.*, in press.

Polyindoloquinoxalines

I. SCHOPOV and N. POPOV, *Institute of Organic Chemistry,*
Bulgarian Academy of Sciences, Sofia 13, Bulgaria

Synopsis

Two polymers, containing 6H-indolo [2,3-b] quinoxaline as a repeating unit, have been prepared by polycyclization of 5,5'-biisatyl with 3,3'-diaminobenzidine, and of 5,5'-diisatyl ether with 3,3',3,4'-tetraaminodiphenyl ether in polyphosphoric acid. Their structure was established by comparing the infrared and electronic spectra of the newly obtained polymers with the corresponding spectra of four model compounds synthesized for the purpose. The electronic spectra showed conjugation along the chain of both the polymer with ether bonds and the one with single bonds between the rings. The two polymers gave an electronic paramagnetic resonance signal. The polyindoloquinoxalines showed good thermal stability in air and in nitrogen, the better stability being manifested by the polymer with single bonds between the rings.

INTRODUCTION

Recent investigations indicate that polymers containing quinoxaline repeating units exhibit excellent thermal stability.[1–4] Furthermore, when the quinoxaline rings form a polymer with a ladder structure, its thermal qualities are even better,[5] a possible explanation being that with the planar ladder structure conjugation is more perfect. This assumption is confirmed by the fact that when conjugation is lacking, thermal stability is very low. Thus, polyquinoxalines obtained from aliphatic tetraketones have low thermal stability despite their ladder structure.[6]

The purpose of the present work was to investigate the synthesis and study the properties of polymers containing 6H-indolo[2,3b]quinoxaline (indophenazine) (I) as a recurring unit:

I
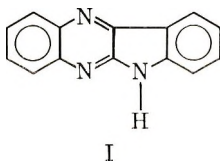
Indoloquinoxaline is a stable compound with a high melting point (294–295°C), which was synthesized a long time ago but has not been extensively studied.[7] Compared with quinoxaline, it has the advantage of possessing two more linear condensed rings and a longer system of conjugation. Polyindoloquinoxalines can upon condition be treated as polymers with an imperfect ladder structure. Theoretical investigations have shown[8] that, even when imperfect, ladder structure leads to greater

thermal stability than the one of ordinary, linear structure. Bearing this in mind, as well as the above considerations about the role of conjugation, one could expect polymers containing indoloquinoxaline rings to manifest good thermal stability.

We synthesized polyindoloquinoxaline polymers by polycyclization reaction of diisatyls with aromatic tetraamines [eq. (1)].

$$(1)$$
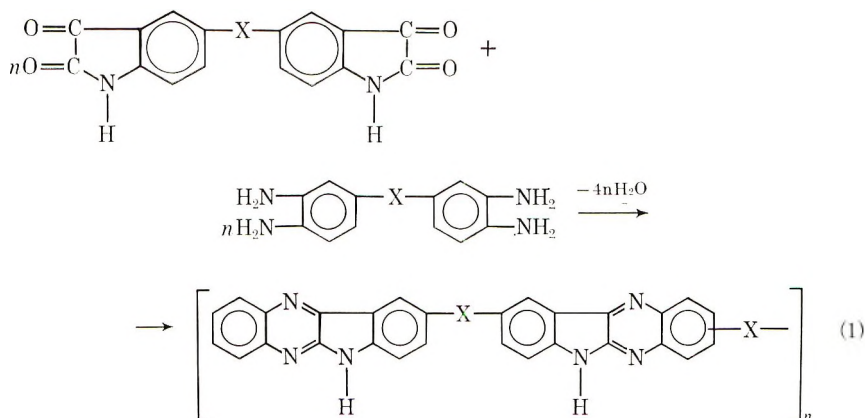
When X is a single bond, one obtains the polymer poly-2(3),9-{9′,2′(3′)— 6H-indolo[2,3-b]quinoxalinyl}-6H-indolo[2,3-b]quinoxaline, which for simplicity will be termed polyindoloquinoxaline. When X is an oxygen atom, the polymer will be poly-2(3),9-{9′,2′(3′)-6H-indolo[2,3-b]quinoxalinyl}- 6H-indolo[2,3-b]quinoxalinyl ether, termed polyindoloquinoxalinyl ether.

EXPERIMENTAL

Monomers and Solvents

Isatin was a commercial product (obtained from P.P.H., POCh, Gliwice, Poland) with a melting point of 202–203°C.

1,2-Diaminobenzene dihydrochloride (purest) was obtained from VEB-Schering, Berlin-Adlershof, Germany.

5,5′-Biisatyl was prepared by the method of Dethloff and Mix[9] and purified by dissolution in 10% sodium hydroxide, quickly acidifying with 10% sulfuric acid to pH 2.3. The precipitate was filtered and then the filtrate was acidified with an excess of the acid. 5,5′-Biisatyl thus precipitated was washed with water till absence of sulfate ions and then dried.

3,3′-Diaminobenzidine (DAB) was used in the form of DAB·4HCl·2H₂O, prepared by a procedure according to Iwakura et al.[10]

5,5′-Diisatyl ether was prepared as described in the previous paper.[11]

3,3′,4,4′-Tetraaminodiphenyl ether (TADE) was prepared according to Foster and Marvel[12] and isolated as the tetrahydrochloride. Elemental analysis showed that it contains two molecules of crystal water.

Polyphosphoric acid (PPA) was used as 110% PPA, prepared from ortho-phosphoric acid and phosphorus pentoxide.

Model Compounds

6H-Indolo[2,3-b]quinoxaline (**I**). 1,2-Diaminobenzene dihydrochloride (1.81 g, 0.01 mole) was added to 30 ml of PPA, heated at 140°C in a nitrogen atmosphere with stirring. After the evolution of hydrogen chloride had stopped, 1.47 g (0.01 mole) isatin was added. Heating was continued for 1 hr, after which time the mixture was poured into 300 ml of water. The precipitate was filtered, washed with water, and left to stand overnight in a solution of 5% ammonium bicarbonate. Then it was again filtered, washed with water, and dried. The yield of indoloquinoxaline thus obtained, mp 294–295°C, was quantitative. By a mixed melting point and the infrared spectrum, it was proved that this product is identical with the one obtained according to Schunck[7] and Badger.[13]

Bi-{2,2′-6H-indolo[2,3-b]quinoxaline} (**II**). DAB · 4HCl · 2H$_2$O (0.79 g, 0.002 mole) was added to 25 ml of PPA, and the mixture was heated at 140°C with stirring and bubbling of a stream of nitrogen through the mixture. After the evolution of hydrogen chloride had stopped, 0.75 g (0.0051 mole) isatin was added, and the mixture was heated with stirring for 1 hr at 140°C and 11 hr at 180°C. The dark-red solution was poured into 250 ml of water, the precipitate was filtered, washed with water, and left to stand overnight in a 5% solution of ammonium bicarbonate. Then the precipitate was again filtered, thoroughly washed, and dried, yielding 0.8 g (92.0% of the theoretical). On sublimation in a bath of 390°C, *in vacuo* (10^{-3} mm Hg), 2,2′-biindoloquinoxaline represents a yellow substance which does not melt below 520°C. According to Tiwari,[14] it is red (not having been sublimated). It dissolves in sulfuric acid, dimethylformamide, dimethyl sulfoxide, and at higher temperature in pyridine.

Anal. Calcd for C$_{28}$H$_{16}$N$_6$ (436.48): C, 77.05%; H, 3.70%; N, 19.25%. Found: C, 76.30%; H, 4.31%; N, 19.28%.

Bi-{9,9′-6H-indolo[2,3-b]quinoxaline} (**III**). This was prepared by following the procedure for obtaining 2,2′-biindoloquinoxaline described above, starting from 2.00 g (0.011 mole) 1,2-diaminobenzene dihydrochloride and 1.46 g (0.005 mole) 5,5′-biisatyl. The yield was 2 g (91.7% of the theoretical). Sublimation as described above, yields 9,9′-biindoloquinoxaline as a yellow substance which does not melt below 500°C. It is soluble in dimethylformamide, dimethyl sulfoxide, and, at elevated temperatures, in pyridine.

Anal. Calcd for C$_{28}$H$_{16}$N$_6$ (436.48): C, 77.05%; H, 3.70%; N, 19.25%. Found: C, 76.44%; H, 4.23%; N, 19.03%.

Bis-{2,2′-6H-indolo[2,3-b]quinoxalinyl} ether (**IV**). This was obtained in an analogous manner from 0.82 g (0.002 mole) TADE·4HCl·2H$_2$O and 0.66 g (0.0045 mole) isatin with a yield of 0.83 g (92% of the theoretical). On sublimation under the conditions described above, a yellow substance was obtained which does not melt below 520°C and dissolves in sulfuric

acid, dimethylformamide, dimethyl sulfoxide and at elevated temperature in pyridine.

Anal. Calcd for $C_{28}H_{16}N_6O$ (452.58): C, 74.31%; H, 3.56%; N, 18.57%. Found: C, 73.63%; H, 4.01%; N, 18.26%.

Bis-{9,9'-6H-indolo [2,3-b] quinoxalinyl} ether (V). This was obtained in a manner similar to the procedure of preparing the other model compounds, from 1.54 g (0.005 mole) 5,5'-diisatyl ether and 2 g (0.011 mole) 1,2-diaminobenzene dihydrochloride, with a yield of 2.1 g (93% of the theoretical). The product obtained on sublimation is a yellow substance, not melting below 520°C and soluble in dimethylformamide, dimethyl sulfoxide, and pyridine.

Anal. Calcd for $C_{28}H_{16}N_6O$ (452.58): C, 74.31%; H, 3.56%; N, 18.57%. Found: C, 74.60%; H, 4.24%; N, 18.14%.

Polymers

Polyindoloquinoxaline. A 1.98-g portion (0.005 mole) DAB·4HCl·2H$_2$O was subdivided and added in small portions to 40 ml PPA, maintained at 140°C with stirring and passage of a stream of nitrogen was passed through the mixture. After the evolution of hydrogen chloride had ceased, 1.46 g (0.005 mole) 5,5'-biisatyl was added and heating was continued at this temperature for 3 hr. The reaction mixture was then further heated for 9 hr at 180°C. The hot solution, which was dark in color, was poured into 400 ml of water, and the precipitate formed was filtered, washed with water, and left to stand overnight in a 5% solution of ammonium bicarbonate. After it had been filtered, thoroughly washed, and dried, the polymer was extracted in a Soxhlet apparatus with ethanol for several days. It was reddish-brown and weighed 1.86 g (86% of the theoretical). The intrinsic viscosity in concentrated sulfuric acid at 20°C was $[\eta] = 0.11$ dl/g. On heating *in vacuo* (10^{-2} mm Hg) at 300°C for $2^1/_2$ hr, the polymer showed no apparent changes, but $[\eta]$ reached 0.30 dl/g.

Polyindoloquinoxaline dissolves in sulfuric acid in the cold, and when heated, in hexamethylphosphoramide, less readily in dimethylacetamide and dimethyl sulfoxide.

Anal. Calcd for $(C_{14}H_7N_3)_n$: C, 77.40%; H, 3.25%; N, 19.35%. Found: C, 74.52%; H, 4.36%; N, 18.51%.

Polyindoloquinoxalinyl Ether. This was prepared by the previous procedure from 1.236 g (0.003 mole) TADE·4HCl·2H$_2$O and 0.924 g (0.003 mole) 5,5'-diisatyl ether, with a yield of 1.23 g (88% of the theoretical). The polymer is green; $[\eta] = 0.33$ dl/g (dissolved in concentrated sulfuric acid at 20°C). On heating for $2^1/_2$ hr at 300°C *in vacuo* (10^{-2} mm Hg), its intrinsic viscosity reached $[\eta] = 0.42$ dl/g. In the cold, the polymer is soluble only in sulfuric acid, while at higher temperature it dissolves in hexamethylphosphoramide and less readily in dimethylacetamide and dimethyl sulfoxide.

ANAL. Calcd for $(C_{14}H_7N_3O)_n$: C, 72.20%; H, 3.03%; N, 18.03%. Found: C, 68.36%; H, 4.16%; N, 17.85%.

Spectroscopic Studies

Infrared spectra were obtained with a Zeiss-Jena UR-10 spectrometer.

Electronic spectra were taken in concentrated sulfuric acid solution in the range 240–800 mμ with a Leres spectrometer.

EPR spectra were obtained with a JES-3B S-X (JEOL) spectrometer. Measurements were carried out with samples carefully evacuated to 2.5×10^{-5} mm Hg. The number of unpaired spins was determined by a comparison with a diphenyl picryl hydrazyl standard.
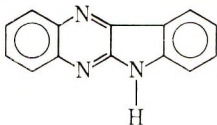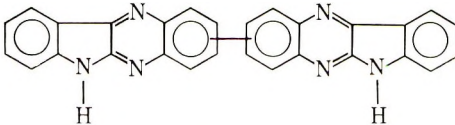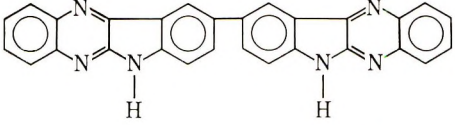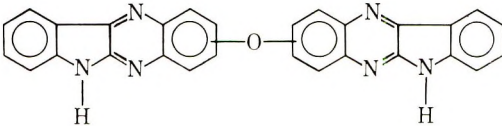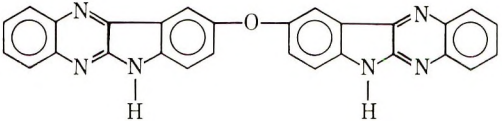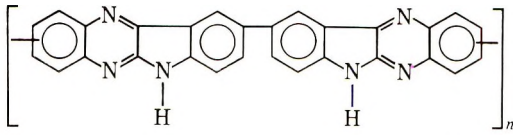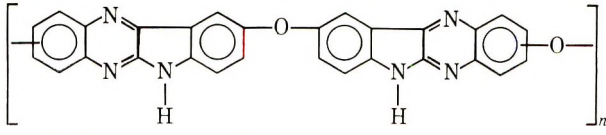
RESULTS AND DISCUSSION

The experiments carried out indicated polyphosphoric acid to be a suitable medium for the synthesis of the indoloquinoxaline ring. Thus, the oxidizing processes are avoided, and one can operate with the more stable hydrochlorides instead of with the free polyamines. The conditions for polycyclization were studied by preparing model compounds I–V (Table I). It should be noted that it is easy to obtain indoloquinoxaline in PPA while there are some difficulties in the preparation of model compounds II–V. In all cases investigated, the infrared spectra of the reaction products display absorption bands at 1715–1730 cm^{-1}, i.e., within a region, characteristic of a carbonyl group. Taking into consideration the greater reactivity of the β-carbonyl group in isatin, one could assume that this group reacts first with one of the two o-amino groups of diamine, while the final closing of the ring represents a second stage in the reaction. It was proved that complete cyclization takes place more easily on heating in vacuo. This process was carried out simultaneously with the sublimation of the biindoloquinoxalines obtained. The structure of the model compounds thus isolated was proved by their infrared and electronic spectra, as well as by elemental analysis for nitrogen. The results of the analysis for carbon and hydrogen are not very accurate because the combustion is rather difficult to carry out. It is of interest that in obtaining polymeric indoloquinoxalines, polycyclization is apparently more perfect, as absorption bands of the carbonyl group are almost lacking in the infrared spectra of the polymers. In all cases, however, the polymers were heated in vacuo to create conditions for the completion of the reaction of polycyclization. It was found that this increased their molecular weight. No changes of infrared or electronic spectra of the polymers occurred on heating. Nevertheless, the presence of incompletely cyclized units cannot be fully excluded.

It should be noted that in the cases of the model compounds II and IV, there is a possibility of formation of three isomers of each compound, i.e., the indoloquinoxaline rings could be linked in three different ways: 2,2'; 3,3'; and 2,3'. In the experimental part these are conditionally indicated as 2,2'. These substances could not be isolated separately. The bonding

in the polymers might also be different, both between the second and the ninth atom and between the third and the ninth ones. Since the differences in the first case are analogous to those in the second, a comparison of the model compounds with the polymers is allowable. The infrared spectra

TABLE I
Electronic Spectra of Model Compounds and Polymers[a]

No.	Compound	λ_{max}, $m\mu$	ϵ
I		271.5 426.8 441.0	61 900 48 200 47 600
II		286.6 478.0	98 600 97 000
III		286.9 424.5 450.5	89 500 96 000 117 000
IV		284.6 480.0	98 500 79 200
V		282.2 422.5 442.0	80 500 86 000 91 000
VI		295.8 500.5	1 700[b] 2 000[b]
VII		288.0 491.5	1 940[b] 1 770[b]

[a] All spectra were taken in sulfuric acid.
[b] $E_{1\%}^{1cm}$.

(Fig. 1) of model compounds II and III are similar, but differ from the infrared spectrum of indoloquinoxaline in the appearance of absorption bands characteristic of 1,2,4-substituted benzene ring,[15] i.e., at 805, 828, and 885 cm^{-1}. The three compounds display absorption bands characteristic

of the o-disubstituted benzene ring, in the range 735–770 cm^{-1}.   With poly-indoloquinoxaline (VI), absorption bands characteristic of a 1,2,4-substituted benzene ring are still more evident.   The absorbance in the range 735–770 cm^{-1} is weaker.   This is actually the difference between poly-indoloquinoxaline (VI) and the model biindoloquinoxalines.   The similarity between these spectra, in all other respects, leads to the conclusion that the polymer consists of indoloquinoxaline rings.

A comparison between the infrared spectrum of model compound V and the spectra of I and III, as well as those of polymers VI and VII shows similarities.   Hence, one has the right to conclude that polyindoloquinox-alinyl ether too, has actually the structure attributed to it.

The electronic spectra of the model compounds and those of the polymers (Figs. 2 and 3 and Table I) are of great interest because they give some idea of the extent of conjugation in the molecules.   These spectra indicate that biindoloquinoxalines II and III, as compared with I, display a batho-chromic shift, meaning that the two rings are conjugated.   In compound II this shift is greater than it is in III.   This shows that conjugation in the molecule of indoloquinoxaline is not uniform.   The conjugated system in the quinoxaline ring is longer than it is in the indole ring condensed with it.   The electronic spectrum of polyindoloquinoxaline shows a greater bathochromic shift than do the model compounds, this being an indication of a large number of recurring units taking part in the conjugation.

The oxygen atom in the biindoloquinoxalinyl ether IV does not interrupt the conjugation.   One observes almost the same bathochromic shift as in II.   With polyindoloquinoxalinyl ether, the absorption maxima are even more shifted into the long-wave region, which indicates that similar to the case with polyindoloquinoxaline, there is conjugation along the chain. Some authors[16] doubt the possibility of conjugation via the oxygen atom, e.g., in 4,4′-diacetyldiphenyl ether.   In our case, one could assume that conjugation is determined by the fact that the oxygen atom is situated between rings, having a system of conjugation with considerable length. This assumption is confirmed also by a comparison between the spectra of model compounds IV and V.   The bathochromic shift is considerable when the oxygen atom joins the indoloquinoxaline rings on the quinoxaline side of the rings, where the system of conjugation is longer.

Polyindoloquinoxaline dissolves in a rather limited number of highly polar solvents.   This is to be expected, taking into consideration the rigid backbone of the polymer (imperfect ladder structure).   One might hope that polyindoloquinoxalinyl ether would be more soluble on account of the presence of oxygen atoms, which increases the flexibility of the polymer chain.   Unfortunately, this polymer dissolves only in the same polar solvents, giving more concentrated solutions.   The solutions of both polymers are of low concentrations, insufficient for casting films.

On heating, the indoloquinoxaline polymers do not melt, but gradually decompose.   It is evident from the thermogravimetric curves that poly-indoloquinoxaline, as compared with the polyquinoxalines,[1] shows a little

better thermal stability (Fig. 3). Furthermore, its rate of decomposition on the air is somewhat lower.

Polyindoloquinoxalinyl ether (Fig. 4) shows a thermal stability which is considerably lower, both in an inert medium and in air. There are contradictory opinions about the role of the oxygen atom, in the chain of polymers which are built of rings. It has been established, on the one hand, that the aromatic ether bond is much less stable upon thermal treatment than is the bond between two benzene rings.[17] On the other hand, in some cases the polymers containing oxygen atoms in their chains have better thermal stability.[4,18] These results are sometimes rather contradictory. Thus, for quinoxaline polymers obtained under different conditions but containing identical recurring units, some authors point out better thermal stability of the polymers with a single bond between the rings,[2,3] whereas others find that it is higher in polymers with an ether bond.[4] For this reason, it is difficult to evaluate the effect of the ether bond on the thermal properties of polymers. In our case, spectroscopic data indicate that conjugation along the polyindoloquinoxalinyl ether chain is less markedly expressed than it is with polyindoloquinoxaline. The difference, however, is insignificant, meaning that presumably the lower
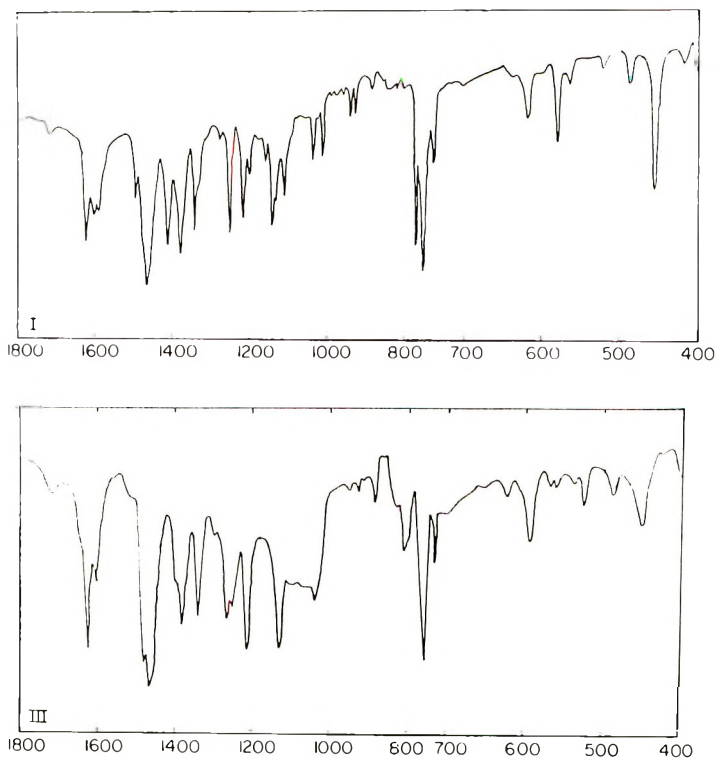
Fig. 1. Infrared spectra of model compounds and polymers. The formulas are given in Table I.
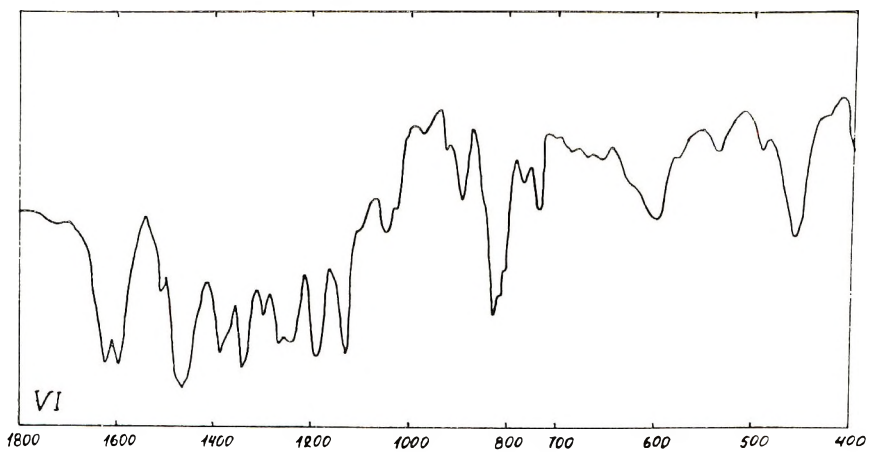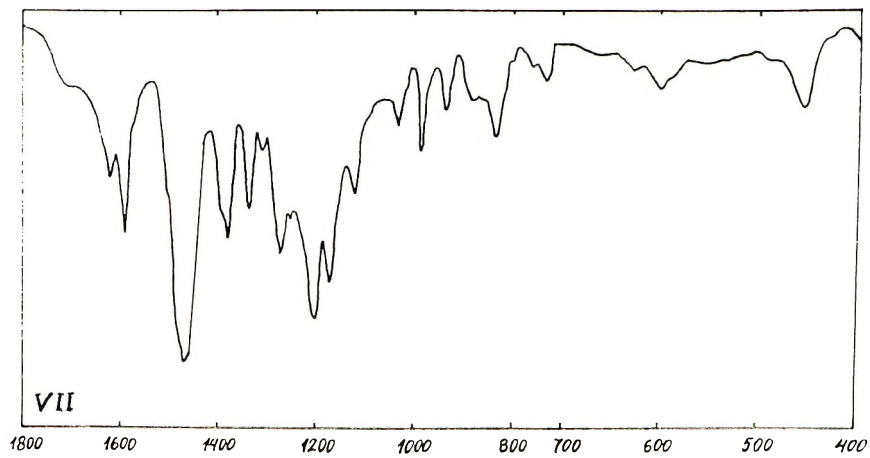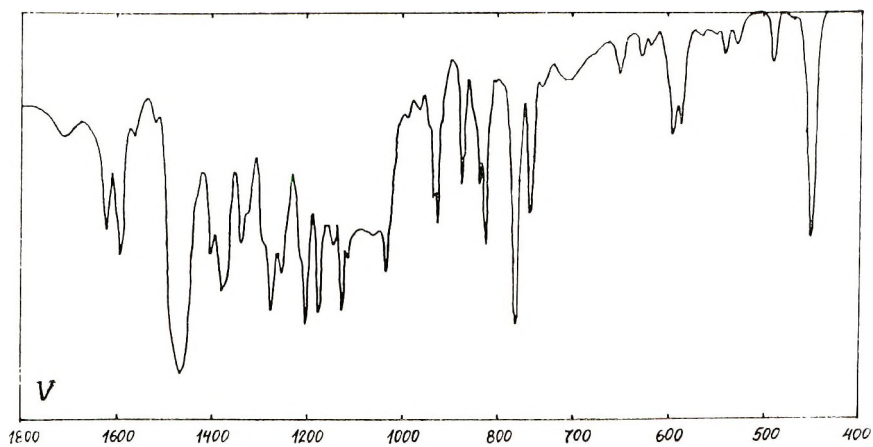
Fig. 1 (continued)

thermal stability is not determined by the conjugation, but by the lower strength of the ether bonds.[17]

The indoloquinoxaline polymers, like some other polymers with quinoxaline rings[19] burn only with great difficulty. For this reason, the results of the analyses, especially those for C and H, are not satisfactory.
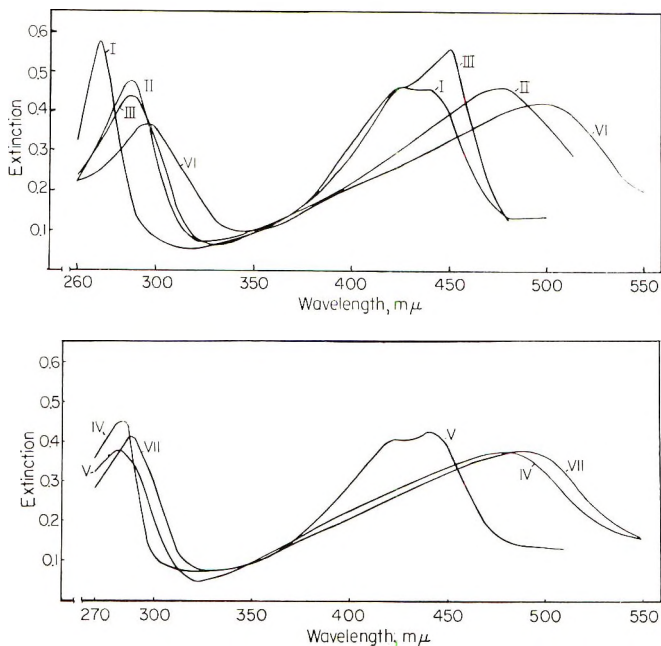
Fig. 2. Electronic spectra of model compounds and polymers. The formulas are given in Table I.
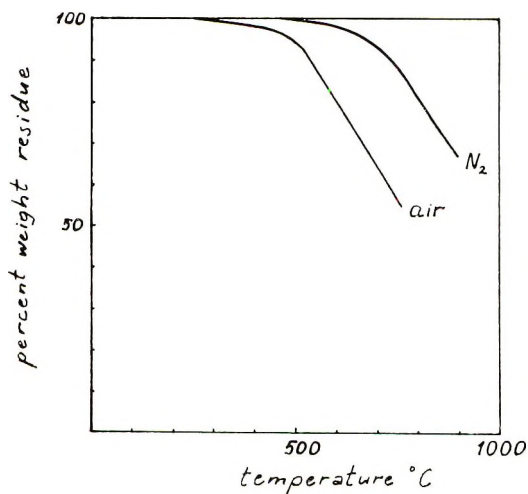
Fig. 3. Thermogravimetric analysis of polyindoloquinoxaline. Temperature rise 5.3°C/min.

The continuous system of conjugation along the chain of the indolo-quinoxaline polymers is confirmed also by the presence of the signal of electronic paramagnetic resonance, characteristic of polyconjugated polymers.[20] This signal is narrow and symmetric, with a g factor close to that
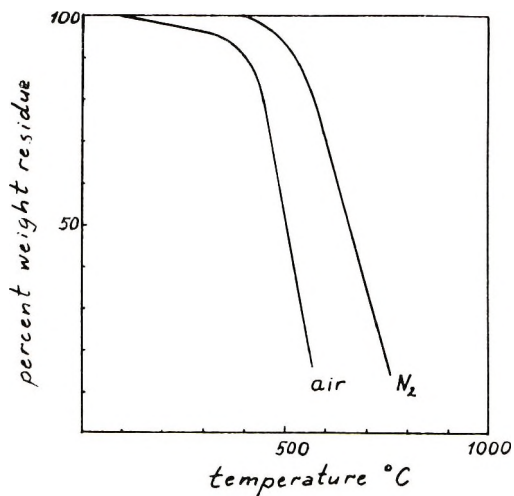
Fig. 4. Thermogravimetric analysis of polyindoloquinoxalinyl ether. Temperature rise, 5.3°C/min.

of the free electron. The number of unpaired spins is 1.86×10^{18} spins/g for polyindoloquinoxaline and 2.02×10^{18} spins/g for polyindoloquinoxalinyl ether.

References

1. J. K. Stille and J. R. Williamson, *J. Polym. Sci. B*, **2**, 209 (1964); *J. Polym. Sci. A*, **2**, 3867 (1964).

2. G. P. de Gaudemaris and B. J. Sillion, *J. Polym. Sci. B*, **2**, 203 (1964).

3. G. P. de Gaudemaris, B. Sillion, and J. Prévé, *Bull. Soc. Chim.*, France **1964**, 1793.

4. J. K. Stille, J. R. Williamson, and F. Arnold, *J. Polym. Sci. A*, **3**, 1013 (1965).

5. J. K. Stille and E. L. Mainen, *J. Polym. Sci. B*, **4**, 665 (1966).

6. J. K. Stille and M. E. Freeburger, *J. Polym. Sci. B*, **5**, 989 (1967).

7. E. Schunck and L. Marchlewski, *Ber.*, **28**, 2528 (1895).

8. M. M. Tessler, *J. Polym. Sci. A-1*, **4**, 2521 (1966).

9. N. Dethloff and H. Mix, *Ber.*, **82**, 543 (1949).

10. Y. Iwakura, K. Uno, and Y. Imai, *J. Polym. Sci. A*, **2**, 2605 (1964).

11. I. Schopov, *Comp. Rend. Acad. Bulg. Sci.*, **21**, 241 (1968).

12. R. T. Foster and C. S. Marvel, *J. Polym. Sci. A*, **3**, 417 (1965).

13. G. M. Badger and P. J. Nelson, *J. Chem. Soc.*, **1962**, 3926.

14. L. D. Tiwari and S. Dutt, *Proc. Nat. Acad. Sci. India*, **7**, 58 (1937); *Chem. Abstr.*, **32**, 2943 (1938).

15. K. Nakanishi, *Infrared Absorption Spectroscopy*, Holden-Day, San Francisco, 1962.

16. M. I. Gugeshashvily, B. E. Davydov, Yu. V. Korshak, and L. D. Rosenshtein, *Izv. Akad. Nauk USSR, Ser. Khim.*, **1964**, 1703.

17. S. S. Hirsch and M. R. Lilyquist, *J. Appl. Polym. Sci.*, **11**, 305 (1967).

18. P. M. Hergenrother and H. H. Levine, *J. Polym. Sci. A-1*, **5**, 1453 (1967).

19. H. Jadamus, F. De Schryver, W. De Winter, and C. S. Marvel, *J. Polym. Sci. A-1*, **4**, 2831 (1966).

20. A. A. Dulov, *Usp. Khim.*, **35**, 1853 (1966).

Anionic Graft Polymerization of Ethylene Oxide on Starch.   I

MENASHE TAHAN and ALBERT ZILKHA, *Department of Organic Chemistry, The Hebrew University, Jerusalem, Israel*

Synopsis

Graft polymers of polyethylene oxide on various starches were obtained by anionic graft polymerization of ethylene oxide on the starch alkoxide derivatives.   The poly-alkoxides were prepared by reaction of potassium naphthalene with starch in DMSO solution.   It was found that increase of monomer or alkoxide concentration led to transformation of the grafts from solids to syrups.   Rice starch, having a more complex structure than soluble starch or wheat starch, led to graft polymers having higher melting ranges than the others.   The graft polymers were very soluble in water or methanol.

INTRODUCTION

Graft polymers of vinyl monomers on starch have been prepared by free-radical methods based on the formation of free-radical active centers on the starch backbone.[1–21]   All these methods are unsuitable for the graft polymerization of ethylene oxide on starch, since alkylene oxides are inert to free-radical polymerization.

We have recently developed a new anionic method for the preparation of graft polymers of vinyl monomers on polyhydroxypolymers.[22–24]   The alkoxide derivative of the latter is used as initiator of the graft polymerization of vinyl monomers.   Thus graft polymers of acrylonitrile, methacrylonitrile, and methyl methacrylate on cellulose,[22] cellulose acetate,[23] and poly(vinyl alcohol)[22] were prepared.   The use of alkali metal naphthalene, for the preparation of the macromolecular alkoxides in solution under anhydrous conditions, was found to have several advantages[23,25–28] for the systematic study of the graft polymerization.

It was shown previously that it is possible to polymerize alkylene oxides by anionic mechanism with the use of alkali metal alkoxides as initiators of polymerization.[29–31]

It is possible that the product obtained in the hydroxyethylation of starch (or cellulose[32–34]) in the presence of alkali contains, besides the hydroxyethyl groups, short graft chains of poly(ethylene oxide).[35]   However, true graft polymers of polyethylene oxide on starch were not described.

We have now studied the anionic graft polymerization of ethylene oxide on various starches (soluble, rice, or wheat starch) using the alkoxide

derivative of starch as initiator of the graft polymerization. The graft polymerizations were carried out in dimethyl sulfoxide (DMSO), and the starch potassium alkoxide was prepared by addition of potassium naphthalene. The effect of alkoxide and monomer concentrations on some physical properties of the graft polymers was studied.

EXPERIMENTAL

Materials

Potassium naphthalene was prepared in tetrahydrofuran, and its concentration was determined by titration with acid.[36] Ethylene oxide gas (Matheson, 99.7% purity) was used.

Preparation of Stock Solution of Starch in DMSO

For systematic investigations of the graft polymerization, it was found convenient to prepare stock solutions of known concentration of dry starch in DMSO.

Into a three-necked 3-l. flask fitted with a high-speed stirrer and containing DMSO (1.8 l.), starch having 15% moisture (70.6 g) was added slowly (about 10 min) with strong stirring, to prevent formation of large aggregates of starch which dissolved with great difficulty afterwards. The starch suspension was heated slowly with a heating mantle until complete solution of the starch occurred. The colorless solution was distilled *in vacuo*, at a temperature not exceeding 60°C, until about 300 ml distillate were collected. This procedure was found to remove the water present as seen by subsequent azeotropic distillation with benzene.

The stirrer and distillation apparatus were removed under argon one after the other and replaced by a standard joint stopper fitted with a self-sealing rubber cap through which a syringe could be introduced. Argon was introduced until a slight positive pressure existed in the flask. The concentration of the starch in the DMSO solution was determined on an aliquot portion by precipitation with methanol.

Graft Polymerization Procedure

The polymerization vessel consisted of a 150-ml three-necked flask equipped with a high-speed stirrer, a thermometer, a self-sealing rubber cap through which the reagents were added by syringes, and an Anschutz fitted with a Teflon stirring gland and a three-way stopcock, which permitted joining the apparatus either to an oil pump or to argon. The Teflon stirring gland permitted stirring under vacuum. The apparatus was joined to a vacuum line, dried while stirring by flaming *in vacuo*, and flushed with argon. This procedure was repeated twice.

The starch solution was introduced by a syringe followed by the required amount of alkali metal naphthalene. The color of the alkali metal naphthalene disappeared almost immediately, and the starch alkoxide derivative

precipitated out as a heavy gel. The reaction mixture was cooled to the required temperature and a required amount (see below) of gaseous ethylene oxide was bubbled in under the surface. After about 1 hr, the polymerization vessel was closed under argon and shaken to complete the polymerization.

The ethylene oxide cylinder was connected, through a trap of solid calcium hydride, to a flowmeter to measure the quantity of gas passing into the polymerization vessel. Another flowmeter was connected to the exit of the polymerization vessel, to measure any ethylene oxide not absorbed in the reaction mixture. The calibration of the flowmeter was checked by passing ethylene oxide for a certain time at a definite flow rate and weighing the gas trapped in cold THF.

Isolation of the Graft Polymers

Preliminary experiments showed that it was almost impossible to isolate without great losses from DMSO solution the graft polymer after the reaction mixture was neutralized. It was found much more convenient to isolate the graft polymer in the form of its alkoxide derivative before neutralization. The alkoxide derivative of the graft polymer was actually not soluble in DMSO, and it was possible by addition of an equal volume of dry benzene and centrifugation, to isolate the graft polymer alkoxide without appreciable losses. This was further washed with dry ether and dried. By this procedure any homopolyethylene oxide present is lost in the filtrate.

Due to the great solubility of the graft polymers in water and the fact that they had a tendency to become insoluble on prolonged heating, it was found convenient to dissolve the graft polymer alkoxide in the minimum amount of absolute methanol, and to add to the solution an equivalent of a $1M$ solution of tartaric acid in methanol. The mixture was left overnight, and the precipitate of monopotassium tartrate was centrifuged. The methanol solution was evaporated *in vacuo* below 40°C, and the residue was left to solidify under acetone. The graft polymers were filtered and dried *in vacuo* over phosphorus pentoxide. They were kept in the dark under anhydrous conditions. Not all the graft polymers were solid, and many of them were syrups.

Proof for the Formation of Graft Polymers

The fact that the graft polymers, contrary to starch, were completely soluble in methanol shows that all the starch was converted to graft polymer. The graft polymers contained starch, as shown by the anthrone test,[37,38] besides poly(ethylene oxide), as seen from the resonance for the —CH_2—O— protons at 222 cps (absent in starch) which is characteristic for poly(ethylene oxide) in the NMR.[39]

Contrary to starch, the graft polymers gave a negative color reaction with iodine. The color reaction is attributed to the formation of a helical complex of amylose with iodine, where the iodine is held in the helix. The

negative reaction obtained with the graft polymers indicates attachment of side chains to the starch which makes difficult helical formation.

Contrary to starch, oxidation with periodic acid of the graft polymers[40] was not quantitative in all cases, indicating that part of the hydroxyl groups at C_2 and C_3 were substituted by poly(ethylene oxide) chains.

TABLE I
Graft Polymerization of Ethylene Oxide on Soluble Starch[a]

[Monomer], mole/l.	$\frac{[M]}{[C]}$	Graft polymer yield[b]		Melting point, °C
		Fraction insoluble in methanol, %	Fraction soluble in methanol, %	
Series A, 10% Starch Alkoxide (58 mmole/l.)				
0.85	14.70	45	32	120–130
0.85	14.70	46	17	—
1.71[c]	29.40	—	55	58–62
Series B, 20% Starch Alkoxide (116 mmole/l.)				
0.34	2.90	68	30	—
0.51	4.40	28	69	220–330
0.68	5.90	0	—	—
0.85	7.40	0	96	140–150
1.02	8.80	0	92	110–115
1.37	11.70	0	—	—
Series C, 30% Starch Alkoxide (174 mmole/l.)				
0.34	1.96	0	100	130–140
0.34	1.96	0	60	—
0.51	2.94	0	—	80–90
Series D. 40% Starch Alkoxide (232 mmole/l.)				
0.34	1.47	0	100	133–140
0.34[d]	1.47	0	64	—
0.51	2.20	0	52	55–60
0.68	2.94	0	33	—
1.37	5.88	0	—	—

[a] Experimental conditions: The starch alkoxide derivative was prepared by adding potassium naphthalene in THF to the starch (2.43 g) in DMSO (50 ml). The volume of THF + DMSO was kept constant (70 ml). Ethylene oxide was bubbled into the reaction mixture at 0 ± 2°C and the reaction mixture was shaken at room temperature. All crude graft polymers were precipitated by benzene. A solution of tartaric acid in methanol was used for termination.
[b] Calculated from the theoretical yield of the graft polymer.
[c] Solubility of graft polymer, 30 g/100 ml (water); 20 g/100 ml (methanol).
[d] Solubility of graft polymer, 85 g/100 ml (water).

The products of the graft polymerization have varying degrees of molar substitution up to $MS \simeq 5$ (Table I), so that they cannot be simple hydroxyethyl derivatives, but graft polymers of poly(ethylene oxide) on starch.

RESULTS AND DISCUSSION

Graft Polymerization on Soluble Starch

The graft polymerization of ethylene oxide on soluble starch was carried out with the use of various concentrations of starch alkoxide and monomer (Table I). The alkoxide derivative of the graft polymers was not soluble in all cases in methanol, and its solubility increased with increasing the monomer or alkoxide concentrations. Thus when 10% of the hydroxyl groups of the starch were converted to alkoxide (DS = 0.3), and a monomer concentration of 0.85 mole/l. was used, about 45% of the alkoxide derivative of the graft polymer was insoluble in methanol. At 20% alkoxide (DS = 0.6), even a smaller concentration of monomer (0.68 mole/l.) was sufficient to bring all the alkoxide derivative of the graft polymer into solution. At DS = 0.6 starch alkoxide, and relatively low monomer concentration (0.34 mole/l.), only 30% of the graft polymer alkoxide was soluble in methanol, while at a higher monomer concentration (0.68 mole/l.) all the graft polymer alkoxide was soluble in methanol.

The pure graft polymers, obtained by neutralization of their alkoxide derivative, were either solid or syrups. Their tendency to solidify depended on the initial alkoxide and monomer concentrations. On increas-

TABLE II
Graft Polymerization of Ethylene Oxide on Rice Starch[a]

[Monomer], mole/l.	Time, hr	$\frac{[M]}{[C]}$	Graft polymer yield[b]		Ethylene oxide polymerized, %[c]
			Fraction soluble in methanol, %	Fraction insoluble in methanol, %	
			Series A		
0.461	48	2.94	46.8	44.5	79.0
0.461	48	2.94	43.8	—	—
0.770	48	4.90	72.5	17.3	81.0
0.770	48	4.90	70.5	—	—
1.535	48	9.80	51.7	—	—
1.535	48	9.80	51.7	3.9	37.0
			Series B		
0.386	24	1.96	5.4	—	—
0.769	17	4.90	10.8	46.3	11.2
1.545	24	9.80	40.0	—	—
1.545	16	9.80	6.0	30.6	10.7
2.320	16	14.70	34.7	—	—

[a] Experimental conditions: The rice starch potassium alkoxide was prepared by addition of potassium naphthalene in THF to the starch in DMSO, (1 g starch/25 ml DMSO). In series A and B, 4 g and 2 g starch were used, respectively; 30% starch alkoxide (157.2 mmole/l.) was used. The volume of THF + DMSO was kept constant; In series A, 140 ml and in series B, 70 ml ethylene oxide was bubbled into the reaction mixture at 0 ± 2°C and the reaction mixture was shaken at room temperature.

[b] The per cent yield is from the theoretical one.

[c] The per cent ethylene oxide polymerized was calculated from the yield assuming total recovery of the starch.

ing the monomer concentration at constant alkoxide concentration, or increasing the alkoxide concentration at constant monomer concentration, the graft polymers became more sticky and more difficult to solidify (Table I). While solid graft polymers were obtained at 10% alkoxide, even with monomer concentrations up to 1.71 mole/l., with 40% alkoxide, they were obtained only with concentrations up to 0.34 mole/l.

Graft Polymerization on Rice Starch

The graft polymerization of ethylene oxide on starch is slow (Table II). Thus after 17 hr, on using a [monomer]/[alkoxide] ratio ([M]/[C] $\simeq$ 5), only 11% of the monomer was converted to graft polymer, while after 48 hr the conversion was 81%. At a still higher [M]/[C] ratio ($\simeq$10), only 6% conversion was observed after 16 hr and 52% after 48 hr. This explains the decrease in yield observed on increasing the monomer concentration for the same reaction time.

Generally the graft polymers on rice starch were solid, and easier to isolate than those obtained from soluble starch under comparable conditions. The alkoxide derivatives of the graft polymers of rice starch were less soluble in methanol than those of soluble starch, and partial loss of graft polymer may have occurred for this reason.

TABLE III
Graft Polymerization of Ethylene Oxide on Wheat Starch[a]

[Monomer], mole/l.	$\dfrac{[M]}{[C]}$	Graft polymer yield, %	Ethylene oxide polymerized, %[b]
Series A			
0.628	4	85	68.5
0.628	4	80[c]	57.4
0.786	5	83	69.7
0.786	5	79[c]	60.1
0.943	6	80	65.3
1.258	8	81	72.7
1.258	8	72	55.6
1.570	10	65	49.8
1.570	10	65	49.9
Series B			
0.628	3	83	61.3
0.836	4	79	61.5
1.045	5	d	—

[a] Experimental conditions: The starch alkoxide derivative was prepared by adding potassium naphthalene in THF to the starch (4.35 g) in DMSO (100 ml). The volume of THF added was kept constant (40 ml). Polymerization time 48 hr. In series A, 27.6% alkoxide (157.2 mmole/l.) and in series B, 36.7% alkoxide (209 mmole/l.) were used. All crude graft polymers were precipitated by benzene.

[b] Calculated from the graft polymer yield, assuming total recovery of the starch.

[c] Crude graft polymer precipitated by acetone.

[d] The polymer was a syrup.

Graft Polymerization on Wheat Starch

Generally the results obtained with wheat starch (Table III) were similar to those obtained with rice starch. The graft polymer alkoxides were more soluble in methanol than those of rice starch and the pure graft polymers were more sticky. Increasing the monomer concentration led to more difficultly crystallizable products.

Physical Properties of the Graft Polymers

The melting ranges of the graft polymers varied between 55 and 230°C, depending on the monomer and alkoxide concentrations (Table I). Increasing either the monomer or alkoxide concentration led to lowering of the melting range.

The graft polymers were very soluble in methanol or water, unlike soluble starch. On heating or on long standing in solution, they became insoluble in a variety of solvents, including methanol, water, and DMSO, but were soluble in 15% ammonia solution on standing. The graft polymers obtained with the use of a relatively high monomer concentration or a high alkoxide concentration had a great tendency to become insoluble.

Graft polymers generally combine the properties of their components, and increasing the amount of one component in respect to the other affects the properties of the graft polymer. Thus the graft polymers which contained a high percentage of starch and a low percentage of poly(ethylene oxide) melted at about 230°C, similar to starch, while those containing a high poly(ethylene oxide) content melted at low temperature, 50–60°C, or were sticky substances which refused to solidify. This effect of the two components is also observed in the solubility of the graft polymers. While the graft polymers having a high starch content were less soluble in water or methanol, those having a high poly(ethylene oxide) content were more soluble.

In addition, the length of the side chains of the poly(ethylene oxide) and the frequency of their grafting on the starch backbone should affect the physical properties of the graft such as solubility and melting range. Starch which is grafted with longer polyethylene oxide side chains, in the range where the homopolymer is liquid, or with a greater number of them, is expected to be more soluble and have a lower melting range than that having shorter grafted side chains or a smaller number of them. This is in accordance with the changes observed with increasing monomer or alkoxide concentration.

It may be mentioned that Kargin[41] has shown that in the graft polymers of poly(ethylene oxide) on nylon 6, there was a continuous lowering of melting point with increasing the polyethylene oxide content of the graft polymers. The side chains interfere with the crystallization of the graft, under conditions which are suitable for the crystallization of the homopolymer.

In the hydroxyethylation of starch, it was found that above DS = 1 these ethers become more solvated by lower alcohols such as methanol or ethanol. At a DS from 0.4 to 1.0, the hydroxyethyl starch becomes more and more soluble in cold water, besides becoming sticky and unfiltrable. At a DS of about 3, the products were thermoplastic and soluble in water or alcohol.[42,43]

The melting range and solubility properties depend naturally on the type of the starch used as polymer backbone. The graft polymers of soluble starch, which is a partially hydrolyzed starch,[44,45] having a relatively low molecular weight, have lower melting points and a smaller tendency to solidify than the graft polymers obtained from rice starch or wheat starch, which are more complex in structure. In turn, rice starch contains more of the higher molecular weight component, amylopectin, and less of the low molecular weight component, amylose, than wheat starch (18.5% amylose as compared to 25–26%), so that it has a higher average molecular weight. Furthermore the branches of the amylopectin of the former are longer than those of the latter.[46-49] This complexity in structure is reflected in the gelatinization temperature range of the various starches, that of rice having the higher one.[50] It may be that for these differences in molecular weight and structure the graft polymers of rice starch had a greater tendency to solidify than the corresponding grafts on wheat starch.

In the present graft polymerization, termination does not seem to take place since there is no possibility of proton transfer from the solvent or monomer. Though it is known[51] that an equilibrium exists between potassium *tert*-butoxide and dimethyl sulfoxide leading to the formation of dimesyl anion, the equilibrium constant is very small ($K = 1.5 \times 10^{-7}$), and furthermore in our case, the basicity of both the alkoxide initiator and that of the growing alkoxide anion is much smaller than potassium *tert*-butoxide, so that no significant transfer to the DMSO should occur. Transfer to the hydroxyl groups of the starch may be possible, but this leads to the formation of new starch alkoxide groups, so that the graft polymerization is a "living" one. Flory has drawn attention to the fact that the anionic polymerization of ethylene oxide by alkoxides is free of termination.[52] No homopolymer could be isolated from the reaction mixture besides the graft polymer, indicating that no initiating centers, other than the starch alkoxides, were participating in the polymerization.

References

1. C. E. Brockway and K. B. Moser, *J. Polym. Sci. A*, **1**, 1025 (1963).

2. C. E. Brockway, *J. Polym. Sci. A*, **2**, 3721 (1964); *ibid.*, **2**, 3733 (1964).

3. E. J. Jones, L. B. Morgan, J. F. L. Roberts, and S. M. Todd, Brit. Pat. 715,194 (1954).

4. G. Mino and S. Kaizermann, *J. Polym. Sci.*, **31**, 242 (1958).

5. S. Kimura and M. Imoto, *Makromol. Chem.*, **42**, 140 (1960).

6. Z. Reyes, C. E. Rist, and C. R. Russell, *J. Polymer Sci. A*, **4**, 1031 (1966).

7. G. F. Fanta, R. C. Burr, C. R. Russell, and C. E. Rist, *J. Appl. Polym. Sci.*, **10**, 929 (1966); *J. Polym. Sci. B*, **4**, 765 (1966); *J. Appl. Polym. Sci.*, **11**, 457 (1967).

8. H. Singh, R. T. Thampy, and V. B. Chipalkatti, *J. Polym. Sci. A*, **3**, 4289 (1965).

9. V. A. Kargin, P. V. Kozlov, N. A. Plate, and I. I. Konoreva, *Vysokomol. Soedin.*, **1**, 114 (1959).

10. V. A. Kargin, N. A. Plate, and E. P. Rebinder, *Vysokomol. Soedin.*, **1**, 154 (1959).

11. V. P. Solomko, I. O. Uskov, and A. O. Galina, *Visu. Kurs'k Univ.* 1962 (5), *Ser. Fiz. Khim., No.* **2**, 106–110 (Ukrain); *Chem. Abstr.*, **62**, 10654 e (1965).

12. J. Borunsky, U. S. Pat. 3,138,564 (1964); *Chem. Abstr.*, **61**, 8478b (1964).

13. K. P. Shen and F. R. Eirich, *J. Polym. Sci.*, **53**, 81 (1961).

14. R. L. Walrath, Z. Reyes, and C. R. Russell, *Advan. Chem. Ser.*, **34**, 87 (1962).

15. A. J. Restaino and W. N. Reed, Belg. Pat. 629,203 (1963); *Chem. Abstr.*, **60**, 13397 (1964).

16. N. Geacintov, V. T. Stannett, E. W. Abrahamson, and J. J. Hermans, *J. Appl. Polym. Sci.*, **3**, 54 (1960).

17. D. J. Angier, R. J. Ceresa, and W. F. Watson, *J. Polym. Sci.*, **34**, 699 (1959).

18. B. H. Thewlis, *Nature*, **190**, 260 (1961); *J. Appl. Chem.*, **13**, 249 (1963); *Starke*, **16**, 279 (1964).

19. R. J. Ceresa, *J. Polym. Sci.*, **53**, 9 (1961).

20. R. L. Whistler and J. L. Goatley, *J. Polym. Sci.*, **62**, S123 (1962).

21. A. A. Berlin, E. A. Penskaya, and G. I. Volkova, *Mezhdunarod. Simpozium po Makromol. Khim., Doklady, Moscow, 1960*, **3**, 334 (1960); *Chem. Abstr.*, **55**, 7898 (1961).

22. B. A. Feit, A. Bar-Nun, M. Lahav, and A. Zilkha, *J. Appl. Polym. Sci.*, **8**, 1869 (1964).

23. Y. Avny, B. Yom-Tov, and A. Zilkha, *J. Appl. Polym. Sci.*, **9**, 3737 (1965).

24. A. Zilkha, B. A. Feit, and A. Bar-Nun, U. S. Pat. 3,341,483 (1967).

25. A. Zilkha and Y. Avny, U. S. Pat. 3,366,614 (1968).

26. Y. Avny and A. Zilkha, *Israel J. Chem.*, **3**, 207 (1965–66).

27. Y. Avny, S. Migdal, and A. Zilkha, *Europ. Polym. J.*, **2**, 355 (1966).

28. Y. Avny and A. Zilkha, *Europ. Polym. J.*, **2**, 367 (1966).

29. G. Gee, W. C. E. Higginson, and G. T. Merrall, *J. Chem. Soc.*, **1959**, 1345.

30. F. Eirich and H. Mark, *J. Colloid Sci.*, **11**, 689 (1956).

31. C. C. Price and D. D. Carmelite, *J. Amer. Chem. Soc.*, **17**, 4039 (1966).

32. P. W. Morgan, *Ind. Eng. Chem. Anal. Ed.*, **18**, 500 (1946).

33. E. T. Reese, R. G. H. Siu, and H. S. Levinson, *J. Bacteriol.*, **59**, 485 (1950).

34. H. H. Brownell and C. B. Purves, *Can. J. Chem.*, **35**, 677 (1957).

35. E. T. Hjermstad, in *Starch: Chemistry and Technology*, R. L. Whistler and E. F. Paschall, Eds., Academic Press, New York-London, 1967, Vol. 2, pp. 423–424, 427–428.

36. A. Zilkha and Y. Avny, *J. Polym. Sci. A*, **1**, 549 (1963).

37. *B. D. H. Book of Organic Reagents*, B. D. H. Publication, England, 1958.

38. F. J. Viles, Jr. and L. Silverman, *Anal. Chem.*, **21**, 950 (1949).

39. T. F. Page, Jr. and W. E. Bressler, *Anal. Chem.*, **36**, 1981 (1964).

40. V. F. Pfiefer, V. E. Sohns, H. F. Conway, C. B. Lancaster, S. Dabic, and E. L. Griffin, Jr., *Ind. Eng. Chem.*, **52**, 201 (1960).

41. V. A. Kargin, in *Macromolecular Chemistry (J. Polym. Sci. C*, **4**), M. Magat, Ed., Interscience, New York, 1963, p. 1601.

42. W. Jarowenko, U. S. Pat. 2,996,498 (1961); *Chem. Abstr.*, **56**, 1658 (1962).

43. E. T. Hjermstad in *Starch: Chemistry and Technology*, R. L. Whistler and E. F. Paschall, Eds., Academic Press, New York-London, 1967, Vol. 2, 427–428.

44. C. J. Lintner, *J. Prakt. Chem.* [2], **34**, 378 (1886).

45. G. C. Small, *J. Amer. Chem. Soc.*, **41**, 113 (1919).

46. D. M. W. Anderson, C. T. Greenwood, and E. L. Hirst, *J. Chem. Soc.*, **1955**, 225.

47. C. T. Greenwood, *Advan. Carbohydrate Chem.*, **2**, 335 (1956).

48. A. W. Arbuckle and C. T. Greenwood, *J. Chem. Soc.*, **1958**, 2626.

49. C. T. Greenwood, *Stärke*, **6**, 169 (1960).

50. H. W. Leach, in *Starch: Chemistry and Technology*, R. L. Whistler and E. F. Paschall, Eds., Academic Press, New York–London, 1965, Vol. 1, p. 292.

51. A. Ledwith and N. K. McFarlane, *Proc. Chem. Soc.*, **1964**, 108.

52. P. J. Flory, *Principles of Polymer Chemistry*, Cornell Univ. Press, Ithaca, N. Y., 1953, p. 336.

Anionic Graft Polymerization of Ethylene Oxide on Starch. II. Structure of the Graft Polymers

MENASHE TAHAN and ALBERT ZILKHA, *Department of Organic Chemistry, The Hebrew University of Jerusalem, Jerusalem, Israel*

Synopsis

Starch–poly(ethylene oxide) graft polymers were prepared in DMSO at various monomer and starch alkoxide concentrations. Complimentary and varied information on the structure of the graft polymers was obtained from NMR and periodic acid oxidation of the polymers. From the NMR spectra of the graft polymers in pyridine containing a trace of HCl, which causes shifting of the resonance of the internal —CH$_2$O— protons from the terminal —CH$_2$OH protons, the polyethylene oxide content, the $\overline{DP}_n$ of the grafted side chains, and the efficiency of the alkoxides were calculated. With increase of the alkoxide concentration there was a small decrease in $\overline{DP}_n$, and in the efficiency of the alkoxides in initiating graft polymerization. With increase of monomer concentration, there was only a small increase in $\overline{DP}_n$ but a large increase in the efficiency, indicating the existence of transfer reactions between the growing anions and the free hydroxyl groups on the starch. The results of the periodic acid oxidation showed that with increase of alkoxide concentration there was no significant change in per cent oxidation of the graft polymers, but with increase of monomer, there was an increase in the participation of the secondary hydroxyl groups in initiation. This supports the NMR evidence for the existence of transfer reactions leading to $\overline{DP}_n$ values much lower than those calculated from [monomer]/[catalyst] ratios.

INTRODUCTION

We have shown[1] that the reaction of ethylene oxide (EO) with starch potassium alkoxide in DMSO solution at suitable monomer/alkoxide molar ratios led to the formation of graft polymers of polyethylene oxide on starch having varying physical properties. It was the object of the present study to obtain information on the structure of these graft polymers and how it is affected by changing the monomer and alkoxide concentrations. Such information might shed light on the properties of the graft polymers, and might also give more information on the graft polymerization process, and the participation of the different hydroxyl groups in initiation. NMR spectroscopy, as well as oxidation by periodic acid, were used to obtain complimentary as well as varied information.

The relative rates of reaction of the three different hydroxyl groups of the starch, determine the mode of distribution of the substituents on the starch backbone, i.e., the location of the grafted side chains, and with it the structure of the graft polymers. Some work in this direction was

carried out before.[2-6] The results were found to depend on the reaction conditions. There is no absolute selectivity, but in many reactions there is preferential participation of the secondary hydroxyl at C_2.

Croon[2] carried out methylation of amylose dissolved in sodium hydroxide by dimethyl sulfate and found that the relative rates of methylation of the hydroxyl groups at C_2, C_3 and C_6 were 6:1:7. Bines and Whelan[3] found in the methylation of monosodio amylose, prepared by heating amylose with sodium hydroxide in butanol, that the molar ratios of the mono-O-methyl-D-glucose fraction was as follows: $C_2:C_3:C_6 = 2.6:1:1.2$. Russell et al.,[4] in the methylation of starch alkoxide, prepared by reaction with sodium in liquid ammonia, at a degree of substitution (DS) of 0.34 and 0.9, found the hydrolysis products to be composed of the following molar ratios of free glucose, mono-, di-, and tri-O-methyl-D-glucose (36:6:2:1) and (6:3:2:1) respectively. At DS = 0.9, the mono-O-methyl-D-glucose fraction was composed of a molar ratio of the 2-methyl to the 6-methyl isomer of 1:1, and at DS = 0.34 this ratio was 3:2. Husemann and Kafka[6] prepared in homogenous solution hydroxyethyl and carboxymethyl ethers of amylose and determined the distribution of the substituents by oxidation with periodic acid and by tritylation. They deduced that in all cases the secondary hydroxyl, probably that at C_2, reacts preferentially at low DS.

RESULTS AND DISCUSSION

The effect of both alkoxide (Table I) and monomer (Table II) concentrations was investigated. The alkoxide content from the total hydroxyl groups of the starch was varied from 31.9% to 63.9%, which is approximately equivalent to conversion of one to two hydroxyl groups of the glucose units to alkoxide. In all experiments (Table I) the yield and composition of the graft polymers were essentially constant, the per cent of ethylene oxide converted to graft polymer was constant about 60% and did not increase with alkoxide concentration (Table III). All the starch was incorporated into the graft polymer even at the low alkoxide concentrations. The effect of monomer concentration was investigated by using 31.9% starch alkoxide, and the monomer concentration was varied fourfold. The graft polymers obtained in all cases were sticky except in expt. 164, where the conversion of ethylene oxide was less than expected. The graft polymers obtained at the high monomer concentrations were partially extracted with acetone. The poly(ethylene oxide) content of the graft polymers increased with increasing monomer concentration (Table IV). The per cent conversion of ethylene oxide to graft polymer was not complete and it decreased slowly with increasing monomer concentration.

The composition of the graft polymers was determined from analyses for starch and for polyethylene oxide (PEO). The starch was determined spectrophotometrically by the anthrone method.[7,8] The poly(ethylene oxide) content could not be determined from ethoxyl determinations, since they were found to be inaccurate and inconsistent, and they were deter-

TABLE I

Effect of Alkoxide Concentration on Graft Polymerization
of Ethylene Oxide on Wheat Starch[a]

Expt. no.	[Alkoxide] mmole/l.	%	[M] [C]	Yield, %	PEO (%)	Graft polymer Composition[b] Starch (anthrone method), %	Starch (by difference), %
154	165	31.9	3.67	80.6	36.5[c]	70.6	63.5
156	196	38.4	3.10	83.0	36.0	67.6	64.0
157	196	38.4	3.10	75.0	38.8	62.5	61.2
158	244	48.0	2.48	78.0	34.5	70.2	65.5
159	244	48.0	2.48	83.0	37.2	66.9	62.8
160	323	63.9	1.84	—	—	—	—

[a] Experimental conditions: The starch alkoxide derivative was prepared by adding potassium naphthalene in THF to the starch in DMSO (100 ml). The volume of THF added was kept constant (50 ml), EO (4 g; 606 mmole/l.) and starch (4.17 g; 171.5 mmole/l. glucose) were used. Polymerization temperature 15-20°C. The polymerization mixture was shaken for 2 weeks.

[b] The poly(ethylene oxide) content was determined from NMR, and the starch content was determined by the anthrone method, and calculated by difference from the PEO content.

[c] The per cent PEO was not determined by NMR in this case due to incomplete solubility of the graft, but was estimated assuming complete incorporation of the starch in the graft. The per cent starch determined by the anthrone method in this case was especially high. See Table III.

mined from NMR.[9] From the composition of the graft polymers, it was possible to carry out a balance of the monomer and starch at the end of the graft polymerization (Tables III and IV).

NMR Study of the Graft Polymers of Poly(ethylene Oxide) on Starch

Based on the work of Page and Bressler,[9] we tried to find out the $\overline{DP}_n$ of the grafted side chains of PEO. Acid hydrolysis of the graft polymers, subsequent isolation of the severed side chains of PEO, and determination of their $\overline{DP}_n$ did not seem feasible, since degradation and scission of the PEO chains might also occur.

The technique of Page and Bressler involved taking advantage of the complex formed between pyridine and —OH groups in the presence of traces of dry HCl, to shift the resonance of the terminal —CH$_2$—OH groups from that of the internal —CH$_2$—O— groups (235 and 222 cps, respectively). Since for every starch alkoxide that initiated polymerization there should be one such endgroup, it is possible by this method to determine also the percentage of alkoxide groups which reacted with ethylene oxide. Thus from one NMR determination on a graft polymer, it is possible to determine the amount of PEO in the graft (from $Y + X$) (where Y represents the integration of the peak area centered at 222 cps and X

TABLE II

Effect of Monomer Concentration on Graft Polymerization
of Ethylene Oxide on Wheat Starch[a]

Expt. no.[b]	Monomer concn [M], mole/l.	$\dfrac{[M]}{[C]}$	Yield, %	Graft polymer Composition[c]	
				Starch, (%)	PEO, %
154	0.606	3.67	80.6	70.6	36.5[d]
164	1.212	7.35	59.2	58.2	(41.8)
165	1.212	7.35	71.5	46.6	(53.4)
167	1.818	11.00	66.0	37.5	(62.5)
167B	—	—	—	38.5	—
168	1.818	11.00	67.0	38.8	(61.2)
168B	—	—	—	38.5	59.8
169	2.424	14.68	62.0	33.3	(66.7)
169B	—	—	—	32.7	67.2
170	2.424	14.68	63.0	32.7	(67.3)
170B	—	—	—	32.7	66.4

[a] Experimental conditions: The starch alkoxide derivative was prepared by adding potassium naphthalene in THF to the starch (4.17 g) in DMSO (100 ml). Starch alkoxide per cent of total hydroxyl groups was 31.9% (0.165 mole/l.). The volume of THF added was kept constant (50 ml). Polymerization temperature 15–20°C. The polymerization mixture was shaken for 2 weeks.

[b] Experiment numbers ending with "B" represent fractions of graft polymer that were extracted with acetone from the respective grafts.

[c] The starch content was determined by the "anthrone method" and that of poly-E.O. given in parentheses was calculated by difference from the starch content, and without brackets was determined by NMR.

[d] Estimated as in Table I.

TABLE III

Effect of Alkoxide Concentration on Balance of the Monomer and Starch
at the End of the Graft Polymerization

Expt. no.	EO in graft, g[a]	EO converted to graft, %	Starch in graft, g[b]		Starch converted to graft, (%)	
			Calculated from starch determination	Calculated from PEO determination	Calculated from starch determination	Calculated from PEO determination
154	2.50[b]	62.6[c]	4.64	4.17[c]	111.2	100.0[c]
156	2.45	61.2	4.60	4.35	110.2	104.5
157	2.48	59.4	3.83	3.75	91.8	90.0
158	2.22	55.6	4.52	4.21	108.4	101.0
159	2.51	62.8	4.51	4.23	108.1	101.5

[a] Out of 4.0 g monomer introduced.

[b] Out of 4.17 g introduced.

[c] See Table I.

TABLE IV
Effect of Monomer Concentration on Balance of the Monomer and Starch
at the End of the Graft Polymerization

Expt. no.	EO in graft, g	EO introduced, g	EO converted to graft, %	Starch in graft, g[a]	Starch converted to graft, %
154	2.50	4.0	62.6	4.64	111.2[b]
164	3.01	8.0	37.6	4.19	100.5
165	4.66	8.0	58.3	4.06	97.5
167	6.68	12.0	55.7	4.01	96.2
168	6.63	12.0	55.3	4.20	100.8
169	8.34	16.0	52.1	4.16	99.8
170	8.55	16.0	53.4	4.15	99.5

[a] Out of 4.17 g introduced.
[b] See Table III, expt. 154.

that at 235 cps), the efficiency of the alkoxide initiator (from X) and $\overline{DP}_n$ of the grafted side chains from the ratio Y/X. Since one terminal methylene group is present, the other being attached to the starch, it follows that $\overline{DP}_n = \frac{1}{2}[(Y/X) + 1]$.

This NMR method can be thus very promising if the starch in pyridine containing a trace of HCl has no resonance at 222 and at 235 cps which can increase the resonance areas, X and Y, and cause an inaccuracy in the determination of EO content of the graft polymers. To verify this point we found out that cellulose acetate (DS = 2.4) in pyridine, under the same conditions as the graft polymers, did not interfere in this region, and the $\overline{DP}_n$ of poly(ethylene oxide) ($\overline{M}_n = 400$), determined by NMR in the presence of cellulose acetate, was essentially the same as that obtained on acetylation. Further the NMR spectrum of a simple D-glucose derivative, namely 3-O-methyl-D-glucose, under these conditions, showed no resonance for the —CH$_2$OH or —CHOH protons in the 222 cps region, but there was a small tailing of the C$_6$ methylene protons in the 235 cps region. Determination of the PEO content of the graft polymers by NMR has shown that the results obtained were essentially in conformation with those deduced from the anthrone method, indicating that the extent of interference of the starch protons is not significant. This showed that it would be possible to estimate the $\overline{DP}_n$ of the PEO side chains, without appreciable interference from the starch, provided that there would be a good resolution of the peak areas, X and Y, as in the case with PEO.[9]

The NMR spectra of the grafts did not have a sharp dividing range between the Y and X areas, but the limits between them were still discernible. To eliminate errors as far as possible, a blank NMR determination of homopoly(ethylene oxide), $\overline{M}_n = 400$, was carried out on the same spectrum.

It may be noted that for the determination of $\overline{DP}_n$ by this method, it is not necessary to know the amount of the graft polymer present in solution, since it is based only on the ratio of the peak areas, X and Y. For this

reason the $\overline{DP}_n$ of partially soluble graft polymers were also determined, in case that most of the polymer dissolved. Provided that the graft polymers were homogeneous, and the fraction that dissolved was identical in structure with the insoluble fraction, this determination should give the true $\overline{DP}_n$ of the grafted side chains. Some of the graft polymers of PEO–starch, especially those containing a high PEO content, were found to become partially insoluble in solvents such as water, methanol, and pyridine, which before aging were good solvents for the graft polymers. For this reason, the PEO content of these graft polymers, as well as the amount of their —CH$_2$OH endgroups, could not be determined accurately. That is why in these samples only the $\overline{DP}_n$ of the PEO side chains was determined. The graft polymers obtained at relatively low monomer concen-

TABLE V
NMR Results of Graft Polymers of PEO–Starch[a]

Expt. no.[b]	X, cm	Y, cm	$\overline{DP}_n$	EO, %	Total —CH$_2$OH mmole[c]	Catalyst efficiency, %[d]	$\dfrac{[M]^e}{[C]}$
				Series A			
154[f]	1.95	6.35	2.13				2.30
156	2.02	5.48	1.85	36.0	21.87	74.6	1.90
157[f]	2.70	7.34	1.86				
157	2.06	6.11	1.98	38.8	20.60	70.2	1.84
158[f]	3.70	7.80	1.55				
158	2.04	4.18	1.52	34.5	21.80	59.5	1.38
159[f]	3.56	7.74	1.56				
159	2.02	4.97	1.73	37.2	23.22	63.4	1.56
				Series B			
154[f]	1.95	6.35	2.13				2.30
164[g]	3.08	6.83	1.61				2.76
165[g]	2.62	9.94	2.38				4.29
167[g]	1.75	7.10	2.53				6.13
168B[h]	1.45	7.09	2.95	60.6	39.5	159.5	6.08
169[g]	1.90	8.02	2.61				7.64
170[g]	1.71	7.56	2.71				7.83
170B[g,h]	2.30	11.95	3.10				—
170B[h]	1.47	8.19	3.28	64.6	46.7	188.6	7.83

[a] Experimental conditions: Weighed samples of the graft polymers were dissolved in 2.5 ml pyridine-HCl reagent, and their NMR spectra taken on a Varian A60 instrument.

[b] Series A: change of alkoxide concentration at constant monomer; series B: change of monomer concentration at constant alkoxide.

[c] The amount of —CH$_2$OH groups present in the total graft polymer obtained in the reaction.

[d] Calculated from the amount of the —CH$_2$OH groups.

[e] Based on the monomer that was incorporated in the graft polymer, [C] is the initial concentration of alkoxide.

[f] The experiments were only qualitative.

[g] The experiments were only qualitative, since not all the graft polymer dissolved.

[h] Fraction of the respective polymer extracted by acetone.

tration (Table I), were all completely soluble in pyridine·HCl and it was possible to calculate from their NMR spectra, their composition, the $\overline{DP}_n$ of the side chains, and the amount of —CH_2OH endgroups.

It is seen (Table V) that the $\overline{DP}_n$ calculated from experiments in which the graft polymers were completely in solution were the same, within experimental error, as those obtained from experiments in which the polymer was not.

Effect of Alkoxide Concentration

With increasing alkoxide concentration (expts. 154–159, Table V) the $\overline{DP}_n$ of the PEO side chains decreased, as expected. These $\overline{DP}_n$ were less than those calculated from the ratio of the initial monomer to alkoxide concentrations [M]/[C]. However, if the amount of monomer that was incorporated in the graft polymer is considered instead of the initial concentration, then the $\overline{DP}_n$ calculated by using the ratio $[M]_{effective}/[C]$ is of about the same order as that deduced from the NMR (Table V).

From determination of the —CH_2OH endgroups of the PEO side chains (Table V) the efficiency of the alkoxide was calculated and was found to decrease with increasing alkoxide concentration (75–60%), which may be expected since not all the alkoxide was found to initiate graft polymerization.

Effect of Monomer Concentration

With increasing monomer concentration, the $\overline{DP}_n$ of the side chains increased as expected, but the increase was much more moderate than that expected from the increase of the [M]/[C] ratios (Fig. 1). (It may be pointed out that the fractions extracted by acetone had a little higher $\overline{DP}_n$
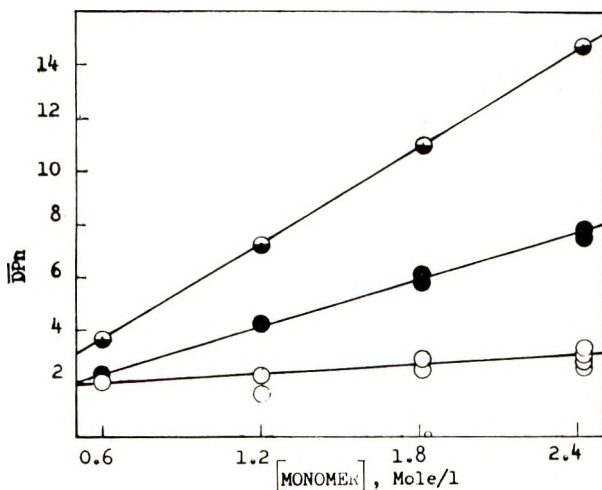
Fig. 1. $\overline{DP}_n$ vs. $[M]_0$ at constant alkoxide$_0$:   (○) determined from NMR; (◒) calculated from initial [M]/[C]; (●) calculated from $[M]_{effective}/[C]$.

than the parent graft polymer. This may be due to the fact that acetone dissolved fractions having longer side chains.) The smaller increase in $\overline{DP}_n$ may be due to the decrease observed in the per cent ethylene oxide which was converted to graft polymer with increasing monomer concentration (Table IV), but this decrease in conversion is not sufficiently large to explain the results completely. Besides, the efficiency of the alkoxide in initiating graft polymerization is expected to increase with increasing monomer concentration. Actually it increased up to about 190% in the range investigated. Using even an efficiency of 100% for the alkoxide, and taking into consideration the per cent conversion of monomer to graft, it can be calculated that for the highest monomer concentration investigated, the $\overline{DP}_n$ obtained should have been 7.8 and not about 3 as deduced from NMR (Fig. 1).

Experimental error cannot be the main cause for this behavior, since if there was considerable interference from the starch in the 235 cps region, thus increasing the X area, this effect should have been similar, since in all samples analyzed by NMR, the amount of starch present was the same. Now since the efficiency was found to increase with monomer concentration from about 70% to 190% (the 70% is estimated from the results of change of alkoxide concentration), it follows that this increase found is not due to interference of the starch but actually to the increase in the monomer concentration. Furthermore if the limits of the integration between the X and Y areas were not well defined, this should have led to random error in the estimation of X and Y, and this cannot explain the systematic increase of the alkoxide efficiency found with increase in monomer concentration. It follows that the low $\overline{DP}_n$ values estimated from the NMR, which were much lower than $[M]_{\text{effective}}/[C]$, and the alkoxide efficiency which approached 190%, can only be explained if it is assumed that starch hydroxyl groups which were not converted to alkoxide also initiated graft polymerization. This assumption can be reasonable if these free hydroxyl groups participate in chain transfer as shown in eq. (1), leading to the formation of new alkoxide groups:

$$Starch-O-(CH_2-CH_2O)_n-CH_2CH_2-O^- + Starch-OH \rightleftharpoons$$
$$Starch-O-(CH_2-CH_2-O)_n-CH_2CH_2-OH + Starch-O^- \quad (1)$$
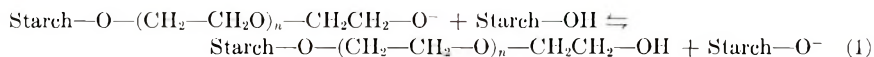
Oxidation of the Graft Polymers by Periodic Acid

To investigate further the structure of the graft polymers and to obtain complimentary as well as new information on that deduced from NMR, we have studied the oxidation of the graft polymers by periodic acid.[10-28] Grafting of a hydroxyethyl group or of a PEO chain on one of the secondary hydroxyl groups of the glucose units is sufficient to prevent oxidation of the starch. Therefore from the extent of oxidation of the graft polymers, it should be possible to determine the percentage of glucose units which have no substitution on the secondary hydroxyl groups, as well as the percentage of glucose units which are substituted at one or both of the secondary hydroxyls, and from this determine the efficiency of the secon-
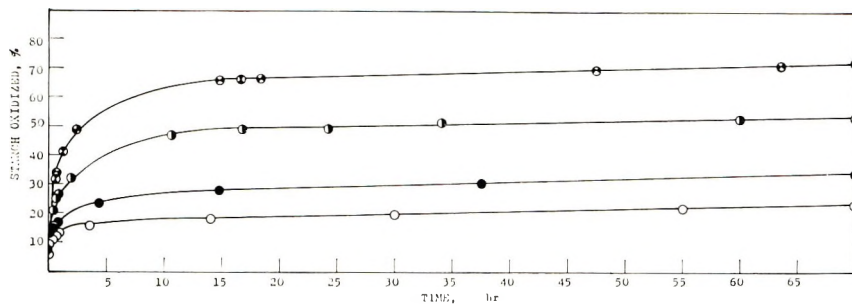
Fig. 2. Effect of monomer concentration on oxidation of graft copolymers of poly-(ethylene oxide)–wheat starch: (◐) expt. 154, 0.606 mole/l.; (◑) expt. 164, 1.212 mole/l.; (●) expt. 168B, 1.818 mole/l.; (○) expt. 170B, 2.424 mole/l.
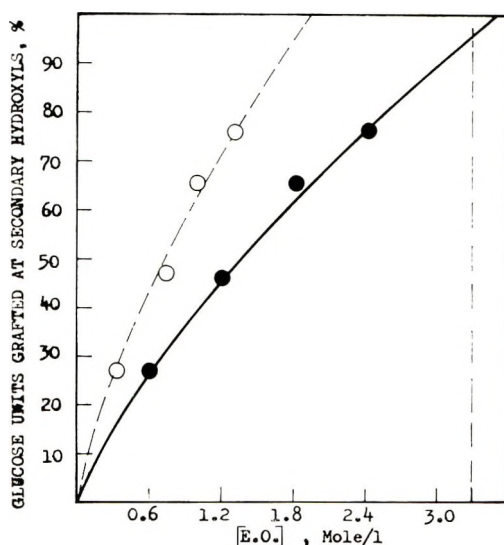
Fig. 3. Dependence of the degree of grafting of the glucose units of the starch on monomer concentration: (●) initial ethylene oxide; (○) effective ethylene oxide.

dary alkoxides in initiating graft polymerization. The oxidation was carried out under homogeneous and optimal conditions[21] in aqueous solution at pH 1.7, with the use of only an equivalent of periodic acid, or a slight excess, based on the starch present in the graft polymer. In all cases, plots of the per cent oxidation versus time gave a curve which approached asymptotically a fixed maximum after a reasonable length of time, showing that there was no over-oxidation.[10]

The per cent oxidation of the glucose units in the graft polymers obtained at constant alkoxide concentration (31.9%) decreased with increasing monomer concentration (Fig. 2), indicating an increase in the extent of grafting at the secondary hydroxyl groups. A graphical presentation of the per cent of glucose units grafted at least at one of the secondary hydroxyl groups versus monomer concentration (Fig. 3) showed that this

increased quite sharply with increasing monomer concentration. From the shape of the curve of Figure 3, it is possible to see by extrapolation that on further increase of the initial monomer concentration, at an alkoxide concentration equivalent to substitution of one alkoxide group per glucose unit, the extent of grafting at the secondary hydroxyl groups will increase further.

The final oxidation results obtained for the different alkoxide concentrations investigated were quite similar. The oxidation curves for graft polymers obtained under the same conditions from two different experiments were almost identical, showing the accuracy of the results.

The oxidation results (especially Fig. 3), showing selectivity of grafting at the secondary hydroxyl groups, may be explained by one of the following two possibilities. Either the reaction of potassium naphthalene with the starch in DMSO is selective, with preferential formation of alkoxide at one of the secondary hydroxyl groups, or it is random, and the increased participation of the secondary hydroxyl groups in initiation with increase in monomer concentration, is due to preferential transfer of the growing anions to the acidic hydrogens of the secondary hydroxyl groups [eq. (1)], most probably to those at C_2 which are known to be more acidic.[29]

In order to distinguish between these possibilities, methylation of the starch alkoxide (prepared as usual with potassium naphthalene) was carried out, the products were hydrolyzed, and the O-methyl-D-glucose derivatives were determined. The results showed that the methylation was completely random.[30] This points out clearly that the second possibility seems to be the most probable.

It follows that on increasing the monomer concentration at 31.9% alkoxide, the extent of the transfer reactions of the growing anions with the secondary hydroxyl groups increased (as seen from the oxidation results), and the new alkoxides, which are selectively formed, can participate in initiation provided that monomer is available, which is the case at high monomer concentrations.

Now the polymerization is very slow, and an equilibrium may be established between the free hydroxyl groups in the starch and the growing alkoxides as shown in eq. (1). Since the hydroxyl group at C_2 is the most acidic, the equilibrium of the transfer reaction will occur preferentially with these hydroxyl groups. Actually the equilibrium shown in eq. (1) is a new metallation reaction by the alkoxide of the growing chains. Now there are various factors besides the acidity of the hydroxyl groups which can lead to preferential metallation at C_2. In the first place the DMSO helps in breaking partially the helical conformation of the starch, and also reduces the intra- and intermolecular hydrogen bonding.[31] This increases the availability of the C_2 hydroxyl groups for reaction. In the second place the hydroxyl groups at C_2 and C_3 in the chair conformation of the anhydroglucose units are equatorial[32-34] and are not so far from each other even though they are in *trans* positions. (It is known from cyclohexane that the equatorial hydrogens are 19°28' above or below the plane of the ring.)

This makes possible the formation of a stable chelate (five-membered ring) of the alkoxide formed at C_2 with the hydroxyl group at C_3.[35,36]

It may be noted that the growing anion $\sim$O—$CH_2CH_2O^-$ seems to be more basic than an alkoxide at C_2, since the latter suffers from electron withdrawal by three oxygen atoms. This fact will favor the transfer reaction, so that in the presence of sufficient monomer, all the C_2 hydroxyl groups may participate in polymer initiation, and the resulting graft polymers will not suffer oxidation by periodic acid. Due to the small differences in the acidities of the compounds participating in equilibrium (1) and the slowness of the transfer reaction, the transfer to the more acidic hydroxyl at C_2 may be highly selective, contrary to the metallation reaction with potassium naphthalene, which is very basic, and can even cause additional metallation at the same glucose unit, which has already a negative charge from alkoxide.

No appreciable change was found in the oxidation results on increasing the starch alkoxide from 31.9 to 48%, indicating that there was essentially no increase in the participation of the secondary alkoxide groups of glucose units in initiation. The methylation results cited,[30] have shown that on increasing the DS of the starch alkoxide from about 31.9 to 48% alkoxide, there was increased di- and tri-metallation of D-glucose units by the potassium naphthalene, and if both the C_2 and C_3 alkoxides on the same D-glucose unit participate, or there is more initiation by the C_6 alkoxides, the oxidation results will not change. A decrease in the efficiency of the secondary alkoxide groups in initiating grafting with increase in alkoxide concentration, as indicated from the NMR results, may also partly explain the oxidation results obtained.

In the previous work[1] it was shown that on increasing either the alkoxide or monomer concentration, the graft polymers became less crystalline and more syrupy. As found in the present work on increasing the monomer concentration, there was an increase in chain transfer to the hydroxyl groups of the starch, leading to more grafting of relatively short polyethylene oxide side chains on the starch. Such short PEO chains are liquid. This increased distribution of poly(ethylene oxide) chains on the starch backbone can explain, at least partly, this behavior of the graft polymers.

EXPERIMENTAL

Purification of reagents and preparation of the graft polymers was carried out as before.[1]

The starch content of the graft polymers was determined by hydrolysis of the polymers in dilute sulfuric acid, and the glucose was determined colorimetrically after heating with a solution of anthrone in sulfuric acid.[7,8]

Determination of PEO in the Graft Polymers by NMR

Amounts of the graft polymers between 70 and 110 mg were dissolved in 2.5 ml pyridine·HCl reagent[9] so that their starch content was the same,

and the PEO content was in the range of a calibration curve prepared from varying amounts of PEO having an $\overline{M}_n = 400$. The NMR spectra were determined on the fresh solutions of the graft polymers, since it was feared that some degradation may occur on standing.

Oxidation of the Graft Polymers with Periodic Acid

Blank determinations on the oxidation of dextrin, were carried out and compared with those of the graft polymers which were also water-soluble and the oxidation was completely homogeneous. Dextrin or graft polymer samples containing about 2.1 mmole glucose were dissolved in 50 ml water in a volumetric flask covered with aluminum foil to exclude light and placed in a thermostat at 25°C. To this was added 50 ml of 0.0422M solution of periodic acid (2.11 mmole), held at the same temperature. The solutions were rigorously mixed and kept in the thermostat. Aliquot portions of 4–5 ml of the reaction mixture were taken at different periods to follow up the oxidation, and these were added to a mixture of 20% potassium iodide solution (3 ml), 6N sulfuric acid (0.5 ml), and water (10 ml) to stop the oxidation.

The liberated iodine formed from excess periodic acid as well as the liberated iodic acid were titrated with 0.1N thiosulfate solution using starch as indicator. Under the same conditions blank determinations on the periodic acid solution were carried out.

References

1. M. Tahan and A. Zilkha, *J. Polym. Sci. A-1*, in press.

2. I. Croon, *Acta Chem. Scand.*, **13**, 1235 (1959).

3. B. J. Bines, and W. I. Whelan, *J. Chem. Soc.*, **1962**, 4232.

4. W. M. Doane, N. L. Smith, C. R. Russell, and C. E. Rist, *Stärke*, **17**, 225 (1965).

5. J. S. Smirnova, A. V. Derevitskaya, and Z. Rogovin, *Vysokomol. Soedin*, **4**, 80 (1962).

6. E. Husemann, and M. Kafka, *Makromol. Chem.*, **41**, 208 (1960).

7. *B. D. H. Book of Organic Reagents*, B. D. H. Publication, England, 1958.

8. F. J. Viles, Jr. and L. Silverman, *Anal. Chem.*, **21**, 950 (1949).

9. T. F. Page, Jr. and W. E. Bressler, *Anal. Chem.*, **36**, 1981 (1964).

10. J. M. Bobbit, *Advan. Carbohydrate Chem.*, **11**, 1 (1956).

11. J. R. Dyer, *Methods Biochem. Anal.*, **3**, 111 (1956).

12. G. Tegge, *Stärke*, **12**, 321 (1961).

13. R. D. Guthrie, *Advan. Carbohydrate Chem.*, **16**, 105 (1961).

14. C. L. Mehltretter, *Stärke*, **15**, 313 (1963).

15. E. L. Jakson and C. S. Hudson, *J. Amer. Chem. Soc.*, **59**, 2049 (1937).

16. E. L. Jakson and C. S. Hudson, *J. Amer. Chem. Soc.*, **60**, 989 (1938).

17. A. V. Derevitskaya, Yu. Koslova, and Z. Rogovin, *J. Gen. Chem. USSR*, **26**, 1649 (1956).

18. A. V. Derevitskaya, Y. Kozlova, and Z. Rogovin, *J. Gen. Chem. USSR*, **26**, 3749 (1956); *ibid.*, **26**, 1649 (1956).

19. E. Husemann, M. Reinhardt, and M. Kafka, *Makromol. Chem.*, **41**, 184 (1960).

20. F. Brown, T. G. Halsall, E. L. Hirst, and J. K. N. Jones, *J. Chem. Soc.*, **1948**, 27.

21. V. F. Pfiefer, E. V. Sohns, H. F. Conway, C. B. Lancaster, S. Dabie, and E. L. Griffin, Jr., *Ind. Eng. Chem.*, **52**, 201 (1960).

22. D. H. Grangaard, J. H. Michell, and C. B. Purves, *J. Amer. Chem. Soc.*, **61**, 1290 (1939).

23. J. H. Michell and C. B. Purves, *J. Amer. Chem. Soc.*, **64**, 585 (1942).

24. D. H. Grangaard, E. K. Gladding, and C. B. Purves, *Paper Trade J.*, **115**, No. 7, 41 (1942).

25. D. J. Bell, *J. Chem. Soc.*, **1948**, 992.

26. D. J. Bell, A. Palmer, and A. T. Johns, *J. Chem. Soc.*, **1949**, 1536.

27. D. J. Bell and G. D. Greville, *J. Chem. Soc.*, **1950**, 1902.

28. A. L. Potter and W. Z. Hassid, *J. Amer. Chem. Soc.*, **70**, 3488, 3774 (1948).

29. A. V. Derevitskaya, G. S. Smirnova, and Z. Rogovin, *Proc. Acad. Sci., USSR Chem. Sect. (English Transl.)*, **136**, 1254 (1961); *Chem. Abstr.*, **56**, 14379 (1962).

30. G. Ezra and A. Zilkha, unpublished results.

31. B. Casu, M. Reggiani, G. G. Gallo, and A. Vigevani, *Tetrahedron*, **22**, 3061 (1966).

32. V. S. R. Rao and J. F. Foster, *J. Phys. Chem.*, **67**, 951 (1963).

33. V. S. R. Rao and J. F. Foster, *J. Phys. Chem.*, **69**, 636 (1965).

34. B. Casu and M. Reggiani, in *Vibrational Spectra of High Polymers, (J. Polym. Sci., C, 7)*, G. Natta and G. Zerbi, Eds., Interscience, New York, 1964, p. 171.

35. J. A. Rendleman, Jr., *J. Org. Chem.*, **31**, 1845 (1966).

36. J. A. Rendleman, Jr., *Advan. Carbohydrate Chem.*, **21**, 209 (1966).

Anionic Graft Polymerization of Methacrylonitrile on Potassium Starch Alkoxide

MENASHE TAHAN and ALBERT ZILKHA, *Department of Organic Chemistry, The Hebrew University, Jerusalem, Israel*

Synopsis

The anionic graft polymerization of methacrylonitrile on potassium starch alkoxide in dimethyl sulfoxide was studied. Factors affecting the graft polymerization such as monomer and alkoxide concentrations as well as temperature were investigated. The yield of the graft polymers was found to increase with alkoxide concentration, and it was possible to incorporate all the starch into graft polymer. On increasing the monomer concentration the graft polymer yield increased to a flat maximum. At the higher monomer concentrations, the efficiency of monomer in giving graft polymer decreased due to increased homopolymer formation. The composition of the graft polymers varied with increasing monomer concentration, graft polymers having about 40–65% of grafted starch were obtained. With increasing temperature (10 to 60°C), the yield of graft polymer decreased, there was more homopolymerization, but the amount of starch incorporated in the graft remained constant. The structure of the graft polymers was deduced from hydrolysis of the starch backbone of the graft polymers by dilute mineral acid and the determination of the molecular weights of the grafted side chains, and from oxidation by periodic acid, which showed the extent of grafting at the secondary hydroxyl groups. These results have shown that by anionic graft polymerization it is possible to obtain graft polymers having more densely packed grafted side chains of relatively low molecular weights than those obtained previously by free-radical graft polymerization.

INTRODUCTION

Grafting of vinyl monomers on starch was carried out by free-radical methods based on the formation of free-radical active centers on the starch backbone by chemical means, such as by reaction with Fenton's reagent,[1–3] persulfates,[4] ceric (IV) ions,[5–10] manganese III ions,[11] ozone–oxygen mixtures,[12–15] and the like, or by physical methods such as irradiation by γ-rays[16–18] or ultraviolet light,[19] or by mastication,[20–22] milling,[23] and freezing–thawing cycles.[24] Generally these methods have several disadvantages. The graft polymers are not homogeneous in structure, due to the fact that the free-radical centers on the starch are formed at random. The molecular weights of the grafted vinyl polymers are high[1,2,8,16] and the number of side chains grafted is very small.[8,16,17] Graft polymers having a large number of small grafted side chains were not obtained.[9,10] Since combination of free radicals is an ordinary termination reaction, insoluble crosslinked graft polymers are liable to be formed.

It was expected that anionic graft polymerization on starch will not have many of these disadvantages. Using the alkoxide derivative of starch as initiator of polymerization, it is possible to influence the density of the grafted side chains by varying the degree of substitution of the alkoxide. The $\overline{DP}$ of the side chains can be governed by the ratio of monomer to initiator, so that graft copolymers having a relatively high density of side chains and low molecular weight can be formed. No dimerization of the growing anions is possible, so that crosslinked polymers will not be formed.

In previous work[25] we have shown that it is possible to use the alkoxide derivative of cellulose or poly(vinyl alcohol), prepared in liquid ammonia, for the initiation of graft polymerization of vinyl monomers. The graft polymerization of acrylonitrile and methacrylonitrile on the alkoxide derivative of cellulose acetate in various solvents was also carried out.[26]

In the present work we have studied in detail the graft polymerization of methacrylonitrile on potassium starch alkoxide derivative. This monomer was taken for the systematic study since it has no acidic hydrogen for chain transfer. The starch alkoxide was prepared in DMSO solution by addition of alkali metal naphthalene.[27] This method was found to be very convenient and had many advantages.[26,27]

The effect of monomer and alkoxide concentrations and of temperature on the graft polymerization were studied. The structure of the graft polymers was investigated by using periodic acid oxidation and acid hydrolysis leading to degradation of the starch backbone thereby permitting isolation of the grafted side chains for molecular weight estimation.

EXPERIMENTAL

Materials

Potassium naphthalene was prepared in dry tetrahydrofuran and its concentration in solution was determined by titration with acid.[28] Methacrylonitrile (Fluka) was purified as described previously.[26] Soluble starch (Analar, B.D.H.) containing 15% moisture was used. Dimethyl sulfoxide pure grade (Fluka) was used. Dry stock solutions of soluble starch were prepared by dissolving the starch in DMSO and distilling about 15% of the solvent *in vacuo* at a temperature not more than 60°C, to ensure distillation of the water present. This procedure was found to remove the water present, as seen by addition of benzene to the dry starch solution and azeotropic distillation.

Graft Polymerization and Isolation Procedure

The polymerization vessel consisted of a 150 ml three-necked flask equipped with a high speed stirrer, a self-sealing rubber cap through which the reagents were added by syringes, a thermometer, a Teflon stirring gland, and a three-way stopcock. The apparatus was joined to the vacuum line, flamed with a gas burner with stirring, and then flushed with argon. This

procedure was repeated twice.   Potassium naphthalene in THF was added
to the starch dissolved in 50 ml DMSO with very strong stirring.   The
characteristic deep color disappeared as the reagent reacted with the starch
to give the alkoxide derivative, which precipitated as a heavy gel.   The
polymerization mixture was cooled to the required temperature, and mono-
mer was added with external cooling to keep the temperature constant.
The light yellow alkoxide solution became brown as the polymerization
progressed.   The reaction mixture was added to 500 ml of a mixture of
ethanol and petroleum ether (2:3) acidified with 1–2 ml acetic acid.   The
precipitate, consisting of crude graft polymer, was filtered, washed with
petroleum ether and ether, followed by water and dried in a vacuum
desiccator over phosphorus pentoxide.   The yellow crude product was
extracted at room temperature with acetone in which polymethacrylonitrile
(PMAN) is soluble until no more material was extracted.   The fraction
soluble in acetone was recovered on evaporation of the solvent *in vacuo*.
It consisted of PMAN homopolymer and small amounts of graft polymers
having a relatively high PMAN content.   The undissolved material, con-
sisting of graft polymer and unreacted starch, was extracted with boiling
water, until the extract contained no solute.   This fraction was recovered
on evaporating the water *in vacuo*.   It consisted of unreacted starch and
graft polymers having a relatively low PMAN content.   The residue con-
sisting of the pure graft polymer was dried *in vacuo*.   The composition of
the graft polymer was determined from nitrogen analysis.

Hydrolysis of the Graft Polymers

Samples of 100–260 mg graft polymer were added to $2N$ hydrochloric
acid (30 ml for every 80 mg starch), and the mixture was heated in a
thermostat at 100°C for 8 hr.   The reaction mixture was cooled, and the
PMAN was filtered, washed with water, followed by alcohol and dried at
50°C.

The intrinsic viscosities of the PMAN were calculated from one-point
viscosity measurement in DMF at 29.2°C at a concentration of 0.1 g
polymer/100 ml, by using the equation,[29] $\eta = \eta_0 e^{[\eta]c}$.   The molecular
weights were calculated by using the relationship,[30] $[\eta] = 3.06 \times 10^{-3} \bar{M}_w^{0.503}$.

Oxidation with Periodic Acid

In periodic acid oxidation,[31,32] to samples of graft polymers containing
starch equivalent to 0.08 mmole glucose, periodic acid ($0.02125M$) (4 ml,
0.085 mmole) was added, and the mixture was shaken in the dark in a
thermostat at 32°C.   After the required time, the reaction was stopped by
addition of potassium iodide (20%); 0.5 ml $6N$ sulfuric acid and 10–20 ml
water were added, and the iodine which was slowly liberated was titrated
with $0.1N$ sodium thiosulfate.   The percentage of glucose units oxidized
was calculated.

Proof for the Formation of Graft Polymers

Since the polymer was insoluble in both hot water and acetone, it is neither starch nor polymethacrylonitrile. The infrared spectrum of the graft showed typical absorptions for both starch (3 370, 1 075, and 1 020 cm^{-1}) and PMAN (2 245 cm^{-1} nitrile). The graft polymers after hydrolysis by hydrochloric acid showed the absorptions for glucose besides those for PMAN, indicating that the PMAN was attached to the starch. The starch in the graft polymer was not totally oxidized by periodic acid, indicating the presence of secondary hydroxyl groups which have undergone substitution by PMAN chains.

RESULTS

Effect of Alkoxide Concentration

Potassium naphthalene easily metallated the starch in DMSO up to about 50% conversion of the hydroxyl groups to alkoxides. The per cent hydroxyl groups out of the total of the starch converted to alkoxide was varied between 10 to 50% (DS 0.3–1.5). Monomer conversion increased with per cent alkoxide and was quantitative at 30% alkoxide (159 mmole/l.). At the lower alkoxide concentrations, difficulties were encountered in the separation of the pure graft polymer. The fraction soluble in hot water which consisted of unreacted starch decreased with increasing the alkoxide concentration and at 40% alkoxide all the starch was converted to graft polymer. The fraction extracted by water contained about 1% nitrogen, indicating that very low graft polymers were extracted with the unreacted starch. The fraction soluble in acetone, which consisted essentially of PMAN homopolymer as seen from nitrogen analysis, decreased with increasing alkoxide concentration. At 40% alkoxide this fraction decreased to a minimum of about 50% of the monomer introduced. The yield of the pure graft polymer, which was insoluble in acetone and boiling water, increased with increasing the alkoxide concentration. At low alkoxide concentrations only low yields of graft polymer were obtained. An optimal yield of about 60% was obtained on using 40% alkoxide which did not increase on increasing the alkoxide to 50%. The composition of the graft polymers did not vary with the alkoxide concentration. In all cases graft polymers consisting of about 55% PMAN and 45% starch were obtained (Table I). The amount of THF present in the reaction mixture did not influence the results in the range investigated (Table I). In order to check the accuracy of the results, a balance of the amounts of monomer and starch before and after the graft polymerization was carried out (Table II). The results obtained showed that the experiments were accurate, and all the monomer and starch introduced could be accounted for. From Table II it is seen that the ratio of the fraction of MAN which gave homopolymer to that incorporated in the graft polymer decreased continuously with increasing the alkoxide until 40% alkoxide

TABLE I
Effect of Alkoxide Concentration on Graft Polymerization of Methacrylonitrile on Soluble Starch[a]

Expt. no.	[Alkoxide], mmole/l.	Alkoxide, % of total hydroxyl groups	Conversion, %	Fraction soluble in acetone, %	Fraction soluble in hot water, %	Graft polymer			
						Yield, %	N, %	PMAN in graft polymer, %	Starch in graft polymer, %
52	52.8	10.0	33	—	—	8	—	—	—
179[b]	56.2	10.3	49	—	—	—	—	—	—
51	105.6	20.0	65	—	—	8	—	—	—
180[b]	112.3	20.6	—	49	25	15	11.82	56.4	43.6
68	159.0	30.0	100	49	25	26	11.51; 11.66	55.2	44.8
50	159.0	30.0	100	50	10	40	—	—	—
181[b]	168.5	30.9	100	44	4	52	—	—	—
57	212.0	40.0	100	33	4	63	11.28; 11.28	53.7	46.3
49	212.0	40.0	88	—	0	62	11.50; 11.46	54.7	45.3
48	264.0	50.0	100	35	4	61	11.50; 11.59	55.0	45.0

[a] Experimental conditions: The starch alkoxide derivative was prepared by adding potassium naphthalene in THF to the starch in DMSO (50 ml). The volume of THF added was kept constant (20 ml) unless otherwise indicated. Methacrylonitrile (5 ml, 0.86 mole/l.) and starch (2 g) were used unless otherwise indicated. Polymerization temperature 20°C; time 1 hr.
[b] Starch (2.06 g) was used. Volume of THF added was 12.5 ml. A different batch of reagents was used.

TABLE II
Balance of the Monomer and Starch at the End of the Graft Polymerization

Expt. no.[a]	Monomer					Starch				
	Homopolymer extracted with acetone, g	MAN in graft polymer, g[b]	Total amount of MAN recovered, g	MAN polymerized, g[c]	MAN homopolymer/MAN in graft polymer	Starch extracted with hot water, g	Starch in graft polymer, g	Total amount of starch recovered, g	Starch introduced, g	Unreacted Starch/starch in graft polymer
68	2.94	0.86	3.80	4.02	3.42	1.50	0.69	2.19	2.00	2.18
57	1.98	2.04	4.02	4.02	0.98	0.24	1.75	1.99	2.00	0.14
48	2.10	2.02	4.12	4.02	1.03	0.24	1.65	1.98	2.00	0.14

[a] The experiment numbers are those of Table I.

[b] Calculated from % N.

[c] In all cases the conversion was quantitative, and in these cases the amount of MAN polymerized is equal to the amount of MAN introduced.

TABLE III

Effect of Monomer Concentration on Graft Polymerization of Methacrylonitrile on Soluble Starch[a]

Expt. no.	[Monomer], mole/l.	Conversion, %	Fraction soluble in acetone, %	Fraction soluble in hot water, %	Yield, %	Graft polymer		
						N, %	PMAN in graft polymer, %	Starch in graft polymer, %
				Series A[b]				
53	0.17	100	11	36	53	7.04; 7.18	33.9	66.1
54	0.34	100	16	23	61	9.58; 9.52	45.5	54.5
55	0.51	100	23	16	61	10.11; 10.11	48.2	51.8
60	0.51	100	22	15	63	9.96; 9.75	47.0	53.0
56	0.68	100	32	9	59	10.29; 10.31	48.8	51.2
57	0.86	100	33	4	63	11.28; 11.28	53.7	46.3
49	0.86	88	—	0	62	11.50; 11.46	54.7	45.3
174[e]	1.15	100	36	1	63	9.76; 9.75	46.5	53.5
175[e]	1.15	100		2	61		—	
176[e]	1.34	100	35	2	63	10.90; —	52.0	48.0
177[c]	1.54	100	40	0	63	10.69; —	50.9	49.1
178[e]	1.54	100		0	59		—	
58	1.71	100	42	0	58	12.73; 12.98	61.2	38.8
				Series B[d]				
61	0.17	—	8	92	0			
62	0.17	—	11	89	0			
63	0.51	—	0	100	0			
64	0.51	16.0	21	79	0			
52	0.86	33.0	—	51	8			
179[a,e]	0.86	49.0	66	—	—			

[a] Experimental conditions: The starch alkoxide derivative was prepared by adding potassium naphthalene in THF to the starch (2 g) in DMSO (50 ml) unless otherwise indicated. The volume of THF added was kept constant (20 ml) unless otherwise indicated. Polymerization temperature 20°C, time 1 hr.

[b] Starch alkoxide, 40% of total hydroxyl groups.

[c] Starch used 2.06 g; THF added 12.5 ml. A different batch of reagents was used.

[d] In series B, starch alkoxide was 10% of total hydroxyl groups.

[e] % alkoxide was 10.3.

was reached.   Above that, this ratio remained constant about 1, indicating that half of the monomer was converted to graft polymer, and half to homopolymer.

Effect of Monomer Concentration

This was investigated at a high (40%) and a low (10%) alkoxide concentration.   At 40% alkoxide (Table III, series A), the conversion was quantitative in all cases.   The fraction of unreacted starch decreased with
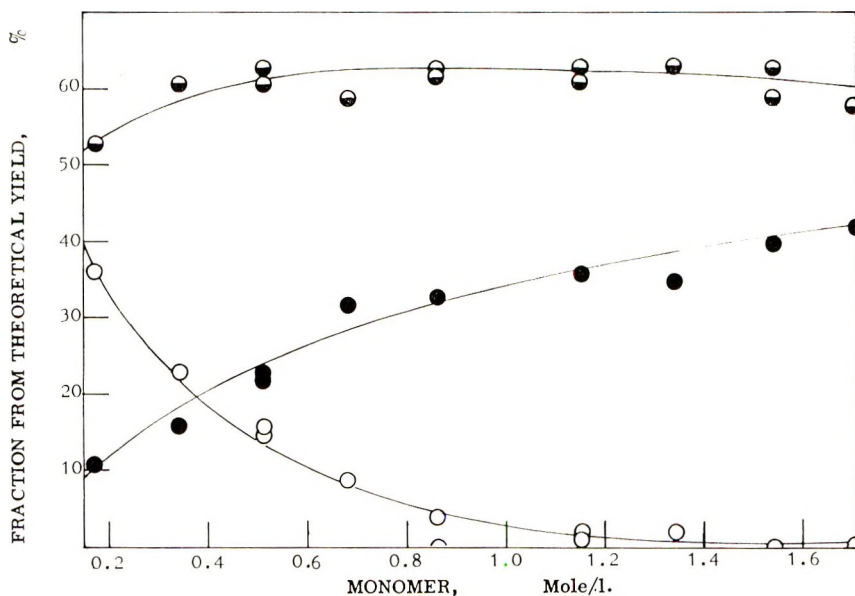
Fig. 1. Effect of monomer concentration on the graft polymerization: (○) fraction soluble in hot water (unreacted starch);   (●) fraction soluble in acetone (PMAN homopolymer);   (◑) graft polymer.

increasing monomer concentration (Fig. 1), and from a monomer concentration of 0.86 mole/l. and higher all the starch was converted to graft polymer.   The fraction of PMAN homopolymer increased with increasing the monomer concentration.   The yield of the pure graft polymer remained constant (61–63%), except at the relatively low and high monomer concentrations.

The composition of the graft polymers changed with increasing the monomer concentration.   The fraction of PMAN in the graft polymer increased with increasing monomer concentration.   This increase was greatest at the low monomer concentrations.   The per cent of starch in the graft decreased correspondingly with increase of monomer concentration.

The balance of the amounts of monomer and starch before and after the graft polymerization showed the experiments were accurate (Table IV).

TABLE IV
Balance of the Monomer and Starch at the End of the Graft Polymerization

	Monomer					Starch				
Expt. no.[a]	Homo-polymer extracted with acetone, g	MAN in graft polymer, g[b]	Total amount of MAN recovered, g	MAN poly-merized, g[c]	MAN homo-polymer/MAN in graft polymer	Starch extracted with hot water, g	Starch in graft polymer, g	Total amount of starch recovered, g	Starch intro-duced, g	Unreacted starch/starch in graft polymer
53	0.31	0.50	0.81	0.80	0.62	1.04	0.97	2.01	2	1.07
54	0.58	1.00	1.58	1.61	0.58	0.83	1.20	2.03	2	0.69
55	1.01	1.29	2.30	2.41	0.77	0.71	1.33	2.04	2	0.53
60	0.97	1.30	2.27	2.41	0.75	0.66	1.46	2.12	2	0.45
56	1.67	1.50	3.17	3.22	1.11	0.47	1.47	1.94	2	0.32
57	1.98	2.04	4.02	4.02	0.97	0.24	1.75	1.99	2	0.14
174	2.48	2.05	4.53	4.82	1.21	0.07	2.36	2.43	2	0.03
176	2.69	2.52	5.21	5.62	1.28	0.15	2.32	2.47	2	0.06
177	3.39	2.72	6.11	6.42	1.25	0.00	2.62	2.62	2	0
58	4.20	3.55	7.75	8.04	1.18	0.00	2.25	2.25	2	0

[a] The experiment numbers are those of Table III.
[b] Calculated from % N.
[c] In all cases the conversion was quantitative, and in these cases the amount of MAN polymerized is equal to the amount of MAN introduced.
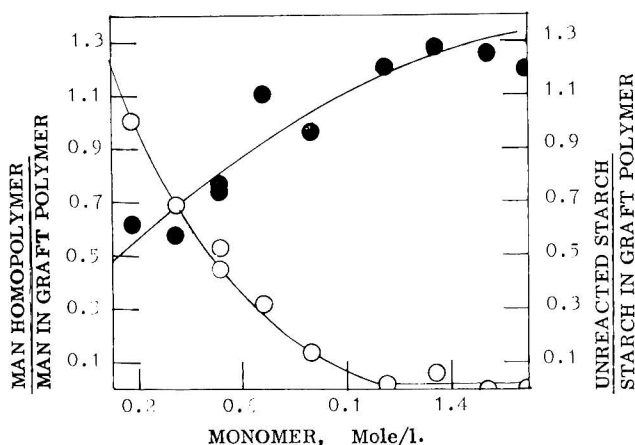
Fig. 2. Dependence of the ratios (●) MAN homopolymer/MAN in graft polymer and (○) unreacted starch/starch in graft polymer on monomer concentration.

It is seen that the amounts of PMAN homopolymer obtained and that of PMAN grafted increased with increasing monomer concentration. The ratio of MAN which gave homopolymer to that incorporated in the graft polymer, also increased (Fig. 2). A tenfold increase of monomer concentration increased this ratio from 0.6 to about 1.2, indicating a decrease in the efficiency of the monomer in giving graft polymer. Increasing the monomer concentration led to increased incorporation of the starch in the graft polymer. At the lowest monomer concentration investigated, about 50% of the starch was grafted, but in order to incorporate the second 50%, it was necessary to increase the monomer concentration at least fivefold. Low monomer concentrations were thus more efficient in the graft polymerization.

From Table III, series B, it is seen that on using a low percentage of alkoxide, the conversion with low monomer concentrations was negligible. The conversion increased with increasing monomer concentration, but the yield of graft polymer was low and the reproducibility was poor.

Effect of Temperature

This was investigated, over the range 10–60°C, at both high and low alkoxide concentrations. Lower temperatures could not be used, as the DMSO crystallized out; higher temperatures were not feasible due to the volatility of the monomer. It is seen (Fig. 3, Table V, series A) that the PMAN homopolymer fraction increased with increasing temperature, while the fraction of graft polymer decreased. The fraction of ungrafted starch was very small and remained practically constant.

The per cent of PMAN in the graft polymer decreased with increasing temperature. The ratio of the fraction of MAN which gave homopolymer to that incorporated in the graft polymer increased with increasing temperature, and at 60°C about 75% of added monomer was converted to

TABLE V

Effect of Temperature on Graft Polymerization of Methacrylonitrile on Soluble Starch[a]

Expt. no.	Temperature, °C	Fraction soluble in acetone, %	Fraction soluble in hot water, %	Yield, %	Graft polymer		
					N, %	PMAN in graft polymer, %	Starch in graft polymer, %
				Series A[b,e]			
71	10	32	5	63	12.30; 12.11	58.2	41.8
49	20	—	0	62	11.50; 11.46	54.7	45.3
57	20	33	4	63	11.28; 11.28	53.7	46.3
65	40	40	5	55	11.62; 11.58	55.3	44.7
66	40	40	7	53	11.16; 11.39	53.7	46.3
69	60	48	6	46	—	—	—
70	60	51	7	42	8.75; 8.66	41.5	58.5
				Series B[d,e]			
61	20	8	92	0			
62	20	11	89	0			
72	60	0	0	0			
73	60	28	72	0			

[a] Experimental conditions: As in Table I.

[b] In series A, conversion in all experiments was quantitative, except in expt. 49, where the conversion was 88%.

[c] In series A, starch alkoxide was 40% of total hydroxyl groups.

[d] In series B, starch alkoxide was 10% of total hydroxyl groups.

[e] Monomer (0.17 mole/l.) was used.

TABLE VI
Balance of the Monomer and Starch at the End of the Graft Polymerization

	Monomer					Starch				
Expt. no.[a]	Homopolymer extracted with acetone, g	MAN in graft polymer, g[b]	Total amount of MAN recovered, g	MAN polymerized, g[c]	MAN homopolymer/MAN in graft polymer	Starch extracted with hot water, g	Starch in graft polymer, g	Total amount of starch recovered, g	Starch introduced, g	Unreacted starch/starch in graft polymer
71	1.93	2.20	4.13	4.02	0.88	0.30	1.57	1.87	2	0.190
57	1.98	2.04	4.02	4.02	0.97	0.24	1.75	1.99	2	0.137
65	2.40	1.83	4.23	4.02	1.31	0.30	1.47	1.77	2	0.220
66	2.40	1.71	4.11	4.02	1.40	0.42	1.47	1.89	2	0.200
70	3.07	1.05	4.12	4.02	2.92	0.42	1.48	1.90	2	0.280

[a] The experiment numbers are those of Table V.
[b] Calculated from % N.
[c] In all cases the conversion was quantitative, and in these cases the amount of MAN polymerized is equal to the amount of MAN introduced.
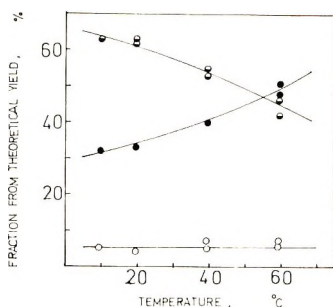
Fig. 3. Effect of temperature on the graft polymerization: (○) fraction soluble in hot water (unreacted starch); (●) fraction soluble in acetone (PMAN homopolymer); (◑) graft polymer.

homopolymer (Table VI, Fig. 4). From Table V, series B, it is seen that at low per cent alkoxide, the conversion was negligible and the reproducibility was poor.
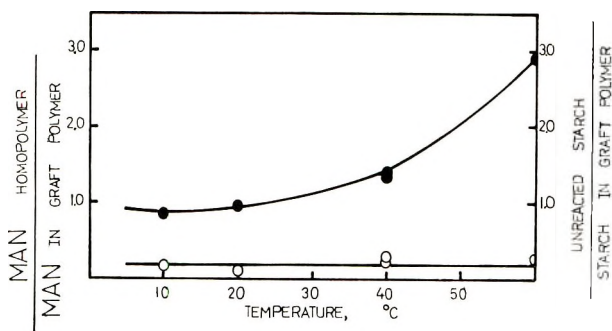
Fig. 4. Dependence of the ratios (●) MAN homopolymer/MAN in graft polymer and (○) unreacted starch/starch in graft polymer on polymerization temperature.

Attempts to Establish the Structure of the Graft Polymers

Hydrolysis. Hydrolysis of the starch backbone is the chief method used in verifying the structure of starch graft polymers.[1,2,6,17] This leaves the grafted side chains; these can be isolated and their molecular weights determined. The graft polymers were subjected to acid hydrolysis with HCl to destroy the starch backbone. The weight of the PMAN isolated after hydrolysis was greater than that calculated from the nitrogen content of the graft polymers before hydrolysis, due to partial hydrolysis of the nitrile groups to amides or carboxyl groups. The nitrogen content of the isolated PMAN was accordingly smaller than that present in the pure PMAN homopolymer (20.9%).

Infrared spectra of the polymers showed the characteristic absorptions for glucose at 3 370 cm and 1 020 cm^{-1}. They showed only a weak absorption at the nitrile region (2 245 cm^{-1}), and sometimes this absorption could

TABLE VII
Hydrolysis Results of the Graft Polymers[a]

Expt. no.	[Monomer], mole/l.	PMAN in graft before hydrolysis, mg	PMAN recovered from hydrolysis, mg	N, %	$[\eta]$, dl/g	$\overline{M}_w$	PMAN in graft, mmole	Alkoxide efficiency, %	No. of glucose units per PMAN chain	$\overline{DP}$
56	0.68	62.5	69.0	15.5	0.192	3 760	22.4	2.70	31.0	56
57	0.86	75.5	80.4	16.1	0.213	4 610	30.2	2.97	28.2	69
176	1.34	71.7	86.4	17.7	0.217	4 790	37.6	3.33	24.1	71
58	1.71	103.3	128.8	15.6	0.284	8 180	—	—	—	122
180	0.86	84.1	68.6	19.0	0.347	12 190	—	—	—	182
50	0.86	—	—	17.1	0.201	4 110	—	—	—	61
70	0.86	46.2	48.7	14.8	0.183	3 410	15.7	2.10	40.0	51

[a] Experimental conditions: The experimental numbers are those given in Tables I–VI. Alkoxide concentration in all experiments was 212 mole/l., except in expts. 180, 50, and 176 where it was 112.3, 159.0, and 218.0 mole/l., respectively. The temperature was 20°C except in expt. 70, where it was 60°C. The hydrolysis was carried out with 2N HCl.

TABLE VIII

Results of the Oxidation of the Graft Polymers of PMAN–Soluble Starch[a]

Expt. no.	[Alkoxide], mole/l.	[Monomer], mole/l.	Glucose units oxidized, %	Glucose grafted, at secondary hydroxyls, %	Secondary alkoxide reacted, mmole	Monomer in graft, mmole	$\overline{DP}_n$	$\overline{M}_n$	No. of glucose units per PMAN chain attached to a secondary hydroxyl
48	264	0.86	89.2	10.8	1.333	30.16	22.6	1 520	9.26
54	212	0.34	91.0	9.0	1.110	14.92	13.5	900	11.11
55	212	0.51	91.3	8.7	1.073	19.25	18.0	1 200	11.50
57	212	0.86	89.0	11.0	1.359	30.22	22.3	1 490	9.10
58	212	1.71	89.3	10.7	1.320	45.50	34.5	2 300	9.36

[a] Experimental conditions: Samples of soluble starch or of the graft polymers containing exactly 0.08 mmole glucose were used. To each sample 4 ml periodic acid (0.02125M, 0.085 mmole) were added. The temperature of oxidation was held constant at 32°C.
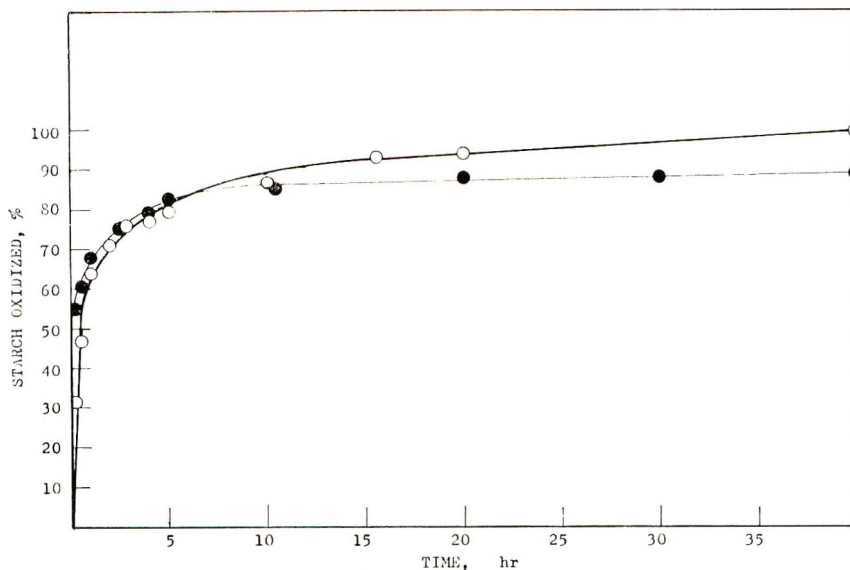
Fig. 5. Heterogeneous oxidation of soluble starch and of PMAN-soluble starch graft polymer: (○) soluble starch; (●) graft polymer (expt. 58).

not be discerned. On the other hand a strong peak for amide or carboxyl appeared at 1 650–1 670 cm^{-1}. Therefore, the molecular weights calculated from the intrinsic viscosity (Table VII) are only very approximate. The results tend to show that the molecular weights of the grafted side chains decreased with increasing alkoxide concentration and temperature and increased with increasing monomer concentration as expected.

From the molecular weights of the side chains and the composition of the graft polymers, (Tables I–VI), the efficiency of the alkoxides in initiating graft polymerization was calculated. This efficiency showed a small increase with increase in monomer concentration but generally it remained low and only 2.1–3.3% of the alkoxide-initiated graft polymerization, and no appreciable differences were found with change of alkoxide concentration.

Oxidation with Periodic Acid. To get further information on the structure of the graft polymers, their oxidation with periodic acid was investigated.[31,32] The periodic acid oxidizes only the glucose units which have no substituents on one of the secondary hydroxyl groups at C_2 or C_3. The degree of oxidation will thus show the extent of grafting at these hydroxyl groups. From these results the secondary alkoxide efficiency in initiating graft polymerization and the density of the grafted side chains attached to the secondary hydroxyl groups of the starch can be calculated.
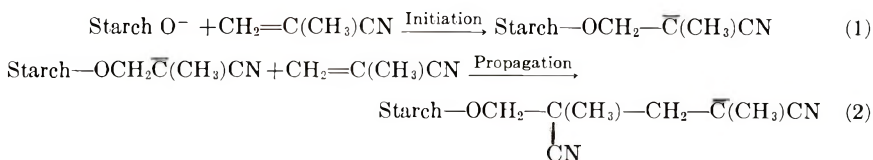
Since the graft polymers of soluble starch were insoluble in water, the reaction was carried out heterogeneously. Blank determinations on soluble starch, which is also insoluble in cold water, were carried out. The results are shown in Table VIII and Figure 5. Every point of the curve was determined in a separate experiment due to the heterogeneous nature

of the oxidation reaction. The oxidation was initially rapid, up to about 10 hr, and then became very slow. The soluble starch was completely oxidized after 40 hr, and no further oxidation was observed after 50 hr. A reaction time of 40 hr was for this reason taken as the time required for complete oxidation of the glucose units of the graft polymers which are open to oxidation. The extent of the oxidation of the graft polymers obtained under various conditions, was about the same 89–91%. This indicates that the efficiency of the secondary alkoxides in initiating graft polymerization was not affected considerably by change in monomer or alkoxide concentration. With increasing monomer from 0.34 to 1.71 mole/l., the efficiency of the secondary alkoxide increased a little (from 9 to 11%).

If it is assumed that the graft polymerization was initiated only by the secondary hydroxyl groups at C_2 or C_3, and that only one such group per glucose unit initiated polymerization, it is possible from the oxidation results to calculate the amount of alkoxide groups which initiated polymerization. From this and from the amount of PMAN in the graft, the $\overline{DP}_n$ and $\overline{M}_n$ of the side chains were calculated. This $\overline{M}_n$ is the maximum possible, since there must be initiation at C_6 and some initiation at both C_2 or C_3 may also occur.

DISCUSSION

The graft polymerization probably proceeds as shown in eqs. (1) and (2).

$$\text{Starch O}^- + CH_2{=}C(CH_3)CN \xrightarrow{\text{Initiation}} \text{Starch}{-}OCH_2{-}\overline{C}(CH_3)CN \qquad (1)$$

$$\text{Starch}{-}OCH_2\overline{C}(CH_3)CN + CH_2{=}C(CH_3)CN \xrightarrow{\text{Propagation}}$$

$$\text{Starch}{-}OCH_2{-}\underset{\underset{\displaystyle CN}{|}}{C}(CH_3){-}CH_2{-}\overline{C}(CH_3)CN \qquad (2)$$

In DMSO, which has a high solvating power, both the positive counterion of the alkoxide and of the growing anion will be highly solvated, leading to an enhanced rate of initiation and propagation. Termination of the graft polymerization can be by transfer to free hydroxyl groups on the starch, but a new alkoxide group will be formed which can continue the polymerization. The polymerization seems to be a "living" one. This is supported by the fact that addition of a second portion of monomer to a system in which the first has polymerized led to complete polymerization. Results as regards yield and composition of graft were the same as those obtained when all the monomer was added in one portion, indicating that the added monomer had polymerized on the "living" ends.

The yield of graft polymer increased with increasing alkoxide concentration due to increase in the possibilities of reaction of the alkoxide with monomer, which also decreases the amount of ungrafted starch and the amount of homopolymer formed. The inefficiency of the graft polymerization at low alkoxide concentration may be related to what is known in

anionic polymerization, that a threshold concentration of initiator exists below which no polymerization occurs.[33]

Increasing the monomer concentration increased the fraction of the starch incorporated in the graft polymer, due to increased possibilities of interaction between the monomer and the alkoxide. At relatively low monomer concentrations, the fraction of monomer which was converted to graft polymer was high, although not all of the starch was converted to graft polymer. At the higher monomer concentrations, although the yields were high they also lead to extensive homopolymerization, pointing to the existence of anions other than the starch alkoxides, competing for monomer.

With increasing temperature more initiator centers can participate in the initiation, so that more densely packed chains of relatively low molecular weight are expected to be formed. That is why the incorporation of starch in the graft polymer did not decrease with increasing the temperature. The increase in the homopolymer fraction and the decrease in the graft polymer yield point to the existence of a termination reaction whose extent increases with temperature.

Homopolymer Formation

Homopolymer formation is due to the presence of active anion centers not connected to the starch which can initiate polymerization. The existence of termination reactions can lead to the formation of such anions. No transfer to monomer involving a proton seems to be possible, since, unlike acrylonitrile, the monomer has no acidic α-hydrogen.[34,35] Overberger et al.[36] suggested hydride ion transfer as shown in eq. (3).

$$\tag{3}$$
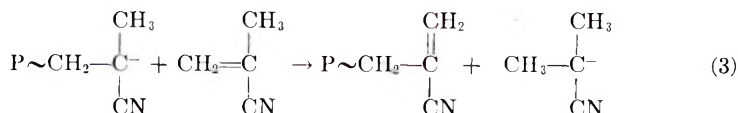
If such a termination reaction is occurring (especially at the higher temperatures investigated) then active anions are formed which can lead to homopolymerization. A cyclization reaction [eq. (4)] which leads to termination,[37] is also possible.
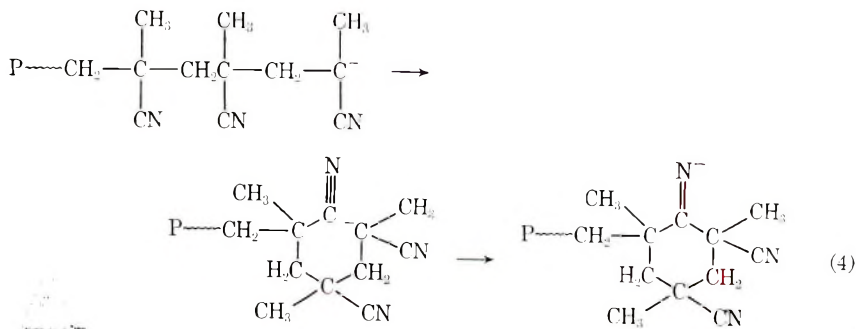
$$\tag{4}$$

Another possibility for homopolymer formation is that the system might not have been completely anhydrous. Traces of water can react with the alkali metal naphthalene to give alkali metal hydroxide which can initiate homopolymerization. Part of the results may be explained on this basis, but there are other facts which seem to contradict this. The fact that, at low alkoxide concentrations, high conversion of monomer occurred with only a small yield of graft polymer may indicate that the water present has acted preferentially with the alkali metal naphthalene, so that at these low concentrations of alkoxide, it was more dominant in initiating polymerization leading to homopolymer formation. On the other hand, the equilibrium (5) may exist, which converts the potassium hydroxide to starch alkoxide.

$$Starch—OH + KOH \rightleftharpoons Starch—OK + H_2O \tag{5}$$
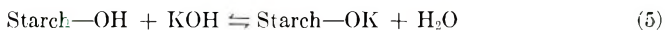
Caldin and Long[38] have shown that the equilibrium of the reaction:

$$EtO^- + H_2O \rightleftharpoons EtOH + OH^- \tag{6}$$

in mixtures containing ethanol and a few per cent water was strongly in favor of alkoxide and not of OH^- formation. Similarly Burus and England[39] have concluded from kinetic results that the conversion of hydroxide to alkoxide is almost complete in ethanol, even if it contained a few per cent of water.

Still another possibility for homopolymer formation is interaction of the growing anions with the DMSO used as solvent to give dimesyl anion, which can initiate homopolymerization.
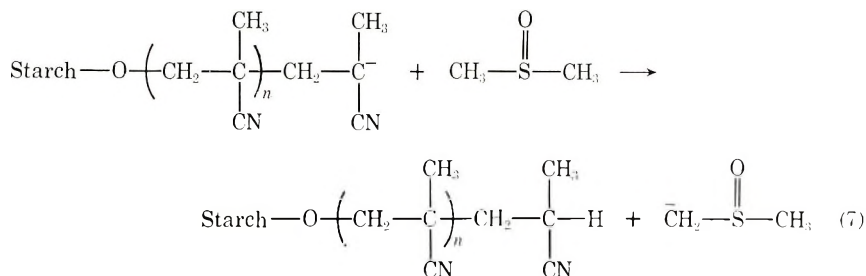
Recently Ledwith et al.[40] showed that in the polymerization of ethylene oxide and methyl methacrylate by potassium *tert*-butoxide in DMSO there is indication that the true catalyst is dimesyl anion formed by the equilibrium (8):

$$(CH_3)_3—C—O^-K^+ + CH_3—SO—CH_3 \rightleftharpoons (CH_3)_3C—OH + \bar{C}H_2—SO—CH_3 \tag{8}$$

It is interesting that although the equilibrium is largely in favor of the *tert*-butoxide ($K = 1.5 \times 10^{-7}$),[41,42] nevertheless, due to the large concentration of DMSO, dimesyl anions seem to initiate polymerization. In our

case, the growing anion is not sufficiently basic, due to the electron-withdrawing effect of the nitrile group, and for this reason the reaction with DMSO will not be appreciable.

Formation of dimesyl anions by interaction of DMSO with starch alkoxide is even less probable, due to the much lower basicity of the alkoxide as compared to *tert*-butoxide. Had there been such an interaction to an appreciable extent, then no graft polymers should have been formed, due to the large excess of DMSO present.

Structure of the Graft Polymers

Although the methods used for investigating the structure of the graft polymers, namely hydrolysis and periodic acid oxidation, may not be very accurate, nevertheless they give important information on the grafting process and on the structure of the graft polymers. The two methods (Tables VII, VIII) show that with increase of monomer concentration, there is an increase in the molecular weight of the grafted side chains, and a small increase in the efficiency of the alkoxide initiator.

It may be noted that the $\overline{M}_w$ found from hydrolysis were much greater than the maximal $\overline{M}_n$ calculated. This may be due on the one hand to the fact that the $\overline{M}_w$ values were determined on PMAN chains which have suffered extensive hydrolysis of the nitrile groups and also have glucose endgroups, and they may be taken only as very approximate. On the other hand, the distribution of the molecular weights of the grafted side chains which is given by $\overline{M}_w/\overline{M}_n$ is not sharp. It should be noted that it is quite possible that there exist besides the grafted PMAN chains also species containing only one MAN unit attached, i.e., in which initiation occurred but not propagation; this will decrease the maximal $\overline{M}_n$ calculated.

The values of the $\overline{DP}_n$ were much higher than the [M]/[C] ratios. They increased with increasing monomer concentration. The density of the PMAN side chains is not great, since the efficiency of the alkoxide is small and does not vary considerably with increasing monomer concentration. Only one PMAN chain for every 10 C_2 or C_3 secondary hydroxyls is present.

These results show that the propagation is much faster than initiation, and monomer prefers to add to a growing polymer chain than react with alkoxide. That is why the secondary alkoxides' efficiency in initiating graft polymerization, as seen from the oxidation results, varied only a little with a fivefold increase in monomer concentration. This behavior led to the large increase in $\overline{DP}_n$ of the side chains with increasing monomer concentration. The low initiator efficiency is the cause for the $\overline{DP}_n$ of the PMAN side chains being much greater than [M]/[C] and for the existence of a relatively small number of side chains on the starch polymer backbone.

The results of the present graft polymerization have shown that it is possible by anionic graft polymerization to obtain graft polymers having

much more densely packed and relatively short side chains than those previously obtained by free-radical polymerization.[2,7]

References

1. C. E. Brockway and K. B. Moser, J. Polym. Sci. A, 1, 1025 (1963).
2. C. E. Brockway, J. Polym. Sci. A, 2, 3721 (1964).
3. C. E. Brockway, J. Polym. Sci. A, 2, 3733 (1964).
4. E. J. Jones, L. B. Morgan, J. F. L. Roberts, and S. M. Todd, Brit. Pat. 715,194 (1954).
5. G. Mino and S. Kaizermann, J. Polym. Sci., 31, 242 (1958).
6. S. Kimura and M. Imoto, Makromol. Chem., 42, 140 (1960).
7. Z. Reyes, C. E. Rist, and C. R. Russell, J. Polym. Sci. A-1, 4, 1031 (1966).
8. G. F. Fanta, R. C. Burr, C. R. Russell, and C. E. Rist, J. Appl. Polym. Sci., 10, 929 (1966).
9. G. F. Fanta, R. C. Burr, C. R. Russell, and C. E. Rist, J. Polym. Sci. B, 4, 765 (1966).
10. G. F. Fanta, R. C. Burr, C. R. Russell, and E. C. Rist, J. Appl. Polym. Sci., 11, 457 (1967).
11. H. Singh, R. T. Thampy, and V. B. Chipalkatti, J. Polym. Sci. A, 3, 4289 (1965).
12. V. A. Kargin, P. V. Kozlov, N. A. Plate, and I. I. Konoreva, Vysokomol. Soedin., 1, 114 (1959).
13. V. A. Kargin, N. A. Plate, and E. P. Rebinder, Vysokomol. Soedin., 1, 154 (1959).
14. V. P. Solomko, I. O. Uskov, and A. O. Galina, Visn. Kuvs'k. Univ. Ser. Fiz. Khim., 1962 (5), No. 2, 106 (Ukrain); Chem. Abstr., 62, 10654c (1965).
15. J. Borunsky, U. S. Pat. 3,138,564 (1964); Chem. Abstr., 61, 8478b (1964).
16. K. P. Shen and F. R. Eirich, J. Polym. Sci., 53, 81 (1961).
17. R. L. Walrath, Z. Reyes and C. R. Russell, Advan. Chem. Ser., 34, 87 (1962).
18. A. J. Restaino and W. N. Reed, Belg. Pat. 629,203 (1963); Chem. Abstr., 60, 13397 (1964).
19. N. Geacintov, V. T. Stannett, E. W. Abrahamson, and J. J. Hermans, J. Appl. Polym. Sci., 3, 54 (1960).
20. O. J. Angier, R. J. Ceresa, and W. F. Watson, J. Polym. Sci., 34, 699 (1959).
21. R. J. Ceresa, J. Polym. Sci., 53, 9 (1961).
22. B. H. Thewlis, Nature, 190, 260 (1961); J. Appl. Chem., 13, 249 (1963); Stärke, 16, 279 (1964).
23. R. L. Whistler and J. L. Goatley, J. Polym. Sci., 62, S123 (1962).
24. A. A. Berlin, E. A. Penskaya, and G. I. Volkova, Mezhdunarod. Simp. Makromolekul. Khim. Dokl., Moscow, 1960, 3, 334 (1960); Chem. Abstr., 55, 7898 (1961).
25. B. A. Feit, A. Bar-Nun, M. Lahav, and A. Zilkha, J. Appl. Polym. Sci., 8, 1869 (1964).
26. Y. Avny, B. Yom-Tov, and A. Zilkha, J. Appl. Polym. Sci., 9, 3737 (1965).
27. Y. Avny and A. Zilkha, Israel J. Chem., 3, 207 (1966).
28. A. Zilkha and Y. Avny, J. Polym. Sci. A, 1, 549 (1963).
29. D. K. Thomas and T. A. J. Thomas, J. Appl. Polym. Sci., 3, 129 (1960).
30. C. G. Overberger, E. M. Pearce, and N. Mayes, J. Polym. Sci., 34, 109 (1959).
31. J. M. Bobbit, Advan. Carbohydrate Chem., 11, 1 (1956).
32. V. E. Pfiefer, V. E. Sohns, H. F. Conway, C. B. Lancaster, S. Dabic, and E. L. Griffin, Jr., Ind. Eng. Chem., 52, 201 (1960).
33. M. Frankel, A. Ottolenghi, M. Albeck, and A. Zilkha, J. Chem. Soc., 1959, 3858.

34. A. Ottolenghi and A. Zilkha, *J. Polym. Sci. A*, **1**, 687 (1963).

35. A. Zilkha and Y. Avny, *J. Polym. Sci. A*, **1**, 549 (1963).

36. C. G. Overberger, H. Yuki, and N. Urakawa, *J. Polym. Sci.*, **45**, 127 (1960).

37. M. Szware, *Fortschr. Hochpolymer. Forsch.*, **2**, 281 (1960).

38. E. F. Caldin and G. Long, *J. Chem. Soc.*, **1954**, 3737.

39. R. G. Burus and B. D. England, *Tetrahedron Letters*, **1960**, No. 24, 1.

40. A. Ledwith, C. E. H. Bawn, and N. K. McFarlane, *Polymer*, **8**, 485 (1967).

41. A. Ledwith and N. K. McFarlane, *Chem. Progr.*, **1964**, 108.

42. A. Ledwith and Y. Shih-Lin, *Chem. Ind.* (London), **1964**, 1867.

# Production of Radicals in Polyoxymethylene by Ultraviolet Photolysis: An EPR Study

O. R. HUGHES and L. C. COARD, *Celanese Research Company, Summit, New Jersey 07901*

Synopsis

Polyoxymethylene (POM) was photolyzed at 2537 and at 3130 Å at −196°C. The EPR spectra of the radical intermediates were recorded. Photolysis *in vacuo* produces a small number of radicals, apparently due to the presence of traces of chromophores. Photolysis in oxygen, however, is a type of photo-oxidation. The radicals $H\dot{C}O$, $\sim O\dot{C}HO\sim$, $CH_3\cdot$, and $HOO\cdot$ were detected and identified as intermediate products of photolysis. Hydrogen atoms and hydroxyl radicals were too reactive (i.e., mobile) at −196°C to be observed. Alkoxy and alkyl radicals and the POM peroxy radical

$$\sim OCH\sim \quad \overset{\displaystyle O-O\cdot}{\underset{\displaystyle |}{}}$$
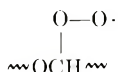
were probably formed as well but could not be characterized with certainty.

INTRODUCTION

Extended tests have indicated that polyoxymethylene (POM) copolymer (without the usual additives) is degraded by sunlight, even though the polyacetal structure itself should not absorb sunlight wavelengths. The photolysis in air has been described as a photo-oxidation.[1,2] In order to understand better the nature of this photolysis, an EPR study was undertaken to detect and identify the dominant radical intermediates produced when polyoxymethylene materials are photolyzed.

There have been several EPR studies of the radicals produced in polyoxymethylene materials by x- and γ-irradiation techniques.[3–7] There has, however, been no EPR study of the radicals generated by ultraviolet photolysis. It should be expected that the types and stabilities of radicals produced by ultraviolet photolysis will differ from those produced by the higher-energy techniques because of the differences in the mechanisms of radical formation.

EXPERIMENTAL

Most of the work reported here is based on the unfiltered ultraviolet light of a G.E. low-pressure (germicidal) G 15T8 lamp which has most of its energy at 2537 Å. Samples in a quartz finger Dewar of liquid nitrogen were

exposed at a distance of 1.5 in. from the two-bulb lamp (incident light intensity of approximately 5×10^{15} quanta/cm^2-sec). The photolysis at 3 130 Å was effected by a 250 watt Mazda ME/D medium pressure Hg point source lamp. An image of the arc was focused through two quartz lenses on an area 0.5×2 cm on the sample held in a quartz finger Dewar at $-196°$C. In order to select the 3 130 Å band, and particularly to eliminate the contribution at 2 537 Å, the beam of ultraviolet light was passed through a quartz two-compartment cell containing 1-cm depths of potassium chromate solution (0.2 g/l.) and a potassium biphthalate solution (5.0 g/l.), and a Corning 7-54 filter (3 mm). The incident light intensity was found to be 2×10^{16} quanta/cm^2-sec. All light intensities were determined by uranyl oxalate actinometry.

All data reported here were obtained from samples in powder form. The samples were not fabricated into films in order to avoid generating chromophoric, thermal degradation products. The sample tubes were flamed and degassed on an oil pumped vacuum line for at least 1.5 hr before the sample was admitted. The tubes were handled in a nitrogen atmosphere when the samples were made up.

The POM homopolymer studied here was a stable polymer whose chains have formate and methoxy endgroups which prevent thermal "unzipping" of formaldehyde. The material was free of any lubricants, thermal stabilizers, or other additives.

The copolymer is a polyoxymethylene material having randomly distributed oxyethylene units ($\sim$1–5 wt-%) similar to that described by Weissermel and co-workers.[8] The copolymer is stable to thermal unzipping but is free of all lubricants, thermal stabilizers, and other additives.

The spectra were recorded on a Varian Associates Model E-3 EPR spectrometer (X-band) which was modified by the insertion of a Hewlett Packard model 532B wavemeter on the waveguide. Spectra could be obtained on samples at $-196°$C by mounting the sample in a quartz Dewar of liquid nitrogen, or spectra could be obtained at temperatures between $-196°$C and room temperature with the use of a Varian variable temperature insert. The g values were checked by using freshly prepared dilute solid mixtures of DPPH in MgO in sealed evacuated capillary tubes.

RESULTS

Photolysis *in vacuo* of copolymer or homopolymer with 2 537 Å light at $-196°$C produces a detectable number of radicals which have an EPR spectrum like that in Figure 1. The radicals contributing to this spectrum are indefinitely stable at $-196°$C if stored in the dark. The spectrum has contributions from formyl radicals, $H\overset{\cdot}{C}O.$, methyl radicals, $CH_3.$, and various other radicals which contribute to a symmetric center band. The formyl radical is indicated by the characteristic asymmetric doublet[9] ($a_H = 125$ oe, $g = 2$) and the methyl radical by the quartet ($a_H = 22$-23 oe, $g = 2$).[10,11] The center band probably results from alkoxy and alkyl radicals.
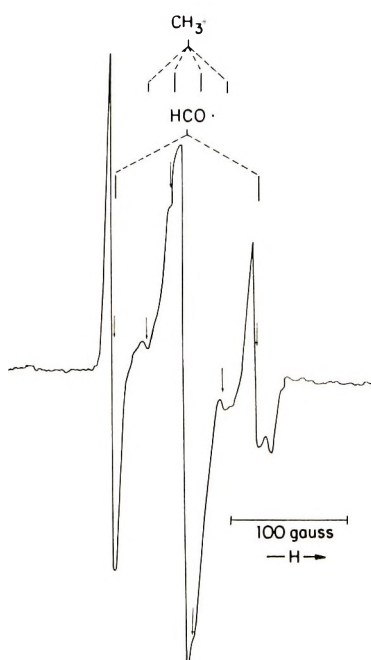
Fig. 1. EPR spectrum of the radicals produced by photolysis of copolymer or homopolymer by 2 537 Å light at −196°C.
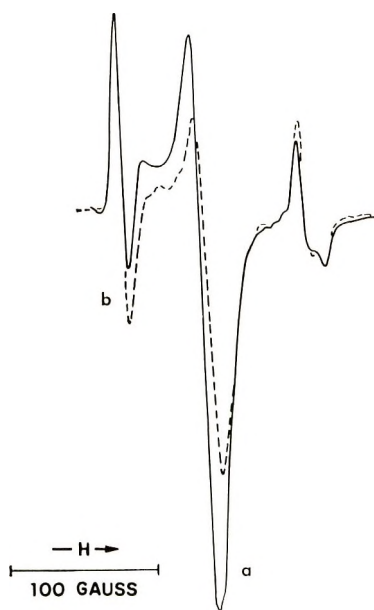
Fig. 2. EPR spectra of radicals generated by photolysis at 2 537 Å at −196°C: (a) just before oxygen depletion; (b) just after oxygen depletion.
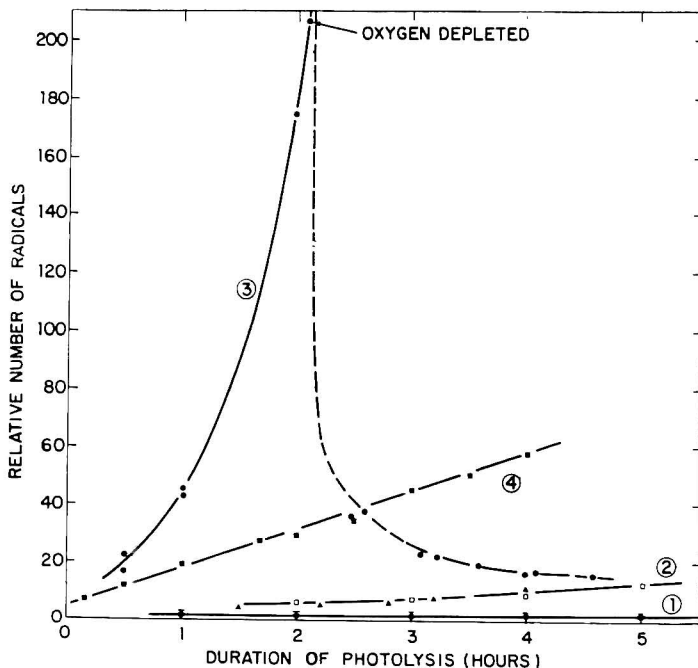
Fig. 3. Rates of radical production (excluding formyl radical) in POM materials on photolysis by 2 537 Å light at −196°C: (1) copolymer, homopolymer, and paraformaldehyde photolyzed *in vacuo*; (2) homopolymer and paraformaldehyde photolyzed under 10 mm oxygen; (3) copolymer photolyzed under 10 mm oxygen, showing the great decrease in the number of radicals when the oxygen is depleted; (4) copolymer photolyzed under 100 mm oxygen.
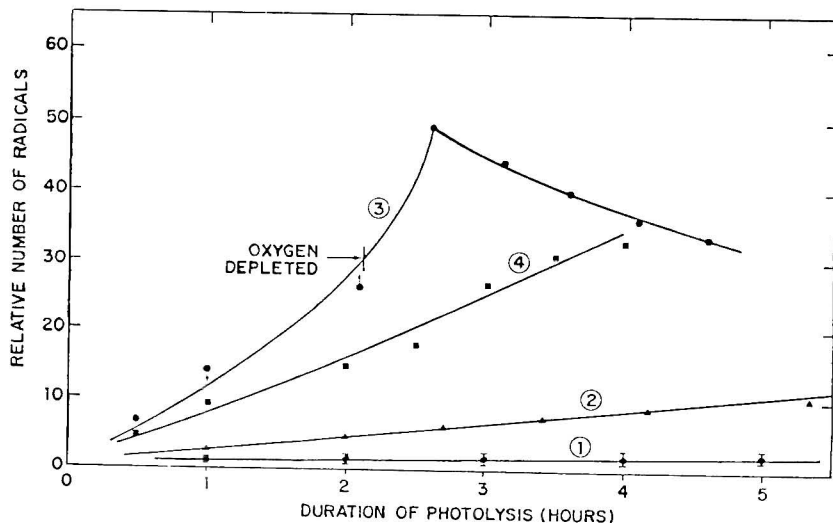
Fig. 4. Rates of formyl radical production in POM materials on photolysis by 2 537 Å light at −196°C: (1) copolymer, homopolymer, and paraformaldehyde photolyzed *in vacuo*; (2) homopolymer photolyzed under 10 mm oxygen; (3) copolymer photolyzed under 10 mm oxygen; (4) copolymer photolyzed under 100 mm oxygen.

A similar photolysis with 3 130 Å light produces fewer radicals (e.g., 1.5 × 10¹⁵ spins/g at 3 130 Å versus 1 500 × 10¹⁵ spins/g at 2 537 Å, corrected to the same total quanta); the formyl radical signal is particularly reduced in intensity relative to the center band, being only barely detectable.

Photolysis of copolymer or homopolymer in oxygen at −196°C (the polymer was sealed in sample tubes under 10 mm of oxygen at room temperature and cooled) produces an EPR spectrum which is initially like that in Figure 5a (i.e., no methyl radical quartet is detected; but one of the
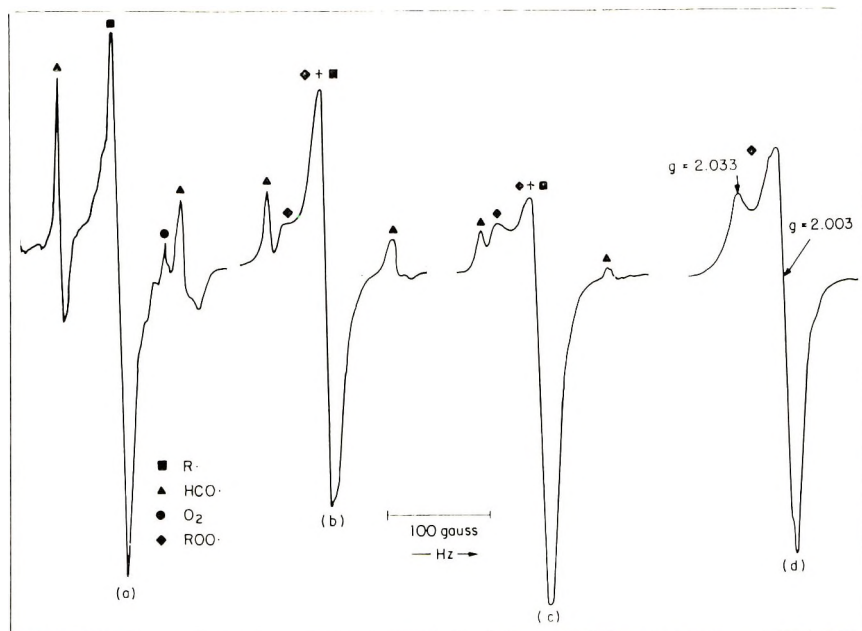
Fig. 5. Formation of hydroperoxy radicals in POM materials on storage at −196°C under fluorescent lighting after ultraviolet photolysis: (a) radicals produced by ultraviolet photolysis at −196°C with 2 537 Å light (a line from the oxygen in the sample is also present); (b) after storage in −196°C for one day; (c) after 2 days; (d) after 4 days storage at −196°C. This spectrum does not undergo further change on standing at −196°C. The transformation does not occur if the original sample is stored in the dark at −196°C.

many oxygen lines appears in the high field region of the spectrum as indicated), in the later stages of photolysis in oxygen the spectrum is more like that in Figure 2a. The quantities of radicals, either formyl or center band radicals, produced on photolysis in vacuo or in oxygen are plotted as a function of the duration of photolysis in Figures 3 and 4. As curve 1 in either figure indicates, photolysis of copolymer or homopolymer in vacuo is limited to an initial generation of radicals but further photolysis does not produce increased radical concentration. This is taken to mean that traces of chromophores, which are unavoidably present, are photolyzed

to radical products which do not undergo further reaction at $-196°C$ *in vacuo*.

Curves *2* and *3* in Figures 3 and 4 show that photolysis of copolymer or homopolymer in oxygen at $-196°C$ produces continuously increasing radical concentrations. The increase is particularly pronounced in the copolymer. This may be due to the lower crystallinity of the copolymer versus the homopolymer. In a limited supply of oxygen, the oxygen line decreases in intensity during such photolysis and eventually disappears indicating that the photolysis is actually a photo-oxidation leading eventually to a depletion of oxygen in the sample tube.

The difference between the initial spectrum of the products of photolysis in oxygen (Fig. 5a) and a later spectrum (Fig. 2a) is identical to the spectrum in Figure 5d. The spectrum in Figure 5d is that of HOO· (see below). The hydrogen atoms, H·, produced in the photolysis (which in the absence of oxygen decay too rapidly at $-196°C$ to be observed), react with oxygen in the sample and are observed as hydroperoxy radicals.

Photolysis beyond the point of oxygen depletion results in a change in the EPR spectrum from that in Figure 2a to that in Figure 2b. Again, the difference is a decrease in the concentration of hydroperoxy radicals present. The decrease in HOO· concentration is sudden (Fig. 3, curve 3) and is accompanied by an increase in formyl radical concentration (Fig. 4, curve *3*). Apparently, after oxygen depletion the hydroperoxy radical is no longer being formed [reactions (1) and (2)] faster than it is being destroyed by photolysis.

The Hydroperoxy Radical

If the radical mixture represented by Figure 5a is stored in the dark at $-196°C$ under vacuum no change occurs. If stored at $-196°C$ under normal laboratory fluorescent lighting, the formyl radical decomposes to carbon monoxide and hydrogen atoms [eq. (1)].

The hydrogen atoms quickly form H_2 and are not observed. The formyl signal eventually disappears leaving the center band signal unaffected.

However, when a similar distribution of radicals is stored at $-196°C$ in oxygen under normal laboratory fluorescent lighting (but not in the dark), a transformation in the EPR spectrum occurs (Figures 5a, b, c, d). The final asymmetric spectrum (Fig. 5d) is indefinitely stable at $-196°C$, but is not observable at temperatures above $-80°C$.

The asymmetric signal has the important spectroscopic feature that it cannot be "saturated" at ordinary microwave power levels. All the other signals can be "saturated" at relatively low power levels. This point helps establish the fact that the asymmetric signal represents a new radical. The fact that the asymmetric signal has a different "saturation" behavior than the other radical signals studied here is seen in the proportionate increase in the intensity of the asymmetric signal with increases in the square root of the microwave power used (Fig. 6).
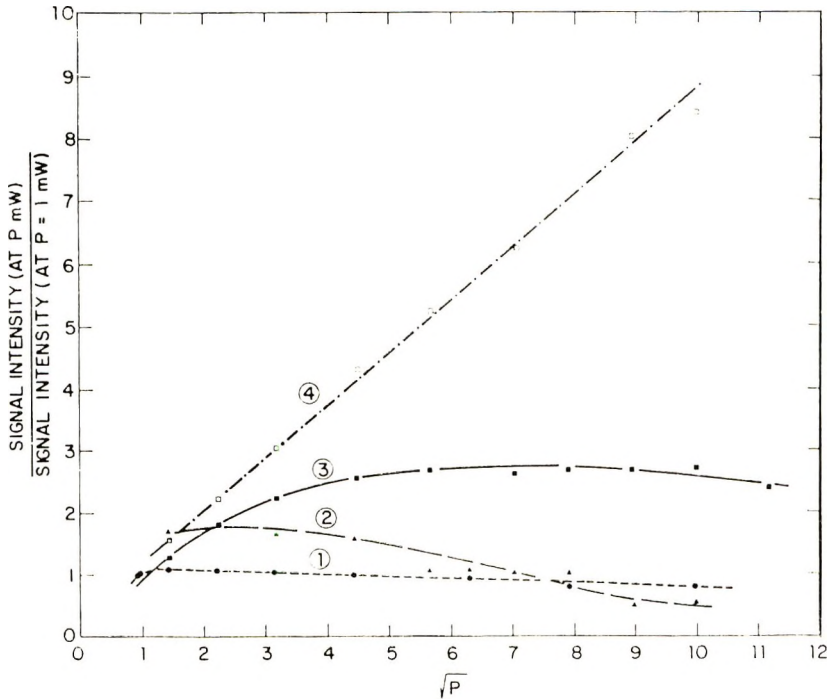
Fig. 6. Response of the signal intensities of the EPR spectra to increases in the applied microwave power P: (1) ~OĊHO~; (2) CH$_3$·; (3) HCO·; (4) peroxy radical.

EPR signals having the asymmetric line shape of Figure 5d, the associated power saturation characteristic, and stability have been previously reported for the hydroperoxy radicals.[12-17] The hydroperoxy radical is produced here by a two-step reaction:

$$HĊO \xrightarrow[\text{(primarily } \lambda > 3000 \text{ Å)}]{UV} H\cdot + CO \tag{1}$$

$$H\cdot + O_2 \rightarrow HO_2\cdot \tag{2}$$
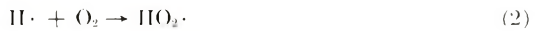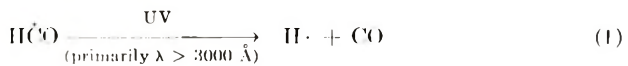
THE ~OĊHO~ Radical

It is known that x- or γ-irradiation of POM materials produces the ~OĊHO~ radical by hydrogen abstraction from the acetal group ~OCH$_2$O~.[5-7] The radical has a doublet spectrum (a_H = 12-13 oe, g = 2) much like that in Figure 7a. The radical when generated in this way is extremely stable even at room temperature in oxygen and therefore must be located deep within the crystalline region of the polymer. Plasma treatment also produces such a doublet spectrum, however, with much decreased stability.[18]

The doublet spectrum in Figure 7a (a_H = 13-15 oe, g = 2) was generated first by ultraviolet photolysis of the copolymer in a limited supply of oxygen to a point beyond the point of oxygen depletion, producing a spectrum like
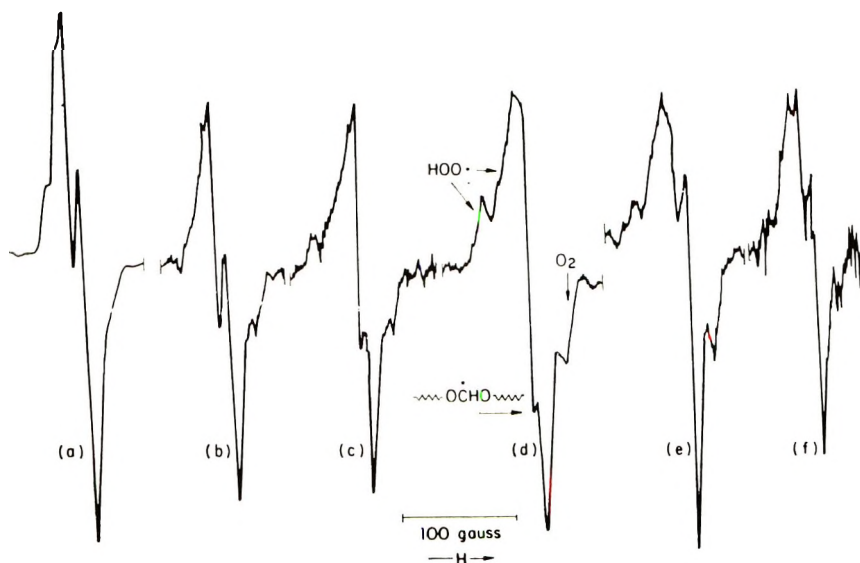
Fig. 7. Reaction of ~OĊHO~ with oxygen: (a) the doublet from ~OĊHO~ at −196°C before addition of oxygen; (b) oxygen added, sample warmed to −110°C, no reaction; (c) warmed to −90°C, reaction has commenced; (d) −80°C, spectrum is composed of contributions from ~OĊHO~ and oxygen, and the reaction product, HOO·; (e) −40°C, some HOO· has been destroyed; (f) some ~OĊHO~ still remains.

that in Figure 2b, then the sample was quickly warmed to room temperature for a moment and recooled to −196°C, a doublet spectrum such as that in Figure 7a was obtained. (It is essential that the photolysis extend beyond the point of oxygen depletion, otherwise the doublet is destroyed by reaction with oxygen.) Very slow warming only resulted in a decay of the original signal. Apparently, on slow warming the original radical mixture achieves sufficient mobility at a relatively low temperature so that radicals decay by radical-radical combination reactions rather than through hydrogen abstraction from the polyacetal matrix. Hydrogen abstraction, because of its higher activation energy, becomes an important mechanism for reactive radical decay only at the higher temperature obtained if the sample is warmed quickly. The product of hydrogen abstraction by the reactive radicals is the more stable ~OĊHO~ radical.

The chain radical, ~OĊHO~, produced by ultraviolet photolysis, has only limited stability at room temperature. The signal decays to one half its original intensity in about 15 min. The fact that this radical has a lower stability when generated by ultraviolet photolysis than when generated by x- or λ-irradiation is not surprising, however. The chromophores which were photolyzed to form the reactive radicals which produced in turn the ~OĊHO~ radical by hydrogen abstraction, are found almost exclusively in the amorphous regions of the polymer. It is therefore to be expected that the ~OĊHO~ radicals will be found in the amorphous regions of the polymer where they are accessible to oxygen.

The direct combination of polymer chain radicals such as the polyethylene radical, $\sim$CH$_2$ĊHCH$_2\sim$, with oxygen is reported to yield rather stable polymer peroxy radicals such as $\sim$CH$_2$—$\overset{\overset{\displaystyle O\text{—}O\cdot}{|}}{\text{CH}}$—CH$_2\sim$.[15] We have attempted an analogous synthesis of a polyacetal peroxy radical $\sim$OCHO$\sim$, $\overset{\overset{\displaystyle O\text{—}O\cdot}{|}}{}$ by direct combination of the chain radical, $\sim$OĊHO$\sim$, with oxygen. The $\sim$OĊHO$\sim$ radical was prepared as described above, then exposed to oxygen briefly at $-196°$C. No reaction occurred until the sample was warmed to $-90°$C in a variable temperature cavity Dewar insert. The transformation in the EPR spectrum which occurred as the temperature was raised is displayed in Figure 7. Finally at room temperature the only surviving signal is that of a low concentration of $\sim$OĊHO$\sim$ which was apparently located in regions of the polymer which were relatively inaccessible to oxygen.

It is tempting to assign one or more of the intermediate spectra (Fig. 7d, 7e) to the polyacetal peroxy radical but the available data do not permit this. The only peroxy radical that could be identified in the spectra of Figure 7 was the hydroperoxy radical. If the polyacetal peroxy radical did form it was unstable and could not be clearly identified in the spectra of Figure 7.

Alkyl and Alkoxy Radicals

The alkyl radical, $\sim$OCH$_2\cdot$, and the alkoxy radical, $\sim$CH$_2$O$\cdot$, are possible intermediates in the photolysis scheme. The alkyl radical should appear in these EPR spectra, if present, as a triplet centered at $g = 2$ with a hyperfine splitting constant of about 22–23 oe. The alkoxy radical would appear as a broadened singlet at $g = 2$, since coupling of the unpaired electron with the hydrogen atoms on the adjacent carbon atom is small.

The center band of the EPR spectrum (in the absence of high HOO$\cdot$ concentration) has an irregular appearance like that in Figure 5a. The peak to peak distance varies from 7 to 17 oe. Such a signal is probably composed of the spectra of more than one radical and could easily include an unresolved triplet from the alkyl radical or the singlet from the alkoxy radical.

DISCUSSION

Initial photolysis of polyoxymethylene materials produces formyl radicals and "center band" radicals; the latter probably include $\sim$OCH$_2\cdot$ and $\sim$OCH$_2$O$\cdot$ as the major contributors. The photolytic generation and subsequent decomposition of formyl radicals is an important process leading to the photolysis of polyoxymethylene materials because hydrogen atoms are produced in the photodecomposition of formyl radicals [eq. (1)].

These hydrogen atoms engage in a variety of radical–radical and hydrogen abstraction reactions. At $-196°C$ the latter are slow but at higher temperatures assume a predominant importance. The reactions of hydrogen atoms proceed so quickly even at $-196°C$ that the doublet spectrum of H· was not detected.

When hydrogen atoms are generated in vacuum reactions (3)–(5) are important.

$$2H· \rightarrow H_2 \tag{3}$$

$$H· + \text{⋙}CH_2O· \rightarrow \text{⋙}CH_2OH \tag{4}$$

$$H· + \text{⋙}OCH_2O\text{⋙} \rightarrow \text{⋙}O\dot{C}HO + H_2 \tag{5}$$
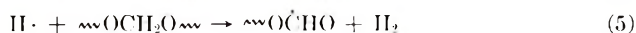
Reaction (5) is particularly important at higher temperatures. At higher temperatures hydrogen abstraction by a variety of other radicals is also important. If oxygen is present, additional reactions occur [eqs. (2), (6), and (7)].

$$H· + O_2 \rightarrow HOO· \tag{2}$$

$$\text{⋙}O\dot{C}HO\text{⋙} + O_2 \rightarrow \text{chain cleavage} \tag{6}$$

$$\begin{array}{ll} H· & + HOO· \rightarrow HOOH \\ \text{(or RH)} & \qquad\qquad (R·) \end{array} \tag{7}$$
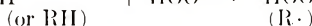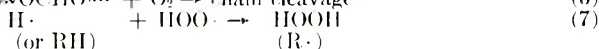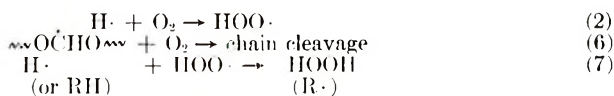
It was expected that the photolysis of the peroxide which can be produced when oxygen is present would lead to the generation of hydroxyl radicals.

$$\begin{array}{ccc} \text{HOOH} & \xrightarrow{\text{UV}} & 2\,\text{HO·} \\ \text{(or ROOH)} & & \text{(or RO· + HO·)} \end{array} \tag{8}$$
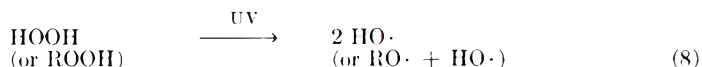
The doublet spectrum which has been reported for the hydroxyl radical was not detected, however, either because it is too mobile and reactive or because of an unfavorable spin orbit coupling.[19] The decay reactions of hydroxyl radicals might explain the formation of H_2O, HCOOH, and $\text{⋙}CH_2OH$ during photolysis.

The stable products of photolysis, i.e., the radical decay products, have been detected by other techniques. Thus, CO, H_2, CH_2O, H_2O, HCOOH, and CO_2 have been detected by mass spectrometry.[2,18] In addition, acetic acid, methane, and ethane were detected. These are possible decay products of the methyl radicals detected by EPR. The production of $\text{⋙}CH_2OH$ groups [reaction (4)] is indicated by the growth of the infrared hydroxyl band at $3450\,\text{cm}^{-1}$.

There are several chromophores which, if present in POM materials, would be photolyzed to formyl radicals. These are: formaldehyde, aldehydes (e.g., $\text{⋙}OCH_2CHO$), formates, and formic acid. The photolysis of formaldehyde proceeds to radical and nonradical products, depending on the photolysis wavelength:[20]

$$CH_2O \xrightarrow{\text{UV}} H\dot{C}O + H· \tag{9}$$

$$\xrightarrow{\text{UV}} H· + CO \tag{1}$$

$$\xrightarrow{\text{UV}} CO + H_2 \tag{10}$$
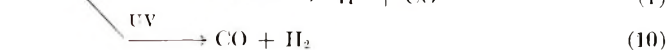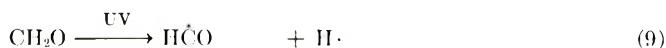
At 2 537 Å reaction (9) is highly favored over reaction (10); at 3 130 Å reactions (9) and (10) occur with equal probability. This and the fact that the formyl radical itself is photolyzed by 3 130 Å and longer wavelength light, largely accounts for the observation of greater radical concentrations on photolysis at 2 537 Å than on photolysis at 3 130 Å. Formate endgroups are known to be present in POM materials and are known to produce formyl radicals on photolysis; however, the extinction coefficient for the absorption at 2 537 Å is small, and at longer wavelengths it is negligible.

In addition, there are various related compounds whose photolysis also results in the production of formyl radicals. Formyl radicals are produced on photolysis of trioxane, ethylene glycol monomethyl ether, ethylene glycol dimethyl ether, triethylene glycol diacetate, poly(ethylene glycol),[18] and purified methanol.[11] Such formyl radicals may result from photochemical reactions which depend on the photolysis of the $ROCH_2 \cdot$ radical. The radical $HOCH_2 \cdot$ is reported to absorb 2 537 Å light and form formyl radicals.[21]

Another attractive source of formyl radicals might be the absorption of ultraviolet light by an acetal oxygen complex. The possible initiation of photooxidation by charge-transfer excitation was discussed by Chien.[22] Stenberg et al. have demonstrated recently[23] that ethyl ether in the presence of oxygen has a substantial ultraviolet absorption at wavelengths longer than $\lambda = 2 200$ Å, whereas ethyl ether–nitrogen solutions do not. Such an absorption might be expected for an acetal–oxygen complex, although this has not yet been demonstrated.

References

1. P. G. Kelleher and L. B. Jassie, *J. Appl. Polym. Sci.*, **9**, 2501 (1965).
2. N. Grassie and R. S. Roche, *Makromol. Chem.*, **112**, 34 (1968).
3. R. Marx and M. C. Chachaty, *J. Chim. Phys.*, **58**, 527 (1961).
4. R. Lenk, *Czech. J. Phys.*, **B12**, 833 (1962).
5. M. B. Neiman, T. S. Fedoseyeva, G. V. Chubarova, A. L. Buchachenko, and Ya. S. Lebedev, *Vysokomol. Soedin.*, **5**, 1339–1344 (1963).
6. V. I. Tupikov and S. Ya. Pshezhetskii, *Russ. J. Phys. Chem.*, **38**, 1310 (1964).
7. H. Yoshida and B. Rånby, *J. Polym. Sci. A*, **3**, 2289 (1965).
8. K. Weissermel, E. Fischer, K. Gutweiler, H. D. Herrman, and H. Cherdron, *Angew. Chem.*, **79**, 512 (1967).
9. F. J. Adrian, E. L. Cochran, and V. A. Bowers, *J. Chem. Phys.*, **36**, 1661 (1962).
10. C. K. Jen et al., *Phys. Rev.*, **112**, 1169 (1958).
11. P. J. Sullivan and W. S. Koski, *J. Amer. Chem. Soc.*, **85**, 384 (1962); *ibid.*, **86**, 159 (1964).
12. J. Kroh, B. C. Green, and J. W. T. Spinks, *J. Chem. Phys.*, **32**, 1249 (1960).
13. S. Siegel, L. H. Baum, S. Skolnik, and J. M., Flournoy, *J. Chem. Phys.*, **32**, 1249 (1960); *ibid.*, **34**, 1782 (1961).
14. C. L. Ayres, E. G. Jansen, and F. J. Johnston, *J. Amer. Chem. Soc.*, **88**, 2610 (1966).
15. J. C. W. Chien and C. R. Boss, *J. Amer. Chem. Soc.*, **89**, 571 (1967).
16. E. E. Beasley, Ph.D. Thesis, U. of Maryland, 1963.
17. K. U. Ingold and J. R. Morton, *J. Amer. Chem. Soc.*, **86**, 3400 (1964).
18. O. R. Hughes and K. C. Hou, unpublished results.

19. M. Bersohn, and J. C. Baird, *An Introduction to Electron Paramagnetic Resonance*, Benjamin, New York, 1966, p. 131.

20. J. G. Calvert and J. N. Pitts, Jr., *Photochemistry*, Wiley, New York, 1966, p. 371.

21. R. S. Alger, T. H. Anderson, and L. A. Webb, *J. Chem. Phys.*, **30**, 695 (1959).

22. J. C. W. Chien, *J. Phys. Chem.*, **69**, 4317 (1965).

23. V. I. Stenberg, R. D. Olson, C.-T. Wang, and N. Kulevsky, *J. Org. Chem.*, **22**, 3227 (1967).

Dilute Solution Studies of Nitrogen-Substituted Polyurethanes

H. C. BEACHELL and JEAN C. PETERSON BUCK,* *Department of Chemistry, University of Delaware, Newark, Delaware 19711*

Synopsis

A high molecular weight linear polyurethane was prepared by the polyaddition of equimolar amounts of ethylene glycol and methylene bis(4-phenyl isocyanate). Varying amounts of the labile carbamate protons of the polyurethane backbone were substituted by a number of groups of varying length and composition. The resultant grafted or nitrogen-substituted polyurethanes were then studied viscometrically in both polymer solvent and in a polymer solvent-nonsolvent mixture. The configuration of the nitrogen-substituted polyurethane was found to be dependent upon the number and length of pendent branches.

INTRODUCTION

At the present time, there is considerable interest in copolymers which can be prepared using a polyurethane as part of the chain. This is true because the resulting polymeric materials have quite a wide spectrum of properties, depending upon the nature of the starting materials.

However, in many of the industrially important polyurethane copolymers, the primary interest is in the preparation of block copolymers. In general, these block copolymers, such as Spandex, are prepared by a simple extension of the synthetic route outlined above. That is, the copolymer is usually prepared from a long-chain diol, a diisocyanate, and a so-called chain-extender, such as a diamine.[1] If desired, a fairly well-characterized, branched polymer can easily be obtained by using a triol in place of some of the diol.[1]

Many different types of block copolymers of polyurethanes are described in the general and patent literature. However, relatively few grafted copolymers involving the polyurethane entity are reported, and practically no reports describing the preparation and properties of grafted species with a linear homopolyurethane backbone have been published.

In this study a linear polyurethane of high molecular weight was prepared in solution by the polyaddition of equimolar amounts of ethylene glycol and methylene bis(4-phenyl isocyanate). The preparation and

characterization of the linear backbone have been described in detail previously.[2]

Nitrogen-substituted derivatives were prepared with the use of the characterized linear polyurethanes described above as backbones. In this procedure the labile carbamate protons of the polyurethane backbones were substituted by a number of groups, of varying length and composition, through a two-step reaction.[3] The substitutions were effected in the following manner. First, sodium hydride was used as a strong base to abstract a proton from the carbamate nitrogen [eq. (1)].

$$-[CO-NH-Ar-NH-COO-R-O]_n + 2NaH \xrightarrow{DMF,0°C}$$
$$-[CO-NNa-Ar-NNa-COO-R-O]_n + 2H_2 \quad (1)$$
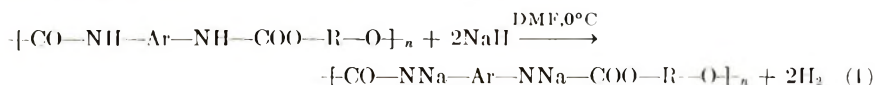
An alkyl halide was then added to form the nitrogen-substituted polymer:

$$-[CO-NNa-Ar-NNa-COO-R-O]_n + 2R'X \xrightarrow{DMF,0°c}$$
$$-[CO-NR'-Ar-NR'-COO-R-O]_n + 2NaX \quad (2)$$
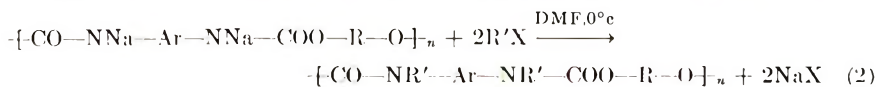
The structure of Ar depends upon the initial isocyanate used, R on the diol, and R' on the alkyl halide.

The reactions (1) and (2) illustrate a complete or 100% degree of substitution. However, partial substitutions can be obtained by using appropriate amounts of the sodium hydride and alkyl halide with the polyurethane backbone.[4]

A polyurethane graft was prepared in a similar manner by using, instead of an alkyl halide in reaction (2), a long-chain halogen-terminated homopolymer. The reaction sequence can be described as shown in eq. (3).

$$-[CO-NNa-Ar-NNa-COO-R-O]_n + 2CH_3-[OCH_2CH_2]_mBr \xrightarrow{DMF,0°c}$$
$$-[CO-N-Ar-N-COO-R-O]_n + 2NaBr \quad (3)$$
$$\underset{CH_3}{\overset{(OCH_2CH_2)_m}{|}} \quad \underset{CH_3}{\overset{(OCH_2CH_2)_m}{|}}$$
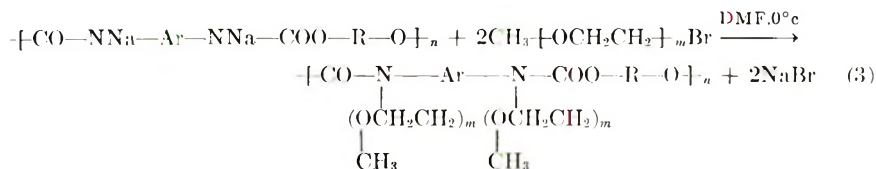
By using this procedure, the length of the backbone and the number of reactive carbamate sites (thus the number of attached chains) and the length of the prepolymerized, attached chains could be controlled.

In order to carry out the substitution reactions described above, special precautions were taken to avoid the possibility of any side reactions of either the sodium hydride, the anionic backbone or the halide end group. This was true in either the simple alkylation reaction or in the preparation of a graft copolymer.

To avoid all such side reactions, the reaction steps were carried out under completely anhydrous conditions with carefully purified reagents and solvents, to assure complete absence of oxygen, moisture and in general, all impurities containing active hydrogen atoms capable of destructive side reactions.

Best results could be obtained by running the reaction at ice temperature and in the highly polar solvent, DMF.[5]

EXPERIMENTAL

Preparation of Nitrogen-Substituted Polyurethane Derivatives

The N-substitution was carried out according to the procedure described by Blumstein.[4] A 500-ml, three-necked, round-bottomed flask was equipped with a stirrer, condenser, dropping funnel, and nitrogen inlet. The system was protected from moisture with calcium chloride drying tubes and the apparatus was flamed out under nitrogen prior to use.

The reaction flask was placed in a sodium chloride–ice bath. An appropriate amount of sodium hydride, as a 50% suspension in mineral oil, was added to the reaction flask with 50 ml of dry and precooled DMF. The polyurethane backbone, dissolved in 50 ml dry DMF, also precooled in a sodium chloride–ice bath, was then added dropwise with vigorous stirring, to the sodium hydride–DMF slurry. After complete addition of the polymer–DMF solution, stirring was continued, at salt–ice temperature, for 1 hr. Initially, hydrogen was evolved, and a green color appeared very rapidly. This color was also noted by Blumstein[4] and is characteristic of the presence of the polyurethane ion in solution. The slurry soon became clear, indicating complete reaction of the sodium hydride.

After 1 hr, alkyl iodide or bromide dissolved in 20 ml of DMF was added to the polyurethane sodium salt. Stirring was maintained for an additional hour at salt–ice temperature. Within 5 min, after the complete addition of the alkyl halide, the green color disappeared from the reaction mixture, yielding a clear grayish solution.

The solution was then filtered to remove any of the sodium halide formed, although some was soluble in the DMF, and the alkylated polyurethane was then recovered by precipitation into a large excess of distilled water. The solid polymer was washed repeatedly with additional portions of distilled water, to eliminate as much as possible, the adsorbed sodium halide and DMF. The resulting polymer was dried in a vacuum oven at room temperature for several days. In each preparation, the extent of N-substitution was determined by infrared and elemental analyses.

The extent of N-substitution was limited, however, to a maximum of approximately 15%. It was found that the backbone was degraded when subjected to amounts of NaH yielding a derivative of higher than 15% N-substitution. One exception to this rule was the N-methylation reaction; elemental analysis (based on carbon content) indicated approximately 50% N-substitution. The product did not appear to be degraded.

The reactive halides used in preparing the N-substituted derivatives included methyl iodide, β-acetoxyethyl bromide, decanoyl chloride, and 1-iodooctadecane.

Preparation of Grafted Copolymers

The reactions used in preparing the grafted polyurethanes are essentially the same as those described previously in the preparation of the N-substituted derivatives. Instead of using halides of low molecular weight to react with the sodium salt of the polyurethane backbone, a long-chain homopolymeric species with a reactive halide endgroup was employed. The homopolymer used was a commercial polyoxyethylene.

The terminal hydroxyl group of the homopolyoxyethylene was halogenated by treatment with bromoacetyl bromide, as described by Griehl and Neue,[6] prior to subsequent grafting reactions.

Intrinsic Viscosity Measurements

Viscosities were measured in a Cannon-Ubbelohde dilution viscometer at a constant temperature of $25 \pm 0.02°C$. All solvents and solutions were filtered, prior to measurement, through fine sintered-glass or solvent-resistant Millipore filters. The initial polymer concentrations were determined by evaporating to dryness an aliquot of the filtered polymer solution. In each determination, four or five dilutions were usually made, and three or four readings were usually taken for each single dilution to obtain flow times within 0.2 sec of one another. The resulting flow times were then averaged. The measurements were made under free fall conditions; no kinetic energy corrections were applied since they were found to be negligible.

Values of the intrinsic viscosity and the Huggins constant k' were determined from the double plot of the Huggins equation:[7,8]

$$\eta_{sp}/c = [\eta] + k'[\eta]^2 c$$

and the Kraemer equation:[9]

$$\eta_{inh} = [\eta] - k''[\eta]^2 c$$

RESULTS AND DISCUSSION

The polyurethane backbone used in all of the N-substitutions described here is linear by the very nature of its preparation.[2] Therefore, any branching present in the resultant N-substituted product was introduced into the backbone purposely.

To determine the final molecular weights of both the N-substituted polyurethane derivatives and the grafted copolymers, the molecular weight of the backbone homopolymer and the total molecular weight of the calculated number of pendent groups were simply added together.

The average molecular weight of the backbone was determined by intrinsic viscosity measurements prior to reaction;[2] the molecular weight of the reactive halide used in the substitution reaction was either known or determined prior to reaction. Since the extent of substitution could be controlled, the number of pendent groups attached to the backbone was

TABLE I
Intrinsic Viscosity Measurements of N-Substituted Derivatives

Substituent	N substitution, %[a]	Solvent system	Temp, °C	$[\eta]$	b[b]	k'[b]
CH_3—	50	DMF	25	0.21	0.016	0.36
$CH_3CO_2C_2H_4$—	1	"	"	0.44$_5$	0.088	0.44
$CH_3CO_2C_2H_4$—	5	"	"	0.40	0.072	0.44
$CH_3CO_2C_2H_4$—	10	"	"	0.30	0.039	0.43
$C_9H_{19}CO$—	5	"	"	0.45	0.077	0.26
$C_9H_{19}CO$—	10	"	"	0.45	0.085	0.42
$C_{18}H_{37}$—	5	"	"	0.36$_5$	0.030	0.23
$C_{18}H_{37}$—	10	"	"	0.22$_8$	0.018	0.35
CH_3—	50	DMF–acetone (71:29)	25	0.21	0.050	0.11
$CH_3CO_2C_2H_4$—	1	"		0.48	0.075	0.33
$CH_3CO_2C_2H_4$—	5	"	"	0.41$_5$	0.065	0.38
$CH_3CO_2C_2H_4$—	10	"	"	0.31	0.035	0.36
$C_9H_{19}CO$—	5	"	"	0.44$_5$	0.079	0.40
$C_9H_{19}CO$—	10	"	"	0.44$_5$	0.070	0.35
$C_{18}H_{37}$—	5	"	"	0.31	0.032	0.33
$C_{18}H_{37}$—	10	"	"	0.24$_7$	0.013	0.21

[a] Actual per cent N-substitution based on elemental carbon analysis.

[b] Determined from the graphical representation of the Huggins equation: $\eta_{sp}/c = [\eta] + k'[\eta]^2c$, where b is the measured slope and k' is $b/[\eta]^2$.

easily determined. The extent of substitution was verified by elemental analyses, and the presence of any N-substitution checked by infrared absorption spectra. Thus, the overall molecular weight of any substituted or grafted polyurethane could be easily evaluated.[10,11]

Significance of the Huggins Constant

The Huggins or viscosity slope constant k', defined in the Huggins equation, $\eta_{sp}/c = [\eta] + k'[\eta]^2c$, is generally used as a measure of the polymer–solvent and polymer–polymer interactions.[12] In conjunction with intrinsic viscosity values, which reflect variations in intramolecular forces, the viscosity slope constants, being indicative of variations in intermolecular forces, can give a general overall view of the macromolecular configuration and behavior in solution.

Many investigators have discussed the dependence of the Huggins constant k' on branching and, in the case of a branched polymer, on the degree of branching. Orofino[13] has shown that in a good solvent k' is not affected by branching, but in a theta solvent the k' value increases slightly over the k' value for the corresponding linear polymer. Morton[14] has observed, however, that for a branched polymer the values of k' are slightly larger than that for a linear polymer in both good and theta solvents. Contrary to both of the above findings, Pollock[15] found no evidence for such a difference in k' due to branching, while Blachford and his co-workers[16]

have observed increases in the value of k' for a branched polymer with the
increase in the degree of branching in a good solvent.

In this work, the viscosity data on the various branched or substituted
polyurethanes, in a good solvent (DMF), give values of k' that increase
with the extent of substitution. This is shown in Tables I–III. In the
same solvent, the intrinsic viscosity values decrease with increased branch-
ing. For both intrinsic viscosity values and k' values, the differences are
generally greater, the longer the chain branches.

TABLE II
Intrinsic Viscosity Measurements of Grafted Polyurethanes

Polymer sample[a]	Extent of grafting, wt-%	Solvent system	$[\eta]$ (25°C)
PU	0	DMF	0.51_0
PU g-POE	5	DMF	0.48_0
PU g-POE	5	DMF–acetone (71:29)	0.48_0
PU g-POE	10	DMF	0.45_0
PU g-POE	10	DMF–acetone (71–29)	0.49_0
POE	0	DMF	0.04_6

[a] Pu designates the polyurethane backbone; POE the polyoxyethylene side chain.

TABLE III
Effect of Extent of Grafting on the Viscosity Constant, k'

Polymer sample	Extent of grafting	Solvent system	$[\eta]$ (25°C)	b	k'
PU	0	DMF	0.48_0	0.118	0.51_3
PU	5	"	0.48_0	0.120	0.52_2
g-POE	10	"	0.45_0	0.103	0.50_8
POE	0	"	0.04_6	0.001	0.66_6
PU	0	DMF–acetone 71:29	0.46_0	0.085	0.40_2
PU	5	"	0.48_0	0.090	0.39_1
g-POE	10	"	0.49_0	0.085	0.35_4

The same measurements were carried out in a polymer solvent–nonsolvent
(71% DMF–29% acetone) mixture. Both the intrinsic viscosity values
and the k' values decreased with an increased extent of branching, and
again in general, the differences were greater, the longer the chain branches.

References

1. H. Sato, *Bull. Chem. Soc.*, Japan, **39**, 2335, 2340 (1966).
2. H. C. Beachell and J. C. Peterson, *J. Polym. Sci.*, in press.
3. C. P. Ngoc Son, Ph.D. Thesis, University of Delaware, Newark, Delaware, June, 1962.
4. R. Blumstein, Ph.D. Thesis, University of Delaware, Newark, Delaware, June, 1965.
5. H. C. Beachell and R. Blumstein, *J. Polym. Sci. C*, **16**, 1403 (1967).
6. W. Griehl and S. Neue, *Faserforsch. u. Textiltech.*, **5**, 423 (1954).
7. M. L. Huggins, *J. Amer. Chem. Soc.*, **64**, 2716 (1942).
8. D. J. Mead and R. M. Fuoss, *J. Amer. Chem. Soc.*, **64**, 277 (1942).
9. E. O. Kraemer, *Ind. Eng. Chem.*, **30**, 1200 (1938).
10. R. Graham, *J. Polym. Sci.*, **24**, 367 (1957).
11. C. E. H. Bawn and M. B. Huglin, *Polym.* [London], **3**, 615 (1962).
12. L. H. Cragg and R. H. Sones, *J. Polym. Sci.*, **9**, 585 (1952).
13. T. A. Orofino and F. Wenger, *J. Phys. Chem.*, **67**, 566 (1963).
14. M. Morton, T. E. Helminiak, S. D. Gadkary, and F. Bueche, *J. Polym. Sci.*, **57**, 471 (1962).
15. D. J. Pollock, L. J. Elyash, and T. W. DeWitt, *J. Polym. Sci.*, **15**, 335 (1955).
16. J. Blachford and R. F. Robertson, *J. Polym. Sci. A*, **3**, 1289 (1965).

Anionic Graft Polymerization of Methyl Methacrylate on Starch and Dextrin

ELIAHU COHEN and ALBERT ZILKHA,
*Department of Organic Chemistry, The Hebrew University,
Jerusalem, Israel*

Synopsis

The anionic graft polymerization of methyl methacrylate on the potassium alkoxide derivative of starch or dextrin in DMSO was studied. The effects of monomer and alkoxide concentrations as well as temperature were investigated. The yield of graft polymer increased with increasing alkoxide concentration. With increasing monomer concentration and with increasing temperature the extent of homopolymer formation increased. The composition of the graft polymers was found to depend on the reaction conditions. Graft polymers having about 10-40% poly(methyl methacrylate) were obtained. There were quantitative differences in yield of isolated graft polymer between starch and dextrin and these were ascribed to differences in the solubility properties of the carbohydrates. Evidence on the structure of the graft polymers and on the mechanism of the graft polymerization was obtained from acid hydrolysis of the graft polymers and determination of the molecular weights of the cleaved side chains.

INTRODUCTION

In previous work we have shown that it is possible to use the alkoxide derivatives of cellulose,[1] cellulose acetate,[2] and poly(vinyl alcohol)[1] as initiators for the anionic graft polymerization of several vinyl monomers. As part of a program for evaluating this grafting process on starch and dextrin,[3] we have studied in detail the graft polymerization of methyl methacrylate on the potassium alkoxide derivative of these carbohydrates.

The alkoxide derivative was conveniently prepared by reaction of the carbohydrate dissolved in DMSO with potassium naphthalene.[2]

The effects of monomer and alkoxide concentrations were investigated, as well as that of temperature. The molecular weights of the grafted side chains as a function of these variables was investigated.

The results obtained with starch and dextrin were compared.

EXPERIMENTAL

Materials

Methyl methacrylate (MMA) was purified as previously described.[4] Soluble starch (Analar, BDH) and dextrin (BDH) containing 15% and 5%

moisture, respectively, were used. Dry stock solutions of starch or dextrin were prepared by dissolving the carbohydrate in DMSO pure grade (Fluka) and distilling off about 15% of the solvent *in vacuo* at a temperature not exceeding 60°C to ensure distillation of the water present.

Graft Polymerization and Isolation Procedure

The polymerizations were carried out in three-necked flasks fitted with a high-speed stirrer, a thermometer, and a self-sealing rubber cap through which the reagents were added with syringes. The flask was flamed twice under vacuum and flushed with argon. Potassium naphthalene in THF was added to 50 ml of the stock solution of starch or dextrin. The characteristic deep color of the reagent disappeared, and the carbohydrate alkoxide formed as a heavy gel.[2] The polymerization mixture was cooled to the required temperature, and monomer was added with external cooling to keep the temperature constant.

At the end of the polymerization, the reaction mixture was diluted with methanol, neutralized with acetic acid, and then was further diluted with methanol (total volume 400 ml). The crude graft polymer was filtered and washed with methanol, in which potassium acetate is soluble. It was dried *in vacuo* over phosphorus pentoxide.

The crude graft polymer was separated from homopoly(methyl methacrylate) by extraction with benzene (3 g crude polymer in 100 ml benzene left to stand for 2 days). The residual fraction, in the case of soluble starch, was extracted with boiling water (200 ml) for 5 min to remove unreacted starch. In the case of dextrin, the extraction was carried out by cold water in which it is soluble. These extraction procedures were repeated until no solute passed over. The residue is the pure graft polymer. A typical infrared spectrum of a graft polymer showed absorptions for the ester groups at 1 740 cm^{-1} and for the carbohydrate at 3 330 and 1 020 cm^{-1}. The composition of the graft polymers was calculated from methoxyl determinations (analysis carried out by Drs. Weiler and Strauss, Oxford).

RESULTS AND DISCUSSION

Effect of Alkoxide Concentration

The percent of hydroxyl groups out of the total of the starch or dextrin converted to alkoxide was varied between 10 and 50% (DS = 0.3–1.5). (Table I). The fraction soluble in methanol (in the process of isolation of the graft polymer) and in benzene decreased with increasing alkoxide concentration. This fraction is composed mainly of MMA homopolymer and some highly grafted polymers. The fraction soluble in water decreased. This fraction was composed of unreacted starch or dextrin and some graft polymers containing small amount of grafted PMMA, which have solubility behavior similar to that of the carbohydrates. The fraction

TABLE I
Effect of Alkoxide Concentration on Graft Polymerization on Soluble Starch[a]

[Alkoxide], mmole/l.	Alkoxide, % of total hydroxyl groups	Crude yield, g[b]	Fraction soluble in methanol and in benzene, %[c]	Fraction soluble in hot water, %[c]	Graft polymer		$[\eta]$, dl/g[e]	$\bar{M}_w^f$
					Yield, %[c]	PMMA in graft polymer, %[d]		
233	50	3.16	57	8	35	26	0.052	9 550
233	50	3.17	54	12	34	23		
186	40	3.03	—	—				
186	40	2.92	60	10	30	25	0.046	8 020
140	30	2.44	66	7	27	10		
140	30	2.52	64	11	25	15	0.039	6 400
93	20	2.07	73	13	14	6		
93	20	2.13	71	12	17	12	0.033	5 050
47	10	1.99	71	25	4	2		
47	10	2.03	70	28	2	8		

[a] Experimental conditions: The starch alkoxide derivative was prepared by adding potassium naphthalene in THF to the starch in DMSO (50 ml). MMA (5 ml, 0.563 mole/l.) and starch (2.04 g, 0.157 mole/l. glucose) were used. Polymerization temperature 20°C, time 1 hr. The total volume of the reaction mixture was 80 ml.

[b] Theoretical yield, 6.54 g.

[c] Calculated from the theoretical yield, based on total conversion of monomer.

[d] Calculated from % OCH₃.

[e] Determined on the PMMA cleaved from the graft polymers by acid hydrolysis.

[f] $\bar{M}_w$ calculated from $[\eta]$ is only approximate (see text).

TABLE II

Effect of Monomer Concentration on Graft Polymerization on Soluble Starch[a]

[Monomer], mole/l.	Crude yield, g	Theoretical yield, g	Fraction soluble in methanol and in benzene, %[c]	Fraction soluble in hot %[b]	Graft polymer			
					Yield, %[b]	PMMA in graft polymer, %[c]	[η], dl/g[d]	$\bar{M}_a$[e]
Series A								
0.225	2.67	3.84	36.9	12	51	20	0.046	8020
0.225	2.60	3.84	34.7	13	52	20		
0.450	2.88	5.64	51.5	16	32	24	0.052	9550
0.450	2.92	5.64	50.3	12	38	27		
0.675	3.69	7.44	—	—	35	27		
0.337 +0337[f]	3.27	7.44	58.0	3	39	29	0.075	15890
0.675	3.00	7.44	61.0	6	33	27	0.052	9550
0.675	3.01	7.44	61.0	8	31	29		
0.900	3.18	9.24	67.3	5	28	30		
0.900	3.20	9.24	67.3	5	29	33	0.058	11070
1.125	3.39	11.04	70.7	4	25	34	0.065	12970
1.125	3.49	11.04	69.5	4	26	37		
Series B								
0.563	2.07	6.54	73.0	13	14	6		
0.563	2.13	6.54	71.2	12	17	12		
1.125	1.98	11.04	83.0	7	10	8		
1.125	2.11	11.04	81.4	6	13	5		

[a] Experimental conditions: The starch alkoxide derivative was prepared by adding potassium naphthalene in THF to the starch (2.04 g, 0.157 mole/l. glucose) in DMSO (50 ml). Starch alkoxide, as percentage of total hydroxyl groups in Series A was 50% and in Series B 20%. Polymerization temperature 20°C, time 1 hr. The total volume of the reaction mixture was 80 ml.

[b] Calculated from the theoretical yield, based on total conversion of monomer.

[c] Calculated from % OCH₃.

[d] Determined on the PMMA cleaved from the graft polymers by acid hydrolysis.

[e] Calculated $\bar{M}_a$ from [η] is only approximate (see text).

[f] Monomer added in two equal portions, the second one being added 10 min. after the first.

TABLE III
Effect of Monomer Concentration on Graft Polymerization on Dextrin[a]

[Monomer], mole/l.	Crude yield, g	Theoretical yield, g	Fraction soluble in methanol and in benzene, %	Fraction soluble in water, %	Graft polymer			$[\eta]$, dl/g[d]	$\bar{M}_w$[e]
					Yield, %[b]	PMMA in graft polymer, %[c]			
				Series A					
0.225	2.60	3.7	33	49	18	19.8			
0.225	2.80	3.7	28	26	46	20.8		0.046	8020
0.450	2.69	5.5	53	19	28	27.1		0.052	9550
0.450	2.85	5.5	51	15	34	26.6			
0.563[f]	3.28	6.4	51	16	33	33.1		0.064	12700
0.563[g]	2.61	6.4	61	27	12	23.7		0.046	8020
0.563[h]	2.59	6.4	62	35	3	18.7			
0.675	3.10	7.3	60	11	29	32.4		0.052	9550
0.675	3.37	7.3	60	11	29	29.4			
0.900	3.45	9.1	67	8	25	34.5		0.058	11070
0.900	3.26	9.1	65	9	26	35.5			
1.125	3.31	10.9	70	6	24	36.3		0.064	12700
1.125	3.41	10.9	71	7	22	36.5			
				Series B					
0.563	1.38	6.4	82	18					
0.563	1.26	6.4	81	19					
1.125	0.46	10.9	96	4					
1.125	0.38	10.9	97	3					

[a] Experimental conditions: The dextrin alkoxide derivative was prepared by adding potassium naphthalene in THF to the dextrin (1.9 g; 0.146 mole/l. glucose) in DMSO (50 ml). Dextrin alkoxide content, as percentage of total hydroxyl groups in Series A was 50%, and in Series B 20%. Polymerization temperature 20°C, time 1 hr. The total volume of reaction mixture was 80 ml.

[b] Calculated from the theoretical yield, based on total conversion of monomer.

[c] Calculated from OCH_3.

[d] Determined on the PMMA cleaved from the graft polymers by acid hydrolysis.

[e] $\bar{M}_w$ calculated from $[\eta]$ is only approximate (see text).

[f] Reaction temp, 10°C.

[g] Reaction temp, 40°C.

[h] Reaction temp, 60°C.

of pure graft polymer as well as its PMMA content increased with increasing the alkoxide concentration. The increase in the number of initiating centers increased the amount of carbohydrate as well as the fraction of monomer incorporated in the graft polymer.

Effect of Monomer Concentration

This was studied at both high (50%) and low (20%) starch or dextrin alkoxide concentrations (Tables II and III). At 50% alkoxide the fraction soluble in methanol and in benzene increased with increasing monomer concentration, the fraction soluble in water decreased, and the pure graft polymer fraction also decreased, due to a relative increase in homopolymerization. However, there was an increase in the quantity of the graft polymer obtained. This increase in the amount of monomer and of carbohydrate grafted may be due to the greater possibility of the monomer reacting with the alkoxide. The composition of the graft polymers showed an increase in the percentage of PMMA in the graft polymer with increasing monomer concentration.

At 20% alkoxide, the homopolymer fraction was greater than that obtained at 50% alkoxide, the fraction soluble in water was similar, and the fraction of the pure graft polymer was much lower. The increase in the homopolymer fraction and the corresponding decrease in the graft polymer fraction may be correlated with losses of graft polymer fractions having side chains of relatively high molecular weight (infrared spectra of the

TABLE IV
Effect of Temperature on Graft Polymerization on Soluble Starch[a]

Temp, °C	Crude yield, g[b]	Fraction soluble in methanol and in benzene, %[c]	Fraction soluble in hot water, %[c]	Graft polymer Yield, %[c]	PMMA in graft polymer, %[d]	$[\eta]$ dl/g[e]	$\bar{M}_w$[f]
10[g]	3.25	51.6	6.4	42	30.6		
10	3.24	53.2	5.8	41	31.0	0.064	12710
40	2.85	58.3	3.7	38	21.3		
40	3.00	55.7	7.3	37	23.9	0.046	8020
60	2.74	59.6	6.4	34	18.9	0.039	6400

[a] Experimental conditions: The starch alkoxide derivative was prepared by adding potassium naphthalene in THF to the starch in DMSO (50 ml). MMA (5 ml; 0.563 mole/l.) and starch (2.04 g; 0.157 mole/l. glucose) were used. Starch alkoxide content as percentage of total hydroxyl groups was 54% unless otherwise indicated. Polymerization time, 1 hr. The total volume of the reaction mixture was 80 ml.

[b] Theoretical yield, 6.54 g.

[c] Calculated from the theoretical yield, based on total conversion of monomer.

[d] Calculated from % OCH₃.

[e] Determined on the PMMA cleaved from the graft polymers by acid hydrolysis.

[f] $\bar{M}_w$ calculated from $[\eta]$ is only approximate (see text).

[g] Starch alkoxide, as percentage of total hydroxyl groups was 50%.

fractions showed the presence of carbohydrate), obtained as a result of the high [monomer]/[alkoxide] ratios, which seem to be soluble in methanol and in benzene.

It is important to note that together with the low yields obtained, the reproducibility of the results were poor at the low alkoxide concentrations.

Effect of Temperature

The temperature was varied from 10 to 60°C. The homopolymer fraction slightly increased with increasing the temperature both in the case of starch and dextrin (Table IV). The water-soluble fraction, in the case of starch was approximately constant (6%) and in the case of dextrin increased from 16 to 35%. The pure graft polymer fraction decreased from 42 to 34% (starch) and from 33 to 2% (dextrin). The percentage of PMMA in the graft polymer decreased with increasing temperature. These results may be explained by an increase of termination of the polymerization with increase of temperature. This, as explained later, causes an increase in the homopolymer fraction and a corresponding decrease in the graft polymer.

Effect of Polymerization Time

The graft polymerizations were very fast, and the yields of the crude graft polymers obtained after even a fraction of a minute were more than 80% of the yields obtained after 48 hr.

Comparison of the Results Obtained with Starch and Dextrin

Generally, the fraction soluble in methanol and in benzene and that soluble in water were greater, and the pure graft polymer fraction was smaller in the case of dextrin as compared to starch. On the other hand, the composition of the pure graft polymer was similar. It is quite possible that the cause for these differences is due to the greater solubility of dextrin (and its graft polymers) as compared to starch. This also explains the fact that even at 30% dextrin alkoxide no pure graft polymer could be isolated.

As evidence for the loss of dextrin graft polymers due to their greater solubility, it was found that at 10% alkoxide, in the case of starch, the fraction soluble in water, which was recovered by evaporation, contained 15.3% PMMA. In the case of dextrin under the same conditions this fraction contained 25% PMMA. With 50% alkoxide the differences between dextrin and starch were much smaller. The fraction soluble in water in the case of starch contained 23.5% PMMA, and in the case of dextrin this fraction contained 24.5% PMMA. It may be noted that the solubility of the graft polymers does not depend only on the composition of the graft polymers but also on the molecular weight of the grafted PMMA, and on the distribution of the grafted chains on the polymer backbone.

Molecular Weight of the Poly(methyl Methacrylate)

In various studies of the anionic polymerization of methyl methacrylate,[4-6] a wide molecular weight distribution was found. To find out the molecular weight of the grafted side chains, the graft polymers were hydrolyzed with $2N$ hydrochloric acid for 6 hr under reflux. Thus all the starch or dextrin backbone was hydrolyzed to glucose units. The insoluble PMMA thus severed from the graft polymers, containing a glucose end-group was isolated, and the molecular weights were calculated from intrinsic viscosities determined in methyl ethyl ketone at 25°C by using the molecular weight–intrinsic viscosity relationship:[7] $[\eta] = 7.1 \times 10^{-5} \bar{M}_w^{0.72}$.

The intrinsic viscosities were calculated from one point viscosity measurement at a concentration of 0.1 g polymer/100 ml by using the equation,[8] $\eta = \eta_0 e^{[\eta]c}$.

The isolated poly(methyl methacrylates) were found to have suffered partial hydrolysis, as seen from methoxyl determination, which were in all cases $20 \pm 2\%$ OCH_3. Therefore the molecular weights calculated by using the above viscosity–molecular weight relationship (Tables I–IV) are only approximate. However, since these polymers had about the same methoxyl content, they may be compared among themselves.

It may be noted that the $\overline{DP}$ of the side chains were very much higher than the monomer to alkoxide ratios used.

From the Mark-Houwink relationship, $[\eta] = K\bar{M}^\alpha$, it follows that $\log [\eta] = \log K + \alpha \log \bar{M}$. Now if there is a direct relationship between the molecular weights obtained, and the monomer concentration, then the plot of $\log [\eta]$ versus $\log [\text{monomer}]$ will be linear. The intrinsic viscosities of the severed PMMA side chains increased with increasing monomer concentration. Plots of $\log [\eta]$ versus $\log [\text{monomer}]$ gave straight lines in the case of both starch and dextrin.

Increase of temperature was found to decrease the molecular weights of the grafted side chains in the case of both starch and dextrin as seen by the lowering of $[\eta]$ of the polymers. This may be due either to the increase of termination which leads to the formation of shorter chains, or to the possibility that more starch alkoxides participate in high polymer formation.

The intrinsic viscosities of the severed chains were found to increase with increasing alkoxide concentration, which is unusual in anionic polymerization. However, these findings may be misleading, since various high molecular weight grafts dissolved in methanol and in benzene and were lost.
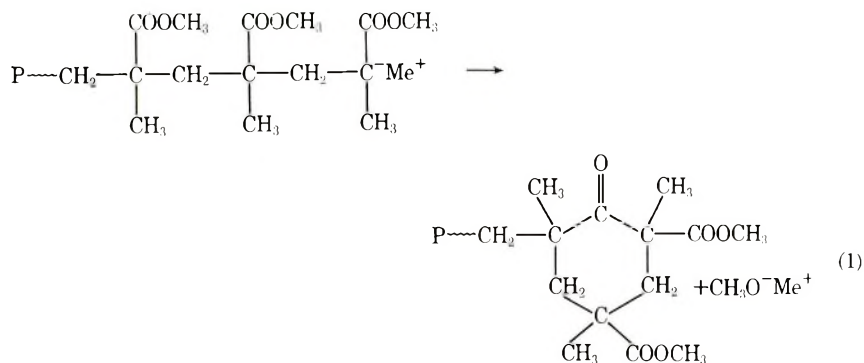
Mechanism of the Graft Polymerization

The fact that a large proportion of the monomer was converted to homopolymer suggested that a termination reaction was occurring. Termination by chain transfer to monomer is not possible, since the monomer has no acidic α-hydrogen. Any termination by chain transfer to the

hydroxyl groups of the starch, if at all possible, does not lead to homo-polymerization.

Another possibility for homopolymer formation is interaction of the growing anions with the DMSO to give dimesyl anion which can initiate homopolymerization. Recently it was shown[9] that in the polymerization of methyl methacrylate by potassium *tert*-butoxide in DMSO there is indication that the true initiator is dimesyl anion formed by an equilibrium reaction between DMSO and potassium *tert*-butoxide. In our case, the growing anion is not sufficiently basic due to the electron-withdrawing effect of the ester group, and for this reason the reaction with DMSO will not be appreciable. Formation of dimesyl anions by interaction of DMSO with starch alkoxide is even less probable, due to the much lower basicity of the alkoxide as compared to *tert*-butoxide.

Another possibility for homopolymer formation is that the system might not have been completely anhydrous. Traces of water can react with the alkali metal naphthalene to give alkali hydroxide which can initiate homopolymerization. However, utmost care was taken in the drying of reagents and apparatus, so that this does not seem to be a major source for homopolymer formation.

It is known[5,10,12] from the anionic polymerization of methyl methacrylate that there exist various possibilities of termination leading to the generation of methoxide ions, such as interaction with the ester groups of the monomer or monomolecular termination by internal cyclization[5,10] as shown in eq. (1).

$$P\text{—}CH_2\text{—}\underset{\underset{CH_3}{|}}{\overset{\overset{COOCH_3}{|}}{C}}\text{—}CH_2\text{—}\underset{\underset{CH_3}{|}}{\overset{\overset{COOCH_3}{|}}{C}}\text{—}CH_2\text{—}\underset{\underset{CH_3}{|}}{\overset{\overset{COOCH_3}{|}}{C}}^-Me^+ \longrightarrow$$

$$ \tag{1} $$

A cyclic ketone (carbonyl absorption at 1712 cm^{-1})[5] and methoxide ion are formed. Attack of the starch or dextrin alkoxide on ester groups of polymer or monomer may also lead to the formation of methoxide.

To find out whether such reactions occurred in the graft polymerization system, we carried out a series of graft polymerization experiments under various conditions, neutralized the reaction mixture with acetic acid, and distilled out *in vacuo* the methanol formed (and THF) which was trapped in a Dry Ice–acetone bath. The amount of methanol was determined by gas chromatography. It was found (Table V) that the quantity of methanol (obtained from the methoxide ions) increased with increasing alkoxide

concentration and with temperature, indicating that the extent of the termination reactions increased. Comparison of the infrared spectra of starch, homopoly(methyl methacrylate), pure graft polymer, polymer fraction soluble in water, and the fraction soluble in the aqueous acid hydrolyzate of the graft polymer showed an absorption at 1 712 cm^{-1} (cyclic ketone)[5] present in the latter two fractions.

Wiles and Bywater[13,14] obtained also methanol in the polymerization of MMA by n-butyllithium at $-30°C$ (Table V). At 10°C they found that the amount of methanol obtained was almost equal to the amount of butyllithium used. In our case the amount of methanol obtained was only about 10% of the alkoxide concentration. This difference may be due to the higher reactivity of the butyllithium, which was found to attack

TABLE V
Determination of Free Methoxide Anions in the Polymerization Mixture
in Graft Polymerization of Methyl Methacrylate on Starch[a]

Starch, g	[Alkoxide]		[Monomer], mmole/l.	Temp, °C	[Methanol], mmole/l.[b]
	%	mmole/l.			
3.33[c]	50	307.8	900	20	25.0
3.33[c]	40	246.2	900	20	15.0
2.00	50	246.2	962	10	21.3
2.00	50	248.2	962	30	24.0
2.00	50	246.2	962	50	25.3
[d]	—	3.8 (BuLi)	250	−30	3.5
[d]	—	7.6 (BuLi)	250	−30	6.7

[a] The reaction mixture was neutralized with acetic acid and the methanol formed was distilled *in vacuo* and determined quantitatively by gas chromatography.

[b] The amount of methanol may be a little higher, since some methanol may have escaped during the distillation.

[c] In these experiments the total volume of the reaction mixture was 100 ml, in the others it was 75 ml.

[d] Values taken from those of Wiles and Bywater[13] for the homopolymerization of MMA by BuLi.

the monomer, generating most of the methoxide ions, as evidenced by their liberation in the early stages of the polymerization. The liberated methoxide ions may be mainly responsible for the homopolymerization observed.

It may be noted that the growing ends may be dissociated more or less completely, due to the high dielectric constant and solvation power of the DMSO. Solvation by complex formation with methoxide ions, formed by the side reactions, may also occur as was found[6,11] previously. These different solvations cause different propagation rates and can lead to the wide molecular weight distribution mentioned.

In the anionic polymerization of methyl methacrylate it was found[10,11]

that after initiation there was a rapid addition of monomer. When the chain reached a $\overline{DP}_n$ of 3–10, there was a great possibility of intramolecular cyclization, leading to termination and formation of a cyclic trimer (cyclic ketone). After this stage the possibility for cyclization became much smaller. This means that the terminated fractions are mainly low molecular weight products which dissolved in the water extractions or after acid hydrolysis, as supported by the infrared spectra. From this it may be concluded that the cleaved side chains, of which the intrinsic viscosities were measured, were composed of the relatively high molecular weight fractions, which were the major part of the total grafted PMMA.

The linear dependence of log $[\eta]$ on log [monomer], meaning that the molecular weights were directly proportional to the monomer concentration, can be explained by one or two ways. (a) Termination is monomolecular[15] where $\overline{DP} = (K_p/K_t)[M]$. The formation of the cyclic ketones supports the existence of monomolecular terminations. (b) The linear increase of molecular weight with monomer concentration may be correlated also with the possibility that the growing ends which have $\overline{DP} > 10$ remain "living," and essentially do not suffer termination during the very short time required for propagation. Obviously in this case increasing the monomer concentration will increase the molecular weight. These "living" ends may eventually terminate, for example by monomolecular termination.

Support for the existence of "living" ends may be seen from the results of the experiment (Table II) in which the monomer was added in two portions to the starch alkoxide. The $[\eta]$ determined on the cleaved side chains was 0.075 dl/g, which was higher than that obtained in a similar experiment in which all the monomer was added in one portion ($[\eta] = 0.052$ dl/g). This may be explained by the possibility that added monomer was polymerized on the "living" ends leading to the higher molecular weights.

Based on the molecular weights of the grafted side chains, and on the content of PMMA and starch or dextrin in the pure graft polymers, it is possible to calculate the average distribution of the side chains on the polymer backbone; thus about one PMMA chain is attached for every 150–200 glucose units of the starch or dextrin molecule. This calculation is based only on the side chains which were insoluble in water and were recovered from hydrolysis. It does not include the small fractions of very low graft polymers which on hydrolysis remained attached to a glucose unit and became soluble in water. Taking these fractions also into consideration, the distribution will be lower than that calculated but nevertheless it would be much less than that calculated from the initial monomer/alkoxide ratios. From this it may be concluded that only a small fraction of the alkoxide was involved in initiation of high molecular weight polymer.

References

1. B. A. Feit, A. Bar-Nun, M. Lahav, and A. Zilkha, *J. Appl. Polym. Sci.*, **8**, 1869 (1964).

2. Y. Avny, B. Yom-Tov, and A. Zilkha, *J. Appl. Polym. Sci.*, **9**, 3737 (1965).

3. M. Tahan, Ph.D. Thesis, The Hebrew University, 1968.

4. M. Tahan, A. Ottolenghi, and A. Zilkha, *Europ. Polym. J.*, **2**, 199 (1966).

5. W. E. Goode, *J. Polym. Sci.*, **47**, 75 (1960).

6. B. J. Cottam, D. M. Wiles, and S. Bywater, *Can. J. Chem.*, **41**, 1905 (1963).

7. S. N. Chinai, J. D. Matlack, A. L. Resnick, and R. J. Samuels, *J. Polym. Sci.*, **17**, 391 (1955).

8. D. K. Thomas and T. A. J. Thomas, *J. Appl. Polym. Sci.*, **3**, 129 (1960).

9. A. Ledwith, C. E. H. Bawn, and N. K. McFarlane, *Polymer*, **8**, 485 (1967).

10. D. L. Glusker, R. A. Galluccio, and R. A. Evans, *J. Amer. Chem. Soc.*, **86**, 187 (1964).

11. D. M. Wiles and S. Bywater, *Polymer*, **3**, 175 (1962).

12. A. A. Korotkov, S. P. Mitsengdler, and V. N. Krasulina, *J. Polym. Sci.*, **53**, 217 (1961).

13. D. M. Wiles and S. Bywater, *Chem. Ind.*, (London), **1963**, 1209.

14. D. M. Wiles and S. Bywater, *J. Phys. Chem.*, **68**, 1983 (1964).

15. A. Ottolenghi and A. Zilkha, *J. Polym. Sci. A*, **1**, 687 (1963).

Properties of PVC.   I.   Properties of PVC Films Prepared by Casting and by Precipitation

JIŘÍ MALÁC, EVA ŠIMŮNKOVÁ, and JIŘÍ ZELINGER,
*Department of Rubber and Plastics Technology, Technical University,
Prague, Czechoslovakia*

Synopsis

This investigation compares the properties of PVC films prepared both by casting from tetrahydrofuran solution and from samples obtained by precipitation with properties of samples from the original PVC.   The differences in properties are explained on the basis of solvent residues remaining in the samples even after tempering at higher temperatures and after extremely long times of drying.   Attention was given to the difficulties caused by this fact, namely, in observing the influence of molecular weight and of distribution of molecular weights of fractions on PVC properties.   Reasons were given for the retention of the tetrahydrofuran by PVC.

INTRODUCTION

A number of investigations have reported on the properties of poly(vinyl chloride) (PVC) samples obtained either by solution casting or by precipitation of PVC from solution.[1-14]   The changes of properties of precipitated samples and of cast films in comparison with properties of the original polymer are usually attributed to the lowering of degree of polymer arrangement,[5-7,9,15] and changes of these properties caused by tempering are similarly explained by an increase in the order of arrangement.

The melting point of PVC crystallites is reported[4,16-18] to be above 200°C. In this temperature range polymer degradation occurs to such an extent that it is practically impossible to prepare the polymer with the lower degree of arrangement by the usual method. i.e., by fusion of the crystallites followed by cooling.   The study of cast films and precipitated polymer properties is therefore the only procedure that can give insight into this tendency of the polymer arrangement to be changed.

EXPERIMENTAL

Materials

The PVC used was Halvic 223 ($[\eta] = 0.63$ dl/g).   Tetrahydrofuran solvent was cleaned by shaking with ferrous sulfate, dried over solid NaOH, distilled, and again dried over sodium.   It was distilled just prior to use.

Cast films were prepared from a 1% (weight) solution of PVC in tetra-hydrofuran, which was heated 30 min at 50–55°C under reflux to disintegrate and dissolve the large aggregates. The solution, after cooling, was poured into an aluminum foil pan and then dried at room temperature first in a fume chamber hood and then under vacuum for a week. The whole drying time took 3 months. Thus films having a thickness of 0.05–0.07 mm and a density of 1.3780 g/cm³ were obtained.

Precipitated PVC was prepared from 2 l. of 10% (volume) solution of Halvic 223 in tetrahydrofuran (THF) by heating 30 min at 50–55°C under reflux. After the solution was cooled to 25°C the polymer was precipitated by the addition of 2 l. distilled water with continual stirring; THF was distilled off at 25–40°C under vacuum. The resultant precipitate in the form of an agglomerate was dried in a fume chamber hood then in a desiccator at 25–30°C.

From the original and precipitated polymer were obtained film and sheet specimens.

Films with a thickness of ca 0.1 mm were cut into samples having dimensions $2 \times 2 \times 0.1$ mm. These were tempered 3 hr at 85°C and then used for density measurements. The preparation of these films entailed either milling at different times and temperatures or pressing at different temperatures for 3 min at 200 kp/cm² between polished aluminum sheets.

Sheet compounds were prepared from a mixture of PVC containing 1% Advastab D 671 (stabilizer). The mixture was milled 5 min at 160°C to give sheets with a thickness of 2.2 mm, which were then compression-molded 3 min at 190°C in a small frame under a pressure of 120 kp/cm². Thicknesses varied between 2 and 4 mm. After tempering 3 hours at 85°C these were used for determination of properties.

Characterization

Density at 20°C was measured by means of a density gradient column. Methanol was used to wet the samples.

Tensile strength corresponding to the upper yield point was measured at deformation velocity of 50 mm/min.

Notch impact strength was determined according to DIN 53 453.

Embrittlement temperature on specimens with a dimension of $20 \times 6 \times 2$ mm was determined in an apparatus described in Czechoslovak Standard CSN 62 1555 in which the sample is bent at a constant deformation velocity at various temperatures.

Dynamic properties, including values of the real component of dynamic elasticity modulus in torsion G' and of mechanical attenuation tan δ were obtained by means of a torsion pendulum, working on the principle of natural oscillations at frequencies of 0.2–2.0 Hz.

Kinetics of density changes were observed on samples of cast films or on samples of sheets of precipitated PVC which were heated for various times and at different temperatures in a test tube in a silicone bath and then rapidly cooled to 20°C.

RESULTS

The densities of milled films of precipitated and of original PVC are compared in Figure 1. The densities of compression-molded films of precipitated and of original PVC are contrasted in Figure 2. The density of the films depends on the time and temperature of milling or on the temperature used in compression molding. The density of milled films is higher than that of compression-molded ones.
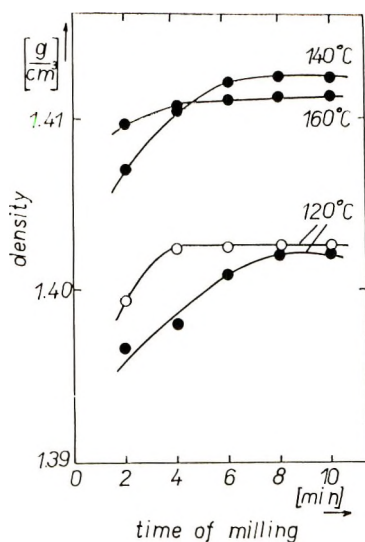

Fig. 1. Density dependence of PVC films on time and on temperature of milling: (O) original polymer; (●) precipitated polymer.

The dependence of density changes of cast films on time and temperature of tempering is shown on Figures 3 and 4. The density changes up to 90°C can be explained by volume relaxation in the zone T_g corresponding to release of tension which remained in the sample after evaporation of solvent.

The dependence of density of samples in the form of 2-mm sheets obtained from precipitated PVC on time and temperature is shown in Figure 5.

TABLE I

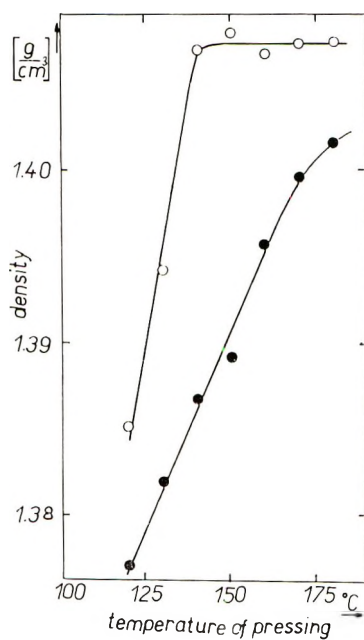|	Original PVC	Precipitated PVC
Tensile strength, kp/cm²	733	696
Notch impact strength, kp/cm	1.9	1.8
Embrittlement temperature, °C	15	46
Density at 20°C, g/cm³	1.4055	1.3940
T_α from dynamic measurement, °C	88	75

Fig. 2. Density dependence of PVC films on compression-molding temperature: (O) original polymer; (●) precipitated polymer.
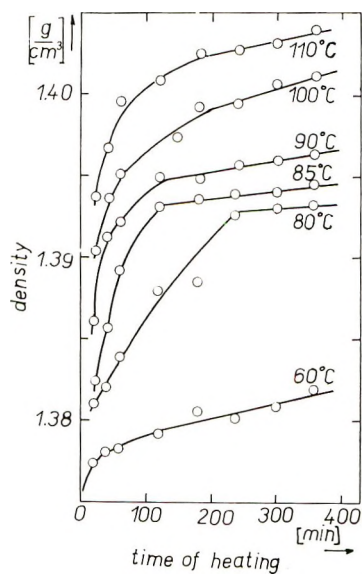

Fig. 3. Density dependence of PVC films cast from tetrahydrofuran solution on time and temperature of tempering.

The properties of sheets prepared in the same way from the original and precipitated polymer are compared in Table I.

Dynamic properties of the original polymer and for precipitated polymer are plotted in Figures 6 and 7, respectively.
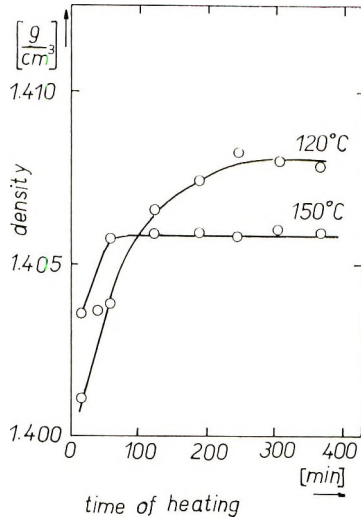

Fig. 4. Density dependence of PVC films cast from tetrahydrofuran solution on time and temperature of tempering.
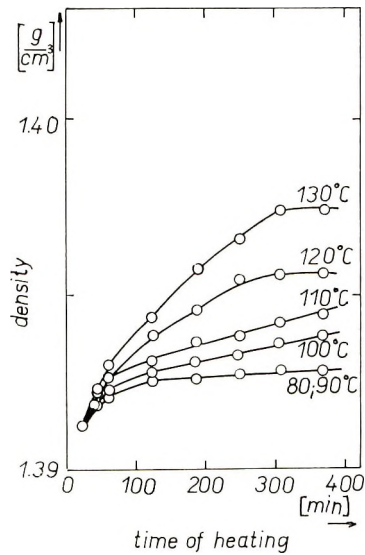
Fig. 5. Density dependence of 2-mm sheets prepared from precipitated PVC on time and temperature of tempering.

Fig. 6. Dependence of G' and tan δ on temperature for a sample of original PVC.

Fig. 7. Dependence of G' and tan δ on temperature for a sample of precipitated PVC.

DISCUSSION

Let us consider the question: What is the reason for the property differences between cast films and samples prepared by precipitation of PVC and samples of the original polymer? As mentioned in the intro-

Fig. 8. Weight loss dependence of 2-mm precipitated PVC samples on time and temperature of tempering.

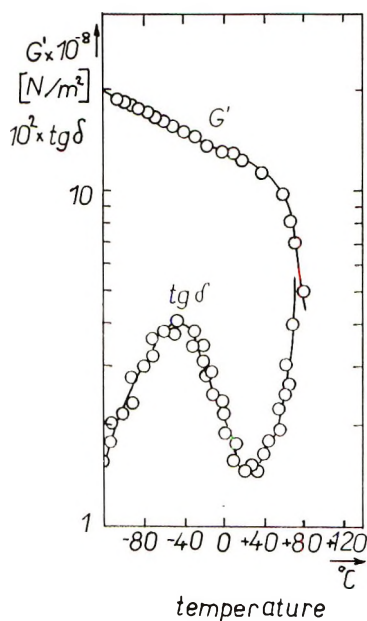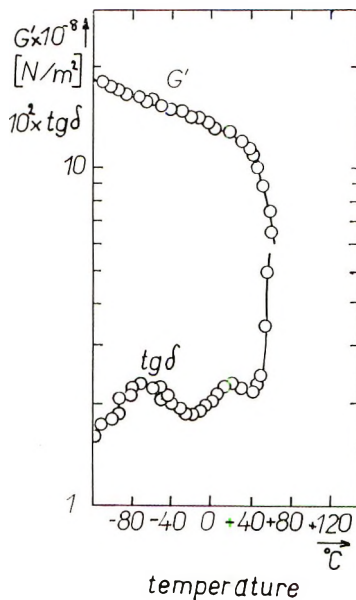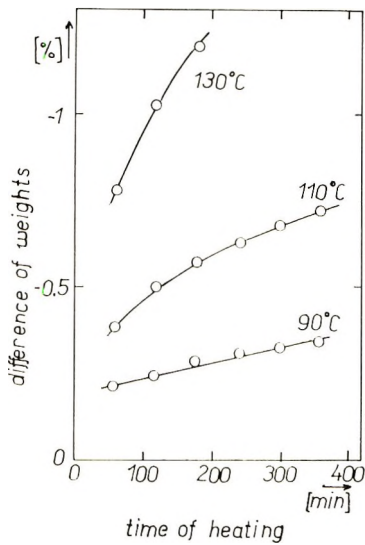duction, these changes are usually ascribed to reduction in the ordered arrangement of the polymer.

This concept is supported by the evidence cited above that the density of precipitated or cast films is lower than that of the original PVC sample. It is also supported by the course of density changes at temperatures above 90°C.

However, inconsistent with this concept is the fact that density changes as a function of time cannot be described by Avrami's equation, which would be the case normally, if it were merely a matter of increased degree of crystallization. This inconsistency is not usual in view of the fact that there are published cases of crystallization processes which do not satisfy the Avrami equation. The fundamental inconsistency may be stated as follows.

The reduction of molecular arrangement should necessitate not only a decrease in density but also an increase of notch impact strength (according to the data in Table I only a slight drop was noted) and a decrease in temperature embrittlement (according to the data in Table I the reverse effect was observed, viz. a significant increase in embrittlement temperature was caused by precipitation).

This inconsistency cannot be explained on the basis of a reduction in ordered molecular arrangement, or at least not on this basis alone.

By comparison of dynamic properties of samples of the original and precipitated PVC we see that precipitation causes the disappearance of the β maximum in the curve of mechanical attenuation as a function of temperature and also T_α is shifted to lower temperatures, which is analogous to the results reported by Bohn[19] for mixtures of PVC with plasticizers.
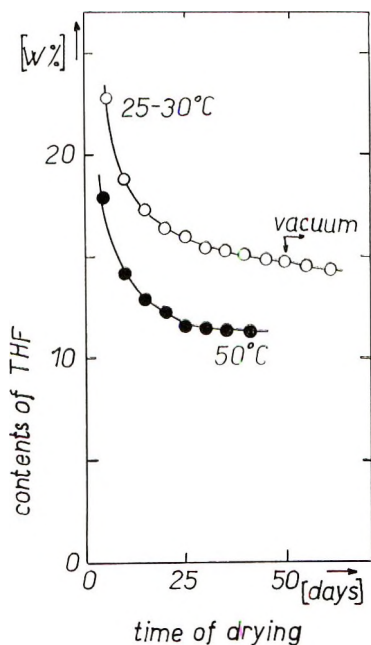
Fig. 9. Quantitative dependence of residual tetrahydrofuran on drying time: (O) at room temperature and (●) at 50°C.

Since our samples contained no added plasticizer, these property changes brought about by precipitation must be a result of the influence of solvent residues, even though one would expect that THF with a boiling point of 65°C would not remain in mixture after long-term drying, milling at 160°C, pressing at 190°C, and 3 hr tempering at 85°C.

The presence of THF in the samples of precipitated PVC and in cast films was demonstrated as follows.

We should point out that the presence of solvent residues in the mixtures could also explain the density drop of precipitated and cast samples, because THF has a density of 0.888 g/cm³ at 20°C.

Presumably if THF is truly present in the samples, it should be possible to demonstrate a weight loss of samples after a sufficiently long time of heating. Samples of 2 mm sheets prepared from precipitated PVC (Halvic 223) were therefore heated at various times at 90, 110, and 130°C. The dependence of weight loss as a function of time and temperature of heating is seen on Figure 8. The weight loss of the samples increases quite naturally with increasing temperature and with tempering time.

For identical time treatments the weight loss of an identically prepared and identically tempered sample of original PVC was compared with a sample of precipitated PVC to check the possibility of polymer degradation. For the 4-mm sheets of original polymer the weight loss after 6 hr at 110°C was 0.062%, while with sheets of precipitated PVC the weight loss was 0.32%.
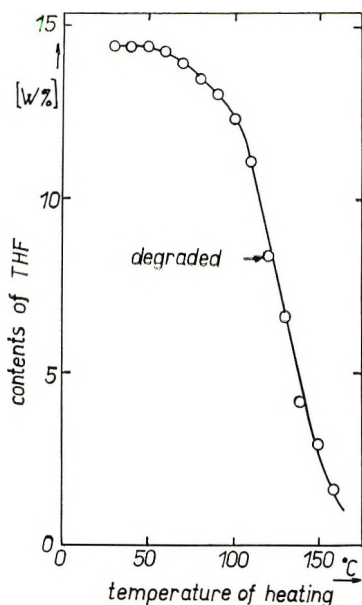
Fig. 10. Quantitative dependence of residual tetrahydrofuran on heating temperature. Heated 1 hr at temperature T, weighed, and then temperature increased by 10°C.

Under identical conditions, viz., after 6 hr at 110°C, the weight loss of powdered original PVC was 0.59%, while the weight loss of precipitated PVC was 8.42%.

Films cast from solution were dried at room temperature first in a fume chamber, then a week under vacuum, and finally for 1 year at room temperature. The weight loss of these films after 6 hr drying at 110°C was 5.8%.

Conclusive evidence that precipitated PVC does lose THF during this heat treatment was demonstrated by means of pyrolytic gas chromatography at 250°C.

Since the weight loss of samples by tempering shows only the presence of residual solvent and gives no idea of the absolute quantity, questions of theoretical and practical importance may be asked: (1) what quantity of THF is present in the PVC samples dried at normal or elevated temperature to constant weight? (2) In case this amount is not zero, is it possible to remove these solvent residues?

In a Petri dish 50 g of PVC was dissolved in 200 ml of THF. The amount of residual THF as a function of drying time at room temperature and at 50°C is shown in Figure 9. From this figure it can be seen that the drying of PVC–THF mixture to constant weight does not mean the total removal of solvent and that use of vacuum is not effectual in reducing the quantity of remaining solvent.

Figure 10 shows the THF residue as a function of temperature for a sample dried at room temperature to constant weight by heating con-

tinuously for 1 hr at temperature T and weighed. Then the drying temperature was increased 10°C. From Figure 10 it can be seen that degradation of the sample occurs in advance of drying. Thus the curve shows not only the solvent loss but also the weight loss of PVC by degradation. The sample of original powder of PVC, which had nearly the same color as the cast sample dried at 120°C (marked degraded) had a weight loss of 2.6%. One might object that PVC without stabilizer was used for drying and that the addition of stabilizer perhaps could delay the
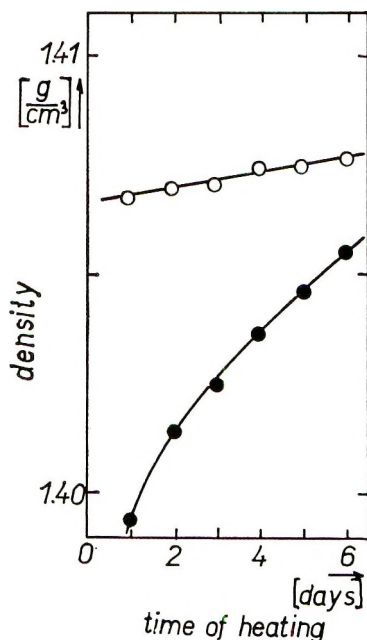
Fig. 11. Density dependence on tempering time at 110°C for samples of (○) original PVC and (●) precipitated PVC.

degradation and permit a more efficient drying of sample. For investigation of this possibility we used samples of 2 mm sheet prepared in the same way but consisting partly of original and partly of precipitated polymer. The plot of density of these samples as a function of tempering time at 110°C is shown in Figure 11. From this figure it can be seen that with increasing time of drying the density of precipitated samples approaches that of samples of original PVC (and may conceivably approach its limit). From a practical point of view, it is impossible to reach the density of original polymer because the samples are quite degraded after 6 days of tempering.

CONCLUSION

It has been proved that the property differences between the original PVC samples and solvent-cast PVC films or samples precipitated from THF solutions is due in part to incomplete removal of solvent and that the residual solvent remains even when the samples are heat-treated at high temperatures for extremely long times.

Due to the impossibility of transformation of precipitated polymer back to the original polymer (because of the impossibility of thoroughly drying PVC) it is concluded that neither samples of precipitated PVC nor samples of cast PVC films can be compared directly to original polymer. It is very important therefore that the authors of some investigations[2-7,10-14] who were unaware of this phenomenon recheck their conclusions. Their studies deal with the influence of molecular weight and of distribution of molecular weights on PVC properties.

It is obvious that properties of cast films or of precipitated PVC will be less dependent on polymer characteristics for example, on molecular weight of comparable fractions than on content of residual solvent.

By comparison of dynamic properties of samples from the original and from precipitated PVC it is apparent that the precipitation processing eliminates the β maximum of mechanical attenuation. Bohn[19] sets down the dissolution of β maximum up to a total locking limitation of movement of chain sections. Quite logically if it is possible to lock the movement of chain segments by interaction of solvent with polymer, it is also possible to cause retention by the same interaction of polymer with solvent, a retention of a significant amount of solvent in sample.

References

1. O. C. Bockman, *J. Polym. Sci. A*, **3**, 3399 (1965).

2. Yu. V. Glazkovskiĭ, V. E. Zgaevskiĭ, S. P. Ruchinskiĭ, and N. M. Bakardinhiev, *Vysokomol. Soedin.*, **8**, 1472 (1966).

3. E. Gallinella and C. Garbuglio, *Chim. Ind. (Milan)*, **47**, 1208 (1965).

4. A. Nakajima, H. Hamada, and S. Hayashi, *Makromol. Chem.*, **95**, 40 (1966).

5. O. Seipold and Th. Marx, *Plaste Kautsch.*, **1**, 11 (1954).

6. V. P. Lebedev, N. A. Okladnov, K. S. Minsker, and B. P. Shtarkman, *Vysokomol. Soedin.*, **7**, 655 (1965).

7. D. N. Bort, Yu. V. Ovchinnikov, and E. E. Rylov, *Vysokomol. Soedin.*, **4**, 935 (1962).

8. V. P. Lebedev, L. E. Derlyukova, I. N. Razinskaya, N. A. Okladnov, and B. P. Shtarkman, *Vysokomol. Soedin.*, **7**, 333 (1965).

9. H. Kaltwasser, F. Krause, and H. Grohn, *Plaste Kautsch.*, **13**, 129 (1966).

10. F. Krasovec and A. Peterlin, *J. Stefan Inst. Repts.* (Ljubljana), **3**, 213 (1956).

11. S. A. Shevlyakov and M. T. Bryk, *Plast. Massy*, **1966**, No. 2, 40; *ibid.*, **1966**, No. 4, 5.

12. M. T. Bryk, A. S. Shevlyakov, and G. A. Puchkovskaya, *Plast. Massy*, **1966**, No. 8, 9.

13. A. Kaminska, *Polimery*, **9**, No. 2, 48 (1964).

14. S. Krozer, *Polimery*, **10**, No. 9, 397 (1965).

15. L. A. Igonin, V. A. Ermolina, Yu. V. Ovchinnikov, and V. A. Kargin, *Vysokomol. Soedin.*, **1**, 1327 (1959).

16. V. Nardi, G. Pisent, and M. Mammi, *Nuovo Cimento* (suppl.), **26**, 1 (1962).

17. D. Kockott, *Kolloid-Z.*, **198**, 17 (1964).

18. F. R. Reding, E. R. Walter, and F. J. Welch, *J. Polym. Sci.*, **56**, 225 (1962).

19. L. Bohn, *Kunststoffe*, **53**, 826 (1963).

Syntheses and Reactions of Functional Polymers. XLVI. Preparation and Reactions of N-Benzyloxyisomaleimide–Styrene Copolymer

MASAYASU AKIYAMA, YASUHIRO YANAGISAWA, and MAKOTO OKAWARA, *Research Laboratory of Resources Utilization, Tokyo Institute of Technology, Ookayama, Meguro-ku, Tokyo, Japan*

Synopsis

Polymerization of N-benzyloxymaleimide(I) was attempted to obtain a polymer with the N-hydroxysuccinimide unit in the chain. In the light of infrared and NMR data the compound reported by Ames as N-benzyloxymaleimide is N-benzyloxyisomaleimide (III). Homopolymerization of III did not give polymer. Copolymerization of III with styrene was carried out in dioxane at 70°C. A strong alternation tendency like that of maleimides was observed. Monomer reactivity ratios and $Q-e$ values were determined. Copolymer having the isoimide structure showed infrared absorptions at 1815 and 1675 cm^{-1} in the carbonyl region. The copolymer was isomerized to N-benzyloxymaleimide type copolymer and debenzylated to N-hydroxymaleimide type copolymer. An insoluble copolymer was prepared by using divinylbenzene as a crosslinking agent and was converted to N-acetoxymaleimide type copolymer, which was used as an insoluble acetylating agent.

INTRODUCTION

Highly reactive and racemization-free N-hydroxysuccinimide esters of the amino acids and peptides are sometimes used as a potent "activated" ester for the peptide synthesis.[1,2] In a study on polymeric reagents, we were interested in the preparation and use of polymers having N-hydroxysuccinimide units in the chain. Use of such polymers, would facilitate various procedures in synthesis, i.e., separation of reaction mixture, purification of the product, and recovery of the original hydroxy polymer. Such a polymer was obtained[3] in previous studies from styrene–maleic anhydride copolymer by means of polymer modifications and was used as a polymeric agent in acylation of amines. In the meantime, another study on the use of linear and crosslinked N-hydroxysuccinimide polymers prepared from ethylene–maleic anhydride copolymer has been reported by Laufer et al.[4]

In order to obtain the crosslinked bead-type polymer which is expected to be much easier in handling, a preparative route via polymerization of a definite monomer should be investigated. In the present study, copoly-

merization of N-benzyloxyisomaleimide with styrene and modifications of the derived polymer to the N-hydroxyimide type polymer are described.

RESULTS AND DISCUSSION

Ames and Grey[5] reported the formation of N-benzyloxymaleimide (I) by thionyl chloride treatment of N-benzyloxymaleamic acid (II), which was derived from maleic anhydride and O-benzylhydroxylamine in benzene.
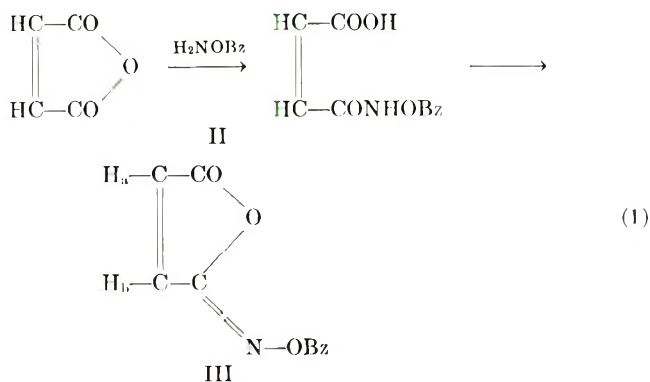
$$\begin{array}{c} \text{HC—CO} \\ \| \qquad\qquad \diagdown \\ \qquad\qquad\qquad \text{N—OBz} \\ \| \qquad\qquad \diagup \\ \text{HC—CO} \end{array}$$

I Bz; —CH₂C₆H₅
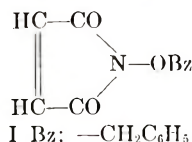
Examination of the product obtained by Ames's procedure revealed that it is N-benzyloxyisomaleimide (III) as shown by eq. (1)

$$\begin{array}{ccc} \text{HC—CO} & & \text{HC—COOH} \\ \| \qquad \diagdown & \xrightarrow{\text{H}_2\text{NOBz}} & \| \qquad \qquad \longrightarrow \\ \qquad\qquad \text{O} & & \\ \| \qquad \diagup & & \| \\ \text{HC—CO} & & \text{HC—CONHOBz} \\ & \text{II} & \end{array}$$

$$\begin{array}{c} \text{H}_\text{a}\text{—C—CO} \\ \| \qquad\qquad \diagdown \\ \qquad\qquad\qquad \text{O} \\ \| \qquad\qquad \diagup \\ \text{H}_\text{b}\text{—C—C} \\ \qquad\qquad \diagdown\!\!\diagdown \\ \qquad\qquad\qquad \text{N—OBz} \\ \qquad \text{III} \end{array} \qquad\qquad (1)$$

Several isoimides are reported in the literature, and the formation seems to depend on the reaction conditions used.[6] The infrared spectrum of the isoimide (III) exhibited a strong absorption due to the carbonyl group at 1 795 cm^{-1} and a weak absorption due to the —C=N— linkage at 1 630 cm^{-1}. These absorptions are observed in isoimides but not in normal imides. The NMR spectrum showed two doublet peaks at 7.20 δ due to H$_\text{a}$, and at 6.30 δ due to H$_\text{b}$, indicating unsymmetrical nature of the molecule.

Attempted isomerization of the isoimide into the imide (I) under thermal, photochemical and catalytic conditions has not yet succeeded. Homopolymerization of the isoimide in dioxane with azobisisobutyronitrile (AIBN) at 70°C did not give a polymer. Copolymerization of the isoimide with styrene produced polymer. The copolymerization was conducted in dioxane with the use of AIBN as an initiator at 70°C. The results are shown in Table I and the copolymerization diagram is presented in Figure 1. A marked tendency for alternation can be observed in the isomaleimide–styrene copolymerization. The monomer reactivity ratios were calculated according to the usual methods yielding values for r_1 for N-benzyloxyisomaleimide of 0.09 ± 0.06 and for r_2 for styrene of 0.22 ± 0.08. Q and e values for the isomaleimide are 0.96 and 1.18, respectively.

TABLE I

Copolymerization of N-Benzyloxyisomaleimide with Styrene[a]

	Initial mixture				Polymer composition	
No.	Styrene, mole-%	Benzyl-oxyiso-male-imide, mole-%	Conver-sion, %	Analysis (found) N, %	Styrene, mole-%	Benzyl-oxyiso-male-imide, mole-%
1	90	10	13	2.63	76	24
2	80	20	14	3.34	68	32
3	60	40	16	4.26	55	45
4	50	50	15	4.45	52	48
5	40	60	13	4.42	52	48
6	20	80	10	4.83	46	54
7	10	90	4	5.47	36	64

[a] Polymerization conditions: 70°C in dioxane; monomer mixture, 2.18 mole/l.; AIBN initiator, 0.18 mole/l.

The Q, e values reported[7] for maleimide–styrene are 1.8 and 1.34, respectively.

The infrared spectrum of the typical alternating copolymer of isomaleimide–styrene (IV) showed two strong absorptions at 1 815 and 1 675 cm^{-1}, of which the former was due to the carbonyl group of the five-membered
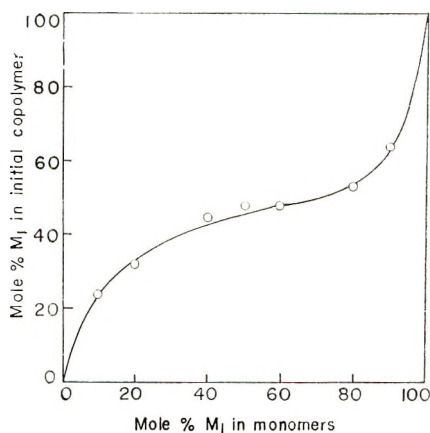

Fig. 1. Copolymerization diagram for N-benzyloxyisomaleimide (M_1) and styrene (M_2).

isoimide ring and the latter might be ascribed to the —C=N— linkage. Literature reports indicate that several attempts to prepare isoimides with a saturated ring system were unsuccessful.[6] In our case, a saturated isoimide structure was easily obtained by polymerization of an unsaturated isoimide.

$$ (2) $$

IV   V

When copolymer IV was treated with hydrochloric acid in dioxane at 70°C, isomerization of the isomaleimide moiety occurred, and normal N-benzyloxyimide type copolymer (V) was produced. The conversion was high but not quantitative. The infrared spectrum of polymer V displayed carbonyl absorptions at 1780 and 1720 cm^{-1} which are characteristic of normal saturated imides. Absorptions due to free N-hydroxyl group were not detected. Treatment of polymer IV with acetic acid alone at 70°C did not cause isomerization. The isomerization might be brought about at first by cleavage of the isoimide ring, and then by cyclization of the resulting amic acid moiety to the imide structure.

In connection with the isomerization, a preparation of a polymer with N-benzyloxymaleamic acid units in the chain was attempted to test the ease of cyclization of the amic acid. Copolymerization of the amic acid with styrene in dioxane at 75°C using AIBN gave polymer V′, whose infrared spectrum showed that most of the carbonyl absorption was due to the imide group and not to the amic acid group.

$$ (3) $$

II   V′

The imide structure was obtained by polymerization at elevated temperature. It was thought that a polymer having the amic acid alone might be difficult to prepare because of the ease of cyclization. On treatment with hydrochloric acid, polymer V′ gave polymer V.

Debenzylation of the N-benzyloxy group is not familiar, although the benzyl group is usually removed by action of hydrogen bromide in acetic acid at room temperature. Treatment of the normal type imide polymer V with hydrogen bromide in acetic acid at elevated temperature for 2 hr gave debenzylated N-hydroxymaleimide type copolymer (VI).

V   VI   VII

$$ (4) $$

The structure of polymer VI was confirmed by the agreement of infrared absorption peaks with those of the polymer obtained previously.[3] By the reaction of polymer VI with acetic anhydride in dimethylformamide (DMF) at room temperature, N-acetoxyimide type copolymer (VII) was easily obtained. The infrared spectrum of polymer VII and the corresponding polymer previously obtained were the same.[3] The hydrogen bromide treatment of the isoimide polymer IV gave N-hydroxyimide polymer VI. In this treatment, isomerization followed by debenzylation took place.

Copolymerization of the isomaleimide with styrene in the presence of divinylbenzene yielded a crosslinked copolymer (VIII). This polymer was isomerized and debenzylated by routine treatment and acetylated with acetic anhydride in DMF to give an insoluble N-acetoxyimide type copolymer (X), which had partly unreacted isomaleimide functions as well as N-acetoxyimide units. The infrared spectrum showed several peaks in the carbonyl region. The transformation of the inner part of the crosslinked polymer was not obtained. The acetoxy imide content of the copolymer X was determined to be 88 mmole/g by a chemical method based on the reaction of polymer X with cyclohexylamine to give N-cyclohexylacetamide. The amide produced was pure enough not to require recrystallization.

This crosslinked polymer can be used as an insoluble polymeric reagent in such solvents as DMF, and use of these polymers simplifies the work-up of acetylation reactions.

EXPERIMENTAL

Infrared spectra of the products were obtained on potassium bromide disks by use of a Hitachi infrared photometer, Model EPI-S2; the NMR spectrum was obtained in carbon tetrachloride solution with tetramethylsilane as an internal standard.

Monomer Preparation

N-**Benzyloxymaleamic Acid (II).** According to Ames' procedure,[4] maleic anhydride was treated with an equimolar amount of O-benzylhydroxylamine in benzene at room temperature for 2 hr to yield II as a precipitate. Recrystallization from chloroform gave crystals of II, mp 122–123°C (Lit.[4] mp, 121–122°C).

ANAL. Calcd for $C_{11}H_{11}O_4N$: N, 6.33%. Found: N, 6.47%.

N-**Benzyloxyisomaleimide (III).** According to Ames' procedure,[4] the amic acid II was treated with thionyl chloride in benzene at refluxing temperature, followed by work-up procedures to give III. Recrystallization from *n*-hexane gave colorless needles, mp 80–80.5°C (Lit.[4] mp, 80–81°C).

ANAL. Calcd. for $C_{11}H_9O_3N$: C, 65.02%; H, 4.46%; N, 6.89%. Found; C, 64.93%, H, 4.60%; N, 6.91%.

Peaks of the NMR spectrum were 7.28 δ (singlet 5H due to aromatic ring hydrogens), 7.22 δ (doublet 1H), 6.30 δ (doublet 1H), and 5.13 δ (singlet 2H due to benzylic methylene hydrogens).

Polymerization

Copolymerization of the isomaleimide with styrene was performed in dioxane with azobisisobutyronitrile (AIBN) as an initiator. The total amount of monomers was 2.18 mole/l, and the amount of initiator was 0.18 mole/l. The polymerization tubes were sealed off under vacuum and heated in a bath thermostatted at 70°C for 0.5–1.0 hr. The polymer solution was then poured in methanol, and the polymer was purified by reprecipitation from tetrahydrofuran to methanol. The polymer composition was determined by nitrogen analysis. The results are shown in Table I and Figure 1. The monomer reactivity ratios were obtained by use of both the Fineman-Ross and the linear line-crossing technique, and the Q-e value was calculated according to the usual copolymerization equation.

Homopolymerization of the isomaleimide (4.06 g, 0.02 mole) in dioxane (10 ml) with AIBN at 70°C gave a trace of precipitate which was insoluble in ether but soluble in methanol.

Preparative-scale polymerization was carried out in an open flask with stirring under an atmosphere of nitrogen. A solution of isomaleimide (15.0 g) and styrene (15 ml) in benzene (230 ml) was heated at 70°C for 6 hr with AIBN (620 mg), and then subjected to the usual work-up procedures; the procedure gave 15.2 g of N-benzyloxyisomaleimide–styrene copolymer (IV). Analysis showed 4.21% N.

The major infrared absorptions were at 1815, 1675, 1495, 1455, 1370, 1125, 1020, 985, 735 and 700 cm^{-1}. The inherent viscosity in DMF (0.5 g/100 ml) was 0.06.

Conversion of Copolymer IV into N-Benzyloxymaleimide–Styrene Copolymer (V)

A mixture of 3.00 g of IV in 40 ml of dioxane and 20 ml of concentrated hydrochloric acid was heated at 60–70°C for 2 hr. The reaction mixture was poured into 500 ml of water, and the separated polymer was collected by filtration, washed with water, and dried. After reprecipitation from dioxane to methanol, the yield was 2.4 g. Analysis showed 3.66% N.

The infrared absorption peaks of polymer V were at 1780, 1720, 1495, 1455, 1380–1345, 1210, 1055, 740, and 700 cm^{-1}. The polymer could not be acetylated with acetic anhydride in DMF.

Conversion of Copolymer V into N-Hydroxymaleimide–Styrene Copolymer (VI) and Its Acetylation

A mixture of 100 mg of polymer V and 5 ml of a solution of hydrogen bromide (20%) in acetic acid was heated at 65°C for 3 hr. The reaction mixture was poured into 100 ml of water, and the precipitated polymer VI

was collected. The infrared absorptions of the polymer were at 3500–2700, 1780, 1705, 1495, 1455, 1070, and 700 cm^{-1}, and the spectrum was identical with that of the N-hydroxymaleimide type copolymer obtained previously.[3]

Polymer VI was further subjected to acetylation. The polymer VI thus obtained (ca. 40 mg) was treated with 1 ml of an acetic anhydride-DMF (1:1) solution at room temperature for 10 hr. The solution was poured into methanol and the product was separated and dried. The product, copolymer of N-acetoxymaleimide–styrene (VII), showed absorption peaks at 1815, 1785, 1740, 1495, 1455, 1370, 1220, 1165, 1050, 830, and 700 cm^{-1}, which were identical with those of the previously obtained N-acetoxyimide copolymer.[3]

Conversion of Polymer IV to Polymer VI in HBr–AcOH

A mixture of 6.0 g of polymer IV and 60 ml of a solution of hydrogen bromide (10%) in acetic acid was heated at 70°C for 2.5 hr. The polymer did not dissolve but was deformed in shape in the acid solution. The reaction mixture was poured into 500 ml of water, and the polymer was collected, washed with water, and dried. Reprecipitation from DMF to methanol–water gave polymer VI. The yield was 4.7 g (theoretical conversion, 4.3 g). Analysis showed 3.91% N.

The infrared spectrum of the product was the same as that of the polymer obtained from polymer V. Detection of a small fraction due to polymer V was difficult. The spectrum showed that the structure was the anticipated one.

Copolymerization of N-Benzyloxymaleamic Acid with Styrene

A mixture of 5.53 g of the amic acid II, 10 ml of styrene and 100 mg of AIBN in 40 ml of dioxane was heated at 75°C for 8 hr in a sealed tube. The polymer solution was poured into 500 ml of methanol. The polymer collected was 3.6 g (polymer V'). The infrared spectrum showed a strong absorption at 1700 cm^{-1} and a small absorption at 1780 cm^{-1}, together with small bands at 1680–1600 cm^{-1}. The strong absorptions of the amic acid in the region 1600–1400 cm^{-1} almost disappeared. When polymer V' was treated with hydrochloric acid, a decrease of absorptions at 1680–1600 cm^{-1} was observed, which showed further conversion of polymer V' to polymer V.

Crosslinked Copolymer of N-Benzyloxyisomaleimide and Styrene(VIII)

A mixture of 5.0 g of N-benzyloxyisomaleimide, 4.0 ml of styrene, 0.5 ml of divinylbenzene, and 0.20 g of benzoyl peroxide in 100 ml of water containing a small quantity of poly(vinyl alcohol) was heated at 80°C for 2 hr with stirring under a stream of nitrogen. The separated polymer was washed by swelling in acetone; then it was collected and dried under vacuum. It was not beadlike in shape. The total yield was 6.21 g.

Reactions of Polymer VIII

Conversion to N-Hydroxyimide Type Polymer (IX) and N-Acetoxyimide Tape Polymer(X). A 2.0-g portion of polymer VIII was added to 5.0 ml of hydrogen bromide (10%)–acetic acid solution, and the mixture was heated at 60°C for 3 hr. The product was collected and washed with water. This was considered to be crosslinked N-hydroxymaleimide–styrene copolymer (IX). The polymer IX was further treated with acetic anhydride–DMF solution at room temperature for 12 hr. The polymer was separated by decantation and washed with methanol. The yield of the polymer was 1.7 g. This polymer was a copolymer of N-acetoxymaleimide–styrene (X). The infrared spectrum showed absorptions in the carbonyl region at 1815, 1785, 1740, 1720, and 1675 cm^{-1}, suggesting that the polymer contained other than the N-acetoxyimide function.

Reaction of Polymer X. A mixture of 1.0 g of polymer X and a slight molar excess of cyclohexylamine in DMF was allowed to react at room temperature for 10 hr and then the polymer was removed by filtration. Evaporation of the filtrate gave 124 mg crude N-cyclohexylamide, mp 103°C Lit.[8] mp, 104°C) without recrystallization. This value corresponded to 0.88 mmole/g of acetoxy content in polymer X.

References

1. G. W. Anderson, J. E. Zimmerman, and F. M. Callahan, *J. Amer. Chem. Soc.*, **89**, 178 (1967).

2. D. A. Laufer and E. R. Blout, *J. Amer. Chem. Soc.*, **89**, 1246 (1967).

3. M. Akiyama, M. Narita, and M. Okawara, *J. Poly. Sci. A-1*, in press.

4. D. A. Laufer, T. M. Chapman, D. I. Marlborough, V. M. Vaidya, and E. R. Blout, *J. Amer. Chem. Soc.*, **90**, 2698 (1968).

5. D. E. Ames and T. F. Grey, *J. Chem. Soc.*, **1955**, 631.

6. E. Hedaya, R. L. Hinman, and S. Theodoropulos, *J. Org. Chem.*, **31**, 1311, 1317 (1966).

7. G. Van Paesschen and D. Timmerman, *Makromol. Chem.*, **78**, 112 (1964).

8. *Dictionary of Organic Compounds*, J. R. A. Pollock, Ed., 4th ed., Eyre and Spottiswoode, London, 1965, p. 790.

Sulfur Modification of Polyethylene Surfaces.   I. Insertion of Sulfur into Polyethylene Surfaces

DOUGLAS A. OLSEN* and A. JEAN OSTERAAS,† *Research Center, Ashland Chemical Co., Minneapolis, Minnesota 55420*

Synopsis

Atomic sulfur generated respectively by the pyrolysis of carbonyl sulfide and by the photolysis of carbonyl sulfide, carbon disulfide, and sulfur vapors has been shown to modify irreversibly the surface of polyethylene as shown by wettability measurements. The nature of the modification is not completely apparent from this portion of the study, however, insertion of the atomic sulfur into a carbon–hydrogen bond to form a surface thiol group appears likely.   The modified surfaces thus formed are shown to undergo several classical organic reactions, as determined by wettability measurements.

INTRODUCTION

It has been shown that substituted carbenes and nitrenes react with polyethylene and other polymer surfaces.[1]   Since atomic sulfur is isoelectronic with both carbenes and nitrenes, it would seem reasonable to expect that atomic sulfur also reacts with the carbon–hydrogen bonds of polymers, thus forming mercaptans (thiols) on the surfaces.   The literature also refers to several instances of insertion of atomic sulfur into carbon–hydrogen bonds with formation of mercaptans.[2]   Atomic sulfur also reacts with olefinic double bonds to give thiiranes.[3]   The latter references, however, are for reactions taking place in the bulk of the material and are not surface reactions.   In the work discussed here the reactions of hydrocarbon surfaces and atomic sulfur are considered.

In the previous studies, the substituted carbenes and nitrenes were first reacted with a polyethylene surface.   The critical surface value γ_c of the new surface was then determined and compared with the critical surface tension values of commonly available polymers.   In this instance, literature data are not available for the critical surface tension values of sulfur-containing polymers.   Thus, the procedure here is: (1) to show that all reactions between atomic sulfur and polyethylene surfaces give consistent critical surface tension values which differ considerably from the critical surface tension value of sulfur, and (2) to show that the sulfur-modified

* Present address: Applied Science Division, Litton Systems, Inc., Minneapolis, Minn. 55413.

† Present address: Research Division, Gould-National Batteries, Inc., Minneapolis, Minn. 55414.

(thiol) surface may be oxidized to a sulfonic acid surface which can undergo further reactions.

An alternate procedure which will be reported later is to form the sulfonic acid surface by direct sulfonation and compare its properties with a sulfonic acid surface prepared by oxidation of the thiol surface.[4]

EXPERIMENTAL PROCEDURE

Preparation of Atomic Sulfur

The literature was searched for probable precursors of atomic sulfur. Among the possibilities found were carbonyl sulfide (COS),[2,3] ethylene episulfide (CH₂—CH₂—S),[5] and carbon disulfide (CS₂);[5] all generated through photolysis. Elemental sulfur also appeared to be a possible precursor for thermolysis, although extremely high temperatures (1 500°C) might be necessary.[6] In most of the work discussed below photolysis was used; however, it will be seen that carbonyl sulfide can also be reacted through thermolysis and elemental sulfur can be used at temperatures much lower than 1 500°C by a combination of heat and photolysis. Ethylene episulfide was not readily available and hence was not considered further.

Pyrolysis and Photolysis Equipment

The pyrolysis experiments with COS or elemental sulfur took place in essentially the same equipment as used for the pyrolysis of carbene/nitrene precursors,[1] viz., in a pyrolysis chamber at about 350°C with a diffusion distance of 1.4 cm and a time of exposure sufficient to soften the polymer substrate. For the gaseous COS the chamber was equipped with entry and exit ports.

In the photolysis experiments, the radiation source was an Hanovia Model 7420 mercury arc lamp. The polymers to be thus modified were suspended in quartz flasks. For exposure to gaseous COS the flasks were equipped with entry and exit ports. For exposure to CS₂ a small amount of liquid in the flask provided sufficient vapor; runs were made both in air and nitrogen. No detectable difference was noted. All reactions were carried out at room temperature; however, the mercury arc generated sufficient heat within the polymer to soften it slightly. The normal time of exposure was 30–60 min. The lamp and sample were generally about 16 cm apart.

For the experiments with elemental sulfur, heat (~125°C) was used to vaporize the sulfur; this, together with simultaneous photolysis, generated the atomic sulfur. In this instance a quartz plate covered the pyrolysis chamber and completely enclosed the polymer to be treated. Other conditions were the same as for photolysis.

Substrate

The polyethylene sheets used in this study were of a commercially available grade (Cadillac Plastic and Chemical Co.). Before exposure to pyrolysis vapors, the sheets were washed in detergent, with subsequent copious rinsing first in tap water and then in distilled water.[7] Wettability measurements on the cleaned polyethylene surfaces gave the expected γ_c values of 31 dyne/cm,[8] thus establishing the suitability of the substrate and the cleaning procedure.

Surface Reactions

Samples of polyethylene exposed to atomic sulfur generated during the pyrolysis of photolysis reaction were subjected to several classical organic reactions and the resulting critical surface tension value measured. Since the surface was immobile, the reaction conditions were more stringent than the classical analogs. The various reaction conditions are given in Table I. Controls were also used; in these runs polyethylene which had not been exposed to atomic sulfur was subjected to the same reaction conditions. No change in the original γ_c value was observed.

TABLE I
Reaction Conditions

Reaction	Type	Chemicals	Conditions
(2)	Oxidation	0.5M KMnO$_4$	pH 10; 4 hr, 99°C, 25 hr, 25°C
(2)	Neutralization	25% HNO$_3$	10 min, 25°C
(3)	Chlorination	POCl$_3$ (undiluted)	10 min, 25°C
(4)	Fluorination	CF$_3$CH$_2$OH	20 min, 25°C
(7)	Oxidation	0.5M KMnO$_4$	pH 10; 11 hr. 99°C; 16 hr. 25°C
(7)	Neutralization	3M HCl	30 min, 25°C
(8)	Chlorination	PCl$_5$ in CCl$_4$ (thick slurry)	30 min, 25°C
(9)	Amination	6M NH$_4$OH	24 hr, 25°C
(10)	Formylation	Formaldehyde	8 hr, 25°C
(11)	Fluorination	Trifluoroacetic anhydride	24 hr, 25°C
(5), (12)	Hydrolysis	10% KOH	10 hr, 100°C

Wettability Measurements

Advancing contact angles were measured directly by using an Eberbach telescopic cathetometer equipped with a circular protractor. The procedure was essentially that described by Schonhorn and Ryan.[9] The wetting liquids were those used previously in this laboratory.[10]

For each drop of wetting liquid, three or more contact angle measurements were made on each side of the drop. The reproducibility was generally about ±3°. Contact angles were also verified on duplicate sur-

faces.   The contact angle values thus obtained for each liquid were aver-
aged with the cosines shown in the figures as circles and triangles, the most
extreme values being given as the error.   In general the standard deviation
would be less than the error shown.

RESULTS AND DISCUSSION

Surface Treatment

As mentioned above, no literature values are available for the γ_c values of
mercaptanlike polymer surfaces.   This is unlike the previous work with
carbenes and nitrenes, where insertion produces surfaces with γ_c values pre-
dictable from a knowledge of existing polymer surfaces.   The procedure
here has been to demonstrate that the reaction of atomic sulfur with poly-
mer surfaces produces a surface with a consistent γ_c value differing from
that of the original polymer and from that of sulfur.   The γ_c value of the
stable room temperature form of sulfur (orthorhombic) is known to be 30
dyne/cm.[10]

The experimental results for the various atomic sulfur precursors are
shown in Figure 1 and are summarized in Table II.   From the data of

TABLE II
Critical Surface Tension Values of Treated Polymer Surfaces

| Substrate | Precursor | γ_c, dyne/cm | | |
		Pyrolysis	Photolysis	Heat and photolysis
Polyethylene	COS	39	38.5	—
(γ_c = 31)	S	30.5[a]	—	39, 40
	CS$_2$	—	38	—

[a] Value is that of elemental sulfur adsorbed on surface.[10]

Table II it is possible to assign a tentative γ_c of 39 $\pm$ 1 dyne/cm to the
sulfur-treated surfaces.   This value is clearly different from the γ_c of 30
dyne/cm of elemental sulfur.   In view of these values, together with the
known chemistry of atomic sulfur, an insertion reaction is indeed reason-
able, viz:

$$\boxed{}\text{--H} + \text{S} \rightarrow \boxed{}\text{--SH}$$
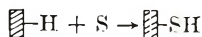
The following discussion further amplifies the likelihood that insertion of
atomic sulfur occurs at the C—H bonds of polyethylene surfaces.

Reactions of Thiol Surfaces

If sulfur is inserted at the polyethylene surface, as suggested above, then
the newly formed thiol surface should react as a mercaptan and undergo the
classical reactions of mercaptans.   Two such reaction schemes are pre-
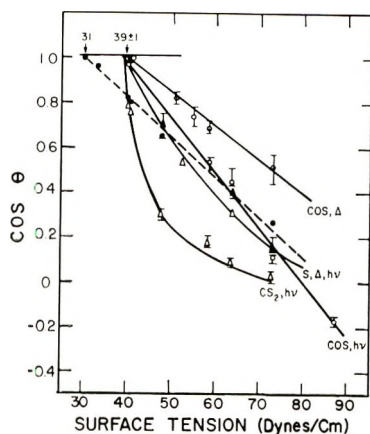sented here.   The general procedure is similar to that used in the previous

Fig. 1. Wettabilities of polyethylene exposed to atomic sulfur generated from the various precursors noted. The curvature of the data for sulfur and carbon disulfide is similar to that observed previously.[10] The dashed line presents data for polyethylene exposed to unphotolyzed sulfur vapor.

investigations of carbenes and nitrenes, in that upon completion of each reaction in the reaction scheme γ_c values were determined and compared with expected values wherever possible.

In the first reaction sequence the polyethylene surface was photolyzed in the presence of CS_2 vapors, oxidized by $KMnO_4$, neutralized with HNO_3, chlorinated with $POCl_3$, and fluorinated with 2,2,2-trifluoroethanol. The reactions, products, and γ_c values (with the reaction conditions given in Table I) are given in eqs. (1)–(5).

$$\text{[PE]}-H \xrightarrow[\Delta,\ h\nu]{CS_2} \text{[PE]}-SH \qquad\qquad \gamma_c = 39 \text{ dyne/cm} \qquad (1)$$

$$\text{[PE]}-SH \xrightarrow[HNO_3]{KMnO_4} \text{[PE]}-SO_2OH \qquad\qquad \gamma_c = 53 \text{ dyne/cm} \qquad (2)$$

$$\text{[PE]}-SO_2OH \xrightarrow{POCl_3} \text{[PE]}-SO_2Cl \qquad\qquad\qquad\qquad (3)$$

$$\text{[PE]}-SO_2Cl \xrightarrow{CF_3CH_2OH} \text{[PE]}-SO_2OCH_2CF_3 \qquad \gamma_c = 35 \text{ dyne/cm} \qquad (4)$$

$$\text{[PE]}-SO_2OCH_2CF_3 \xrightarrow{KOH} \text{[PE]}-SO_2OH \qquad \gamma_c = 42 \text{ dyne/cm} \qquad (5)$$
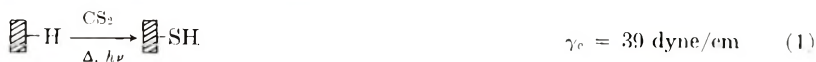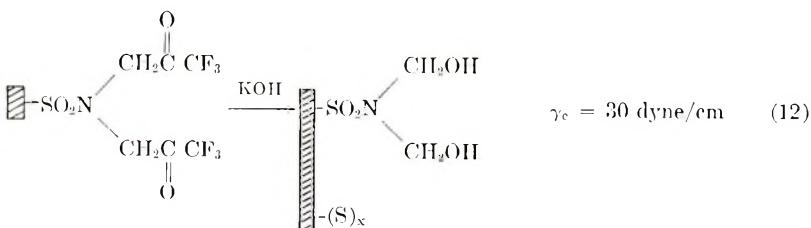
Figure 2 shows the wettability measurements for reactions (1), (2), (4), and (5). These results are in general agreement with expected results, i.e., upon oxidation of the thiol surface to the more polar sulfonic acid surface an increase in the critical surface tension is observed. Treatment with 2,2,2-trifluoroethanol produces a fluorinated surface which, as expected, exhibits a lowered critical surface tension value. This latter γ_c value, while lowered, does not approach the γ_c value of polytetrafluorethylene ($\gamma_c = 18$ dyne/cm) as closely as an analogous step did in previous work with carbethoxycarbene.[1] These results, however, will be shown in a later publica-

tion to be consistent with other similar data.[4]   Finally the γ_4 value for the regenerated sulfonic acid surface is only 42 dyne/cm rather than an expected 50 dyne/cm.   This might indicate only partial hydrolysis or possibly desulfonation with the formation of colloidal sulfur on the polymer surface.   Sulfur having a low critical surface tension would, if present, undoubtedly depress the observed critical surface tension.

In the next reaction sequence the polyethylene surface was photolyzed in the presence of sulfur vapors, oxidized, neutralized, chlorinated, aminated, formylated, fluorinated, and hydrolyzed.   The reactions products and critical surface tension values are given in eqs. (6)–(12).

$$\boxed{}\text{–H} \xrightarrow[\Delta, h\nu]{S} \boxed{}\text{–SH} \qquad\qquad \gamma_c = 39 \text{ dyne/cm} \qquad (6)$$

$$\boxed{}\text{–SH} \xrightarrow[HCl]{KMnO_4} \boxed{}\text{–SO}_2\text{OH} \qquad\qquad \gamma_c = 53 \text{ dyne/cm} \qquad (7)$$

$$\boxed{}\text{–SO}_2\text{OH} \xrightarrow{PCl_5} \boxed{}\text{–SO}_2\text{Cl} \qquad\qquad\qquad (8)$$

$$\boxed{}\text{–SO}_2\text{Cl} \xrightarrow{NH_4OH} \boxed{}\text{–SO}_2\text{NH}_2 \qquad\qquad \gamma_c = 45 \text{ dyne/cm} \qquad (9)$$

$$\boxed{}\text{–SO}_2\text{NH}_2 \xrightarrow{H\overset{O}{\overset{\|}{C}}H} \boxed{}\text{–SO}_2\text{N}\begin{smallmatrix}\text{CH}_2\text{OH}\\ \\ \text{CH}_2\text{OH}\end{smallmatrix} \qquad \gamma_c = 39 \text{ dyne/cm} \qquad (10)$$

$$\boxed{}\text{–SO}_2\text{N}\begin{smallmatrix}\text{CH}_2\text{OH}\\ \\ \text{CH}_2\text{OH}\end{smallmatrix} \xrightarrow{(CF_3C)_2O} \boxed{}\text{–SO}_2\text{N}\begin{smallmatrix}\text{CH}_2\overset{O}{\overset{\|}{C}}\text{ CF}_3\\ \\ \text{CH}_2\text{C CF}_3\\ | \\ O\end{smallmatrix} \qquad \gamma_c = 28 \text{ dyne/cm} \qquad (11)$$

$$\boxed{}\text{–SO}_2\text{N}\begin{smallmatrix}\text{CH}_2\overset{O}{\overset{\|}{C}}\text{ CF}_3\\ \\ \text{CH}_2\text{C CF}_3\\ \| \\ O\end{smallmatrix} \xrightarrow{KOH} \boxed{}\text{–SO}_2\text{N}\begin{smallmatrix}\text{CH}_2\text{OH}\\ \\ \text{CH}_2\text{OH}\end{smallmatrix} \quad \gamma_c = 30 \text{ dyne/cm} \qquad (12)$$

$$-(S)_x$$

Figure 3 shows the wettability measurements for reaction (7), (9), (10), (11), and (12).   Reactions (6)–(8) are identical eqs. (1)–(3) of the previous shorter reaction sequence.

After chlorination and amination of the sulfonated polyethylene, the critical surface tension decreased from 53 to 45 dyne/cm for the sulfonamide surface of reaction (9).   On reaction with formaldehyde, a dimethylol sulfonamide surface is formed, and the critical surface tension is further decreased to 39 dyne/cm; this is close to the value expected (37 dyne/cm) for a poly(vinyl alcohol) surface.[11]   Furthermore, treating the pre-
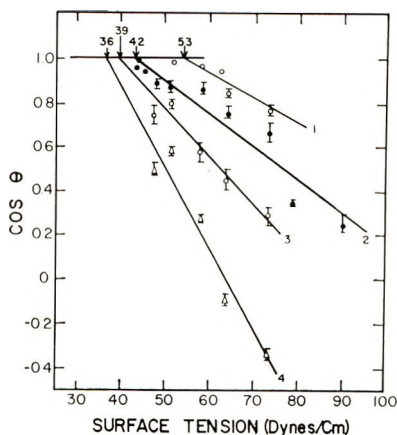
Fig. 2. Wettabilities of polyethylene exposed as follows (see text): (3) formation of surface thiol groups; (1) oxidation of thiol groups to sulfonic acid groups; (4) reaction with POCl₃ and CF₃CH₂OH to give a fluorinated methyl surface; (2) final hydrolysis to partially regenerate sulfonic acid surfaces.
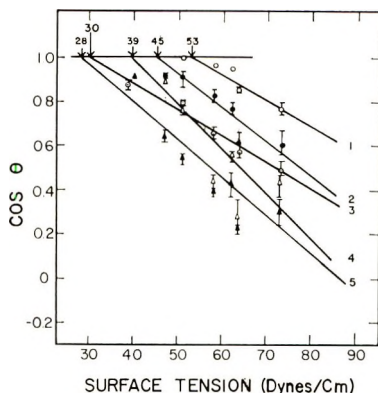

Fig. 3. Wettabilities of polyethylene exposed as follows (see text): (1) sulfonic acid surface groups; (2) further reaction with PCl₅ and NH₄OH to give sulfonamide surfaces; (4) formylation to give a dimethylol sulfonamide surface; (5) reaction with trifluoracetic anhydride to give a fluorinated methyl surface; (3) final hydrolysis regenerating the dimethylol sulfonamide surface along with partial desulfonation.

sumed dimethylol sulfonamide surface with 2,2,2-trifluoroacetic anhydride results in a lower energy surface, since the critical surface tension decreased from 39 dyne/cm for the dimethylol sulfonamide surface to 28 dyne/cm for the N,N-di(trifluoroacetoxymethyl)sulfonamide surface. Hydrolysis of this latter surface gave a γ_c value of 30 dyne/cm which is that of sulfur. This may indicate, as suggested above, that desulfonation may have taken place. (Reflectance spectra results[4] show this to be partially true.)

All of the foregoing results are strong evidence that sulfur does indeed insert into the carbon–hydrogen bonds of the polyethylene surfaces. There is another possibility, though that must also be considered here, viz., that

diffusion of the various reactants into the surface layers of the polyethylene accounts for the observed changes in γ_c values. This possibility is unlikely, since controls were used where the original unmodified polyethylene ($\gamma_c = 31$ dyne/cm) was subjected to the various reactions with no change observed in the γ_c value. Thus, this possibility was not considered further.

In conclusion, it seems highly likely that atomic sulfur does insert into polyethylene surfaces. The thiol surface thus formed has a γ_c value of 39 ± 1 dyne/cm.

References

1. D. A. Olsen and A. J. Osteraas, *J. Appl. Polym. Sci.*, in press.

2. A. R. Knight, O. P. Strausz and H. E. Gunning, *J. Am. Chem. Soc.*, **85**, 1207, 2349 (1963).

3. O. P. Strausz, and H. E. Gunning, *J. Am. Chem. Soc.*, **84**, 4080 (1962).

4. D. A. Olsen and A. J. Osteraas, *J. Polym. Sci. A-1*, in press.

5. H. E. Gunning, in *Elemental Sulfur*, B. Meyer, Ed., Interscience, New York, 1965, Chap. 14.

6. B. Meyer, in *Elemental Sulfur*, B. Meyer, Ed., Interscience, New York, 1965, Chap. 4.

7. M. K. Bernett and W. A. Zisman, *J. Phys. Chem.*, **63**, 1241 (1959).

8. W. A. Zisman, *Adv. Chem. Ser.*, **43**, 1 (1964).

9. H. Schonhorn and F. W. Ryan, *J. Phys. Chem.*, **70**, 3811 (1966).

10. D. A. Olsen, R. W. Moravec, and A. J. Osteraas, *J. Phys. Chem.*, **71**, 4464 (1967).

11. B. R. Ray, J. R. Anderson, and J. J. Scholtz, *J. Phys. Chem.*, **62**, 1220 (1958).

Sulfur Modification of Polyethylene Surfaces.   II. Modification of Polyethylene Surfaces with Fuming Sulfuric Acid

DOUGLAS A. OLSEN* and A. JEAN OSTERAAS,† *Research Center, Ashland Chemical Co., Minneapolis, Minnesota 55420*

Synopsis

Previous work has shown that atomic sulfur irreversibility modifies polyethylene, presumably through an insertion reaction into carbon–hydrogen bonds with formation of surface thiol groups. The thiol groups were then oxidized to sulfonic acid surface groups, which were further reacted chemically as shown by wettability measurements. In this work the thiol group was bypassed and the surface sulfonic acid groups were obtained by exposing the polyethylene surface directly to fuming sulfuric acid. The sulfonic acid groups were reacted further. Critical surface tension values identical with those in the previous work with atomic sulfur were obtained, thus substantiating the previous work.

INTRODUCTION

The first publication in this series[1] showed that atomic sulfur does indeed appear to be inserted into the carbon–hydrogen bonds of polyethylene surfaces to give surface thiol groups which then may be further reacted to give a variety of surface groups.   As was discussed in the previous study, no polymer prototype surfaces existed against which critical surface tension values might be compared.   As will be shown here, it is possible to prepare the same surface groups of the previous study by the alternate procedure of direct sulfonation.   In this study the thiol intermediate was bypassed and the polyethylene surface was converted directly to a sulfonic acid by immersing the film in either fuming sulfuric acid[2] or chlorosulfonic acid[3] with the net reactions shown in eqs. (1) and (2).

$$\boxtimes\text{—H} \xrightarrow{\text{H}_2\text{SO}_4.\text{SO}_3} \boxtimes\text{—SO}_2\text{OH} \tag{1}$$

$$\boxtimes\text{—H} \xrightarrow{\text{ClSO}_3\text{H}} \boxtimes\text{—SO}_2\text{OH} \tag{2}$$

* Present address: Applied Science Division, Litton Systems, Inc., Minneapolis, Minn. 55413.

† Present address: Research Division, Gould-National Batteries, Inc. Minneapolis, Minn. 55414.

EXPERIMENTAL PROCEDURE

Sulfonation

The polyethylene surfaces were sulfonated directly either with reagent grade fuming sulfuric acid or reagent grade chlorosulfonic acid. The optimum degree of surface sulfonation was taken to be that point for which the maximum critical surface tension value was obtained without visible signs of charring. This point corresponded to a critical surface tension γ_c of about 55 ± 3 dyne/cm. Some brown coloration was acceptable, however. The reaction condition necessary to obtain this degree of sulfonation with fuming sulfuric acid was found to be 5 min immersion at 25°C. The chlorosulfonic acid reacted more slowly, and a similar degree of sulfonation occurred after 60 min at 25°C.

Substrate

The polyethylene sheets used in this study were of a commercially available grade (Cadillac Plastic and Chemical Co.) The sheets were washed in detergent, with subsequent copious rinsing first in tap water and then in distilled water before exposure to the sulfonating agents.[4] Wettability measurements on the cleaned polyethylene surfaces gave the expected γ_c value of 31 dyne/cm,[5] thus establishing the suitability of the substrate and the cleaning procedure.

Surface Reactions

Samples of sulfonated polyethylene surfaces were subjected to several classical organic reactions and the critical surface tension value of the surfaces measured. Since the surface was immobile, the reaction conditions were of necessity more stringent than the classical analogs.

For the "short" series, polyethylene film was immersed in fuming sulfuric acid at room temperature for 5 min, rinsed in water, dried, and immersed in a thick slurry of PCl_5 in CCl_4 at 25°C for 15 hr, then immersed in 2,2,2-trifluoroethanol at 25°C for 24 hr, and finally hydrolyzed in 10% KOH for 10 hr at 100°C.

In the "long" series, polyethylene film was immersed in fuming sulfuric acid at 25°C for 5 min, rinsed in water, dried, and immersed in a thick slurry of PCl_5 in CCl_4 at 25°C for 72 hr. This step was carried out in a closed chamber containing a magnetic stirring bar. Constant agitation was necessary to keep the PCl_5 in suspension. After 72 hr, the polyethylene film was immersed in $6M$ NH_4OH at room temperature for 8 hr. At this point, the functional group at the surface presumably is a sulfonamide. The sulfonamide-modified polyethylene film was immersed in formaldehyde at 25°C for 18 hr. At this point, the functional group presumably is dimethylol sulfonamide. The dimethylol sulfonamide-modified polyethylene film was then immersed in 2,2,2-trifluoracetic anhydride at 25°C for 70 hr. This step was followed by hydrolysis in 10% KOH for 10 hr at 100°C.

The reaction conditions for these series are somewhat more stringent than the conditions for the thiol sequences of the previous publication.[1] While this does not appear to affect the critical surface tension values of this study it does appear to result in material giving better frustrated multiple internal reflection spectra (FMIR).[6]

Controls were also used; in these runs polyethylene which had not been sulfonated was subjected to the foregoing reaction conditions. No change in the original γ_c value was observed.

Wettability Measurements

Advancing contact angles were measured directly by using an Eberbach telescopic cathetometer equipped with a circular protractor. The procedure was essentially that described by Schonhorn and Ryan.[7] The wetting liquids were those used previously in this laboratory.[8]

For each drop of wetting liquid, three or more contact angle measurements were made on each side of the drop. The reproducibility was generally about $\pm 3°$. Contact angles were also verified on duplicate surfaces. The contact angle values thus obtained for each liquid were averaged with the cosines shown in the figures as circles and triangles with the most extreme values being given as the error. In general, the standard deviation would be less than the error shown.

RESULTS AND DISCUSSION

Surface Treatment

As discussed above, both fuming sulfuric acid and chlorosulfonic acid were used to sulfonate the polyethylene surfaces. The critical surface tension value of polyethylene treated by fuming sulfuric acid at 25°C for 5 min was found to be 57 dyne/cm; after 10 min the γ_c value was increased to 64 dyne/cm, however considerable charring resulted. The critical surface tension value of polyethylene treated by chlorosulfonic acid at 25°C for 30 min is 52 dyne/cm; after 60 min the γ_c value is increased to 55 dyne/cm. Because of the rather slow reaction rate chlorosulfonic acid was not used in any subsequent studies.

It was found experimentally that sulfonated surfaces with critical surface tension values between 52 and 58 dyne/cm could be used in the reaction sequences discussed below. Thus a tentative γ_c value of 55 $\pm$ 3 dyne/cm has been assigned to sulfonated polyethylene surfaces. This is in reasonable agreement with the γ_c value of 53 dyne/cm for a sulfonated surface obtained by the oxidation of a thiol surface.

It should also be noted that frustrated multiple internal reflection (FMIR) spectra of the sulfonic acid surfaces obtained via fuming sulfuric acid, chlorosulfonic acid, and a thiol intermediate all show infrared bands at 1 165 and 1 040 cm^{-1} which are attributed to the presence of an SO_2 group.

Surface Reactions

The sulfonated polymer was further modified according to the two reaction series (3) and (4) which are identical to the thiol sequences developed in the first publication in this series.[1] The reaction conditions are given in the experimental section.

Short Series:

$$\boxed{}-SO_2OH \xrightarrow{PCl_5} \boxed{}-SO_2Cl \xrightarrow{CF_3CH_2OH} \boxed{}-SO_2OCH_2CF_3$$

$$\downarrow KOH;\ HCl$$

$$\boxed{}-SO_2OH \qquad\qquad (3)$$

Long Series:

$$\boxed{}-SO_2OH \xrightarrow{PCl_5} \boxed{}-SO_2Cl \xrightarrow{NH_4OH} \boxed{}-SO_2NH_2$$

$$\downarrow \overset{O}{\overset{\|}{H\,C\,H}}$$

$$\boxed{}-SO_2N\begin{array}{l}CH_2OCCF_3 \\[2pt] \quad \overset{\|}{O} \\[6pt] CH_2OCCF_3 \\[2pt] \quad \overset{\|}{O}\end{array} \xleftarrow{(CF_3C)_2O} \boxed{}-SO_2N\begin{array}{l}CH_2OH \\[6pt] CH_2OH\end{array}$$

$$\downarrow KOH$$

$$\boxed{}-SO_2N\begin{array}{l}CH_2OH \\[6pt] CH_2OH\end{array}$$

$$\boxed{}-(S)_x \qquad\qquad (4)$$

The critical surface tension values for these various surfaces were determined (Figs. 1 and 2) and are summarized in Tables I and II, where they are compared to the values obtained for the thiol sequences.[1] As is seen,

TABLE I
Summary of Short Reaction Series

Surface	γ_c, dyne/cm	
	Thiol sequence	Sulfonic sequence
$\boxed{}$—H	31	31
$\boxed{}$—SH	39	—
$\boxed{}$—SO$_2$OH	53	58
$\boxed{}$—SO$_2$OCH$_2$CF$_3$	36	35
$\boxed{}$—SO$_2$OH	42[a]	42[a]

[a] Value is low; incomplete hydrolysis?

Fig. 1. Wettabilities of polyethylene exposed as follows (see text): (*2*) polyethylene surface sulfonated with fuming sulfuric acid; (*3*) reaction with PCl₅ and CF₃CH₂OH to give a fluorinated methyl group; (*1*) final hydrolysis to partially regenerate the sulfonic acid surface.

the values are essentially the same for the thiol and sulfonic acid sequences. Thus any differences between the two sequences are presumably minor and the conclusions of the thiol work likewise pertain to this study. It is also possible to assign critical surface tension values to the various surfaces with

TABLE II
Summary of Long Reaction Series

Surface	γ_c, dyne/cm	
	Thiol sequence	Sulfonic sequence
▨—H	31	31
▨—SH	39	—
▨—SO₂OH	53	58
▨—SO₂NH₂	45	42
▨—SO₂N(CH₂OH)(CH₂OH)	39	38.5
▨—SO₂N(CH₂OCCF₃)(CH₂OCCF₃) O, O	28	35
▨—SO₂N(CH₂OH)(CH₂OH)	30[a]	30[a]

[a] γ_c value is that of colloidal sulfur.
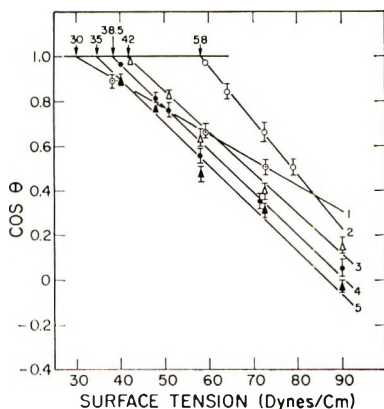
Fig. 2. Wettabilities of polyethylene exposed as follows (see text): (2) surface sulfonated with fuming sulfuric acid; (3) further reaction with PCl₅ and NH₄OH to give sulfonamide surfaces; (4) formylation to give a dimethylol sulfonamide surface; (5) reaction with trifluoroacetic anhydride to give a fluorinated methyl surface; (1) final hydrolysis regenerating the dimethylol sulfonamide surface along with partial desulfonation.

more certainty than on the basis of the thiol work alone. Thus a sulfonamide surface is likely to have a γ_c value of 42 dyne/cm.

The fluorinated sulfonic ester surface with a seemingly high γ_c of 35 dyne/cm has been reproduced. Evidently the SO_2 structure makes a substantial contribution to the γ_c value. In comparison there is considerably more shielding from the SO_2 group in the fluoroacetylated methylol surface. As might be expected on this basis, the observed γ_c value of 28 dyne/cm is considerably lower. Evidently there is also shielding in the methylol structure, since the observed γ_c value of 39 dyne/cm is close to the value (37 dyne/cm) observed[9] for poly(vinyl alcohol), a similar surface structure.

Finally, the close relationship between the results of this study and of the thiol study provides additional evidence that atomic sulfur was originally inserted into the C–H bonds at the surface of polyethylene.

References

1. D. A. Olsen and A. J. Osteraas, *J. Polym. Sci. A-1*, in press.
2. W. E. Walles, U.S. Pat. 2,832,696 (1958).
3. J. A. Nelson and W. K. Vollmer, U. S. Pat. No. 2,879,177 (1959).
4. M. K. Bernett and W. A. Zisman, *J. Phys. Chem.*, **63**, 1241 (1959).
5. See, for example, W. A. Zisman, *Advan. Chem. Ser.*, **43**, 1 (1964).
6. D. A. Olsen and A. J. Osteraas, *J. Polym. Sci. A-1*, in press.
7. H. Schonhorn and F. W. Ryan, *J. Phys. Chem.*, **70**, 3811 (1966).
8. D. A. Olsen, R. W. Moravec, and A. J. Osteraas, *J. Phys. Chem.*, **71**, 4464 (1967).
9. B. R. Ray, J. R. Anderson, and J. J. Scholtz, *J. Phys. Chem.*, **62** 1220 (1958).

Sulfur Modification of Polyethylene Surfaces.   III. Frustrated Multiple Internal Reflection Spectroscopy of Sulfonated Polyethylene Surfaces

DOUGLAS A. OLSEN* and A. JEAN OSTERAAS,† *Research Center, Ashland Chemical Co., Minneapolis, Minnesota 55420*

Synopsis

The previous publications of this series show by indirect means that atomic sulfur inserts into the carbon–hydrogen bonds of polyethylene surfaces. In this study, frustrated multiple internal reflection (FMIR) spectroscopy was used to obtain direct evidence of the nature of the surface groups of the modified polyethylene. The FMIR spectra of surfaces consisting of the products of sulfonic acid groups were virtually identical, regardless of whether the original sulfonic acid surface had been prepared by direct sulfonation or by oxidation of surface thiol groups. The latter groups resulted from the insertion of atomic sulfur into the carbon–hydrogen bonds of the surface. These results establish that sulfur is indeed inserted into polyethylene surfaces.

INTRODUCTION

The first publication in this series[1] showed that atomic sulfur can be reacted with a polyethylene surface to give a new surface consisting of thiol groups which may be further oxidized to sulfonic acid groups. The sulfonic acid groups were then further reacted. The second publication showed that similar results can be obtained by direct sulfonation.[2] In both instances, critical surface tension data were developed, and the internal consistency of the data was used to establish the presence of various functional groups on the polymer surface.

In the work reported here, infrared spectra of the modified surfaces were obtained by means of frustrated multiple internal reflection (FMIR) techniques. As is well known, FMIR techniques permit the spectra of films a few molecular layers thick to be obtained; the resulting spectra closely resemble conventional transmission spectra.[3,4]

The surfaces studied were those reported previously.[1] As has been shown, sulfonic acid groups may be formed on a polyethylene surface by sulfur insertion and subsequent oxidation thus initiating the thiol sequence:

$$\boxed{}—H \xrightarrow[\Delta,\ h\text{-}\nu]{S} \boxed{}—SH \xrightarrow{[O]} \boxed{}—SO_2OH$$
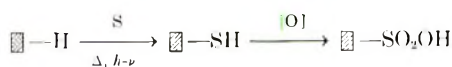
or by direct sulfonation to initiate the sulfonic sequence:

$$\boxed{}—H \xrightarrow{H_2SO_4 \cdot SO_3} \boxed{}—SO_2OH$$
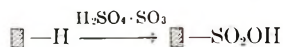
Once the sulfonic acid surface has been formed by either sequence it may be further modified. The reaction series ("short" or "long" series) used in this study were the same as those given previously.[1,2]

Short Series:

$$\boxed{}—SO_2OH \xrightarrow{PCl_5} \boxed{}—SO_2Cl \xrightarrow{CF_3CH_2OH} \boxed{}—SO_2OCH_2CF_3$$

$$\downarrow KOH;\ HCl$$

$$\boxed{}—SO_2OH$$

Long Series:

$$\boxed{}—SO_2OH \xrightarrow{PCl_5} \boxed{}—SO_2Cl \xrightarrow{NH_4OH} \boxed{}—SO_2NH_2$$

$$\downarrow \overset{O}{\underset{}{\overset{\|}{HCH}}}$$

$$\boxed{}—SO_2N\overset{CH_2OCCF_3}{\underset{CH_2OCCF_3}{\big\langle}} \xleftarrow{(CF_3C)_2O} \boxed{}—SO_2N\overset{CH_2OH}{\underset{CH_2OH}{\big\langle}}$$

$$\downarrow KOH$$

$$\boxed{}—SO_2N\overset{CH_2OH}{\underset{CH_2OH}{\big\langle}}$$
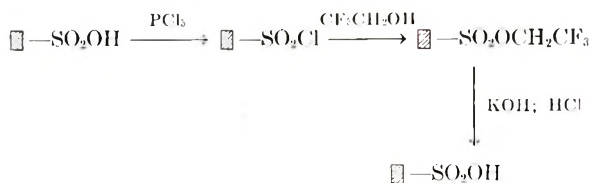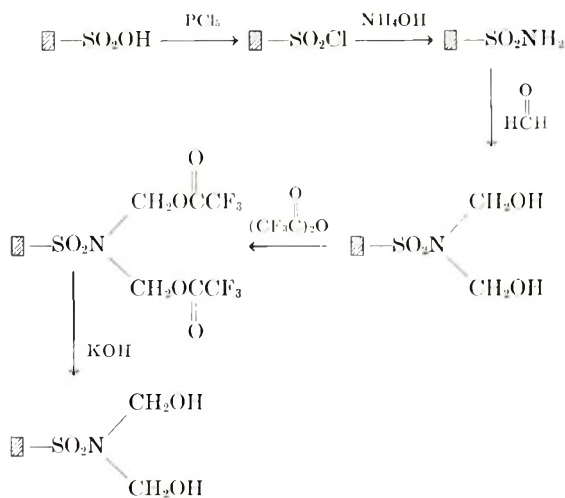
Thus there are four sets of spectra reported here, viz., for products of "long" and "short" series for both the thiol and sulfonic sequences.

EXPERIMENTAL PROCEDURE

Surfaces

The procedure for modifying the surfaces of this study have been reported in detail in the previous publications of this series.[1,2]

Spectra

FMIR spectra were obtained by using a Perkin-Elmer Model 421 infrared spectrometer equipped with a Wilkes Model 12 double-beam internal

reflection attachment (Wilkes Scientific Corp., South Norwalk, Conn.). The FMIR sample preparation was essentially that described by McCall et al.[5]

RESULTS AND DISCUSSION

The spectra obtained for the short series are shown in Figures 1 and 2 for the sulfonic sequences and thiol sequences, respectively. It should be noted here that it is not possible to obtain a spectrum of the actual thiol surface showing a band due to the S–H bond. This band which occurs at $2\,600$–$2\,550$ cm^{-1} is quite weak in the infrared.[6a] As will be shown, the presence of subsequent reaction products of the thiol surface substantiates that such a surface was indeed formed. Figure 1 shows the reaction of the short series on a sulfonic surface. The salient features are bands at $1\,165$ cm^{-1} ($8.58\,\mu$) and $1\,040$ cm^{-1} ($9.61\,\mu$) due to the vibrations of the sulfonic acid which appear only after sulfonation. These values compare well with those of Bellamy.[7] The C–F band at $1\,210$ cm^{-1} ($8.26\,\mu$) appears after formation of the sulfonyl chloride and its subsequent reaction with trifluoroethanol. The band is at about the center of the range given by Colthup et al.,[8] $1\,350$ cm^{-1} ($7.40\,\mu$) to $1\,120$ cm^{-1} ($8.94\,\mu$). Upon the final hydrolysis, it is obvious that the sulfonic acid is again regenerated.

Figure 2 shows essentially the same spectra for the thiol sequence as Figure 1 does for the sulfonic sequence. The presence of bands due to sulfonic acid groups after the first hydrolysis is excellent evidence that sulfur was indeed inserted into the polyethylene surface. The final hydrolysis was evidently not quite as complete as for Figure 1. This is due to the more vigorous reaction conditions for the sulfonic sequence.

Figures 3 and 4 show spectra obtained for the long series starting from sulfonic acid and thiol surfaces, respectively. For the sulfonic acid long series, Figure 3 shows the same bands as discussed above after sulfonation. The sulfonamide surface retains the sulfur–oxygen bands and also shows a
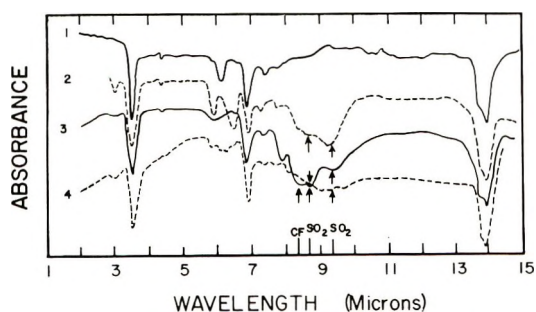
Fig. 1. FMIR spectra of polyethylene exposed first to fuming sulfuric acid followed by subsequent reactions: (1) unexposed polyethylene; (2) polyethylene exposed to fuming sulfuric acid forming surface sulfonic acid groups; (3) further reaction with PCl$_5$ and CF$_3$CH$_2$OH to give a fluorinated methyl surface; (4) final hydrolysis regenerating the original sulfonic acid surface.

pronounced N–H stretch at 3 350 cm^{-1} (2.98 μ). The methylol surface which is formed next shows an O–H stretch also at 3350 cm^{-1} and a very strong C–OH stretching vibration at about 1 000 cm^{-1} (10.0 μ).[6b] The possibility of adsorption of the reagents on the surface rather than true
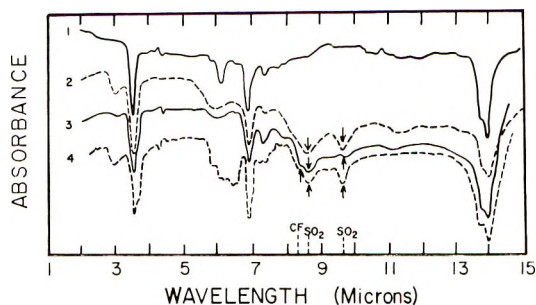
Fig. 2. FMIR spectra of polyethylene exposed to atomic sulfur followed by oxidation to give surface sulfonic acid groups. The identification of the traces is analogous to that of Figure 1.
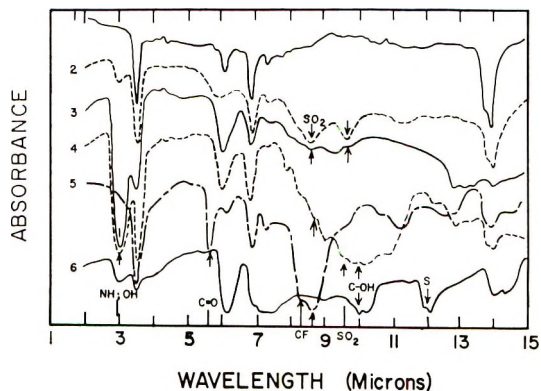
Fig. 3. FMIR spectra of polyethylene exposed first to fuming sulfuric acid followed by subsequent reactions: (1) unexposed polyethylene; (2) polyethylene exposed to fuming sulfuric acid forming surface sulfonic acids; (3) further reaction with PCl$_5$ and NH$_4$OH to give sulfonamide surfaces; (4) formylation to give a dimethylol sulfonamide surface; (5) reaction with trifluoroacetic anhydride to give a fluorinated methyl surface; (6) final hydrolysis to regenerate the dimethylol sulfonamide surface along with partial desulfonation.

reaction can also be refuted by the spectrum of the methylol surface. Formaldehyde is used in forming this step and if only adsorption were taking place the characteristic carbonyl vibration of formaldehyde would be observed. No such band is observed, however. Upon further reaction of the methylol surface with trifluoroacetic anhydride, the O–H and C–OH bands disappear and are replaced by a carbonyl vibration at 1 770 cm^{-1} (5.65 μ) and a C–F band at 1 210 cm^{-1} (8.26 μ). The final hydrolysis, which
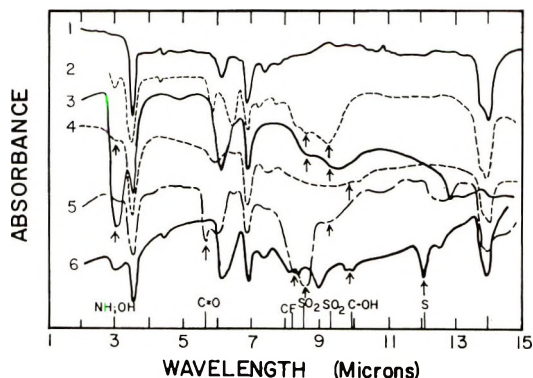
Fig. 4. FMIR spectra of polyethylene exposed to atomic sulfur followed by oxidation to give surface sulfonic acid groups. The identification of the traces is analogous to that of Fig. 3.

should regenerate a methylol surface, does appear to do so. However, the C–OH vibration at about 1 400 cm^{-1} (7.2 μ) cannot be assigned. The band at about 840 cm^{-1} (12.0 μ) corresponds to a vibrational band present in several allotropic forms of sulfur.[9] Thus, it appears that in addition to regeneration of the methylol surface, the carbon–sulfur bond is also attacked, with formation at colloidal sulfur resulting. Critical surface tension data substantiate this view. The presence of colloidal sulfur undoubtedly scatters the incident infrared radiation and would also partially account for the weakened intensities[10] of the bands obtained in the last hydrolysis.

In conclusion, we have shown that for both the long and short series almost identical spectra are obtained, regardless of whether the sulfonic acid surface was formed by direct sulfonation or by oxidation of a thiol group. These results, together with the supporting wettability data of the preceding publications, establish that atomic sulfur is indeed inserted into polyethylene surfaces.

References

1. D. A. Olsen and A. J. Osteraas, *J. Polym. Sci. A-1*, in press.
2. D. A. Olsen and A. J. Osteraas, *J. Polym. Sci. A-1*, in press.
3. T. S. Hermann, *J. Appl. Polymer Sci.*, **9**, 3953 (1965).
4. P. A. Wilks, Jr. and T. Hirschfeld, *Appl. Spectry. Rev.*, **1**, 99 (1967).
5. E. R. McCall, S. H. Miles, and R. T. O'Connor, *Am. Dyestuff Reptr.*, **56**, 13 (1967).
6. R. N. Jones and C. Sandorfy, *Chemical Applications of Spectroscopy*, W. West, Ed., Interscience Publishers, Inc., New York, 1956; (a) p. 546; (b) p. 432.
7. L. J. Bellamy, *The Infra-Red Spectra of Complex Molecules*, 2nd Ed., J. Wiley and Sons, Inc., New York, 1958, p. 350.

8. N. D. Colthup, I. H. Daly, and S. E. Wiberly, *Introduction to Infrared and Raman Spectroscopy*, p. 314, Academic Press, New York, 1964.

9. H. L. Strauss and J. A. Greenhouse, *Elemental Sulfur*, B. Meyer, Ed., Interscience Publishers, New York, 1965, chap. 12.

10. C. G. Ford, *Nature*, **212**, 72 (1966).

Stereospecific Polymerization of o-Methoxystyrene by Anionic Initiators

HEIMEI YUKI, YOSHIO OKAMOTO, YOSHITERU KUWAE, and KOICHI HATADA, *Department of Chemistry, Faculty of Engineering Science, Osaka University, Toyonaka, Osaka, Japan*

Synopsis

o-Methoxystyrene was polymerized with n-butyllithium (n-BuLi), Na naphthalene, and K dispersion as initiators in tetrahydrofuran (THF) and toluene. The stereoregularity of the polymer was investigated by means of the NMR spectroscopy. The methoxy resonance of the spectrum split into ten components due to the tactic pentads. It was found by x-ray examination that the polymer obtained by n-BuLi in toluene at −45°C was crystalline and highly isotactic. In THF, the stereospecificity of the polymerization was independent of the initiator, and the isotacticity of the polymer increased with increasing reaction temperature. In toluene, the stereospecificity depended on the initiator; i.e., n-BuLi gave a polymer with higher isotacticity than that given by phenylsodium. The fraction of isotactic triad of the polymer obtained by n-BuLi in toluene at −78°C was more than 90%, but 50% at 50°C. The presence of ca. 1% THF in toluene led to a steep decrease in the isotacticity even at −78°C. The tacticity of the polymer given by Na naphthalene was not affected by the existence of NaB(C_6H_5)$_4$ in THF. The polymerization in THF could be explained by Bovey's "single σ" process, while a penultimate effect was observed in the polymerization by n-BuLi in toluene.

INTRODUCTION

Natta et al.[1] studied the stereospecific polymerization of o-methoxystyrene (o-MeOSt) with EtAlCl$_2$. Recently, Higashimura et al.[2] investigated the cationic polymerization of o-MeOSt and examined the stereoregularity of the polymer using NMR spectroscopy.

On the other hand, the stereospecific polymerization of this monomer has not been studied with an anionic initiator. It is well known that a compound containing ether oxygen can easily coordinate with alkali metal cations such as Li$^+$ and Na$^+$. Therefore, it is expected that in the anionic polymerization of o-MeOSt the ether oxygen in the monomer or in the chain end of the growing polymer anion may interact with the counter ion to affect sterically the addition of the monomer. In the present work, the anionic polymerization of o-MeOSt is studied, and the relationships between the polymerization conditions and the stereoregularity of the polymer (P-o-MeOSt) are discussed on the basis of the NMR spectroscopy.

EXPERIMENTAL

Materials

o-MeOSt was synthesized by dehydration of methyl(2-methoxyphenyl)-carbinol over KHSO$_4$ at 220–230°C, which was prepared by Grignard reaction of acetaldehyde and o-bromoanisole. The monomer obtained was fractionally distilled, and then redistilled from lithium aluminum hydride; bp 80–81°C/10 mm Hg, n_D^{20} 1.5605. No impurity was detected by gas chromatography and NMR spectroscopy.

Tetrahydrofuran (THF) which had previously refluxed over metallic sodium and then over lithium aluminum hydride was distilled onto Na–K alloy and naphthalene. From the green solution the solvent was transferred to a reaction vessel on a vacuum line just before use.

Toluene was purified by the usual method and was stored over sodium. Before use, the solvent was transferred to a flask containing a small amount of n-butyllithium (n-BuLi) in toluene, from where it was distilled under high vacuum.

n-BuLi was synthesized from n-butyl chloride and metallic lithium in n-heptane according to the method of Ziegler.[3] The concentration was determined by double titration.[4]

Na naphthalene (Na-Naph) was prepared in THF; the concentration was determined by the titration of a hydrolyzed sample with standard hydrochloric acid.

Phenyl sodium (Ph-Na) was obtained according to the method of Gilman from chlorobenzene and sodium dispersion in n-heptane.[5]

Potassium dispersion (K dispersion) was prepared in a n-heptane medium.

Polymerization

Solvent was first transferred on the vacuum line to a glass ampoule which had been evacuated and heated with a gas burner. Then monomer and initiator were added with hypodermic syringes to the ampoule, which was kept in a thermostat under an atmosphere of dry argon. After the polymerization was terminated by adding a small portion of methanol, the reaction mixture was poured into a large amount of methanol. The precipitated polymer was filtered, washed with methanol, and dried.

Measurement

The NMR spectrum of the polymer was obtained at 60°C with a JNM-4H-100 spectrometer at 100 MHz by using chloroform or carbon tetrachloride as a solvent. The concentration of the sample was ca. 20% (w/v), and tetramethylsilane was used as an internal standard. The spectrum was analyzed with a du Pont 310 curve resolver for the determination of pentad sequences. The Lorentzian was assumed in the shape of resonance, and the half width of each peak was given tentatively. The relative

intensity of the peak was determined with an integration meter fitted to the curve resolver.

The x-ray diffraction measurement was made with a Rigakudenki 4001 x-ray diffractometer.

The solution viscosity of the polymer was determined in toluene or in chloroform at $30.0 \pm 0.03°C$.

RESULTS

The polymerizations of o-MeOSt were carried out with n-BuLi, Na naphthalene, and K dispersion as initiators in THF at 0 and $-78°C$. The results are shown in Table I. All of the polymerizations proceeded smoothly to give quantitative yields of polymers, the softening points of which were 120–130°C.

TABLE I
Anionic Polymerization of o-Methoxystyrene in THF[a]

| Mono-mer, mmole | Initiator | | Temp, °C | Time, hr | Yield, % | η_{sp}/c, dl/g[b] |
	Type	Amt, mmole				
4.42	n-BuLi	0.073	−78	2.5	98	0.16
4.52	n-BuLi	0.073	0	2.5	97	—
4.28	Na-Naph.	0.063	−78	1.0	95	0.13
4.72	Na dispersion	0.086	0	2.5	97	0.78
4.28	Na-Naph.	0.063[c]	0	1.0	96	—
4.28	K dispersion	0.125	−78	1.0	95	0.15
3.81	K dispersion	0.114	0	2.5	98	—

[a] Solvent, 15 ml.

[b] Toluene solution, $c = 0.50$ g/dl.

[c] NaBPh₄ (0.29 mmole) was added.

TABLE II
Anionic Polymerization of o-Methoxystyrene in Toluene[a]

| Monomer, mmole | Initiator | | Temp, °C | Time, hr | Yield, % | η_{sp}/c, dl/g[b] |
	Type	Amt, mmole				
4.72	n-BuLi	0.073	−78	144	Trace	—
4.60	n-BuLi	0.056	−78	600	4.2	3.1
4.59[c]	n-BuLi	0.113	−78	144	96	—
11.4	n-BuLi	0.056	−45	168	80	7.0
4.25	n-BuLi	0.073	0	24	100	0.24
4.25	Na dispersion	0.107	30	96	0	—
4.34	K dispersion	0.114	30	96	0	—
3.27	Ph-Na	0.050	0	72	71	—

[a] Solvent, 15 ml.

[b] Chloroform solution, $c = 0.50$ g/dl.

[c] Solvent contained 1.3 vol-% of THF.
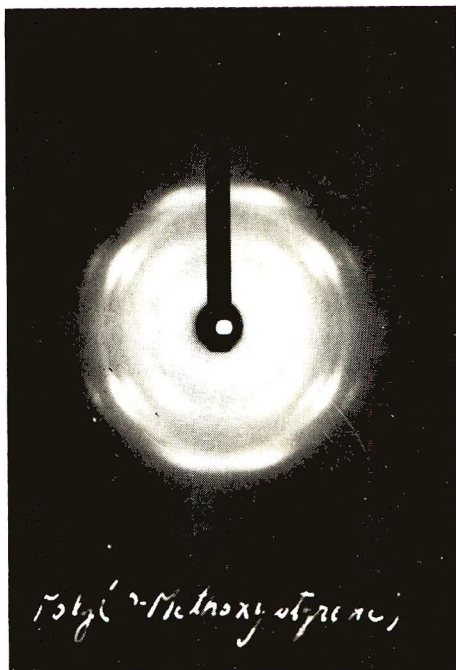
Fig. 1. X-ray diagram of orientated film of crystalline P-o-MeOSt.

Table II shows the results of the polymerization of o-MeOSt in toluene. The rate of polymerization by n-BuLi at low temperature was much slower than that in THF. The solution viscosity of the polymer obtained at low temperature was high, even if the yield of the polymer was low. No polymer was obtained with Na or K dispersions in toluene, but the polymerization was initiated with Ph-Na to form the polymer in a good yield.

When the solution of the reaction mixture either in THF or in toluene was allowed to stand above 0°C for one or two days, the color of the solution gradually disappeared, although the polymerization had already finished. It is considered that the carbanion reacted with the methoxy group to give a phenolate anion,[6] but the amount was so small that no effect was observed on the polymer produced.

The polymer obtained with n-BuLi in toluene at low temperature showed a high crystallinity under a polarizing microscope. It was insoluble in n-hexane and diethyl ether, partially soluble in toluene, and soluble in chloroform and THF. Its melting point was 290–295°C. The x-ray diffraction (Fig. 1) showed the fiber period of this polymer to be 8.0 Å. The value is well consistent with the fiber period (8.10 Å) of isotactic poly-o-methylstyrene,[7] which is similar to P-o-MeOSt in chemical structure, suggesting that crystalline P-o-MeOSt is isotactic.

The NMR spectrum of P-o-MeOSt prepared with n-BuLi in THF at −78°C is shown in Figure 2. Since the intensity ratio of the peaks at 3.5, 6.7, 7.5, and 8.6τ is $4:3:1:2$, these peaks can be attributed to the protons of
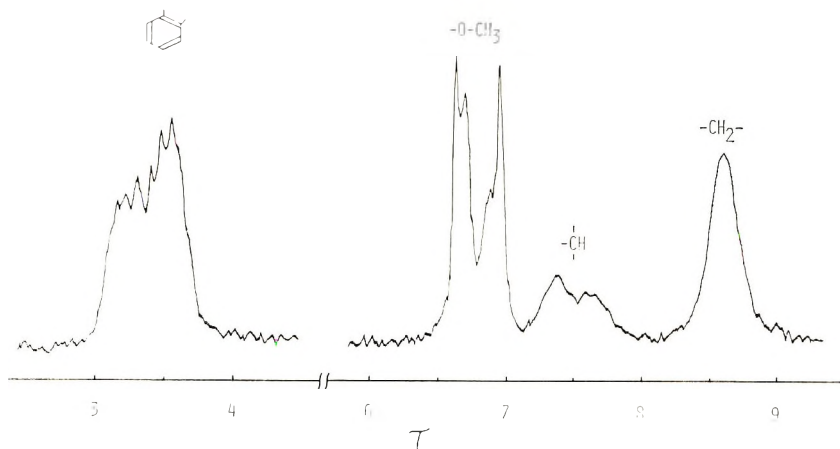
Fig. 2. NMR spectrum of P-o-MeOSt in CCl₄ at 60°C.

phenyl, methoxy, methine, and methylene groups, respectively, with increasing magnetic field.

Figure 3 shows the spectra of the methoxy groups in the polymers obtained under various reaction conditions. The polymers obtained in THF at the same temperature gave very similar spectra, regardless of the initiators used. The polymerization temperature, however, affected the NMR spectrum of the polymer (A and B in Fig. 3). The crystalline polymer obtained with n-BuLi in toluene at $-45°C$ showed a very narrow peak at 6.78τ (C in Fig. 3), but the spectrum was broaden by elevating the polymerization temperature (D in Fig. 3). The spectrum of the polymer prepared at $-78°C$ with n-BuLi in toluene containing ca. 1% THF (E in Fig. 3) is similar to those of the polymers prepared with Ph-Na in toluene at $0°C$ and with EtAlCl₂ in toluene at $-78°C$.

The complicated splits in the spectra of the methoxy protons must be due to the differences of stereochemical structures of the protons because splits by spin-spin coupling can not be considered. Furthermore, the differences seem not to be conformational, because the spectra measured in o-dichlorobenzene at 150°C were very similar to those shown in Figure 3.

We can expect that the methoxy resonance is resolved into ten peaks, corresponding to ten configurationally different pentad sequences.[8] Then, assignments of the fine peaks of the methoxy resonance in the NMR spectrum were attempted, it being assumed that the split is due to the pentad signals and that the crystalline polymer is isotactic. Detailed observations of the spectra indicate that the peaks are divided into three groups; i.e., at 6.60–6.75τ, 6.75–6.88τ, and 6.88–6.95τ. Consequently, the peaks at 6.75–6.88τ were assigned to the isotactic triad (I), which was split into three components (6.78, 6.82, and 6.86τ) by pentad sequences. Then, it is anticipated that if the peaks at the lower fields are the components of the heterotactic triad (H), those at the higher fields belong to the syndiotactic one (S), or vice versa. Some polymers showed spectra composed of
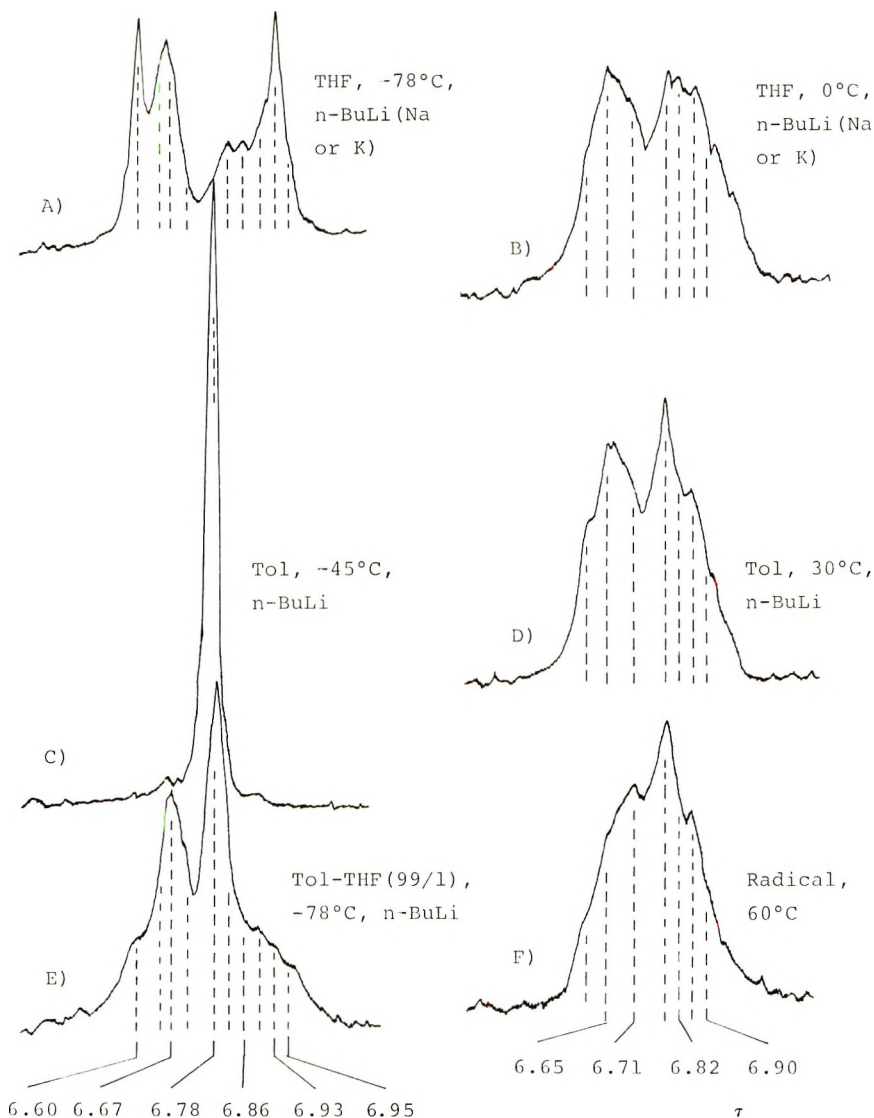
Fig. 3. NMR spectrum of P-o-MeOSt in CHCl₃ at 60°C.

isotactic peaks and peaks in the lower fields, but only small peaks in the higher fields, e.g., spectrum D in Figure 3. If the peaks in the lower fields belong to the syndiotactic triad, the polymer having such a spectrum is composed mainly of isotactic and syndiotactic sequences with only a small portion of heterotactic triad, as is the case with a stereoblock polymer composed of isotactic and syndiotactic blocks. The formation of such a polymer is unlikely in the homogeneous polymerization system employed in this work. Accordingly, the peaks at 6.60, 6.65, 6.67, and 6.71τ are assigned to the four components of the heterotactic triad and the peaks at 6.90, 6.93,

and 6.95τ to the components of the syndiotactic one.   The fractions I, H, and S were determined by the relative intensities of the corresponding absorptions; i.e. the absorption areas.   When the absorptions overlapped, some of the spectra which were typical were analyzed with the curve resolver into ten pentad peaks and the others were resolved into triads as was the case for the analogous spectra already analyzed with the resolver.

The effect of polymerization temperature on the tacticity of P-o-MeOSt was investigated in THF with n-BuLi as an initiator, the tacticity being analyzed on the basis of the assignments described above.   The results are shown in Figure 4.   Although the fraction H was about 50% independently
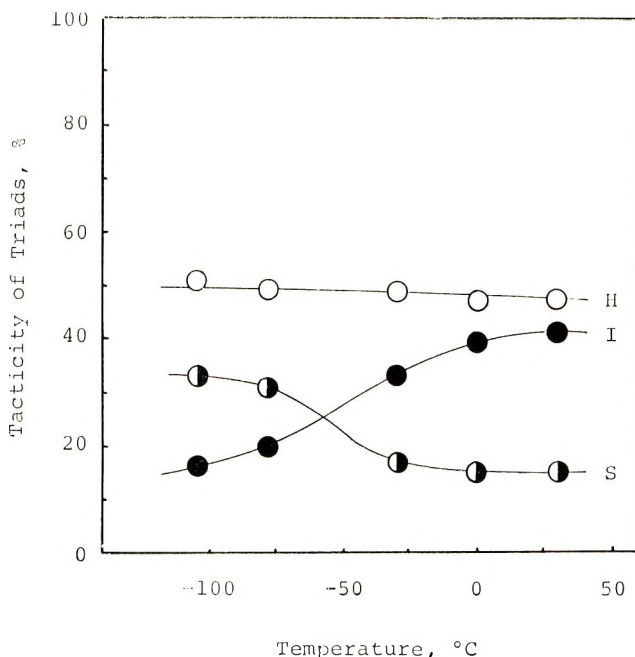
Fig. 4. Dependency of tacticity on the polymerization temperature (in THF). Solvent, 15 ml; monomer, ca. 0.6 g; n-BuLi, ca. 1 mole-% based on monomer.

of the temperature, the isotactic fraction I increased and S decreased with a rise in the temperature.

The results of the polymerization in toluene with n-BuLi are shown in Figure 5.   With raising the temperature, the fraction of I decreased to 50%, and H and S, especially the former, increased steeply.

The tacticity of P-o-MeOSt which was polymerized in a toluene–THF mixture with n-BuLi at $-78°C$ is shown in Figure 6.   The presence of ca. 1% of THF in toluene led to a drastic decrease in the fraction of I and to increases in those of H and S.

The influence of $NaB(C_6H_5)_4$ on the tacticity was studied in the polymerization initiated by Na naphthalene in THF at 0 and $-78°C$.   The
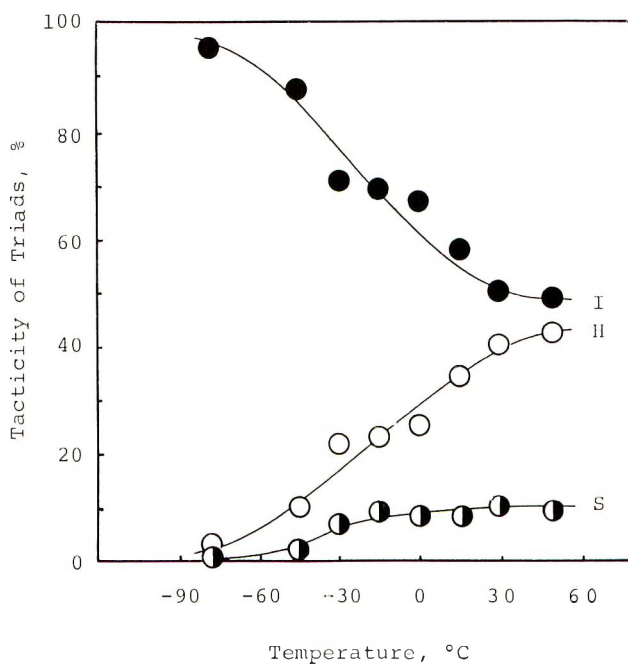
Fig. 5. Dependence of tacticity on the polymerization temperature (in toluene). Solvent, 15 ml; monomer, ca. 0.6 g; n-BuLi, ca. 1 mole-% based on monomer.
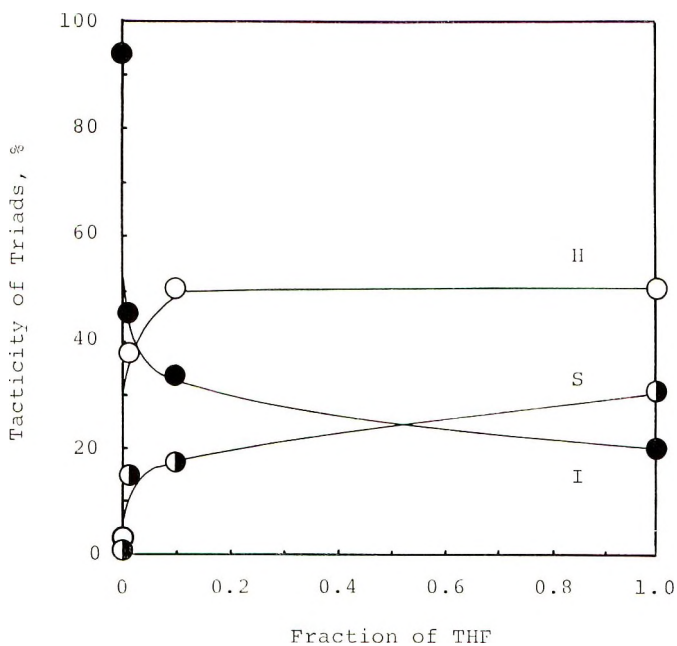
Fig. 6. Relationship between the tacticity of P-o-MeOSt and solvent composition of toluene–THF mixture. (Toluene + THF), 15 ml; monomer, ca. 0.6 g; n-BuLi, ca. 1 mole-% based on monomer.

TABLE III

Tacticity of Poly-o-methoxystyrene Initiated by Na
Naphthalene in the Presence of NaB(Ph)₄ in THF[a]

NaB(Ph)₄, mmole	Temp, °C	Time, hr	Yield, %	Tacticity, %		
				H	I	S
0	−78	1.0	95	50	22	28
0.29	−78	24.0	90	51	21	28
0	0	1.0	95	46	39	15
0.29	0	1.0	96	46	40	16

[a] Solvent, 15 ml; monomer, 4.3–4.7 mmole; initiator, 0.063 mmole.

TABLE IV

Tacticity of Poly-o-methoxystyrene Obtained with Various Initiators

Solvent	Initiator	Temp, °C	Yield, %	Tacticity, %		
				H	I	S
THF	n-BuLi	0	95	47	39	14
THF	Na-Naph.	0	95	46	39	15
THF	K dispersion	0	98	44	41	15
Toluene	n-BuLi	0	100	25	67	8
Toluene	Ph-Na	0	71	39	43	18
Toluene	EtAlCl₂	−78	31	33	43	23
Toluene	BF₃·OEt₂	0	45	47	38	15
Bulk	None	60	26	43	38	10

results are listed in Table III. No influence on the tacticity of P-o-MeOSt was observed.

In Table IV are shown the fractions of the triad sequences in the polymer obtained with various initiators. The tacticity of the polymer obtained in THF was not affected by the initiators used. In toluene, however, n-BuLi gave a more isotactic polymer than Ph-Na. For comparison, the tacticities of the polymers which were prepared by the cationic and radical polymerizations are also shown.

The methoxy resonance in the NMR spectra of the polymers prepared in THF was analyzed by means of the curve resolver as ten components in pentad sequences. One of the results is shown in Figure 7, and the assignment of each component and its relative intensity measured are shown in Table V. If the polymerization in THF can be expressed by a Bernoulli-trial process or a Bovey's "single σ" process[9] with regard to the configurational sequence, the relative intensities of ten components of the pentads can be calculated from the fractions of triad sequences. Table V shows that the observed values are in accord with the calculated ones. The positions of the components seemed to be slightly shifted by the polymerization conditions.

The NMR spectrum of poly-p-methoxystyrene prepared under the same conditions of the polymerization as of o-MeOSt gave no information about
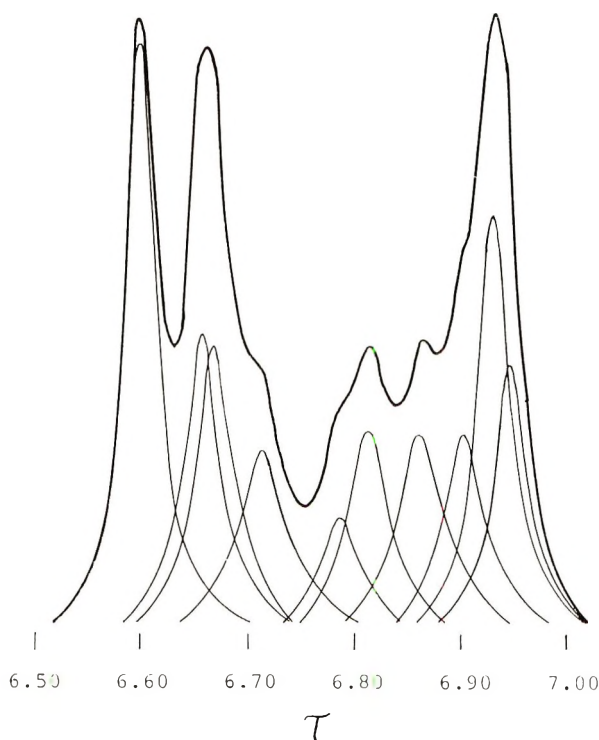
Fig. 7. Curve resolution of methoxy resonance in the NMR spectrum of P-o-McOSt initiated by n-BuLi in THF at −78°C.

TABLE V

Curve Resolution of Methoxy Peaks in NMR Spectrum of P-o-McOSt[a]

Pentads	τ	A		B		C	
		Calcd	Found	Calcd	Found	Calcd	Found
HHS	6.60	16.8	17.8	15.2	18.5	6.6	5.3
HHH	6.65	13.0	13.4	12.0	11.5	11.3	9.4
HHS	6.67	13.0	14.3	12.0	10.7	11.3	8.6
HHH	6.71	8.2	7.4	9.8	8.2	18.3	18.1
III	6.78	2.6	2.5	4.0	3.9	15.2	15.3
HH	6.82	8.2	7.9	9.8	8.7	18.3	17.1
HH	6.86	5.3	4.3	6.2	8.6	5.5	7.5
HSH	6.90	5.3	4.0	6.2	7.6	5.5	7.7
SSH	6.93	16.8	17.0	15.2	13.5	6.6	6.4
SSS	6.95	10.9	11.6	9.6	8.7	2.0	3.9

[a] Obtained with n-BuLi in THF at (A) −105°C, (B) −78°C, and (C) 0°C. The assignments were made in such a way that the calculated intensities agree with the found values, except for the peak at 6.78τ, which was assigned as III from x-ray diffraction.

the tacticity of the polymer, because the methoxy resonance was not split satisfactorily.

DISCUSSION

Since in THF the alkali metal counterion is solvated[10] and the coordination by THF may be stronger than that by ether groups of P-o-MeOSt and o-MeOSt, the steric course of the monomer addition may be determined only by the chain end, as has been found in many radical polymerizations.
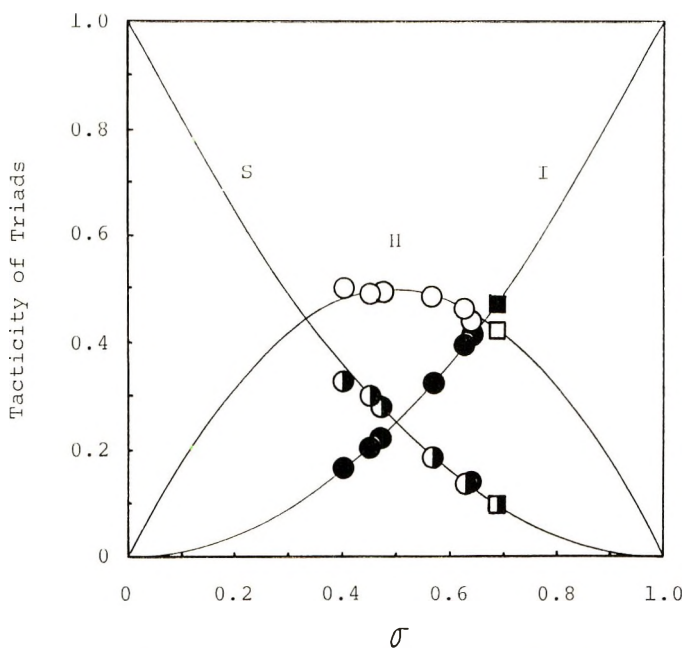
Fig. 8. Bovey plot for P-o-MeOSt obtained with n-BuLi in THF: (□) radical polymerization.

As expected for this mechanism, the tacticity of the polymer was independent of the initiator. Bovey single-σ plots for P-o-MeOSt prepared in THF are shown in Figure 8, where σ is defined as the probability that an adding monomer generates the same configuration as that of the end of a growing chain. The observed values are consistent with the theoretical curves. This, together with the results shown in Table V, may support the correctness of the assignments of the peaks in the NMR spectra, although the assignments were rather tentative.

Two propagating species, a free ion and an ion pair, have been found in the anionic polymerizations of styrene and α-methylstyrene in THF.[11–13] The propagations by these two species may yield configurationally different polymers. The existence of sodium tetraphenylboran which depresses the

dissociation of an ion pair into free ions, did not affect the tacticity of P-o-MeOSt obtained in the polymerization in THF with Na naphthalene. It may be that the above two species give configurationally the same polymers or that the predominant propagating species is an ion pair.

The Bovey single-σ plots for P-o-MeOSt prepared with n-BuLi in toluene are shown in Figure 9. The experimental results deviate from the theoretical curves. In this polymerization the ether groups of the monomer units
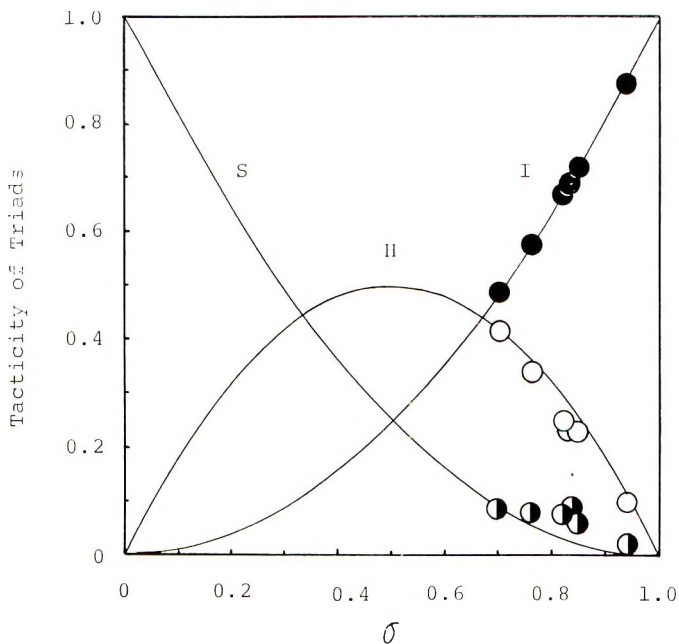
Fig. 9. Bovey plot for P-o-MeOSt obtained with n-BuLi in toluene.

at the chain end and/or of the adding monomer may interact with the lithium counterion. The interaction should be a cause for isotactic polymerization at low temperatures. However, the energy of the interaction may be so small that the stereospecificity of the polymerization decreases steeply with a small rise of the reaction temperature.

Figure 10 shows that Chujo's[14] $\Delta\epsilon = -kT \times \ln(4IS/H^2)$ is almost zero in the polymerization in THF regardless of the temperature. However, $\Delta\epsilon$ in the polymerization in toluene with n-BuLi decreased with a decrease in the polymerization temperature, suggesting that a penultimate effect exists and increases with decreasing temperature.

In a mixture of toluene and THF, THF coordinates preferentially with lithium counterion, preventing the isotactic propagation of the polymer chain. The effect of THF is similar to that on the polymerization of isoprene with n-BuLi in a hydrocarbon solvent, where the 1,4-cis-structure
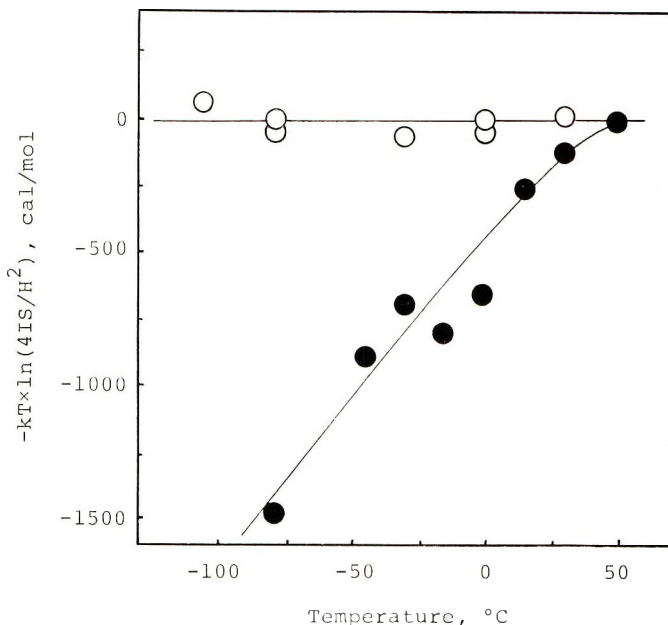
Fig. 10. Relationship between $\Delta\epsilon = -kT \times \ln(4IS/H^2)$ and polymerization temperature for P-o-MeOSt obtained by anionic initiators: (○) in THF with n-BuLi or by Na-Naph.; (●) in toluene with n-BuLi.

steeply decreased by the addition of a small amount of THF in toluene.[15] The interaction of Na$^+$ with the methoxy groups may be weaker than that of Li$^+$, and the former may give a less isotactic polymer than that given by the latter.

References

1. G. Natta, G. Dall' Asta, G. Mazzanti, and A. Casale, *Makromol. Chem.*, **58**, 217 (1962).

2. Y. Ohsumi, S. Tani, T. Higashimura, and S. Okamura, paper presented at the 13th Meeting of Polymer Science, Kobe, Japan July 1967.

3. K. Ziegler and A. Colonius, *Ann.*, **479**, 135 (1930).

4. H. Gilman and A. H. Haubein, *J. Amer. Chem. Soc.*, **66**, 1515 (1944).

5. H. Gilman, H. A. Pacevitz, and O. Baine, *J. Amer. Chem. Soc.*, **62**, 1514 (1940).

6. R. A. Finnegan and J. W. Altschuld, *J. Organometal. Chem.*, **9**, 193 (1967).

7. P. Corradini and P. Ganis, *Nuovo Cimento*, [10], **15**, 96 (1960).

8. H. L. Frisch, C. L. Mallows, and F. A. Bovey, *J. Chem. Phys.*, **45**, 1565 (1966).

9. F. A. Bovey and G. V. D. Tiers, *J. Polym. Sci.*, **44**, 173 (1960).

10. T. E. Hogan-Esch and J. Smid, *J. Amer. Chem. Soc.*, **88**, 307 (1966).

11. D. N. Bhattacharyya, C. L. Lee, J. Smid, and M. Szwarc, *J. Phys. Chem.*, **69**, 612 (1965).

12. H. Hostalka and G. V. Schulz, *J. Polym. Sci. B*, **3**, 175 (1965).

13. J. Comyn, F. S. Dainton, G. A. Harpell, K. M. Hui, and K. J. Ivin, *J. Polym. Sci. B*, **5**, 965 (1967).

14. R. Chujo, *J. Phys. Soc. Japan*, **21**, 2669 (1966); *Makromol. Chem.*, **107**, 142 (1967).

15. A. V. Tobolsky and C. E. Rogers, *J. Polym. Sci.*, **40**, 73 (1959).

Silyl Celluloses: A New Class of Soluble Cellulose Derivatives

J. F. KLEBE and H. L. FINKBEINER, *General Electric Research and Development Center, Schenectady, New York 12301*

Synopsis

Two general methods for the silylation of cellulose have been developed. Silyl amides undergo silyl–proton exchange reactions with cellulose in polar solvents leading to displacement of 80–90% of the hydroxyl protons by silyl groups. The same products are obtained by reaction of the corresponding chlorosilanes with cellulose in pyridine; however, di- and trifunctional impurities present in commercial chlorosilanes have to be removed by scavenging with a carbohydrate in order to avoid crosslinking. Cellulose derivatives with trimethylsilyl, dimethylphenylsilyl, methyldiphenylsilyl, and γ-cyanopropyldimethylsilyl substituents have been prepared by both methods. The properties of the new soluble polymers are largely dependent on the nature of the silyl substituents. The silyl celluloses exhibit a relatively high degree of hydrolytic stability; methyldiphenylsilyl cellulose is hydrolytically stable even under severe conditions.

INTRODUCTION

The silylation* of numerous natural products, including various sugars, has been reported in the literature, and this procedure has become a commonplace operation whenever the effects of hydrogen bonding on the physical properties are undesirable for purposes of separation and analysis.[1]

One of the most ubiquitous and important natural products with an abundance of free hydroxyl groups which significantly determine its physical properties is cellulose. Replacement of some or all of the hydroxyl protons of cellulose by silyl groups can be expected to alter radically the properties of this polymer, just as esterification or alkyl ether formation drastically modify the parent cellulose. The effects of polymer modification by silylation have been demonstrated in at least two cases;[2,3] the increased solubility of silylated polymers in nonpolar solvents is particularly noteworthy.[2]

A search of the literature revealed that cellulose was silylated successfully many years ago.[4] The analysis of cellulose treated with trimethylchlorosilane and pyridine in a heterogeneous reaction indicated that 91% of the hydroxyl protons had indeed been replaced by trimethylsilyl groups. Most surprising to us, however, was the statement that the resulting

---

* The term "silylation" is used here in the general sense of substitution with triorganosilyl groups.

polymer was entirely insoluble in organic solvents just as the parent cellulose is, and moreover, that increasing replacement of acetate groups by trimethylsilyl groups in cellulose acetate led to increasingly less soluble polymers.

The favorable results obtained with bis(trimethylsilyl)-acetamide (BSA) as a silylating agent for various classes of compounds with reactive protons[5] prompted us to attempt the silylation of cellulose with this reagent and to reinvestigate the properties of the product.

RESULTS AND DISCUSSION

Trimethylsilylation with Si—N Compounds

The silylation of cellulose with BSA turned out to be straightforward once a suitable solvent was found. It is characteristic of highly hydrogen-bonded materials of high molecular weight that their silylation is very sluggish, even when the material in the silylated form is quite soluble in the solvent used for the reaction. Solvent systems in which the parent polymer is somewhat soluble or in which at least some swelling occurs are preferable even if the solubility of the silylated product is only marginal in the particular solvent.

With such considerations in mind, silylations were carried out by suspending various grades of natural cellulose in polar solvents such as dimethyl sulfoxide (DMSO), dimethylformamide (DMF), N-methylpyrrolidone (NMP), and hexamethylphosphoramide (HMPA), with addition of an excess of 20–30% over the calculated amount of BSA and on heating the agitated mixtures under anhydrous conditions at temperatures of 100 to 150°C. HMPA and NMP were found particularly useful; in the latter solvent the fibers of a wood pulp cellulose turned into a transparent tan-colored gel within 1 hr at a temperature of 150°C. This NMP-insoluble gel yielded a viscous solution upon addition of xylene or benzene to the mixture.

The choice of the grade of cellulose proved to be of some consequence in these reactions. Depending on the prior history of the cellulose, the silylations go more or less readily to completion; in some cases, although most of the starting material appeared to have reacted, some insoluble gel remained which made filtration extremely difficult. Some commercially available wood pulp celluloses (types V-60 and V-90, Buckeye Cellulose Corp., Memphis, Tennessee) are very readily silylated; cotton linter pulps from the same source were generally of higher molecular weight and, although they left no unreacted insoluble material, gave extremely viscous solutions.

The nature of the hydroxyl groups in cellulose suggests that any resistance to silylation may be due more to steric reasons and lack of solubility than to intrinsic "chemical" difficulties in displacing these particular protons by trimethylsilyl groups. Weaker silylating agents like silylamines and silazanes could be expected to suffice once suitable reaction conditions

were found. Treatment of cellulose in NMP with *N*-trimethylsilyl-piperidine or hexamethyldisilazane at 140–150° C for 3–5 hr indeed gave viscous solutions with very little insoluble residue.

The polymeric product prepared with any of these silylating agents and solvents could be recovered either by vacuum distillation of volatile matter, or more conveniently, by precipitation with polar solvents like acetone, acetonitrile, or alcohols which yielded the polymer in the form of white fibers. The products were in all cases soluble in aromatic, chlorinated, and a number of aliphatic solvents. The yields of recovered material ranged from 80 to 90% calculated on the basis of complete silylation; the elemental analyses indicated that the polymer (I) contained 2–3 trimethylsilyl groups per repeating unit.
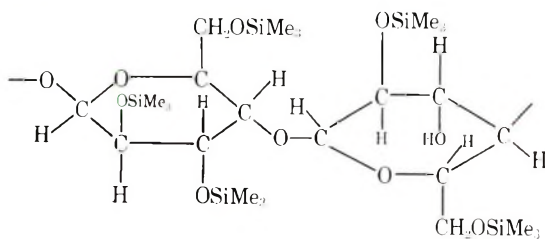
I

Silylation with Trimethylchlorosilane

The composition of the soluble trimethylsilyl cellulose must be virtually identical (according to the elemental analysis) with the totally insoluble product which Schuyten and co-workers[4] obtained by treatment of cellulose with trimethylchlorosilane in pyridine. Freshly distilled commercial trimethylchlorosilane and a sample of the cellulose which had yielded soluble product with BSA also gave us an insoluble product. The cross-linking of the polymer therefore occurred as a result of either some secondary mode of reaction of trimethylchlorosilane itself or the presence of some impurity in the chlorosilane. The most likely impurities in this commercial product are higher chlorinated silanes; dimethyldichlorosilane and methyl-trichlorosilane boil at 70 and 66°C, respectively, and it should be very difficult to remove by fractionation traces of these compounds from tri-methylchlorosilane with a boiling point of 57°C. Pure trimethylchloro-silane was then prepared by reaction of anhydrous hydrogen chloride with hexamethyldisilazane and allowed to react with cellulose suspended in a mixture of pyridine and xylene. A completely soluble product was indeed obtained after a reaction time of 4 hr at 110°C. Thus, the insolu-bility of the product in the earlier experiments had evidently been caused by impurities in the commercial trimethylchlorosilane.

The likely culprits in this undesirable crosslinking reaction, dimethyl-dichlorosilane and methyltrichlorosilane, are known to be considerably more reactive than trimethylchlorosilane. Addition of a small amount of sugar to the mixture of commercial trimethylchlorosilane and pyridine

and heating for a few minutes prior to the addition of the cellulose proved to be sufficient to remove the impurities from the solution in the form of an easily filterable brown lump of solid. Cellulose added at this point was silylated to a completely soluble product. This "sweetened" procedure provides a more economical synthesis of silyl cellulose than the silylations with silicon–nitrogen compounds.

We found it necessary to remove pyridine hydrochloride completely from the polymer; otherwise the trimethylsilyl cellulose became partially insoluble upon drying after the precipitation with a nonsolvent. The insolubilization may be caused by a reverse reaction in which the silyl ether bond is cleaved by the hydrochloride with formation of trimethyl-chlorosilane and cellulose. Removal of traces of pyridine hydrochloride was best accomplished by filtration of the crude product solution through aluminum oxide or by precipitation of the filtered polymer solution with methanol containing a small amount of sodium acetate.

Trimethylsilyl Ethyl Cellulose

It appeared of interest to us to attempt a modification of cellulose derivatives by replacing residual hydroxy protons by silyl groups. It was possible to trimethylsilylate under mild conditions an ethyl cellulose containing an average of 0.7–0.8 hydroxyl groups per anhydroglucose unit. The product which contained 0.6–0.7 trimethylsilyl groups per ring was insoluble in alcohols but soluble in aliphatic hydrocarbons in contrast to the unsilylated ethyl cellulose.

Substitution With Other Silyl Groups

We found that the two methods developed for trimethylsilylating cellulose provided general routes to other silyl celluloses as well. Reaction of cellulose with N-(dimethyl-γ-cyanopropylsilyl)acetamide in NMP or with the corresponding silyl chloride in pyridine allowed the substitution of 80–90% of the hydroxyl protons by dimethyl-γ-cyanopropylsilyl groups. In the same fashion, an average of 2.5 of the three hydroxyl protons of the anhydroglucose unit was replaced by the bulky methyldiphenylsilyl group, whereas substitution with triphenylsilyl groups did not prove to be possible by either method. The infrared spectra of three silyl celluloses are shown in Figure 1.

The proportion of the silyl groups in the resulting polymer ranges from about 55 wt-% for trimethylsilyl cellulose to about 75 wt-% for methyl-diphenylsilyl cellulose. It is not surprising then, that the properties exhibited by the various silyl celluloses are largely determined by the nature of the silyl substituents.

Properties of Silyl Celluloses

Trimethylsilyl Cellulose. The polymer is colorless and is soluble in aromatic and chlorinated solvents and also in a number of aliphatic hydrocarbons. It is insoluble in alcohols, ketones, esters, nitriles, and other

TABLE I
Silyl Celluloses

Substituent	Analysis				Substitution, %	Tensile strength, psi	Elongation to break, %	Electrical Data		
	C, %	H, %	Si, %	N, %				Frequency, cps	Tan δ	Dielectric constant
Me_3Si[a]	47.8	9.1	21.0	—	89	4500	30	60	0.0007	2.8
								10^3	0.0016	2.8
								10^4	0.002	2.8
								10^5	0.003	2.8
$Me(C_6H_5)_2Si$	70.20	6.32	10.75	—	83	—	—			
$NC(CH_2)_3Me_2Si$	53.45	7.94	14.78	7.48	88	1500	198	60	0.169	14.5
								10^3	0.0192	14.1
								10^4	0.0315	13.8
								10^5	0.0811	12.7
$\dfrac{NC(CH_2)_3Me_2Si}{Me_2C_6H_5Si} = \dfrac{1}{3}$	65.77	6.58	11.85	1.62	~85	3200	20			
$\dfrac{NC(CH_2)_3Me_2Si}{Me_2C_6H_5Si} = \dfrac{1}{1}$	61.78	7.05	11.92	3.04	~85	2500	30			
$\dfrac{NC(CH_2)_3Me_2Si}{Me_2C_6H_5Si} = \dfrac{3}{1}$	57.34	7.37	11.93	5.30	~85	2200	100			

[a] Prepared by the silylamide method.
[b] Corona resistance in needle point electrode corona test: failure after 1 600 ∓ 50 hr (105°C, 15 mil air gap, 3 000 cycles, 2 500 V, sample thickness 30 ∓ 2 mils).
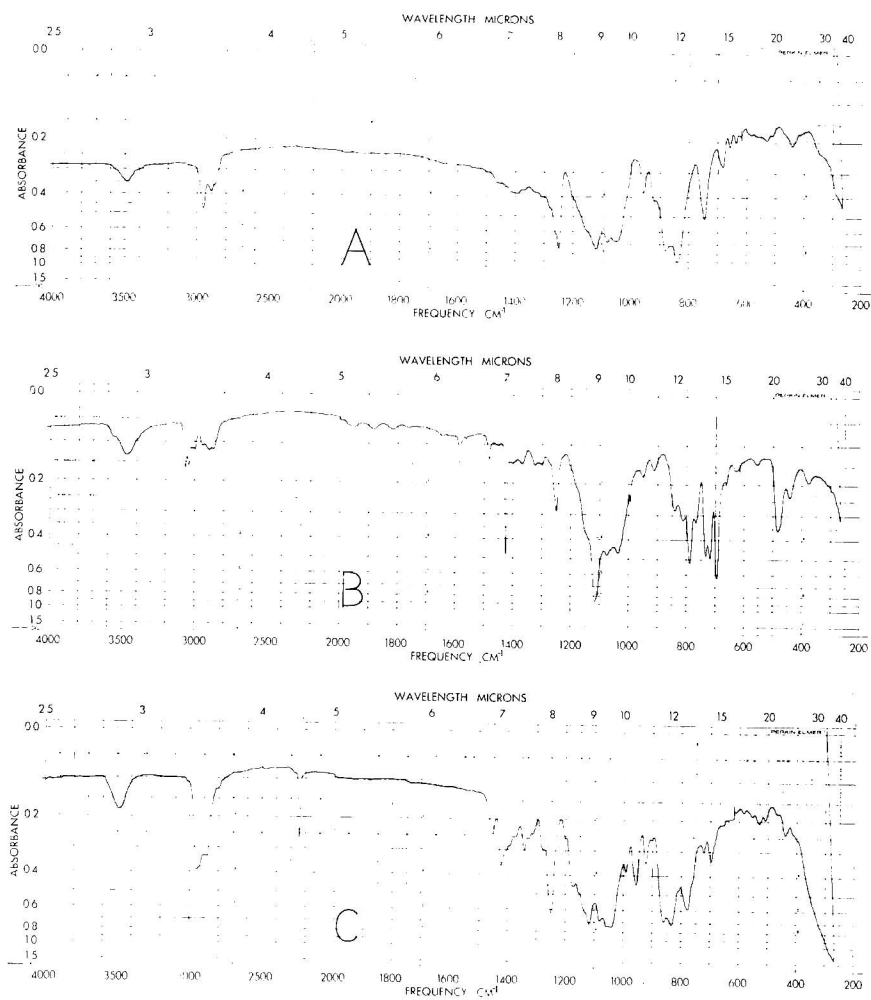
Fig. 1. Infrared spectra of: (A) trimethylsilyl cellulose in KBr); (B) methyldiphenyl-silyl cellulose (in KBr); C) dimethyl-γ-cyanopropylsilyl cellulose (film cast from CHCl₃ solution).

polar solvents. Solution-cast films are clear, flexible, and moderately strong (see Table I). The polymer does not melt; decomposition starts around 300°C in air. Electrical measurements show a low dielectric loss. The high corona resistance is noteworthy; it is characteristic of polymers with a relatively high silicon content.

Of great surprise to us was the relatively high hydrolytic stability of trimethylsilyl cellulose. Polymer samples left in ambient air were completely soluble in benzene up to three months. Even after 3 hr in boiling water, the polymer was nearly completely soluble in benzene; after several days in boiling water, 98% of the silyl groups were gone; however, the shape and clarity of the film sample was essentially unchanged after this treatment.

The hydrolytic stability of trimethylsilyl cellulose is particularly remark-able in view of the fact that poly(trimethylsilyl vinyl ether) is solvolyzed by methanol to poly(vinyl alcohol) under mild conditions,[3] whereas repeated precipitations and prolonged treatment of trimethylsilyl cellulose with methanol had no effect on this polymer. The bonding of the silyl groups is quite similar in these two poly(silyl alkyl ethers); the enhanced hydrolytic stability of silyl cellulose must be attributed to steric hindrance.
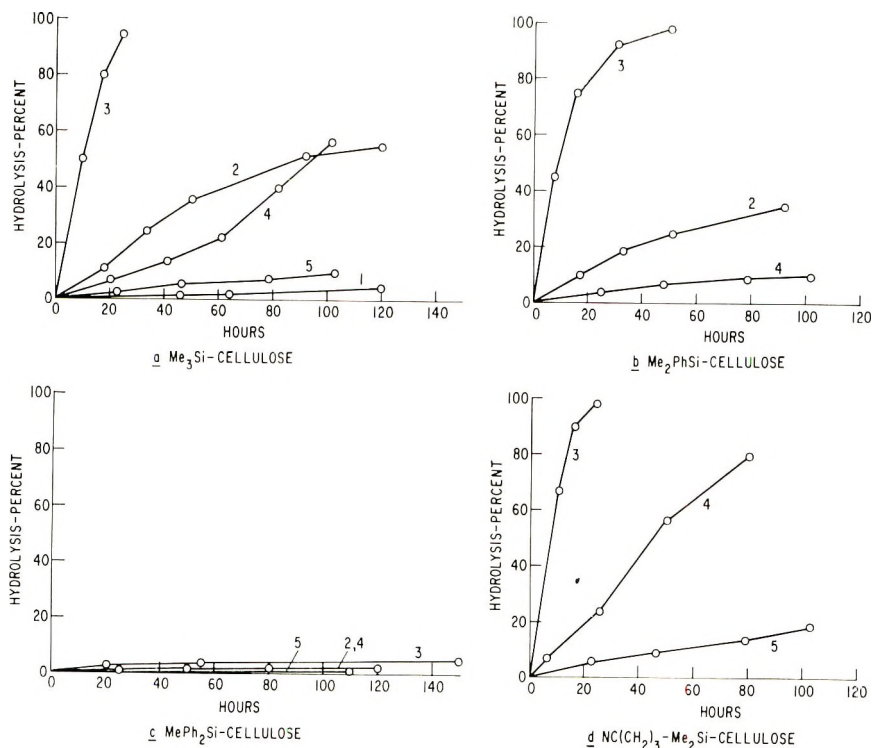
Fig. 2. Hydrolysis of silyl celluloses: (1) in water, 27°C.; (2) in water, 70°C.; (3) in water, 100°C.; (4) 1 atm. of water vapor, 120°C; (5) 1 atm. of water vapor, 150°C.

In order to determine the relative hydrolytic stability of a number of different silyl celluloses, weighed film samples of 3 mils thickness were subjected to water or 1 atm of water vapor (above 100°C) at different temperatures for certain lengths of time and then reweighed after thorough drying at 200°C/0.2 mm for 15 hr. The extent of hydrolysis that had occurred was calculated from the weight loss of the film. Figure 2a shows that 50% of the trimethylsilyl groups were lost by hydrolytic cleavage after 10 hr in water or water vapor of 100°C. Exposure to water of 70°C or water vapor of 120°C leads to 50% hydrolysis after about 80 hr. After 80 hr exposure to water vapor of 150°C or water of 27°C 7% and 2% hydrolysis, respectively, results.

The rather slow rate of hydrolysis in water vapor at high temperature, which was also observed with cellulose substituted with dimethyl-γ-cyanopropylsilyl, dimethylphenylsilyl, and methyldiphenylsilyl groups is peculiar, even considering the lower water content of the vapor, which is at 150°C about one fifth of that at 100°C.

Dimethylphenylsilyl Cellulose. This polymer resembles trimethylsilyl cellulose in all properties investigated. Monophenyl substitution on silicon does not lead to enhanced hydrolytic stability, as shown in Figure 2b.

Methyldiphenylsilyl Cellulose. Like the trimethylsilyl and the dimethylphenylsilyl analog, methyldiphenylsilyl cellulose is a colorless polymer, soluble in aromatic solvents, in chlorinated hydrocarbons and in pyridine. The polymer does not melt; beginning decomposition is noted around 350°C. Cast films are rather stiff, like those of the other two members of the silyl cellulose family, but less flexible; sharp creasing does not break films of trimethylsilyl and dimethylphenylsilyl cellulose, whereas the diphenylmethylsilyl derivative fractures when treated in this way.

The outstanding property of methyldiphenylsilyl cellulose is its hydrolytic stability (Fig. 2c). Film samples appeared entirely unaffected after 120 hr in boiling water; the slight weight loss after this treatment corresponded to hydrolytic cleavage of approximately 5% of the silyl ether bonds.

Dimethyl-γ-cyanopropylsilyl Cellulose. Silylation with dimethyl-γ-cyanopropylsilyl chloride or amide provides this polymer which, as may be expected by the presence of the alkyl chain and the polar cyano group, differs drastically in physical and solution properties from the three other silyl celluloses. The colorless polymer is soluble in polar solvents like nitriles and ketones; it is insoluble in aliphatic and aromatic hydrocarbons. Cast films are slightly opaque and very soft; they can be shaped to some degree by hand without tearing. The hydrolytic stability of this polymer is somewhat lower than that of trimethylsilyl cellulose as shown in Figure 2d, although the hydrolysis under ambient conditions is insignificant.

Blending of γ-cyanopropyldimethylsilyl cellulose with other silyl celluloses leads to incompatible mixtures; however, cellulose can be cosilylated with γ-cyanopropyldimethylchlorosilane and methyldiphenylchlorosilane in various relative proportions. Cast films of the resulting polymers rich in methyldiphenylsilyl groups are nearly clear whereas a large proportion of the polar silyl group results in opacity. Tensile and elongation data (Table I) of these mixed substituted silyl celluloses also reflect the apparently additive effect of the two different substituents on the properties of the polymers.

Surface Silylation of Cellulose Fibers

The silylation of cellulose with Si–N compounds proceeds under relatively mild conditions which should be nondestructive for woven cotton fabric

in contrast to silylation with chlorosilanes and pyridine which deteriorates cotton. When a piece of white cotton fabric was heated in a 1:2 mixture of BSA and N-methyl-pyrrolidone at 140°C for 1 hr and then rinsed with alcohol, the fabric appeared entirely unchanged. The elemental analysis showed the presence of 1.6% Si which corresponds to substitution of 7% of the available hydroxyl protons by trimethylsilyl groups. The silyl groups are presumably located on or near the surface of the individual cotton fibers which was reflected by the fact that the fabric had become highly water repellent. Refluxing of the fabric in a 1:1 benzene–methylene chloride mixture for 3 days did not affect the water repellency. Likewise, three cycles in an automatic washer with regular detergent did not destroy the water repellent properties of the fabric, although extended treatment under basic aqueous conditions can be expected to remove the surface layer of silyl substituents.

EXPERIMENTAL

Silylations with Silylamides

Trimethylsilyl Cellulose. A 34-g portion of wood pulp cellulose V-90 of Buckeye Corporation (dried at 100°C/20 mm overnight) was stirred with 82 g BSA and 300 g of N-methylpyrrolidone (minimum amount to get a stirrable mixture after reaction has set in) at 150–160°C bath temperature. A transparent, tan-colored gel was formed within 1 hr. A 400-cc portion of xylene was now added; another 400-cc portion of xylene was added 2 hr later. Stirring was continued at 150°C for a total of 4 hr. Benzene was added after cooling to give a total of 2.5 liters in order to lower the viscosity. The solution was completely free of solids; it was run from a separation funnel into stirred methanol. The polymer precipitated in the form of a white thread. It was washed with methanol until free of benzene and dried at 50°C/20 mm; the yield was 67 g (91% of the theory).

Completely soluble silyl cellulose prepared by this method has been obtained from wood pulps V-60 and V-90 and from cotton linter pulps 1AY500-2, 1A500, 12HME-1, 6N35, and 1AR500 of Buckeye Cellulose Corporation. Silyl cellulose solutions prepared from wood pulps had lower viscosities than those derived from cotton linter pulps; the intrinsic viscosities measured in chloroform ranged from 2 to 7 dl/g.

Dimethyl(γ-cyanopropyl)silyl cellulose. A mixture of 12.5 g V-60 Buckeye wood pulp, 55 g of N-[dimethyl(γ-cyanopropyl)-silyl]-N-methyl-acetamide and 250 g of N-methylpyrrolidone was stirred under N_2 in a bath heated at 150–160°C. After about 30 min, all solids had gone into solution. Stirring and heating at 150°C was continued for a total of 2 hr; a clear viscous tan-colored solution was obtained. Toluene (200 cc) was now added and the solution run slowly into stirred methanol; the polymer precipitated as nearly white fiber. It was thoroughly washed with CH_3OH and dried at 100°C/200 mm overnight; 36 g product was obtained (87% of the theory based on complete silylation). The polymer is soluble

in chloroform, pyridine, acetonitrile, and other polar solvents; it is insoluble in aliphatic and aromatic hydrocarbons.

Dimethyl(γ-cyanopropyl)silyl methylacetamide used as the silylating agent was prepared as follows.

To a mixture of 73 g of N-methylacetamide (1 mole), 120 g of triethylamine, and 200 cc of toluene was slowly added 155 g of dimethyl-γ-cyanopropylchlorosilane (1 mole). The temperature was kept below about 50°C by proper rate of addition. Et$_3$NHCl was formed; the mixture became dark purple soon after the reaction had started. Stirring at room temperature was continued for one hour after the addition was complete. After filtration, the product was distilled on a spinning band column; the main product boils at 90–93°C/0.03 mm as a colorless liquid which turns yellowish pink on contact with air. After redistillation, a yield of 93 g was obtained.

ANAL. Calcd: C, 54.5%; H, 9.1%; N, 14.1%. Found: C, 54.6%; H, 9.4%; N, 14.0%.

Methyldiphenylsilyl Cellulose. A mixture of 3.2 g of V-60 wood pulp cellulose of Buckeye Corporation (20 mmole), 20 g of N-diphenylmethylsilylacetamide (78 mmole), and 50 g of N-methylpyrrolidone was heated under N$_2$ with stirring in an oil bath at 160–170°C. A clear, very viscous solution was obtained after about 75 min. The mixture was heated at 160–170°C for a total of 2 hr then cooled and diluted with benzene; total volume 200 cc. The solution which was slightly hazy but contained no solids was poured slowly into stirred methanol; the polymer precipitated as a white fiber. After drying at 150°C/20 mm overnight, a yield of 10.0 g was obtained, corresponding to 78% of the theory, based on an average of 2.5 silyl groups per repeating unit. The polymer is soluble in chlorinated and aromatic solvents; it is insoluble in solvents of higher polarity like acetonitrile, acetone, etc. The intrinsic viscosity of a solution of the polymer in chloroform was 3.55 dl/g.

Methyldiphenylsilyl acetamide used as the silylating agent was prepared as follows.

One mole of methyldiphenylchlorosilane (232 g) was added slowly to the stirred mixture of 60 g of acetamide (1 mole), 120 g of triethylamine, and 450 g of benzene. A mildly exothermic reaction occurred, and triethylamine hydrochloride precipitated. The stirred mixture was heated at reflux for about 1 hr after the addition was complete, then allowed to cool to about 50°C and filtered. The product crystallized while being filtered; some was lost with the hydrochloride. The filtrate was kept in the refrigerator overnight. The product was then filtered off and recrystallized from hot benzene; it was in the form of colorless, fine crystals, mp 121–123°C.

ANAL. Calcd: C, 70.5%; H, 6.7%; Si, 11.0%. Found: C, 69.3%; H, 6.8%; Si, 11.0%.

Trimethylsilyl Ethyl Cellulose. A mixture of 5.0 g of Hercules G-50 ethyl cellulose with 0.7–0.8 hydroxyl groups per anhydroglucose unit, 5.0 g of bis(trimethylsilyl)acetamide, 5 g of N-methylpyrrolidone, and 50 cc of benzene was stirred in an anhydrous atmosphere in a bath heated at 85–90°C for 1 hr. A clear colorless solution was obtained. The polymer was precipitated by pouring into stirred methanol. The colorless fibrous product weighed 5.2 g after drying overnight at 80°C/20 mm. The product is soluble in aliphatic hydrocarbons and insoluble in alcohols, in contrast to the starting ethylcellulose. Silylated ethylcellulose is also soluble in chlorinated and in aromatic solvents.

ANAL. Found: C, 55.39%; H, 9.10%; Si, 6.30%. The data correspond to 2.25 C_2H_5O—, 0.65 Me_3SiO—, and 0.1 HO— per repeating unit.

Silylations with Chlorosilanes

Trimethylsilyl Cellulose. A mixture of 4 g of sucrose, 105 g of trimethylchlorosilane (SC-3001 of the General Electric Silicone Products Department), 80 g of pyridine, and 1.4 l. of toluene was heated at 100–110°C for 1.5 hr; the sucrose had turned into a light brown semisolid after this time. V-60 wood pulp cellulose (Buckeye), 26 g, which had been dried at 100°C/20 mm for 15 hr was added and the mixture stirred under anhydrous conditions for 4 hr in an oil bath heated at 105–110°C. All cellulose had gone into solution after this time and pyridine hydrochloride was suspended in the viscous mass. One liter of toluene was added and the mixture filtered through a coarse sintered glass filter funnel holding a 1-in. layer of Harshaw alumina with a layer of tightly packed glass wool on top. The clear, nearly colorless filtrate was free of pyridine hydrochloride and clear films could be cast from this solution without subsequent cross-linking. The polymer could be obtained in the form of white fibers by precipitation with methanol. The product was identical in all respects with silylcellulose prepared with BSA.

Dimethyl(γ-cyanopropyl)silyl Cellulose. Al-500 Buckeye cotton linters (5.0 g) were heated at reflux with stirring with 35 g of dimethyl-γ-cyanopropylchlorosilane and 200 g of pyridine. After about 5 hr at reflux, a viscous, brown solution was obtained with very little solid material left. The solution was diluted with 1 liter of pyridine, filtered, precipitated with CH_3OH, and the nearly colorless fibrous material washed with CH_3OH until the pyridine odor was gone. A yield of 13.5 g was obtained after drying at 100°C/20 mm overnight. The material is identical with the product obtained by silylation with the corresponding silylamide.

Methyldiphenylsilyl Cellulose. Similar to the previous experiment, 5.0 g of Al-500 was heated at reflux with stirring with 40 g of diphenylmethylchlorosilane and pyridine. A clear, light tan-colored solution was obtained after about 15 hr of heating. Filtration left no solid material behind. The product was precipitated with methanol; 16 g of white fibrous material was obtained after drying at 100°C/20 mm. Again, no

difference was detected between polymer prepared by this route and product obtained via silylation with silylamide.

Methyldiphenylsilyl/Dimethyl-γ-cyanopropylsilyl Cellulose. In three separate experiments, 5.0 g (90 mmole of hydroxyl) of V-60 wood pulp (Buckeye) was mixed with: (a) 15.7 g of methyldiphenylchlorosilane (67.5 mmole), 3.6 g of dimethyl-γ-cyanopropylchlorosilane (22.5 mmole) and 200 cc of pyridine; (b) 10.5 g of methyldiphenylchlorosilane (45 mmole), 7.3 g of dimethyl-γ-cyanopropylchlorosilane (45 mmole) and 200 cc of pyridine; (c) 5.3 g of methyldiphenylchlorosilane (22.5 mmole), 10.9 g dimethyl-γ-cyanopropylchlorosilane (67.5 mmole) and 200 cc of pyridine. The three mixtures were heated with stirring under anhydrous conditions in a bath at 130–140° for about 2 hr. The clear solutions were added to methanol, the white polymer precipitates dissolved in chloroform and reprecipitated with methanol. The three experiments (a), (b), and (c) yielded 15.2 g, 14.0 g, and 12.5 g of product, respectively. The analyses shown in Table I indicate that the obtained substituent ratios approximate the molar ratios of the two chlorosilanes employed in the experiments.

References

1. A. E. Pierce, *Silylation of Organic Compounds*, Pierce Chemical Company, Rockford, Ill., 1968.

2. J. F. Klebe, *J. Polym. Sci. B*, **2**, 1079 (1964).

3. S. Murahashi, S. Nozakura and M. Sumi, *J. Polym. Sci. B*, **3**, 245 (1965).

4. H. A. Schuyten, J. W. Weaver and J. D. Reid, U. S. Patent 2,562,955 (August 1951).

5. J. F. Klebe, H. Finkbeiner, and D. M. White, *J. Amer. Chem. Soc.*, **88**, 3390 (1966).

Cocatalysis by Epoxides in the Polymerization of Tetrahydrofuran with Trityl Hexachloroantimonate Initiator*

IRVING KUNTZ and M. T. MELCHIOR, *Esso Research and Engineering Company, Linden, New Jersey 07036*

Synopsis

The polymerization of tetrahydrofuran (THF) with $(C_6H_5)_3C^+SbCl_6^-$ initiator is markedly accelerated by small concentrations of propylene oxide or other epoxides. Molar concentrations of propylene oxide 4 to 10 times those of the carbonium-ion salt showed increasing conversion to polymer. The equilibrium conversion level at different temperatures with epoxides is the same as in their absence; the approach to equilibrium is first-order in THF. NMR experiments in the presence of propylene oxide indicate the formation of a trityl ether intermediate. The cocatalysis effect is interpreted on the basis of an acceleration in the initiation process in the system.

INTRODUCTION

The polymerization of tetrahydrofuran (THF) to high molecular weight products by using carbonium ion salts such as triphenylmethyl (trityl) hexachloroantimonate, $(C_6H_5)_3C^+SbCl_6^-$ (I, referred to later as Ph_3C^+-$SbCl_6^-$) was first reported by Bawn and his associates.[1] More recent studies of this system have concentrated on specific anion effects[2] and the details of the initiation process.[3,4] In this communication, we report our observations that the THF polymerization rate using this initiator is markedly increased by trace amounts of propylene oxide or other epoxides.

EXPERIMENTAL

Experimental procedures were similar to those described previously.[3] The method of purification of the THF affects the rate of polymerization in uncocatalyzed experiments.[5] The THF (J. T. Baker Co.) used in most of the experiments in this research was purified by distillation from lithium dispersion or calcium hydride. Hazards in the purification of THF have recently been reviewed.[6] Polymerizations were carried out in screw-capped ampules and were prepared in a glove box under nitrogen. Epoxides were commercial samples redistilled before use, and when used as cocatalysts were premixed with the THF before addition to the initiator. Polymers

were isolated by precipitation into ice water; this isolation procedure would not collect very low molecular weight, water-soluble products. After drying in the vacuum oven at 40°C, inherent viscosities were determined in benzene at 25°C (0.1 g/dl concentration).

In the NMR experiments with precooled reagents, Dry Ice–acetone was used to cool the PO–THF solution and the flask containing I, before mixing. The solution was rapidly transferred to a NMR tube, which was then kept in a Dry Ice bath until insertion in the NMR spectrometer.

NMR spectra were obtained on a Varian HA-100 instrument operating in the frequency-sweep internal lock mode, a THF peak being used as internal reference. Signal-to-noise enhancement was accomplished by using the C-1024 time-averaging computer. It was generally necessary to obtain 10–40 scans in order to obtain sufficient signal-to-noise. All spectra were run at room temperature, except for one experiment at −30°C.

sec-Butyl triphenylmethyl ether was prepared from 2-butanol by the procedure described earlier.[3] The material had a boiling point of 175–180°C/0.01 mm.

ANAL. Calcd. for $C_{23}H_{24}O$: C, 87.30%; H, 7.64. Found: C, 87.50; H, 7.33.

RESULTS

Figure 1 shows the polymerization of the THF in benzene at 7°C with $Ph_3C^+SbCl_6^-$ as initiator. Results of another experiment, in which propylene oxide (PO) was present at a concentration about 20 times that of the trityl salt, are shown. The increase in polymerization rate is dramatic.
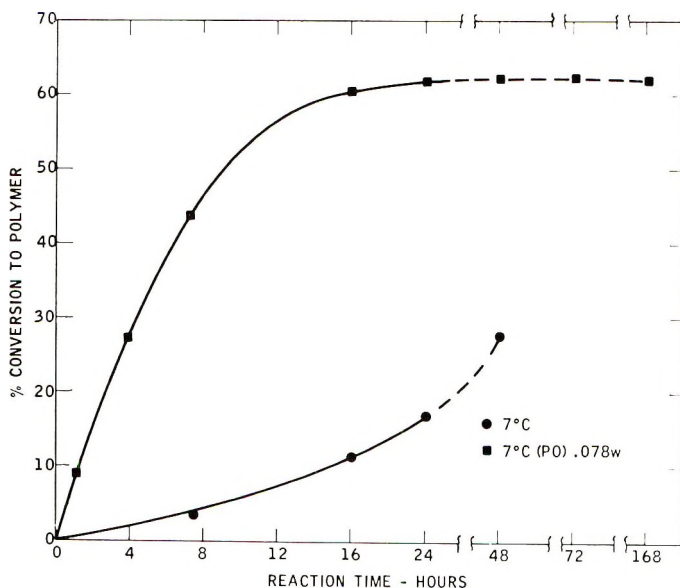
Fig. 1. THF polymerizations at 7°C: THF 10M, benzene 2M. $Ph_3C^+SbCl_6^-$, 3.5 × 10^{-3} M; (■) PO present, 0.071M; (●) no PO.
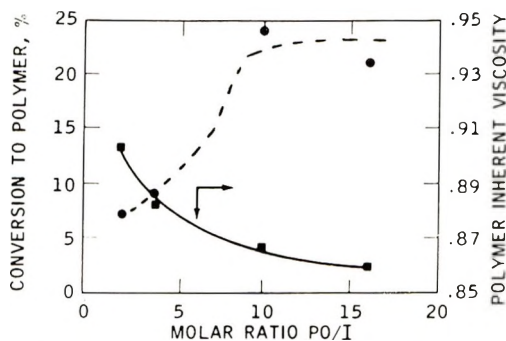
Fig. 2. Effects of PO initiator ratio in THF bulk polymerizations at 7°C: (●) conversion values; (■) polymer inherent viscosities in bezene. $Ph_3C^+SbCl_6^-$ 3.5 × 10^{-3} M, 3 hr experiments, (PO) as shown.

Under our conditions where, for example, in the absence of PO only about 3% conversion to polymer had taken place, a conversion of 45% was found when PO was used. This increase in polymerization rate by small amounts of PO is observed in polymerizations at other temperatures and in bulk polymerizations as well as those containing a solvent. We interpret these results as indicating that the small amount of PO is serving a cocatalyst function in the carbonium-ion salt–THF polymerization system.

Experiments were carried out with varied concentrations of PO to study the stoichiometry of the cocatalyst effect. Figure 2 shows that with molar ratios of PO to carbonium ion salt of 2,4, and 10 conversion to polymer increases regularly. Increasing the epoxide/initiator ratio beyond about 10 seems to give no further increase in rate. Other experiments gave similar results. On the same figure are plotted the inherent viscosities of the polymers isolated in these experiments. The data show decreasing inherent viscosity with increasing concentration of PO.

When $Ph_3C^+SbCl_6^-$ is used to polymerize THF, the solution develops an amber color immediately. The color persists and darkens during the course of the polymerization to ultimately reach very dark brown colors. In experiments with a cocatalyst the color observations are different. When a small amount of an epoxide such as PO is present, the solution is colorless and remains so for a long time. However, if the solution containing the PO is allowed to stand, after significant polymerization has taken place it will become first yellow, then amber, and ultimately reach the same very dark colors observed in the experiment without the cocatalyst. It has been reported that in the polymerization of THF with preformed trialkyl-oxonium-ion salts colored solutions are not produced.[7]

The THF–$Ph_3C^+SbCl_6^-$ system is one showing equilibrium polymerization behavior. Conversion to polymer need not be complete, but reaches an equilibrium value determined by polymerization temperature.[8] Experiments such as that shown in Figure 3 at different temperatures indicate that when PO is used at small concentrations as a cocatalyst the equilibrium

conversion level observed is the same as that in the uncocatalyzed poly-
merization. Figure 3 shows that the approach to equilibrium follows first-
order kinetics.
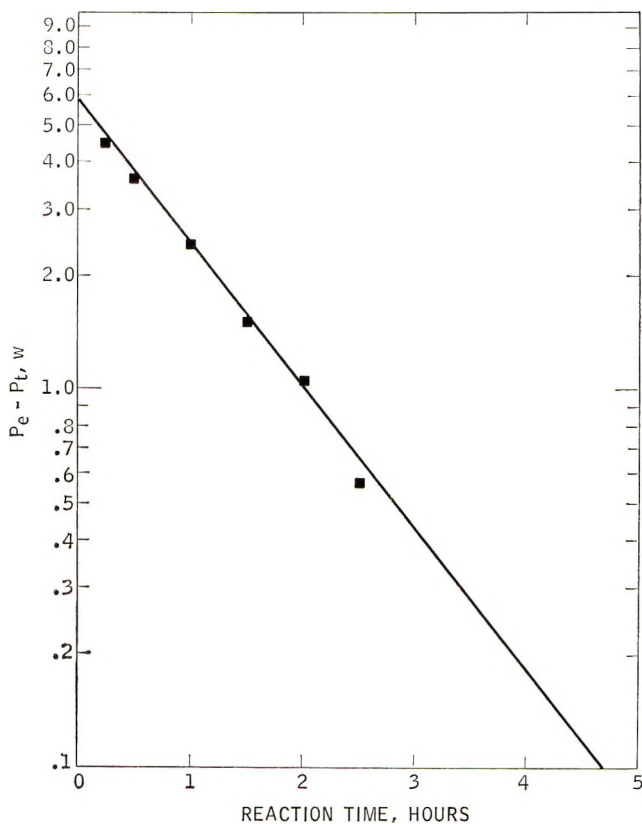
Fig. 3. Approach to equilibrium conversion. THF, 10 M in benzene, $Ph_3C^+SbCl_6^-$
$3.5 \times 10^{-3}M$, PO $0.069M$, $25°C$. Ordinate is the difference between equilibrium poly-
mer concentration and the instantaneous polymer concentration.
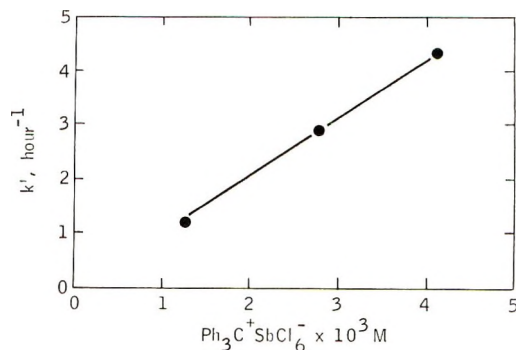
Fig. 4. Dependence of polymerization rate on $(Ph_3C^+SbCl_6^-)$. Initial first-order
rate constants from dilatometric experiments. THF $12M$, PO $0.057\ M$, $25°C$.

TABLE I
Polymerization of THF with $Ph_3C^+SbCl_6^-$ at 23°C
with Various Epoxide Cocatalysts[a]

| Epoxide | Reaction time = 1.25 hr | | Reaction time = 4.25 hr | |
	Con- version, %	Inherent viscosity[b]	Con- version, %	Inherent viscosity
None	3, 3	1.27, 1.31	9, 9	1.91, 2.01
Propylene oxide	48, 48	1.89, 1.87	70, 71	1.76, 1.98
Epichlorohydrin	44, 45	1.78, 1.81	67, 67	2.29, 2.28
Octene-1 epoxide	46	1.50	69	1.72
2,3-Epoxybutane[c]	44	1.50	68	1.83
Isobutylene oxide	1	0.56	2	0.81
Cyclohexene oxide	44	1.44	63	2.02
Cyclododecene oxide	41	1.18	60	1.31
3,4-Epoxyvinylcyclo- hexane	44	1.44	66	1.56
1,2-Epoxy-5,6-*trans*- 9,10-*cis*-cyclodo- decadiene	41	1.25	61	1.33
3,3-Bis(chloromethyl)- oxetane	32	1.35	66	1.67

[a] Reactants were 0.07 mmole $Ph_3C^+SbCl_6^-$, 1.4 mmole epoxide, and 20 ml THF.
[b] Determined in benzene at 25°C.
[c] Approximately equal proportions of the *cis* snd *trans* isomers.

In Figure 4 we show that the initial first-order polymerization rate constant at constant PO concentration shows a first-order dependence on carbonium-ion salt concentration.

So far, we have described only experiments with PO as the cocatalyst epoxide component. Experiments were also carried out with a large number of epoxides with varied structural features. Table I shows these results for two different reaction times. The molar ratio of epoxide to $Ph_3C^+SbCl_6^-$ was 20 in these experiments. It is surprising that so many of these epoxides show the cocatalyst effect to such a similar degree, even those with quite complicated structural features. Terminal epoxides or those derived from internal or cyclic olefins show similar behavior. Experiments with an epoxide/$Ph_3C^+SbCl_6^-$ ratio of 5 did not lead to a significant broadening of the range of cocatalyst effects. However, the data in Table I do show that one epoxide is very different from the others; isobutylene oxide does not behave as a cocatalyst but actually reduces the amount of polymer obtained, compared to that isolated when no cocatalyst at all is used.

Shown in Table II are results of studies designed to determine if the cocatalyst effect could be observed if the epoxide was added to a polymerization that had been proceeding in the conventional way. Experiments 2 and 3 compare an uncocatalyzed and a cocatalyzed polymerization, respectively. We see the conversion and intrinsic viscosity effects we anticipate.

TABLE II
Cocatalytic Effect with Propylene Oxide

Expt. no.	Temp, °C	$Ph_3C^+SbCl_6^-$, mg	THF, ml	PO, ml	Special treatment	Total polymerization time, hr	Polymer yield		Inherent viscosity
							g	%	
1	23	40	20	—	None	2	0.9	5	1.78
2	23	40	20	—	None	24	6.4	36	3.35
3	23	40	20	0.1	None	24	11.9	67	2.23
4	23	40	20	—	0.1 ml PO after 2 hr	24	11.1	62	2.09
5	6	40	20	—	None	24	3.4	20	3.07
6	6	40	20	—	None	4	0.3	2	1.20
7	6	40	20	0.1	None	24	15.0	91	3.29
8	6	40	20	—	0.1 ml PO after 2 hr	24	14.1	85	3.15
9	6	40	20	—	0.1 ml PO after 4 hr	24	13.4	81	2.93
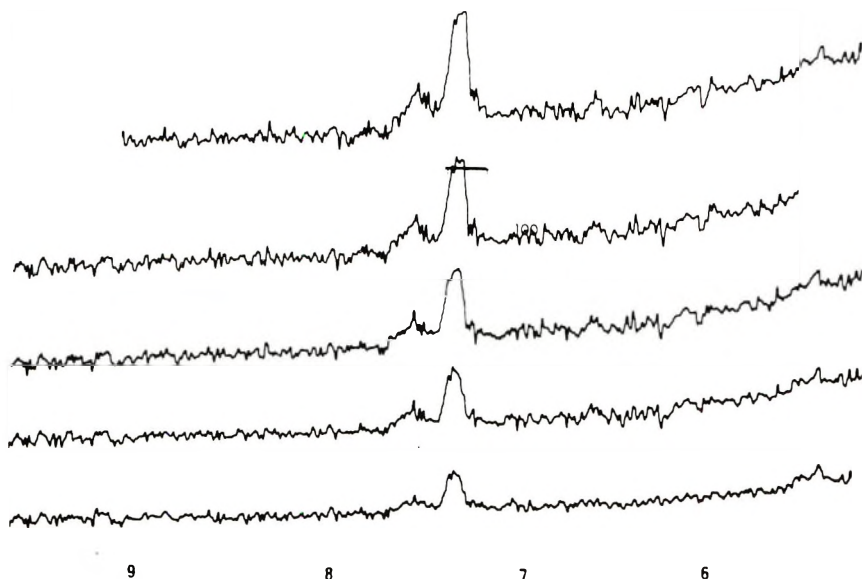
Fig. 5. THF polymerization with PO cocatalyst. I, 6.9 × $10^{-3}M$, PO 7.1 × $10^{-2}M$. Ratio PO/I, 10. Traces are for, from bottom to top, 2, 3, 5, 7 scans.

In experiment 4 of Table II we allowed an uncocatalyzed experiment to proceed for 2 hr. From the data in experiment 1, we note that the amount of polymer produced in this time interval is more than twenty times the amount of $Ph_3C^+SbCl_6^-$ originally used as initiator. In experiment 4 PO was added after this 2-hr period, and the charge allowed to stand. From the amount of polymer isolated in experiment 4 we see that the cocatalyst effect is observed when the epoxide is added to the system after the polymerization has been allowed to proceed in the normal way for some time. Similar results were observed in a series of experiments carried out at 6°C, as also shown in Table II.

NMR experiments have given valuable information about the cocatalytic effect. In initial experiments to obtain samples that did not polymerize explosively at the relatively high initiator concentrations, the molar ratio of PO to $Ph_3C^+SbCl_6^-$ was about 0.7. In these polymerizations we could detect the formation of Ph_3CH as described earlier for the uncocatalyzed system.[3]

Using the time-averaging technique we were able to obtain NMR data at concentrations similar to those used in our polymerization studies. Figure 5 shows the initial NMR traces of an experiment in which PO was used as cocatalyst at a concentration ten times that of the $Ph_3C^+SbCl_6^-$. The aromatic protons at about 7.3 δ (ppm downfield from tetramethylsilane) show a pattern quite different from that observed in a polymerization without cocatalyst, shown in Figure 6. In the latter case the methine peak of Ph_3CH is seen at 5.7 δ. In examining these results, the patterns obtained from authentic mixtures of Ph_3CH and $Ph_3COsec-C_4H_9$ in THF shown in

Figure 7 are helpful.   Our observations are consistent with the formation of
a trityl ether in THF polymerizations containing PO cocatalyst.

As we examined many samples containing PO cocatalyst by the NMR
technique it became clear that the pattern observed for the aromatic pro-
tons changed with time.   No change was noted for the THF polymeriza-
tions without cocatalyst.   Experiments were carried out in which the PO-
THF mixture was cooled in Dry Ice before addition to $Ph_3C^+SbCl_6^-$.
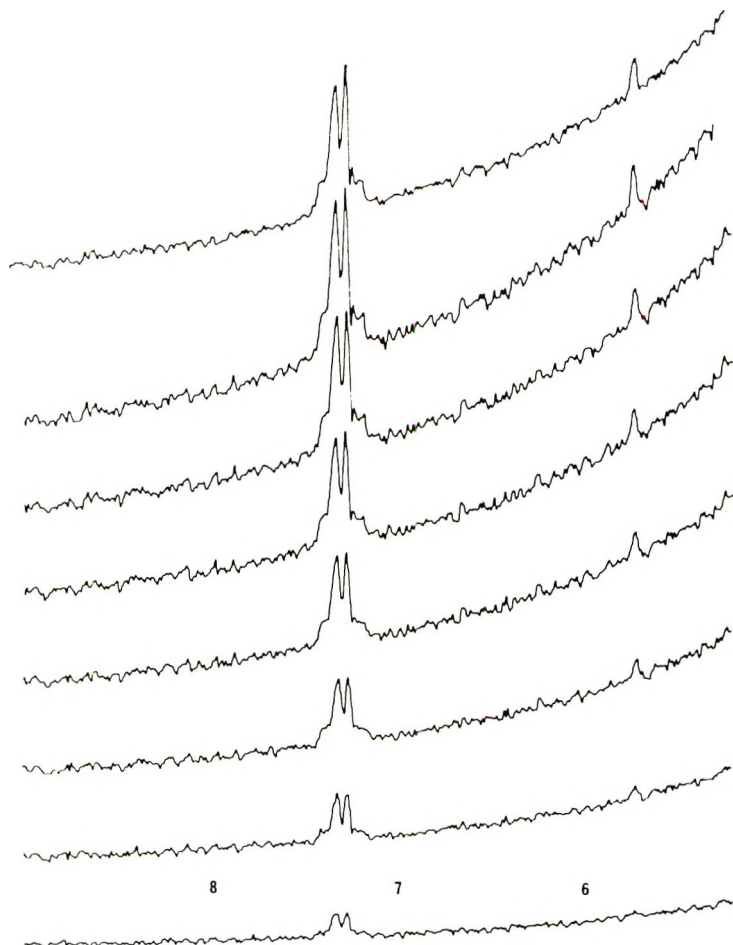
Fig. 6. THF polymerization without cocatalyst.   I, $6.9 \times 10^{-3} M$.   The curves, from
bottom to top, represent 1, 2, 3, 4, 5, 7, 11 scans.

The solution was maintained in a similar bath before insertion into the
NMR instrument, where warming to ambient temperature took place.
This procedure permitted study of the change of the aromatic proton pat-
tern.   Figure 8 shows the results of such an experiment.   There is a
definite change from a pattern expected for a trityl ether structure to one

indicating a significant proportion of Ph_3CH. However, the NMR trace is not that anticipated from Ph_3CH alone.

In another experiment, an NMR sample was prepared with a PO/I ratio of 18; the Dry Ice cooling procedure was followed by insertion into the instrument with the probe maintained at $-30°C$.

Up to this time, examination of the NMR pattern of the THF protons showed that no polymerization had taken place in the colorless solution. After 5.1 hr at $-30°C$ the aromatic proton pattern was consistent with a trityl ether structure and 16% conversion to poly(THF) had taken place.
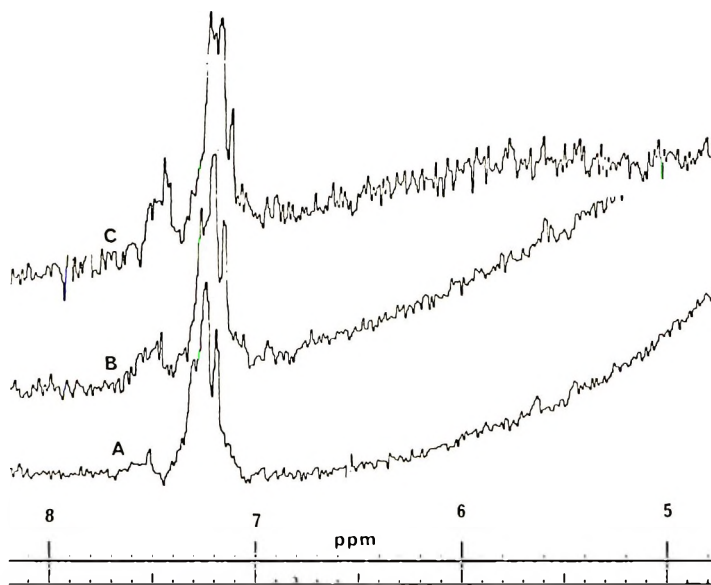
Fig. 7. NMR results with authentic mixtures in THF: (A) Ph_3CH 8.4×10^{-3} M, $Ph_3COsec\text{-}C_4H_9$ $4.4 \times 10^{-3}M$; (B) Ph_3CH $6.7 \times 10^{-3}M$, $Ph_3COC_4H_9$ 6.3×10^{-3} M; (C) Ph_3CH 4.3×10^{-3} M, $Ph_3COC_4H_9$ $8.9 \times 10^{-3}M$. Tracings result from 20–30 scans.

The sample temperature was then raised to $25°C$. After 1 hr at this temperature 38% conversion to polymer had occurred, the aromatic proton pattern still was that of a trityl ether, and the solution was still colorless. The next day the NMR pattern had changed in the fashion previously observed and the solution was dark amber. The NMR traces are shown in Figure 9.

An NMR experiment, similar to those described in Table II, was also carried out; PO was added to a THF polymerization already under way by initiation with $Ph_3C^+SbCl_6^-$. Originally, the pattern of PH_3CH was observed as anticipated. After the PO addition we could observe the enhanced polymerization rate by examining the increase in the peak ascribable to methylene groups alpha to the ether oxygen in the polymer. However, we could not detect any change in the aromatic proton pattern.

Fig. 8. Precooled polymerization. Solution was $4.5 \times 10^{-3}M$ in I, $7.1 \times 10^{-2}M$ in PO. Molar ratio PO/I 16. Successive NMR traces from bottom to top. 1, 2, 16, and 35 scans. Uppermost trace obtained approximately 5 hr after mixing.

DISCUSSION

The experimental results presented have clearly shown that small amounts of propylene oxide or other epoxides significantly increase the polymerization rate of THF when $Ph_3C^+SbCl_6^-$ is used as initiator. The propagation reaction in this system is considered to involve oxonium ions [eq. (1)]. We do not believe that the observed cocatalytic effect of epoxides involves

the propagation reaction. Rather, we believe that the cocatalytic effect must result from an increase in the concentration of propagating centers. This focuses attention on the initiation process in this system. One step in

Fig. 9. NMR studies of polymerization at $-30°C$, I $0.0082M$, PO $0.15M$, THF $13M$, PO/I ratio 18: (A) after 4.5 hr, 14 scans, 14% conversion to polymer; (B) after 5.1 hr, 23 scans, 16% conversion; (C) after 1 hr at $25°C$, 14 scans, 38% conversion; (D) after 24 hr at $25°C$, 67 scans.

the initiation of polymerization of THF with $Ph_3C^+SbCl_6^-$ has been shown to involve the production of triphenylmethane [eq. (2)].[3]
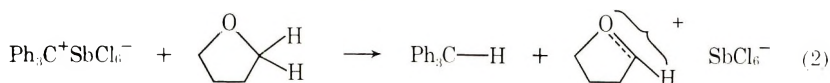
When an epoxide is present, a new species can be formed in solution as shown in eq. (3).
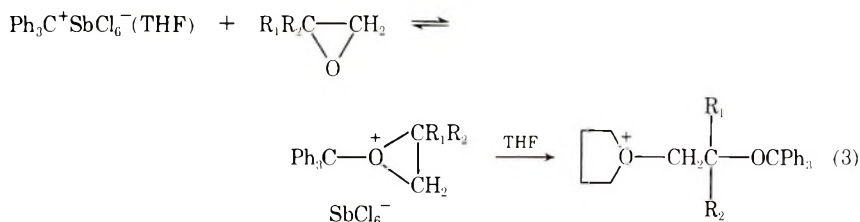
The oxonium ion derived from the epoxide can now react with THF to generate the growing chain. If sufficient epoxide is present to convert all the carbonium ion to the epoxide derived oxonium ion, a complete change of mechanism is obtained and no Ph_3CH is formed. More than 1 mole of epoxide per mole of $Ph_3C^+SbCl_6^-$ is required for this change of mechanism since THF is a stronger Lewis base and present in much higher concentration and more effective in solvating Ph_3C^+ than is PO. Thus, at lower $PO/Ph_3C^+SbCl_6^-$ ratios, both the Ph_3CH-forming initiation process and that shown in eq. (3) proceed simultaneously. The initiation process involving the three-membered oxonium ion is very much faster than that in the uncocatalyzed reaction. More propagating species are generated early in the reaction which are able to react with monomer and cause the observed increase in polymerization rate. The NMR spectra we observe in the presence of PO is consistent with that anticipated from examination of an authentic trityl ether, II, synthesized as a model compound. If the cocatalyst effect is to operate with a particular epoxide there are requirements for the derived oxonium ion of eq. (3). With isobutylene oxide the intermediate must have sufficient carbonium ion character to make the reaction with THF difficult. Thus, this epoxide does not show cocatalytic behavior.

$$\underset{II}{Ph_3COCHCH_2CH_2CH_3}\overset{\overset{\displaystyle CH_3}{|}}{}$$

If this reasoning is correct, it demands that the initiation reaction in the normal polymerization, in the absence of cocatalyst, must be slow. Evidence that initiation of polymerization in this system is slow has been reported.[2,4,9]

Our NMR observations show that the trityl ether group is unstable in the polymerization mixture. It is reasonable that the ether group is cleaved to regenerate the Ph_3C^+ ion. The carbonium ion can now abstract a hydride ion from a THF molecule to form Ph_3CH. The color formation observed on standing in cocatalyzed experiments can be caused by this behavior. The positive fragment of eq. (2) must be a precursor in the color-forming reaction.

The inherent viscosity of the polymers isolated in the cocatalyzed reaction is generally lower (at the same conversion level) than polymers obtained in the absence of a cocatalyst. This behavior may be the result of several effects. Rapid initiation would yield fewer high molecular weight species whose effect is magnified in the inherent viscosity measurement. Chain transfer and cyclization reactions due to the presence of epoxide group residues may also be contributing to this behavior. The generation of new polymer chains by the Ph_3C^+ liberated by the ether cleaving reaction also affects molecular weight.

Much more difficult to explain is the cocatalytic effect observed when PO was added to a polymerization initiated in the normal way. The enhanced polymerization rate was clearly observed in these experiments. Ledwith

has found that the hydride abstraction reaction of $Ph_3C^+SbCl_6^-$ with THF to form Ph_3CH is rapid, even at low temperatures.[10] Thus, there can be no carbonium salt still present to react as shown in eq. (3).

The Ph_3CH-forming reaction of eq. (2) is recognized to be only the first step in the initiation process in the normal reaction. It has been considered that this fragment might be involved in the initiation of the propagation process as shown in eq. (4).[3] This may be a slow process.

$$(4)$$
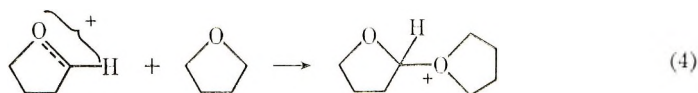
Based on NMR studies of the uncocatalyzed reaction Dreyfuss et al.[4] believe that the first formed positive fragment of eq. (2) loses one or more protons to form a furan derivative and a new cationic species. Some observations indicate that this species is relatively long lived. Their mechanism is shown in eqs. (5) and (6).

$$(5)$$

$$(6)$$
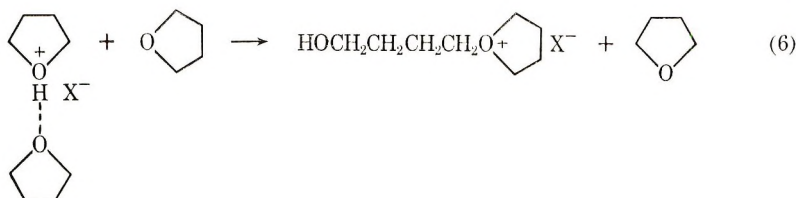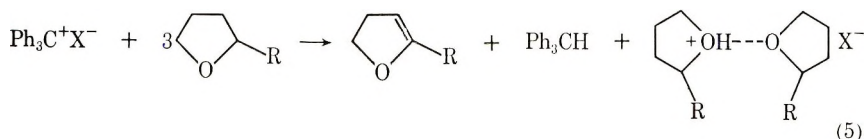
We have duplicated the NMR observations of Dreyfuss at relatively high concentrations of $Ph_3C^+SbCl_6^-$ in THF. At the lower concentrations used in our NMR experiments, similar to those used in our polymerization experiments, we were able to observe only a very broad weak absorption.

However, to explain the cocatalytic effect observed after polymerization has been initiated in the normal way, we are forced to conclude that some passive species present is activated by the addition of epoxide to increase the concentration of growing chains.

References

1. C. E. H. Bawn, C. Fitzsimmons, and A. Ledwith, *Proc. Chem. Soc.*, **1964**, 391.
2. C. E. H. Bawn, R. M. Bell, C. Fitzsimmons, and A. Ledwith, *Polymer*, **6**, 661 (1965).
3. I. Kuntz, *J. Polym. Sci. A-1*, **5**, 193 (1967).
4. M. P. Dreyfuss, J. C. Westfahl, and P. Dreyfuss, *Macromolecules*, **1**, 437 (1968).

5. I. Kuntz, paper presented at 155th American Chemical Society Meeting, April 1968; *Polymer Preprints*, **9**, No. 1, 398 (1968).

6. *Org. Syn.*, **46**, 105 (1967).

7. P. Dreyfuss and M. P. Dreyfuss, paper presented at 155th Meeting, American Chemical Society, San Francisco, April 1968; *Abstracts*, L-35.

8. C. E. H. Bawn, R. M. Bell, and A. Ledwith, *Polymer*, **6**, 95 (1965).

9. P. Dreyfuss and M. P. Dreyfuss, *Adv. Polym. Sci.*, **4**, 528 (1967).

10. A. Ledwith, private communication.

Stereoblock Polymerization of Methyl Methacrylate with VOCl$_3$–Al(C$_2$H$_5$)$_3$ Catalyst System

S. S. DIXIT, A. B. DESHPANDE, L. C. ANAND, and S. L. KAPUR,
National Chemical Laboratory,
Poona, India

Synopsis

Kinetics of the polymerization of methyl methacrylate with the VOCl$_3$–AlEt$_3$ catalyst system at 40°C in *n*-hexane have been studied. A linear dependence of rate of polymerization on the monomer and catalyst concentrations as well as an overall activation energy of 5.87 kcal/mole were found. Characterization of the structure of the polymer by NMR spectra revealed the presence of stereoblock units. The mechanism of polymerization is discussed in relation to the kinetic data obtained.

INTRODUCTION

The polymerization of methyl methacrylate with free radical,[1,2] anionic,[1,3] and Ziegler-Natta type catalysts[4–7] is well known.

The VOCl$_3$–AlEt$_3$[7] TiCl$_4$–AlEt$_3$,[4,7] and Ti(i-C$_3$H$_7$O)$_4$–AlEt$_3$[5] catalyst systems have been extensively used for the polymerization of methyl methacrylate under various conditions by Furukawa[7] and Abe[4,5] and co-workers, respectively. These studies revealed that the polymers obtained have mainly syndiotactic structures. Since free-radical catalysts are known to produce predominantly syndiotactic poly(methyl methacrylate), it has been pointed out[7] that polymerizations with VOCl$_3$–AlEt$_3$ and TiCl$_4$–AlEt$_3$[7] may also follow a free-radical mechanism. This has been supported by results of EPR and infrared studies of the poly(methyl methacrylate) as well as by reactivity ratios of copolymerization reactions.

In this paper kinetic studies of the polymerization of methyl methacrylate with VOCl$_3$–AlEt$_3$ in *n*-hexane at 40°C are reported, and the mechanism of the reaction has been discussed on the basis of results of infrared and NMR spectra. The infrared spectra of the polymers show the presence of syndiotacticity, whereas the NMR data exhibit confirmatory evidence for the presence of stereoblock poly(methyl methacrylate).

EXPERIMENTAL

The reagents and solvents were purified and stored as mentioned in the earlier communication from this laboratory[8] for the polymerization of styrene with VOCl$_3$–AlEt$_3$.

Methyl methacrylate was purified according to the accepted technique, particular attention being paid to removing traces of water.

1,1-Diphenylpicrylhydrazyl was recrystallized from a 1:1 ligroin–benzene mixture and dried before use.
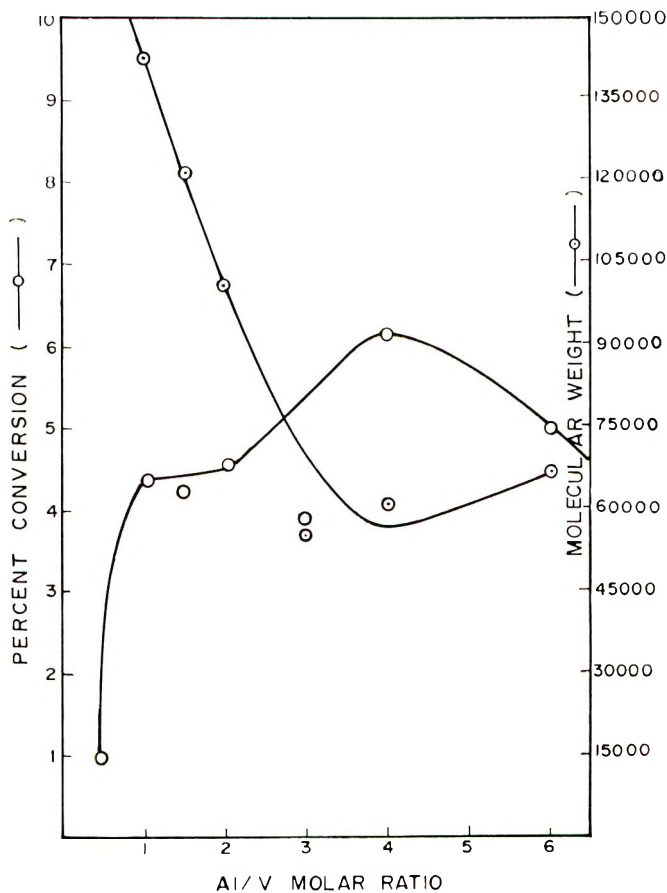
Fig. 1. Effect of Al/V ratio on (O) conversion and (⊙) molecular weight of PMMA with VOCl₃–AlEt₃ catalyst system.   [VOCl₃] = 0.05 mole/l., [MMA] = 1.88 mole/l., total volume = 25 ml, aging time = 20 min, reaction time = 180 min, temperature = 40°C.

The procedure of the polymerization followed was as reported in the earlier communication,[8] except that the catalyst system was prepared in the absence of the monomer in all cases.

The average molecular weights were obtained from viscosity measurement in benzene at 30°C by using the following equations:[9]

$$[\eta] = 1.95 \times 10^{-3} \bar{M}_v^{0.41} \qquad \bar{M} \leqslant 34\,000$$

$$[\eta] = 5.2 \times 10^{-5} \bar{M}_v^{0.76} \qquad \bar{M}_v > 34\,000$$

NMR spectra of 10% (w/v) solutions of the polymers in chlorobenzene were recorded on A-60 Varian spectrophotometer at 85°C, tetramethyl-silane being used as an internal reference.

RESULTS and DISCUSSION

As reported earlier,[8] the catalyst components on mixing turned into a dark brown solution containing fine precipitate which did not change with
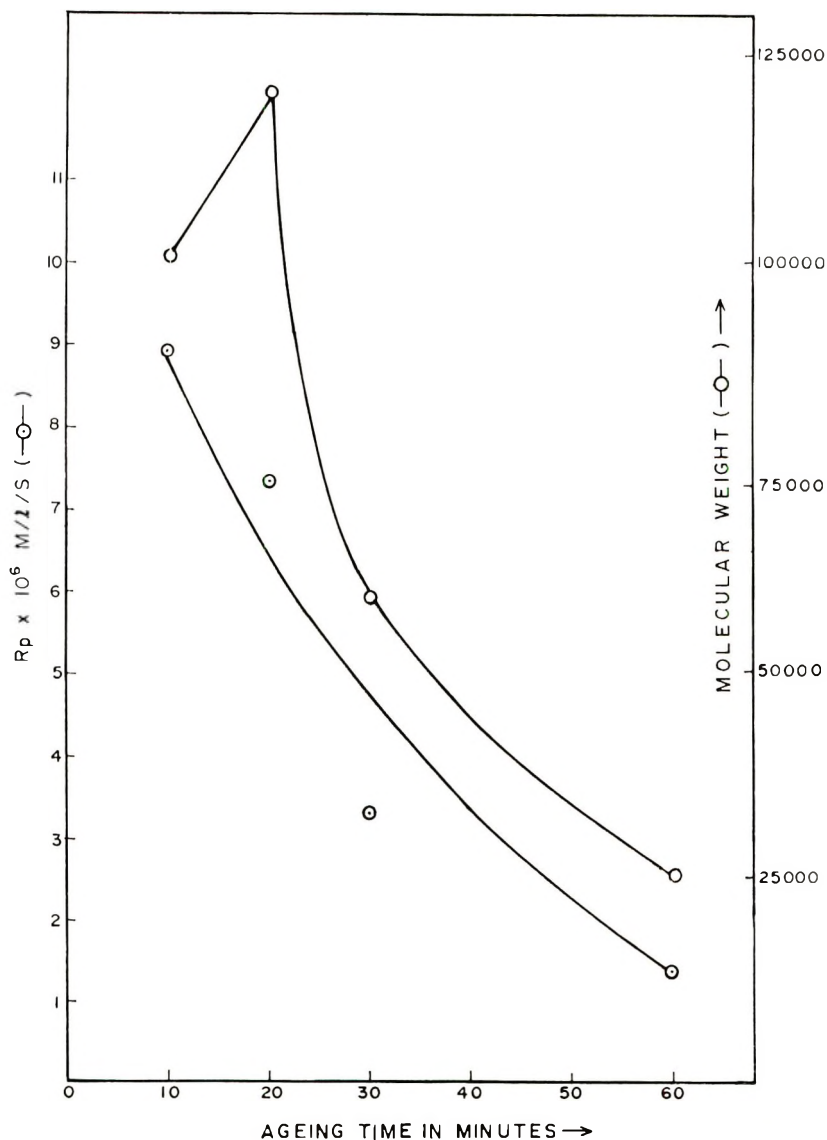
Fig. 2. Effect of aging time on (⊙) R_p and (○) molecular weight of PMMA with VOCl$_3$–AlEt$_3$ catalyst system.   [VOCl$_3$] = 0.05 mole/l., [AlEt$_3$] = 0.075 mole/l., Al/V molar ratio = 1.5, [MMA] = 1.88 mole/l., reaction time = 180 min, temperature = 40°C.
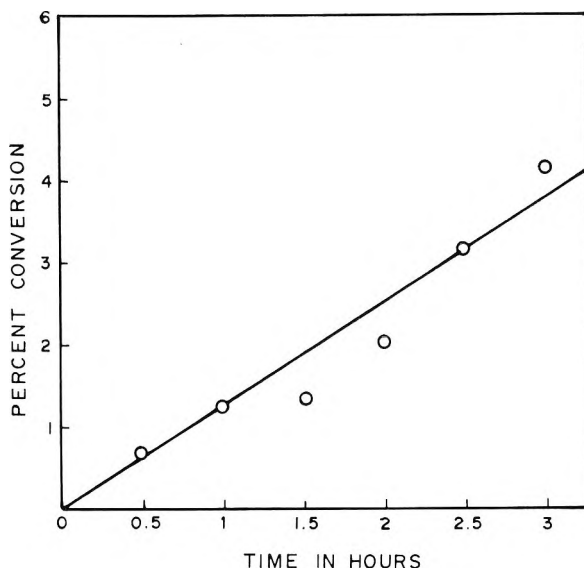
Fig. 3. Effect of time on conversion of MMA with the VOCl$_3$–AlEt$_3$ system. [VOCl$_3$] = 0.05 mole/l., Al/V molar ratio = 1.5, [MMA] = 1.88 mole/l., aging time = 20 min, temperature = 40°C.

variation of the concentration of the respective components; on addition of methyl methacrylate it becomes light brown.

In this case, it can then be assumed that the catalyst sites formed may be independent of the concentrations of the catalyst components. Further, the ratio of the catalyst components was varied in order to determine the ratios of optimum activity; these depend on the nature of the monomer added. It was observed that with an Al/V ratio in the range of 1–2, the rate of polymerization (Fig. 1) is almost constant and at the same time molecular weights are higher than at an Al/V ratio of 4, where the yield is maximum. Subsequent studies were therefore conducted at a mean Al/V ratio of 1.5.

Heterogeneous catalyst systems are often unstable, due either to decomposition or degradation of the catalyst complex in the presence of various components formed. In view of this, the catalyst was aged in absence of monomer for 10–60 min; the monomer was then polymerized with the aged catalyst system at a fixed ratio of Al/V. It was noted that the catalyst aged for 20 min is very active, and the polymer produced with it has a very high molecular weight (Fig 2). At the same time, the rate of polymerization increased linearly with time even up to 3 hr (Fig. 3).

In the light of the above observations, conditions for studying the kinetics were established as (1) Al/V ratio of 1.5, (2) polymerization time of 3 hr, (3) aging time of 20 min. Under these conditions, a fixed amount of methyl methacrylate was polymerized with the varying concentrations of the catalyst components. The rate of polymerization varied linearly with
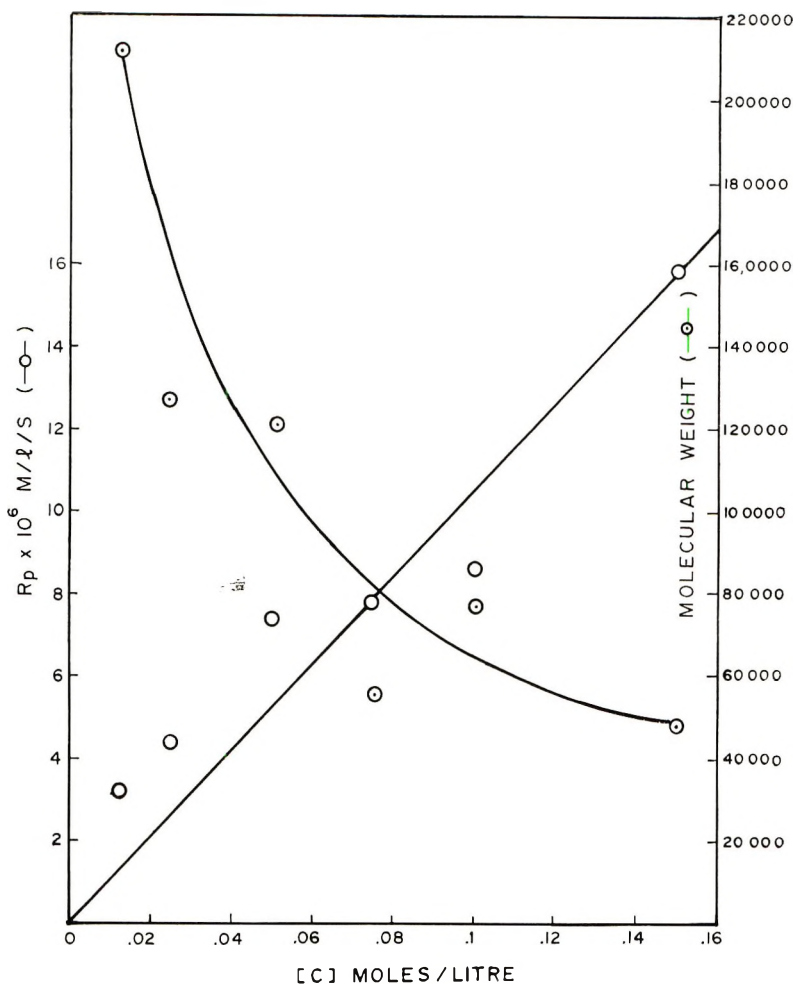
Fig. 4. Effect of catalyst concentration [C] on (O) R_p and (⊙) molecular weight of PMMA with VOCl₃–AlEt₃ system. Al/V molar ratio = 1.5, [MMA] = 1.88 mole/l., aging time = 20 min, reaction time = 180 min, temperature = 40°C.

catalyst concentration (Fig. 4). However, the molecular weight decreased with increasing concentration of catalyst components, indicating chain transfer with the complex formed. Similarly, when the monomer concentration was changed (Fig. 5) at constant concentration of catalyst components, both the rate of polymerization and the molecular weight increase with increasing concentration of monomer, indicating that the monomer has not taken part in the chain transfer reaction. This shows that, as with other Ziegler catalyst systems, the rate of polymerization is first-order with respect both to the monomer and catalyst concentrations. However, the catalyst is highly active because rate constants calculated as $K = 4.634 \times 10^{-5}$ l./mole-sec with respect to monomer and $K = 5.614 \times 10^{-5}$ l./mole-sec with respect to catalyst are comparatively large. The overall
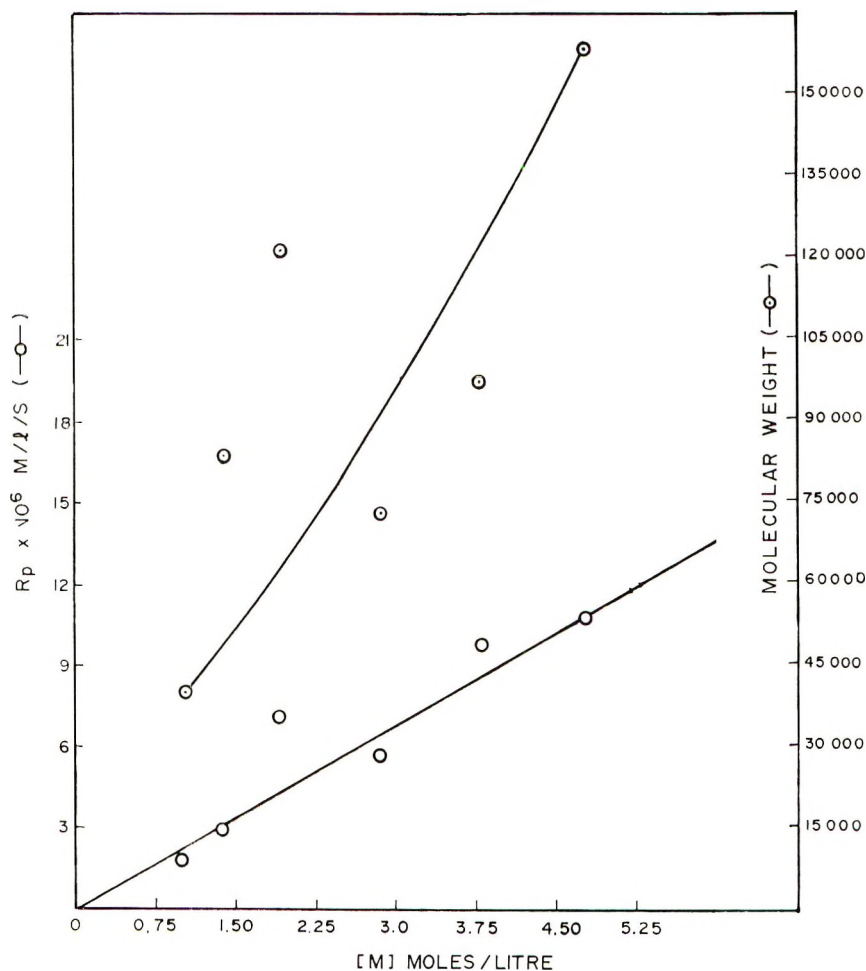
Fig. 5. Effect of monomer concentration [M] on (O) R_p and (⊙) molecular weight of PMMA with VOCl$_3$–AlEt$_3$ system.   [VOCl$_3$] = 0.05 mole/l.; Al/V molar ratio = 1.5, aging time = 20 min, reaction time = 180 min, temperature = 40°C.

activation energy calculated from plots of log R_p versus $1/T$ (Fig. 6) is o the order of 5.870 kcal/mole, which is in the range of values usually reported for Ziegler type catalysts.

In the earlier report,[6] it has been observed from the infrared spectra that poly(methyl methacrylate) obtained with this catalyst system is syndiotactic in structure but the J values calculated approximately[6] fell between the conventional and the stereoblock character of the polymer. In order to confirm the structure of the polymer, NMR spectra were recorded of the polymer obtained at various ratios of Al/V (Fig. 7).   These spectra indicated that these polymers contain a larger percentage of syndiotactic units than isotactic and atactic.   It is also observed that besides the appearance of I and S peaks, a prominent peak at 8.79 τ due
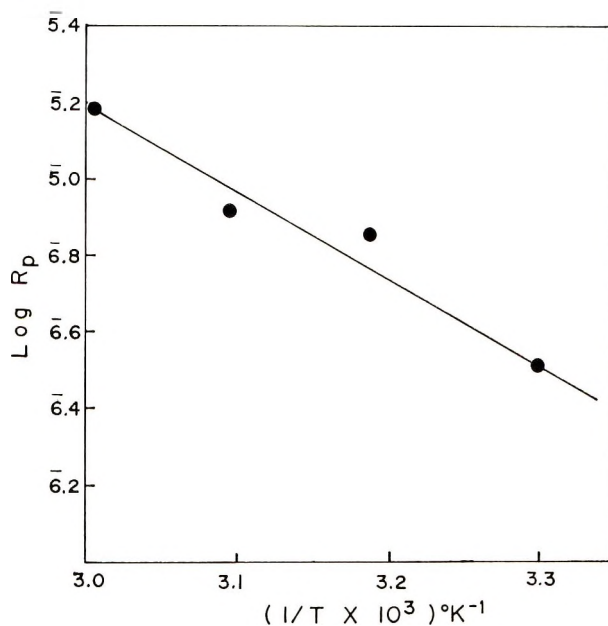
Fig. 6. Effect of temperature on R_p for $VOCl_3$–$AlEt_3$ system. [$VOCl_3$] = 0.05 mole/l., [MMA] = 1.88 mole/l., Al/V molar ratio = 1.5, aging time = 20 min, reaction time = 180 min.

TABLE I
Comparison of Values of Stereoblock Obtained with Different Catalyst Systems

Catalyst system	Mole ratio of catalyst components	Relative areas for the α-methyl peak in the NMR spectra[a]			Reference
		S (8.90 ppm)	H (8.79 ppm)	I (8.67 ppm)	
9-Fluorenyllithium, −60°C in toluene– THF (95:5) solvent	—	0.33	0.33	0.33	10
PhMgBr + CoCl₂, −20°C	CoCl₂/PhMgBr = ¹/₂	0.39	0.17	0.44	11
PhMgBr + CoCl₂, +20°C	CoCl₂/PhMgBr = 1/6	0.45	0.21	0.36	11
VOCl₃–AlEt₃, 40°C	Al/V = 1.5	0.42	0.30	0.27	Present study
VOCl₃–AlEt₃, 40°C	Al/V = 2	0.41	0.29	0.29	"

[a] For evaluation of the areas the syndiotactic S, heterotactic H, and isotactic I, α-CH₃ triad peaks of Bovey and Tiers[14] were used.

to hetero (*H*) units in our samples indicates a relatively short block length. This clearly means that these polymers contain a stereoblock structure. The percentage of syndiotactic, isotactic, and atactic units calculated with the planimeter agreed very well with the values obtained for polymers prepared by other anionic catalyst systems by Smets and Berghmans[10] or a Liquori et al.[11] (Table I). Coleman and Fox[12] have
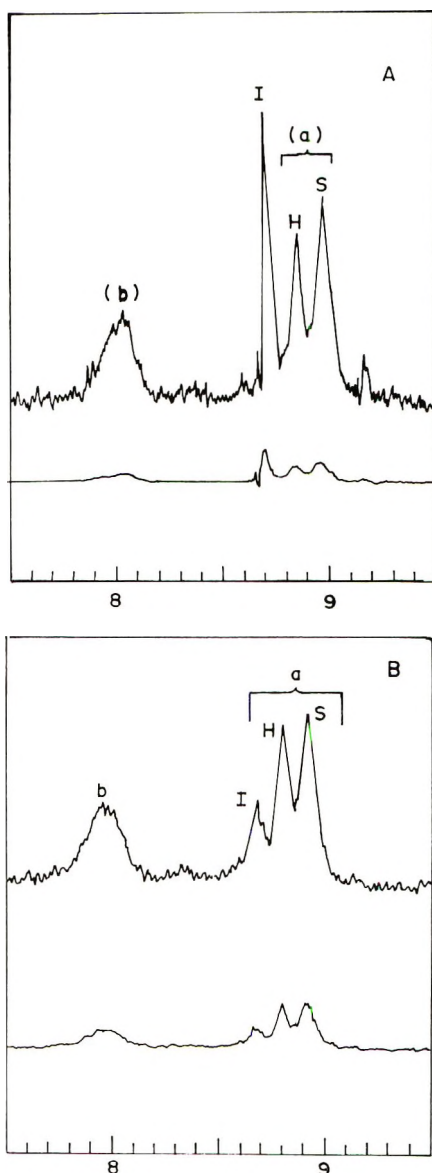
Fig. 7. Nuclear magnetic resonance spectra of PMMA in 10% chlorobenzene solutions: (*A*) PMMA with VOCl$_3$–AlEt$_3$, Al/V ratio = 2; (*B*) PMMA with VOCl$_3$–AlEt$_3$, Al/V ratio = 1.5.

proposed that stereoblock polymers are produced by two-stage anionic polymerization. Very recently, stereoblock formation of methyl methacrylate polymer with anionic initiators has been supported by the work of Lim et al.[13]

It can be understood that $VOCl_3$–$AlEt_3$ catalyst system does not appear to be a free-radical type, even though inhibitors like 1,1-diphenylpicryl-hydrazyl reduce the rate of polymerization and the molecular weights and the colour of the 1,1 diphenylpicrylhydrazyl did not change (Table II). This is also evident from studies with diethyl zinc which show a molecular weight decrease with increasing amount of diethyl zinc (Table III).

TABLE II

Effect of Diphenylpicrylhydrazyl on Polymerization
of Methyl Methacrylate with $VOCl_3$–$AlEt_3$ at $Al/V = 1.5$[a]

Expt.	Amount of DPPH, mg	Conversion, %	$[\eta]$, dl/g	$\bar{M}_v \times 10^{-3}$
1	—	4.243	0.3806	121.9
2	7.5	3.113	0.3330	102.1
3	15.0	2.555	0.2736	78.7
4	20.0	2.341	0.2560	71.94

[a] $[VOCl_3] = 0.05$ mole/l., Al/V ratio $= 1.5$, Aging time $= 20$ min, reaction time $= 3.0$ hr, temperature $= 40°C$, $[MMA] = 1.88$ mole/l. DPPH added just after the addition of monomer.

TABLE III

Effect of $ZnEt_2$ on Polymerization of Methyl Methacrylate with
$VOCl_3$–$AlEt_3$ at $Al/V = 1.5$[a]

Expt.	Concn. of $ZnEt_2$ M/l	$R_p \times 10^6$, mole/l.-sec	$[\eta]$, dl/g	$M_v \times 10^{-3}$
1	—	7.386	0.3806	121.9
2	0.003	10.530	0.2274	61.52
3	0.005	11.360	0.2735	78.70
4	0.010	15.790	0.1775	44.58
5	0.020	20.960	0.2038	53.58
6	0.030	20.600	0.2020	52.84
7	0.040	26.120	0.2017	51.65

[a] $[VOCl_3] = 0.05$ mole/l., aging time $= 20$ min, $[MMA] = 1.88$ mole/l., temperature $= 40°C$, reaction time $= 3$ hr. $ZnEt_2$ was added just after the addition of monomer.

It has been already established that the $VOCl_3$–$AlEt_3$ catalyst system is not only heterogeneous but contains vanadium in the valence state of three[8] and polymerizes all the hydrocarbon monomers by the coordinate ionic mechanism. Our kinetic studies and the stereoblock structure of poly(methyl methacrylate) as determined from NMR studies, provide support for polymerization of methyl methacrylate with $VOCl_3$–$AlEt_3$ by a coordinate anionic mechanism.

References

1. T. G Fox, B. S. Garret, W. E. Goode, S. Gratch, J. F. Kincaid, A. Spell, and J. D. Stroupe, *J. Am. Chem. Soc.*, **80**, 1768 (1958).

2. T. G Fox, W. E. Goode, S. Gratch, C. M. Hugget, J. F. Kincaid, A. Spell, and J. D. Stroupe, *J. Polym. Sci.*, **31**, 173 (1958).

3. D. L. Glusker, E. Stiles, and B. Yoncoskie, *J. Polym. Sci.*, **49**, 297 (1961).

4. H. Abe, K. Imai, and M. Matsumoto, *J. Polym. Sci. B*, **3**, 1053 (1965).

5. H. Abe, K. Imai, and M. Matsumoto, *J. Polym. Sci B*, **4**, 589 (1966).

6. L. C. Anand, S. S. Dixit, A. B. Deshpande and S. L. Kapur, *Indian J. Chem.*, **5**, 517 (1967).

7. S. Inoue, T. Tsuruta and J. Furukawa, *Makromol. Chemie*, **49**, 13 (1961).

8. L. C. Anand, A. B. Deshpande, and S. L. Kapur, *J. Polym. Sci. A-1*, **5**, 2079 (1967).

9. D. L. Glusker, L. Lysloff, and E. Stiles, *J. Polym. Sci.*, **49**, 315 (1961).

10. H. Berghmans and G. Smets, *Makromol. Chemie*, **115**, 187 (1968).

11. A. M. Liquori, G. Anzuino, M. Dalagni, V. Vitagliano, and L. Costantino, *J. Polym. Sci. A-2*, **6**, 509 (1968).

12. B. D. Coleman and T. G Fox, *J. Chem. Phys.*, **38**, 1065 (1963).

13. D. Lim, J. Coupek, K. Juzt, J. Baca, S. Sykora, and B. Schneider, *J. Polym. Sci. C*, **23**, 21 (1968).

14. F. A. Bovey and G. V. D. Tiers, *J. Polym. Sci.*, **44**, 173 (1960).

Anionic Polymerization of Cyanoacetylene (Propiolnitrile)

J. WALLACH and J. MANASSEN,

Plastics Research Laboratory, The Weizmann Institute of Science, Rehovot, Israel

Synopsis

Cyanoacetylene can be polymerized into linear polymers at low temperatures by anionic initiators. The polymers are brown to black amorphous powders, soluble in polar organic solvents. Their molecular weights are of the order of several thousands and the presence of the acidic acetylenic hydrogen does not seem to be an inhibiting factor in polymerization. Some general features of the polymerization and the products obtained are discussed. It is possible to synthesize copolymers with acrylonitrile, which show spectral and solution properties intermediate between those of the two homopolymers. The difference in structure between the materials obtained after pyrolysis of polyacrylonitrile and polycyanoacetylene is discussed.

INTRODUCTION

Reports on the polymerization of acetylenic monomers are few in the literature and are mostly concerned with metal–organic catalyst systems.[1,2] As the acetylenic hydrogen, which is bound to carbon by a sp-hybridized bond, is quite acidic, anionic polymerization of acetylenic monomers, having a free hydrogen, was for a long time considered to be impractical.[3] In the course of our work on the catalytic properties of pyrolyzed polyacrylonitrile,[4] in which we tried polycyanoacetylene as a model polymer, we discovered that the complex catalyst $TiCl_3/BuLi$ did not polymerize the monomer, but that BuLi alone did.

We want to report here some general studies about the phenomena encountered when cyanoacetylene is polymerized by anionic initiators. The only known example of anionic polymerization of acetylenic monomers containing free hydrogen is that of acetylene itself and some of its homologs, by alkali acetylides in aprotic solvents at 40–80°C.[5] Cyanoacetylene polymerizes instantaneously at very low temperatures with BuLi in heptane, and special precautions are necessary to prevent polymerization.[6] Convenient initiators appeared to be alkoxides and cyanides in dimethylformamide (DMF) solution, where rates could be more or less controlled.

EXPERIMENTAL

Synthesis of Cyanoacetylene

This was performed by the dehydration of propargyl aldoxime as reported elsewhere.[4]

Polymerization

Dimethylformamide (BDH, analytical reagent) was dried over activated alumina (12–25 mesh) for 3 days. The alumina was pretreated by heating at 400°C in a nitrogen stream for 2 hr. The dry DMF was distilled at 30–35 mm pressure (bp 65–66°C) and collected as three equal fractions, only the middle fraction being used.

Sodium cyanide (6 g, BDH analytical reagent, dried over P_2O_5) was introduced into a 250-ml round-bottomed flask and attached to a vacuum line (pressure lower than 1μ). By gently heating with a flame the last traces of water were removed.

Dry distilled DMF (150 ml) was introduced into a 250-ml round-bottomed flask together with $^1/_{18}$-in. pellets of molecular sieves (5 Å) which had been dried in a nitrogen stream at 400°C for 2 hr. Subsequently the DMF was distilled into the flask containing the sodium cyanide, which was dissolved by stirring.

Pure cyanoacetylene (18 g) was introduced into a small container attached to the vacuum line and after degassing was distilled into the reaction mixture by way of a P_2O_5 tower. During the distillation the reaction mixture was kept immersed in liquid air. After introduction of the cyanoacetylene, the temperature was raised to −60°C by immersion in an acetone–Dry Ice mixture and kept at this temperature for 3 hr. The solution was divided into two equal parts. One part was poured into 3 l. of methylene chloride and the other part into 3 l. of methylene chloride containing 7 ml of concentrated HCl. After standing for 2 days the polymer had precipitated sufficiently to be recovered by decantation of the solvent and subsequent filtration. Although the two methods of recovery yielded polymer of slightly different properties, their infrared spectra were identical. The polymer, recovered under nonacidic conditions, was soluble in water and could be precipitated from its aqueous solution by dilute acid. It could be dissolved again by the addition of dilute alkali.

Copolymerization

Sodium cyanide (1 g) was introduced into a round-bottomed flask (250 ml) and DMF (100 ml) distilled into it as described above.

Acrylonitrile (15 ml, 0.28 mole), which had been freed of inhibitor in the conventional manner, was distilled into the reaction flask which was held at −60°C. Afterwards cyanoacetylene (3 ml, 0.047 mole) was distilled into the mixture as described above. After stirring at −40°C for 3 hr and at room temperature of 3 hr, the copolymer was precipitated by pouring

the mixture into 3 l. of methylene chloride containing 7 ml of concentrated HCl. After filtration the copolymer was ground in a mortar with dilute HCl and after that with distilled water. It was dried in a desiccator under vacuum over P_2O_5.

After extraction in a Soxhlet apparatus with acetone for 12 hr, one third could be recovered from the acetone phase, and two thirds appeared to be insoluble in acetone.

Solvent Fractionation

The polymer of cyanoacetylene was extracted in a Soxhlet apparatus for 24 hr with each solvent in the order given in Table II.

Molecular Weight Determination

A vapor osmometer (Mechrolab) was used with acetone as the solvent.

RESULTS

Table I shows the dependence of polymer yield and molecular weight on the ratio of monomer to initiator.

TABLE I
Correlation between Ratio of Monomer to Initiator, Polymer Yield,
and Molecular Weight during Anionic Polymerization of Cyanoacetylene in DMF

Initiator	Monomer to initiator ratio	Polymer yield, %	Molecular weight
CH_3ONa[a]	5/1	90	1 640
"	10/1	50	1 430
"	20/1	35	1 640
KCNS[b]	1/1	95	1 100
"	5/1	80	1 430
"	10/1	75	1 000
"	100/1	2	770

[a] $T = -60\,°C$.
[b] $T = 0\,°C$.

It is clear from the table that a direct correlation exists between yield of polymer and the ratio of monomer to initiator, but that the molecular weight is not influenced in any predictable manner. This is also found with other types of initiators[7] and seems to be a general phenomenon in the polymerization of acetylenes into linear polymers.

Description of the Polymer

The polymers are red-brown to black amorphous powders, readily soluble in most polar solvents. By means of thin-layer chromatography, they can be separated into many components whose colors range from bright yellow to green to red and brown. Refinement of the technique enables every

fraction to be separated again and again into other fractions, a fact that can only be explained by the occurrence of many *cis/trans* configurations and conformations. The polymers are also soluble in dilute alkali, from which they can be precipitated by the addition of acid, and thus they behave as weak acids. A more practical way of fractionation is by extraction by different solvents, results of which are given in Table II.

TABLE II
Fractionation of a Polymer of Cyanoacetylene by Means of Solvent Extraction

Solvent	Weight of fraction, %	Molecular weight	Remarks
Chloroform	10		Yellow syrup; no MW determination possible
Isopropanol	29	625	Brown powder
Ethanol	20	1 050	Brown powder
Acetone	41	2 000	Brown/black powder

A molecular weight of 2000 corresponds to a degree of polymerization of 39. The highest ever reported for an acetylenic monomer is a degree of polymerization of 49 initiated by a metal organic catalyst with phenylacetylene.[8] Most reported values are much lower. From this it can be concluded that the acidic acetylenic hydrogen is apparently not an impeding factor during the anionic polymerization and that reaction (1)

$$R^- + HC{\equiv}C{-}C{\equiv}N \rightarrow RH + {}^-C{\equiv}C{-}C{\equiv}N \tag{1}$$
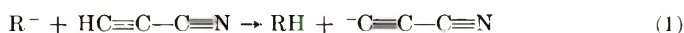
does not seriously compete with reaction (2).

$$R^- + HC{\equiv}C{-}C{\equiv}N \rightarrow R{-}C{=}C^- \diagdown C{\equiv}N \tag{2}$$
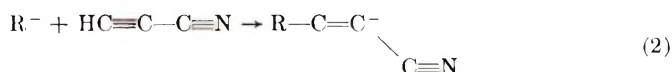
The high solubility of the polymer precludes a serious degree of crosslinking. In principle one may expect that in anionic acetylene polymerization the propagating anion attacks the conjugated chain formed [eq. (3)],

$$\tag{3}$$
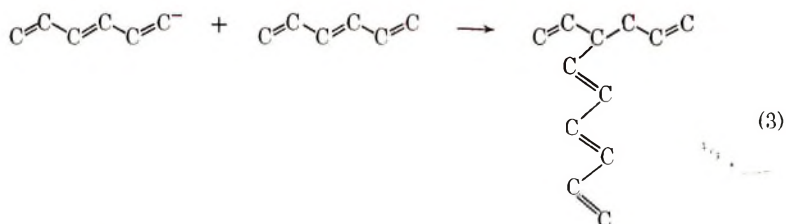
which is reflected in the fact, that in many cases insoluble products are obtained. This is sometimes taken as proof of a high degree of polymerization.[9] We tried to check this possibility by using the rhodanide anion as the initiator, and by analyzing for sulfur in the end product. If

the sulfur content found is higher than that calculated from the molecular weight for one endgroup, attack on the conjugated chain has occurred. Table III gives the results.

TABLE III
Calculated and Measured Sulfur Content of Polymers
Obtained at Different Monomer to CNS⁻ Ratios

M/I	MW	Sulfur content	
		Calculated for one endgroup, %	Found %
1/1	950	3.3	7.6
10/1	1 000	3.2	6.3
100/1	770	4.1	5.3

The sulfur content is greater than that calculated for one endgroup in all cases, but is seen to decrease with increasing monomer to initiator ratio. This suggests attack by the strong nucleophile CNS⁻ rather than cross-linking.
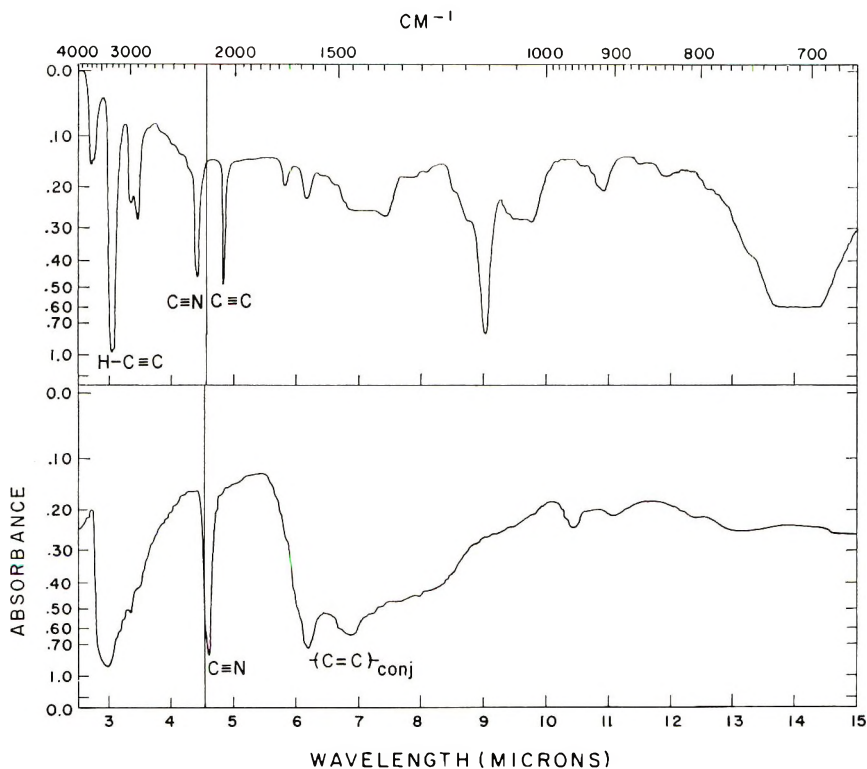
Fig. 1. Comparison between the infrared spectra of (A) cyanoacetylene monomer and (B) its polymer.

Spectra

Since the polymers are a mixture of many isomers, optical as well as NMR spectra are very diffuse, and not much information can be obtained from them. The infrared spectrum, on the other hand, gives valuable information, as can be seen from Figure 1.

It can be seen that the absorption for nitrile appears also in the polymer, but has shifted to a somewhat longer wavelength. The two peaks for acetylene have disappeared entirely, which is proof that polymerization occurs only by way of the C≡C triple bond, and not by way of the C≡N triple bond. Polymerizations through the C≡N moiety have been found to be possible recently in the anionic polymerization of dicyan.[10]

Reactions on the Polymer

The polymers of cyanoacetylene are very resistant to most reactions that can be performed on conjugated molecules. Neither hydrogenation nor
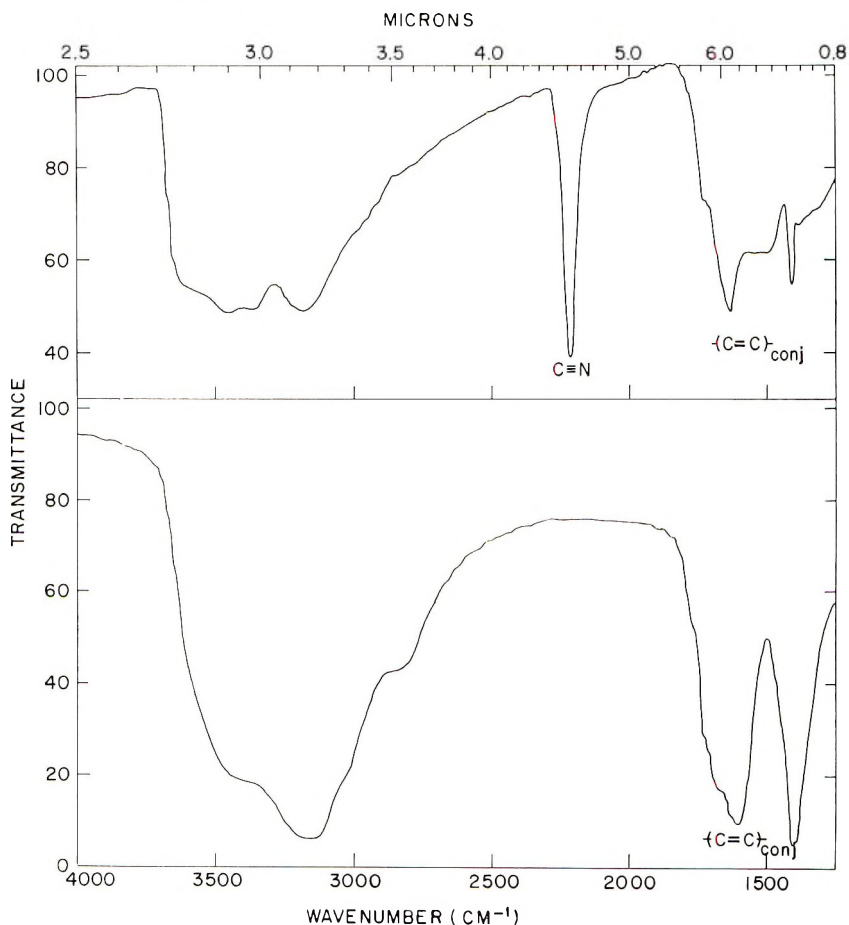
Fig. 2. Comparison between the infrared spectra of polycyanoacetylene (A) before and (B) after treatment with hydrogen peroxide.

chlorination gives a colorless substance. Hydrolysis of the cyano groups is difficult and cannot be forced to completion. For example, treatment of 0.5 g of polymer with 2.5 g of KOH for 12 hr in triethylene glycol at 180°C gives a material that still contains 8% nitrogen and shows cyano absorption in the infrared. One reaction, however, that went to completion under mild conditions, was treatment with hydrogen peroxide in a weakly alkaline medium. The mechanism of this reaction has been studied, and the product is known to be the amide:[11]

$$C_6H_5-C\equiv N + 2H_2O_2 \rightarrow C_6H_5-\overset{\overset{\displaystyle O}{\parallel}}{C}-NH_2 + O_2 + H_2O \qquad (4)$$
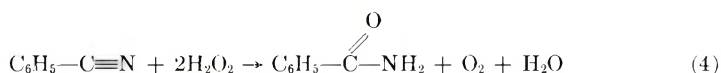
If the polymer is shaken in aqueous solution with H_2O_2 and potassium carbonate at room temperature for 2 days, the black color disappears, and the polymer isolated from the mixture is insoluble in organic solvents but very soluble in water, to such a degree that when exposed to the atmosphere it immediately becomes deliquescent. Polyacrylamide is also known to behave in this manner. In Figure 2, it can be seen that, in the treated polymer, the cyano absorption in the infrared has disappeared, but the absorption at 1 600 cm^{-1} for the conjugated chain has remained unchanged.

Acetylide Initiation

If an acidic monomer like cyanoacetylene is polymerized by an anionic initiator, one would expect chain transfer to occur according to
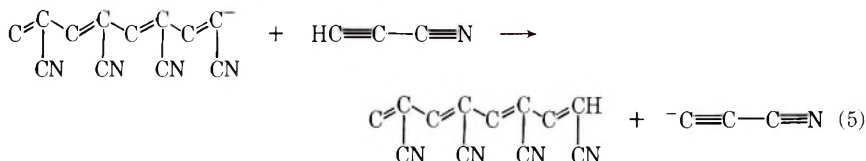
In a previous communication,[12] we reported that studies on the chloroform fraction of the polymer obtained from $DC\equiv C-C\equiv N$, seemed to indicate the occurrence of chain transfer. It is dubious, however, whether this result also applies to the other fractions. The data in Table I showed that the molecular weight is independent of the ratio of initiator to monomer. This can only occur when the chain transfer is degradative, which means that the cyanoacetylide ion $-^-C\equiv C-C\equiv N$ does not initiate a new polymerization chain. Unfortunately we did not succeed in preparing the cyanoacetylide, but we could show that the phenyl-acetylide does initiate polymerization of cyanoacetylene at $-50°C$ in ether. The polymer obtained shows a clear acetylene absorption in the infrared, as can be seen from Figure 3, which never occurred in the polymers obtained by other initiators. This indicates that with other initiators the cyanoacetylide either is not formed, or when formed does not initiate a new chain.
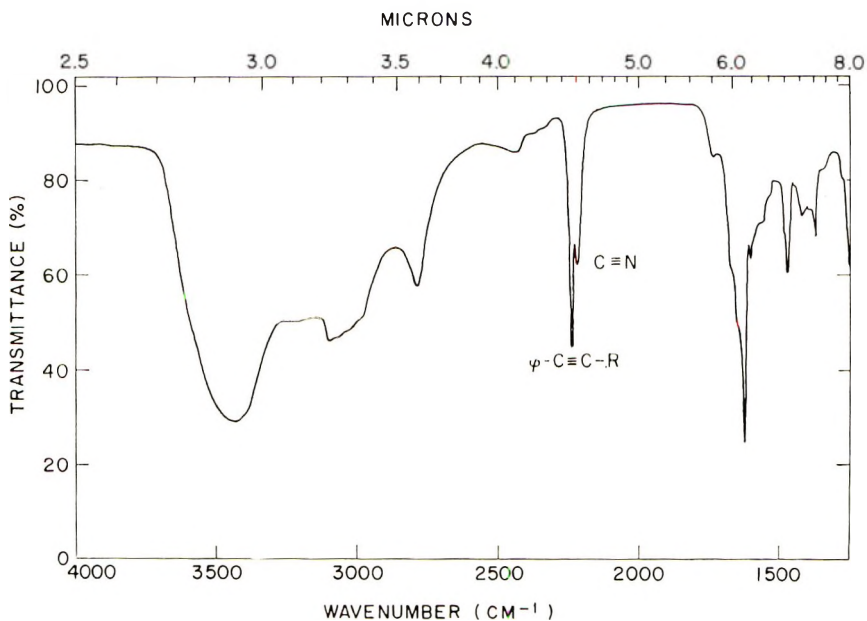
MICRONS

Fig. 3. Infrared spectra of the polymer obtained from cyanoacetylene after initiation by phenylacetylide.

Pyrolysis

Because polycyanoacetylene may serve as a model for pyrolyzed polyacrylonitrile it is interesting to check its behavior on heat treatment. Figure 4 gives a typical example of a differential thermal analysis experiment under nitrogen.

The first exotherm starts at 200°C. At this temperature the polymer becomes insoluble and the cyano absorption in the infrared starts to disappear, which suggests an internal addition like the one proposed for polyacrylonitrile.

$$\tag{6}$$
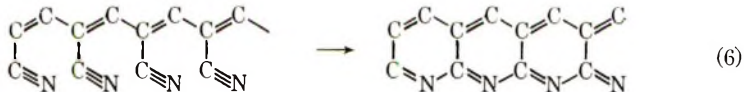
The structure thus formed is the one proposed for pyrolyzed polyacrylonitrile. In a previous report,[4] we showed that pyrolyzed polyacrylonitrile is a good catalyst for the heterogeneous dehydrogenation of cyclohexene; the pyrolyzed polycyanoacetylene shows only a very weak activity for this reaction. We shall discuss the importance of this difference in the next section.

The second exotherm is probably connected with a crosslinking of the conjugated carbon to carbon chain, as at this temperature the infrared

adsorption at $1\,600\ cm^{-1}$ for a conjugated chain starts to disappear. The first endotherm can probably be associated with the loss of water and the second one with the thermal decomposition of the polymer.
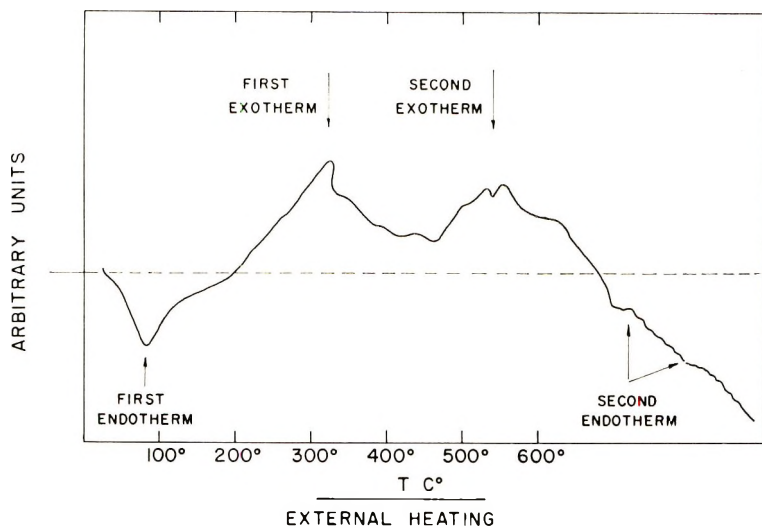
Fig. 4. Diagram of differential thermal analysis of polycyanoacetylene under nitrogen.
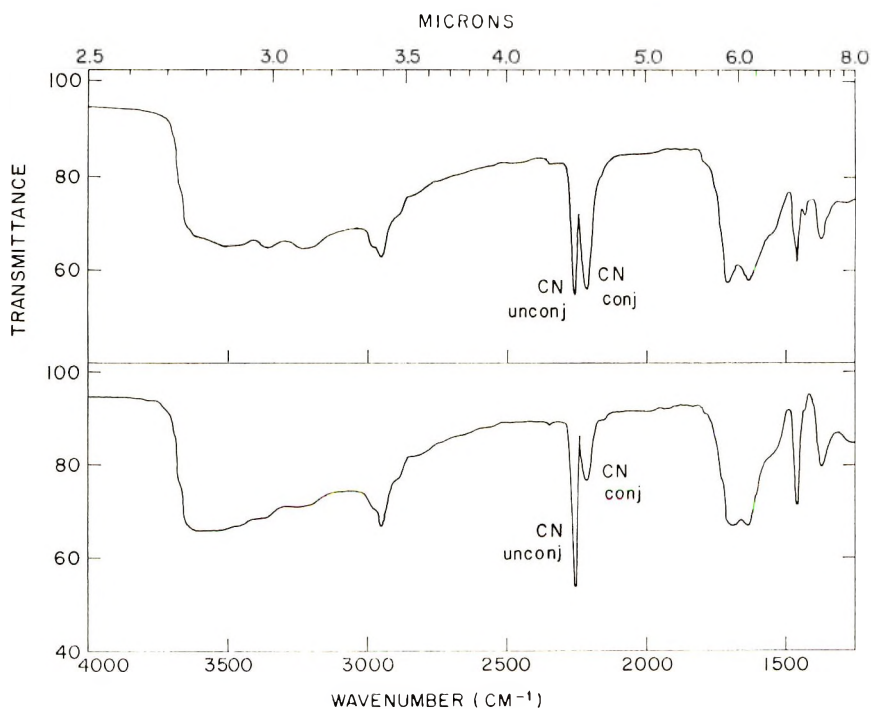
Fig. 5. Infrared spectrum of the acrylonitrile–cyanoacetylene copolymer: (A) fraction soluble in acetone; (B) fraction insoluble in acetone.

Copolymerization

It is possible to prepare copolymers of cyanoacetylene and acrylonitrile by anionic initiation. The materials obtained are grey in color and only partially soluble in acetone. The most interesting phenomenon is the appearance of two cyano peaks in the infrared, one for a cyano group attached to a conjugated chain, and one attached to a saturated chain. From Figure 5 it can be seen that the soluble copolymer is rich in the conjugated component while the insoluble part is rich in the saturated component, which is in accordance with the solubility properties of both
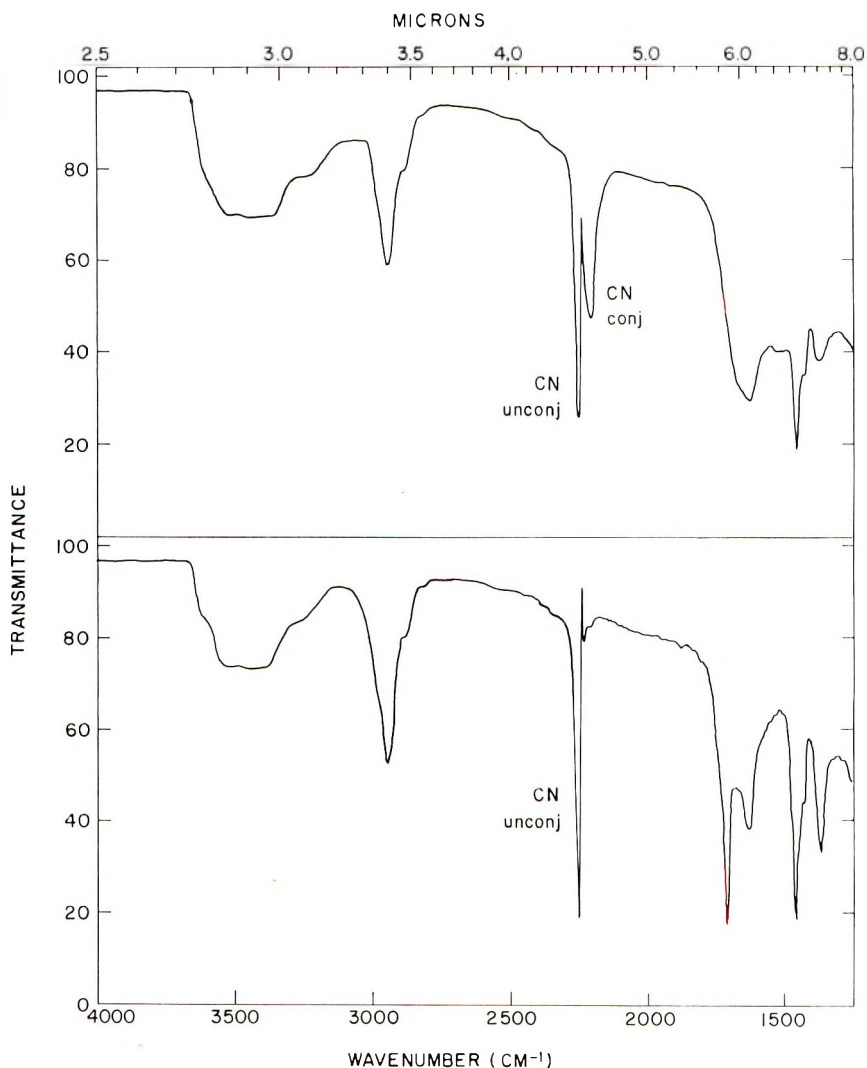
Fig. 6. Infrared spectra of the insoluble acrylonitrile–cyanoacetylene copolymer fraction: (*A*) before chlorination; (*B*) after chlorination.

homopolymers in acetone.   In Figure 6 it can be seen that the acrylonitrile-rich copolymer, unlike the homopolymer of cyanoacetylene, can be chlorinated, whereby the infrared absorption of the cyano group attached to a conjugated chain disappears.   In addition, the grey color of the copolymer disappears with this treatment.

DISCUSSION

The solubilities of the polymers and the sulfur contents given in Table III preclude a serious degree of crosslinking, and it may be assumed that we are dealing with more or less linear polymers.   Several facts suggest that the polymerization occurs only by way of the C≡C— triple bond.   As already mentioned the infrared absorption spectrum does not show peaks for acetylene, but does show the absorption characteristic for cyano groups and a conjugated chain.   This cyano absorption disappears entirely on treatment with H_2O_2, the conjugated chain remaining intact, after which the polymer exhibits properties resembling those of polyacrylamide.   Therefore, the initiation and propagation steps [eqs. (7) and (8)] seem to be straightforward.

$$R^- + HC≡C—C≡N \xrightarrow{k_i} \quad (7)$$

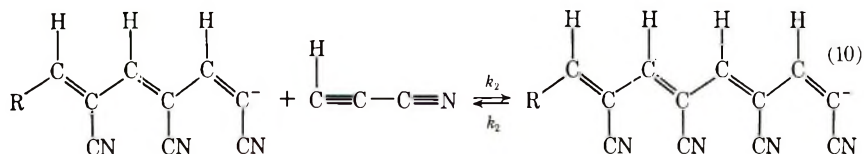$$+ HC≡C—C≡N \xrightarrow{k_p} \quad (8)$$
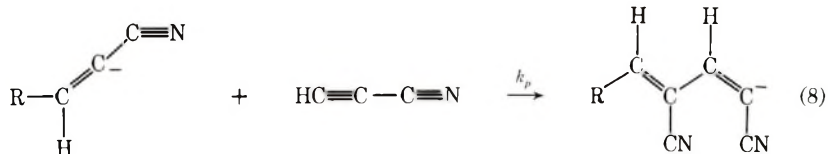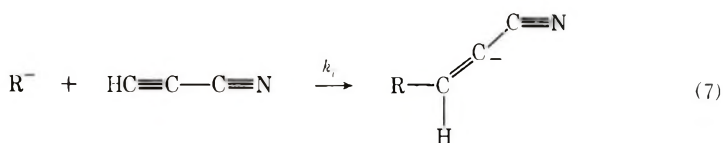
The polymers are formed with a degree of polymerization of almost 40. These results are in qualitative agreement with those found on anionic polymerization of acetylene itself at much higher temperatures.[5]   The degree of polymerization found there is about 11 at 50°C and the different polymerization states are in equilibrium.   Furthermore, it could be shown that the polymers are living and capable of initiating the polymerization of vinyl monomers.   The higher the degree of polymerization of the living anion, the less it was capable of initiating polymerization.   We have done some quantum mechanical calculations on these conjugated anions, which show an appreciable π-electron delocalization, which is more extensive in a longer chain.[13]   This suggests that a correlation exists between this delocalization and the decrease of activity with the length of the living anion. In order to illustrate the effect of the introduction of a cyano group into the acetylene molecule we can compare the two propagating steps [eqs. (9) and (10)].

Acetylene

$$\text{(structure)} + \text{(structure)} \underset{k_1}{\overset{k_1}{\rightleftharpoons}} \text{(structure)} \quad (9)$$

Cyanoacetylene

$$\text{(structure)} + \text{(structure)} \underset{k_2}{\overset{k_2}{\rightleftharpoons}} \text{(structure)} \quad (10)$$
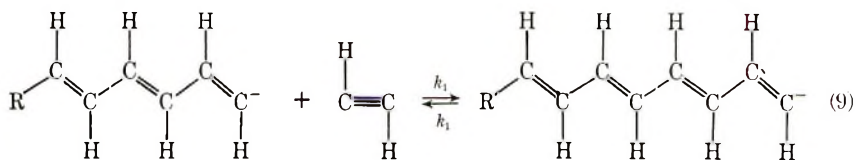
The presence of the electron-attracting cyano groups in the propagating anion, makes the latter less reactive towards protons, which is reflected in the experimental fact that the presence of a considerable quantity of methanol during polymerization does not influence the molecular weight of the polycyanoacetylene, while the propagating ion in the case of acetylene is destroyed instantaneously by the addition of methanol.[5] The presence of the cyano group in the monomer will enhance its acidity as well as the reactivity of the triple bond towards nucleophilic attack. The fact that polymerization of cyanoacetylene occurs at a much lower temperature than observed in the case of acetylene shows that the effect of cyano substitution on the reactivity of the triple bond in the monomer outweighs the influence of the cyano groups on the reactivity of the propagating anion. Here there is an interesting example of how basicity and nucleophility can be influenced in a different way by substituents.

Although the values in Table I suggest that also in the case of cyanoacetylene there is some kind of equilibrium polymerization, much more exact measurements will have to be made to decide this matter.

It remains to be explained why no sign of chain transfer can be found, considering the fact that cyanoacetylene certainly is a stronger acid than acetylene itself. The polymer is soluble in water at high pH, and methanol does not influence the molecular weight during polymerization. This suggests that the propagating anion is a weaker base than the methoxy anion, which could be an explanation for the absence of chain transfer. Potentiometric titrations of the polymer in dimethylformamide solution did not yield much additional information however.

The fact that pyrolyzed polyacrylonitrile is a better catalyst for dehydrogenation than pyrolyzed polycyanoacetylene gives an interesting clue to the structure of both materials, which is difficult to obtain by other means. The structure which is thought responsible for the catalytic activity is the annelated naphthyridine structure.[4]

$$\text{(11)}$$
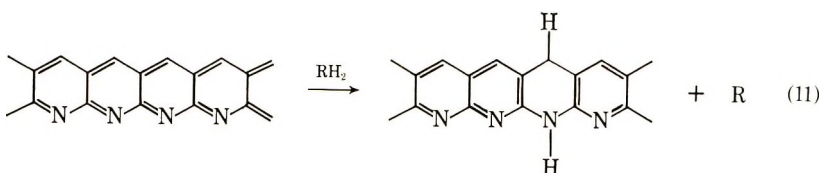
The longer such an annelated system, the more unstable it is and the more it tends to stabilize itself by taking up hydrogen. This means that a longer system is a better dehydrogenator, which suggests that in pyrolyzed polyacrylonitrile the annelated system is longer than in pyrolyzed polycyanoacetylene. This seems plausible, if one considers how these structures and assumed to be formed.

Polyacrylonitrile:

$$\text{(12)}$$

$$\text{(13)}$$

Polycyanoacetylene:

$$\text{(14)}$$
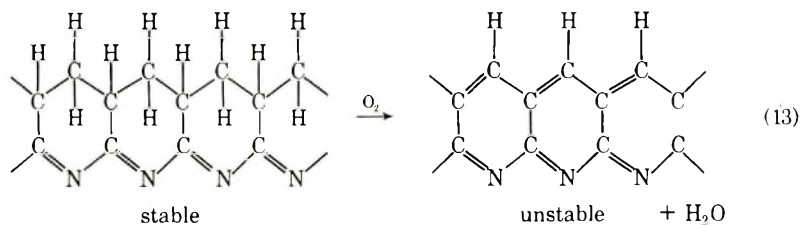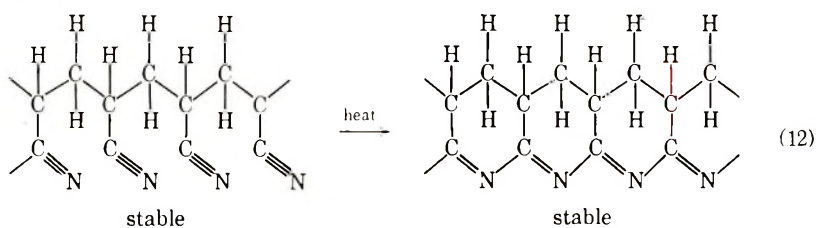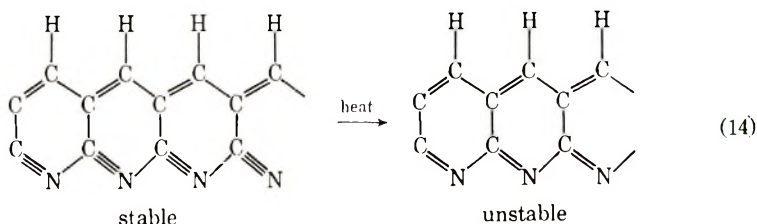
In the case of polyacrylonitrile, the conjugated C=N—system is formed, while the C—C system is still saturated. The structure thus formed is not inherently unstable, and rather long stretches of C=N—conjugation are energetically feasible. The annelated structure is then formed by dehydrogenation of an already closed system and the extension of annelation will be regulated by the thermodynamic stability of the system at the given temperature. In the case of polycyanoacetylene, however, the energetically unfavorable annelated structure has to be formed by closure of an open system, and many energetically more favorable reaction paths, like

crosslinking for instance, are open to the molecule. Thus, it is entirely plausible that the annelation in pyrolyzed polycyanoacetylene will be less extended, as is reflected in its lower dehydrogenating activity.

The experimental results show that greater difference in behavior may exist between an acetylenic monomer and a vinyl monomer during anionic polymerization. This can be illustrated by the fact that, in the presence of an equivalent quantity of methanol, acrylonitrile does not polymerize at all,[14] while the degree of polymerization of cyanoacetylene is hardly affected. In the absence of methanol on the other hand, the degree of polymerization of acrylonitrile is higher than that of its acetylenic counterpart.

References

1. W. H. Watson, Jr., W. C. McMordie, Jr., and L. G. Lands, *J. Polym. Sci.*, **55**, 137 (1961).

2. L. S. Meriwether, M. F. Leto, E. C. Colthup, and G. W. Kennerly, *J. Org. Chem.*, **27**, 3930 (1962).

3. M. Benes, J. Peska, and O. Wichterle, *Chem. Ind.* (*London*), **1962**, 562.

4. J. Manassen and J. Wallach, *J. Amer. Chem. Soc.*, **87**, 2671 (1965).

5. J. Kriz, M. J. Benes, and J. Peska, *Collect. Czech. Chem. Commun.*, **32**, 4043 (1967).

6. E. K. Jensen, *Acta Chem. Scand.*, **18**, 1629 (1964).

7. I. M. Barkalov, A. A. Berlin, et al., *Vysokomol Soedin.*, **5**, 368 (1963).

8. A. A. Berlin, et al., *Vysokomol Soedin.*, **6**, 1773 (1964).

9. B. J. MacNulty, *Polymer*, **7**, 275 (1966).

10. J. Peska, M. J. Benes, and O. Wichterle, *Collect. Czech. Chem. Commun.*, **31**, 243 (1966).

11. K. B. Wiberg, *J. Amer. Chem. Soc.*, **75**, 3961 (1953).

12. J. Wallach and J. Manassen, Preprints of Scientific Papers, International Symposium on Macromolecular Chemistry, Tokyo (1966), 2-1-15, p. I-88.

13. J. Manassen and R. Rein, in press.

14. A. Zilkha, et al., *J. Polym. Sci.*, **49**, 231 (1961).

Studies on the Biaxial Stretching of Polypropylene Film. III. Electron Microscopic Observation of the One-Step Biaxial Stretching of Isotactic Polypropylene Spherulites

HIROSHI TANAKA, TORU MASUKO, KEISUKE HOMMA, and SABURO OKAJIMA, *Faculty of Technology, Tokyo Metropolitan University Tokyo, Japan*

Synopsis

Polypropylene films of various isotacticities and crystallinities were stretched biaxially in one step in air at 140–152°C or polyaxially in poly(ethylene glycol) at 130–160°C, and the morphological changes were studied by electron microscopy (replica). In the initial stage of stretching, with $v_A = 1.4$, the spherulites of one of the films used for the experiment were broken both from the centers and boundaries, and those of another film were broken mainly from the center. This difference in the deformation behavior seems to be characteristic of the film properties and independent of the method of stretching, although the factors involved are still unknown. On further stretching ($v_A = 22$), well annealed spherulites were broken into many small blocklike fragments with unfolded fibrils running among them, particularly at the low stretching temperature (140°C), and fibrillation proceeded at the expense of the residual fragments. In the case of quenched or slightly crystallized material, the fragments were dendritic and divided into finer and finer fibrils on stretching. At elevated temperature, however, even for well annealed spherulites, the deformation behavior resembles that of the quenched material, and at a high degree of stretching the spherulites take on the fibrillar net structure in every case. In films containing a high amount of atactic fraction, radial, tangential, and boundary cracking occurred more easily, and broad fibrils were observed across the cracks.

INTRODUCTION

Many papers have been written about the deformation behavior of isotactic polypropylene spherulites during uniaxial stretching[1–5] or the morphological changes brought about during crystallization[2,6] or heat aging[7,8] at the spherulite boundaries and between radial fibrils, but there are few reports on the biaxial stretching of the spherulites. We have therefore carried out polyaxial stretching[9] and one-step biaxial stretching of isotactic polypropylene films and observed the deformation behavior of the spherulites on the surface of these films by using an electron microscope of the transmission type and/or the scanning type. The stretching was carried out at various temperatures in poly(ethylene glycol) or in air.

Results were not simple, and the type of deformation varied according to the characteristics of the polymer and conditions of stretching. This paper reports the qualitative trend of the deformation behavior. The effects of characteristics of polymer such as molecular weight, isotacticity, and crystallinity as well as the stretching conditions on the deformation behavior will be described in detail elsewhere.

EXPERIMENTAL

Sample

The characteristics of the polymer samples used are listed in Table I.

In Table I, the designation C represents samples supplied by Chisso Corporation, and B denotes another commercial film. The subscripts in-

TABLE I
Characteristics of Polymer Samples Used

Polymer sample	$\overline{M}_v \times 10^{-4}$	Isotacticity, %
B$_1$	31	97
B$_3$	36	96
C$_1$	30	95
C$_3$	28	85
C$_4$	27	80
C$_5$	23	74

TABLE II
Conditions of Preparing Sample Films for Stretching

Sample film number	Sample preparation
1	Commercial undrawn film as received, sample B$_1$
2	A piece of sample B$_3$, 12 cm $\times$ 12 cm, was melted at 190°C for 5 min on a stainless steel plate 3 mm in thickness, crystallized at 140°C for 5 min in poly(ethylene glycol), and quenched in ice water.
3	Film 2 was annealed at 130°C for 1 hr and subsequently at 150°C for 4 hr in poly(ethylene glycol) and quenched in ice water.
4	8 sheets of sample C$_1$, 12 cm $\times$ 12 cm, were piled up and melted between stainless steel plates 0.5 mm in thickness at 190°C for 5 min under pressure of 10 kg/cm² and then quenched in ice water. In order to obtain a free surface this film was remelted at 190°C for 5 min on a stainless steel plate 3 mm in thickness, crystallized in poly(ethylene glycol) at 80°C for 5 min and quenched in ice water.
5	A piece of sample C$_3$ was treated in a similar manner as film 4
6	A piece of sample C$_4$ was treated in a similar manner as film 4
7	A piece of sample C$_5$ was treated in a similar manner as film 4

dicate lot numbers. C_3–C_5 were blends of C_1 and the atactic fraction which was produced in the ordinary manufacturing process. The molecular weight of each sample was evaluated from the reduced viscosity at 135°C of a decalin solution by using the equation of Kinsinger and Hughes,[10] and the isotacticity was obtained after extraction with boiling n-heptane. The sample films for stretching were prepared from the above samples by the methods summarized in Table II.

All the films prepared were about 400 μ in thickness.

Stretching

Biaxial Stretching. Film 1 was stretched polyaxially in poly(ethylene glycol) as reported in the previous paper (method A)[9] after 5 min preheating, while the other films were stretched in the air biaxially in one step at various temperatures by an apparatus constructed in our laboratory, which will be reported elsewhere in detail.[11] The rate of stretching in the air was about 3 mm/sec, and the films were stretched by the same amount in all directions.

Uniaxial Stretching. In order to compare the deformation behavior in biaxial stretching with that in uniaxial stretching, films 1 and 2 were stretched uniaxially in the air at 140°C at a stretching rate of 3 mm/sec.

This paper, however, deals mainly with the deformation behavior in biaxial stretching and the word stretching in subsequent sections refers to biaxial stretching unless otherwise specifically noted.

Electron Microscopy. Morphological changes of the spherulites in stretching were studied by using electron microscopes from Japan Electron Optics Laboratory Co. Ltd. Electron microscopes of the transmission type (JEM-T-4 and JEM-30B) were mainly employed (replica method); a scanning type (JSM-2) was also used.

RESULTS AND DISCUSSION

Figure 1 shows the spherulites of film 1 before stretching and Figure 2 those after stretching to $v_A = 1.4$, where v_A is the degree of stretching expressed as the ratio of area after stretching to that before stretching.

It is clearly seen that the deformation occurs in both the center and boundaries of each spherulite, the latter being dominant. The type of deformation at boundaries is necking.

On elevating the stretching temperature, such a local deformation becomes gradually less remarkable. Figure 3 shows a film stretched at 160°C ($v_A = 1.4$), where the changes in the centers and boundaries of the spherulites are considerably obscure compared with those at 130°C. It seems likely that the deformation of the spherulites becomes more homogeneous at a higher temperature.

It was confirmed that similar local deformation also occurred when film 1 was stretched biaxially in one step in the air, so the phenomenon seems to
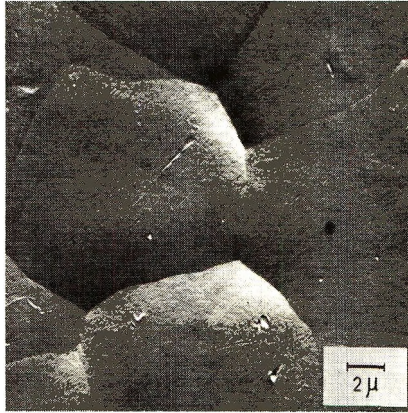
Fig. 1. Electron micrograph of film 1; $v_A = 1.0$.

Fig. 2. Electron micrograph of film 1 stretched polyaxially at 130°C in poly(ethylene glycol); $v_A = 1.4$.
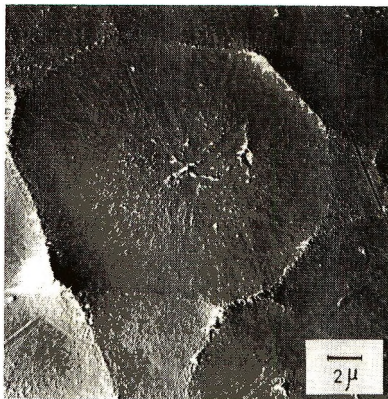

Fig. 3. Electron micrograph of film 1 stretched polyaxially at 160°C in poly(ethylene glycol); $v_A = 1.4$.

be independent of the type of stretching and the medium employed for stretching.

When film 2 was stretched at 140°C, the deformation occurred at the center of each spherulite and spread outward with increasing v_A, the boundaries remaining unbroken.   Figure 4 shows film 2 stretched to $v_A = 1.2$.
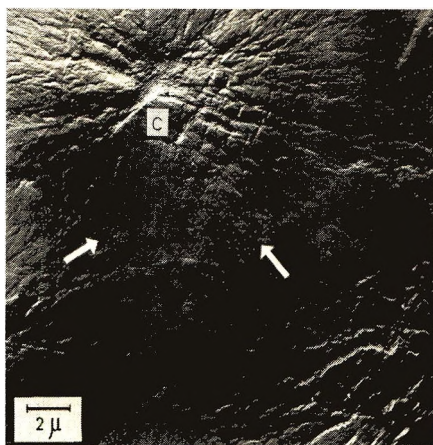
Fig. 4. Electron micrograph of film 2 stretched biaxially in the air in one step at 140°C; $v_A = 1.2$.   Breaking occurs at the center (C) but the boundaries (indicated by arrows) are kept unbroken.
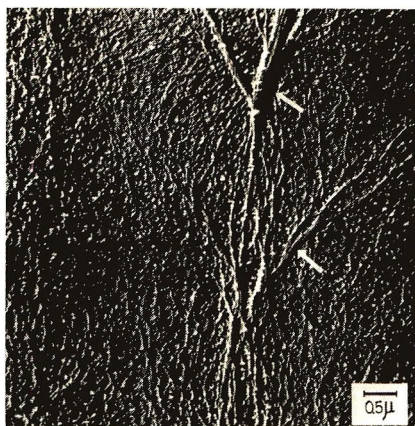
Fig. 5. Electron micrograph of film 2 stretched biaxially at 140°C in air; $v_A = 19$. Dendritic fragments of spherulites (indicated by arrows) are seen in the net structure of fibrils.

At an intermediate degree of stretching, spherulites were broken into many small fragments which were connected by fibrils unfolded from the fragments.   The fibrillation proceeded with increasing v_A at the expense of the residual fragments.   Figure 5 shows the state of $v_A = 19$, where the dendritic fragments of the spherulites can be seen in the center of the net
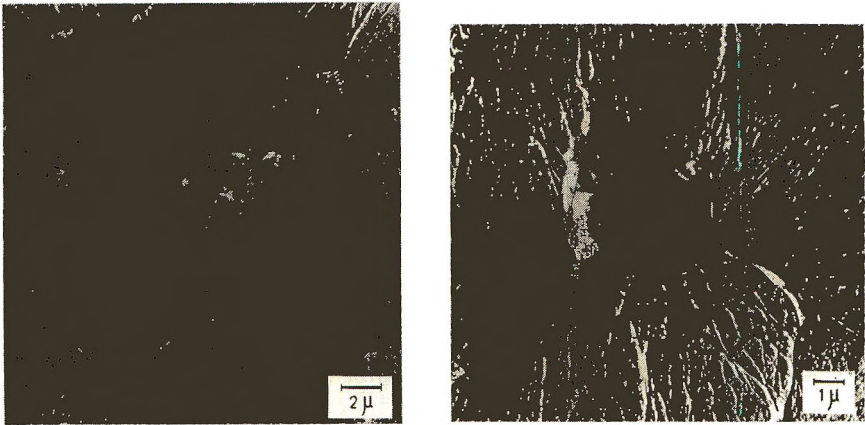
Fig. 6. Electron micrographs of film 3 stretched biaxially at 140°C in air; $v_A = 22$:   (a) blocklike fragments are seen; (b) high magnification of a blocklike fragment.
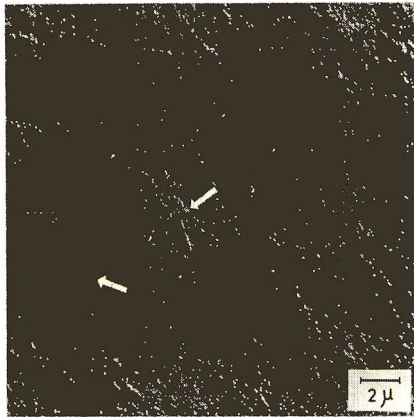

Fig. 7. Surface of film 3 stretched biaxially at 152°C in air; $v_A = 19$.   Fragments are fibrillar as shown by arrows.

Fig. 8. Spherulites of film 4 stretched biaxially in air at 140°C; $v_A = 1.2$.

Fig. 9. Boundaries between three spherulites, I, II, and III of film 5 stretched biaxially at 140°C in air; $v_A = 1.2$. Breaking can be seen between the boundaries (I,II) and (I,III) but not at the boundary (II,III). Also cracking occurs radially on I and II but tangentially on III.
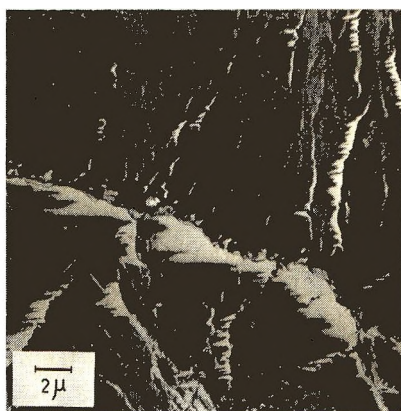

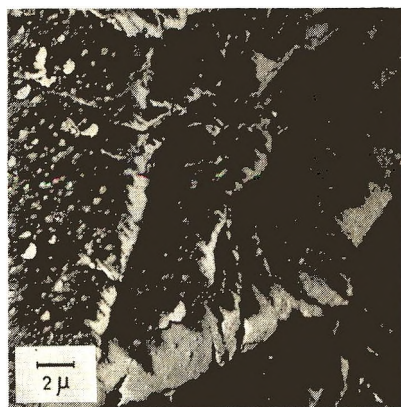Fig. 10. Spherulites of film 6 stretched biaxially in air at 140°C; $v_A = 1.2$.

Fig. 11. Spherulites of film 7 stretched biaxially in air at 140°C; $v_A = 1.2$.
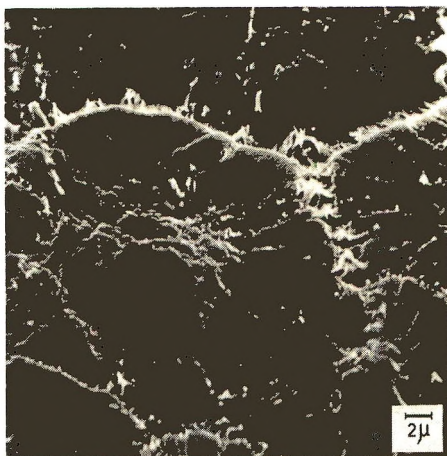
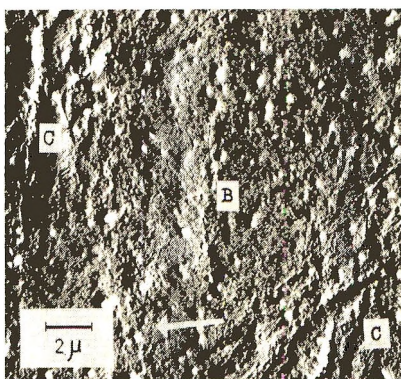Fig. 12. Scanning type electron micrograph of film 7 stretched biaxially in air at 140°C; $v_A = 1.4$.

Fig. 13. Electron micrograph of film 2 stretched uniaxially in air at 140°C; degree of stretching = 1.2. Breaking occurs at the centers (C) of the spherulites and their boundaries (B) are not so broken. The direction of stretching is indicated by an arrow.

structure of fibrils, the finest one being about 400 μ in width. Dendritic fragments are fibrillated more finely as v_A increases.

This phenomenon was more prominent in the case of film 3. Figure 6a shows the film stretched at 140°C to $v_A = 22$, where fibrils are running among block-like fragments. One of the fragments is shown in high magnification in Figure 6b. It is clearly seen that the fragment is not structureless and fibrillates into fringes from the edge.

When stretching is carried out at a higher temperature (152°C), the fragments are transformed to dendritic fibrils as is shown in Figure 7.

It would seem that the deformation of the spherulites annealed at a higher temperature is heterogeneous, and the spherulites break into block-like fragments and finer fibrils connecting the fragments after a stretching of medium degree ($v_A = 22$). On the other hand, quenched and not well
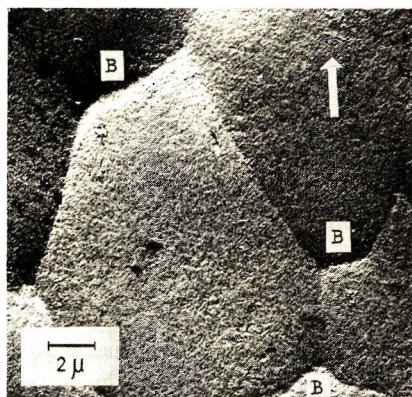
Fig. 14. Electron micrograph of film 1 stretched uniaxially in air at 140°C; degree of stretching = 1.2. Breaking occurs at the boundaries (B) of the spherulites. The direction of stretching is indicated by an arrow.

developed spherulites suffer comparatively homogeneous deformation and fibrillate finely through the stage of coarse dendritic fragments instead of that of the blocklike ones.

When the stretching temperature is elevated, the thermal motion of the segments constituting the spherulite becomes violent and makes it easy to split fibrillar lamellae from blocklike fragments; the deformation of the annealed film then becomes similar in type to that of the quenched film.

Electron micrographs of films 4–7, each stretched to $v_A = 1.2$, are shown in Figures 8–11, respectively. In the case of film 4, which has the highest isotacticity of these films, the spherulite boundaries are not broken, but tangential breakings are observed on the spherulite. In Figure 9 the boundaries between three spherulites, I, II, and III, are shown, where breaking occurs between I and II as well as I and III, but not between II and III. Also, radial cracks can be seen on I and II but not on III. These phenomena may be due to differences in the structure of I and II compared to III. We have often observed that morphologically different spherulites exist in contact within a small area of a film as in Figure 9. The reason is not clear at present. As the isotacticity decreases further (Figs. 10 and 11), the cracks at the boundaries as well as the radial cracks become progressively more prominent.

Figure 12 is a scanning electron micrograph of film 7 ($v_A = 1.4$). It can be noticed that fibrils extend across the cracks between the spherulites and some oblong cavities exist parallel to the fibrils among them. This is because the stretching force acts radially and tangentially on the spherulites. The force brings about also many small radial and tangential cracks in the spherulites, and many unfolded fibrils can be seen to cross these cracks. Moreover, the crystalline lamellae stack in a rooflike fashion.

The boundary and radial cracks may be due to the fact that atactic polymer molecules or low molecular weight fractions are segregated between the spherulites and between the lamellae during crystallization.[2]

This trend becomes marked with increasing atactic content of the film. When the isotacticity is sufficiently high, however, the spherulites are so strong that the cracks are apt to occur tangentially. It is noted that the deformation type of film 1 is different from that of film 4, irrespective of nearly equal value of isotacticity. So these phenomena are dependent not only on isotacticity but also on other factors such as crystallization conditions.

Figure 13 shows an example of the deformation of the spherulites of film 2 stretched uniaxially in the air at 140°C. The centers of the spherulites are preferentially broken similar to the case of biaxial stretching (Fig. 4), while in film 1 (Fig. 14) deformation occurs mainly at the spherulite boundaries. These deformation types correspond well to those in biaxial stretching.

References

1. H. D. Keith and F. J. Padden, Jr., *J. Polym. Sci.*, **41**, 525 (1959).
2. L. Barish, *J. Appl. Polym. Sci.*, **6**, 617 (1962).
3. Y.-F. Yu and R. Ullman, *J. Polym. Sci.*, **60**, 55 (1962).
4. N. Takashima, *Kobunshi*, **12**, 663 (1963).
5. K. Kamide, *Sen-i Gakkaishi*, **22**, 408 (1966).
6. F. J. Padden, Jr., and H. D. Keith, *J. Appl. Phys.*, **30**, 1479 (1959).
7. M. Inoue, *J. Polym. Sci.*, **55**, 443 (1960).
8. J. Schooten, *J. Appl. Polym. Sci.*, **10**, 122 (1960).
9. S. Okajima and K. Homma, *J. Appl. Polym. Sci.*, **12**, 411 (1968).
10. J. B. Kinsinger and R. E. Hughes, J. Phys. Chem., *63*, 2022 (1959).
11. S. Okajima and T. Masuko, Sen-i Gakkoishi, to be published.

Received: January 17, 1969

Polymerization of Methyl Methacrylate Under Ultrasonic Irradiation. Part IV. Effect of Ultrasonic Irradiation on Grignard Catalyst and Stereoregularity of the Polymers Produced in Dioxane–tetrahydrofuran Mixed Solvent

ZENJIRO OSAWA, TAKAO KIMURA, and TAKAO KASUGA,*

*Faculty of Technology, Gunma University, Kiryu City, Gunma, Japan*

Synopsis

Two series of polymerization of methyl methacrylate with Grignard reagent in dioxane–tetrahydrofuran mixed solvent was carried out under ultrasonic irradiation. In series A, catalyst was added to the mixture of monomer and solvent, and in series B, catalyst was previously mixed with solvent. The effect of ultrasonic irradiation on Grignard catalyst and the microstructure in reacting sites were discussed on the basis of the stereoregularity of the polymers produced. The stereoregularity of the polymers in series A was higher than that in series B. The effect of ultrasonic irradiation on the stereoregularity was completely reversed in series A and B and it increased in the former and decreased in the latter. It was, therefore, assumed that ultrasonic irradiation affected the microstructure in the reacting sites in series A, while it increased the relative amount of R_2Mg which gave polymers with poor stereoregularity in series B.

INTRODUCTION

In previous papers of this series[1–3] the effect of ultrasonic irradiation on the microstructure in the transition state of the polymerization of methyl methacrylate has been discussed on the basis of the stereoregularity of the polymers produced. It is assumed that the ultrasonic irradiation affects the initiator as well as the reacting sites in anionic polymerization. This paper presents our efforts to examine the effect of ultrasonic irradiation on Grignard catalyst and stereoregularity of the polymers produced in mixed solvent of dioxane and tetrahydrofuran.

The chemical equilibrium shown in eq. (1) has been presented for Grignard reagents in solution.[4–7] The equilibrium is affected by solvent, concentration of catalyst, temperature, and substituents (R or X).[5,6]

$$2RMgX \rightleftarrows R_2Mg + MgX_2 \rightleftarrows R_2Mg \cdot MgX_2 \tag{1}$$
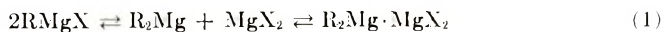
* Present address: Research Institute, Nissan Kagaku Ltd., Ichihara City, Chiba, Japan.

Ashby and Smith[8] confirmed the propriety of the equilibrium in diethyl ether recently, and reported that phenylmagnesium bromide was in the monomeric form in dilute solution (ca. 0.05 mole/l.), and approached a dimeric form at relatively high concentration (0.5–1.0 mole/l.). It was also reported[9] that the dimeric structure, $R_2Mg \cdot MgX_2$, could not be formed in tetrahydrofuran, since a strong coordination of basic tetrahydrofuran with magnesium made it impossible to form halogen bridges. Thus, the actual chemical equilibrium was as given by eq. (2).

$$2RMgX \rightleftharpoons R_2Mg + MgX_2 \tag{2}$$

Schlenk[4,5] reported that all MgX_2 and some $RMgX$ or $R_2Mg \cdot MgX_2$ formed precipitants of the addition compounds of dioxane when dioxane was added to diethyl ether solution of Grignard reagents, and dialkyl magnesium remained in ether solution. Further studies on this problem by Kullman[10] showed that the amount of dialkyl magnesium in diethyl ether was affected by the rate of the addition of dioxane. For examples, if the addition of dioxane was made slowly for a long time the concentration of dialkyl magnesium became higher than for a short time. Furthermore, if mechanical agitation was supplied to the system, the amount of dialkyl magnesium also increased.[10,11]

Goode et al.[12] and Kawabata et al.[13] reported that dialkyl magnesium was an active species for the initiation of methyl methacrylate polymerization and gave polymers with poor stereoregularity, while the other active species, $RMgX$, gave polymers with good stereoregularity.

The facts described above indicate that the relative amount of active species, $RMgX$ and R_2Mg is reflected in the stereoregularity of the polymers produced. If externally supplied energy such as ultrasonic irradiation affects the chemical equilibrium of Grignard reagent and increases the amount of dialkyl magnesium, polymers with poor stereoregularity would be produced. In addition, if reacting sites are affected by ultrasonic irradiation, this would be indicated by a change in the stereoregularity of the polymers produced. For the experimental approach, two series of experiments in which the order of addition of catalyst was reversed, were carried out with and without ultrasonic irradiation.

EXPERIMENTAL

Preparation of Reagents

Purification of the monomer and synthesis of the initiator were described in previous papers.[1–3] Dioxane was first refluxed with $0.4N$ aqueous hydrochloric acid to remove acetaldehyde and was dried over potassium hydroxide pellets and then distilled under dry nitrogen. Tetrahydrofuran was refluxed with sodium wire and then distilled under dry nitrogen.

Polymerization

Polymerizations were divided into two series, namely, the series A (no ripening of initiator system) and series B (ripening of initiator system). Polymerization techniques are described below.

Series A (No Ripening of Initiator System).   A solution of 4 ml of methyl methacrylate and 16 ml of mixed solvent of dioxane and tetrahydrofuran was placed in a 100 ml flask which was previously flushed with dry nitrogen, and the contents were kept at 20°C.   Then 3 ml of phenyl-magnesium bromide in toluene solution $(2.8 \times 10^{-3}M)$ was introduced by means of syringe.

Series B (Ripening of Initiator System).   The same amount of solvent and initiator as in the series A were added to a 100-ml flask and the contents were left for 10 min.   Then 4 ml of monomer was introduced by means of a syringe and polymerization was started.

Polymerization was carried out at constant temperatures, 20 or 28°C for 30 min, and termination was made with methanol containing a small amount of hydrochloric acid.   Methanol-insoluble portions were purified by the methanol–chloroform system.   The amount of tetrahydrofuran in mixed dioxane–tetrahydrofuran solvent was 0, 1, 3, 5, 10, 15, 20, 60, 80, 90, 95, and 100 vol-%.   Parallel runs were carried out under ultrasonic irradiation at a frequency of 500 kcps and input power of 100 W.   The temperature of the system was raised to 28°C by the ultrasonic irradiation.

Characterization of the Products

Intrinsic viscosity was determined in benzene solution at 25°C and viscosity-average molecular weight was calculated by the relationship, $[\eta] = 5.7 \times 10^{-5} \bar{M}_v^{0.76}$ derived from measurements of conventional poly(methyl methacrylate).[14]   Determination of the structure of the polymers was made by NMR spectral analysis.[15]   The NMR instrument used was a Hitachi Model R-20.

RESULTS AND DISCUSSION

Polymerization conditions and results are listed in Table I.

Although a distinct tendency in conversion is not observable from Table I, the conversion generally decreases with increasing amount of tetrahydrofuran in mixed solvent for each series.   In the case of series A, where initiator was added to the monomer–solvent mixture, the conversion without ultrasonic irradiation was higher than that with ultrasonic irradiation series.   However, the opposite results were obtained in series B, where initiator was previously mixed with solvent for 10 min.

On the other hand, the degree of polymerization in series B is lower than that in series A.   In both series A and B, the degree of polymerization of the polymers produced under ultrasonic irradiation is lower than without it. This is probably ascribed to the degradation of the polymers by ultrasonic

TABLE I
Polymerization Conditions and Results

THF:dioxane (by vol)	Series A (no ripening)				Series B (ripened)			
	Conversion, %		$\overline{DP} \times 10^{-3}$		Conversion, %		$\overline{DP} \times 10^{-3}$	
	Without US[a] (20°C)	With US (28°C)[b]	Without US (20°C)	With US (28°C)[b]	Without US (28°C)	With US (28°C)[b]	Without US (28°C)	With US (28°C)[b]
0:100	12.8	3.8	3.21	2.14	4.8	8.9	1.30	0.78
1:99	10.9	2.8	2.76	1.35	5.3	9.4	1.18	0.73
3:97	9.9	—	2.14	—	—	—	—	—
5:95	10.6	5.7	3.16	1.23	4.5	8.9	0.99	0.72
10:90	12.5	3.4	1.91	1.29	4.6	8.5	1.15	0.59
15:85	7.1	1.3	2.34	1.59	—	—	—	—
20:80	7.5	6.0	2.04	1.32	3.7	6.0	1.15	0.53
60:40	2.4	4.6	1.32	1.20	4.0	4.3	0.91	0.47
80:20	—	—	0.81	—	0.5	4.5	—	0.87
90:10	0.7	0.6	0.55	0.67	0.1	0.1	—	—
95:5	0.4	—	—	—	—	—	—	—
100:0	1.6	0.2	6.17	1.66	trace	—	—	—

[a] Ultrasonic irradiation (100 W).
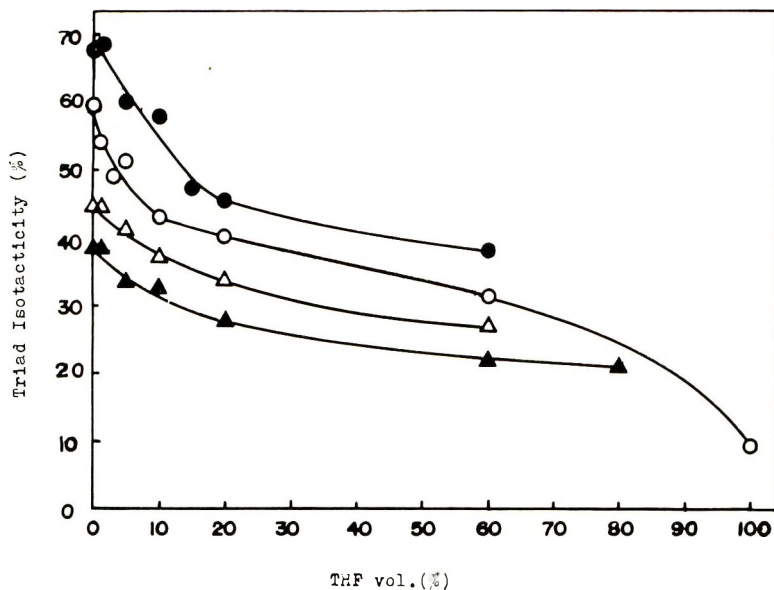[b] Temperature was raised to 28°C by ultrasonic irradiation.

Fig. 1. Isotacticity: (○) series A (no ripening of initiator system), without ultrasonic irradiation; (●) series A (no ripening), with ultrasonic irradiation; (△) series B (ripening of initiator system), without ultrasonic irradition;   (▲) series B (with ripening), with ultrasonic irradiation.
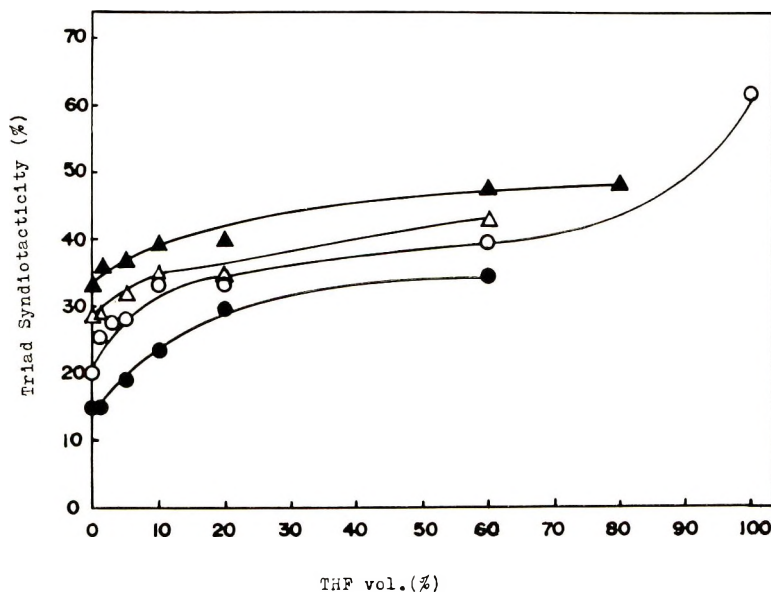

Fig. 2. Syndiotacticity: (○) series A (no ripening of initiator system), without ultrasonic irradiation; (●) series A (no ripening), with ultrasonic irradiation; (△) series B (ripening of initiator system), without ultrasonic irradiation;   (▲) series B (with ripening), with ultrasonic irradiation.

irradiation. To confirm this assumption, ultrasonic treatment of poly-(methyl methacrylate) was carried out in benzene at a concentration of 0.75 wt-%, and we observed that degradation of the polymers occurred.[1] Similar experiments on preformed polymers was also carried out to check the possibility of degradation in dioxane at a concentration of 0.82 wt-%. The initial intrinsic viscosity, 0.57 dropped to 0.50, 0.49, and 0.32 dl/g after 30, 60, and 180 min, respectively. Therefore, the assumption that the lower degree of polymerization in the series receiving ultrasonic treatment is due to the degradation of polymer by ultrasonic irradiation seems to be valid under the conditions used in this experiment.

The stereoregularity of the polymers determined by NMR spectral analysis and plots of isotacticity and syndiotacticity against the concentration of tetrahydrofuran in mixed solvent are shown in Figures 1 and 2, respectively.

It is well known that the stereoregularity of the polymers polymerized by an anionic initiator decreases with increasing polarity of the solvent used.[16-19] Nishioka et al. reported that the stereoregularity of the polymers polymerized with Grignard reagents in dioxane was different from that in toluene.[20] Our experimental results, shown in Figures 1 and 2, demonstrate that polymers with relatively low stereoregularity were produced in dioxane.

As described above, one goal in this experiment was to examine the microstructure of the reacting sites and also to obtain information on the structure of the active species for the polymerization of methyl methacrylate with Grignard reagent. For our purpose, an indirect method, namely, the analysis of the stereoregularity of the polymers produced, seems to offer helpful information.

As shown in Figures 1 and 2, plots of isotacticity and syndiotacticity against the concentration of tetrahydrofuran in mixed solvent give four separate curves in which isotacticity decreases with increasing polar solvent (tetrahydrofuran), and naturally a reverse tendency is observed in syndiotacticity. When one compares the stereoregularity of series A and B, the former, in which initiator was added to the monomer–solvent mixture, gives better stereoregularity than the latter, in which initiator was mixed previously with solvent. For examples, in the case without ultrasonic irradiation series, isotacticity of the polymer polymerized in 100% dioxane is 59.5% in series A and is 44.6% in series B. In the case with the ultrasonic-irradiated systems it is 67.0% in series A and is 38.4% in series B. On the basis of the results described above and the facts that the chemical equilibrium of Grignard reagents is affected by various factors, for examples, solvent, concentration of catalyst, temperature, time, and so on, it is quite probable that the relative amount of dialkyl magnesium is higher in series B (ripening system) than that in series A (no ripening), since dialkyl magnesium gives polymers with less stereoregularity.[12,13]

Therefore the results described above suggest that the relative amount of

active species, namely, RMgX and R_2Mg, in the polymerization of methyl methacrylate is extensively affected by the conditions applied to the polymerization system, in other words, it is reflected in the stereoregularity of the polymers produced. Thus, it is advisable to take into consideration the relative amount of active species when one discusses the structure of the polymers produced by Grignard reagents.

The opposite effect of ultrasonic irradiation on the stereoregularity of the polymers was observed between series A and B. In series A, isotacticity of the polymers produced with ultrasonic irradiation was higher than that without it, while in series B, isotacticity with ultrasonic irradiation was lower than without it.

In the previous papers,[1-3] we reported that the ultrasonic irradiation gave no effect on the stereoregularity of the polymers polymerized in nonpolar solvent such as toluene and it increased isotacticity of the polymers polymerized in a mixed solvent of toluene and dimethyl sulfoxide. In general, it is known that the predominant structure of the reacting sites is contact ion-pairs in nonpolar solvent such as toluene, and solvent-separated ion-pairs appear in accordance with the increase of polarity of solvent.[21,22] Therefore we concluded that solvation of reacting sites by polar solvent was weakened, and a chelating bond between propagating polymer end and gegenion was rather strengthened by the externally supplied ultrasonic irradiation.

In the case of series A, isotacticity with ultrasonic irradiation was higher than that without it. This was consistent with the results reported in previous papers. For examples, at a concentration of 1% tetrahydrofuran, the isotacticity of the polymers produced without ultrasonic irradiation was 53.7%, while it increased to 68.4% on ultrasonic irradiation. Similar results were also observed in all pairs of experiment runs. Therefore the explanation of the previous papers[1-3] seems to be valid in this study of the dioxane–tetrahydrofuran solvent system.

When the initiator was mixed with solvent for 10 min previously (series B), stereoregularity of the polymers polymerized under ultrasonic irradiation was lower than that without it. For examples, at a concentration of 1% tetrahydrofuran, the isotacticity of the polymer produced without ultrasonic irradiation was 44.7%; with ultrasonic irradiation it was 38.2%. Similar results were also observed in all pairs of experiment runs. Since Kullman reported that the agitation increased the concentration of dialkyl magnesium, it was probable that the chemical equilibrium of Grignard reagent was influenced by the application of ultrasound during the ripening of catalyst and solvent, and the increased dialkyl magnesium gave polymers with less stereoregularity.

References

1. Z. Osawa and N. Igarashi, *J. Appl. Polym. Sci.*, **9**, 3171 (1965).

2. Z. Osawa, *J. Appl. Polym. Sci.*, **10**, 1863 (1966).

3. Z. Osawa and M. Kusumoto, *Kogyo Kagaku Zasshi*, **71**, 168 (1968).

4. W. Schlenk, and W. Schlenk, Jr., *Ber.*, **62**, 92 (1929).

5. W. Schlenk Jr., *Ber.*, **64**, 734 (1931).

6. Association of Kinki Kagaku Kogyo, Division of Organic Metals *Handbook of Organic Metals*, Asakura Shoten, 1967, p. 39.

7. S. Murahashi, *Chemistry of Organic Metals*, Kagaku Dojin, 1966, p. 62.

8. E. C. Ashby and M. B. Smith, *J. Am. Chem. Soc.*, **85**, 118 (1963).

9. E. C. Ashby and M. B. Smith, *J. Am. Chem. Soc.*, **86**, 4363 (1964).

10. R. Kullman, *Compt. Rend.*, **231**, 866 (1950).

11. C. R. Noller and W. R. White, *J. Am. Chem. Soc.*, **59**, 1354 (1937).

12. W. E. Goode, F. H. Owens, R. P. Fellmann, W. H. Snyder, and J. E. Moore, *J. Polym. Sci.*, **46**, 317 (1960).

13. N. Kawabata and J. Furukawa, *Kogyo Kagaku Zasshi*, **70**, 1423 (1967).

14. P. J. Flory, *Principles of Polymer Chemistry*, Cornell Univ. Press, 1953, p. 312.

15. F. A. Bovey and G. V. D. Tiers, *J. Polym. Sci.*, **44**, 173 (1960).

16. D. Braun, M. Herner, U. Johnsen, and W. Kern, *Makromol. Chem.*, **51**, 15 (1962).

17. D. L. Glusker, R. A. Galluccio, and R. A. Evans, *J. Am. Chem. Soc.*, **86**, 187 (1964).

18. T. Tsuruta, T. Makimoto, and Y. Nakayama, *Makromol. Chem.*, **90**, 12 (1966).

19. C. Schuerch, *Ann. Rev. Phys. Chem.*, **13**, 195 (1962).

20. A. Nishioka, H. Watanabe, K. Abe, and Y. Sono, *J. Polym. Sci.*, **48**, 241 (1960).

21. W. Fowells, C. Schuerch, F. A. Bovey, and F. P. Hood, *J. Am. Chem. Soc.*, **89**, 1396 (1967).

22. T. E. Hogen-Esch and J. Smid, *J. Am. Chem. Soc.*, **87**, 669 (1965).

NOTE

Dead-End Polymerization of Styrene and Methyl Methacrylate in the Benzoyl Peroxide–Dimethylaniline Redox System

Reaction between benzoyl peroxide (BPO) and dimethylaniline (DMA) has been studied extensively by Horner et al.,[1-3] Imoto et al.,[4-6] and others[7,8]. Since this reaction system produces free radicals which can initiate polymerization of vinyl monomers such as styrene and methyl methacrylate (MMA), Imoto et al.[9], Meltzer and Tobolsky,[10] and Walling and Indictor[7] applied the redox system to the polymerization of styrene.

Imoto et al. found that the initial rate of polymerization R_0, can be expressed as

$$R_0 = k[\text{BPO}]_0^{1/2}[\text{DMA}]_0^{1/2}[\text{M}]_0 \tag{1}$$

Although they carried out the polymerization to completion, the rate was extrapolated to zero time. They thought that the steady-state kinetics did not hold in the later stage of polymerization. Kinetic formulations over the whole course of polymerization had not been established until Tobolsky[11] developed a theory of dead-end polymerization in 1958, and showed that free-radical polymerizations proceed only to a limiting conversion, short of unity.

Soon after, O'Driscoll and McArdle[12] applied the theory to the BPO–DMA redox system and carried out a mathematical treatment for the system in which free radicals are produced by a second-order rate process. O'Driscoll[13] gave an explanation for the results of Imoto et al. in terms of the dead-end theory.

Although we did not use the term "dead-end" explicitly at that time, we analyzed the polymerization of vinyl acetate in the BPO–Fe(II)–benzoin redox system by means of a similar concept.[14]

O'Driscoll and McArdle[12] extended eq. (1) to the whole course of polymerization, the rate of which can be expressed by

$$-dM/dt = (f/A')^{1/2}(k_d ab)^{1/2}M \tag{2}$$

where $A' = k_t/k_p^2$, f is the catalyst efficiency; a, b, and M are the concentrations of DMA, BPO, and monomer, respectively. They assumed that the decomposition of BPO by a second-order rate process yields two free radicals effective for polymerization, and that 1:1 stoichiometry holds for the process. If half of the fragments from BPO are effective,[9] f in this paper and in reference 5 may be regarded as half of the true efficiency.

On the basis of this stoichiometry assumption, eq. (2) can be integrated to yield eq. (3).[12]

$$M_0/M_t = \left\{\left[\frac{(a_0/b_0)^{1/2}\exp\{k_d t(a_0 - b_0)/2\} - 1}{(a_0/b_0)^{1/2}\exp\{k_d t(a_0 - b_0)/2\} + 1}\right] \times \left[\frac{(a_0/b_0)^{1/2} + 1}{(a_0/b_0)^{1/2} - 1}\right]\right\}^{(f/A'k_d)^{1/2}} \tag{3}$$

At infinite time, eq. (3) reduces to eq. (4):

$$M_0/M_\infty = [\{(a_0/b_0)^{1/2} + 1\}/\{(a_0/b_0) - 1\}]^{(f/A'k_d)^{1/2}} \tag{4}$$

It is very interesting to note that eq. (4) suggests that in the redox system, infinite conversion is determined only by the ratio a_0/b_0 and not by their absolute values, and that the maximum limiting conversion of unity should be obtained when $a_0 = b_0$. We have examined these equations for various values of a_0/b_0. The conversion was determined gravimetrically. The number-average degree of polymerization was estimated by means

TABLE I

Conversion, Degree of Polymerization, and Catalyst Efficiency for
Bulk Polymerization of Styrene at 0°C in BPO–DMA Redox System

b_0, mole/l.	a_0, mole/l.	x_i[a]			$\bar{P}_n$	f[b]
		Found	Calcd. by eq. (3)	Calcd. by eq. (11)		
0.00	0.10	0.00	0.00	0.00	—	—
0.01	0.09	—	0.067	0.066	—	—
0.02	0.08	0.097	0.103	0.100	496	0.0863
0.03	0.07	0.127	0.137	0.134	424	0.0887
0.04	0.06	0.163	0.167	0.170	408	0.0885
0.045	0.055	0.187	—	—	415	0.0887
0.05	0.05	0.203	0.200	0.206[c]	345	0.104
0.055	0.045	0.222	—	—	383	0.0935
0.06	0.04	0.228	0.167	0.220	362	0.0934
0.07	0.03	0.201	0.137	0.198	409	0.0971
0.08	0.02	0.165	0.103	0.153	441	0.110
0.09	0.01	—	0.067	0.100	—	—
0.10	0.00	0.011	0.00	0.00	3540	
					Avg.	0.0945

[a] Polymerization time: 185 hr.

[b] Calculated by eqs. (14) and (15).

[c] Calculated by eq. (11').

of the following equations: $\bar{P}_n = 1770[\eta]^{1.40}$ for polystyrene; $[\eta] = 2.87 \times 10^{-3} \bar{P}_n^{0.80}$ for PMMA. Experimental details have been given elsewhere.[5] A part of the results are summarized in Table I.

If one substitutes the numerical values, $k_d = 2.5 \times 10^{-4}$ l./mole-sec, $f = 0.10$, given by O'Driscoll and McArdle,[12] $A' = 4 \times 10^4$ mole/l.-sec (average value of Tobolsky et al.[16] and Bamford et al.[17]), $t = 6.66 \times 10^5$ sec, and initial concentrations of BPO and DMA all into eq. (3), one obtains predicted values of conversion as given in Table I. Figure 1 shows experimental points and the predicted curve at 0°C. In the figure the conversions are plotted against the molar fraction of DMA. This is because eq. (3) can be approximated to eq. (4) in our experimental conditions. The calculation of the conversion at $a_0 = b_0$ was made using eq. (5) instead of eq. (3).

$$M_0/M_t = (k_d a_0 t + 1)^{(f/A'k_d)^{1/2}} \tag{5}$$

Appearance of a maximum in the experimental plot suggests that the dead-end theory based on the bimolecular decomposition of the catalyst is in a right direction. However, to judge from the assymmetry of the points, the exact maximum does not correspond to $a_0 = b_0$ but appears at $b_0 > a_0$. Similar results were obtained at 25°C., as seen in Figure 2. Data of Imoto et al.[9] are also plotted in the figure. Due to the lack of the data, the maximum limiting conversion at 50°C is uncertain. It seems, however, that the maximum is shifting to larger b_0/a_0 ratio the higher the temperature is, and vice versa.

In case of MMA polymerization, acceleration in rate occurred in bulk and with equivolume solution of MMA and benzene, and the limiting conversions approached to unity, irrespective of b_0/a_0 ratios. However, when MMA was diluted to 20 vol-% by benzene, dead-end polymerization was observed as shown in Figure 3.

In spite of strong support for the dead-end theory, these experimental data clearly show the eq. (3) to be modified. In our system, a complete treatment of the decomposition of BPO would have to solve the following kinetic scheme:

$$-db/dt = k_1 ab + k_2 b + k_3 [a \cdot] b + k_4 [P \cdot] b + \ldots \tag{6}$$

where [a·] is the concentration of a radical fragment from the the amine, which cannot initiate polymerization but is assumed to exist as an intermediate product of the primary reaction between DMA and BPO.[9] The fourth term is induced decomposition by living polymer chains.[18] It would be necessary to examine which of these terms is predominant.
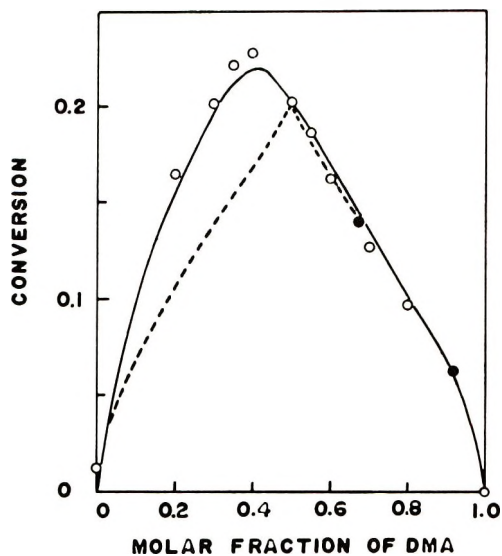

Fig. 1. Relationship between molar fraction of DMA and limiting conversion of styrene in BPO–DMA redox system at 0°C: (———) theoretical plot of eq. (11); (- - -) eq. (3); (O) data of this work; (●) data of O'Driscoll and McArdle.[12]
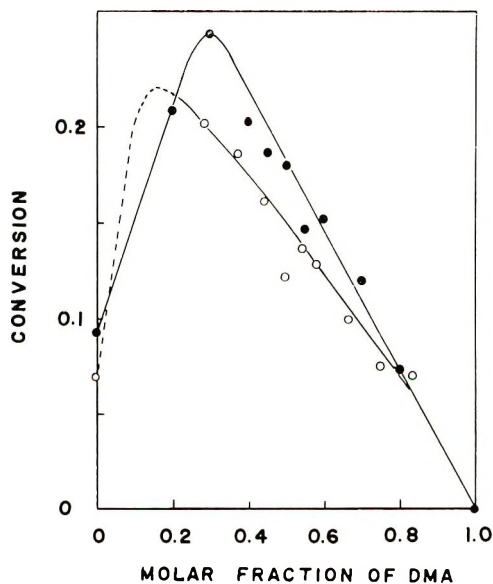

Fig. 2. Plot of molar fraction of DMA vs. limiting conversion of styrene at 25 and 50°C: (●) this work, 25°C; (O) data of Imoto et al.,[9] 50°C.
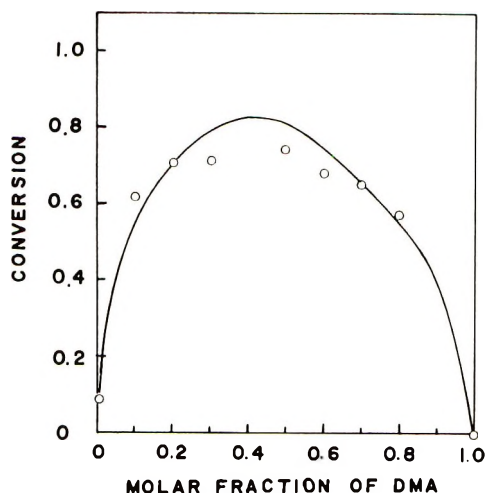
Fig. 3. Limiting conversion as a function of molar fraction of DMA in the solution polymerization of MMA in the BPO–DMA redox system at 0°C: (——) predicted by eq. (11) with $r = 1.5$; (O) experimental points. Polymerization time = 161 hr.

(1) The activation energy of k_2 is known to be about 30 kcal/mole. At lower temperatures, the second term may be negligible as far as we use comparable amount of DMA and BPO ($k_2 \approx 10^{-10}$ sec^{-1} at 0°C). However, this term cannot be neglected at higher temperatures, since we are interested in a long-time polymerization. (see Fig. 2).

(2) If the first and the third terms in eq. (6) are predominant as may be the case at lower temperatures, these terms are combined to be $k_1ab + k_3[a\cdot]b = k_dab$, where $k_d = rk_1$. The r may be regarded as the ratio of the reacting number of BPO to that of DMA. As far as other terms can be neglected, the ratio r should take values between 1 and 2: $r = 1$ if $k_1 \gg k_3$, and 2 if $k_3 \gg k_1$. Owing to this restriction, k_d can be regarded as approximately constant in the following calculations.

(3) Assuming a steady-state radical concentrations which are taking part in the polymerization, the concentration of the living polymer, $[P\cdot]$, is given by

$$[P\cdot] = (fk_dab/k_t)^{1/2} \tag{7}$$

where f is the total efficiency of BPO produced by the processes described in (2). On combining eqs. (6) and (7), it follows that

$$-db/dt = k_dab\{1 + (k_4/k_t^{1/2})(f/k_d)^{1/2}(b/a)^{1/2}\} \tag{8}$$

By inspection one finds that f and k_d in this note are the same as those in the paper of O'Driscoll and McArdle.[12] The value $k_4/k_t^{1/2}$ at 90°C is presumed to be[18] (5–10) $\times$ 10^{-3} l./mole sec with the activation energy of about 2.5 kcal/mole. Hence $k_4/k_t^{1/2}$ at 0°C may be 3.5×10^{-4} l./mole-sec at most. Substituting this value and $f = 0.1$, $k_d = 2.5 \times 10^{-4}$ l./mole-sec into eq. (8), one obtains

$$-db/dt = k_dab\{1 + 0.007(b/a)^{1/2}\} \tag{8'}$$

Hence the time when the second term of eq. (8) becomes 10% of the first term may be about 70 hr, with $b_0 = 0.09$ and $a_0 = 0.01$ mole/l., and $r = 1.5$, rough calculation being made by means of eq. (10). Thus, it is evident that under our experimental conditions, the second term in eq. (8) can be neglected. Therefore, the rate of decomposition of BPO may be written as

$$dx/dt \cong k_d(b_0 - x)(a_0 - x/r) \tag{9}$$

Integration of eq. (9) leads to eq. (10):

$$b/a = (b_0/a_0)\exp\{k_d t(b_0 - a_0 r)/r\} \tag{10}$$

Thus we have the following equations:

$$M_0/M_t = \left\{ \left[\frac{(b_0/a_0)^{1/2}\exp\{k_d t(b_0 - a_0 r)/2r\} - r^{1/2}}{(b_0/a_0)^{1/2}\exp\{k_d t(b_0 - a_0 r)/2r\} + r^{1/2}} \right] \times \right.$$
$$\left. \left[\frac{(b_0/a_0)^{1/2} + r^{1/2}}{(b_0/a_0)^{1/2} - r^{1/2}} \right] \right\}^{(fr/A'k_d)^{1/2}} \quad b_0 \neq a_0 r \tag{11}$$

and

$$M_0/M_t = (k_d a_0 t + 1)^{(fr/A'k_d)^{1/2}} \qquad b_0 = a_0 r \tag{11'}$$

At infinite time,

$$M_0/M_\infty = \left[\{(b_0/a_0)^{1/2} + r^{1/2}\} / \{(b_0/a_0)^{1/2} - r^{1/2}\} \right]^{(fr/A'k_d)} \tag{12}$$

According to eq. (12), the maximum limiting conversion of unity should appear at $b_0/a_0 = r$. As seen in Figure 1, $r \cong 1.5$ at $0°C$. The solid line in Figure 1 is drawn with the use of eq. (11) with this r value. However, the experimental limiting conversion is far less than unity for styrene. Inspection of eq. (11') shows that this is only because our polymerization time is too short at $b_0/a_0 = r$.

In the case of MMA, the exponent in eq. (11) is large compared for styrene, and therefore high limiting conversions were obtained. The predicted curve in Figure 3 was drawn with $f = 0.086$ as obtained from the $\bar{P}_n$ value, $A' = 600$ mole/1.-sec.[19,20]

As may be seen from above discussion, the term "limiting conversion" used in this note is restricted in the sense that t is sufficiently large for the verification of eq. (12). However, if t approaches infinity, the neglected terms would play important roles, making this kinetic treatment ambiguous.

The number-average degree of polymerization for polymers cumulatively formed up to a conversion x is given by[15]

$$\bar{P}_n = \bar{s}M_0 x/2f(b_0 - b) \tag{13}$$

where $\bar{s}$ is the average number of fragments of initiator in one polymer molecule. At infinite time, DMA alone remains if $a_0 r > b_0$. In this case eq. (13) becomes

$$\bar{P}_n = \bar{s}M_0 x/2fb_0 \tag{14}$$

On the other hand, if $b_0 > a_0 r$, there is a complete depletion of DMA as $t \to \infty$. The number of moles of BPO reacted per unit volume should then be $a_0 r$ if we neglect the spontaneous decomposition etc. In this case eq. (13) becomes

$$\bar{P}_n = \bar{s}M_0 x/2fa_0 r \tag{15}$$

If f is unknown, this simple relationship may be useful for the determination of f. With all values other than f known, the f were calculated by means of eqs. (14) and (15), numerical values being listed in Table I. The average value, 0.0945, is in fair agreement with the reported value, 0.10–0.11.[12] A similar calculation was made to give $f_{av.} = 0.086$ for MMA, the fraction of disproportionation being assumed to be 0.60.[20]

In summary, the limiting conversion of styrene and MMA is well explained in terms of the dead-end theory in case of the DMA–BPO redox system. However, a better fit is obtained if we introduce a parameter r which measures an average value of the reacted BPO to DMA ratio. From the dead-end theory applied to the degree of polymerization, the catalyst efficiency f was shown to be calculated in a simple way.

References

1. L. Horner and E. Schwenk, *Angew. Chem.*, **61**, 411 (1949).
2. L. Horner and K. Scherf, *Ann.*, **573**, 35 (1951).
3. L. Horner and H. Junkermann, *Ann*, **591**, 53 (1955).
4. M. Imoto and S. Choe, *Kobunshi Kagaku*, **11**, 396 (1954).
5. M. Imoto and S. Choe, *J. Polym. Sci.*, **15**, 485 (1955).
6. M. Imoto and K. Takemoto, *Kobunshi Kagaku*, **13**, 331 (1959).
7. C. Walling and N. Indictor, *J. Amer. Chem. Soc.*, **80**, 5814 (1958).
8. R. Huisgen, W. Heydkamp, and F. Bayerlein, *Ber.* **93**, 363 (1960).
9. M. Imoto, T. Otsu, and T. Ota, *Makromol. Chem.*, **16**, 10 (1955).
10. T. H. Meltzer and A. V. Tobolsky, *J. Amer. Chem. Soc.*, **76**, 5178 (1954).
11. A. V. Tobolsky, *J. Amer. Chem. Soc.*, **80**, 5927 (1958).
12. K. F. O'Driscoll and S. A. McArdle, *J. Polym. Sci.*, **40**, 557 (1959).
13. K. F. O'Driscoll, *J. Polymer Sci.*, **47**, 520 (1960).
14. S. Hasegawa, N. Hirai, N. Nishimura, and T. Kawano, *Bull. Chem. Soc. Japan*, **31**, 696 (1958).
15. N. Nishimura, *J. Macromol. Chem.*, **1**, 257 (1966).
16. A. V. Tobolsky and J. Offenbach, *J. Polym. Sci.*, **16**, 311 (1955).
17. C. H. Bamford and M. J. S. Dewar, *Proc. Roy. Soc. (London)*, **A192**, 309 (1948).
19. K. F. O'Driscoll and P. J. White, *J. Polym. Sci. A*, **3**, 283 (1965).
19. J. P. Van Hook and A. V. Tobolsky, *J. Polym. Sci.*, **33**, 429 (1958).
20. J. C. Bevington and H. W. Melville, *J. Polym. Sci.*, **14**, 463 (1954).

Department of Chemistry   NORIO NISHIMURA
Faculty of Science
Okayama University
Okayama, Japan